

AD-787 517

**PHASE DIAGRAMS OF SILICATE SYSTEMS:
HANDBOOK; THIRD ISSUE; TERNARY SYSTEMS**

N. A. Toropov, et al

**Army Foreign Science and Technology Center
Charlottesville, Virginia**

10 June 1974

DISTRIBUTED BY:



**National Technical Information Service
U. S. DEPARTMENT OF COMMERCE
5285 Port Royal Road, Springfield Va. 22151**

Best Available Copy



DEPARTMENT OF THE ARMY
U.S. ARMY FOREIGN SCIENCE AND TECHNOLOGY CENTER
220 SEVENTH STREET, N.W.
CHARLOTTESVILLE, VIRGINIA 22901

TRANSLATION

Date: 30 June 1974

AD782517

In Reply Refer to:
FSTC-HT-23-750-74
DIA Task No. T741801

ENGLISH TITLE: Phase Diagrams of Silicate Systems: Handbook;
Third Issue; Ternary Systems

SOURCE: Nauka, Leningrad, 1972, 448 pp.

AUTHOR: N.A. Toropov, Barzakovskiy, V.P., Lapin, V.V.
Kurtseva, N.N., Boykova, A.I.

LANGUAGE: Russian

COUNTRY: USSR

REQUESTOR: AMXBR

TRANSLATOR: Leo Kanner Associates, Redwood City, California (DPS)

ABSTRACT: The handbook contains information on the phase relationships of around two hundred ternary systems containing the oxides of silicon and two other elements, as well as some ternary systems in which there are fluorides, sulfides or water, instead of one or both of the other oxides. Equilibrium phase diagrams are presented, the phases present in the subsolidus region, as well as under high pressure conditions, are described. Information is given on low temperature synthesis and compatibility triangles are presented, characterizing the coexistence of phases below the liquid temperature. The handbook includes diagrams and data on ternary systems containing oxides which have become important in recent years, such as those of germanium, titanium, zirconium, thorium, vanadium, niobium, tantalum, molybdenum and many others. An alphabetical index of the systems is included.

Reproduced by
NATIONAL TECHNICAL
INFORMATION SERVICE
U S Department of Commerce
Springfield VA 22151

NOTICE

The contents of this publication have been translated as presented in the original text. No attempt has been made to verify the accuracy of any statement contained herein. This translation is published with a minimum of copy editing and graphics preparation in order to expedite the dissemination of information.

Approved for public release. Distribution unlimited

ANNOTATION

In the third issue of the handbook Phase Diagrams of Silicate Systems, information is included on the phase relationships in systems containing silica and two other oxides (for example, Al_2O_3 , B_2O_3 , MgO , CaO , BaO , Na_2O , K_2O , Ln_2O_3 , GeO_2 , TiO_2 , ZrO_2 , P_2O_5 , Cr_2O_3 , MnO , FeO , Fe_2O_3 , H_2O , fluorides and others). The systems examined are the physico-chemical basis for production of refractories, various types of ceramics, glass, materials for radioelectronics, nuclear engineering, etc. Not only are equilibrium phase diagrams presented in the handbook, but the phases existing in the subsolidus region, as well as under high pressure conditions, are described. Some physical constants are given (optical properties, structural characteristics, etc.) of the major compounds existing in the corresponding systems. About 200 systems overall are described in the book. Bibliography -- 1087 titles, 101 figures, 80 tables.

FOREWORD

Modern technology requires more and more new materials based on refractory oxides. Oxides which quite recently were considered to be only objects of laboratory studies have acquired industrial importance. In recent years, study has expanded considerably on systems which include the di-oxides of germanium, titanium, zirconium and thorium, the oxides of vanadium, niobium and tantalum, molybdenum and tungsten and many others. The result of all this has been that the number of 3-oxide systems studied has increased considerably. While the number of 3-component silicate systems is 55 in the handbook of D. S. Belyankin, V. V. Lapin and N. A. Toropov, Physicochemical Systems in Silicate Technology (Moscow, 1954), about 200 systems are described in the edition offered. Two issues have been published for ternary systems. The next, fourth issue will be devoted to 3-component nonsilicate systems.

In the handbook, the principal attention is given to examination of equilibrium phase diagrams: crystal-liquid equilibria, polymorphic conversions and solid solutions in the systems. As in the preceding issues, information is given here on the properties of crystalline phases synthesized in the systems examined (crystal constants, X-ray parameters).

In practice (in ceramic engineering, metallurgical processes, etc.), the subsolidus region, the region of solid phase reactions, becomes of great importance. In the handbook, besides information on low-temperature synthesis, phase coexistence triangles are presented (also called compatibility triangles or elementary triangles in the literature), characterizing the co-existence of phases below the liquidus temperature.

At the present time, more and more attention is being given to the studies of phase conversions at high pressures. The work existing in this field is reflected in the handbook.

There is no necessity for proving the importance of the results of studies of 3-component oxide systems for many branches of modern technology. Compositions of various degrees of complexity are used in practice, but a base can usually be distinguished in these compositions, representing a three-component system, and the remaining oxides are additives, as a matter of fact, which sometimes significantly affect the physical properties of the corresponding materials.

V. P. Barzakovskiy

EXPLANATIONS FOR THE THIRD ISSUE

In the handbook, together with the complete formulas of the chemical compounds, abbreviations for them are used (if special stipulations are not made); in this case, the numerical coefficients are written in the form of subscripts, for example $N_4B_2S_5$, or molecular ratios, 4:2:5 (= $4Na_2O \cdot 2BaO \cdot 5SiO_2$).

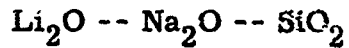
The temperature is given everywhere in degrees Centigrade, and exceptions are accompanied by the appropriate indications (for example, °K).

The legends on the figures usually are abbreviated. The most frequently used abbreviations are L -- liquid, ss -- solid solution.

The unit cell parameters of chemical compounds and solid solutions are given in the same units of measurements which were used by the authors of the corresponding literature sources. Such units are: Å and kX.

1. Å -- angström -- 10^{-8} cm.
2. kX -- kiloX = $1000X = 1.002063 \pm 0.000007$ Å; X is the X-ray standard of wave length, determined by means of the Wolfe-Bragg formula, on the basis of measurement of d(200) of rock salt.

ALKALI SILICATE SYSTEMS



The system has been studied by Kracek [2]. He has plotted phase diagrams for the following partial systems: $\text{Na}_2\text{O}\cdot\text{SiO}_2$ -- $\text{Li}_2\text{O}\cdot\text{SiO}_2$ -- SiO_2 (Fig. 1), $\text{Na}_2\text{O}\cdot\text{SiO}_2$ -- $\text{Li}_2\text{O}\cdot\text{SiO}_2$ (Fig. 2), $\text{Na}_2\text{O}\cdot 2\text{SiO}_2$ -- $\text{Li}_2\text{O}\cdot\text{SiO}_2$ (Fig. 3), $\text{Na}_2\text{O}\cdot 2\text{SiO}_2$ -- $\text{Li}_2\text{O}\cdot 2\text{SiO}_2$ (Fig. 4).

The solid solutions found in the partial system $\text{Na}_2\text{O}\cdot\text{SiO}_2$ -- $\text{Li}_2\text{O}\cdot\text{SiO}_2$ extend from pure Na_2SiO_3 to the limiting composition, corresponding to the formula NaLiSiO_3 . This compound, which can be considered as a sodium-lithium metasilicate actually is the final member of a series of solid solutions of the class Na_2SiO_3 -- $\text{Na}_2\text{Li}_2\text{Si}_2\text{O}_6$. Of course, there is no field for this compound in the ternary diagram.

The fusibility diagram of the partial system $\text{Na}_2\text{O}\cdot\text{SiO}_2$ -- $\text{Li}_2\text{O}\cdot\text{SiO}_2$, from the data of Bergman and colleagues [1], is presented in Fig. 5. The compound NaLiSiO_3 (final member of the solid solutions) has the following crystallographic characteristics: rhombic prisms with definite cleavage in two directions; elongation is parallel to Y; $2V^0$ is very large; refraction in Na light: $\text{Ng} = 1.571$, $\text{Nm} = 1.557$, $\text{Np} = 1.552$.

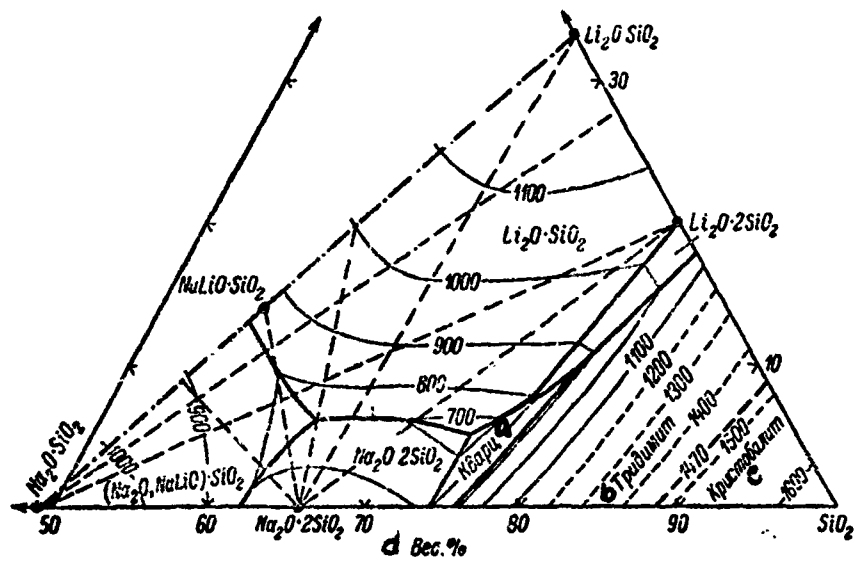


Fig. 1. Phase diagram of Na_2SiO_3 -- Li_2SiO_3 -- SiO_2 system (from Kracek).

Key:

- | | |
|--------------|-----------------|
| a. Quartz | c. Cristobalite |
| b. Tridymite | d. Weight % |

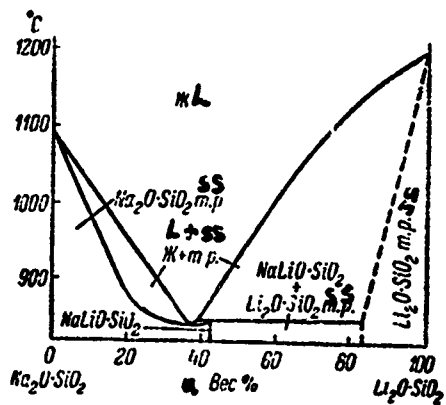


Fig. 2. Phase diagram of partial system
 $\text{Na}_2\text{O} \cdot \text{SiO}_2$ -- $\text{Li}_2\text{O} \cdot \text{SiO}_2$ (from Kracek).

Key:

a. Weight %

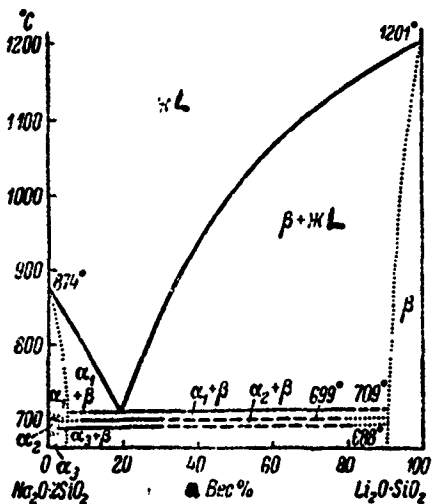


Fig. 3. Phase diagram of partial system
 $\text{Na}_2\text{O}\cdot 2\text{SiO}_2$ -- $\text{Li}_2\text{O}\cdot \text{SiO}_2$ (from Kracek).

Key: a. Weight %

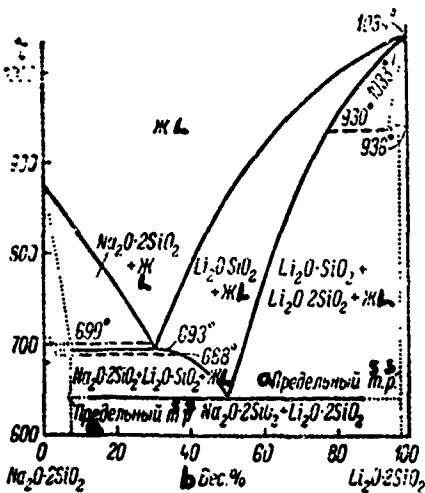


Fig. 4. Phase diagram of partial system
 $\text{Na}_2\text{O}\cdot 2\text{SiO}_2$ -- $\text{Li}_2\text{O}\cdot 2\text{SiO}_2$ (from Kracek).

Key: a. Saturated solid solution
 b. Weight %

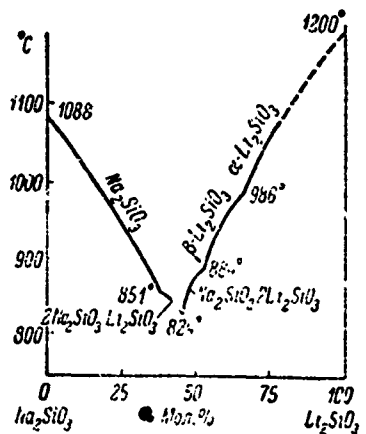


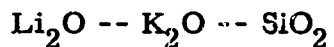
Fig. 5. Fusibility diagram of partial system $\text{Na}_2\text{O}\cdot\text{SiO}_2$ -- $\text{Li}_2\text{O}\cdot\text{SiO}_2$ (from Bergman and colleagues).

Key:

a. Mole %

BIBLIOGRAPHY

1. Bergman, A. G., A. K. Nesterova, N. A. Bychkova, DAN SSSR, 101, No. 3, 483, 1955.
2. Kracek, F.C., J Amer. Chem. Soc., 61, No. 8, 2157; No. 10, 2363, 1939.



The system has been studied by Sheybany [2]. The existence of five ternary compounds has been established: $\text{Li}_2\text{O}\cdot\text{K}_2\text{O}\cdot 4\text{SiO}_2$ (1:1:4), $\text{Li}_2\text{O}\cdot 2\text{K}_2\text{O}\cdot 6\text{SiO}_2$ (1:2:6), $2\text{Li}_2\text{O}\cdot 5\text{K}_2\text{O}\cdot 7\text{SiO}_2$ (2:5:7), $\text{Li}_2\text{O}\cdot 5\text{K}_2\text{O}\cdot 7\text{SiO}_2$ (1:5:7) and $\text{Li}_2\text{O}\cdot 3\text{K}_2\text{O}\cdot 4\text{SiO}_2$ (1:3:4). A phase diagram, bounded by the triangle

$\text{Li}_2\text{O} \cdot \text{SiO}_2$ -- $\text{K}_2\text{O} \cdot \text{SiO}_2$ -- SiO_2 , is presented in Fig. 6. Compound 1:2:6 exists in the form of 4 polymorphic modifications with regions of stability: α from the melting temperature (815°) to 500° ; β from 500 to 250° ; γ from 250 to 40° ; the δ modification is stable below 40° . Compound 2:5:7 forms two modifications, with a transition temperature of 390° .

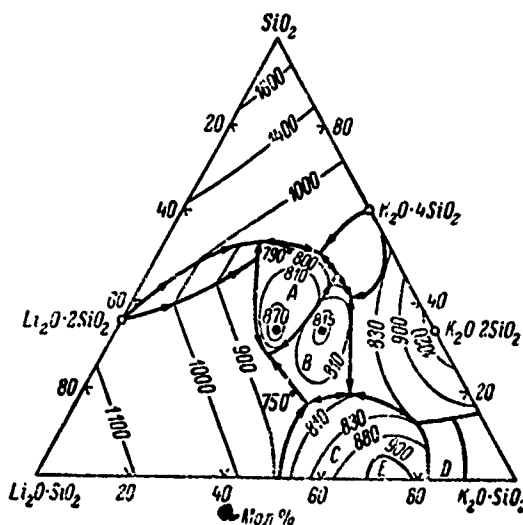


Fig. 6. Phase diagram of $\text{Li}_2\text{O} \cdot \text{SiO}_2$ -- $\text{K}_2\text{O} \cdot \text{SiO}_2$ -- SiO_2 system (from Sheybany):

- A. $\text{Li}_2\text{O} \cdot \text{K}_2\text{O} \cdot 4\text{SiO}_2$; B. $\text{Li}_2\text{O} \cdot 2\text{K}_2\text{O} \cdot 6\text{SiO}_2$;
- C. $2\text{Li}_2\text{O} \cdot 5\text{K}_2\text{O} \cdot 7\text{SiO}_2$; D. $\text{Li}_2\text{O} \cdot 5\text{K}_2\text{O} \cdot 7\text{SiO}_2$;
- E. $\text{Li}_2\text{O} \cdot 3\text{K}_2\text{O} \cdot 4\text{SiO}_2$.

Key:

a. Mole %

Bergman and colleagues [1] visually studied crystallization of the binary profile of Li_2SiO_3 -- K_2SiO_3 (Fig. 7). Two ternary compounds were found here: $\text{Li}_2\text{O} \cdot 3\text{K}_2\text{O} \cdot 4\text{SiO}_2$ and $3\text{Li}_2\text{O} \cdot 2\text{K}_2\text{O} \cdot 5\text{SiO}_2$. The latter compound was not noted by Sheybany.

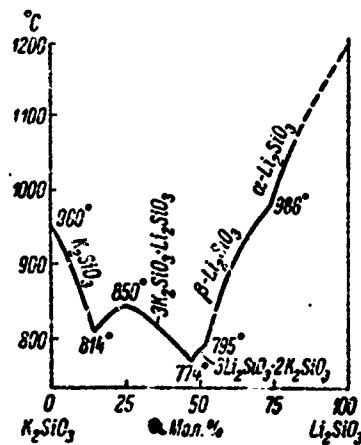


Fig. 7. Fusibility diagram of partial system $\text{Li}_2\text{O} \cdot \text{SiO}_2$ -- $\text{K}_2\text{O} \cdot \text{SiO}_2$ (from Bergman and colleagues).

Key:

a. Mole %

BIBLIOGRAPHY

1. Bergman, A.G., A.K. Nesterova, N.A. Bychkova, DAN SSSR, 101, No. 3, 483, 1955.
2. Sheybany, H.A., Verres et refr., 2, No. 6, 368, 1948; 3, No. 1, 3, 1949.

$\text{Na}_2\text{O} \text{ -- } \text{K}_2\text{O} \text{ -- } \text{SiO}_2$

Kracek [1] has studied the part of the system encompassing the region located between potassium and sodium metasilicates and silica (Fig. 8-10). Formation of ternary compounds within these limits was not detected. A low mutual solubility of potassium and sodium disilicates ($\text{K}_2\text{Si}_2\text{O}_5$ and $\text{Na}_2\text{Si}_2\text{O}_5$) was established.

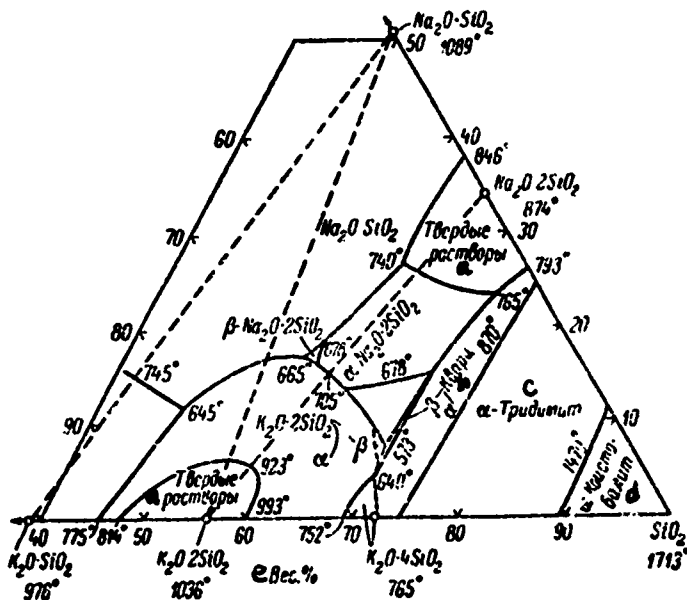


Fig. 8. Phase diagram of $\text{Na}_2\text{O}\cdot\text{SiO}_2 \text{ -- } \text{K}_2\text{O}\cdot\text{SiO}_2 \text{ -- } \text{SiO}_2$ system (from Kracek)

Key:

- a. Solid solutions
- b. Quartz
- c. Tridymite
- d. Cristobalite
- e. Weight %

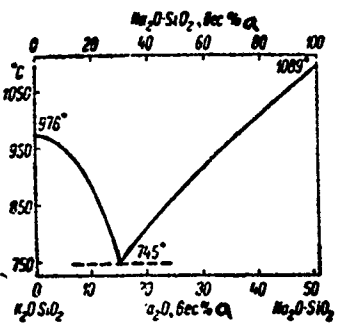


Fig. 9. Phase diagram of partial system of $\text{Na}_2\text{O} \cdot \text{SiO}_2$ -- $\text{K}_2\text{O} \cdot \text{SiO}_2$ (from Kracek).

Key: a. Weight %

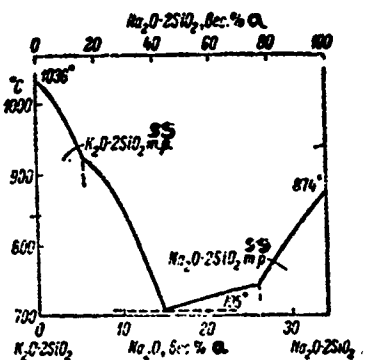


Fig. 10. Phase diagram of partial system $\text{Na}_2\text{O} \cdot 2\text{SiO}_2$ -- $\text{K}_2\text{O} \cdot 2\text{SiO}_2$ (from Kracek).

Key: a. Weight %

BIBLIOGRAPHY

1. Kracek, F.C., J. Phys. Chem., 36, No. 8, 2529, 1932.

CUPRITE-SILICATE SYSTEMS



Borchert and Krämer [1] obtained solid solutions of the metasilicate series MgSiO_3 -- "CuSiO₃," where "CuSiO₃" is a hypothetical compound, by the solid phase synthesis method (at 800-1050°).

50% of the Mg²⁺ ions can be replaced by Cu²⁺ ions and, therefore, the solid solution formulas should be represented as $(.1g\text{Cu})\text{O} \cdot \text{MgO} \cdot 2\text{SiO}_2$. The formation of the solid solutions examined takes place better in the presence of Cu₂O, but Cu²⁺ ions do not enter the lattice. Beginning at 800-850°, the copper content in the solid solution decreases and, at 1075°, practically pure protoenstatite is obtained.

BIBLIOGRAPHY

1. Borchert, W., V. Krämer, Neues Jahrb. Mineral. Monatshefte, No. 1, 6, 1969.

MAGNESIA-SILICATE SYSTEMS



The system has been studied by Murthy and Hummel [1], in the region bounded by the triangle SiO_2 -- Li_2SiO_3 -- Mg_2SiO_4 . Silicate glasses containing small amounts of lithium and magnesium cations, are promising for production of crystalline glass materials, sitalls, from them. One ternary compound $\text{Li}_2\text{O} \cdot \text{MgO} \cdot \text{SiO}_2$ has been found, which crystallizes with difficulty, with indices of refraction $N_g = 1.599$ and $N_p = 1.590$.

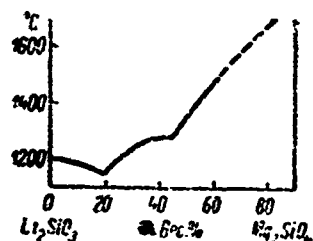


Fig. 11. Phase diagram of partial system Li_2SiO_3 -- Mg_2SiO_4 (from Murthy and Hummel).

Key:

a. Weight %

The Li_2SiO_3 - Mg_2SiO_4 profile is presented in Fig. 11. Formation of the ternary compound $\text{Li}_2\text{O} \cdot \text{MgO} \cdot \text{SiO}_2$ is visible here.

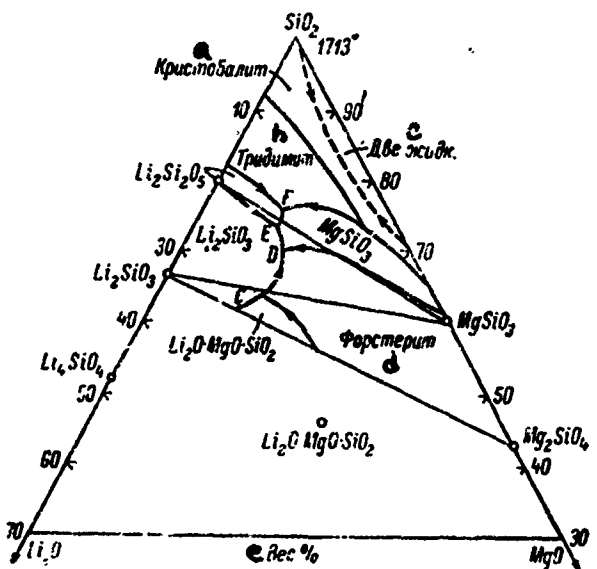


Fig. 12. Phase diagram of partial system Li_2SiO_3 -- MgSiO_4 -- SiO_2 (from Murthy and Hummel).

Key:

- a. Cristobalite
- b. Tridymite
- c. Two liquids
- d. Forsterite
- e. Weight %

A ternary diagram is shown in Fig. 12. The ternary compound field is located predominately below the Li_2SiO_3 - Mg_2SiO_4 profile, and only a small part of this field is above this profile, within the Li_2SiO_3 - MgSiO_4 triangle. The immiscibility region of the two liquids, characteristic

of the MgO-SiO₂ system, extends only insignificantly into the ternary system in the Li₂O direction.

INVARIANT POINTS OF Li₂O -- MgO -- SiO₂ SYSTEM

a Точка (рис. 12)	b Фазы	c Процесс	Состав, вес. %			e Темпера- тура, °C
			Li ₂ O	MgO	SiO ₂	
F	Li ₂ SiO ₃ + MgSiO ₃ + SiO ₂ + + жидкость†	g Эвтек- тика	13.7	10.6	75.7	930 ± 10
E	Li ₂ SiO ₃ + Li ₂ SiO ₄ + + MgSiO ₃ + жидкость†	h То же	15.5	11.3	73.2	935 ± 10
D	Li ₂ SiO ₃ + MgSiO ₃ + + Mg ₂ SiO ₄ + жидкость†	l Реакция	16.4	13.4	70.2	975 ± 10
C	Li ₂ SiO ₃ + Mg ₂ SiO ₄ + Li ₂ O · · Mg ₂ SiO ₄ + жидкость†	»	22.3	14.1	63.6	1070 ± 10

Key:

- | | |
|--------------------------|--------------|
| a. Points (Fig. 12) | f. Liquid |
| b. Phases | g. Eutectic |
| c. Process | h. Same |
| d. Composition, weight % | i. Reactions |
| e. Temperature, °C | |

BIBLIOGRAPHY

1. Murthy, M. K., F. A. Hummel, Amer. Ceram. Soc., 38, No. 2, 55, 1955.

Na₂O -- MgO -- SiO₂

The system has been studied by Botvinikin and Popova [1] and by Manuylova [2], in the region adjacent to SiO₂ (Fig. 13). The existence of the following ternary compounds has been established: Na₂O · MgO · SiO₂, Na₂O · 2MgO · 2SiO₂, Na₂O · 2MgO · 6SiO₂.

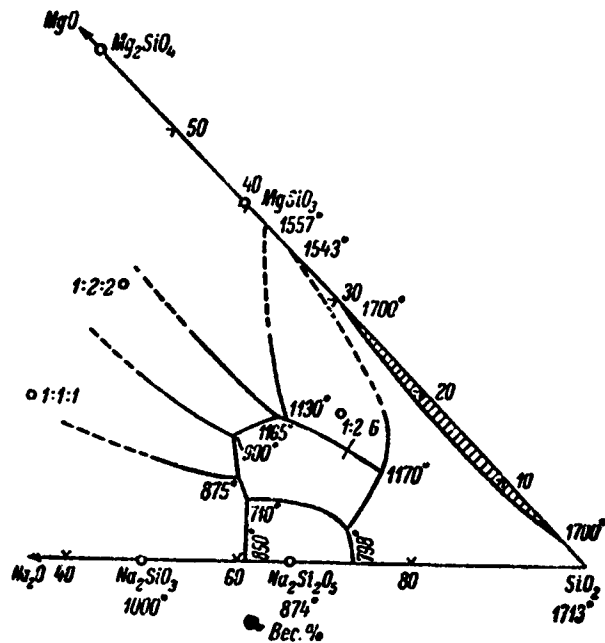


Fig. 13. Phase diagram of $\text{Na}_2\text{O} - \text{MgO} - \text{SiO}_2$ system (from Botvinikin, Popova and Manuylova).

Key: a. Weight %

Schreyer and Schairer [4] describe the compound $\text{Na}_2\text{O} \cdot 5\text{MgO} \cdot 12\text{SiO}_2$, of the osumilite type. Borchert and Petzenhauser [3] obtained this compound in the pure form, by annealing a mixture of $2\text{Na}_2\text{CO}_3 + 5\text{MgO} + 12\text{SiO}_2$ at 1100°; upon annealing a mixture composed of $\text{Na}_2\text{CO}_3 + 5\text{MgO} + 12\text{SiO}_2$, together with the osumilite phase, a new hexagonal phase of unknown stoichiometry was obtained.

TABLE I
INVARIANT POINTS OF $\text{Na}_2\text{O} - \text{MgO} - \text{SiO}_2$ SYSTEM

a Фазы	b Процесс	Температура, °C
$\text{SiO}_2 + \text{MgO} \cdot \text{SiO}_2 + \text{Na}_2\text{O} \cdot 2\text{MgO} \cdot 6\text{SiO}_2 +$ жидкость d	—	1170
$\text{SiO}_2 + \text{Na}_2\text{O} \cdot 2\text{MgO} \cdot 6\text{SiO}_2 + \text{Na}_2\text{O} \cdot 2\text{SiO}_2 +$ жидкость d	Эвтектика	740
$\text{Na}_2\text{O} \cdot \text{SiO}_2 + \text{Na}_2\text{O} \cdot 2\text{MgO} \cdot 6\text{SiO}_2 + \text{Na}_2\text{O} \cdot 2\text{SiO}_2 +$ жидкость d	—	710 (?)
$\text{Na}_2\text{O} \cdot \text{SiO}_2 + \text{Na}_2\text{O} \cdot 2\text{MgO} \cdot 6\text{SiO}_2 + \text{Na}_2\text{O} \cdot \text{MgO} \cdot \text{SiO}_2 +$ жидкость d	Эвтектика	815
$\text{Na}_2\text{O} \cdot \text{MgO} \cdot \text{SiO}_2 + \text{Na}_2\text{O} \cdot 2\text{MgO} \cdot 2\text{SiO}_2 + \text{Na}_2\text{O} \cdot 2\text{MgO} \cdot 6\text{SiO}_2 +$ жидкость d	—	900
$2\text{MgO} \cdot \text{SiO}_2 + \text{Na}_2\text{O} \cdot 2\text{MgO} \cdot 2\text{SiO}_2 + \text{Na}_2\text{O} \cdot 2\text{MgO} \cdot 6\text{SiO}_2 +$ жидкость d	—	1200
$2\text{MgO} \cdot \text{SiO}_2 + \text{MgO} \cdot \text{SiO}_2 + \text{Na}_2\text{O} \cdot 2\text{MgO} \cdot 6\text{SiO}_2 +$ жидкость d	—	1165

Key:

- a. Phases
- b. Process
- c. Temperature °C
- d. Liquid
- e. Eutectic

TABLE II. CRYSTALLINE PHASES OF $\text{Na}_2\text{O} - \text{MgO} - \text{SiO}_2$ SYSTEM

a Соединение	b Система кристаллов	<i>N_g</i>	<i>N_p</i>	<i>2V°</i>	c Оптический знак	Оптическая ориентировка
$\text{Na}_2\text{O} \cdot \text{MgO} \cdot \text{SiO}_2$	^e Кубическая	1.523	—	—	(—)	
$\text{Na}_2\text{O} \cdot 2\text{MgO} \cdot 2\text{SiO}_2$	^f Моноклиническая	1.654	1.641	Большой	(+)	$Z \wedge c = 38^\circ$
$\text{Na}_2\text{O} \cdot 2\text{MgO} \cdot 6\text{SiO}_2$	^g То же	1.546	1.540	—	(+)	$Z \wedge c = 24^\circ$

Key:

- a. Compound
- b. Crystal system
- c. Optical sign
- d. Optical orientation
- e. Cubic
- f. Monoclinic
- g. Same
- h. Large

BIBLIOGRAPHY

1. Botviri^kin, O. K., T. N. Popova, Trudy 2-go soveshch. po eksper. mineralogii [Proceedings, 2d Conference on Experimental Mineralogy], Moscow, 87, 1937.
2. Manuylova, N. S., Ibid., p. 97.
3. Borchert, W., I. Petzenhauser, Ber. Dtsch. keram. Ges., 43, No. 10, 572, 1966.
4. Schreyer, W., J. F. Schairer, Amer. Mineralogist, 47, No. 1, 90, 1962.



The system has been studied by Roedder [2]. The formation of four ternary chemical compounds has been established: $\text{K}_2\text{O} \cdot \text{MgO} \cdot \text{SiO}_2$, $\text{K}_2\text{O} \cdot 5\text{MgO} \cdot 12\text{SiO}_2$, $\text{K}_2\text{O} \cdot \text{MgO} \cdot 3\text{SiO}_2$ and $\text{K}_2\text{O} \cdot \text{MgO} \cdot 5\text{SiO}_2$. The general phase diagram of the system, with isotherms and invariant points applied, is presented in Fig. 14. Binary partial systems are shown in Fig. 15. In this case, the dashed lines characterize, not binary, but ternary equilibria in the sections indicated. The partial binary system $\text{MgO} \cdot \text{SiO}_2$ -- " $\text{K}_2\text{O} \cdot 7\text{SiO}_2$ " is given in Fig. 16.

Borchert and Petzenhauser [1] obtained the compound $\text{K}_2\text{O} \cdot 5\text{MgO} \cdot 12\text{SiO}_2$, osumilite type, with unit cell parameters $a_0 = 10.22 \pm 0.02$, $c_0 = 14.25 \pm 0.02$ Å, by annealing an appropriate mixture of K_2CO_3 , MgO and SiO_2 at 1130° , for a period of six days. In this case, a new hexagonal phase of unknown composition (phase KX) was obtained simultaneously. Annealing at 1200° led to formation of only the KX phase.

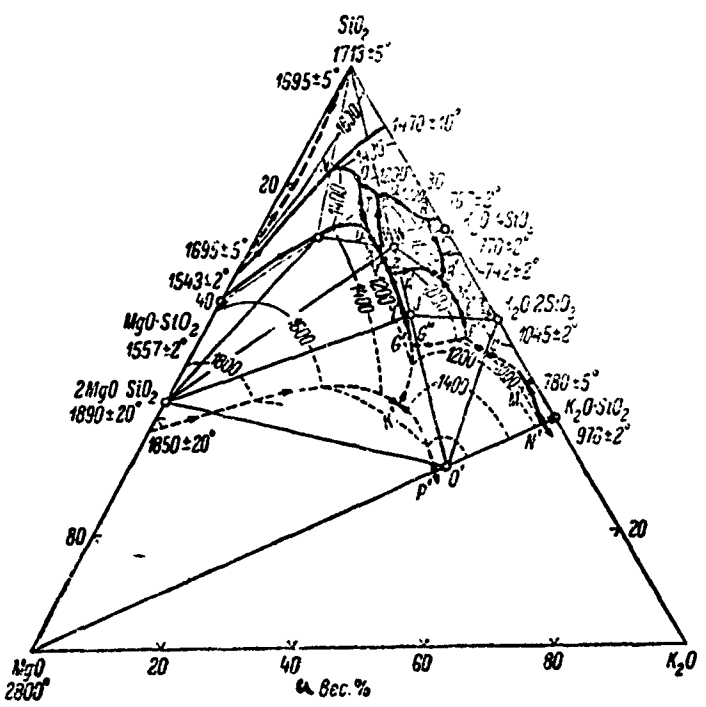


Fig. 14. Phase diagram of K_2O -- MgO -- SiO_2 system (from Roedder).

Key:

a. Weight %

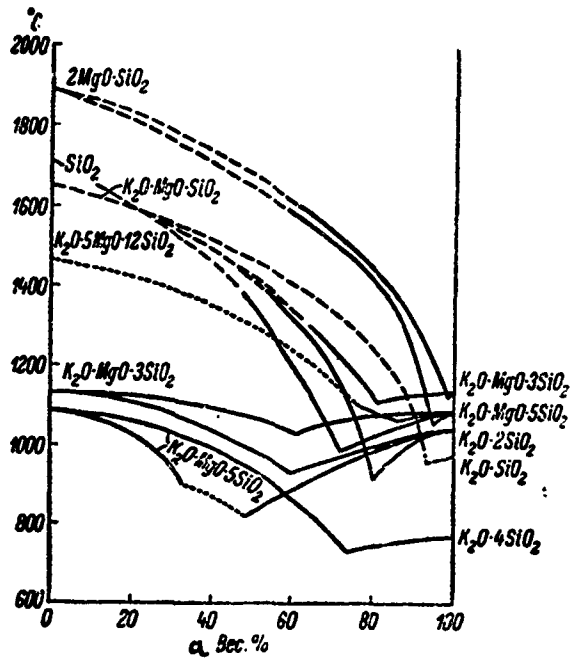


Fig. 15. Phase diagram of partial systems related to the ternary system K_2O -- MgO -- SiO_2 (from Roedder).

Key:

a. Weight %

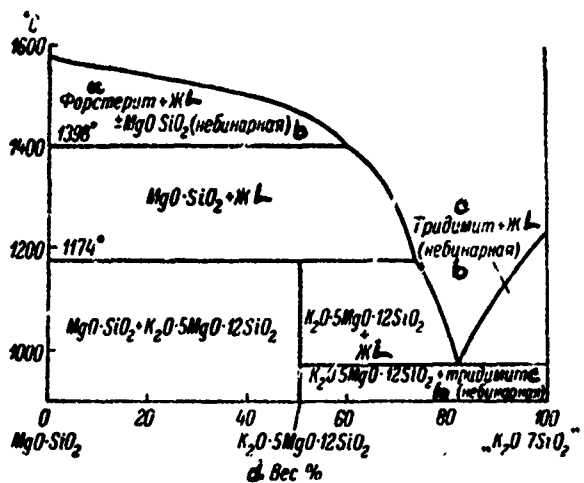


Fig. 16. Phase diagram of partial system $\text{MgO} \cdot \text{SiO}_2$ -- " $\text{K}_2\text{O} \cdot 7\text{SiO}_2$ " (from Roedder).

Key:

- a. Forsterite
- b. Nonbinary
- c. Tridymite
- d. Weight %

TABLE I
INVARIANT POINTS OF $K_2O - MgO - SiO_2$ SYSTEM

• Точка (рис. 14)	б Фазы	с Процесс	д Состав, вес. %			Темпера- тура, °C
			К ₂ O	MgO	SiO ₂	
W	$K_2O \cdot MgO \cdot 5SiO_2 +$ жидкость	г. Плавление	21.66	9.27	69.07	1089 ± 1
J'	$K_2O \cdot MgO \cdot 3SiO_2 +$ жидкость	»	29.93	12.81	57.26	1134 ± 1
P'	$K_2O \cdot MgO \cdot SiO_2 (?) +$ жидкость	»	48.91	20.22	30.87	1650
Q	Тридимит + $K_2O \cdot MgO \cdot 5SiO_2 +$ жидкость	и. Эвтектика	15.5	6.7	77.8	987 ± 5
T	$\alpha \cdot MgO \cdot SiO_2 + K_2O \cdot 5MgO \cdot 12SiO_2 +$ жидкость	ж. Реакция	13.5	10.5	76.0	1174 ± 2
V	$K_2O \cdot MgO \cdot 5SiO_2 + K_2O \cdot 5MgO \cdot 12SiO_2 +$ жидкость	и. Эвтектика	20.0	10.7	69.3	1063 ± 3
Y	$K_2O \cdot MgO \cdot 5SiO_2 + 2MgO \cdot SiO_2 +$ жидкость	»	20.5	11.8	67.7	1053 ± 2
A'	$K_2O \cdot MgO \cdot 5SiO_2 + K_2O \cdot MgO \cdot 3SiO_2 +$ жидкость	»	24.8	10.7	64.5	1030 ± 5
D'	$K_2O \cdot MgO \cdot 5SiO_2 + K_2O \cdot 4SiO_2 +$ жидкость	»	26.5	2.4	71.1	730 ± 5
E'	$K_2O \cdot MgO \cdot 3SiO_2 + K_2O \cdot 2SiO_2 +$ жидкость	»	38.3	5.2	56.5	933 ± 5
I'	$K_2O \cdot MgO \cdot 3SiO_2 + 2MgO \cdot SiO_2 +$ жидкость	»	29.5	13.5	57.0	1131 ± 1
L'	$K_2O \cdot MgO \cdot SiO_2 (?) + K_2O \cdot 2SiO_2 +$ жидкость	»	41.8	4.2	51.0	910
N'	$K_2O \cdot MgO \cdot SiO_2 (?) + K_2O \cdot SiO_2 +$ жидкость	»	60.1	1.7	38.2	950
O'	$K_2O \cdot MgO \cdot SiO_2 (?) + MgO +$ жидкость	»	—	—	—	1650
G'	$K_2O \cdot MgO \cdot SiO_2 (?) + K_2O \cdot MgO \cdot 3SiO_2 +$ жидкость	»	33.0	14.0	53.0	1110 ± 20 (?)
O	$\alpha \cdot MgO \cdot SiO_2 +$ тридимит + $K_2O \cdot 5MgO \cdot 12SiO_2 +$ жидкость	ж. Реакция	11.6	8.8	79.6	1165 ± 2
Z	Тридимит + $K_2O \cdot 5MgO \cdot 12SiO_2 + K_2O \cdot MgO \cdot 5SiO_2 +$ жидкость	и. Эвтектика	15.1	7.2	77.7	963 ± 3
R	Тридимит + $K_2O \cdot MgO \cdot 5SiO_2 + K_2O \cdot 4SiO_2 +$ жидкость	»	24.5	2.0	73.5	715 ± 10
U	$2MgO \cdot SiO_2 + MgO \cdot SiO_2 + K_2O \cdot 5MgO \cdot 12SiO_2 +$ жидкость	ж. Реакция	16.4	11.5	72.1	1155 ± 2

Key:

- a. Points (Fig. 14)
- b. Phases
- c. Process
- d. Composition, weight %
- e. Temperature, °C
- f. Liquid
- g. Tridymite
- h. Melting
- i. Eutectic
- j. Reactions

TABLE I (continued)

α Точка (рис. 16)	β Фазы	С Процесс	δ Состав, вес. %			С Темпера- тура, °C
			K ₂ O	MgO	SiO ₂	
X	2MgO·SiO ₂ +K ₂ O·5MgO· ·12SiO ₂ +K ₂ O·MgO· ·5SiO ₂ +жидкость ⁺	Эвтектика	20.2	11.8	68.0	1042±5
Z	2MgO·SiO ₂ +K ₂ O·MgO· ·3SiO ₂ +K ₂ O·MgO· ·5SiO ₂ +жидкость ⁺	»	23.9	12.0	64.1	1013±3
B'	K ₂ O·MgO·3SiO ₂ +K ₂ O· ·MgO·5SiO ₂ +K ₂ O· ·2SiO ₂ +жидкость ⁺	Реакция	31.6	4.8	63.6	795±15
C'	K ₂ O·MgO·5SiO ₂ +K ₂ O· ·2SiO ₂ +K ₂ O·4SiO ₂ + +жидкость ⁺	Эвтектика	30.0	2.5	67.5	685±20
F'	K ₂ O·MgO·3SiO ₂ +K ₂ O· ·MgO·SiO ₂ (?)+K ₂ O· ·2SiO ₂ +жидкость ⁺	»	40.5	6.0	53.5	905±5
G'	K ₂ O·MgO·3SiO ₂ +K ₂ O· ·MgO·SiO ₂ (?)+2MgO· ·SiO ₂ +жидкость ⁺	»	33.0	15.0	52.0	1105±10
K'	K ₂ O·MgO·SiO ₂ (?)+ +2MgO·SiO ₂ +MgO+ +жидкость ⁺	Реакции	36.0	22.0	42.0	1350±50
M'	K ₂ O·MgO·SiO ₂ (?)+ +K ₂ O·2SiO ₂ +K ₂ O· ·SiO ₂ +жидкость ⁺	Эвтектика	54.2	0.5	45.3	720

TABLE II. CRYSTALLINE PHASES OF K₂O -- MgO -- SiO₂ SYSTEM

α Соединение	β Система пространств	γ Габитус	Ng	Nm	Np
K ₂ O·MgO·SiO ₂ (?)	Кубическая	Округлые зерна ^f	—	1.54	—
K ₂ O·MgO·3SiO ₂	Гексаго- нальная	Шестигранные ^g таблички	1.530	—	1.524
α-K ₂ O·MgO·5SiO ₂	Кубическая	Кубы и октаэдры ^h	—	1.501	—
β-K ₂ O·MgO·5SiO ₂	—	Волокна ⁱ	—	1.505	—
K ₂ O·5MgO·12SiO ₂	Гексаго- нальная	Таблички, приз- мы, пирамиды ^j	1.550	—	1.543

Key:

- a. Compound
- b. Crystal system
- c. Appearance
- d. Cubic
- e. Hexagonal
- f. Round grains
- g. 6-sided tablets
- h. Cubes and octahedra
- i. Fibers
- j. Tablets, prisms, pyramids.

BIBLIOGRAPHY

1. Borchert, W., I. Petzenhauser, Ber. Dtsch. keram. Ges., 43, No. 10, 572, 1966.
2. Roedder, E.W., Amer. J. Sci., 249, No. 2, 81; No. 3, 224, 1951.

CALCIUM SILICATE SYSTEMS



Certain partial regions of this system have been studied. Schwarz and Haacke [2] have studied the Li_4SiO_4 -- Ca_2SiO_4 profile. Bergman, Nesterova and Bychkova [1] present some information of the fusibility of the Li_2SiO_3 -- CaSiO_3 profile. The latter system was studied as early as 1909 by Wallace [3]. Schwarz and Haacke present a phase diagram of the $2\text{Li}_2\text{O} \cdot \text{SiO}_2$ -- $2\text{CaO} \cdot \text{SiO}_2$ system, within up to 30 mole % of calcium orthosilicate (Fig. 17). $2\text{Li}_2\text{O} \cdot \text{SiO}_2$ base solid solutions form in the system, with the $2\text{CaO} \cdot \text{SiO}_2$ content reaching up to 20 mole %. With a higher calcium silicate content solid solutions with maximum and minimum melting temperatures form. Schwarz and Haacke think that, at low temperatures as a result of polymorphic conversions of the solid solutions, the ternary compound $\text{Li}_2\text{O} \cdot \text{CaO} \cdot \text{SiO}_2$ forms. The density curve with this composition discloses a sharp maximum.

Using the visual-polythermal method, Bergman and colleagues came to the conclusion that the CaSiO_3 - Li_2SiO_3 system forms a simple eutectic, with a melting temperature of 1024° and a content of 45.5 mole % CaSiO_3 ; according to Wallace, 979° and 43.7 mole % CaSiO_3 , respectively.

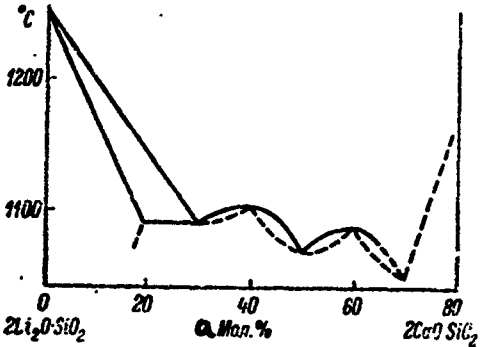


Fig. 17. Phase diagram of partial system $2\text{Li}_2\text{O}\cdot\text{SiO}_2$ -- $2\text{CaO}\cdot\text{SiO}_2$ (from Schwarz and Haacke).

Key:

a. Mole %

1. Bergman, A.G., A.K. Nesterova, N.A. Bychkova, DAN SSSR, 101, No. 3, 483, 1955.
2. Schwarz, R., A. Haacke, Zs. anorgan. allgem. Chem., 115. No. 1/2, 87, 1921.
3. Wallace, R., Zs. anorgan. allgem. Chem., 63, No. 1, 1, 1909.

$\text{Na}_2\text{O} \text{-- CaO} \text{-- SiO}_2$

The system has been studied by Morey and Bowen [6] and Segnit [8].

The major crystalline phases of the system are: devitrite ($\text{Na}_2\text{O} \cdot 3\text{CaO} \cdot 6\text{SiO}_2$), wollastonite and cristobalite. They are found in the composition of the "rocks" of crystallized ("devitrified") technical glass.

A phase diagram of this system, from the data of Morey and Bowen, is presented in Fig. 18. A part of the diagram of importance for glass technology is presented in Fig. 19. Partial profiles of $\text{Na}_2\text{O} \cdot \text{SiO}_2 \text{-- CaO} \cdot \text{SiO}_2$ and $\text{Na}_2\text{O} \cdot 2\text{SiO}_2 \text{-- Na}_2\text{O} \cdot 2\text{CaO} \cdot 3\text{SiO}_2$ are presented in Figs. 20 and 21. Morey and Bowen found four ternary compounds: $\text{Na}_2\text{O} \cdot 3\text{CaO} \cdot 6\text{SiO}_2$ (devitrite), $\text{Na}_2\text{O} \cdot 2\text{CaO} \cdot 3\text{SiO}_2$, $2\text{Na}_2\text{O} \cdot \text{CaO} \cdot 3\text{SiO}_2$ and $\text{Na}_2\text{O} \cdot \text{CaO} \cdot \text{SiO}_2$.

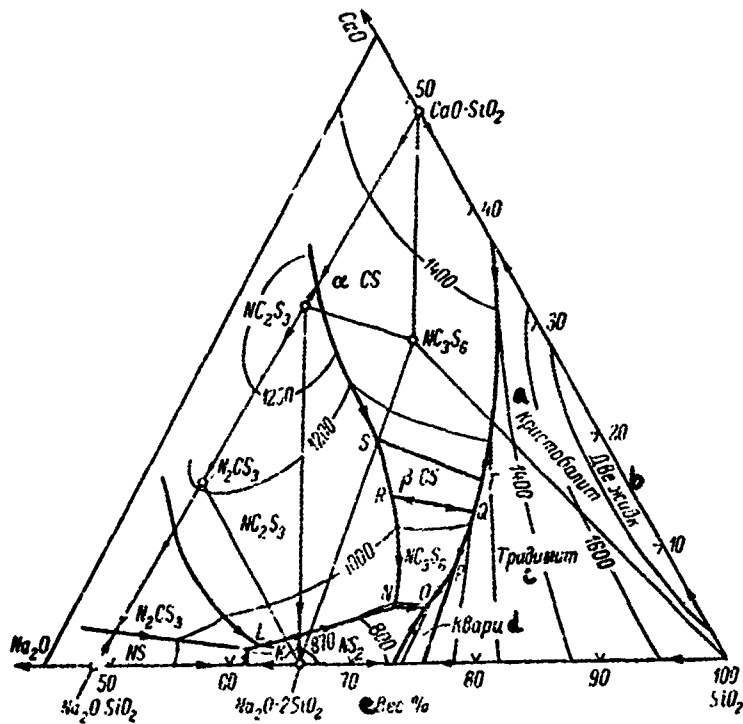


Fig. 18. Phase diagram of $\text{Na}_2\text{O} \text{-- CaO} \text{-- SiO}_2$ system; region enriched in silica (from Morey and Bowen).

Key:

- a. Cristobalite
- b. Two liquids
- c. Tridymite
- d. Quartz
- e. Weight %

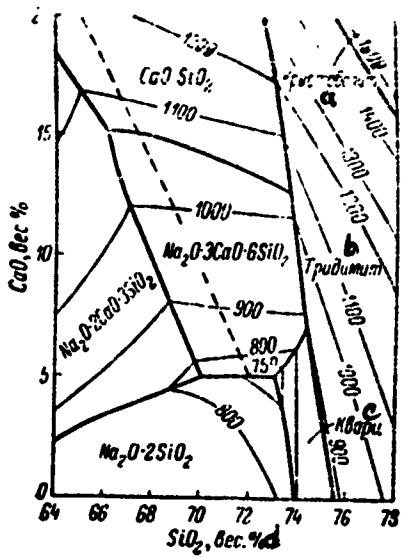


Fig. 19. Phase diagram of part of $\text{Na}_2\text{O} - \text{CaO} - \text{SiO}_2$ ternary system, of importance for glass technology (from Morey): Amount of Na_2O (weight %) is obtained by subtraction from 100% of the total amount of CaO and SiO_2 .

Key:

- a. Cristobalite
- b. Tridymite
- c. Quartz
- d. Weight %

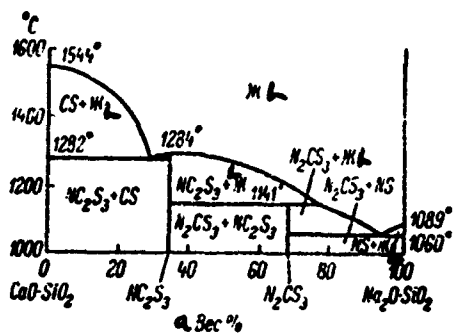


Fig. 20. Phase diagram of partial system Na_2O - SiO_2 -- $\text{CaO}\cdot\text{SiO}_2$ (from Morey and Bowen).

Key:

a. Weight %

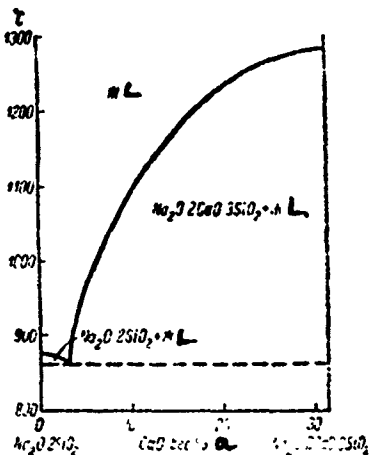


Fig. 21. Phase diagram of partial system Na_2O - 2SiO_2 -- $\text{Na}_2\text{O}\cdot 2\text{CaO}\cdot 3\text{SiO}_2$ (from Morey and Bowen).

Key:

a. Weight %

Toropov and Arakelyan [2] have described two compounds, $2\text{Na}_2\text{O} \cdot 8\text{CaO} \cdot 5\text{SiO}_2$ and $2\text{Na}_2\text{O} \cdot 4\text{CaO} \cdot 3\text{SiO}_2$, which, as was demonstrated eventually, are solid solutions of alkali silicates in calcium orthosilicate.

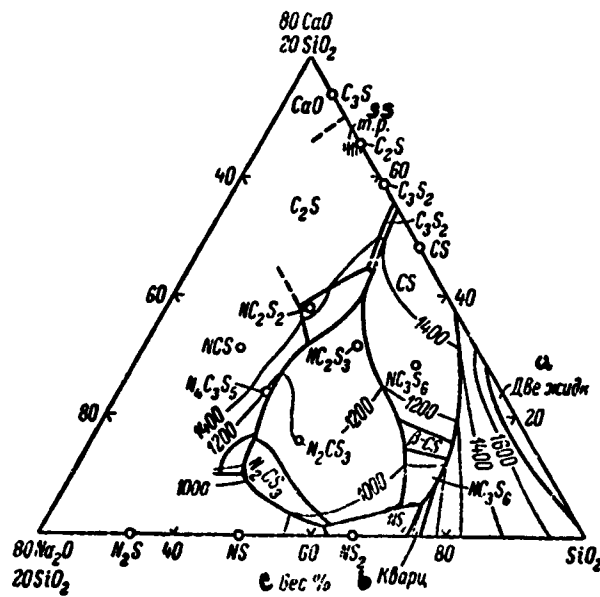


Fig. 22. Phase diagram of $\text{Na}_2\text{O} - \text{CaO} - \text{SiO}_2$ system: Primary phase fields and liquidus isotherms (from Segnit): N, Na_2O ; C, CaO ; S, SiO_2 .

Key:

- a. Two liquids
 - b. Quartz
 - c. Weight %

Segnit, [8] has studied the richer CaO and Na₂O (Fig. 22) part of the system, and he has obtained the new compounds 4Na₂O·3CaO·5SiO₂ and

$\text{Na}_2\text{O} \cdot 2\text{CaO} \cdot 2\text{SiO}_2$. He has shown that Na_2O forms solid solutions with dicalcium silicate. The invariant points of the system are presented in Tables 1 and 2 and the optical properties of the compounds obtained by Morey and Bowen, in Table 3.

Wyckoff and Morey [9], on the basis of X-ray data, assert that only $\text{Na}_2\text{O} \cdot \text{CaO} \cdot \text{SiO}_2$ is actually cubic, and that $2\text{Na}_2\text{O} \cdot \text{CaO} \cdot \text{SiO}_2$ and $\text{Na}_2\text{O} \cdot 2\text{CaO} \cdot 3\text{SiO}_2$ have a pseudocubic structure. The compound $4\text{Na}_2\text{O} \cdot 3\text{CaO} \cdot 5\text{SiO}_2$ melts at approximately 1450° . Refraction of the solid solutions of Na_2O in $2\text{CaO} \cdot \text{SiO}_2$ decreases in proportion to increase in Na_2O content (Table 4).

Toropov and Arakelyan present the following data for the solid solution of the composition $2\text{Na}_2\text{O} \cdot 8\text{CaO} \cdot 5\text{SiO}_2$, which crystallizes in the form of hexagons: $\text{Ng} = 1.674$, $\text{Np} = 1.668$; direct extinction, polysynthetic twins. The compound $\text{Na}_2\text{O} \cdot 4\text{CaO} \cdot 3\text{SiO}_2$ forms irregular and elongated grains, with $\text{Ng} = 1.634$ and $\text{Np} = 1.627$.

Fedorov and Brodkina [3] have studied the profile of $2\text{CaO} \cdot \text{SiO}_2$ -- $\text{Na}_2\text{O} \cdot \text{CaO} \cdot \text{SiO}_2$, proceeding from the previously synthesized γ - $2\text{CaO} \cdot \text{SiO}_2$ and sodium-calcium orthosilicate. Annealing a mixture of these compounds was conducted at 1300° . The phases formed were identified by crystallooptic and X-ray methods. The formation of limited β - $2\text{CaO} \cdot \text{SiO}_2$ base solid solutions has been established. With a $\text{Na}_2\text{O} \cdot \text{CaO} \cdot \text{SiO}_2$ content of up to 10 weight %, the solid solutions have the β - $2\text{CaO} \cdot \text{SiO}_2$ structure; in a mixture with 15 weight % $\text{Na}_2\text{O} \cdot \text{CaO} \cdot \text{SiO}_2$, complex solid solutions form, in which the solvent is the β and the α' forms of $2\text{CaO} \cdot \text{SiO}_2$. The maximum concentration of $\text{Na}_2\text{O} \cdot \text{CaO} \cdot \text{SiO}_2$ in the solid solution at 1300° can be estimated at approximately

TABLE I
INVARIANT POINTS OF $\text{Na}_2\text{O} - \text{CaO} - \text{SiO}_2$ SYSTEM (from Morey & Bowen)

a Точка (рис. 18)	b Фазы	c Процесс	d Состав, вес. %			e Темпера- тура, °C
			Na ₂ O	CaO	SiO ₂	
K	$\text{Na}_2\text{O} \cdot 2\text{SiO}_2 + \text{Na}_2\text{O} \cdot \text{SiO}_2 + 2\text{Na}_2\text{O} \cdot \text{CaO} \cdot 3\text{SiO}_2 + \text{жидкость}$	Эвтектика	37.5	1.8	60.7	821
L	$2\text{Na}_2\text{O} \cdot \text{CaO} \cdot 3\text{SiO}_2 + \text{Na}_2\text{O} \cdot 2\text{CaO} \cdot 3\text{SiO}_2 + \text{Na}_2\text{O} \cdot 2\text{SiO}_2 + \text{жидкость}$	—	36.6	2.0	61.4	827
N	$\text{Na}_2\text{O} \cdot 2\text{SiO}_2 + \text{Na}_2\text{O} \cdot 2\text{CaO} \cdot 3\text{SiO}_2 + \text{Na}_2\text{O} \cdot 3\text{CaO} \cdot 6\text{SiO}_2 + \text{жидкость}$	—	24.1	5.2	70.7	740
O	$\text{Na}_2\text{O} \cdot 3\text{CaO} \cdot 6\text{SiO}_2 + \text{кварц} + \text{Na}_2\text{O} \cdot 2\text{SiO}_2 + \text{жидкость}$	Эвтектика	21.3	5.2	73.5	725
P	Кварц + $\text{Na}_2\text{O} \cdot 3\text{CaO} \cdot 6\text{SiO}_2 +$ тридимит + жидкость	Инверсия	18.7	7.0	73.3	870
Q	Тридимит + $\beta\text{-CaO} \cdot \text{SiO}_2 + \text{Na}_2\text{O} \cdot 3\text{CaO} \cdot 6\text{SiO}_2 + \text{жидкость}$	—	13.7	12.9	73.4	1035
R	$\text{Na}_2\text{O} \cdot 3\text{CaO} \cdot 6\text{SiO}_2 + \text{Na}_2\text{O} \cdot 2\text{CaO} \cdot 3\text{SiO}_2 + \beta\text{-CaO} \cdot \text{SiO}_2 + \text{жидкость}$	—	19.0	14.5	66.5	1030
S	$\beta\text{-CaO} \cdot \text{SiO}_2 + \text{Na}_2\text{O} \cdot 2\text{CaO} \cdot 3\text{SiO}_2 + \alpha\text{-CaO} \cdot \text{SiO}_2 + \text{жидкость}$	—	17.7	19.5	62.8	1110
T	$\alpha\text{-CaO} \cdot \text{SiO}_2 + \text{SiO}_2 + \beta\text{-CaO} \cdot \text{SiO}_2$	Инверсия	11.4	15.6	73.0	1110
—	$\text{Na}_2\text{O} \cdot 2\text{CaO} \cdot 3\text{SiO}_2 + \text{жидкость}$	Плавление	17.5	31.6	50.9	1284
—	$2\text{Na}_2\text{O} \cdot \text{CaO} \cdot 3\text{SiO}_2 + \text{жидкость}$	Инконгруэнтное плавление	34.4	15.6	50.0	1141
—	$\text{Na}_2\text{O} \cdot 3\text{CaO} \cdot 6\text{SiO}_2 + \text{жидкость}$	To же	10.5	28.5	61.0	1047

Key:

- a. Points (Fig. 18)
- b. Phases
- c. Process
- d. Composition, weight %
- e. Temperature, °C
- f. Liquid
- g. Quartz
- h. Tridymite
- i. Eutectic
- j. Inversion
- k. Melting
- l. Incongruent melting
- m. Same

TABLE II
TRIPLE INVARIANT POINTS OF $\text{Na}_2\text{O} - \text{CaO} - \text{SiO}_2$
(from Segnit)

a Фазы	b Процесс	c Состав, вес.%			d Темпера- тура, °C
		Na ₂ O	CaO	SiO ₂	
$2\text{CaO}\cdot\text{SiO}_2 + 3\text{CaO}\cdot 2\text{SiO}_2 + \text{Na}_2\text{O} \cdot 2\text{CaO}\cdot 2\text{SiO}_2 + \text{жидкость}$ e	f Растворение	8.8	44.5	46.7	1280
$\alpha\text{-CaO}\cdot\text{SiO}_2 + 3\text{CaO}\cdot 2\text{SiO}_2 + \text{Na}_2\text{O} \cdot 2\text{CaO}\cdot 2\text{SiO}_2 + \text{жидкость}$ e	g Эвтектика	8.2	44.5	47.3	1270
$\text{Na}_2\text{O}\cdot 2\text{CaO}\cdot 3\text{SiO}_2 + 2\text{CaO}\cdot \text{SiO}_2 + \text{Na}_2\text{O} \cdot 2\text{CaO}\cdot 2\text{SiO}_2 + \text{жидкость}$ e	»	12.5	39.5	48.0	1255
$\text{Na}_2\text{O}\cdot 2\text{CaO}\cdot 3\text{SiO}_2 + \text{Na}_2\text{O}\cdot \text{CaO} \cdot \text{SiO}_2 + \text{Na}_2\text{O}\cdot 2\text{CaO}\cdot 2\text{SiO}_2 + \text{жидкость}$ e	»	24.0	32.0	44.0	1260
$2\text{CaO}\cdot \text{SiO}_2 + \text{Na}_2\text{O}\cdot \text{CaO} \cdot \text{SiO}_2 + \text{Na}_2\text{O}\cdot 2\text{CaO}\cdot 2\text{SiO}_2 + \text{жидкость}$ e	»	23.0	37.6	39.4	1140
$\text{Na}_2\text{O}\cdot 2\text{CaO}\cdot 3\text{SiO}_2 + \text{Na}_2\text{O}\cdot \text{CaO} \cdot \text{SiO}_2 + 4\text{Na}_2\text{O}\cdot 3\text{CaO}\cdot 5\text{SiO}_2 + \text{жидкость}$ e	f Растворение	39.8	16.7	43.5	1130
$\text{Na}_2\text{O}\cdot 2\text{CaO}\cdot 3\text{SiO}_2 + 2\text{Na}_2\text{O}\cdot \text{CaO} \cdot 3\text{SiO}_2 + 4\text{Na}_2\text{O}\cdot 3\text{CaO}\cdot 5\text{SiO}_2 + \text{жидкость}$ e	»	40.0	16.0	44.0	1120
$2\text{Na}_2\text{O}\cdot \text{CaO} \cdot 3\text{SiO}_2 + \text{Na}_2\text{O}\cdot \text{SiO}_2 + 4\text{Na}_2\text{O}\cdot 3\text{CaO}\cdot 5\text{SiO}_2 + \text{жидкость}$ e	»	45.0	10.5	44.5	990
$\text{Na}_2\text{O}\cdot \text{SiO}_2 + \text{Na}_2\text{O}\cdot \text{CaO} \cdot \text{SiO}_2 + 4\text{Na}_2\text{O}\cdot 3\text{CaO}\cdot 5\text{SiO}_2 + \text{жидкость}$ e	»	48.0	10.5	41.5	950

Key:

- a. Phases
- b. Process
- c. Composition, weight %
- d. Temperature, °C
- e. Liquid
- f. Solution
- g. Eutectic

TABLE III
CRYSTALLINE PHASES OF $\text{Na}_2\text{O} - \text{CaO} - \text{SiO}_2$ SYSTEM
(from Morey and Bowen)

a Соединение	b Система кристаллов	c Габитус	<i>N_g</i>	<i>N_p</i>	$2V^\circ$	d Плот- ность, $\text{г}/\text{см}^3$
$\text{Na}_2\text{O} \cdot 3\text{CaO} \cdot 6\text{SiO}_2$ (девитрит) <i>e</i>	Ромбиче- ская	Призмы	1.579	1.564	+75	—
$\text{Na}_2\text{O} \cdot 2\text{CaO} \cdot 3\text{SiO}_2$	Псевдокуби- ческая	Полисинтети- ческие двойники	1.599	1.596	—	—
$2\text{Na}_2\text{O} \cdot \text{CaO} \cdot 3\text{SiO}_2$	Кубическая	(111) и дру- гие формы	1.571	—	—	2.775
$\text{Na}_2\text{O} \cdot \text{CaO} \cdot \text{SiO}_2$			1.600	—	—	2.79

Key:

- | | |
|------------------------------------|---------------------------|
| a. Compound | g. Pseudocubic |
| b. Crystal system | h. Cubic |
| c. Appearance | i. Prisms |
| d. Density, g/cm^3 | j. Polysynthetic twins |
| e. Devitrite | k. (111) and other shapes |
| f. Rhombic | |

15 weight %, since, with a higher content of it in the mixture, pure sodium-calcium silicate is found after annealing. The authors consider that the phase composition of $2\text{Na}_2\text{O} \cdot 8\text{CaO} \cdot 5\text{SiO}_2$ is not the individual compounds, but is a mixture of a solid solution in β , $\alpha' \text{-} 2\text{CaO} \cdot \text{SiO}_2$ and $\text{Na}_2\text{O} \cdot \text{CaO} \cdot \text{SiO}_2$. In their opinion, the compound $2\text{Na}_2\text{O} \cdot 4\text{CaO} \cdot 3\text{SiO}_2$ does not exist.

Yeremin and colleagues [1] annealed a mixture with added Na_2CO_3 (from 0.6 to 3.0 weight %) at 1400° , with subsequent quenching. Very low solubility of Na_2O in $\beta\text{-}2\text{CaO} \cdot \text{SiO}_2$ (about 0.6 weight %) is noted. The index

TABLE IV
INDICES OF REFRACTION OF SOLID SOLUTIONS OF
 Na_2O IN DICALCIUM SILICATE

a Состав, вес.%			<i>Np</i>	<i>Ng</i>	<i>b</i> Двупре- доминение
Na_2O	CaO	SiO_2			
—	65.1	34.9	1.716	1.736	0.020
—	62.0	38.0	1.703	1.731	0.028
—	64.0	36.0	1.698	1.727	0.029
—	66.0	34.0	1.712	1.734	0.022
0.5	62.4	37.1	1.712	1.733	0.021
0.8	63.2	36.0	1.709	1.729	0.020
1.5	66.4	32.1	1.708	1.729	0.021
1.7	63.3	35.0	1.705	1.720	0.015
2.1	63.6	34.3	1.712	1.731	0.019
2.1	62.0	35.9	1.709	1.728	0.019
2.2	65.5	32.3	1.710	1.725	0.015
2.7	62.3	35.0	1.698	1.713	0.015

Key:

- a. Composition, weight %
- b. Birefringence

of refraction of these solid solutions is 1.728-1.730. Sodium oxide stabilizes $\beta\text{-}2\text{CaO}\cdot\text{SiO}_2$.

Maki and Sugimura [5] have shown that the compound $\text{Na}_2\text{O}\cdot 2\text{CaO}\cdot 3\text{SiO}_2$ discloses a reversible phase conversion at approximately 485° . The low temperature modification has a hexagonal unit cell with parameters: $a = 10.471$, $c = 13.174 \text{ \AA}$, $Z = 6$ (at room temperature). At 485° , the unit cell apparently becomes centered rhombohedral, with parameters: $a = 7.53 \text{ \AA}$, $\alpha = 89^\circ 7'$,

$Z = 2$ (at 550°). The compound $2\text{Na}_2\text{O} \cdot \text{CaO} \cdot 3\text{SiO}_2$, having a similar structure, is characterized by a cubic cell, with $a = 15.10 \text{ \AA}$, $Z = 16$. The authors found solid solutions between $\text{Na}_2\text{O} \cdot 2\text{CaO} \cdot 3\text{SiO}_2$ and $\text{Na}_2\text{O} \cdot \text{CaO} \cdot 2\text{SiO}_2$, in which the latter compound is isomorphic, with the high temperature modification $\text{Na}_2\text{O} \cdot 2\text{CaO} \cdot 3\text{SiO}_2$. For a solid solution rich in Na_2O , a polymorphic conversion is not observed. The compounds $\text{Na}_2\text{O} \cdot \text{CaO} \cdot 2\text{SiO}_2$ and $2\text{Na}_2\text{O} \cdot \text{CaO} \cdot 3\text{SiO}_2$ are nonisomorphic.

Maki [4] has studied the structure of devitrite $\text{Na}_2\text{O} \cdot 3\text{CaO} \cdot 6\text{SiO}_2$. Crystals of this compound are in the triclinic system, unit cell parameters: $a = 10.202 \pm 0.003$, $b = 10.680 \pm 0.003$, $c = 7.232 \pm 0.004 \text{ \AA}$, $\alpha = 109^\circ 48' \pm 3'$, $\beta = 99^\circ 46' \pm 5'$, $\gamma = 95^\circ 31' \pm 2'$, $V = 720.5 \pm 0.6 \text{ \AA}^3$, $Z = 2$. The experimental density is 2.726 g/cm^3 , calculated 2.722 g/cm^3 . The devitrite structure is characterized by the presence of wollastonite chains. Wollastonite is formed by thermal decomposition of devitrite.

BIBLIOGRAPHY

1. Yeremin, N.I., A.I. Yegereva, A.M. Dmitriyeva, I.B. Farfarova, Zhurn. prikl. khim., 43, No. 1, 18, 1970.
2. Toropov, N.A., O.I. Arakelyan, DAN SSSR, 72, No. 2, 356, 1950.
3. Fedorov, N.F., E.R. Brodkina, Izv. AN SSSR, Neorg. mater., 3, No. 7, 1283, 1967.
4. Maki, I., J. Ceram. Assoc. Japan, 76, No. 874, 203, 1968.
5. Maki, I., I. Sugimura, J. Ceram. Assoc. Japan, 76, No. 873, 144, 1968.
6. Morey, G., N. Bowen, J. Soc. Glass Techn., 9 226, 1925.
7. Morey, G.W., H.E. Merwin, J. Optic. Soc. Amer., 22, 632, 1932.
8. Segnit, E.R., Amer. J. Sci., 251, No. 8, 586, 1953.
9. Wyckoff, R.W., G.W. Morey, Amer. J. Sci., (5), 12, No. 71, 419, 1926.

K_2O -- CaO -- SiO_2

A part of the system, included in the triangle $K_2O \cdot SiO_2$ -- $CaO \cdot SiO_2$ -- SiO_2 , has been studied by Morey and colleagues [5]. Taylor [8] has studied the partial system $2CaO \cdot SiO_2$ -- $K_2O \cdot CaO \cdot SiO_2$. See also [4, 6].

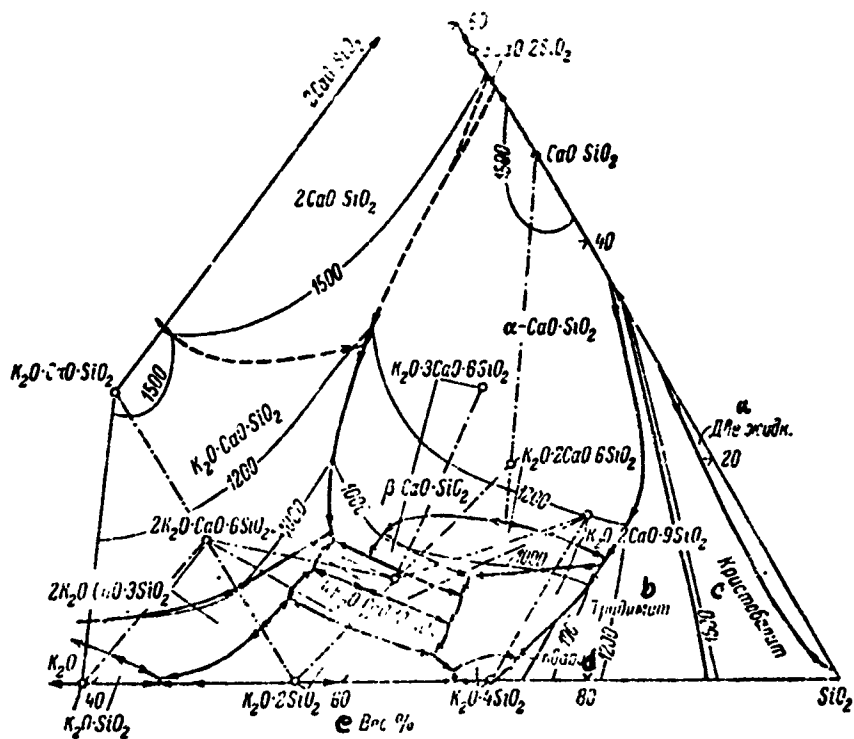


Fig. 23. Phase diagram of K_2O -- CaO -- SiO_2 system, region enriched in silica (from Morey, Kracek and Bowen).

Key:

- a. Two liquids
- b. Tridymite
- c. Cristobalite
- d. Quartz
- e. Weight %

Morey and colleagues give a ternary diagram (Fig. 23), as well as four profiles: 1. from $K_2O \cdot 2SiO_2$ to the side of the $SiO_2 - CaO$ triangle, to a point, corresponding to a content of approximately 32 weight % CaO (Fig. 24); 2. $K_2O \cdot SiO_2 - CaO \cdot SiO_2$ (Fig. 25); 3. $K_2O \cdot CaO \cdot SiO_2 - K_2O \cdot 2SiO_2$ (Fig. 26); 4. $K_2O \cdot 4SiO_2 - CaO \cdot SiO_2$ (Fig. 27). The partial system $2CaO \cdot SiO_2 - K_2O \cdot CaO \cdot SiO_2$ has been studied by Taylor, who found the compound $K_2O \cdot 23CaO \cdot 12SiO_2$ here.

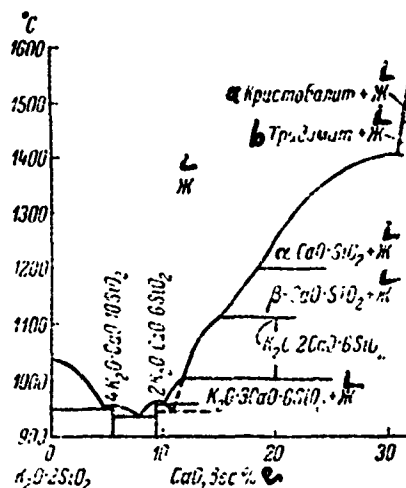


Fig. 24. Ternary system profile, going from compound $K_2O \cdot 2SiO_2$ through compound $K_2O \cdot 2CaO \cdot 6SiO_2$ to the side of triangle $CaO \cdot SiO_2$ (from Morey and colleagues).

Key:

- a. Cristobalite
- b. Tridymite
- c. Weight %

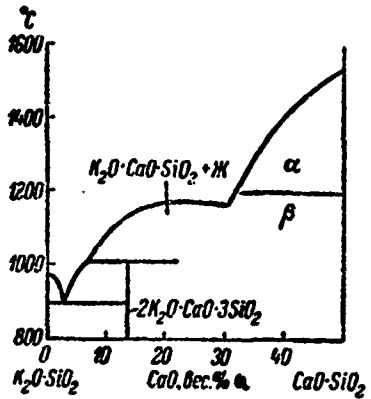


Fig. 25. Phase diagram of partial system $K_2O \cdot SiO_2$ -- $CaO \cdot SiO_2$
(from Morey and colleagues).

Key: a. Weight %

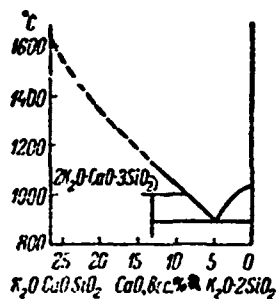


Fig. 26. Phase diagram of partial system $K_2O \cdot CaO \cdot SiO_2$ -- $K_2O \cdot 2SiO_2$ (from Morey and colleagues).

Key:

a. Weight %

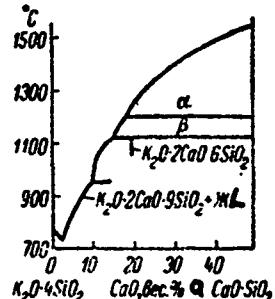


Fig. 27. Phase diagram of partial system $K_2O \cdot 4SiO_2$ -- $CaO \cdot SiO_2$ (from Morey and colleagues).

Key:

a. Weight %

A considerable number of crystalline ternary compounds has been found in the system. Morey and colleagues found six compounds: $2K_2O \cdot CaO \cdot 3SiO_2$, $K_2O \cdot CaO \cdot SiO_2$, $4K_2O \cdot CaO \cdot 10SiO_2$, $K_2O \cdot 3CaO \cdot 6SiO_2$, $K_2O \cdot 2CaO \cdot 9SiO_2$, and $2K_2O \cdot CaO \cdot 6SiO_2$. Toropov and Borisenko [2] and Yung and colleagues [3], on the basis of X-ray studies, confirm the existence of the compound $K_2O \cdot 23CaO \cdot 12SiO_2$. The index of refraction of this compound is close to that of dicalcium silicate: according to Toropov [1], $Ng = 1.703$, $Np = 1.695$ and, according to Suzukawa [7], $Ng = 1.711$, $Np = 1.703$.

TABLE I
INVARIANT POINTS OF K_2O -- CaO -- SiO_2 SYSTEM

a фазы	b Процесс	c Состав, вес.%			d Темпера- тура, °C
		K_2O	CaO	SiO_2	
$\alpha\text{-}K_2O\cdot3CaO\cdot6SiO_2 + \beta\text{-}CaO\cdot SiO_2 + SiO_2 +$ жидкость e	f Реакция	13.3	10.8	75.9	1080
$K_2O\cdot2CaO\cdot9SiO_2 + \sigma\text{-}K_2O\cdot3CaO\cdot6SiO_2 +$ $+ SiO_2 +$ жидкость e	»	13.8	10.5	75.7	1050
$K_2O\cdot2CaO\cdot9SiO_2 + K_2O\cdot4SiO_2 + SiO_2 +$ $+$ жидкость e	g Эвтектика	25.1	1.9	73.0	720
$K_2O\cdot2CaO\cdot9SiO_2 + K_2O\cdot2SiO_2 + K_2O\cdot$ $\cdot4SiO_2 +$ жидкость e	»	30.8	0.9	68.3	720
$K_2O\cdot2CaO\cdot9SiO_2 + 4K_2O\cdot CaO\cdot$ $\cdot10SiO_2 + K_2O\cdot2SiO_2 +$ жидкость e	f Реакция	31.6	2.3	66.1	710
$K_2O\cdot2CaO\cdot9SiO_2 + 4K_2O\cdot CaO\cdot$ $\cdot10SiO_2 + 2K_2O\cdot CaO\cdot6SiO_2 +$ жидкость e	»	28.8	5.3	65.9	825
$K_2O\cdot2CaO\cdot9SiO_2 + 2K_2O\cdot CaO\cdot$ $\cdot6SiO_2 + \beta\text{-}K_2O\cdot3CaO\cdot6SiO_2 +$ жидкость e	»	26.8	7.8	65.4	910
$\beta\text{-}K_2O\cdot3CaO\cdot6SiO_2 + \alpha\text{-}K_2O\cdot3CaO\cdot$ $\cdot6SiO_2 +$ жидкость e	h Превраще- ние	23.6	11.0	65.4	1000
$2K_2O\cdot CaO\cdot6SiO_2 +$ жидкость e	i Таяние	31.1	9.3	59.6	959
$4K_2O\cdot CaO\cdot10SiO_2 +$ жидкость e	»	36.5	5.4	58.1	916
$2K_2O\cdot CaO\cdot6SiO_2 + \beta\text{-}K_2O\cdot3CaO\cdot$ $\cdot6SiO_2 + \beta\text{-}CaO\cdot SiO_2 +$ жидкость e	f Реакция	32.3	11.3	56.4	930
$2K_2O\cdot CaO\cdot3SiO_2 + 4K_2O\cdot CaO\cdot$ $\cdot10SiO_2 + 2K_2O\cdot CaO\cdot6SiO_2 +$ жидкость e	g Эвтектика	37.2	10.2	52.6	890
$2K_2O\cdot CaO\cdot3SiO_2 + 2K_2O\cdot CaO\cdot$ $\cdot6SiO_2 + \beta\text{-}CaO\cdot SiO_2 +$ жидкость e	»	34.2	13.0	52.8	860
$K_2O\cdot CaO\cdot SiO_2 + \beta\text{-}CaO\cdot SiO_2 + 2CaO\cdot$ $\cdot SiO_2 +$ жидкость e	f Реакция	22.5	31.0	46.5	1160
$2K_2O\cdot CaO\cdot3SiO_2 + \beta\text{-}CaO\cdot SiO_2 +$ $+ K_2O\cdot CaO\cdot SiO_2 +$ жидкость e	»	34.1	13.7	52.2	830
$3K_2O\cdot CaO\cdot3SiO_2 + K_2O\cdot2SiO_2 + 4K_2O\cdot$ $\cdot CaO\cdot10SiO_2 +$ жидкость e	g Эвтектика	40.5	7.7	51.8	835
$K_2O\cdot5O_2 + 2K_2O\cdot CaO\cdot3SiO_2 + K_2O\cdot$ $\cdot SiO_2 +$ жидкость e	»	51.7	0.2	45.1	770
$\beta\text{-}CaO\cdot SiO_2 +$ жидкость e	i Таяние	44.8	26.7	28.5	1030
$\alpha\text{-}CaO\cdot SiO_2 ; K_2O\cdot23CaO\cdot42SiO_2 +$ $+$ не	g Эвтектика	44.2	29.7	29.1	1595

Key:

- a. Phases
- b. Process
- c. Content, weight %
- d. Temperature, °C
- e. Liquid
- f. Reactions
- g. Eutectic
- h. Conversion
- i. Melting

TABLE II
CRYSTALLINE PHASES OF K_2O -- CaO -- SiO_2 SYSTEM

a Соединение	b Система кристаллов	c Габитус	N_g	N_m	N_p	$N_g - N_p$	$2V^{\circ}$
$2K_2O \cdot CaO \cdot 3SiO_2$	Кубическая	Октаэдры	—	1.572	—	—	—
$K_2O \cdot CaO \cdot SiO_2$	Гексагональная	Пирамиды	1.603	—	1.600	0.005	(+)
$4K_2O \cdot CaO \cdot 10SiO_2$	f To же	Пластинки	1.548	—	1.537	0.011	—
$\alpha-K_2O \cdot 3CaO \cdot 6SiO_2$	Ромбическая	Призмы	1.59	?	1.575	0.015	(+) большой
$\beta-K_2O \cdot 3CaO \cdot 6SiO_2$	f To же	Нады и пластинки	1.57	—	1.56	0.010	(-)?
$K_2O \cdot 2CaO \cdot 9SiO_2$	Моноклинико- триклиническая	Призмы и пластинки	1.535	?	1.515	0.020	(-) большой
$2K_2O \cdot CaO \cdot 6SiO_2$	f To же	—	1.543	1.541	1.535	0.008	(-) 60±5

Key:

- | | |
|-------------------|----------------------------|
| a. Compound | h. Monoclinic or triclinic |
| b. Crystal system | i. Octahedra |
| c. Appearance | j. Pyramids |
| d. Cubic | k. Plates |
| e. Hexagonal | l. Prisms |
| f. Same | m. Needles and plates |
| g. Rhombic | n. Prisms and plates |
| | o. Large |

BIBLIOGRAPHY

1. Toropov, N. A., Khimiya tsementov [Cement Chemistry], Promstroyizdat Press, Moscow, 1956, p. 72.
2. Торопов, Н. А., А. И. Борисенко, Tsement, No. 5, 16, 1950.
3. Yung, V. N., Yu. M. Butt, V. V. Myshlyayev, Ibid., No. 6, 9, 1951.
4. Bredig, M. A., Amer. Mineralogist, 28, No. 11-12, 594, 1943; J. Phys. Chem., 49, No. 11/12, 537, 1945.

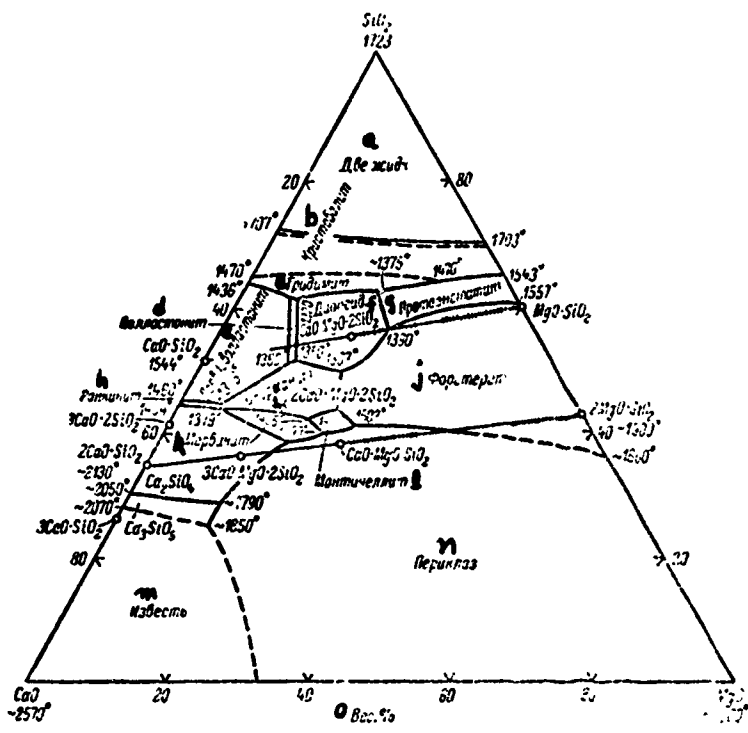
5. Morey, G.W., F.C. Kracek, N.L. Bowen, J. Soc. Glass Techn., 14, No. 54, 149, 1930.
6. Nurse, R.W., Proc. 3rd Intern. Symp. Chem. Cement, London, 169, 1952.
7. Suzukawa, Y., Zement -- Kalk -- Gips, 9, No. 9, 390, 1956.
8. Taylor, W.C., J. Res. Nat. Bur. Stand., 27, No. 3, 311, 1941.



As early as the first works of Day and colleagues [17], Bowen and Anderson [9], Bowen [8] and Ferguson and Merwin [19], the basic characteristics of the system had been ascertained and the existence of the predominant phases had been established. The following three-component compounds crystallize in the system: $\text{CaO} \cdot \text{MgO} \cdot 2\text{SiO}_2$, diopside; $\text{CaO} \cdot \text{MgO} \cdot \text{SiO}_2$, monticellite; $3\text{CaO} \cdot \text{MgO} \cdot 2\text{SiO}_2$, merwinite; $2\text{CaO} \cdot \text{MgO} \cdot 2\text{SiO}_2$, ockermanite and the compound $5\text{CaO} \cdot 2\text{MgO} \cdot 6\text{SiO}_2$.

A phase diagram of the $\text{MgO} \text{ -- } \text{CaO} \text{ -- } \text{SiO}_2$ system, according to Osborn and Muan [30], who studied the preceding work (up to 1960), mainly of Ricker and Osborn [33], is presented in Fig. 28. Separate partial systems are presented in Fig. 29-33.

Solid solutions have been found among the many compounds in the $\text{CaO} \text{ -- } \text{MgO} \text{ -- } \text{SiO}_2$ system. Solid solutions apparently are absent among monticellite, merwinite, ockermanite and wollastonite. The partial system diopside ($\text{CaO} \cdot \text{MgO} \cdot 2\text{SiO}_2$) -- silica has been studied by Bowen. The system is a simple eutectic, with a liquid phase immiscibility region. Ehrenberg [18] showed that only diopside forms from the "dry" components, as a result of solid phase reaction, and not tremolite as was proposed by Bowen.



Reproduced from
best available copy.

Fig. 28. Phase diagram of MgO -- CaO -- SiO₂ system (from Osborn and Muan).

Key:

- a. Two liquids
 - b. Cristobalite
 - c. Tridymite
 - d. Wollastonite
 - e. Pseudowollastonite
 - f. Diopside
 - g. Protoenstatite
 - h. Rankinite
 - i. Ockermanite
 - j. Forsterite
 - k. Merwinite
 - l. Monticellite
 - m. Lime
 - n. Periclase
 - o. Weight %

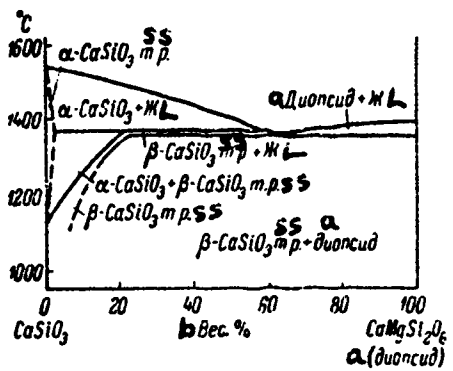


Fig. 29. Phase diagram of partial system $\text{CaO} \cdot \text{SiO}_2$ -- $\text{CaO} \cdot \text{MgO} \cdot 2\text{SiO}_2$ (from Schairer and Bowen).

Key:

- a. Diopside
- b. Weight %

The partial system diopside -- calcium metasilicate has been studied by Schairer and Bowen [35]. A very flat primary crystallization curve is observed for diopside (Fig. 29). Diopside forms a solid solution with CaSiO_3 , in which the conversion temperature of the calcium metasilicate in this crystalline solution increases considerably, from 1125 to 1368°. At a temperature of 1368°, the β phase (wollastonite) dissolves much more diopside (up to 22%) than the α phase (pseudowollastonite).

In the partial system calcium metasilicate -- ockermanite, the latter does not form a solid solution with either the α or β calcium metasilicate. The partial systems dicalcium silicate -- ockermanite and merwinite --

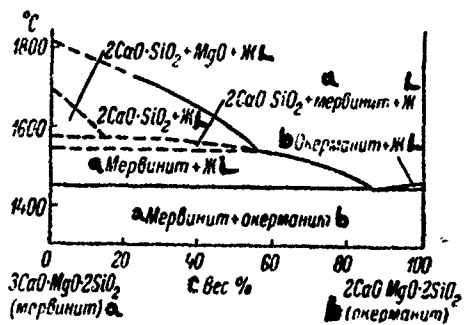


Fig. 30. Phase diagram of partial system $3\text{CaO} \cdot \text{MgO} \cdot 2\text{SiO}_2$ (merwinite) -- $2\text{CaO} \cdot \text{MgO} \cdot 2\text{SiO}_2$ (ockermanite) (from Osborn).

Key:

- a. Merwinite
- b. Ockermanite
- c. Weight %

ockermanite (Fig. 30) have been studied by Osborn [29], and ciopside -- ockermanite by Ferguson and Merwin [19].

Ockermanite apparently can produce solid solutions with some compounds. Schairer and colleagues [36] investigated solid solutions formed from ockermanite with merwinite (considerably less than 5 weight % dissolves), rankinite (less than 7.5% and more than 5 weight % dissolves at 1380°), monticellite (less than 2% at 1340°), forsterite (possibly about 1% at 1340°) and d.calciumsilicate (considerably less than 5%, and it is even possible that there is quite negligible solubility here). In connection with this, it is noted that, over a certain temperature range, the composition of ockermanite can deviate from stoichiometric (2:1:2).

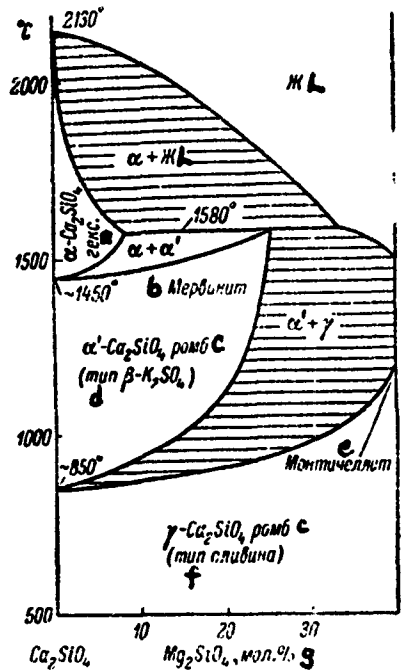


Fig. 31. Phase diagram of partial system $2\text{CaO}\cdot\text{SiO}_2$ -- $2\text{MgO}\cdot\text{SiO}_2$ (from Bredig).

Key:

- a. Hexagonal
- b. Merwinite
- c. Rhombic
- d. $\beta\text{-K}_2\text{SO}_4$ type
- e. Monticellite
- f. Olivine type
- g. Mole %

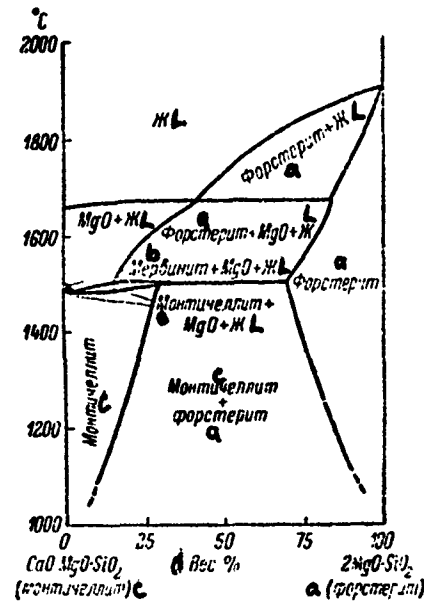


Fig. 32. Phase diagram of partial system $2\text{MgO}\cdot\text{SiO}_2$ -- $\text{CaO}\cdot\text{MgO}\cdot\text{SiO}_2$ (monticellite) (from Ricker and Osborne).

Key:

- a. Forsterite
- b. Merwinite
- c. Monticellite
- d. Weight %

The partial system Ca_2SiO_4 -- Mg_2SiO_4 (Fig. 31) has been studied by Bredig [13]. Bredig considers merwinite $3\text{CaO}\cdot\text{MgO}\cdot 2\text{SiO}_2$ to be an individual compound, similar to Ca_2SiO_4 in its crystalline aspect, with a

K_2SO_4 type rhombic structure. Merwinite decomposes at $1975 \pm 5^\circ$, with formation of a melt, periclase and dicalcium silicate.

Solid solutions in the monticellite ($CaO \cdot MgO \cdot SiO_2$) -- forsterite ($2MgO \cdot SiO_2$) series have been studied by Ricker and Osborn [33]. Close to the liquidus temperature, a broad region of solid solutions is observed, but, nevertheless, solid solutions are not continuous in the monticellite -- forsterite series (Fig. 32). Despite belonging to one and the same space group and the close dimensions of the unit cells, even at elevated temperatures, limited solubility is observed. Thus, at 1500° , when liquid and periclase appear, as a result of congruent melting, the coexisting solid phases on both sides contain approximately 30 weight % dissolved forsterite and monticellite. The merwinite $3CaO \cdot MgO \cdot 2SiO_2$ formed does not form a solid solution with monticellite.

The partial system $MgSiO_3$ -- $MgO \cdot CaO \cdot 2SiO_2$ (Fig. 33) has been studied by Atlas [6].

The partial binary system MgO -- $2CaO \cdot SiO_2$, according to Ricker and Osborn, is a simple eutectic, with a eutectic melting temperature of 1800° .

Butt and colleagues [2] have shown that magnesium oxide, dissolving in tricalcium silicate up to a content of 4 weight %, forms a solid intrusion solution.

Biggar and O'Hara [7] have studied the partial profile of forsterite -- monticellite by the quenching method. It has been shown that monticellite is unstable at atmospheric pressure. The stability region of monticellite solid solutions (for the monticellite-forsterite profile) is extended at elevated temperatures: at 1200° , the stability is limited between 89 and 93 mole %

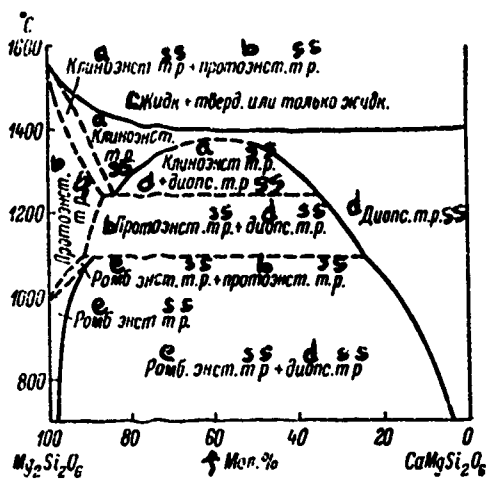


Fig. 33. Phase diagram of partial system $\text{CaO} \cdot \text{MgO} \cdot 2\text{SiO}_2$ -- $\text{Mg}_2\text{Si}_2\text{O}_6$ (from Atlas).

Key:

- a. Clinonestatite
- b. Protoenstatite
- c. Liquid + solid or only liquid
- d. Diopside
- e. Rhombic enstatite
- f. Mole %

monticellite, at 1490° , from 75 to 92 mole % and, for 800° , from 95 to 96 mole % in all.

The authors have precisely defined the region of existence of forsterite-base solid solutions. The highest monticellite content in this solid solution, reaching 19 mole %, is observed at 1490° . With increase or decrease in temperature, the maximum content of monticellite decreases, amounting to 7 mole %, for example, at 1200° .

Spencer and Coleman [37] determined the density of the chemical compounds in the system, using a pycnometer filled with xylol.

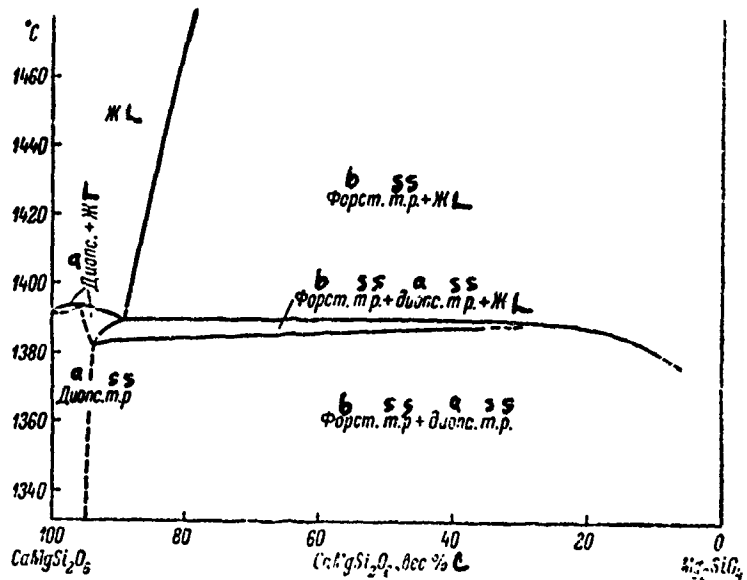


Fig. 34. Phase diagram of diopside (CaO·MgO·SiO₂) -- forsterite (2MgO·SiO₂) system (from Kushiro and Schairer).

Key:

- a. Diopside
- b. Forsterite
- c. Weight %

In the first works on the diopside -- forsterite system, it was assumed that it is a simple eutectic, with a very flat diopside crystallization curve. Kushiro and Schairer [24] determined that CaMgSi₂O₆ and Mg₂SiO₄ base solid solutions exist here. The low temperature region of this system is

shown in Fig. 34. The liquidus " diopside solid solutions has a maximum approximately 2° higher than the melting temperature of diopside, 1391.5°. Diopside can contain about 5 weight % of forsterite in solid solution.

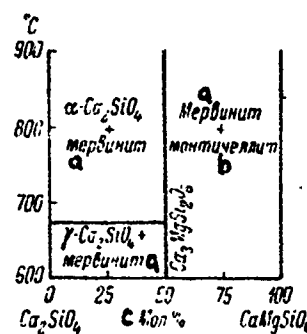


Fig. 35. Phase diagram of $2\text{CaO} \cdot \text{SiO}_2$ -- $\text{CaO} \cdot \text{MgO} \cdot \text{SiO}_2$ system in the subsolidus region at 140 kgf/cm^2 water vapor pressure (from D. Roy).

Key:

- a. Merwinite
- b. Monticellite
- c. Mo%e %

D. Roy [34] studied the low temperature region (600-900°) of the $2\text{CaO} \cdot \text{SiO}_2$ -- $\text{CaO} \cdot \text{MgO} \cdot \text{SiO}_2$ (monticellite) system, using the hydrothermal method at water vapor pressures of 70-1000 kgf/cm^2 . She observed monticellite, Ca_2SiO_4 , and merwinite everywhere, in the form of pure phases, and she did not observe solid solutions. A subsolidus equilibrium phase diagram for water vapor pressure of 140 kgf/cm^2 is presented in Fig. 35.

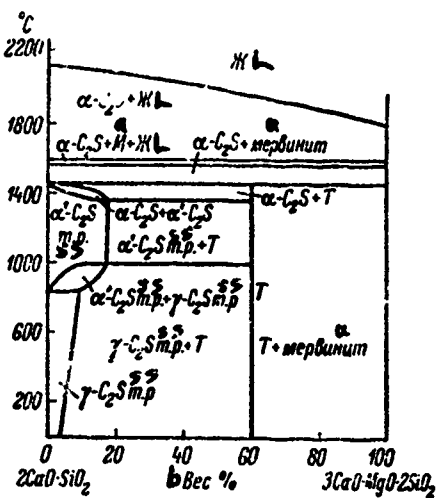


Fig. 36. Phase diagram of partial system $2\text{CaO} \cdot \text{SiO}_2$ -- $3\text{CaO} \cdot \text{MgO} \cdot \text{SiO}_2$ (merwinite) system (from Gutt):
T, new magnesium-calcium silicate.

Key:

- a. Merwinite
- b. Weight %

Carefully (prolonged annealing) studying the $2\text{CaO} \cdot \text{SiO}_2$ -- $3\text{CaO} \cdot \text{MgO} \cdot 2\text{SiO}_2$ (merwinite) system, Gutt [20] discovered a new, complex compound $(2\text{CaO} \cdot \text{SiO}_2)_{5.6} (3\text{CaO} \cdot \text{MgO} \cdot 2\text{SiO}_2)_{4.4}$ (T in Fig. 36), and he proposed a new variant of the $2\text{CaO} \cdot \text{SiO}_2$ -- merwinite system (Fig. 36). The liquidus curve, obtained by means of a heating microscope, reaches from 1800 to 2130° . Only $\alpha\text{-}2\text{CaO} \cdot \text{SiO}_2$ is separated from the liquid as the primary phase here; at 1575° , decomposition of merwinite takes place, with formation of $\alpha\text{-}2\text{CaO} \cdot \text{SiO}_2$, periclase (MgO) and liquid. At 1590° , magnesium oxide dissolves and only

the dicalcium silicate remains in the liquid. In this region, where periclase is present, the system cannot be considered to be a binary one.

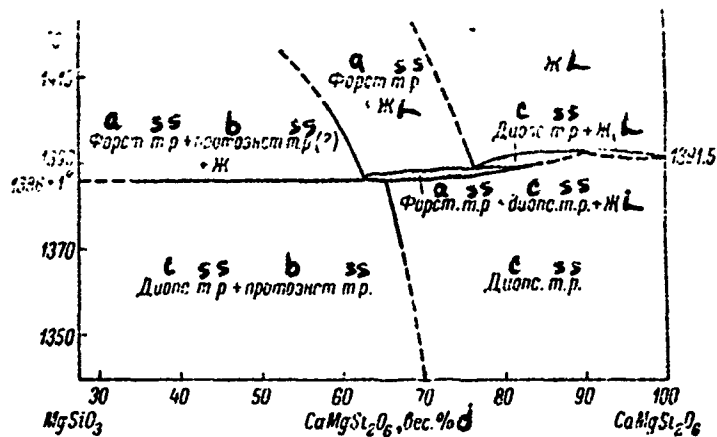


Fig. 37. Refined phase diagram of diopside-enriched portion of $\text{MgO} \cdot \text{SiO}_2$ -- $\text{CaO} \cdot \text{MgO} \cdot 2\text{SiO}_2$ system (from Kushiro and Schairer).

Key:

- a. Forsterite
- b. Protonstatite
- c. Diopside
- d. Weight %

Kushiro and Schairer [24] recently refined the diopside-enriched region of the diopside-enstatite system (Fig. 37).

A three-phase triangular system, according to Berezhnoy [1], is presented in Fig. 38. The phase relationships for temperatures of 1600 and 1700°, from Muan and Osborn, are shown in Fig. 39a and b.

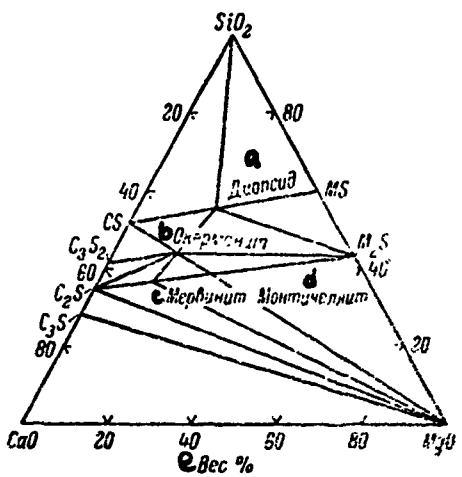
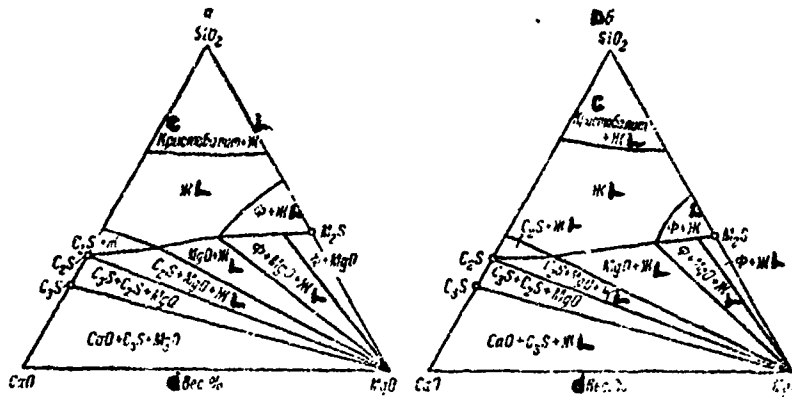


Fig. 38. Phase co-existence triangle of $MgO - CaO - SiO_2$ system (from Berezhnaya).

Key:

- a. Diopside
- b. Ockermanite
- c. Merwinite
- d. Monticellite
- e. Weight %

The question of stability of ockermanite at normal pressure has been touched on in a number of works, for example, Carstens and Kristoffersen [14], Bowen, Schairer and Posnjak [10], Osborn and Schairer [31], Nuuvonen [27], Christie [15], and at elevated pressures, in the works of Harker and Tuttle [21], Kushiro [22] and Kushiro and Yoder [25] and others. The thermal behavior of ockermanite has been studied in greatest detail at high temperatures and normal pressures by Lapin and Solovova [4], in which the study was carried



Reproduced from
best available copy.

Fig. 39. Phase relationships (isothermal sections) of
 $MgO - CaO - SiO_2$ system at 1600 (a) and 1700° (b)
(from Muan and Osborn): ϕ forsterite.

Key:

- c. Cristobalite
- d. Weight %

out both by an approach "from below," at temperatures from 900 to 1280° and holding from 4 hours 30 minutes to 20 hours, and "from above," with preliminary melting of the synthesized ockermanite and holding it then at various temperatures in the 1200-1350° range for periods of 2-233 hours. Partial decomposition of ockermanite was established, with appearance of crystals of grains of other phases within it. Thus, at 1325°, $2CaO \cdot SiO_2$ and merwinite appear, at 1275° and holding for two and four hours, a small amount of monticellite is combined with the latter, and upon holding 20 hours at 1275°, diopside and wollastonite solid solutions were found within the ockermanite

crystals; the diopside and wollastonite phases, with predominance of diopside, were observed at all holding times (from 2 to 233 hours) at 1200° and lower (down to 1050°).

The phase ratios and melting temperatures in the $\text{MgO} - \text{CaO} - \text{SiO}_2$ system has been studied at elevated pressures. Yoder [38] determined the increase in melting temperature of diopside ($\text{CaO} \cdot \text{MgO} \cdot 2\text{SiO}_2$) with pressure. He introduces the equation $t_{\text{melt}} = 1391.5 + 0.01297 P$, where t_{melt} is the melting temperature (in °C) and P is the pressure (in bars). Boyd and England [11, 12] have studied the relation of melting temperature of diopside up to a pressure of 60 kbar.

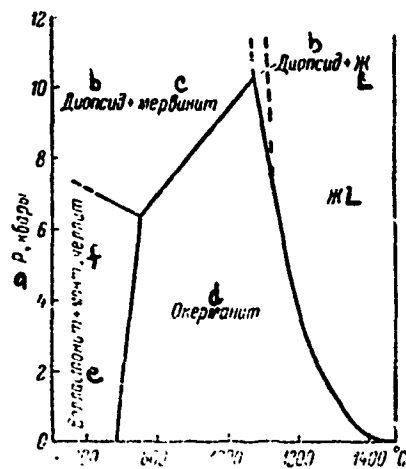


Fig. 40. Phase ratios for the compound $\text{Ca}_2\text{MgSi}_2\text{O}_7$ vs. temperature and pressure (from Yoder).

Key:

- a. Pressure P , kbar
- b. Diopside
- c. Merwinite
- d. Ockermanite
- e. Wollastonite
- f. Monticellite

Yoder [39] has determined the stability region of ockermanite in the ternary system under high pressure conditions. A diagram showing the stability field of ockermanite $\text{Ca}_2\text{MgSi}_2\text{O}_7$ (the possibility is admitted of formation of solid solutions based on ockermanite) is presented in Fig. 40. Yoder studied the reaction ockermanite + forsterite = diopside + monticellite under high pressure conditions.

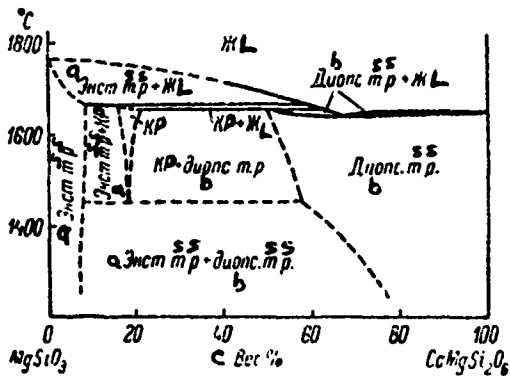


Fig. 41. Phase diagram of partial system diopside -- enstatite at pressure of 20 kbar (from Kushiro): KP clino-pyroxene.

Key:

- a. Enstatite
 - b. Diopside
 - c. Weight %

Kushiro [23] has studied the system forsterite -- diopside -- silica at a pressure of 20 kbar. Partial diagrams of Mg_2SiO_4 -- $\text{CaMgSi}_2\text{O}_6$ and MgSiO_3 -- $\text{CaMgSi}_2\text{O}_6$ for the pressure indicated are presented in Figs. 41 and 42. See also [16].

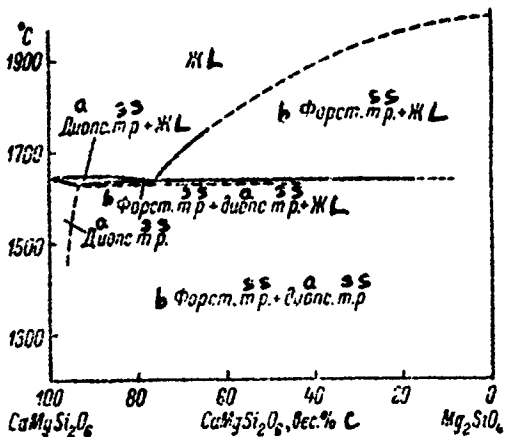


Fig. 42. Phase diagram of partial system forsterite -- diopside at pressure of 20 kbar (from Kushiro).

Key:

- a. Diopside
- b. Forsterite
- c. Weight %

Kalinina and Filipovich [3] and Toropov and Khotimchenko [5] have shown that crystallization of glass forms metastable phases, sometimes including solid solutions.

According to the new definitions of Onken [28], relating to the olivine group, monticellite has the following unit cell parameters: $a = 4.822 \pm 0.001$, $b = 11.108 \pm 0.003$, $c = 6.382 \pm 0.002$ Å.

INVARIANT POINTS OF CaO -- MgO -- SiO₂
(from Parker and Nurse)

α Фазы	б Состав, вес. %			с Темпера- тура, °C
	CaO	MgO	SiO ₂	
2CaO · MgO · 2SiO ₂ + 2CaO · SiO ₂ + 3CaO · MgO · · 2SiO ₂ + жидкость d	47.2	9.2	43.6	1400
2CaO · MgO · 2SiO ₂ + 2CaO · SiO ₂ + MgO + жидкость d	42.6	21.9	35.5	1580

Key:

- a. Phases
- b. Composition, weight %
- c. Temperature, °C
- d. Liquid

Ferguson and Merwin [19] have determined the optical properties of solid solutions of the clinoenstatite (MgSiO₃) -- diopside system.

BIBLIOGRAPHY

1. Berezhnoy, A. S., Mnogokomponentnyye sistemy okislov [Multicomponent Oxide Systems], Naukova dumka Press, Kiev, 1970.
2. Butt, Yu. M., V. V. Timashev, V. Ye. Kaushanskiy, Izv. AN SSSR, Neorg. mater., 1, 7, 1965, p. 1201.
3. Kalinina, A. M., V. N. Filipovich, Ibid., p. 1189.
4. Lapin, V. V., I. P. Solovova, in the book Eksperimental'nyye issledovaniya mineraloobrazovaniya [Experimental Research in Mineral Formation], Moscow, 1971.
5. Toropov, N. A., V. S. Khotimchenko, Izv. AN SSSR, neorg. mater., 2, 4, 1966, p. 738.

6. Atlas, L., J. Geol., 60, No. 2, 125, 1952.
7. Biggar, G.M., M.J. O'Hara, J. Amer. Ceram. Soc., 52, No. 5, 249, 1969.
8. Bowen, N.L., Amer. J. Sci., (4) 38, 207, 225, 1914.
9. Bowen, N.L., O. Andersen, Amer. J. Sci., (4), 37, 487, 1914.
10. Bowen, N.L., J.F. Schairer, E. Posnjak, Amer. J. Sci., (5), 26, No. 153, 1933.
11. Boyd, F.R., J.L. England, Carnegie Inst. Washington Year Book, 57, 173, 1957-1958.
12. Boyd, F.R., J.L. England, Carnegie Inst. Washington Year Book, 60, 113, 1960-1961.
13. Bredig, M.A., J. Amer. Ceram. Soc., 33, No. 6, 190, 1950.
14. Carstens, C.W., K. Kristoffersen, Neues Jahrb. Mineral., Geol., Paläontol., Beilage-Band, 62A, 163, 1931.
15. Christie, O.H., Skr. Norske Vidensk.-Akad. Oslo, 1, Matem.-Naturv. Kl., Ny-ser., No. 15, 1, 1964.
16. Davis, T.C., Carnegie Inst. Washington Year Book, 62, 103, 1961-1963.
17. Day, A.L., E.C. Shepherd, F.E. Wright, Amer. J. Sci., (4), 22, No. 130, 265, 1906.
18. Ehrenberg, H., Zbl. Mineral., Geol. u. Paläontol., Abt. Mineral. u. Petrogr., 129, 1932.
19. Ferguson, J.B., H.E. Merwin, Amer. J. Sci., (4), 48, No. 284, 81, 1919.
20. Gutt, W., Nature, 190, No. 4773, 339, 1961: 207, No. 4993, 184, 1965.
21. Harker, R.I., O.F. Tuttle, Amer. J. Sci., 254, No. 8, 468, 1956.
22. Kushiro, I., Carnegie Inst. Washington Year Book, 63, 84, 1963-1964.
23. Kushiro, I., Amer. J. Sci., 267A, Schairer vol., 269, 1969.
24. Kushiro, I., J.F. Schairer, Carnegie Inst. Washington Year Book, 62, 94, 1962-1963.
25. Kushiro, I., Yoder, H.S., Carnegie Inst. Washington Year Book, 63, 81, 1963-1964.

26. Muan, A., E.F. Osborn, Phase Equilibria among Oxides in Steelmaking, Addison Wesley, Reading, 93, 1965.
27. Nuuvonen, K.J., Bull. Commision geol. Finlande, No. 158, 57, 1952.
28. Onken, H., Naturwissenschaften, 51, No. 14, 334, 1964.
29. Osborn, E.F., J. Amer. Ceram. Soc., 26, No. 10, 321, 1943.
30. Osborn, E.F., A. Muan, in: E.M. Levin, C.R. Robbins, H.F. McMurdie. Phase Diagrams for Ceramists, USA, Columbus, fig. 598, 1964.
31. Osborn, E.F., J.F. Schairer, Amer. J. Sci., 239, No. 10, 715, 1941.
32. Parker, T.W., R.W. Nurse, J. Iron a. Steel. Inst., 148, No. 2, 475, 1943.
33. Ricker, R.W., E.F. Osborn, J. Amer. Ceram. Soc., 37, No. 4, 133, 1954.
34. Roy, D.M., Mineral. Magaz., 31, No. 233, 187, 1956.
35. Schairer, J.F., N.L. Bowen, Amer. J. Sci., 240, No. 10, 725, 1942.
36. Schairer, J.F., H.S. Yoder, C.E. Tilley, Carnegie Inst. Washington Year Book, 65, 217, 1965-1966.
37. Spencer, D.R.F., D.S. Coleman, Trans. Brit. Ceram. Soc., 68, No. 3, 125, 1969.
38. Yoder, H.S., J. Geol., 60, No. 4, 364, 1952.
39. Yoder, H.S., Carnegie Inst. Washington Year Book, 66, 471, 1966-1967.



The system has not been studied fully. Eskola [5] has studied the partial CaSiO_3 -- SrSiO_3 profile, and Toropov and Konovalov [2], the partial Ca_2SiO_4 -- Sr_2SiO_4 profile. In both cases, continuous solid solutions are observed. The phase diagram of the partial system $\text{CaO}\cdot\text{SiO}_2$ -- $\text{SrO}\cdot\text{SiO}_2$, from the data of Eskola, is presented in Fig. 43. Toropov and Konovalov have determined the indices of refraction of solid solutions of the orthosilicate profile, and Buckner

and Roy [4], the regions of existence of the α - and β -wollastonite solid solutions. The temperature-concentration ratios between the α - and β -solid solutions of wollastonite are shown in Fig. 44. Henning and Päiselt [6] have studied the solid solutions in the series Ca_2SiO_4 -- Sr_2SiO_4 by infrared spectroscopy.

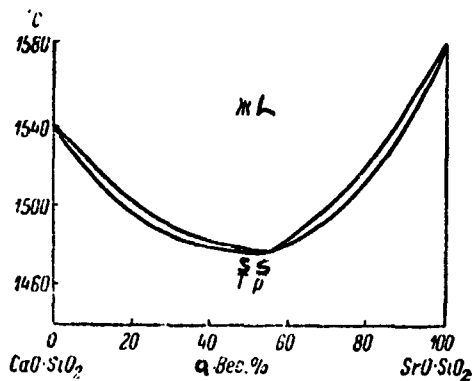


Fig. 43. Phase diagram of partial system $\text{CaO} \cdot \text{SiO}_2$ -- $\text{SrO} \cdot \text{SiO}_2$ (from Eskola).

Key: a. Weight %

Toropov and colleagues [1], in study of the partial system of $3\text{CaO} \cdot \text{SiO}_2$ -- $3\text{SrO} \cdot \text{SiO}_2$, found that the solubility limit of the tristrontium silicate in the tricalcium is approximately 7.5 weight %. The same polymorphic conversions are found for the solid solution as for pure $3\text{CaO} \cdot \text{SiO}_2$; however, the temperatures of these conversions decreases. Thus, for a solid solution containing 7.5 weight % $3\text{SrO} \cdot \text{SiO}_2$, the polymorphic conversions took place:

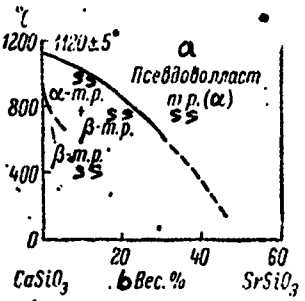


Fig. 44. Diagram illustrating the regions of existence of the α - and β -wollastonite solid solutions in the $\text{CaO} \cdot \text{SiO}_2$ -- $\text{SrO} \cdot \text{SiO}_2$ system (from Buckner and Roy).

Key:

- a. Pseudowollastonite
- b. Weight %

the first at 850° (for pure $\text{CaO} \cdot \text{SiO}_2$ at 900°), the second at 920° (for pure $3\text{CaO} \cdot \text{SiO}_2$ at 950°).

Brisi and Appendino [3] have studied the system in the subsolidus region, at 1200 and 1350° . The phases were identified by X-ray methods in samples quenched after prolonged annealing at the temperatures indicated. The phase diagrams for 1200 and 1350° , respectively, are represented in Fig. 45 a and b. Three series of solid solutions are continuous. These are solid solutions between calcium oxide and strontium oxide, between α' - Ca_2SiO_4 and α' - Sr_2SiO_4 and between pseudowollastonite and strontium metasilicate.

Sr_2SiO_4 stabilizes various modifications of Ca_2SiO_4 . The first portions of Sr_2SiO_4 entering the solid solution stabilizes α' - Ca_2SiO_4 . The solid solution of the composition $\text{Ca}_{1.9}\text{Sr}_{0.1}\text{SiO}_4$ corresponds to the γ - Ca_2SiO_4 structure.

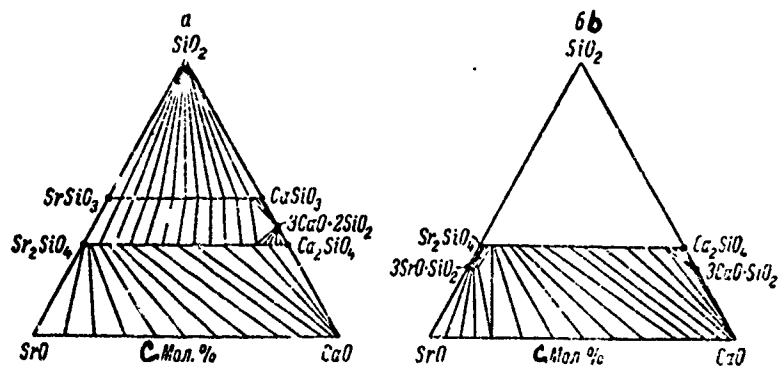


Fig. 45. Diagram of phase ratios in $\text{CaO} - \text{SrO} - \text{SiO}_2$ system, in subsolidus region (from Brisi and Appendino):
a. 1200° ; b. 1350° .

Key:

c. Mole %

For the composition $\text{Ca}_{1.8}\text{Sr}_{0.2}\text{SiO}_4$, a structure corresponding to the α' - Ca_2SiO_4 form is characteristic. Attention is drawn to the three-phase field, in which the compound $3\text{CaO} \cdot 2\text{SiO}_2$ is in equilibrium with the solid solution $(\text{CaSr})\text{SiO}_3$, containing about 3 mole % of strontium metasilicate, and with the solid solution $(\text{CaSr})_2\text{SiO}_4$, containing about 15 mole % Sr_2SiO_4 . Two two-phase fields, in which the $3\text{CaO} \cdot 2\text{SiO}_2$ content is in equilibrium with the calcium meta-and orthosilicate solid solutions, are in direct proximity to the three-phase field. Brisi and Appendino studied the phase ratios at 1350° only in the region rich in CaO and SrO . The compounds $3\text{CaO} \cdot \text{SiO}_2$ and $3\text{SrO} \cdot \text{SiO}_2$ existing here form limited solid solutions of low concentration.

The solubility of $3\text{CaO}\cdot\text{SiO}_2$ in tristrontium silicate is approximately 5 mole % at 1350°. Solubility of $3\text{SrO}\cdot\text{SiO}_2$ in tricalcium silicate is not over 1 mole %. The partial system $3\text{CaO}\cdot\text{SiO}_2$ -- $3\text{SrO}\cdot\text{SiO}_2$ is not binary. Free calcium oxide and the $(\text{Ca}, \text{Sr})\text{O}$ solid solution, as well as the dicalcium silicate $(\text{Ca}, \text{Sr})_2\text{SiO}_4$ solid solution, apparently exist here.

BIBLIOGRAPHY

1. Toropov, N.A., A.I. Boykova, A.F. Iyevin'sh, S.K. Apinitis, DAN SSSR, 137, 4, 1961, p. 882.
2. Toropov, N.A., P.F. Konovalov, Ibid., 40, 4, 1943, p. 178.
3. Brixi, C., P. Appendino, Ann. Chim. (Roma), 55, No. 12, 1213, 1965.
4. Buckner, D.A., R. Roy, J. Amer. Ceram. Soc., 43, No. 1, 53, 1960.
5. Eskola, P., Amer. J. Sci., (5), 4, No. 23, 353, 1922.
6. Henning, O., G. Päseilt, Zs. Chem., 5, No. 12, 468, 1965.

STRONTIUM SILICATE SYSTEMS



The system has been studied by Botvinkin and colleagues [1] by the quenching method. The authors restricted the investigation to the Na_2SiO_3 -- SrSiO_3 -- SiO_2 region, which includes the Na_2SiO_3 -- SrSiO_3 binary profile. One ternary compound $\text{Na}_2\text{O} \cdot 2\text{SrO} \cdot 3\text{SiO}_2$ (1:2:3) melting with decomposition at about 1200° , was found in the system. According to Chetverikov and Manuylova [2], this compound forms rectangular plates and prisms in the tetragonal system; the crystals are optically positive, and the indices of refraction: $\text{Ng} = 1.556$, $\text{Np} = 1.552$, $\text{Ng-Np} = 0.004$.

A phase diagram of the partial section of Na_2SiO_3 -- SrSiO_3 is presented in Fig. 46. The portion of the ternary system studied is presented in Fig. 47.

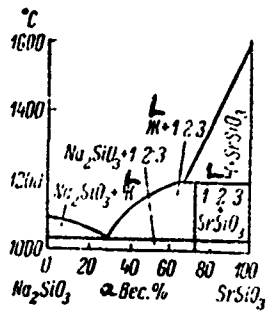


Fig. 46. Phase diagram of partial system Na_2SiO_3 -- SrSiO_3 (from Botvinkin and colleagues).

Key: a. Weight %

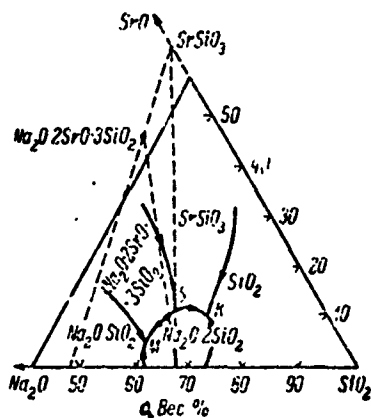


Fig. 47. Silica-rich portion of phase diagram of Na_2O -- SrO -- SiO_2 system (from Botvinkin and colleagues).

Key: a. Weight %

INVARIANT POINTS OF $\text{Na}_2\text{O} \cdot \text{SiO}_2$ -- $\text{SrO} \cdot \text{SiO}_2$ -- SiO_2 SYSTEM

Точка (рис. 47)	Фазы	Процесс	Состав, вес. %			Темпера- тура, °C
			Na ₂ O	SrO	SiO ₂	
K	$\text{SiO}_2 + \text{SrO} \cdot \text{SiO}_2 + \text{Na}_2\text{O} \cdot 2\text{SiO}_2 +$ + жидкость f	Эвтектика ^g	21	11	68	742
δ	$\text{Na}_2\text{O} \cdot 2\text{SrO} \cdot 3\text{SiO}_2 + \text{SrO} \cdot \text{SiO}_2 +$ + $\text{Na}_2\text{O} \cdot 2\text{SiO}_2 +$ жидкость f	Реакция ^h	27.5	10	62.5	837
M	$\text{Na}_2\text{O} \cdot \text{SiO}_2 + \text{Na}_2\text{O} \cdot 2\text{SiO}_2 +$ + $\text{Na}_2\text{O} \cdot 2\text{SrO} \cdot 3\text{SiO}_2 +$ жидкость f	Эвтектика ^g	35	4.5	60.5	845

Key:

- | | |
|--------------------------|--------------------|
| a. Points (Fig. 47) | e. Temperature, °C |
| b. Phases | f. Liquid |
| c. Process | g. Eutectic |
| d. Composition, weight % | h. Reactions |

BIBLIOGRAPHY

1. Botvinkin, O. K., T. A. Popova, A. P. Zak, in the collection Noveyshiye raboty po fizikokhimii stekla [Recent Work in the Physical Chemistry of Glass], Gizlegprom Press, Moscow, 1936, p. 86.
2. Chetverikov, S. D., N. S. Man'ylova, Ibid., p. 95.

$\text{BeO} \text{ -- } \text{SrO} \text{ -- } \text{SiO}_2$

Shteynberg [1], carrying out crystallization of glass, studied the incomplete partial $\text{SrSiO}_3 \text{ -- BeSiO}_3$ profile, since BeSiO_3 was not obtained in pure form. The ternary compound $2\text{SrO} \cdot \text{BeO} \cdot 3\text{SiO}_2 = \text{Sr}_2\text{BeSi}_3\text{O}_9$, melting incongruently at 1435° , with decomposition into SrSiO_3 and liquid, and having indices

of refraction $N_g = 1.675$, $N_p = 1.665$, was obtained for the first time; the extinction angle is 20° and the optical sign is positive.

BIBLIOGRAPHY

1. Shteynberg, Yu. G., Strontsiyevyye glazuri [Strontium Glazes], 2d ed., Stroyizdat Press, Moscow-Leningrad, 1967.



Some efforts to ascertain the existence of ternary compounds have been undertaken by Eskola [2], who studied crystallization of glass, of the composition $\text{MgO} \cdot \text{SrO} \cdot \text{SiO}_2$ and $2\text{SrO} \cdot \text{MgO} \cdot 3\text{SiO}_2$. However, only binary compounds were found.

Shteynberg [1] has studied the partial profile $\text{MgSiO}_3 \text{ -- SrSiO}_3$, using the quenching method. One ternary compound was found, $\text{MgO} \cdot 3\text{SrO} \cdot 4\text{SiO}_2$, melting incongruently at 1430° , with decomposition into SrSiO_3 and melt. Thin plate and needle-shaped crystals of the new compound are uniaxial, positive, with direct extinction, perfect cleavage, and indices of refraction $N_g = 1.645$, $N_p = 1.632$.

Shteynberg expressed doubt as to the correctness of the assertion of Massazza [3], of the existence of the compound $\text{MgO} \cdot 2\text{SrO} \cdot 2\text{SiO}_2$ (ockermanite analog), and he considers that the crystalline phase in his tests was the compound 1:3:4 described above.

BIBLIOGRAPHY

1. Shteynberg, Yu. G., Strontsiyevyye glazuri [Strontium Glazes], 2d ed., Stroyizdat Press, Moscow-Leningrad, 1967, p. 41.
2. Eskola, P., Amer. J. Sci., (5), 4, No. 23, 363, 1923.
3. Massazza, F., Ann. Chim. (Roma), 52, No. 7, 589, 1962.

BARIUM SILICATE SYSTEMS



The system has been studied by the quenching method by Dietzel and colleagues [2], in the concentration region bounded by the compounds $\text{Li}_2\text{O}\cdot\text{SiO}_2$ -- $\text{BaO}\cdot\text{SiO}_2$ -- SiO_2 . Ternary compounds were not obtained. Solid solutions between $\text{BaO}\cdot 2\text{SiO}_2$ and $2\text{BaO}\cdot 3\text{SiO}_2$ are widespread in the three-component region. A phase diagram of the $\text{Li}_2\text{O}\cdot\text{SiO}_2$ -- $\text{BaO}\cdot\text{SiO}_2$ -- SiO_2 system is presented in Fig. 48.

According to the data of Bergman and colleagues [1], using the visual method, the partial system Li_2SiO_3 -- BaSiO_3 is a simple eutectic. The eutectic contains 55 mole % BaSiO_3 , and it melts at 960° . A polymorphic conversion was noted at 986° for lithium metasilicate.

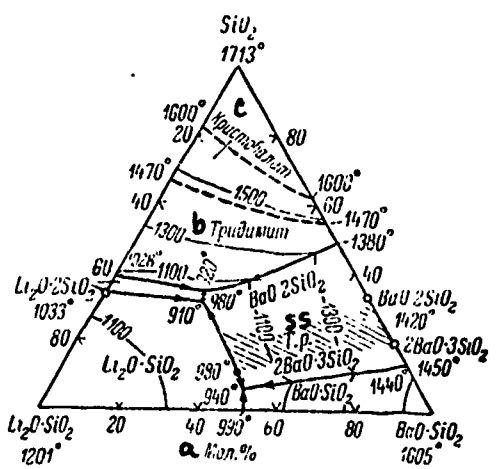


Fig. 48. Phase diagram of $\text{Li}_2\text{O}\cdot\text{SiO}_2$ -- $\text{BaO}\cdot\text{SiO}_2$ system (from Dietzel and colleagues).

Key:

- a. Mole %
- b. Tridymite
- c. Cristobalite.

INVARIANT POINTS OF $\text{Li}_2\text{O} - \text{BaO} - \text{SiO}_2$
SYSTEM²

a Фазы	b Процесс	c Состав, мол. %			d Темпера- тура, °C
		SiO_2	BaO	Li_2O	
$\text{Li}_2\text{O} \cdot \text{SiO}_2 + \text{BaO} \cdot \text{SiO}_2 +$ жидкость e	Эвтектика	50.0	26.0	24.0	990
$\text{Li}_2\text{O} \cdot \text{SiO}_2 + \text{BaO} \cdot \text{SiO}_2 + 2\text{BaO} \cdot \text{SiO}_2 +$ жидкость e	,	53.0	24.5	22.5	940
$\text{Li}_2\text{O} \cdot \text{SiO}_2 + \text{Li}_2\text{O} \cdot 2\text{SiO}_2 + \text{BaO} \cdot 2\text{SiO}_2 +$ жидкость e	,	65.5	12.5	22.0	910
$\text{Li}_2\text{O} \cdot 2\text{SiO}_2 + \text{BaO} \cdot 2\text{SiO}_2 + \text{SiO}_2$ (тридимит) + жидкость e	,	67.0	12.0	21.0	920
$\text{Li}_2\text{O} \cdot 2\text{SiO}_2 + \text{BaO} \cdot 2\text{SiO}_2 +$ жидкость e (псевдобинарная система)	,	66.5	12.0	21.5	960

Key:

- | | |
|------------------------|------------------------|
| a. Phases | e. Liquid |
| b. Process | f. Tridymite |
| c. Composition, mole % | g. Pseudobinary system |
| d. Temperature, °C | h. Eutectic |

BIBLIOGRAPHY

1. Bergman, A.G., A.K. Nesterova, N.S. Bychkova, DAN SSSR, 101, 3, 1955, p. 483.
2. Dietzel, A., H. Wickert, N. Köppen, Glastechn. Ber., 27, No. 5, 147, 1954.

$\text{Na}_2\text{O} - \text{BaO} - \text{SiO}_2$

The system has been studied by Kumanin and colleagues [1], encompassing the region rich in silica (up to 35 mole % SiO_2). Greene and Morgan [2] present some data. Kumanin and colleagues discovered the formation of

two ternary compounds: $4\text{Na}_2\text{O} \cdot 2\text{BaO} \cdot 5\text{SiO}_2$ and $\text{Na}_2\text{O} \cdot 2\text{BaO} \cdot 2\text{SiO}_2$. The phase diagram of the portion of the system studied is presented in Fig. 49.

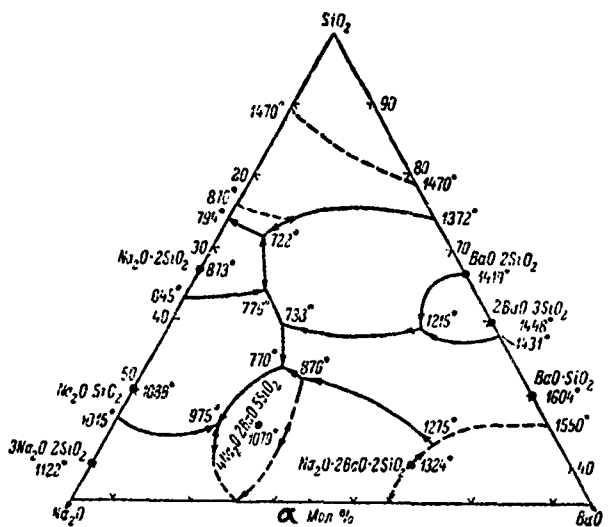


Fig. 49. Phase diagram of $\text{Na}_2\text{O} - \text{BaO} - \text{SiO}_2$ system (from Kumanin and colleagues).

Key: a. Mole %

The authors studied 15 partial binary profile-sections of the diagram in detail. These sections were taken at a constant content of one of the components: Na_2O , SiO_2 or BaO . Two profiles represent the partial binary systems $\text{Na}_2\text{O} \cdot \text{SiO}_2$ -- $\text{BaO} \cdot 2\text{SiO}_2$ (Fig. 50) and $\text{Na}_2\text{O} \cdot \text{SiO}_2$ -- $2\text{BaO} \cdot 3\text{SiO}_2$ (Fig. 51).

Greene and Morgan have studied the partial system $\text{Na}_2\text{O} \cdot 2\text{SiO}_2$ -- $\text{BaO} \cdot 2\text{SiO}_2$, which is a simple eutectic. The eutectic melts at 797° , and it contains 68 weight % $\text{Na}_2\text{O} \cdot \text{SiO}_2$ (Fig. 52).

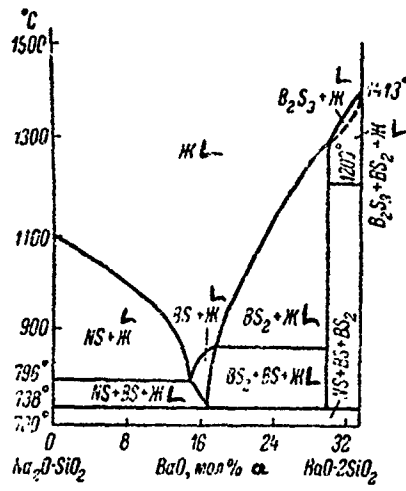


Fig. 50. Phase diagram of partial system $\text{Na}_2\text{O} \cdot \text{SiO}_2$ -- $\text{BaO} \cdot 2\text{SiO}_2$ (from Kumanin and colleagues).

Key: a. Mole %

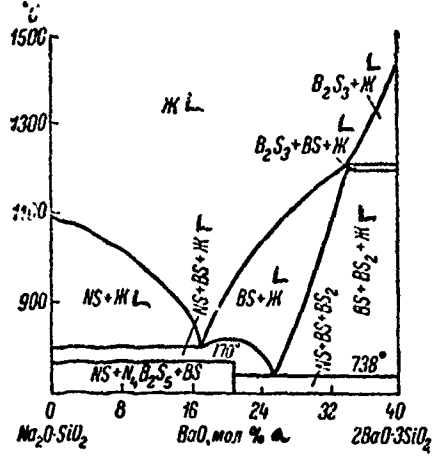


Fig. 51. Phase diagram of partial system $\text{Na}_2\text{O} \cdot \text{SiO}_2$ -- $2\text{BaO} \cdot 3\text{SiO}_2$ (from Kumanin and colleagues).

Key: a. Mole %

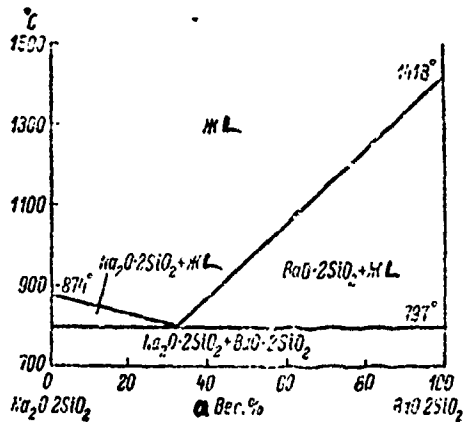


Fig. 52. Phase diagram of partial system $\text{Na}_2\text{O} \cdot 2\text{SiO}_2$ -- $\text{BaO} \cdot 2\text{SiO}_2$ (from Greene and Morgan).

Key: a. Weight %

INVARIANT POINTS OF $\text{Na}_2\text{O} - \text{BaO} - \text{SiO}_2$ SYSTEM
(from Kumanin and colleagues)

a Фазы	b Процесс	c Состав, вес. %			d Темпера- тура, °C
		Na O	BaO	SiO ₂	
e Тридимит + BaO · 2SiO ₂ + кварц + жидкость	h Реакция	18.0	8.0	74.0	870
α-Кварц + Na ₂ O · 2SiO ₂ + BaO · 2SiO ₂ + жидкость g	i Эвтектика	23.0	5.5	71.5	722
Na ₂ O · 2SiO ₂ + BaO · 2SiO ₂ + Na ₂ O · SiO ₂ + жидкость g	j Плавление	26.6	9.4	64.0	776
Na ₂ O · SiO ₂ + BaO · 2SiO ₂ + BaO · SiO ₂ + жидкость g	i Эвтектика	26.7	13.5	59.8	738
2BaO · 3SiO ₂ + BaO · 2SiO ₂ + BaO · SiO ₂ + жидкость g	h Реакция	9.1	31.7	59.2	1215
Na ₂ O · SiO ₂ + 4Na ₂ O · 2BaO · 5SiO ₂ + BaO · SiO ₂ + жидкость g	i Эвтектика	29.3	17.0	53.7	770
4Na ₂ O · 2BaO · 5SiO ₂ + BaO · SiO ₂ + Na ₂ O · 2BaO · 2SiO ₂ + жидкость g	h Реакция	27.5	20.5	52.0	876
Na ₂ O · SiO ₂ + 3Na ₂ O · 2SiO ₂ + 4Na ₂ O · 2BaO · 5SiO ₂ + жидкость g	i Эвтектика	41.6	12.6	45.8	975
4Na ₂ O · 2BaO · 5SiO ₂ + жидкость g	j Инконгруэнтное плавление	36.38	18.18	45.44	1079
BaO · SiO ₂ + Na ₂ O · 2BaO · 2SiO ₂ + 2BaO · SiO ₂ + жидкость g	h Реакция	15.7	41.8	43.5	1275
Na ₂ O · 2BaO · 2SiO ₂ + жидкость g	j Инконгруэнтное плавление	20	40.0	40.0	1324
Na ₂ O · 2SiO ₂ + 4Na ₂ O · 2BaO · 5SiO ₂ + 4O · 2BaO · 2SiO ₂ + жидкость g	i Эвтектика	44.0	20.5	35.5	860

Key:

- | | |
|-------------------------|------------------------|
| a. Phases | g. Liquid |
| b. Process | h. Reactions |
| c. Composition weight % | i. Eutectic |
| d. Temperature, °C | j. Melting |
| e. Tridymite | k. Incongruent melting |
| f. Quartz | l. Congruent melting |

BIBLIOGRAPHY

1. Kumanin, K. G., N. L. Dilaktorskiy, R. L. Nemirovskaya, G. S. Krasikov, Trudy Gos. optich. inst., 22, No. 135, 1950, p. 3
2. Greene, K. T., W. R. Morgan, J. Amer. Ceram. Soc., 24, No. 4, 111, 1941.

BeO -- BaO -- SiO₂

The system has been studied by Isupova and Keler [3], with products obtained by reactions in the solid state (annealing at 1350°). Two ternary compounds were obtained: BeO·BaO·SiO₂ and 2BeO·BaO·2SiO₂. The first was synthesized still earlier by Odelevskiy and Strel'tsina [4]. The compound 2BeO·BaO·2SiO₂ corresponds to the rare mineral barylite, described by Aminoff [5]. The compound BaBeSiO₄ melts at 1675°, has a density $d_4^{25} = 4.11 \text{ g/cm}^3$ (according to the data of Odelevskiy and Strel'tsina, $d_4^{20} = 4.23 \text{ g/cm}^3$); indices of refraction $Ng = 1.665 \pm 0.002$, $Np = 1.662 \pm 0.002$; the crystals are biaxial, negative, and polysynthetic twins are characteristic. Natural barylite 2BeO·BaO·2SiO₂ is in the rhombic system, and it forms prisms along c and forms plates along (001). The following data are presented in the handbooks [2] for the indices of refraction of barylite: $Ng = 1.703$ (1.708), $Nm = 1.696$ (1.702), $Np = 1.691$ (1.695); $(+2V = 81^\circ \text{ and } -2V = 70^\circ)$. Artificial barylite melts at 1600°, it has $Ng = 1.690 \pm 0.002$, $Np = 1.675 \pm 0.002$, and it is biaxial, positive crystals. The density of natural barylite, according to Ygberg [6] is 4.03 g/cm^3 , of artificial (according to Isupova), 4.02 g/cm^3 . Abrasheva and Belov [1] have studied the structure of barylite. The coexisting phase triangle (I-VIII) is presented in Fig. 53.

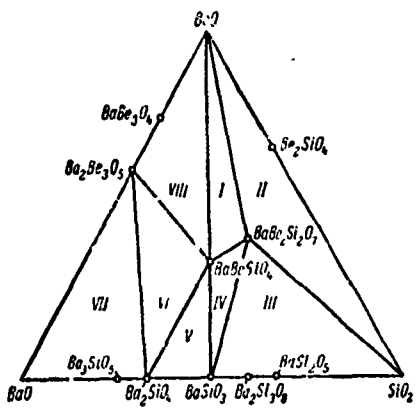


Fig. 53. Coexisting phase triangle of $\text{BeO} - \text{BaO} - \text{SiO}_2$ system (from Isupova and Keler).

BIBLIOGRAPHY

1. Abrasheva, K. K., N. V. Belov, DAN SSSR, 144, No. 3, 1962, p. 638.
2. Winchell, A. N., G. Winchell, Opticheskiye svoystva isskustvennykh mineralov [Optical Properties of Synthetic Minerals], transl. from English, Mir Press, Moscow, 1967.
3. Isupova, Ye. N., E. K. Keler, Zhurn. neorg. khim., 9, No. 2, 1964, p. 403.
4. Odelevskiy, V. I., R. N. Strel'tsina, Izv. Tomsk. politekhn. inst., 91, 1956, p. 323.
5. Aminoff, G., Förh. Geol. Föreningen i Stockholm, 45, 124, 1923.
6. Ygberg, E. R., Förh. Geol. Föreningen i Stockholm, 63, No. 427, 394, 1941.

$\text{MgO} - \text{BaO} - \text{SiO}_2$

The system has been studied by Yasuno [8], in the region bounded by sanbornite, forsterite and silica. The partial system $\text{BaSi}_2\text{O}_5 - \text{Mg}_2\text{SiO}_4$ (Fig. 54) is a simple eutectic, with eutectic melting temperature $1170 \pm 5^\circ$.

with a composition of 85.5 weight % BaSi_2O_5 and 14.5 weight % Mg_2SiO_4 .

The eutectic partial system BaSi_2O_5 -- MgSiO_3 has a eutectic composition of 78.5 weight % BaSi_2O_5 and 21.5 weight % MgSiO_3 , with a melting temperature of $1135 \pm 5^\circ$. The BaSi_2O_5 -- Mg_2SiO_4 -- SiO_2 triple diagram (Fig. 55) is characterized by the presence of two triple eutectics: E_5 (between the sanbornite, protoenstatite and tridymite fields), with a melting temperature of $1110 \pm 5^\circ$ and a composition of 8.7 weight % MgO , 41.0 weight % BaO and 50.3 weight % SiO_2 , and E_6 (between the sanbornite, forsterite and protoenstatite fields), with a melting temperature of $1125 \pm 5^\circ$ and composition 8.7 weight % MgO , 44.8 weight % BaO and 46.5 weight % SiO_2 .

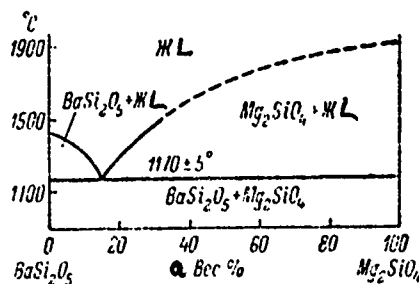


Fig. 54. Phase diagram of partial system sanbornite (BaSi_2O_5) -- forsterite (Mg_2SiO_4) (from Yasuno).

Key: a. Weight %

Argyle and Hummel [4] have studied the system in the subsolidus region. To better obtain equilibrium, small quantities of MgF_2 or LiF were added to the mixtures during annealing. The formation of five ternary compounds was established: $3\text{BaO} \cdot \text{MgO} \cdot 2\text{SiO}_2$, $2\text{BaO} \cdot \text{MgO} \cdot 2\text{SiO}_2$, $\text{BaO} \cdot 2\text{MgO} \cdot 2\text{SiO}_2$,

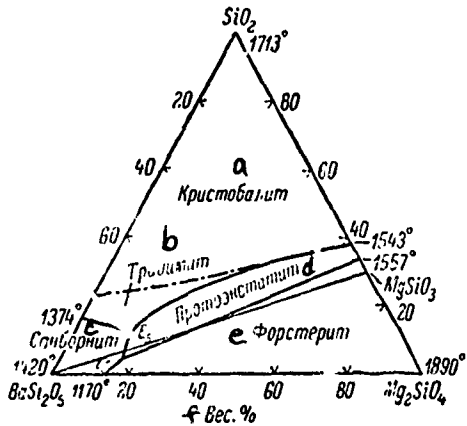


Fig. 55. Phase diagram of BaSi_2O_5 -- Mg_2SiO_4 -- SiO_2 system (from Yasuno).

Key:

- a. Cristobalite
- b. Tridymite
- c. Sanbornite
- d. Protoenstatite
- e. Forsterite
- f. Weight %

$\text{BaO} \cdot \text{MgO} \cdot \text{SiO}_2$ and $\text{BaO} \cdot \text{MgO} \cdot 5\text{SiO}_2$ (Fig. 56). The compounds 1:1:1 and 1:2:2 melt congruently at 1640 and 1600°, respectively. For the remaining three incongruently melting compounds, the following reactions were observed during melting: $2\text{BaO} \cdot \text{MgO} \cdot 2\text{SiO}_2$ at 1425° forms $\text{BaO} \cdot \text{MgO} \cdot \text{SiO}_2$ and liquid; $\text{BaO} \cdot \text{MgO} \cdot 3\text{SiO}_2$ at 1015° forms $\text{BaO} \cdot 2\text{MgO} \cdot 2\text{SiO}_2$ and liquid; the compound $3\text{BaO} \cdot \text{MgO} \cdot 2\text{SiO}_2$ begins to melt at 1620°, with formation of $\text{BaO} \cdot \text{MgO} \cdot \text{SiO}_2$ and $2\text{BaO} \cdot \text{SiO}_2$. Solid solutions were not found in the system.

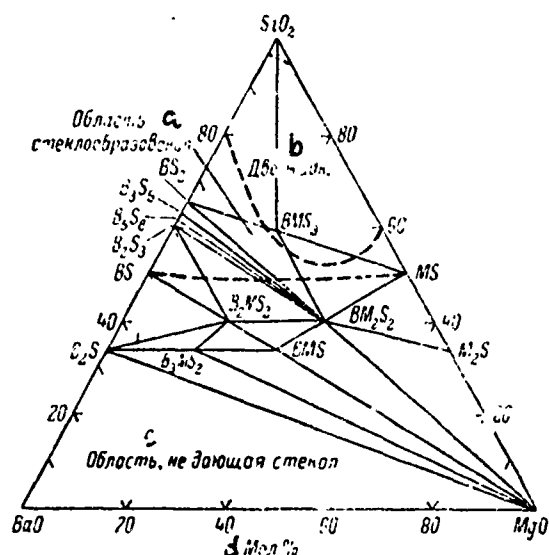


Fig. 56. Diagram of phase ratios of $MgO - BaO - SiO_2$ system in the subsolidus region (from Argyle and Hummel).

Key:

- a. Glass formation region
- b. Two liquids
- c. Region not producing glass
- d. Mole %

The compound $BaO \cdot 3MgO \cdot 2SiO_2$, to which Grylicki and Nadochowski referred [6], is actually a mixture of $BaO \cdot 2MgO \cdot 2SiO_2$ and MgO .

Besides the compounds indicated above, Grebenshchikov [1, 2] synthesized a new lamellar silicate $MgO \cdot BaO \cdot 4SiO_2 = MgBaSi_4O_{10}$, which is the crystallochemical analog of gillespite ($FeBaSi_4O_{10}$). The synthesis was accomplished

by prolonged crystallization (7 days and more) of the corresponding glass, in the 900-1000° range, with addition of 2% MgF_2 . The indices of refractions of the crystals in the sodium D line: $N_g = 1.585$, $N_p = 1.573$. The tetragonal cell parameters of $MgBaSi_4O_{10}$: $a = 7.46$, $c = 16.1$ kX, $c:a = 2.16$, $Z = 4$. The density, calculated from X-ray data, is 3.22 g/cm^3 .

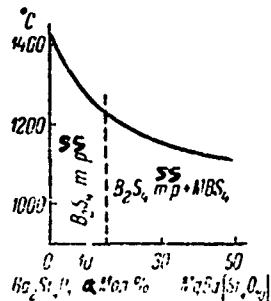


Fig. 57. Schematic diagram of phase ratios of partial system $Ba_2Si_4O_{10}$ -- $MgBaSi_4O_{10}$ (from Grebenschchikov).

Key: a. Mole %

Toropov and Grebenschchikov [3] studied the subsolidus region of the system $Ba_2Si_4O_{10}$ -- $MgBaSi_4O_{10}$, heating the mixtures (up to 50 mole % $MgBaSi_4O_{10}$) almost to the start of fusion (1110-1200°). A schematic phase diagram in the subsolidus region of $Ba_2Si_4O_{10}$ -- $MgBaSi_4O_{10}$ is presented in Fig. 57. The solubility limit of $MgBaSi_4O_{10}$ in barium disilicate is estimated at 15 mole %. This comparatively low replaceability of Ba^{2+} by Mg^{2+} apparently is connected with the considerable difference in structure of sanbornite

($\text{Ba}_2\text{Si}_4\text{O}_{10}$) and the gillespite-like silicate. It is interesting that the index of refraction of the limiting solid solution is only 0.004 less than the corresponding value for sanbornite.

Klasens and colleagues [7] describe the ternary compounds $\text{BaO} \cdot \text{MgO} \cdot \text{SiO}_2$, $\text{BaO} \cdot 2\text{MgO} \cdot 2\text{SiO}_2$, $2\text{BaO} \cdot \text{MgO} \cdot 2\text{SiO}_2$ and $3\text{BaO} \cdot \text{MgO} \cdot 2\text{SiO}_2$, obtained by annealing mixtures of BaCO_3 , MgO and SiO_2 at 1000 and 1200°.

Borchert and Petzenhauser [5], by annealing a mixture of $\text{BaO} + 5\text{MgO} + 12\text{SiO}_2$ (about 1300°), obtained a new hexagonal phase of unknown composition, with unit cell parameters $a_0 = 13.24$, $c_0 = 13.33 \pm 0.05$ Å.

BIBLIOGRAPHY

1. Grebenschchikov, R.G., Zap. Vsegozduzn. mineral. obshch., 2-ya ser., Part 91, 1962, p. 211.
2. Grebenschchikov, R.G., Trudy 6-go soveshch. po eksper. i tekhn. mineral i petrogr. [Proceedings, 6th Conference on Experimental and Engineering Mineralogy and Petrography], AN SSSR Press, Moscow, 1962, p. 295.
3. Toropov, N.A., R.G. Grebenschchikov, Zhurn. neorg. khim., 7, No. 2, 1962, p. 337
4. Argyle, J.F., F.A. Hummel, Glass Industry, 46, No. 12, 710, 1965.
5. Borchert, W., I. Petzenhauser, Ber. Dtsch. keram. Ges., 43, No. 10, 572, 1966.
6. Grylicki, M., F. Nadochowski, Prace Inst. Hutniczych, 10, No. 5, 243, 1958.
7. Klasens, H.A., A.H. Hoekstra, A.P.M., Cox, J. Electrochem. Soc., 104, No. 2, 93, 1957.
8. Yasuno, F., Ceram. Assoc. Japan, 67, No. 12, 403, 1959.

$\text{CaO} - \text{BaO} - \text{SiC}_2$

The first investigation of the system is that of Eskola [8], who studied the metasilicate profile $\text{CaSiO}_3 - \text{BaSiO}_3$ presented in Fig. 58. Eskola did not find any solid solutions here. He obtained the ternary compound $2\text{CaO} \cdot \text{BaO} \cdot 3\text{SiO}_2$.

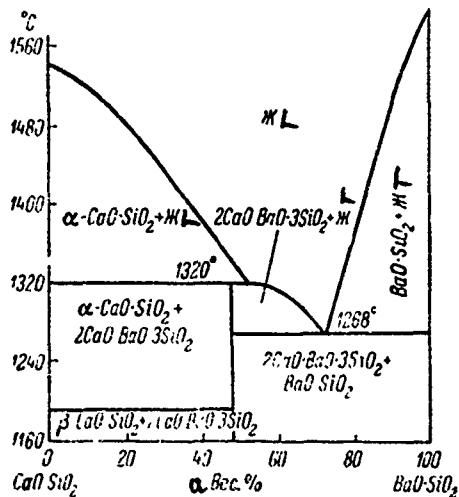


Fig. 58. Phase diagram of partial system $\text{CaO} \cdot \text{SiO}_2 - \text{BaO} \cdot \text{SiO}_2$ (from Eskola).

Key:

a. Weight %

Toropov and Konovalov [3] demonstrated complete miscibility in the $2\text{BaO} \cdot \text{SiO}_2 - 2\text{SrO} \cdot \text{SiO}_2$ system, and they determined the indices of refraction and density of the solid solutions.

Toropov and colleagues [1, 2] plotted a complete phase diagram of the ternary system, which is presented in Fig. 59. In the presence of barium

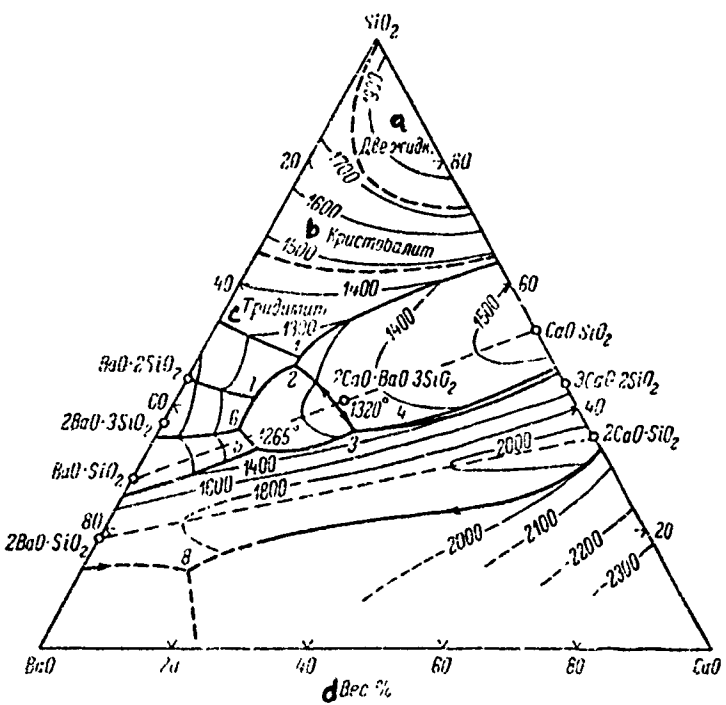


Fig. 59. Phase diagram of $\text{BaO} - \text{CaO} - \text{SiO}_2$ system (from Toropov, Galakhov and Bondar').

Key:

- a. Two liquids
- b. Cristobalite
- c. Tridymite
- d. Weight %

oxide, the compound $3\text{CaO} \cdot 2\text{SiO}_2$ melts, with decomposition into a solid solution of calcium and barium orthosilicates and liquid. The figurative point of this compound is outside its field of primary crystallization.

The region of solid solutions of the series $\text{Ca}_2\text{SiO}_4 - \text{Ba}_2\text{SiO}_4$ represents a broad band, the boundaries of which and liquidus temperature of the field have been determined precisely.

In the binary system $\text{CaO} - \text{SiO}_2$, the region of phase separation of the liquids encompasses the composition 72.0-99.5 weight % SiO_2 , and the equilibrium temperature of the three phases is 1698° . In the ternary system, this region extends up to 11 weight % BaO . A schematic three-dimensional model of the phase separation region, having the appearance of a cupola, at the base of which is the plane of coexistence of two liquid (glass) and one crystalline phase, and the peak of which is the critical phase-separation temperature in the $\text{CaO} - \text{SiO}_2$ system, is presented in Fig. 60. The position of the K' point is defined by the coordinates: CaO 5 weight %, BaO 11 weight %, SiO_2 84 weight % and the temperature 1690° . The values of the critical phase separation temperatures are presented in Table 2.

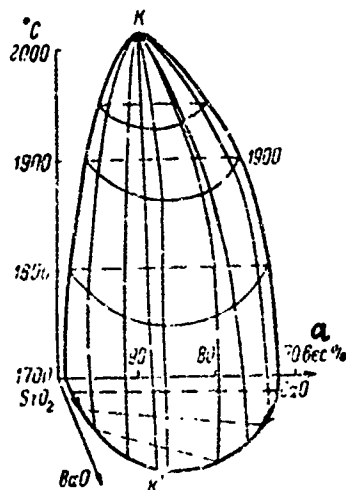


Fig. 60. Immiscibility cupola of melts in $\text{BaO} - \text{CaO} - \text{SiO}_2$ system (from Toropov, Galakhov and Bondar').

Key:

a. Weight %

TABLE 1
INVARIANT POINTS OF CaO -- BaO -- SiO₂ SYSTEM
(from Toropov and colleagues)

a точка (рис. 59)	b Фазы	c Процесс	d Состав, вес. %			e Темпера- тура, °C
			CaO	BaO	SiO ₂	
1	BaO·2SiO ₂ +CaO·SiO ₃ +SiO ₂ +жидкость f	г. Эвтектика	14.5	38.0	47.5	1150
2	BaO·2SiO ₂ +CaO·SiO ₃ +2CaO·BaO·3SiO ₂ +жидкость f	»	14.0	39.5	46.5	1190
3	2CaO·BaO·3SiO ₂ +CaO·SiO ₃ +твердый раствор+жидкость f	и. Реакция	29.5	34.5	36.0	1300
4	CaO·SiO ₂ +3CaO·2SiO ₂ +твердый раствор+жидкость f	»	31.0	33.0	36.0	1310
5	BaO·SiO ₂ +2CaO·BaO·3SiO ₂ +твердый раствор+жидкость f	г. Эвтектика	15.5	51.5	33.0	1255
6	2BaO·3SiO ₂ +2CaO·BaO·3SiO ₂ +BaO·SiO ₃ +жидкость f	»	11.5	52.5	36.0	1235
7	BaO·2SiO ₂ +2CaO·BaO·3SiO ₂ +2BaO·3SiO ₂ +жидкость f	»	11.0	48.0	41.0	1210
8	твердый раствор+BaO+CaO+жидкость f	»	15.0	72.0	13.0	--

Key:

- | | |
|--------------------------|-------------------|
| a. Points (Fig. 59) | f. Liquid |
| b. Phases | g. Solid solution |
| c. Process | h. Eutectic |
| d. Composition, weight % | i. Reactions |
| e. Temperature, °C | |

It was found in works [5, 9] that solid solutions of the Ca₂SiO₄ -- Ba₂SiO₄ system are not continuous. Formation of an individual ternary compound, the composition of which was not determined, also is indicated.

Brisi [6] proposes that, in the pseudobinary system of Ba₂SiO₄ -- Ca₂SiO₄, besides solid solutions of limited concentration, based on Ca₂SiO₄, a uniform phase with hexagonal symmetry, similar to glaserite in structure, exists in the concentration range from 0.8 CaO · 1.2 BaO · SiO₂ to 0.45 CaO · 1.55 BaO · SiO₂.

TABLE 2
CRITICAL PHASE SEPARATION TEMPERATURES
OF LIQUIDS IN CaO -- BaO -- SiO₂ SYSTEM

a Состав, вес. %			b Критическая температура разделения, °C
CaO	BaO	SiO ₂	
10	—	90	2110
5	5	90	1950
5	10	85	1840
10	5	85	1965
15	5	90	1925
20	5	75	1900
15	10	75	1825

Key:

- a. Composition, weight %
- b. Critical phase separation temperature, °C

Brisi and Appendino [7] found that the maximum solubility of Ba₂SiO₄ in Ca₂SiO₄ is 20 mole % at 1100° (Fig. 61). Substitution of calcium atoms by barium atoms leads to stabilization of the high temperature forms of Ca₂SiO₄. For the composition 1.8 CaO · 0.2BaO · SiO₂, X-ray photos indicate a rhombic unit cell (characteristic of the α modification), with parameters $a_0 = 6.86$, $b_0 = 5.57$ and $c_0 = 9.37$ Å.

Toropov and Fedorov [4], using the quenching method, plotted a phase diagram of the Ca₂SiO₄ -- Ba₂SiO₄ system, which is presented in Fig. 62. The ternary compound found has the composition of approximately 6BaO · 4CaO · 5SiO₂, and it melts without decomposing at a temperature of 1875°. Its density is 4.86 g/cm³, and the indices of refraction: Ng = 1.771 ± 0.004, Np = 1.767 ± 0.004.

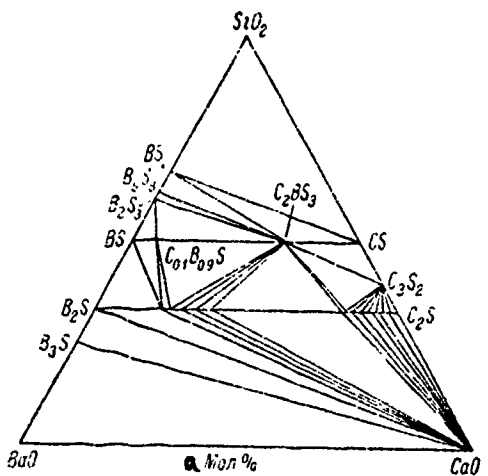


Fig. 61. Diagram of phase ratios in
CaO -- BaO -- SiO₂ system in subsolidus
region at 1100° (from Brisi and Appendino).

Key: a. Mole %

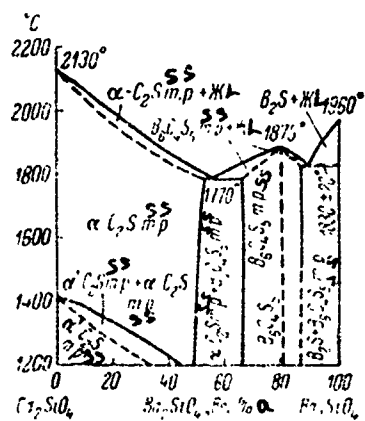


Fig. 62. Phase diagram of partial system
Ca₂SiO₄ -- Ba₂SiO₄ (from Toropov and
Fedorov).

Key: a. Weight %

Two solid solution regions were identified in the system: based on dicalcium silicate and based on the barium-calcium silicate found. The maximum solubility of the barium-calcium silicate in Ca_2SiO_4 corresponds to a content of 54 weight % Ba_2SiO_4 , and of Ca_2SiO_4 solubility in the barium-calcium silicate, to a content of 67.5 weight % Ba_2SiO_4 , the limiting solubility of Ba_2SiO_4 in the barium-calcium silicate, to a content of 87 weight % Ba_2SiO_4 . Ba_2SiO_4 base solid solutions were not found.

The Ca_2SiO_4 and $6\text{BaO} \cdot 4\text{CaO} \cdot 5\text{SiO}_2$ eutectic contains 55.8 weight % Ba_2SiO_4 and 44.2 weight % Ca_2SiO_4 , and it has a melting temperature of $1770 \pm 20^\circ$. The barium-calcium silicate and Ba_2SiO_4 eutectic contains approximately 90 weight % Ba_2SiO_4 , and it melts at $1830 \pm 20^\circ$.

Formation of Ca_2SiO_4 base solid solutions of various concentrations leads to successive stabilization of the β -, α' -, and α -forms of Ca_2SiO_4 . Rhombic Ba_2SiO_4 , depending on its content in the solid solution, stabilizes both the hexagonal α - and the rhombic α' -, and even the monoclinic β - Ca_2SiO_4 .

A discontinuity is found in the concentration dependences of the indices of refraction and of microhardness, which corresponds to a content of approximately 81 weight % Ba_2SiO_4 , which confirms the accepted formula for barium-calcium silicate.

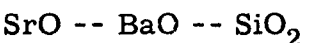
The composition of the ternary compound presented by Toropov and Fedorov is very close to the composition given by Grylicki and Nadochowski, and it differs considerably from the data of Kholin and colleagues, who apparently give a composition of the limiting solid solution of Ca_2SiO_4 in barium-calcium silicate, and not of the complex silicate itself.

In the pseudobinary CaSiO_3 -- BaSiO_3 system, Brisi and Appendino, beside the previously known compound $2\text{CaO} \cdot \text{BaO} \cdot 3\text{SiO}_2$, found a new compound,

close to the formula $0.9\text{BaO}\cdot 0.1\text{CaO}\cdot \text{SiO}_2$. This compound, probably having a certain region of uniformity, cannot be considered to be a modification of BaSiO_3 , stabilized by calcium (Fig. 61).

BIBLIOGRAPHY

1. Bondar', I. A., Zhurn. neorg. khim., 1, 7, 1956, p. 1539.
2. Toropov, N. A., F. Ya. Galakhov, I. A. Bondar', Izv. AN SSSR, OKhN, No. 6, 1956, p. 64.
3. Toropov, N. A., P. F. Konovalov, DAN SSSR, 20, No. 9, 1938, p. 663.
4. Toropov, N. A., N. F. Fedorov, Zhurn. neorg. khim., 9, No. 8, 1964, p. 1939.
5. Kholin, I. I., Yu. S. Malinin, Z. B. Entin, Zhurn. prikl. khim., 34, No. 7, 1961, p. 1419.
6. Brisi, C., Industr. Ital. Cemento, 33, No. 6, 397, 1963.
7. Brisi, C., P. Appendino, Science of ceramics, vol. 3, London, 1967, p. 183.
8. Eskola, P., Amer. J. Sci., (5), 4, No. 23, 353, 1922.
9. Nadochowski, F., M. Grylicki, Silikattechnik, 10, No. 2, 77, 1959.



Shteynberg [1] has studied the partial profile $\text{SrSiO}_3 \text{ -- BaSiO}_3$, by carrying out crystallization of the corresponding glasses, with subsequent quenching. He describes three ternary compounds: $\text{SrO}\cdot\text{BaO}\cdot 2\text{SiO}_2$, $\text{SrO}\cdot 2\text{BaO}\cdot 3\text{SiO}_2$ and $\text{SrO}\cdot 5\text{BaO}\cdot 6\text{SiO}_2$, which crystallize in the form of poly-synthetic twins, hampering their differentiation. The existence of solid solutions of the series $\text{SrO}\cdot\text{BaO}\cdot 2\text{SiO}_2 \text{ -- SrO}\cdot 2\text{BaO}\cdot 3\text{SiO}_2$ is proposed (on the basis of data of the indices of refraction). The compound $\text{SrO}\cdot\text{BaO}\cdot 2\text{SiO}_2$

apparently is an analog of diopside, which is seen from the similarity of the infrared absorption spectra. For the compound $\text{SrO} \cdot \text{BaO} \cdot 2\text{SiO}_2$, indices of refraction are presented of $\text{Ng} = 1.653$, $\text{Np} = 1.648$; the crystals are biaxial, and extinction is direct. The compound $\text{SrO} \cdot 2\text{BaO} \cdot 3\text{SiO}_2$ is characterized by indices of refraction $\text{Ng} = 1.666$, $\text{Np} = 1.661$, and the crystals are biaxial. For the compound $\text{SrO} \cdot 5\text{BaO} \cdot 6\text{SiO}_2$, $\text{Ng} = 1.663$, $\text{Np} = 1.659$, the crystals are biaxial and extinction is oblique.

Brisi and Appendino [3] studied the partial profile $3\text{BaO} \cdot \text{SiO}_2$ -- $3\text{SrO} \cdot \text{SiO}_2$. At 1500° , according to X-ray data, formation of a continuous solid solution takes place. At 1200° , limiting solid solutions, based on tribarium silicate, are found, which are connected, as Massazza [4] showed, with instability of $3\text{SrO} \cdot \text{SiO}_2$ below 1280° .

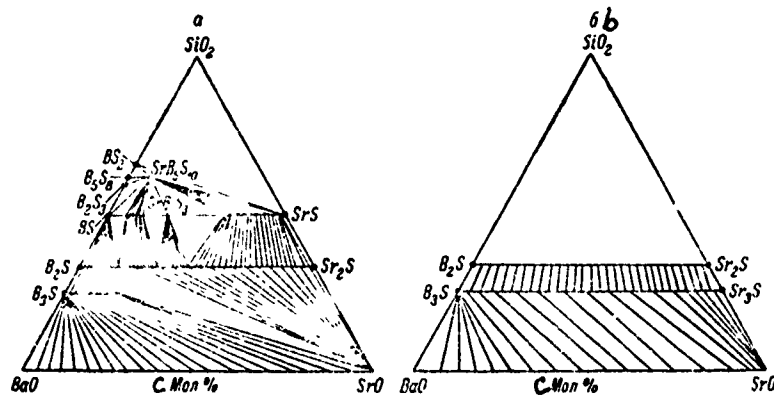


Fig. 63. Diagram of phase ratios of $\text{SrO} \text{-- BaO} \text{-- SiO}_2$ system in subsolidus region (from Appendino and Appendino-Montorsi); a. 1100° ; b. 1400° .

Key:

c. Mole %

Appendino and Appendino-Montorsi [2] confirmed the formation of a solid solution of the type $3(\text{Ba}, \text{Sr})\text{O} \cdot \text{SiO}_2$, and they found that, at 1100° , approximately one-fifth of the barium atoms can be replaced by strontium atoms (Fig. 63a). In the section bounded by the compounds BaO , B_2S , Sr_2S and SrO , there are four regions: 1. a region containing two solid solutions based on $3\text{BaO} \cdot \text{SiO}_2$ and $2\text{BaO} \cdot \text{SiO}_2$, in which substitution of barium by strontium reaches 20-25%; 2. a region, in which there is SrO and a solid solution of the type $2(\text{SrBa})\text{O} \cdot \text{SiO}_2$, with a predominantly strontium content; 3. a region of two solid solutions, $\text{Ba}(\text{Sr})\text{O}$ and $3(\text{BaSr})\text{O} \cdot \text{SiO}_2$; 4. one three-phase region (white field in the figure).

From a study of the region in which the $(\text{SrO} + \text{BaO}) : \text{SiO}_2$ ratio is between 2 and 1 (within the limits included between the compounds BS , SrS , Sr_2S and B_2S), at 1100° , low solubility of $\text{SrO} \cdot \text{SiO}_2$ in barium metasilicate (not over 2%) was found. A solid solution region also was found in the metasilicate profile, in the interval between $0.9\text{BaO} \cdot 0.1\text{SrO} \cdot \text{SiO}_2$ and $0.8\text{BaO} \cdot 0.2\text{SrO} \cdot \text{SiO}_2$. The authors did not study stability of these solid solutions at temperatures higher than 1100° .

The $\text{SrO} \cdot \text{SiO}_2$ base solid solution corresponds approximately to the formula $2\text{SrO} \cdot \text{BaO} \cdot 3\text{SiO}_2$ at 1100° . This is considered to be a discrete compound, which is stable below 1250° . In the region rich in silica, the compound $\text{SrO} \cdot 5\text{BaO} \cdot 10\text{SiO}_2$ has been found, for which a set of interplane distances is introduced.

The authors have studied, at 1400° , the system bounded by the region between the compounds BaO , B_2S , Sr_2S and SrO . Here, a continuous series of solid solutions has been found of $3\text{BaO} \cdot \text{SiO}_2$ -- $3\text{SrO} \cdot \text{SiO}_2$ and $2\text{BaO} \cdot \text{SiO}_2$ -- $2\text{SrO} \cdot \text{SiO}_2$. Two two-phase fields are shown in Fig. 63b.

BIBLIOGRAPHY

1. Shteynberg, Yu. G., Strontsiyevyye glazuri [Strontium Glazes], 2d ed., Stroyizdat Press, Moscow-Leningrad, 1967.
2. Appendino, P., M. Appendino-Montorsi, Ann. Chim. (Roma), 59, No. 8-9, 1969.
3. Brisi, C., P. Appendino, Ricer. Sci., 36, No. 1, 369, 1966.
4. Massazza, F., Chim. Industr., 37, No. 12, 939, 1955.

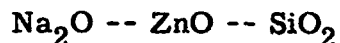
ZINC SILICATE SYSTEMS



The rough investigation of Stewart and Buchi [1] was restricted to the region adjoining SiO_2 : up to 70 mole % ZnO and 70 mole % Li_2O . Two ternary compounds were found: $\text{Li}_2\text{O} \cdot \text{ZnO} \cdot \text{SiO}_2$ and $4\text{Li}_2\text{O} \cdot 10\text{ZnO} \cdot 7\text{SiO}_2$. X-ray studies showed that the compound $\text{Li}_2\text{O} \cdot \text{ZnO} \cdot \text{SiO}_2$, structurally is similar to $\text{Li}_2\text{O} \cdot \text{MgO} \cdot \text{SiO}_2$, can be indexed on the basis of a primitive tetragonal cell, with parameters $a = 11.47$, $c = 10.78 \text{ \AA}$, $c:a = 0.94$, and the compound $4\text{Li}_2\text{O} \cdot 10\text{ZnO} \cdot 7\text{SiO}_2$ correspondingly, on the basis of a rhombic cell, with parameters $a = 7.93$, $b = 9.13$, $c = 12.80 \text{ \AA}$, $a:b:c = 0.87:1:1.40$.

BIBLIOGRAPHY

1. Stewart, I. M., G. J. P. Buchi, Trans. Brit. Ceram. Soc., 61, No. 10, 623, 1962.



The phase equilibria in the system have not been studied. Litvin and colleagues [1] have studied crystallization in the $\text{Na}_2\text{O} \text{ -- } \text{ZnO} \text{ -- } \text{SiO}_2$ system in the $350\text{--}550^\circ$ temperature range, in steel autoclaves lined with titanium, with a solvent of a water solution of caustic soda. They were the first to

obtain five sodium zinc silicates, the chemical formulas and properties of which are presented in the table. The first two phases have a significant piezoelectric effect, which makes their practical use possible, especially in combination with bright luminescence (in the yellow-green portion of the spectrum, with activation by manganese).

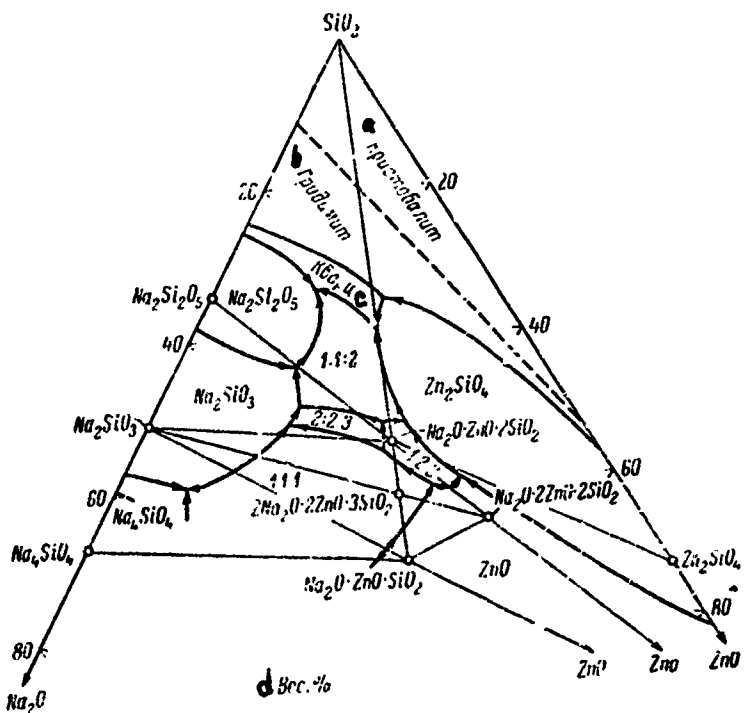


Fig. 64. Phase diagram of $\text{Na}_2\text{O} - \text{ZnO} - \text{SiO}_2$ system in high-silica region (from Holland and Segnii).

Key:

- a. Cristobalite
- b. Tridymite
- c. Quartz
- d. Weight %

Holland and Segnit [2] have studied the system (excluding the section adjacent to the Na_2O -- ZnO side) by the quenching method (Fig. 64). Four ternary compounds were obtained: $\text{Na}_2\text{O} \cdot \text{ZnO} \cdot \text{SiO}_2$, $\text{Na}_2\text{O} \cdot \text{ZnO} \cdot 2\text{SiO}_2$, $\text{Na}_2\text{O} \cdot 2\text{ZnO} \cdot 2\text{SiO}_2$ and $2\text{Na}_2\text{O} \cdot 2\text{ZnO} \cdot 3\text{SiO}_2$, melting incongruently at 1340 (with formation of ZnO and liquid), 860 (with formation of 1:2:2, 2:2:3 and liquid; at 900°, compound 2:2:3 disappears and final melting is observed at 945°), 1090 (with formation of ZnO and liquid, final melting at 1325°) and 975° (with formation of compounds 1:1:1 and 1:2:2 and liquid; at 1010°, compound 1:2:2 dissolves and the final melting takes place at 1175°), respectively.

PROPERTIES OF SODIUM ZINC SILICATES

a Состав	b Сингония	c Параметры одноцентрической ячейки, Å			d Плотность, г/см ³	e Твердость по Моосу	Ng	Nm	Np
		a	b	c					
$\text{Na}_2\text{O} \cdot \text{ZnO} \cdot 3\text{SiO}_2$	f Моноклин- ная	6.5	8.8	6.7	3.0	5	1.582	1.571	1.558
$\text{Na}_2\text{O} \cdot 2\text{ZnO} \cdot 2\text{SiO}_2$	g Ромбиче- ская	9.16	13.6	5.07	3.8	4.5	1.633	1.615	1.614
$\text{Na}_2\text{O} \cdot 3\text{ZnO} \cdot 2\text{SiO}_2$	h То же	5.05	14.9	10.2	3.5	1.5	1.654	1.640	1.633
$\text{Na}_2\text{O} \cdot \text{ZnO} \cdot 2\text{SiO}_2$	» »	22.60	7.20	7.45	3.6	5.0	1.574	1.565	1.562
$\text{Na}_2\text{O} \cdot \text{ZnO} \cdot \text{SiO}_2$	f Моноклин- ная	5.0	7.07	5.33	3.4	1.0	1.663	1.655	1.640

Key:

- a. Composition
- b. Crystal system
- c. Unit cell parameters, Å
- d. Density, g/cm³
- e. Moos hardness
- f. Monoclinic
- g. Rhombic
- h. Same

The compound $\text{Na}_2\text{O} \cdot \text{ZnO} \cdot \text{SiO}_2$ exists in four polymorphic forms, with transition temperatures of 620 ± 10 , 815 ± 10 and $1055 \pm 5^\circ$. For the low temperature form, biaxial negative crystals, with indices of refraction $\text{Ng} = 1.618 \pm 0.002$, $\text{Np} = 1.606 \pm 0.002$, are characteristic. Crystals of compound 1:1:2 are monoclinic, biaxial and negative, with a large optical axis angle and indices of refraction $\text{Ng} = 1.580 \pm 0.002$, $\text{Np} = 1.557 \pm 0.002$. Crystals of compound 1:2:2 are biaxial and negative, with a medium optical axis angle and indices of refraction $\text{Ng} = 1.650 \pm 0.003$, $\text{Np} = 1.633 \pm 0.002$. Compound 2:2:3 forms poorly expressed pseudocubic crystals, frequently appearing to be isotropic, with an index of refraction 1.587 ± 0.002 ; however, X-ray data indicate that this compound belongs to the tetragonal crystal system, with parameter c three times greater than a .

Holland and Segnit discovered a mixture of several phases in efforts to obtain compound 1:1:3.

A X-ray photo of compound 1:3:2, made by Litvin and colleagues, in the opinion of Holland and Segnit, actually is a X-ray photo of 2:2:3, in a mixture with other phases.

BIBLIOGRAPHY

1. Litvin, B. N., O. K. Mel'nikov, V. V. Ilyukhin, A. V. Nikitin, Kristallografiya, 9, 6, 1954, p. 943.
2. Holland, A. E., E. R. Segnit, Austr. J. Chemistry, 19, No. 6, 905, 1966.



A rough study of the system has been made by Ingerson and colleagues [1]. Determination of the liquidus temperature and the primary phases in the system

has been accomplished only for points 1-7 (Fig. 65). The ternary compound $K_2O \cdot ZnO \cdot SiO_2$ apparently exists in the system, separating out in the form of isotropic (cubic) crystals, with $N = 1.622$ and decomposing with melting at 1300° . Moreover, the possibility is suggested of formation of two compounds: $K_2O \cdot 2ZnO \cdot 3SiO_2$ (isotropic crystals, $N > 1.591$) and $K_2O \cdot ZnO \cdot 2SiO_2$ (uniaxial crystals, $N \sim 1.544$). Field A, noted on Fig. 65, possibly belongs to one of these compounds.

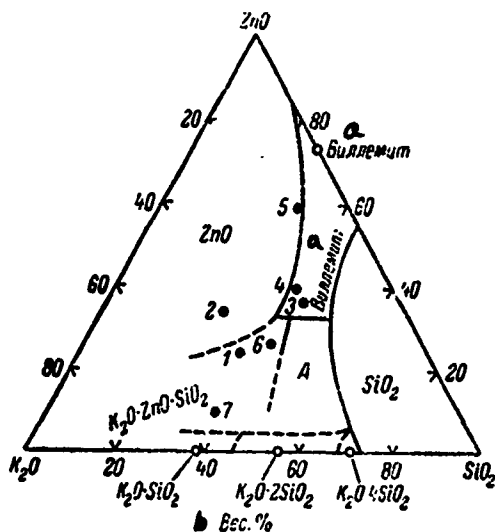


Fig. 65. Phase diagram of K_2O -- ZnO -- SiO_2 system (from Ingerson and colleagues).

Key:

- a. Willemite
- b. Weight %

BIBLIOGRAPHY

1. Ingerson, E., G.W. Morey, O.F. Tuttle, Amer. J. Sci., 246, No. 1, 31, 1948

$\text{MgO} \text{ -- } \text{ZnO} \text{ -- } \text{SiO}_2$

The system has been studied by Sarver and Hummel [1] and Segnit and Holland [2]. The first authors studied the subsolidus relationships in the pseudobinary system Zn_2SiO_4 -- Mg_2SiO_4 (annealing up to $\sim 1450^\circ$). For determination of the mutual solubility at reduced temperatures (down to 850°), the study was conducted under hydrothermal conditions (water vapor pressure reached 1000 psi). It is evident from the phase diagram of the Zn_2SiO_4 -- Mg_2SiO_4 system presented in Fig. 66 that the mutual solubility of these silicates in the subsolidus region increases with increase in temperature. Thus, the solubility of Zn_2SiO_4 in Mg_2SiO_4 increases from 16 mole % at 850° to 24 mole % at 1460° , and the solubility of Mg_2SiO_4 in Zn_2SiO_4 for these same temperatures increases from 20 to 44 mole %.

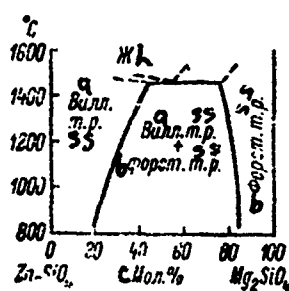


Fig. 66. Phase diagram of partial system Mg_2SiO_4 -- Zn_2SiO_4 (from Sarver and Hummel).

Key:

- a. Willemite
- b. Forsterite
- c. Mole %

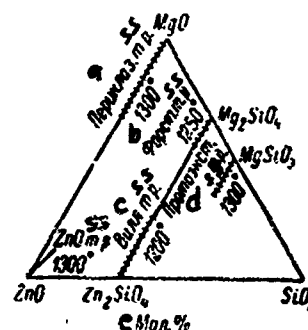


Fig. 67. Solid solutions in $\text{MgO} \text{ -- } \text{ZnO} \text{ -- } \text{SiO}_2$ system (from Sarver and Hummel).

Key:

- a. Periclase
- b. Forsterite
- c. Willemite
- d. Protoenstatite
- e. Mole %

Sarver and Hummel also determined the solubility of $ZnSiO_3$ in $MgSiO_3$. The solid solutions existing in the MgO -- ZnO -- SiO_2 system, the concentrations of which are given for 1200-1300°, are shown in Fig. 67.

Segnit and Holland [2] employed the quenching method, using a high-temperature microscope. Ternary compounds were not found. The phase diagram of the complete MgO -- ZnO -- SiO_2 system is presented in Fig. 68. Considerable areas in the diagram belong to solid solutions of the pseudobinary system Mg_2SiO_4 -- Zn_2SiO_4 and the MgO -- ZnO system.

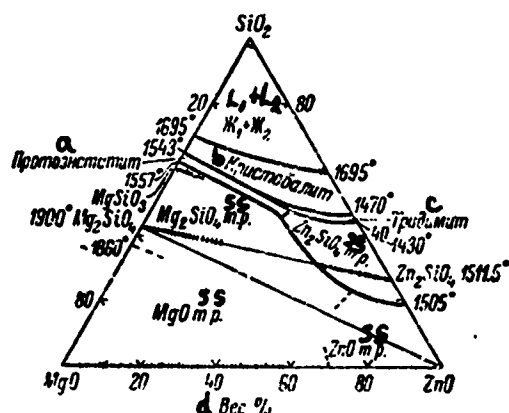


Fig. 68. Phase diagram of MgO -- ZnO -- SiO_2 system (from Segnit and Holland).

Key:

- a. Protoenstatite
- b. Cristobalite
- c. Tridymite
- d. Weight %

A eutectic in the pseudobinary Mg_2SiO_4 -- Zn_2SiO_4 profile crystallizes at about 1500° , and it contains 29 weight % Mg_2SiO_4 and 71 weight % Zn_2SiO_4 . The position of this eutectic gives an indication of lower solubility of Mg_2SiO_4 in Zn_2SiO_4 than that presented by Sarver and Hummel¹, going up to 26 weight % at 1480° . The maximum solubility of $ZnSiO_3$ in $MgSiO_3$ was found to equal 11 weight %. The region adjacent to the MgO apex remains unstudied, and still another invariant point is possible here, in which the phases based on forsterite, zincite (ZnO) and periclase, will be found in equilibrium with the liquid.

INVARIANT POINTS OF MgO -- ZnO -- SiO_2 SYSTEM

a Фазы	b Процесс	c Состав, вес. %			d Темпера- тура, $^\circ C$
		MgO	ZnO	SiO_2	
e $MgSiO_3$ (protoenstatite) + SiO_2 (три- димит) + Zn_2SiO_4 твердый раствор	f Эвтектика	15.5	37.0	47.5	1370 ± 5
e Mg_2SiO_4 твердый раствор + proto- енстатит + Zn_2SiO_4 твердый рас- твор	i Точка диойного подъема	19.5	35.5	45.0	1395 ± 5
MgO твердый раствор + ZnO твер- дый раствор + Zn_2SiO_4 твердый раствор	f Эвтектика	12.5	64.5	23.0	1500

Key:

- | | |
|----------------------------|---------------------------|
| a. Phases | f. Tridymite |
| b. Process | g. Solid solution |
| c. Composition, weight % | h. Eutectic |
| d. Temperature, $^\circ C$ | i. Double elevation point |
| e. Protoenstatite | |

BIBLIOGRAPHY

1. Sarver, J. E., F. A. Hummel, J. Amer. Ceram. Soc., 45, No. 6, 301, 1962.
 2. Segnit, E. R., A. E. Holland, J. Amer. Ceram. Soc., 48, No. 8, 409, 1965.



The study has been studied by Segnit [2], by the quenching method (Fig. 69). One ternary compound $2\text{CaO} \cdot \text{ZnO} \cdot 2\text{SiO}_2$ has been found, corresponding to the mineral lardystonite, with a congruent melting temperature of 1425° . It forms negative, uniaxial crystals, with indices of refraction $\text{Ne} = 1.661$ and $\text{No} = 1.673$.

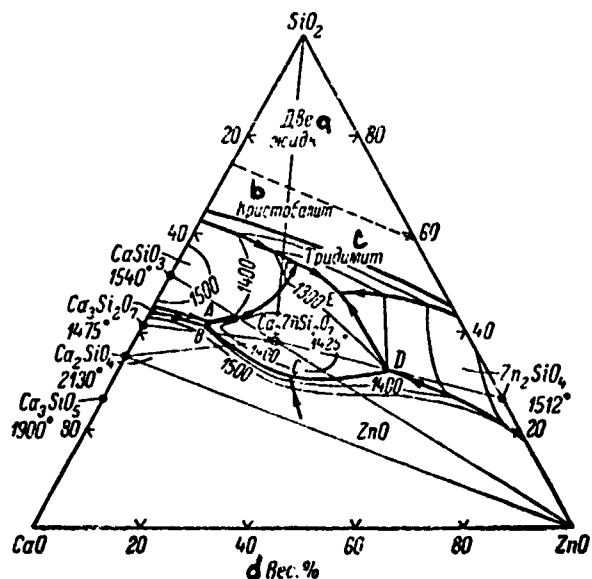


Fig. 69. Phase diagram of CaO -- ZnO -- SiO₂ system (from Segnit).

Key:

- a. Two liquids
 - b. Cristobalite
 - c. Tridymite
 - d. Weight %

Bigaré and colleagues [1] have studied a section of the $3\text{CaO}\cdot\text{SiO}_2$ -- ZnO profile (up to 5 weight % ZnO), where solid solutions form in a certain region. The results of thermographic studies of polymorphic conversions of modifications of Ca_3SiO_5 , stabilized by zinc oxide, i.e., the region of existence of solid solutions, corresponding to various modifications of $3\text{CaO}\cdot\text{SiO}_2$, are shown in Fig. 70. The maximum concentration of ZnO in the solid solution is somewhat in excess of 2 weight %.

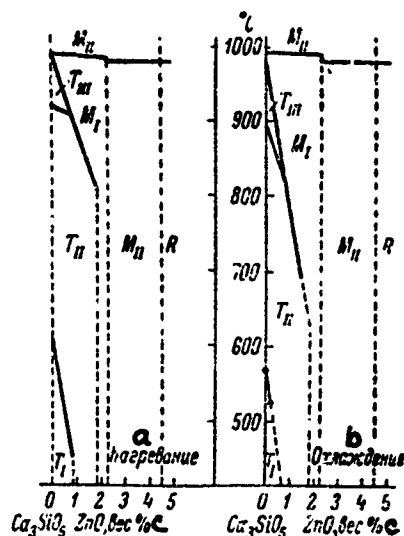


Fig. 70. Change in conversion temperature of solid solutions of the $3\text{CaO}\cdot\text{SiO}_2$ -- ZnO series (from Bigaré and colleagues): M monoclinic solid solutions, T tetragonal, R rhombic.

Key:

- a. Heating
- b. Cooling
- c. Weight %

INVARIANT POINTS OF CaO -- ZnO -- SiO₂ SYSTEM

a Точки (рис. 69)	b Фазы	c Процесс	d Состав, вес. %			e Темпера- тура, °C
			CaO	ZnO	SiO ₂	
A	3CaO·2SiO ₂ +CaO·SiO ₂ +2CaO·ZnO·2SiO ₂ +жидкость	и Эвтектика	40.4	11.5	42.1	1360
B	3CaO·2SiO ₂ +2CaO·SiO ₂ +2CaO·ZnO·2SiO ₂ +жид- кость	и Реакционная точка	46.9	11.5	41.6	1365
C	ZnO+2CaO·SiO ₂ +2CaO·ZnO·2SiO ₂ +жидкость	и Эвтектика	36.6	32.4	31.0	1345
D	ZnO+2ZnO·SiO ₂ +2CaO·ZnO·2SiO ₂ +жидкость	и	18.0	50.0	32.0	1297
E	SiO ₂ (тридимит)+2ZnO·SiO ₂ +2CaO·ZnO·2SiO ₂ +жидкость	и	19.6	32.4	48.0	1170
F	SiO ₂ (тридимит)+CaO·SiO ₂ +2CaO·ZnO·2SiO ₂ +жид- кость	и Реакционная точка	24.1	21.9	54.0	1223

Key:

- a. Points (Fig. 69)
- b. Phases
- c. Process
- d. Composition, weight %
- e. Temperature. °C
- f. Liquid
- g. SiO₂ (tridymite)
- h. Eutectic
- i. Reaction point.

BIBLIOGRAPHY

1. Bigaré, M., A. Guinier, C. Mazieres, M. Regourd, N. Yannquis, W. Eysel, Th. Hahn, E. Woermann, J. Amer. Ceram. Soc., 50, No. 11, 609, 1967.
2. Segnit, E.R., J. Amer. Ceram. Soc., 37, No. 6, 273, 1954.

SrO -- ZnO -- SiO₂

Shteynberg [1] presents some information on the system, having studied the partial SrSiO₃ -- ZnSiO₃ profile by the quenching method. One ternary compound 3SrO·ZnO·4SiO₂ was found, melting incongruently at 1390°, with

decomposition into SrSiO_3 and liquid. The crystals, obtained in the form of rectangular prisms, were uniaxial, positive, with indices of refraction $\text{Ng} = 1.677$, $\text{Np} = 1.672$. A region of immiscible liquids was found close to zinc metasilicate.

The existence of the ternary compounds $\text{SrO} \cdot 2\text{ZnO} \cdot 2\text{SiO}_2$ and $2\text{SrO} \cdot \text{ZnO} \cdot 2\text{SiO}_2$, described by Klasens and colleagues [2], cannot be considered to be conclusively established. These authors carried out synthesis by sintering at 1000-1200°.

According to the data of Shteynberg, a X-ray photo of the composition $2\text{SrO} \cdot \text{ZnO} \cdot 2\text{SiO}_2$ is similar to $3\text{SrO} \cdot \text{ZnO} \cdot 4\text{SiO}_2$, and the X-ray photo of $\text{SrO} \cdot 2\text{ZnO} \cdot 2\text{SiO}_2$ is similar to that of SrSiO_3 .

BIBLIOGRAPHY

1. Shteynberg, Yu. G., Strontsiyevyye glazuri [Strontium Glazes], Stroyizdat Press, Moscow-Leningrad, 1967, p. 56.
2. Klasens, H. A., A. H. Hoekstra, A. P. M. Cox, J. Electrochem. Soc., 104, No. 2, 93, 1957.



Klasens and colleagues [1], annealing a mixture of BaCO_3 , ZnO and SiO_2 at 1000-1200° obtained three ternary compounds: $\text{BaO} \cdot \text{ZnO} \cdot \text{SiO}_2$, $\text{BaO} \cdot 2\text{ZnO} \cdot 2\text{SiO}_2$ and $2\text{BaO} \cdot \text{ZnO} \cdot 2\text{SiO}_2$. The interplane distances and X-ray line intensities are presented for these compounds.

BIBLIOGRAPHY

1. Klasens, H. A., A. H. Hoekstra, A. P. M. Cox, J. Electrochem. Soc., 104, No. 2, 93, 1957.

LEAD SILICATE SYSTEMS



The system has been studied by Krakau and colleagues [3-5], who restricted themselves to the $\text{Na}_2\text{O} \cdot \text{SiO}_2$ -- $\text{PbO} \cdot \text{SiO}_2$ -- SiO_2 triangle. Five ternary compounds were found: the compounds $\text{Na}_2\text{O} \cdot 3\text{PbO} \cdot 6\text{SiO}_2$ (lead devitrite) and $\text{Na}_2\text{O} \cdot 2\text{PbO} \cdot 3\text{SiO}_2$, melting congruently at 717 and 615°, respectively (the first of these compounds undergoes an enantiotropic $\leftarrow \rightleftharpoons \rightarrow$ conversion at 540°), and the compounds $\text{Na}_2\text{O} \cdot 2\text{PbO} \cdot 4\text{SiO}_2$, $\text{Na}_2\text{O} \cdot 3\text{PbO} \cdot 7\text{SiO}_2$ and $3\text{Na}_2\text{O} \cdot 3\text{PbO} \cdot 11\text{SiO}_2$, melting incongruently at 635, 725 and 645°, respectively. In Fig. 71, where the complete phase diagram of the system, plotted by Levin and colleagues [8], combining existing data in the literature, is presented, these compounds are designated by Roman numbers: I (1:2:4), II (1:3:6), high-temperature modification), III (1:2:3), IV (1:3:7) and V (3:3:11). The system has five ternary eutectics, designated a, b, c, d and e.

Krakau [3] has studied several partial binary systems: $\text{PbO} \text{ -- Na}_2\text{O} \cdot \text{SiO}_2$ (Fig. 72), $\text{PbO} \cdot \text{SiO}_2 \text{ -- Na}_2\text{O} \cdot \text{SiO}_2$ (Fig. 73), $2\text{PbO} \cdot \text{SiO}_2 \text{ -- Na}_2\text{O} \cdot \text{SiO}_2$ (Fig. 74), $3\text{PbO} \cdot \text{SiO}_2 \text{ -- Na}_2\text{O} \cdot \text{SiO}_2$ (Fig. 75) and $3\text{PbO} \cdot 2\text{SiO}_2 \text{ -- Na}_2\text{O} \cdot \text{SiO}_2$ (Fig. 76).

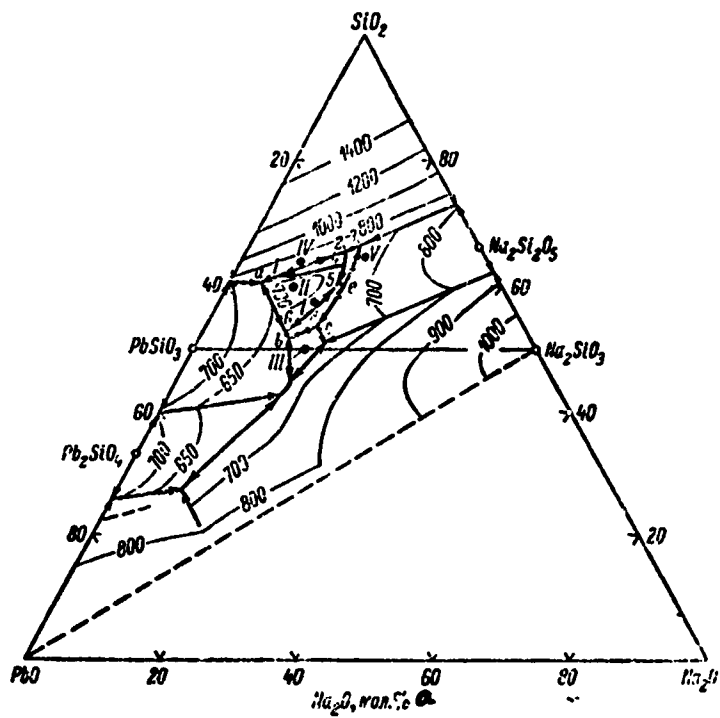


Fig. 71. Phase diagram of $\text{Na}_2\text{O} - \text{PbO} - \text{SiO}_2$ system:
 region bounded by $\text{PbSiO}_3 - \text{Na}_2\text{SiO}_3 - \text{SiO}_2$ triangle
 (from Krakau and colleagues): invariant point temperatures:
 a. 670° , b. 580° , c. 575° , d. 570° , e. 610° , 1. 685° , 2. 640° ,
 3. 643° , 4. 630° , 5. 620° , 6. 630° ; I. $\text{Na}_2\text{O} \cdot 2\text{PbO} \cdot 4\text{SiO}_2$; II.
 $\text{Na}_2\text{O} \cdot 3\text{PbO} \cdot 6\text{SiO}_2$; III. $\text{Na}_2\text{O} \cdot 2\text{PbO} \cdot 3\text{SiO}_2$; IV. $\text{Na}_2\text{O} \cdot 3\text{PbO} \cdot 7\text{SiO}_2$;
 V. $3\text{Na}_2\text{O} \cdot 3\text{PbO} \cdot 11\text{SiO}_2$.

Key:

a. Mole %

Glasses of the $\text{Na}_2\text{O} - \text{PbO} - \text{SiO}_2$ system have been studied in detail
 by I. V. Grebenschchikov and his colleagues [1, 2, 6, 7].

CRYSTALLINE PHASES OF $\text{Na}_2\text{O} - \text{PbO} - \text{SiO}_2$ SYSTEM

a Соединение	b Система кристаллов	c Габитус	d Спайность	Ng	Np	e Оптический знак	f Температура, °C
$\text{Na}_2\text{O} \cdot 2\text{PbO} \cdot 4\text{SiO}_2$	Ромбическая	l Иглы	g Совершенная // удлнению	1.782	1.744	?	Плавится никонгруэнтно при 635°
$\alpha\text{-Na}_2\text{O} \cdot 3\text{PbO} \cdot 6\text{SiO}_2$	h Тетрагональная	m Призмы, пирамиды	n Чистая	1.707	1.704	(+) ?	Плавится при 717°
$\beta\text{-Na}_2\text{O} \cdot 3\text{PbO} \cdot 6\text{SiO}_2$	Ромбическая	p Пирамиды	s Чистая	1.744	1.719	?	При 540° — превращение в α -форму
$\text{Na}_2\text{O} \cdot 3\text{PbO} \cdot 7\text{SiO}_3$	Гексагональная	o Ромбоэдры	t По (0001) ясная	1.750	1.726	(-)	Плавится никонгруэнтно при 725°
$\text{Na}_2\text{O} \cdot 2\text{PbO} \cdot 3\text{SiO}_3$	Моноклинная	j ?	u Совершенная	1.790	1.691	—	Плавится при 615°
$3\text{Na}_2\text{O} \cdot 3\text{PbO} \cdot 11\text{SiO}_2$	k То же	r Таблицы	v Совершенная по одному направлению	1.681	1.617	—	Плавится никонгруэнтно при 645°

Key:

- | | |
|--------------------|---|
| a. Compound | n. Pyramids |
| b. Crystal system | o. Rhombohedra |
| c. Appearance | p. Plates |
| d. Cleavage | q. Perfectly parallel elongation |
| e. Optical sign | r. Indistinct |
| f. Temperature, °C | s. Distinct |
| g. Rhombic | t. Distinct along (0001) |
| h. Tetragonal | u. Perfect |
| i. Hexagonal | v. Perfect in one direction |
| j. Monoclinic | w. Melts incongruently at |
| k. Same | x. Melts at |
| l. Needles | y. At 540°, conversion to α form |
| m. Prisms | |

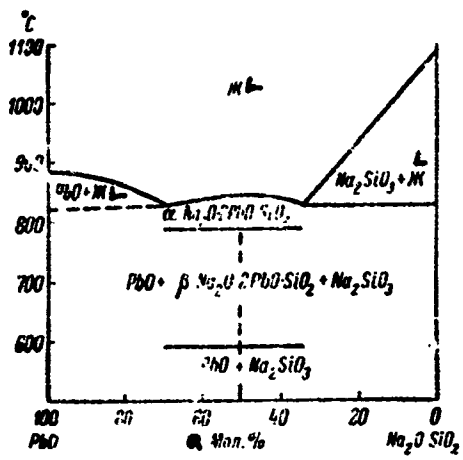


Fig. 72. Phase diagram of partial system $\text{PbO} - \text{Na}_2\text{O} \cdot \text{SiO}_2$ (from Krakau and colleagues).

Key: a. Mole %

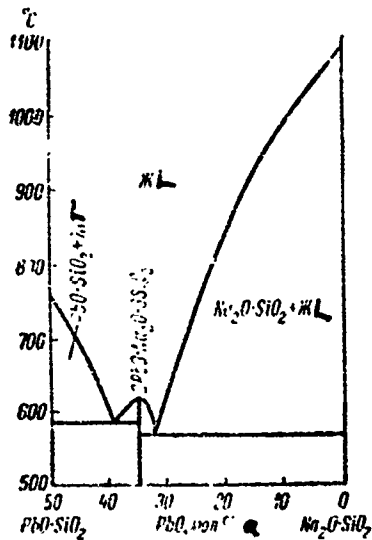


Fig. 73. Phase diagram of partial system $\text{Na}_2\text{O} \cdot \text{SiO}_2 - \text{PbO} \cdot \text{SiO}_2$ (from Krakau and colleagues).

Key: a. Mole %

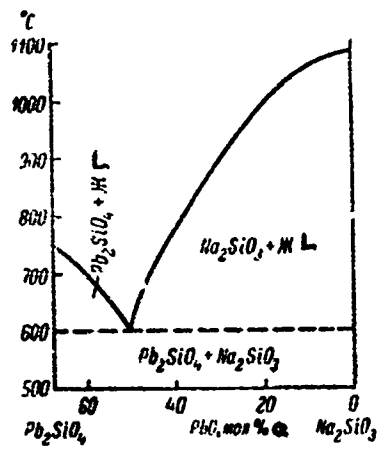


Fig. 74. Phase diagram of partial system $\text{Na}_2\text{O} \cdot \text{SiO}_2$ -- $2\text{PbO} \cdot \text{SiO}_2$
(from Krakau and colleagues).

Key: a. Mole %

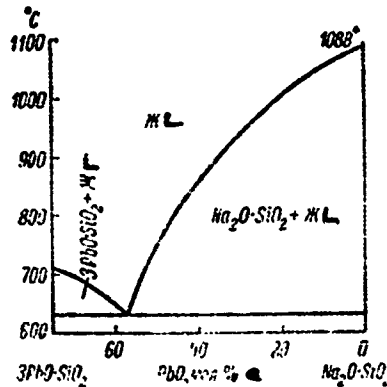


Fig. 75. Phase diagram of partial system $\text{Na}_2\text{O} \cdot \text{SiO}_2$ -- $3\text{PbO} \cdot \text{SiO}_2$
(from Krakau and colleagues).

Key: a. Mole %

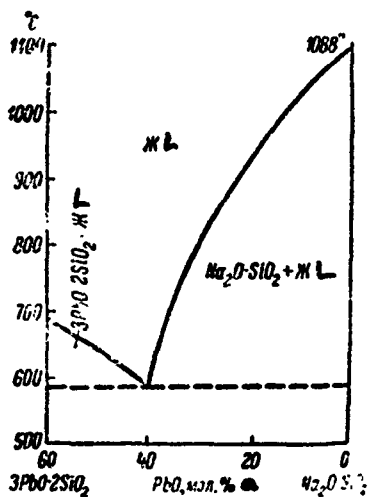


Fig. 76. Phase diagram of partial system $\text{Na}_2\text{O} \cdot \text{SiO}_2$ -- $3\text{PbO} \cdot 2\text{SiO}_2$
(from Krakau and colleagues).

Key: a. Mole %

BIBLIOGRAPHY

1. Yevstrop'yev, K. S., in the collection Fiziko-khimicheskiye svoystva troynoy sistemy Na_2O -- PbO -- SiO_2 [Physicochemical Properties of the Na_2O -- PbO -- SiO_2 Ternary System], AN SSSR Press, Moscow, 1949, p. 83.
2. Yevstrop'yev, K. S., N. A. Toropov, Khimiya kremniya i fizicheskaya khimiya silikatov [Chemistry of Silicon and Physical Chemistry of Silicates], Promstroyizdat Press, Moscow, 1950, p. 355.
3. Krakau, K. A., Izv. Sektora fiziko-khimich. analiza inst. obshch. khim., 8, 1936, p. 331.
4. Krakau, K. A., in the collection Fiziko-khimicheskiye svoystva troynoy sistemy Na_2O -- PbO -- SiO_2 [Physicochemical Properties of the Na_2O -- PbO -- SiO_2 Ternary System], AN SSSR Press, Moscow, 1949, p. 15.
5. Krakau, K. A., Ye. Ya. Mukhin, M. S. Genrikh, DAN SSSR, 14, No. 5, 1937, p. 281.

6. Pospelov, B. A., K. S. Yevstrop'yev, in the collection Fiziko-khimicheskiye svoystva troynoy sistemy Na₂O -- PbO -- SiO₂ [Physicochemical Properties of the Na₂O -- PbO -- SiO₂ Ternary System], AN SSSR Press, Moscow, 1949, p. 70.
7. Skornyakov, M. M., Ibid., p. 39.
8. Levin, E. M., C. R. Robbins, H. F. McMurdie, Phase Diagrams for Ceramists, USA, Columbus, Fig. 494, 1964.



The system has been studied by Geller and Bunting [2]. In accordance with the diagram presented (Fig. 77), four ternary compounds of a complex stoichiometric composition have been found: K₂O·2PbO·2SiO₂, K₂O·4PbO·3SiO₂, K₂O·PbO·4SiO₂ and 2K₂O·PbO·3SiO₂. It is interesting that, in the Na₂O -- PbO -- SiO₂ system, in which many compounds also are found, their composition is completely different from that of the lead-potassium silicates.

The compounds 1:2:2, 1:4:8 and 1:1:4 melt congruently at 918, 779 and 757°. Compound 2:1:3 melts incongruently at 735°, with crystallization of compound 1:2:2. The authors assert the existence of a fifth, more acid compound of unknown formula, melting incongruently at about 750°, with crystallization of silica.

In study of glasses, phase separation was found below the line of PbO -- K₂O·SiO₂, in the region adjacent to K₂O. Viscosity of melts of the system was determined by Frohberg and Rohde [1].

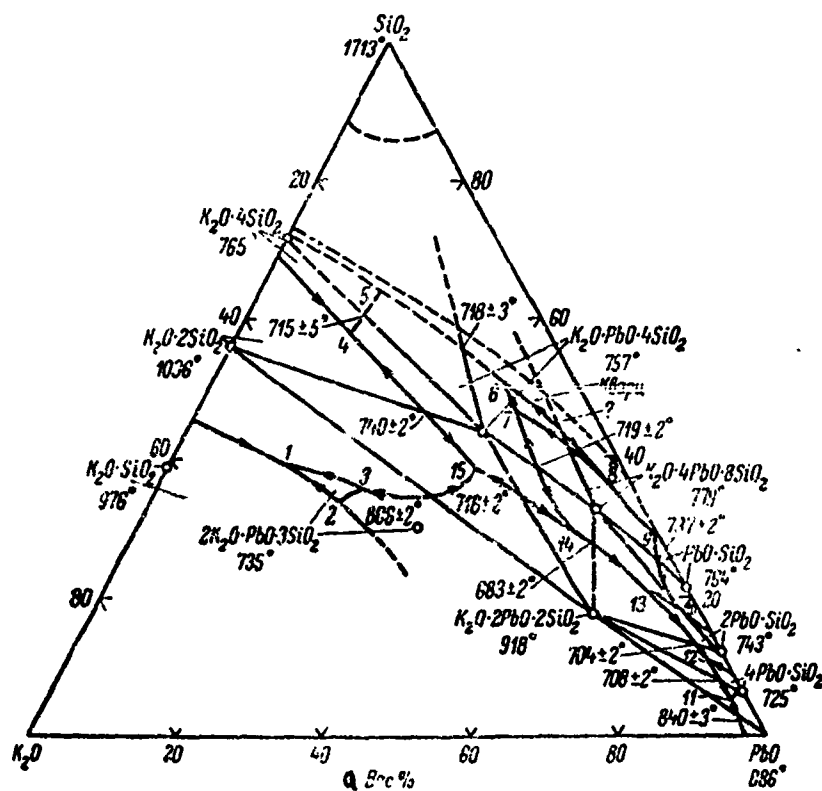


Fig. 77. Phase diagram of K_2O -- PbO -- SiO_2 system (from Geller and Bunting).

Key: a. Weight %

TABLE 1
INVARIANT POINTS OF K_2O -- PbO -- SiO_2 SYSTEM

a Соединение	b Процесс	c Состав, вес. %			d Темпера- тура, °C
		K_2O	PbO	SiO_2	
$K_2O \cdot 2PbO \cdot 2SiO_2 +$ жидкость e	1. Мягкое плавление	14.3	67.5	18.2	918
$K_2O \cdot 4PbO \cdot 8SiO_2 +$ жидкость	"	6.4	60.8	32.8	779
$K_2O \cdot PbO \cdot 4SiO_2 +$ жидкость	"	16.9	40.0	43.1	757
$2K_2O \cdot PbO \cdot 3SiO_2 +$ жидкость	2. Инконгруэнтное плавление	31.8	37.7	30.5	735 ± 5

Key:

- | | |
|--------------------------|------------------------|
| a. Compound | e. Liquid |
| b. Process | f. Melting |
| c. Composition, weight % | g. Incongruent melting |
| d. Temperature, °C | |

TABLE 2
DOUBLE EUTECTICS WITHIN K_2O -- PbO -- SiO_2 TERNARY SYSTEM

a Фазы	b Состав, вес. %			c Темпера- тура, °C
	K_2O	PbO	SiO_2	
$K_2O \cdot 2SiO_2 + K_2O \cdot 2PbO \cdot 2SiO_2 +$ жидкость d	27.2	38.0	34.8	806
$K_2O \cdot 2SiO_2 + K_2O \cdot PbO \cdot 4SiO_2 +$ жидкость	22.6	31.8	45.6	740
$K_2O \cdot 4SiO_2 + K_2O \cdot PbO \cdot 4SiO_2 +$ жидкость	23.5	16.5	60.0	715 ± 5
$SiO_2 + K_2O \cdot PbO \cdot 4SiO_2 +$ жидкость	12.6	30.1	57.0	718
$K_2O \cdot 4PbO \cdot 8SiO_2 + K_2O \cdot PbO \cdot 4SiO_2 +$ жидкость	11.5	50.7	37.8	719
$K_2O \cdot 2PbO \cdot 2SiO_2 + K_2O \cdot PbO \cdot 4SiO_2 +$ жидкость	16.0	49.3	34.7	716
$K_2O \cdot 2PbO \cdot 2SiO_2 + K_2O \cdot 4PbO \cdot 8SiO_2 +$ жидкость	9.2	63.2	27.6	683
$PbO \cdot SiO_2 + K_2O \cdot 4PbO \cdot 8SiO_2 +$ жидкость	1.8	73.7	24.5	734
$2PbO \cdot SiO_2 + K_2O \cdot 2PbO \cdot 2SiO_2 +$ жидкость	2.0	85.2	12.8	704
$PbO + K_2O \cdot 2PbO \cdot 2SiO_2 +$ жидкость	2.0	95.5	2.5	810

Key:

- | | |
|--------------------------|--------------------|
| a. Phases | c. Temperature, °C |
| b. Composition, weight % | d. Liquid |

TABLE 3
TRIPLE INVARIANT POINTS OF K_2O -- PbO -- SiO_2 SYSTEM

a Точка (рис. 77)	b Фазы	c Процесс	d Состав, в.с. %			e Темпера- тура, °C
			K_2O	PbO	SiO_2	
1	$K_2O \cdot SiO_2 + K_2O \cdot 2SiO_2 +$ +2 : 1 : 3 + жидкость f	Эвтектика	46	15	39	725 (?)
2	$K_2O \cdot SiO_2 + 2 : 1 : 3 +$ +1 : 2 : 2 + жидкость f	—	37	27	36	—
3	2 : 1 : 3 + $K_2O \cdot 2SiO_2 +$ +1 : 2 : 2 + жидкость f	—	40	26	34	—
4	$K_2O \cdot 2SiO_2 + K_2O \cdot 4SiO_2 +$ +1 : 1 : 4 + жидкость f	Эвтектика	26	16	58	705 (?)
a Точка (рис. 77)	б Фазы	в Процесс	Состав, вес. %			г Темпера- тура, °C
			K_2O	PbO	SiO_2	
5	$K_2O \cdot 4SiO_2 + 1 : 1 : 4 +$ + SiO_2 + жидкость f	Эвтектика	18	19	63	—
6	1 : 1 : 4 + ? + SiO_2 + жидк. f кость	—	40	39	51	—
7	1 : 1 : 4 + ? + 1 : 4 : 8 + жидк. f кость	—	40	43	47	700 ± 5
8	1 : 4 : 8 + SiO_2 + ? + жидк. f кость	—	3.2	60.0	36.8	742
9	1 : 4 : 8 + $SiO_2 + PbO \cdot SiO_2 +$ + жидкость f	—	0.5	71.0	28.5	730
10	$PbO \cdot SiO_2 + 1 : 4 : 8 +$ + 2 $PbO \cdot SiO_2$ + жидкость f	—	3.0	78.0	19.0	676
11	1 : 2 : 2 + 4 $PbO \cdot SiO_2 +$ + PbO + жидкость f	—	1.5	91.7	6.8	705
12	4 $PbO \cdot SiO_2 + 2PbO \cdot SiO_2 +$ + 1 : 2 : 2 + жидкость f	—	1.8	88.0	10.2	693
13	2 $PbO \cdot SiO_2 + 1 : 2 : 2 +$ + 1 : 4 : 8 + жидкость f	—	5.0	74.5	20.5	637
14	1 : 2 : 2 + 4 : 4 : 8 + + 1 : 1 : 4 + жидкость f	—	11.0	59.5	29.5	682
15	1 : 2 : 2 + $K_2O \cdot 2SiO_2 +$ + 1 : 1 : 4 + жидкость f	—	26.0	41.7	38.3	708

Key:

- a. Points (Fig. 77)
- b. Phases
- c. Process
- d. Composition, weight %
- e. Temperature, °C
- f. Liquid
- g. Eutectic

TABLE 4
CRYSTALLINE PHASES OF K_2O -- PbO -- SiO_2 SYSTEM

a Соединение	b Система кристал- лов	c Габитус	d Спай- ность	<i>N_g</i>	<i>N_m</i>	<i>N_p</i>	<i>2V°</i>	e Опти- ческий знак
$K_2O \cdot 2PbO \cdot 2SiO_2$	g Гексаго- нальная	—	—	1.93	—	1.72	0	(—)
$K_2O \cdot 4PbO \cdot 8SiO_2$?	h —	—	1.79	—	1.63	0	(—)
$K_2O \cdot PbO \cdot 4SiO_2$?	Пластин- ки, пря- моуголь- ные зерна	—	1.65	1.612	1.590	75	(+)
$2K_2O \cdot PbO \cdot 3SiO_2$?	Пласти- ники	—	около k	—	—	—	—
Состав неизвест- ного	?	то же j	—	1.67	—	—	k около 80	(—)

Key:

- | | |
|---------------------------------|-----------------------|
| a. Compound | g. Hexagonal |
| b. Crystal system | h. Plates |
| c. Appearance | i. Rectangular grains |
| d. Cleavage | j. Same |
| e. Optical sign | k. About |
| f. Phase of unknown composition | |

BIBLIOGRAPHY

1. Frohberg, M.G., W. Rohde, Glastechn. Ber., 37, No. 10, 453, 1964.
2. Geller, R.F., E.N. Bunting, J. Res. Nat. Bur. Stand., 17, No. 2, 283, 1936.

MgO -- PbO -- SiO_2

The system has been studied by Argyle and Hummel [1], predominantly in the subsolidus region. The study was limited to a temperature of 900°. Some mixtures (adjacent to the SiO_2 apex) were heated in closed, platinum tubes (pressure 5000 psi).

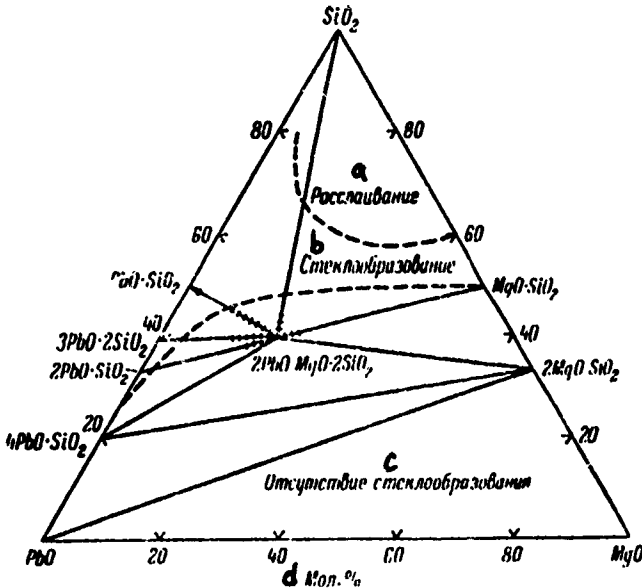


Fig. 78. Diagram of subsolidus phase relationships of $\text{MgO} \text{-- PbO} \text{-- } \text{SiO}_2$ system (from Argyle and Hummel).

Key:

- a. Phase separation
- b. Glass formation
- c. Absence of glass formation
- d. Mole %

One ternary compound was found $2\text{PbO} \cdot \text{MgO} \cdot 2\text{SiO}_2$, which melts congruently at 832° . This compound forms solid solutions with $2\text{PbO} \cdot \text{SiO}_2$, $3\text{PbO} \cdot 2\text{SiO}_2$, $\text{PbO} \cdot \text{SiO}_2$, $\text{MgO} \cdot \text{SiO}_2$ and SiO_2 . A schematic phase diagram with concentration regions, of which glass formation, the absence of glass and phase separation of the liquids are characteristic, is presented in Fig. 78. Two partial binary profiles are presented in Figs. 79 and 80.

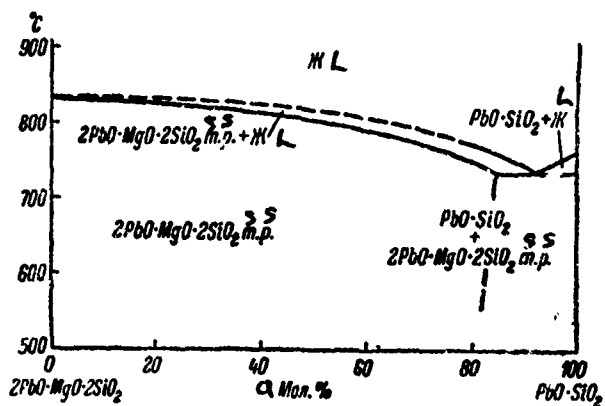


Fig. 79. Diagram of phase relationships of $2\text{PbO}\cdot\text{MgO}\cdot2\text{SiO}_2$ -- $\text{PbO}\cdot\text{SiO}_2$ partial system (from Argyle and Hummel).

Key: a. Mole %

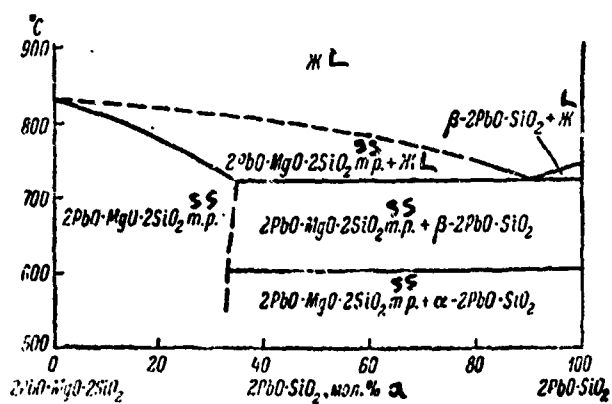


Fig. 80. Diagram of phase relationships of $2\text{PbO}\cdot\text{MgO}\cdot2\text{SiO}_2$ -- $2\text{PbO}\cdot\text{SiC}_2$ partial system (from Argyle and Hummel).

Key: a. Mole %

It was determined, by means of density measurements, that a cation deficit is characteristic of the solid solutions. The most extensive region of solid solutions is observed in the $2\text{PbO}\cdot\text{MgO}\cdot 2\text{SiO}_2$ -- $\text{PbO}\cdot\text{SiO}_2$ series; a constant $\text{PbO}:\text{SiO}_2$ ratio is present there. This ratio is of decisive importance for formation of solid solutions.

Billhardt [2] considers that the ternary compound existing in the system is a magnesia barysilite, with the formula $8\text{PbO}\cdot\text{MgO}\cdot 6\text{SiO}_2$, and he described a X-ray photo, similar to that obtained by Argyle and Hummel for the ternary compound. Further research is necessary to precisely determine the formula of the magnesium lead silicate.

BIBLIOGRAPHY

1. Argyle, J.F., F.A. Hummel, Glass Industry, **46**, No. 10, 583, No. 12, 710, 1965.
2. Billhardt, H.W., Amer. Mineralogist, **54**, No. 3-4, 510, 1969.

$\text{BaO} \text{-- } \text{PbO} \text{-- } \text{SiO}_2$

The system has been studied by Argyle and Hummel [1], predominantly in the subsolidus region (up to 1200°). The existence of two ternary compounds has been established: $\text{PbO}\cdot\text{BaO}\cdot 2\text{SiO}_2$ and $3\text{PbO}\cdot\text{BaO}\cdot 2\text{SiO}_2$. The compound $\text{PbO}\cdot\text{BaO}\cdot 2\text{SiO}_2$ forms solid solutions with $\text{PbO}\cdot\text{SiO}_2$ and $\text{BaO}\cdot\text{SiO}_2$. A considerable area of solid solutions based on $2\text{BaO}\cdot\text{SiO}_2$ (in a series with $2\text{PbO}\cdot\text{SiO}_2$) has been established. The authors have determined the concentration region in which transparent glass is obtained. Phase separation of the liquids is observed near the silica apex. Glass-forming and nonglass-forming regions and the phases existing in the subsolidus region are shown in Fig. 81.

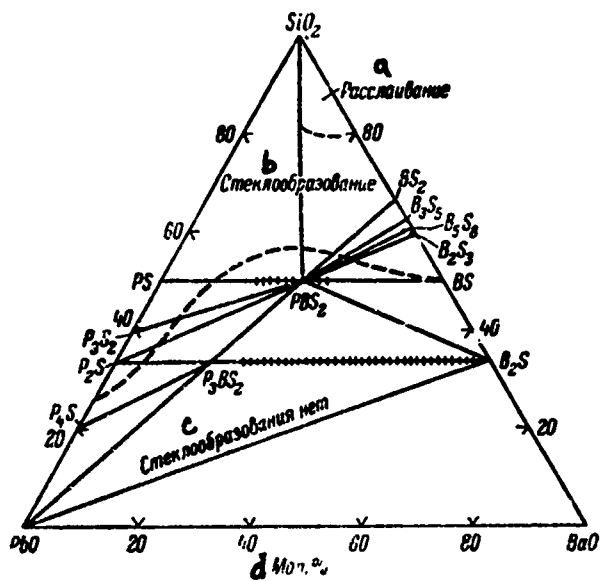


Fig. 81. Diagram of subsolidus phase relationships of $\text{BaO} - \text{PbO} - \text{SiO}_2$ system (from Argyle and Hummel).

Key:

- | | |
|---------------------|-----------------------|
| a. Phase separation | c. No glass formation |
| b. Glass formation | d. Mole % |

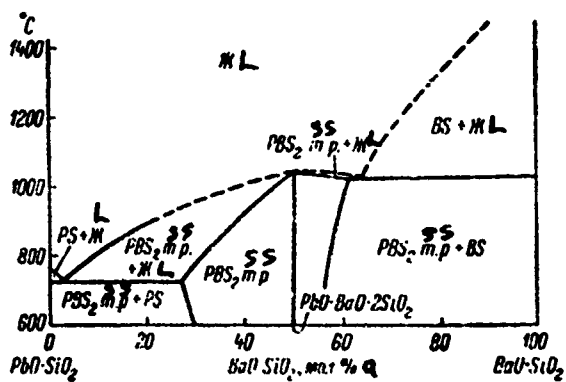


Fig. 82. Diagram of phase relationships of $\text{PbO-SiO}_2 - \text{BaO-SiO}_2$ partial system (from Argyle and Hummel).

Key: a. Mole %

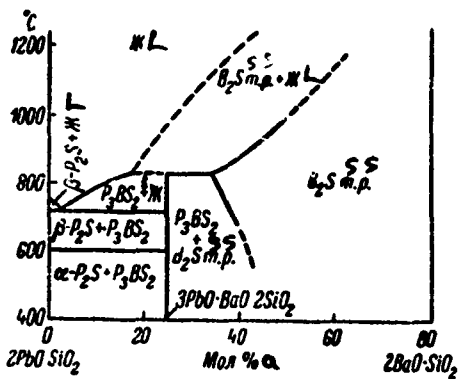


Fig. 83. Diagram of phase relationships of $2\text{PbO}\cdot\text{SiO}_2$ -- $2\text{BaO}\cdot\text{SiO}_2$ partial system (from Argyle and Hummel).

Key: a. Mole %

A phase diagram of the pseudobinary system $\text{PbO}\cdot\text{SiO}_2$ -- $\text{BaO}\cdot\text{SiO}_2$ is presented in Fig. 82. In the compound $\text{PbO}\cdot\text{BaO}\cdot 2\text{SiO}_2$, 45 mole % of the BaO is replaced by lead oxide and 23 mole % of the PbO is replaced by barium oxide. The pseudobinary profile $2\text{PbO}\cdot\text{SiO}_2$ -- $2\text{BaO}\cdot\text{SiO}_2$ is presented in Fig. 83. The authors draw attention to an anomaly in the change of interplane distance d of the solid solutions at 30 mole % $2\text{PbO}\cdot\text{SiO}_2$, which is connected with conjectural structural conversions.

The phase diagram of the partial system $2\text{PbO}\cdot\text{SiO}_2$ -- $2\text{BaO}\cdot 3\text{SiO}_2$ is characterized by the presence of the compound $\text{PbO}\cdot\text{BaO}\cdot 2\text{SiO}_2$. The compound $\text{PbO}\cdot 3\text{BaO}\cdot 4\text{SiO}_2$, to which Butler and Cassanos referred [2], was not found.

BIBLIOGRAPHY

1. Argyle, J.F., F.A. Hummel, Glass Industry, 46, No. 10, 583, No. 12, 710, 1965.
2. Butler, K.H., J.G. Cassanos, J. Electrochem. Soc., 97, No. 3, 83, 1950.

MANGANESE SILICATE SYSTEMS



Hay and colleagues [1] have studied the portion of the system adjacent to the silica apex. A diagram of the liquidus surface of this part of the system, with the boundaries of the region of existence of two liquid phases plotted, is depicted in Fig. 84. One ternary compound is found here $\text{Na}_2\text{O} \cdot \text{MnO} \cdot 2\text{SiO}_2$, which melts with decomposition into tephroite and liquid. The immiscibility region is located in the $\text{MnO} \cdot \text{SiO}_2$ field. Five tie lines are shown here.

The two layers formed in samples quenched from 1200° were isolated separately, and a chemical analysis of each layer was carried out; in one of the layers, for example, the outer layer has the composition (weight %) 41.5 MnO, 10 Na₂O and 48.5 SiO₂ and the inner layer, 50.4 MnO, 4 Na₂O and 45.6 SiO₂.

The miscibility discontinuity apparently has an upper limit at temperatures above 1300 - 1350° .

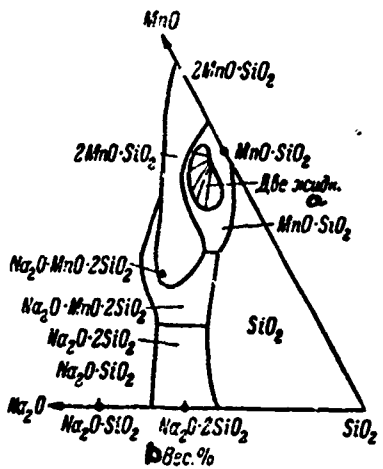


Fig. 84. Liquidus surface of silica-rich part of $\text{Na}_2\text{O} - \text{MnO} - \text{SiO}_2$ system; region of immiscibility of two liquids is shown for 1200° (from Hay and colleagues).

Key:

- a. Two liquids
- b. Weight %

BIBLIOGRAPHY

1. Hay, R., P. T. Carter, S. K. Kabi, J. Soc. Glass Techn., 40, No. 196, 429T, 1956.



A phase diagram of the system, from data of Glasser and Osborn [2], is shown in Fig. 85. It is characterized by the absence of ternary eutectics and by three liquidus invariant points; M, E and N. Point N (1470°) is an inversion point, in which tridymite and cristobalite coexist in equilibrium with a rhodonite solid solution and a liquid of the composition $\text{MgO} - 21.5$, $\text{MnO} - 22.5$ and

SiO_2 -- 56 weight %. At point M (1536°), high-temperature enstatite and rhodonite solid solutions and cristobalite are found in equilibrium with a liquid of the composition $\text{MgO} = 32$, $\text{MnO} = 5$ and $\text{SiO}_2 = 63$ weight %. At point E (1538°), an olivine solid solution is in equilibrium with rhodonite, high-temperature enstatite and a liquid of the composition $\text{MgO} = 36$, $\text{MnO} = 5.5$ and $\text{SiO}_2 = 58.5$ weight %.

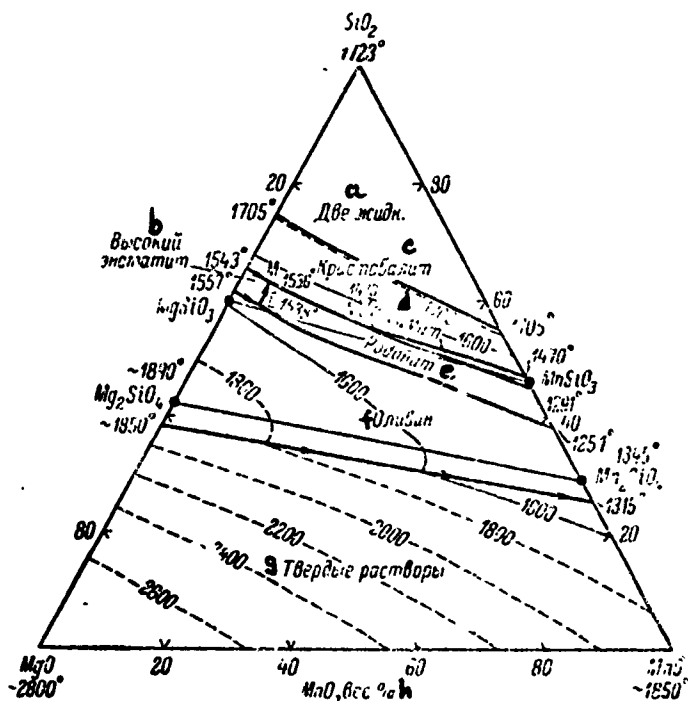


Fig. 85. Phase diagram of $\text{MgO} - \text{MnO} - \text{SiO}_2$ system (from Glasser and Osborn).

Key:

- | | |
|-------------------------------|--------------------|
| a. Two liquids | e. Rhodonite |
| b. High-temperature enstatite | f. Olivine |
| c. Cristobalite | g. Solid solutions |
| d. Tridymite | h. Weight % |

A diagram of an orthosilicate binary system is presented in Fig. 86. Mn_2SiO_4 , identical with natural tephroite, melts congruently at 1345° .

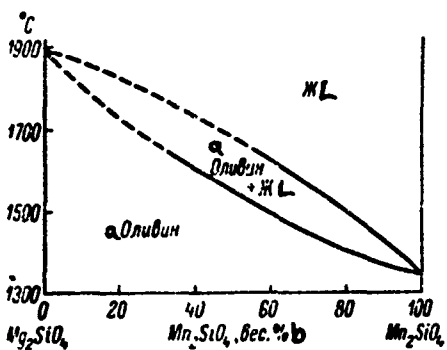


Fig. 86. Phase diagram of partial system Mg_2SiO_4 -- Mn_2SiO_4 (from Glasser and Osborn).

Key:

- a. Olivine
- b. Weight %

A phase equilibrium diagram of MnSiO_3 -- MgSiO_3 , according to Glasser and Osborn [2], is presented in Fig. 87. Rhodonite solid solutions form a continuous isomorphic series from MnSiO_3 to 94.5 weight % MgSiO_3 at solidus temperatures. At a temperature of 1300° , the rhodonite solid solution contains only 78 weight % MgSiO_3 . During the investigation, the presence of a very narrow, two-phase region (solid solution of high-temperature enstatite + solid solution of rhodonite) was discovered.

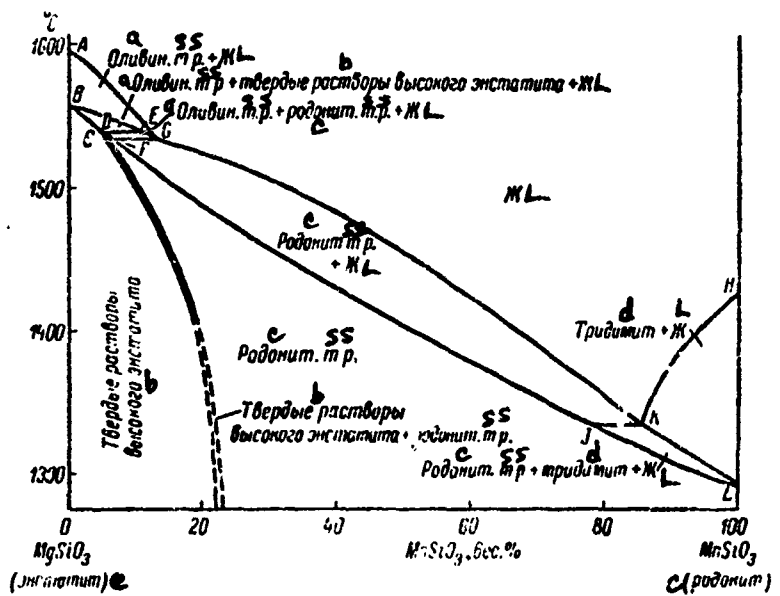


Fig. 87. Phase diagram of partial system MgSiO_3 -- MnSiO_3 (from Glasser and Osborn): A. 1595°; B. 1557°; C. D. E. 1538°; F. G. 1533°; H. 1425°; J. K. 1333°; L. 1291°

Key:

- a. Olivine
- b. High-temperature enstatite solid solutions
- c. Rhodonite
- d. Tridymite
- e. Enstatite
- f. Weight %

SiO_2 gives two compounds with MnO : MnSiO_3 (1292°) and Mn_2SiO_4 (1345°); the latter is identical to the Mn-olivine, tephroite. MnSiO_3 is not isostructural with a single one of the three forms of MgSiO_3 or with a single one of the forms of CaSiO_3 .

MnSiO_3 polymorphism has been studied by Liebau and colleagues [3, 4], according to whom there are three modifications of manganese metasilicate.

γ MnSiO_3 (triclinic) is stable at room temperature and is structurally identical to the natural mineral rhodonite, which is a five-fold infinite chain of $[\text{SiO}_4]$ tetrahedra. At 1160° , γ MnSiO_3 changes to the ρ modification, which is isostructural with the natural mineral bustamite (triclinic crystal system), and the latter, in turn, is close in structure to wollastonite (three-fold chain of silicate tetrahedra).

α MnSiO_3 is a metastable phase at normal pressures and in all temperatures, and it is isostructural with pseudowollastonite.

X-ray data from Liebau for MnSiO_3 are presented in the table.

LINEAR PARAMETERS OF MnSiO_3 MODIFICATION UNIT CELLS

a Модификации MnSiO_3	$a, \text{\AA}$	$b, \text{\AA}$	$c, \text{\AA}$
$\gamma\text{-MnSiO}_3$	6.71	7.6 ₈	12.3 ₃
Родонит природный с 19 мол. % CaSiO_3	6.68	7.66	12.20
$\beta\text{-MnSiO}_3$	2×8.03	7.11	2×6.84
Бустамит природный	2×7.73	7.18	2×6.92
ρ -ролластонит природный	7.94	7.32	7.07

Key:

- a. MnSiO_3 modification
- b. Natural rhodonite with 19 mole % CaSiO_3
- c. Natural bustamite
- d. Natural ρ wollastonite

No manganese compounds analogous to $\text{Ca}_3\text{Si}_2\text{O}_7$ or Ca_3SiO_5 have been found in the ternary system [1].

BIBLIOGRAPHY

1. Glasser, F.P., Silikattechnik, 11, No. 8, 362, 1960.
2. Glasser, F.P., E.F. Osborn, J. Amer. Ceram. Soc., 43, No. 3, 132, 1960.
3. Liebau, F., W. Hilmer, G. Lindemann, Acta crystallogr., 12, No. 3, 182, 1959.
4. Liebau, F., M. Sprung, E. Thilo, Zs anorgan. allgem. Chem., 297, No. 3-4, 213, 1958.



A diagram of the ternary system, according to Glasser [2], who used an atmosphere with a low oxygen partial pressure to maintain manganese in the divalent form, is depicted in Fig. 88. There are three ternary liquidus minima, with the following CaO, MnO and SiO₂ content (weight %): 1. 5.0, 48.4, 46.6; 2. 17.5, 45.0, 37.5; 3. 15.0, 53.0, 32.0, and temperatures of 1256, 1195 and 1204°, respectively.

Of the eleven crystalline phases, six have a variable composition: two metasilicates, based on βCaSiO_3 and MnSiO_3 , three orthosilicates, based on $\alpha\text{Ca}_2\text{SiO}_4$, $\alpha'\text{Ca}_2\text{SiO}_4$ and Mn_2SiO_4 , and a (Ca, Mn)O phase. There is no Ca_3SiO_5 in the ternary system in contact with the liquid: it disappears at $t > 1700^\circ$, as a result of the peritectic reaction $\text{Ca}_3\text{SiO}_5 + \text{liquid} = \alpha(\text{Ca}, \text{Mn})_2\text{SiO}_4 + (\text{Ca}, \text{Mn})\text{O} + \text{liquid}$. Mn^{2+} is concentrated preferentially, in the distribution between the existing phases, in the more basic phases. $\text{Ca}_3\text{Si}_2\text{O}_7$ and Ca_3SiO_5 do not accept appreciable amounts of Mn^{2+} in their lattices. Below 1250°, Ca_3SiO_5 gradually (7-10 days) changes to Ca_2SiO_4 and (Ca, Mn)O solid solutions.

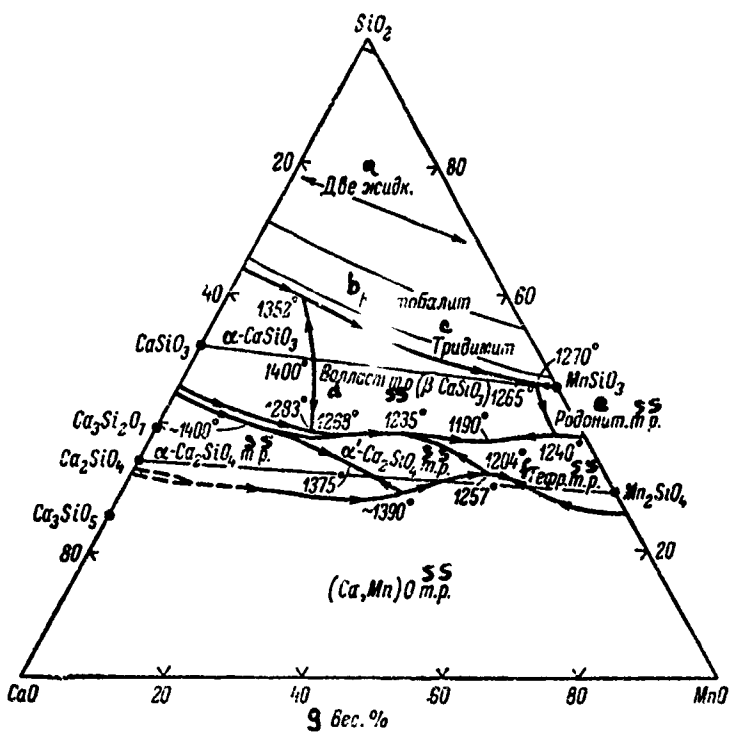


Fig. 88. Diagram of phase relations of CaO -- MnO -- SiO₂ system (from Glasser).

Key:

- | | |
|-----------------|--------------|
| a. Two liquids | e. Rhodonite |
| b. Cristobalite | f. Tephroite |
| c. Tridymite | g. Weight % |
| d. Wollastonite | |

Partial orthosilicate profiles are presented in Fig. 89a and b. A glaucochroite phase composition, the natural analog of which is isostructural with olivine, is shown by the vertical dashed line.

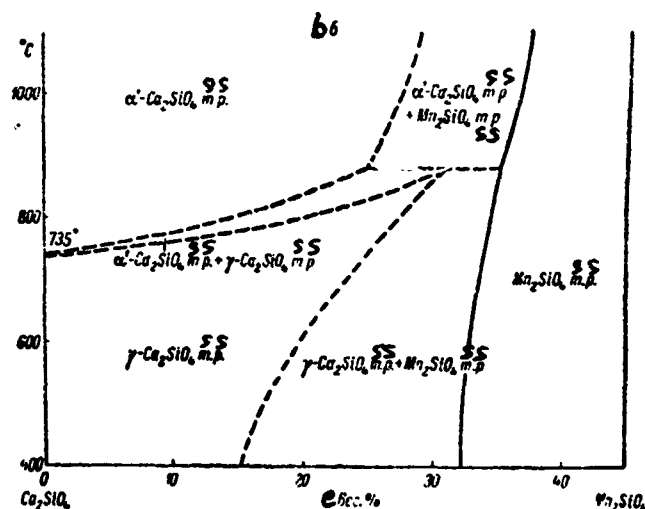
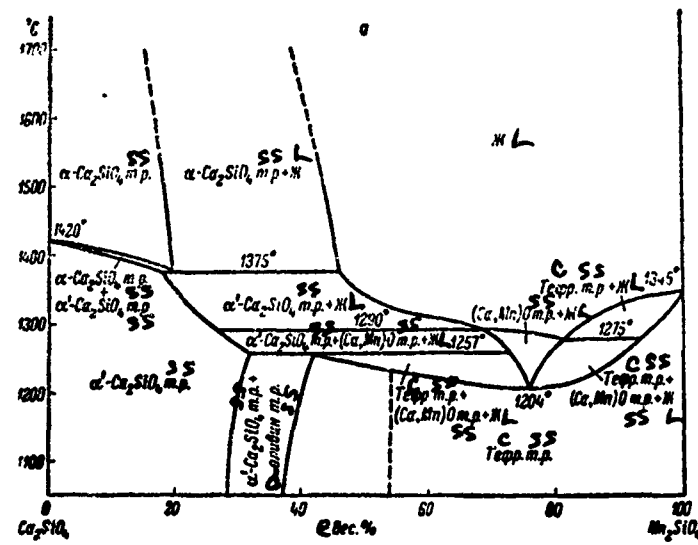


Fig. 89. Phase diagram of partial system Ca_2SiO_4 -- Mn_2SiO_4 (from Glasser): a. complete diagram; b. region adjacent to Ca_2SiO_4 .

Key:

- c. Tephroite
 - d. Olivine
 - e. Weight %

According to Hurlbut [6], for tephroite, $a = 4.90$, $b = 10.60$ and $c = 6.25$ Å, and for glaucochroite, $a = 4.92$, $b = 11.19$ and $c = 6.51$ Å.

Of the three orthosilicate phases, $\gamma \text{Ca}_2\text{SiO}_4$, CaMnSiO_4 and Mn_2SiO_4 , the latter two form completely isomorphic mixtures. A large two-phase region exists between $\gamma \text{Ca}_2\text{SiO}_4$ and the region of olivine solid solutions of the Mn_2SiO_4 -- CaMnSiO_4 type [1, 3]. With respect to limited solubility, these data contradict the early works of Greer [5], who observed a broader isomorphic replacement.

The high-temperature form of Ca_2SiO_4 includes 20-25 weight % Mn_2SiO_4 in solid solution [1, 3]. Mn^{2+} , replacing Ca, stabilizes the high-temperature form of Ca_2SiO_4 .

Goldschmidt and Rait [4], in a reducing medium, obtained manganese merwinite, having a perovskite structure.

A diagram of the phase interrelationships in the partial system CaSiO_3 -- MnSiO_3 , according to L. Glasser [3], is presented in Fig. 90. The dashed line designates the subsolidus interrelationships between johansenite and wollastonite, which are similar to those between hedenbergite and wollastonite. Johansenite synthesis was not successful. The upper limit of its stability region (578°) is based on data of decomposition of the natural mineral.

Liebau and colleagues [7, 8], studying the phase relationships in the MnSiO_3 -- $\text{MnCa}(\text{SiO}_3)_2$ system, established the presence of three types of solid solutions: pseudowollastonite, based on αMnSiO_3 , bustamite, based on βMnSiO_3 and rhodonite, based on γMnSiO_3 . In the latter, the CaSiO_3 content is limited to 20 mole %. The high-temperature forms of α and βMnSiO_3 form a continuous solid solution with CaSiO_3 . The optical properties of the metasilicates of the solid solutions have been studied by Sundius [9] and Voos [10].

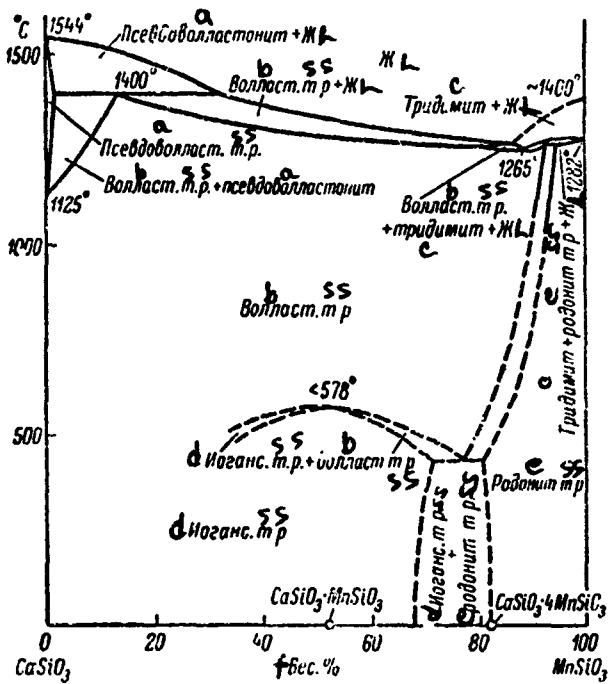


Fig. 90. Diagram of phase relationships of partial system CaSiO_3 -- MnSiO_3 (from L. Glasser).

Key:

- a. Fseudowollastonite
- b. Wollastonite
- c. Tricymite
- d. Johansenite
- e. Rhodonite
- f. Weight %

BIBLIOGRAPHY

1. Glasser, F.P., Silikattechnik, 11, No. 8, 362, 1960.
2. Glasser, F.P., J. Amer. Ceram. Soc., 45, No. 5, 242, 1962.
3. Glasser, L.S.D., F.P. Glasser, Silikattechnik, 11, No. 8, 363, 1960
4. Goldschmidt, H.J., J.R. Rait, Nature, 152, No. 3856, 356, 1943.
5. Greer, W.L., Amer. Mineralogist, 17, No. 4, 135, 1932.
6. Hurlbut, C.S., Amer. Mineralogist, 46, No. 5-6, 549, 1961.
7. Liebau, F., M. Sprung, E. Thilo, Zs. anorgan. allgem. Chem., 297, No. 3-4, 213, 1958.
8. Liebau, F., W. Hilmer, G. Lindemann, Acta crystallogr., 12, No. 3, 182, 1959.
9. Sundius, N., Amer. Mineralogist, 16, No. 10-11, 411, 488, 1931.
10. Voos, E., Zs. anorgan. allgem. Chem., 222, No. 2, 201, 1935.

FERROSILICATE SYSTEMS



The system has been studied by Carter and Ibrahim [1]. One ternary compound, melting incongruently at 975°, has been found, which could be considered to be alkaline fayalite. A phase diagram is presented in Fig. 91. There is a remarkably strong drop in the melting temperature (by several hundred degrees), upon addition of 1 % Na₂O total to a FeO + SiO₂ mixture.

Carter and Ibrahim present a number of diagrams of partial binary systems, of which 2FeO·SiO₂ -- 2Na₂O·SiO₂ (Fig. 92) and 2FeO·SiO₂ -- Na₂O·SiO₂ (Fig. 93) are not true binaries.

A phase coexistence triangle (referred to room temperature), dividing the diagram into seven phase triangles, in each of which three phases are present, is presented in Fig. 94: in the first triangle, Fe₂SiO₄ + Na₂O·2SiO₂ + SiO₂; in the second, FeO + Na₂O·2SiO₂ + Fe₂SiO₄; in the third, FeO + Na₂O·FeO·SiO₂ + Na₂O·2SiO₂; in the fourth, Na₂O·FeO·SiO₂ + Na₂O·2SiO₂; in the fifth, Na₂O·FeO·SiO₂ + 2Na₂O·SiO₂ + Na₂O·SiO₂; in the sixth, FeO + 2Na₂O·SiO₂ + Na₂O·FeO·SiO₂, and, in the seventh, FeO + Na₂O + 2Na₂O·SiO₂.

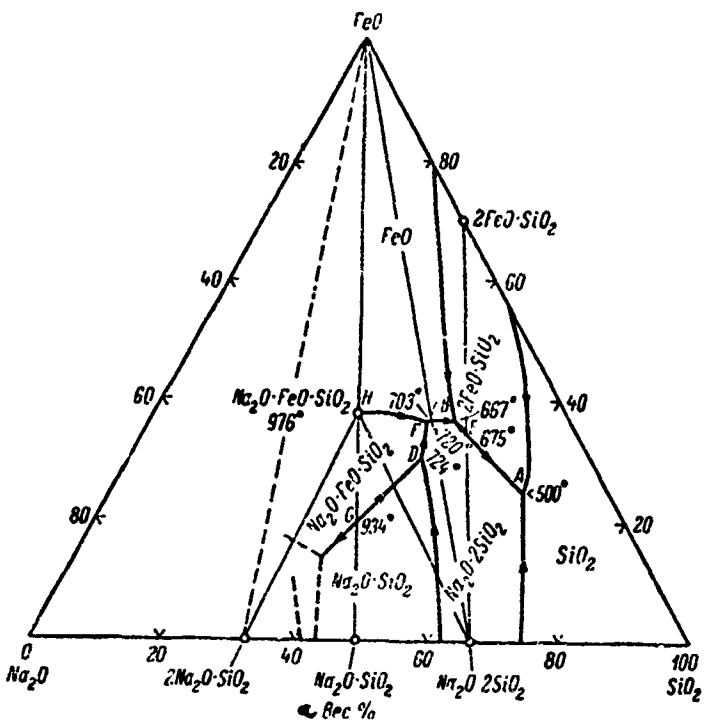


Fig. 91. Phase diagram of $\text{Na}_2\text{O} - \text{FeO} - \text{SiO}_2$ system; primary phases of system (from Carter and Ibrahim).

Key: a. Weight %

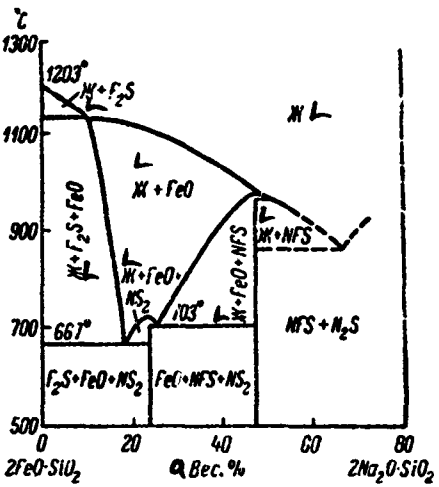


Fig. 92. Phase diagram of partial system $2\text{FeO}\cdot\text{SiO}_2$ -- $2\text{Na}_2\text{O}\cdot\text{SiO}_2$; system is not a true binary (from Carter and Ibrahim).

Key: a. Weight %

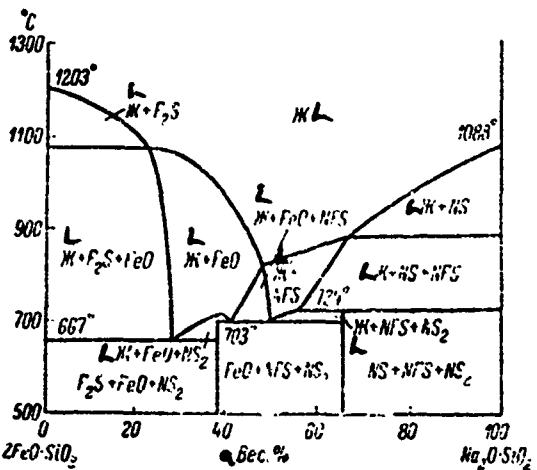


Fig. 93. Phase diagram of partial system $2\text{FeO}\cdot\text{SiO}_2$ -- $\text{Na}_2\text{O}\cdot\text{SiO}_2$; system is not a true binary (from Carter and Ibrahim).

Key: a. Weight %

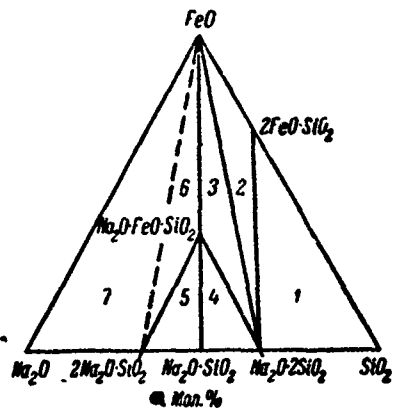


Fig. 94. Phase coexistence triangle of $\text{Na}_2\text{O} - \text{FeO} - \text{SiO}_2$ system (from Carter and Ibrahim).

Key: a. Mole %

INVARIANT POINTS OF $\text{Na}_2\text{O} - \text{FeO} - \text{SiO}_2$ SYSTEM

Точка (рис. 91)	Фазы <i>b</i>	Процесс <i>c</i>	Состав, вес.%			Темпера- тура, °C <i>e</i>
			Na ₂ O <i>d</i>	FeO <i>d</i>	SiO ₂ <i>d</i>	
A	$\text{Na}_2\text{O} \cdot 2\text{SiO}_2 + 2\text{FeO} \cdot \text{SiO}_2 +$ + $\text{SiO}_2 +$ жидкость <i>f</i>	Эвтектика <i>a</i>	Определен приблизительно			Ниже 500
B	$\text{FeO} \cdot \text{Na}_2\text{O} \cdot 2\text{SiO}_2 + 2\text{FeO} \cdot$ + $\text{SiO}_2 +$ жидкость <i>f</i>		18.5	35.5	46	667
C	$\text{FeO} + \text{Na}_2\text{O} \cdot \text{FeO} \cdot \text{SiO}_2 +$ + $\text{Na}_2\text{O} \cdot 2\text{SiO}_2 +$ жидкость <i>f</i>		23	35.5	41.5	703
D	$\text{Na}_2\text{O} \cdot \text{SiO}_2 + \text{Na}_2\text{O} \cdot \text{FeO} \cdot$ + $\text{SiO}_2 + \text{Na}_2\text{O} \cdot 2\text{SiO}_2 +$ жидкость <i>f</i>	Реакция <i>b</i>	26.5	29.5	44	724
E	$2\text{FeO} \cdot \text{SiO}_2 + \text{Na}_2\text{O} \cdot 2\text{SiO}_2 +$ + жидкость <i>f</i>	Бинарная эвтектика <i>c</i>	18	33.5	48.5	675
F	$\text{FeO} + \text{Na}_2\text{O} \cdot 2\text{SiO}_2 +$ жидкость <i>f</i>	То же <i>d</i>	22	36	42	720
G	$\text{Na}_2\text{O} \cdot \text{FeO} \cdot \text{SiO}_2 + \text{Na}_2\text{O} \cdot$ + $\text{SiO}_2 +$ жидкость <i>f</i>		40.5	19.5	40	934
H	$\text{FeO} + \text{Na}_2\text{O} \cdot \text{FeO} \cdot \text{SiO}_2 +$ + жидкость <i>f</i>	Реакция <i>b</i>	32	36.5	31.5	976

Key:

- a. Points (Fig. 91)
- b. Phases
- c. Process
- d. Composition, weight %
- e. Temperature, °C
- f. Liquid
- g. Eutectic
- h. Reactions
- i. Binary eutectic
- j. Same
- k. Determined approximately
- l. Below 500

BIBLIOGRAPHY

1. Carter, P. T., M. Ibrahim, J. Soc. Glass Technol., 36, No. 170, 142, 1952.

$\text{K}_2\text{O} - \text{FeO} - \text{SiO}_2$

The system has been studied by Roedder [1], in the region encompassing compositions with the $\text{K}_2\text{O}:\text{SiO}_2$ ratio $< 1:2$. The melt contains Fe_2O_3 , the amount of which reaches 6 weight % in the region rich with FeO. Two ternary

compounds have been found: $K_2O \cdot SeO \cdot 3SiO_2$ and $K_2O \cdot FeO \cdot 5SiO_2$. A diagram of the phase relationships, under conditions of equilibrium with metallic iron, is presented in Fig. 95. Crystals of $K_2O \cdot FeO \cdot 3SiO_2$ form round, colorless grains, with an average index of refraction $N_m = 1.575$ and birefringence on the order of 0.01; they melt without decomposition at approximately 900°. Crystals of $K_2O \cdot FeO \cdot 5SiO_2$ form isotropic, birefringent grains, with an average index of refraction $N_m = 1.535$. An anomalous interference color with reddish and bluish tones sometimes is observed. The compound melts without decomposition at about 900°.

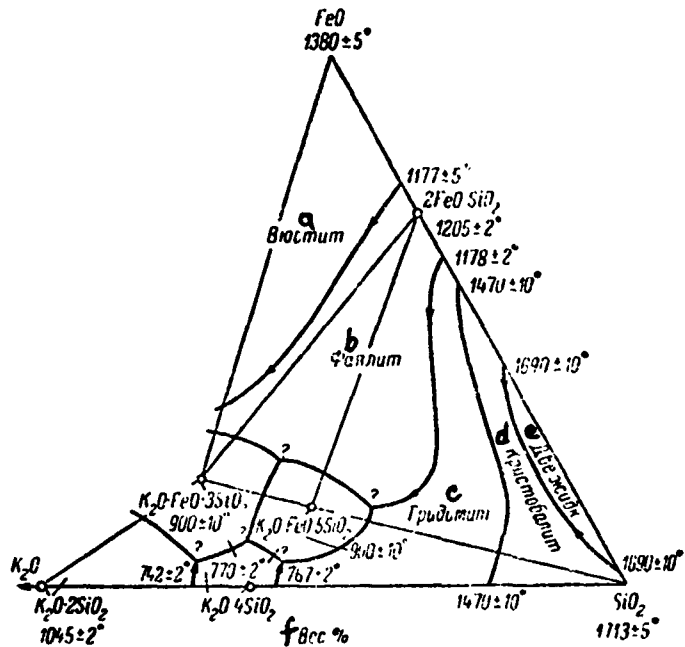


Fig. 95. Approximate phase diagram of K_2O -- FeO -- SiO_2 system (from Roedder); all iron oxides are assumed to be FeO .

Key:

- | | |
|--------------|-----------------|
| a. Wüstite | d. Cristobalite |
| b. Fayalite | e. Two liquids |
| c. Tridymite | f. Weight % |

BIBLIOGRAPHY

1. Roedder, E.W., Amer. J. Sci., Bowen vol., pt. 2, 435, 1952.



The system has been studied in detail by Bowen and Schairer [4], by the quenching method. The tests were preformed in an iron crucible in a stream of nitrogen. Quantitatively, Fe_2O_3 reached 2 % (close to Fe_2SiO_4). The complete phase diagram of the system is presented in Fig. 96, from Osborn and Muan [11], with certain temperature values refined. The phase ratios for temperatures of 1550, 1450 and 1150°, are presented in Fig. 97. Phase transformations in the system are seen graphically at the points designated by letters. There is a considerable region of phase separation of melts in the system, located close to the silica apex.

Phase diagrams of the partial systems Mg_2SiO_4 -- Fe_2SiO_4 and MgSiO_3 -- "FeSiO₃" are given in Figs. 98 and 99. The complexity of the MgSiO_3 -- FeSiO₃ system is caused by the fact that pyroxenes rich in magnesium metasilicate (like MgSiO₃ itself), melt with decomposition and liberation of a forsterite crystalline phase. Pyroxenes containing a large amount of ferrous metasilicate melt, with crystallization of tridymite or cristobalite. According to Bowen and Schairer, at liquidus temperatures, pyroxene solutions containing at least 55 mole % FeSiO₃ can exist. At lower temperatures, solid solutions containing up to 84 mole % FeSiO₃ become stable. Noting the prevalence of rhombic and not monoclinic pyroxenes of the MgSiO_3 -- FeSiO₃ series in nature, Bowen indicates that the latter are stable only at high temperatures, and that monoclinic and rhombic pyroxenes are enantiotropic forms, with an

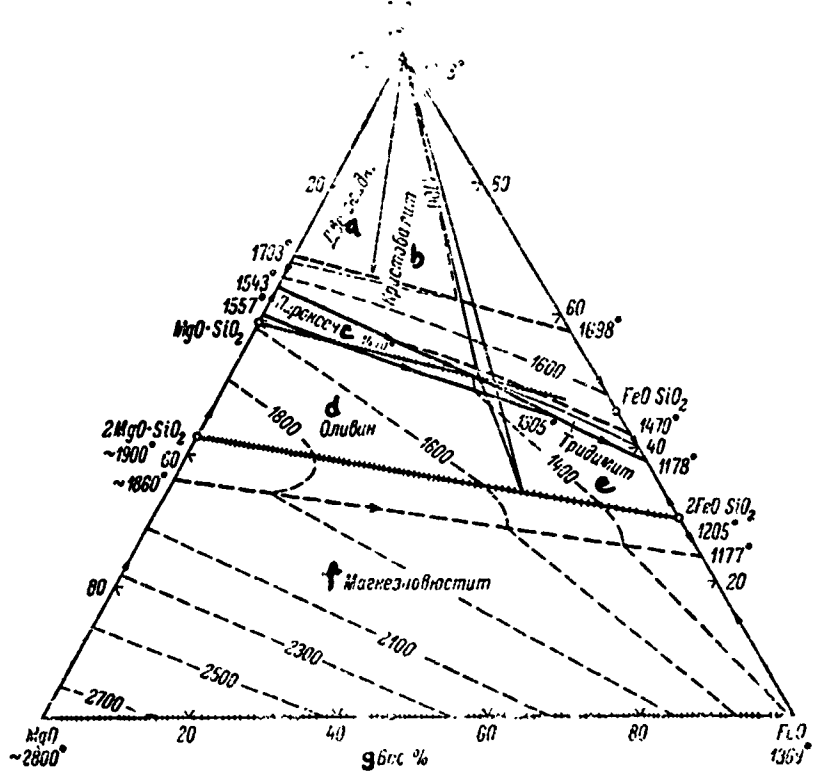


Fig. 96. Phase diagram of $\text{MgO} - \text{FeO} - \text{SiO}_2$ system
(from Osborn and Muan).

Key:

- a. Two liquids
- b. Cristobalite
- c. Pyroxene
- d. Olivine
- e. Tridymite
- f. Magneziowüstite
- g. Weight %

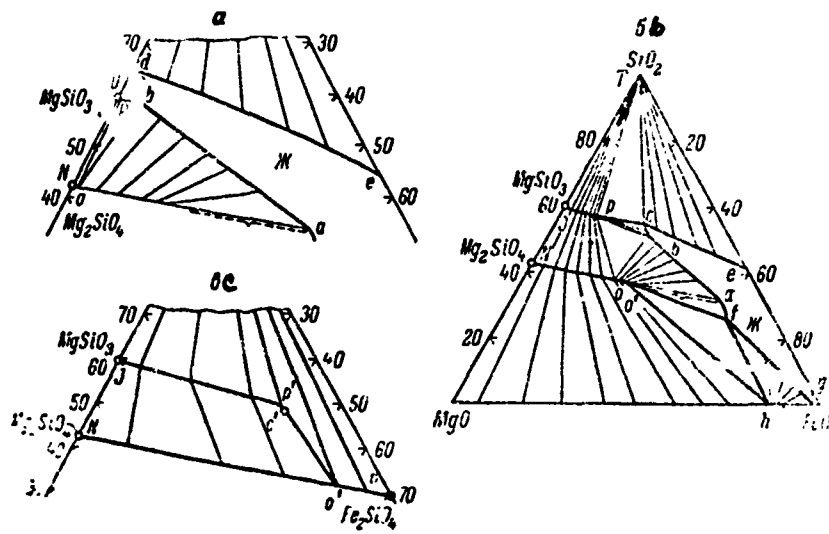


Fig. 97. Diagram of phase relationships of MgO -- "FeO" -- SiO_2 system, for temperatures of 1550 (a), 1450 (b) and 1150° (c)(from Bowen and Schairer).

inversion range of 995-1140°. The temperature of conversion of enstatite (MgSiO_3) into clinoenstatite is 1145°, and it decreases with increase in ferrous oxide content in the crystal solution (Fig. 99). The lowest temperature 995° corresponds to solid solutions, which are richest in iron silicate. A triple eutectic between the olivine, pyroxene and tridymite fields, with a melting temperature of 1305°, has the composition: $\text{MgO} \sim 9$, $\text{FeO} \sim 46$, $\text{SiO}_2 \sim 45$ weight %. Sahama and Torgeson [13] and Mueller [7, 8] have taken up problems of thermodynamic treatment of solid solutions in the $\text{MgO} \sim \text{FeO} \sim \text{SiO}_2$ system. The indices of refraction of the olivine and pyroxene solid solutions are presented in Tables 1 and 2.

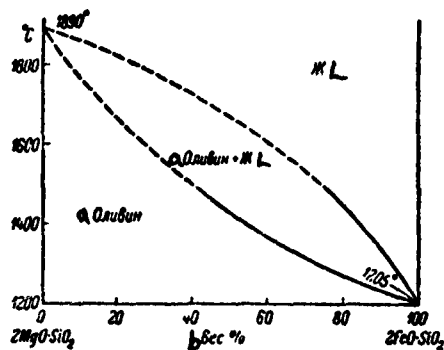


Fig. 98. Phase diagram of partial system $2\text{MgO}\cdot\text{SiO}_2$ -- $2\text{FeO}\cdot\text{SiO}_2$ (from Bowen and Schairer).

Key:

- a. Olivine
- b. Weight %

TABLE 1
INDICES OF REFRACTION OF Mg_2SiO_4 -- Fe_2SiO_4
SOLID SOLUTIONS

Cocration, weight % a. Fe_2SiO_4	N_g	N_m	N_p	$2V^\circ$
100	1.875	1.864	1.824	-47
90	1.848	1.835	1.793	-
75	1.807	1.794	1.762	-
50	1.752	1.738	1.712	-
25	1.709	-	1.671	-
0	1.6688	1.6507	1.6359	+81

Key:

- a. Composition, weight % Fe_2SiO_4

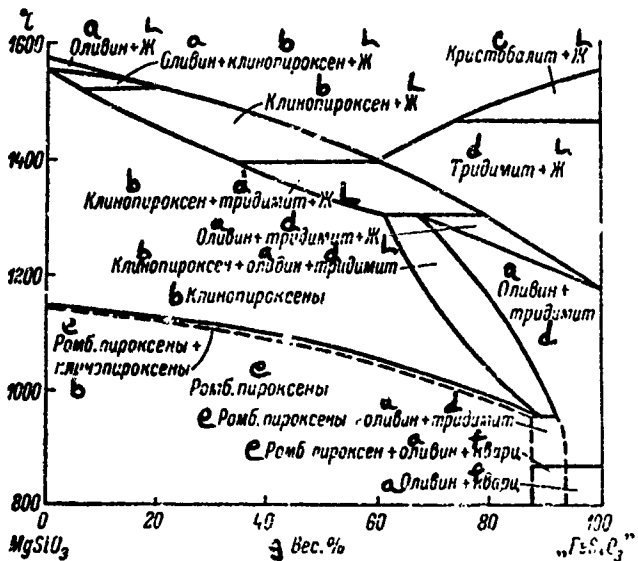


Fig. 99. Phase diagram of partial system MgSiO_3 -- "FeSiO₃"; in some regions of the system, there are no true binaries, as a consequence of the presence of Fe_2O_3 (from Bowen and Schairer).

Key:

- | | |
|------------------|----------------------|
| a. Olivine | e. Rhombic pyroxenes |
| b. Clinopyroxene | f. Quartz |
| c. Cristobalite | g. Weight % |
| d. Tridymite | |

Akimoto and colleagues [2, 3] have shown that, at pressures when iron silicate becomes a stable phase, i. e., 17.4 kbar, there is a continuous series of MgSiO_3 -- FeSiO_3 solid solutions. The pressure at which the corresponding Mg-Fe pyroxenes form can be calculated from the formula $P = 109x - 92$ kbar (where x is the mole fraction of FeSiO_3 in the pyroxene). Thus, for $x = 0.90$, the pressure will be 6 kbar.

TABLE 2
INDICES OF REFRACTION OF $MgSiO_3$ -- $FeSiO_3$
SOLID SOLUTIONS

Состав, вес.% $\approx FeSiO_3$	N_g	N_m	N_p	$2V^\circ$	б Плотность, g/cm^3
0	1.658	1.653	1.650	+31	3.175
13.2	1.675	1.670	1.666	+34	3.20
25.0	~1.700	1.689	1.682	-82	3.37
47.0	1.731	1.728	1.715	-63	3.49
64.2	1.739	1.734	1.723	-48	--
83.7	1.763	1.756	1.746	--	--

Key:

- a. Composition, weight % $FeSiO_3$
- b. Density, g/cm^3

Ringwood and Major [12] have studied transformation of the solid solutions of the $MgSiO_3$ -- $FeSiO_3$ series under high pressure conditions. Pure $FeSiO_3$ at a pressure of 130 kbar is transformed into Fe_2SiO_4 (spinel) and SiO_2 (stishovite). Solid solutions with a high $FeSiO_3$ content (up to a composition $(Mg_{0.5}Fe_{0.5})SiO_3$), at a pressure of 180 kbar, is completely transformed into a mixture of spinel + stishovite. With a higher $MgSiO_3$ content, pyroxene is found, in addition to spinel and stishovite.

Akimoto and Fujisawa [2] have determined the maximum concentration of Fe_2SiO_4 in spinelide and olivine solid solutions $(Mg, Fe)_2SiO_4$. At a temperature of 800° and pressures between 45 and 95 kbar, the mole fraction of Fe_2SiO_4 in the spinel phase equals 0.73 and, in the olivine, 0.37.

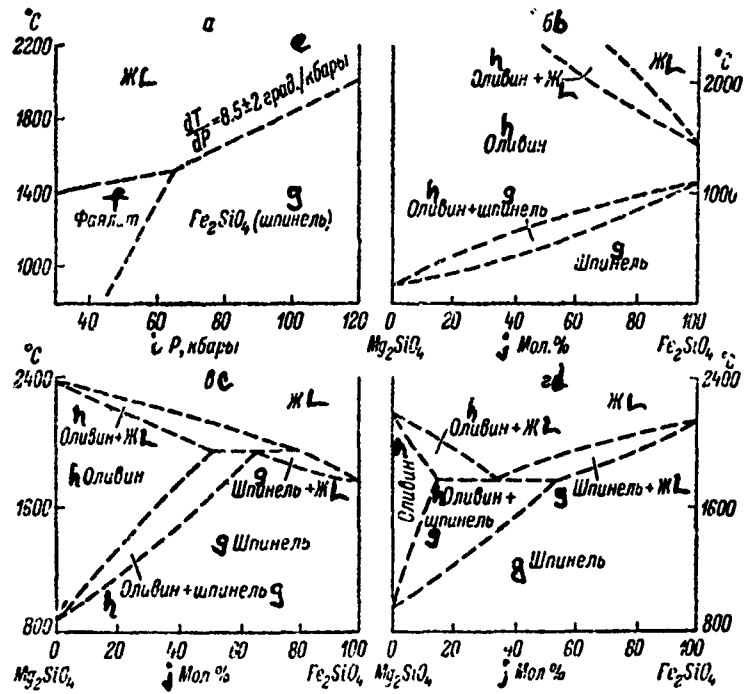


Fig. 100. Phase relationships of partial system Mg_2SiO_4 -- Fe_2SiO_4 at various pressures (from Lindsley): a. $P-t$ diagram for Fe_2SiO_4 ; b. $P \sim 50$ kbar; c. $P \sim 100$ kbar; d. $P \geq 100$ kbar;

Key:

- e. Degree/kbar
- f. Fayalite
- g. Spinel
- h. Olivine
- i. P, kbar
- j. Mole %

A thermodynamic study of the coexisting olivine and pyroxene solid solution has been done by Nafziger and Muan [9]. According to Olsen and Mueller [10], an increase in $MgSiO_3$ content in the solid solution reduces the equilibrium pressure for the reaction forming rhombic pyroxene $(Mg, Fe)SiO_3$ from fayalite and quartz.

Phase equilibrium constants for the system are introduced by Kern and Weisbrod [5].

Bereznoy [1] produced only a provisional triangulation of the system, assuming the coexistence of FeO and Mg_2SiO_4 , as well as of Fe_2SiO_4 and $MgSiO_3$.

BIBLIOGRAPHY

1. Berezhnoy, A. S., Trudy Ukr. inst. ogneuporov, No. 6, 1962, p. 5.
2. Akimoto, Sh., H. Fujisawa, Earth Planetary Sci. Lett., 1, No. 4, 237, 1966.
3. Akimoto, Sh., H. Fujisawa, T. Katsura, Y. Ida, J. Geophys. Res., 70, No. 20, 5269, 1965.
4. Bowen, N. L., J. F. Schairer, Amer. J. Sci., (5), 29, No. 170, 151, 1935.
5. Kern, M. R., M. A. Weisbrod, Thermodynamique de base pour mineralogistes, petrographes et geologues [Basic Thermodynamics for Mineralogists, Petrographers and Geologists], Paris, 1964.
6. Lindsley, D. H., Carnegie Inst. Washington Year Book, 65, 226, 1965-1966.
7. Mueller, R. F., Geochim. cosmochim. acta, 25, No. 4, 287, 1961.
8. Mueller, R. F., Mineral. Magaz., 33, No. 266, 1015, 1964.
9. Nafziger, R. H., A. Muan, Amer. Mineralogist, 52, No. 9-10, 1364, 1967.
10. Olsen, E., R. F. Mueller, J. Geol., 74, No. 5, pt. 1, 620, 1966.
11. Osborn, E. F., A. Muan, in: E. M. Levin, C. R. Robbins, H. F. McMurdie, Phase diagrams for ceramists, USA, Columbus, fig. 682, 1964.

12. Ringwood, A. E., A. Major, Earth Planetary Sci. Lett., 1, No. 5, 351, 1966.

13. Sahama, Th. G., D.R. Torgeson, J. Geol., 57, No. 3, 255, 1949.



The initial data on the system were obtained by Konstantinov and Selivanov [3]. The system has been studied in detail by Bowen and colleagues [5, 16]. Three ternary compounds have been found: $2\text{CaO} \cdot \text{FeO} \cdot 2\text{SiO}_2$, ferruginous ockermanite; $\text{CaO} \cdot \text{FeO} \cdot \text{SiO}_2$, ferruginous monticellite or kirstenite; $\text{CaO} \cdot \text{FeO} \cdot 2\text{SiO}_2$, hedenbergite. The results of Bowen and colleagues are presented in the form of three partial systems: $\text{CaSiO}_3 \text{ -- CaFeSiO}_4$ (Fig. 101), $\text{CaSiO}_3 \text{ -- "FeSiO}_3\text{"}$ (Fig. 102) and $\text{Ca}_2\text{SiO}_4 \text{ -- Fe}_2\text{SiO}_4$ (Fig. 103). Solid solutions formed between the following compounds: hedenbergite and ferruginous monticellite, ferruginous monticellite, fayalite ($2\text{FeO} \cdot \text{SiO}_2$) and dicalcium silicate ($2\text{CaO} \cdot \text{SiO}_2$), hedenbergite and wollastonite ($\text{CaO} \cdot \text{SiO}_2$) and hedenbergite and iron metasilicate ("FeSiO₃").

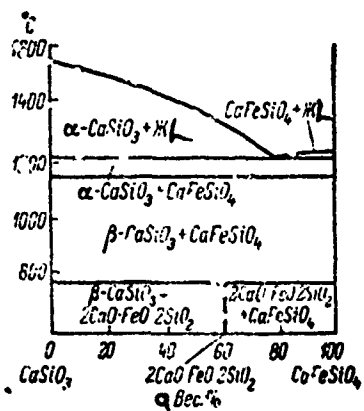


Fig. 101. Phase diagram of partial system $\text{CaO} \cdot \text{SiO}_2 \text{ -- CaO} \cdot \text{FeO} \cdot \text{SiO}_2$ (from Bowen and colleagues).

Kev. a. Weight %

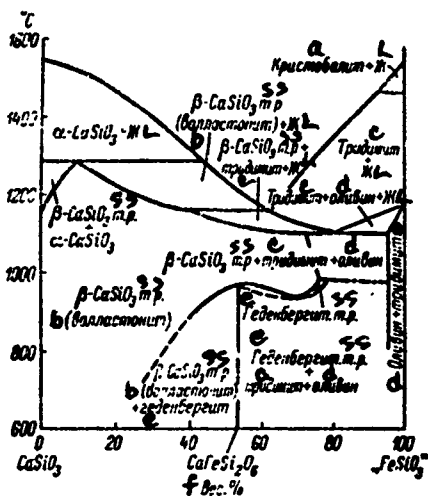


Fig. 102. Phase diagram of partial system $\text{CaO} \cdot \text{SiO}_2$ -- " $\text{FeO} \cdot \text{SiO}_2$ " (from Bowen and colleagues).

Key:

- a. Cristobalite
- b. Wollastonite
- c. Tridymite
- d. Olivine
- e. Hedenbergite
- f. Weight %

Phase diagrams for the partial systems $2\text{CaO} \cdot \text{SiO}_2$ -- FeO and $\text{CaO} \cdot \text{FeO} \cdot \text{SiO}_2$ -- FeO , obtained by Allen and Snow [4], are introduced in Figs. 104 and 105. The data of other authors were taken in plotting these diagrams.

A complete phase diagram of the CaO -- " FeO " -- SiO_2 system, plotted by Osborn and Muan [15], taking account of work performed up to 1960, is presented in Fig. 106.

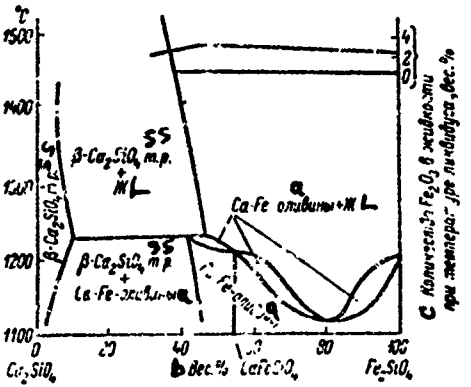


Fig. 103. Phase diagram of calcium-iron olivines $2\text{CaO} \cdot \text{SiO}_2$ -- $2\text{FeO} \cdot \text{SiO}_2$ (from Bowen and colleagues).

Key:

- a. Olivines
- b. Weight %
- c. Amount of Fe_2O_3 in liquid at liquidus temperature, weight %

Lindsley and Munoz [11], in studying the partial system $\text{CaFeSi}_2\text{O}_6$ -- FeSiO_3 , obtained data introducing certain additions to the diagram proposed by Bowen and colleagues. The authors directed attention to the reaction:

$$\text{FeSiO}_3\text{-rich hedenbergite} + \text{FeSiO}_3\text{-poor hedenbergite} = \text{fayalite (olivine)} + \text{quartz (or tridymite)}.$$

The positions of the lines characterizing the equilibrium of this reaction is shown in Fig. 107.

Lindsley and colleagues [10] have studied the hedenbergite solid solution (hedenbergite clinopyroxene) -- wollastonite solid solution inversion, as a function of pressure. Data on the quartz-tridymite inversion were taken from Kennedy and colleagues [8].

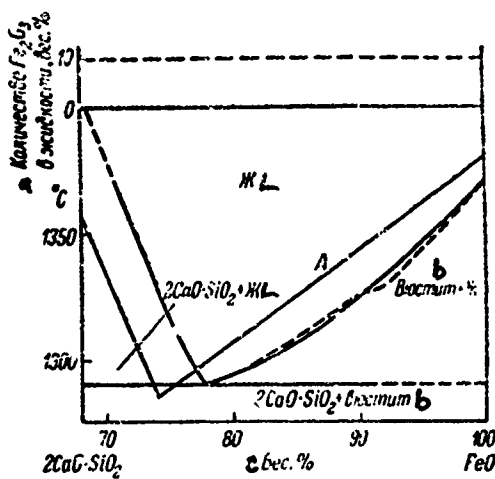


Fig. 104. Phase diagram of partial system
 $2\text{CaO}\cdot\text{SiO}_2$ -- FeO (from Allen and Snow;
 curve A, from Osborne and Muan).

Key:

- a. Amount of Fe_2O_3 in liquid, weight %
- b. Wustite
- c. Weight %

Lindsley [9] has studied the phase transformations of hedenbergite $\text{CaSiO}_3\cdot\text{FeSiO}_3$, as well as the solid solutions of the latter with ferrosillite (FeSiO_3), under high pressure conditions. The results obtained for hedenbergite are presented in Fig. 108. The tests were conducted under conditions of equilibrium with metallic iron, and the presence of Fe_2O_3 was disregarded. A phase diagram of the $\text{CaFeSi}_2\text{O}_6$ -- FeSiO_3 system, for a pressure of 15 kbar, is presented in Fig. 109. The phases which are stable at high pressures (over 10 kbar) are pyroxenoid and clinopyroxene.

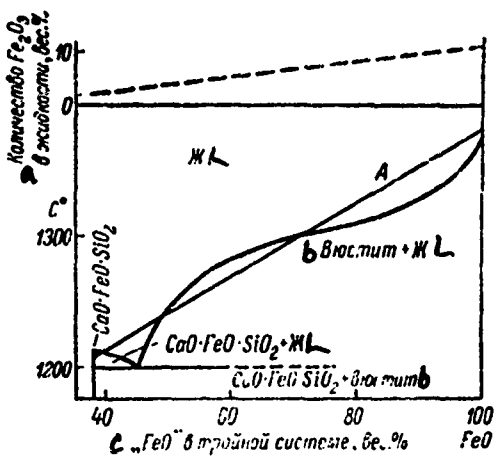


Fig. 105. Phase diagram of partial system
 $\text{CaO} \cdot \text{FeO} \cdot \text{SiO}_2$ -- FeO (from Allen and Snow;
curve A from Schairer).

Key:

- a. Amount of Fe_2O_3 in liquid, weight %
- b. Wüstite
- c. "FeO" in ternary system, weight %

Lindsley and Munoz [12] have studied the subsolidus region of the system $\text{Ca}_{0.50}\text{Fe}_{0.50}\text{SiO}_3$ -- FeSiO_3 , under conditions of reduced (2 kbar and below) and increased (20 kbar) pressures. At 20 kbar, two coexisting pyroxenes, orthopyroxene and clinopyroxene, were found as independent phases. Orthopyroxene has the approximate composition 95 mole % FeSiO_3 + 5 mole % CaSiO_3 . The composition of clinopyroxene under high pressure conditions is variable, and it changes from 60 mole % FeSiO_3 + 40 mole % CaSiO_3 at 800° to 92 mole % FeSiO_3 + 8 mole % CaSiO_3 at 950°.

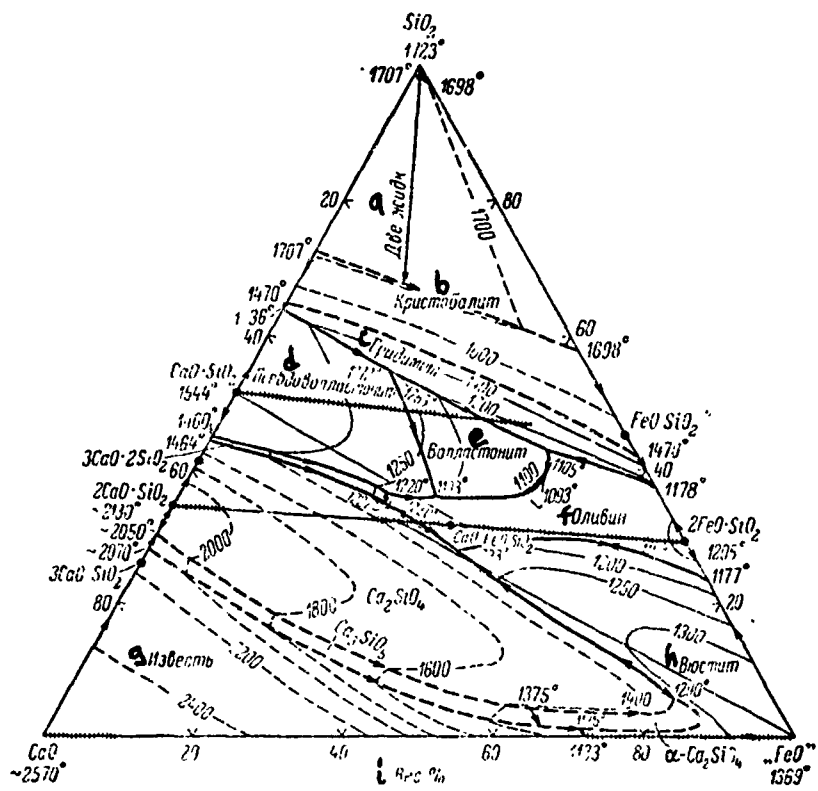


Fig. 106. Phase diagram of CaO -- "FeO" -- SiO₂ system (from Osborn and Muan).

Key:

- | | |
|-----------------------|-------------|
| a. Two liquids | f. Olivine |
| b. Cristobalite | g. Lime |
| c. Tridymite | h. Wüstite |
| d. Pseudowollastonite | i. Weight % |
| e. Wollastonite | |

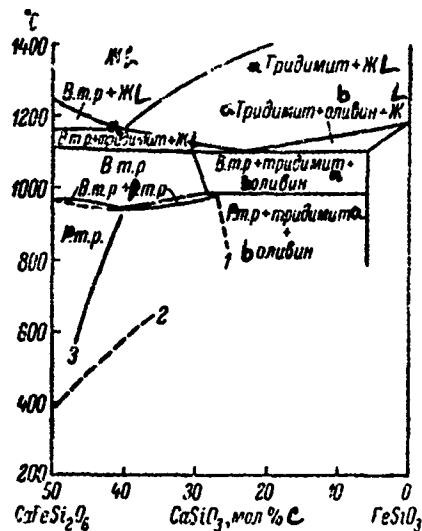


Fig. 107. Phase diagram of partial system $\text{CaFeSi}_2\text{O}_6$ -- FeSiO_3 : B. m. p. wollastonite solid solution; P. m. p. hedenbergite solid solution; 1. from Bowen and colleagues; 2. from Ernst (on the basis of hydrothermal tests); 3. from Lindsley and Muan.

Key:

- a. Tridymite
- b. Olivine
- c. Mole %

Myer and Lindsley [14] have determined the optical properties of solid solutions of the $\text{Ca}_{0.5}\text{Fe}_{0.5}\text{SiO}_3$ -- FeSiO_3 profile, synthesized at pressures of 20 kbar and higher, which permitted reaching pure FeSiO_3 . Lindsley and colleagues [13] have determined the unit cell parameters of solid solutions of the hedenbergite ($\text{Ca}_{0.5}\text{Fe}_{0.5}\text{SiO}_3$) -- ferrosillite (FeSiO_3) profile.

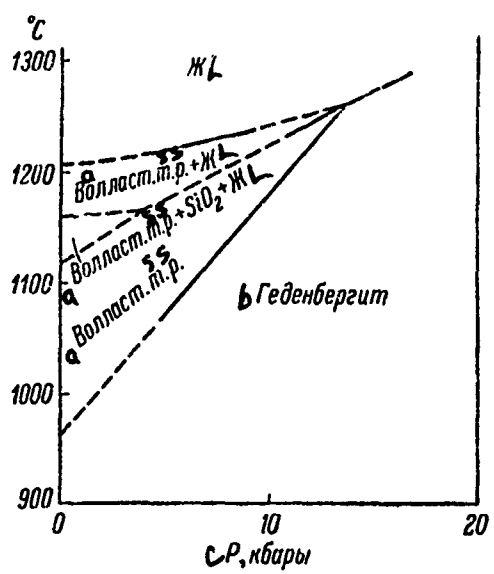


Fig. 108. P-t diagram for hedenbergite
(from Lindsley).

Key:

- a. Wollastonite
- b. Hedenbergite
- c. P, kbar

Bas'yas [1, 2] proposes considering the compound $\text{Ca}_3\text{Fe}(\text{SiO}_4)_2$ (a merwinite analog), in the Ca_2SiO_4 -- Fe_2SiO_4 series of solid solutions, as a chemical individual with a melting temperature of 1250°.

Wyderko and Mazanek [17] have studied the index of refraction, density and microhardness of solid solutions of the isomorphic series Ca_2SiO_4 -- Fe_2SiO_4 (up to a content of 59 weight % Ca_2SiO_4). The indices of refraction decrease from values $\text{Ng} = 1.880$, $\text{Nm} = 1.868$, $\text{Np} = 1.830$ (for pure

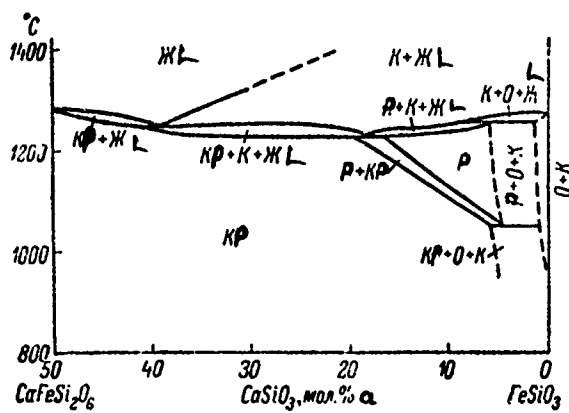


Fig. 109. Phase diagram of partial system hedenbergite -- ferrosillite, for 15 kbar pressure (from Lindsley): K quartz; KP clinopyroxene; O olivine; P pyroxenoid.

Key:

a. Mole %

Fe_2SiO_4) to Ng = 1.732, Nm = 1.720 and Np = 1.685 for the solid solution containing 58.18 weight % Ca_2SiO_4 ; the density decreased correspondingly from 4.29 to 3.40 g/cm³.

Johnson and Muan [7], using data in the literature, plotted an approximate schematic diagram of the phase ratios (coexisting phase triangles) of the CaO -- FeO -- SiO₂ system at 1080° (Fig. 110). The authors determined the activity of the components in the solid solutions of the system at 1080° (study of the equilibrium ratios of CO₂:CO in the presence of metallic iron).

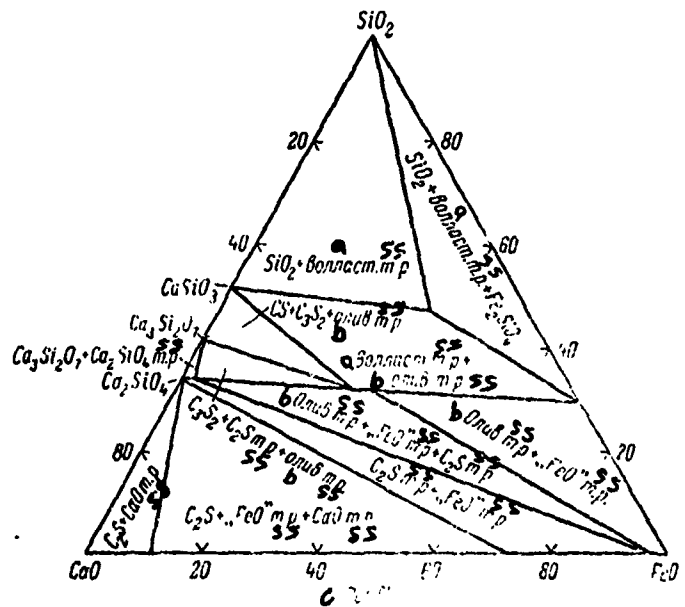


Fig. 110. Diagram of phase relationships of $\text{CaO} - \text{FeO} - \text{SiO}_2$ system in subsolidus region at 1080° (from Johnson and Muan).

Key:

- a. Wollastonite
- b. Olivine
- c. Weight %

CRYSTALLINE PHASES OF CaO -- FeO -- SiO₂ SYSTEM

^a Соединение	^b Система кристаллов	<i>N_g</i>	<i>N_p</i>
2CaO·FeO·2SiO ₂ (железистый окерманит) ^c	Тетрагональ- ^f вая (?)	1.690	1.673
CaO·FeO·SiO ₂ (железистый монтicеллит) ^d	Ромбическая ^g	1.743	1.696
CaO·FeO·2SiO ₂ (гедонбергит) ^e	Моноклинная ^h	1.757	1.732

Key

- a. Compound
- b. Crystal system
- c. Ferruginous ockermanite
- d. Ferruginous monticellite
- e. Hedenbergite
- f. Tetragonal
- g. Rhombic
- h. Monoclinic

BIBLIOGRAPHY

1. Bas'yas, I. P., Trudy 6-go soveshch. no eksper. i tekhn. mineral. i petrogr. [Proceedings, 6th Conference on Experimental and Engineering Mineralogy and Petrography], AN SSSR Press, Moscow, 1962, p. 359.
2. Bas'yas, I. P., Trudy Vostochn. inst. ogneuporov, No. 4, 1963, p. 131.
3. Konstantinov, N. S. and E. P. Selivanov, Izy. SPb. politekhn. inst., 17, 1912, p. 127.
4. Allen, W. C., R. B. Snow, J. Amer. Ceram. Soc., 38, No. 8, 266, 1955.
5. Bowen, N. L., J. F. Schairer, E. Posnjak, Amer. J. Sci., (5), 26, No. 153, 193, 1933.
6. Ernst, W. G., Amer. J. Sci., 264, No. 1, 37, 1966.
7. Johnson, R. E., A. Muan, Trans. Metal. Soc. AIME, 239, No. 12, 1931, 1967.

8. Kennedy, G.C., G. Wasserburg, H.C. Heard, R.C. Newton, Amer. J. Sci., 260, No. 7, 501, 1962.
9. Lindsley, D.H., Carnegie Inst. Washington Year Book, 65, 230, 1965-1966.
10. Lindsley, D.H., G.M. Brown, J.D. Muir, Carnegie Inst. Washington Year Book, 66, 359, 1966-1967.
11. Lindsley, D.H., J.L. Munoz, Carnegie Inst. Washington Year Book, 66, 363, 1966-1967.
12. Lindsley, D.H., J.L. Munoz, Amer. J. Sci., 267A, Schairer vol., 295, 1969.
13. Lindsley, D.H., J.L. Munoz, L.W. Finger, Carnegie Inst. Washington Year Book, 67, 91, 1967-1968.
14. Myer, G.H., D.H. Lindsley, Carnegie Inst. Washington Year Book, 67, 92, 1967-1968.
15. Osborn, E.F., A. Muan, in: E.M. Levin, C.R. Robbins, H.F. McMurdie, Phase diagrams for ceramists, USA, Columbus, fig. 586, 1964.
16. Schairer, J.F., J. Amer. Ceram. Soc., 25, No. 10, 241, 1942.
17. Wyderko, M., E. Mazanek, Mineral. Magaz., 36, No. 283, 955, 1968.



The first study of the system was made by Chizhikov and colleagues [3]. The authors note the presence of trivalent iron in the melt. Ternary compounds were not found.

Dobrotsvetov and colleagues [1, 2], carrying out the melting in sealed iron crucibles, plotted an approximate phase diagram of the partial system Zn_2SiO_4 -- Fe_2SiO_4 . It is seen from Fig. 111 that, at high temperatures, a continuous series of solid solutions forms and that, at decreased temperatures of 850-900°, decomposition of them takes place. The dashed lines indicate the approximate nature of the diagram in this region. At low temperatures,

two solid solution regions exist in the Zn_2SiO_4 -- Fe_2SiO_4 system: 1. a willemite base, with from 0 to 27 weight % Fe_2SiO_4 content and 2. a fayalite base, with from 0 to 25 weight % Zn_2SiO_4 content.

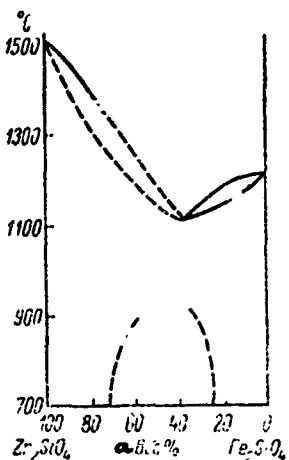


Fig. 111. Phase diagram of partial system Zn_2SiO_4 -- Fe_2SiO_4 (from Dobrotsevov and colleagues).

Key:

a. Weight %

The refraction of willemite increases significantly with inclusion of iron in its structure, from $N_e = 1.717 \pm 0.001$ and $N_o = 1.696 \pm 0.001$ for pure willemite to $N_e = 1.745 \pm 0.002$ and $N_o = 1.715 \pm 0.001$, with a 27 weight % Fe_2SiO_4 content in the solid solution. With inclusion of zinc in the fayalite structure, the index of refraction of the latter decreases noticeably.

BIBLIOGRAPHY

1. Dobrotsvetov, B. L., Vestn. Mock univ., Geologiya, No. 3, 1965, p. 37.
2. Dobrotsvetov, B. L., Ye. I. Bogoslovskaya, Ye. I. Sobel'man, DAN SSSR, 158, 1, 1964, p. 189.
3. Chizhikov, D. M., V. P. Schastlivyy, L. I. Blokhina, Ibid., 129, 6, 1959, p. 1353.



The system has been studied by a number of investigators [1-7, 9, 10].

A three-dimensional model of the phase diagram of the ternary system, from the data of Hay and colleagues [5, 10], is presented in Fig. 112. The region of two immiscible liquids is seen well here, as well as the trough-shaped depression descending from the rhodonite-tephrolite eutectic (1208°) to the fayalite- SiO_2 eutectic (1178°).

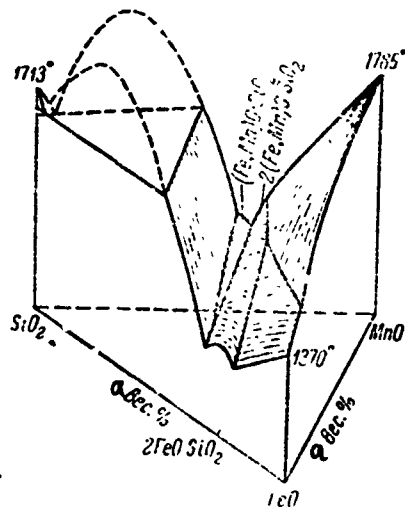


Fig. 112. Three-dimensional model of $\text{MnO} \text{ -- } \text{FeO} \text{ -- } \text{SiO}_2$ system (from Hay and colleagues).

Key: a. Weight %

A phase diagram of the $\text{MnO} - \text{FeO} - \text{SiO}_2$ system, according to Maddocks [6], is introduced in Fig. 113. The triple eutectic has the composition $\text{FeO} = 50$, $\text{MnO} = 20$ and $\text{SiO}_2 = 30$ weight % and a temperature of 1170° . The composition $\text{FeO} = 36$, $\text{MnO} = 36$, $\text{SiO}_2 = 28$ weight % corresponds to the point of the ternary pseudocompound knebelite, which enters the solid solution region and is, as Maddocks thinks, tephrolite saturated with fayalite.

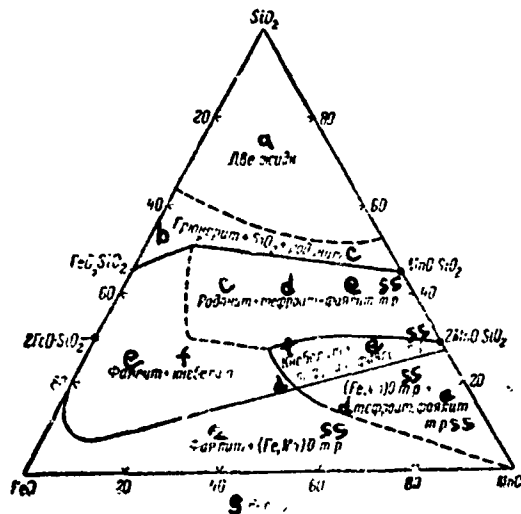


Fig. 113. Phase diagram of $\text{MnO} - \text{FeO} - \text{SiO}_2$ system (from Maddocks).

Key:

- Two liquids
- Grunerite
- Rhodonite
- Tephroite
- Fayalite
- Knebelite
- Weight %

A possible diagram of the partial system "FeO·SiO₂" -- MnO·SiO₂, according to White [10], is given in Fig. 114. Since pure FeSiO₃ does not exist, tridymite and olivine are distinguished in the left side of the profile instead of it.

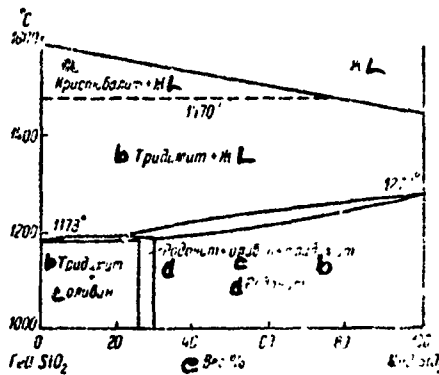


Fig. 114. Hypothetical phase diagram of partial system "FeO·SiO₂" -- MnO·SiO₂ (from White).

Key:

- a. Cristobalite
- b. Tridymite
- c. Olivine
- d. Rhodonite
- e. Weight %

A phase diagram for the orthosilicate profile, according to Carter *et al* is presented in Fig. 115. Fayalite and tephrolite form a continuous series of solid solutions. Judging from this diagram, knebelite should be one of the members of the solid solution, and not an independent compound. However, the temperatures of the start and end of melting of the solid solutions in this

system are difficult to determine accurately; therefore, Carter et al accept a modified phase diagram for the orthosilicate profile.

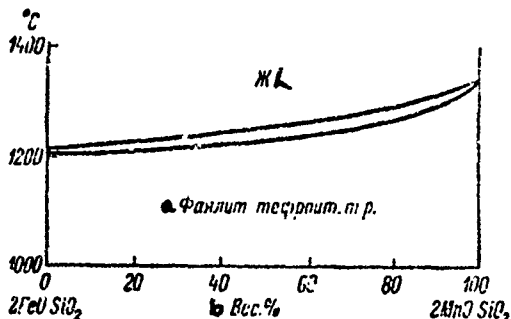


Fig. 115. Phase diagram of partial system $2\text{FeO}\cdot\text{SiO}_2$ -- $2\text{MnO}\cdot\text{SiO}_2$ (from Carter and colleagues).

Key:

- a. Fayalite-tephroite solid solution
- b. Weight %

Scimar [9], applying the laws of thermodynamics to the existing data in the literature for the FeO -- MnO -- SiO_2 system, determined the shape and position of the isoactivity curves of FeO , MnO and SiO_2 in this system, which is important for study of the equilibrium between liquid steel and slag.

Riboud and Muan [7] have studied the phase ratios in the $2\text{FeO}\cdot\text{SiO}_2$ -- $\text{FeO}\cdot\text{SiO}_2$ -- $\text{MnO}\cdot\text{SiO}_2$ -- $2\text{MnO}\cdot\text{SiO}_2$ region and the iron oxide ("FeO") -- $\text{MnO}\cdot\text{SiO}_2$ system, by the quenching method, under strongly reducing conditions, in a mixture of gases consisting of equal parts of CO_2 and H_2 . The liquidus

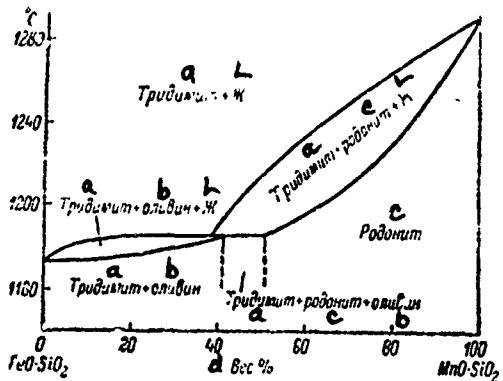


Fig. 116. Diagram of phase ratios for $\text{FeO} \cdot \text{SiO}_2$ -- $\text{MnO} \cdot \text{SiO}_2$ profile (from Riboud and Muaz).

Key:

- a. Tridymite
- b. Olivine
- c. Rhodonite
- d. Weight %

and solidus temperatures of the majority of the mixtures studied were between 1173 and 1345°. A diagram of the phase ratios for the $\text{FeO} \cdot \text{SiO}_2$ -- $\text{MnO} \cdot \text{SiO}_2$ profile is given in Fig. 116. The diagram in Fig. 117 represents a projection of the liquidus surface of part of the $\text{FeO} \cdot \text{MnO} \cdot \text{SiO}_2$ system in a CO_2 and H_2 (1:1) atmosphere. Fig. 118 illustrates the phase ratios for a series of isothermal sections in the $\text{FeO} \cdot \text{MnO} \cdot \text{SiO}_2$ system, in an atmosphere of a mixture of CO_2 and H_2 (1:1).

Cameron [2] has plotted an equilibrium diagram of the oxygen potentials in the $\text{Fe} \cdot \text{Mn} \cdot \text{Si} \cdot \text{O}$ system at 1600°.

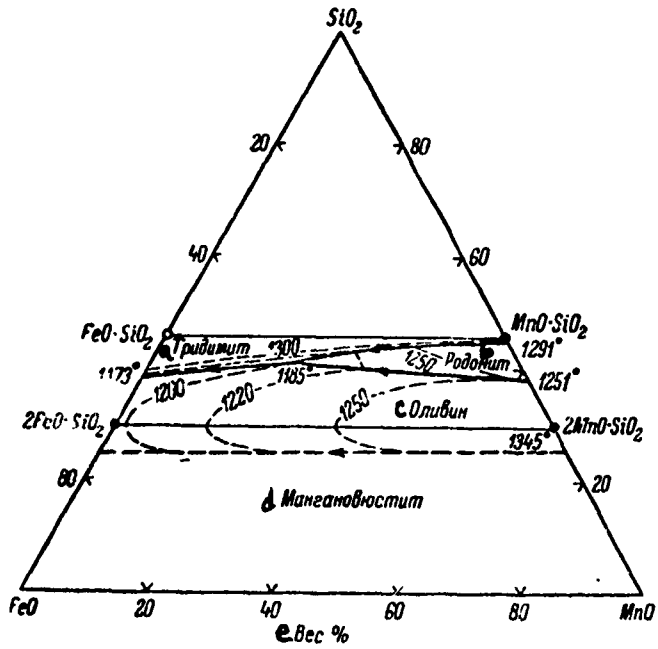


Fig. 117. Phase diagram of part of $\text{FeO} - \text{MnO} - \text{SiO}_2$ system in atmosphere containing CO_2 and H_2 in a 1:1 ratio (from Riboud and Muan).

Key:

- a. Tridymite
- b. Rhodonite
- c. Olivine
- d. Manganowüstite
- e. Weight %

Schwerdtfeger and Muan [8], determining the CO/CO_2 equilibrium ratio in the gas phase, coexisting with a system of oxides and metallic iron, found the activity of the components of the olivine ($\text{Fe}_2\text{SiO}_4 - \text{Mn}_2\text{SiO}_4$) and pyroxenoid ($\text{FeSiO}_3 - \text{MnSiO}_3$) solid solutions.

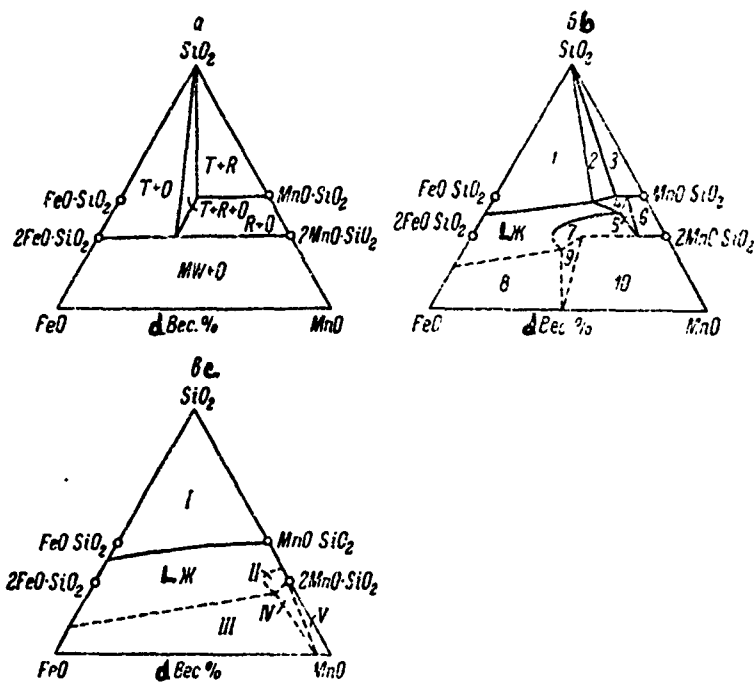


Fig. 118. Phase relationships in $\text{FeO} - \text{MnO} - \text{SiO}_2$ system, in an atmosphere containing CO_2 and H_2 in a 1:1 ratio (from Riboud and Muan): a. 1170° , b. 1240° , c. 1300° ; T. tridymite, R. rhodonite solid solution, O. olivine solid solution, MW. manganowüstite solid solution; 1. T + liquid, 2. T + R + liquid, 3. T + R, 4. R + liquid, 5. R + O + liquid, 6. R + O, 7. O + liquid, 8. MW + liquid, 9. O + MW + liquid, 10. O + MW; I. T + liquid, II. O + liquid, III. MW + liquid, IV. O + MW + liquid, V. O + MW.

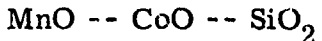
Key:

d. Weight %

BIBLIOGRAPHY

1. Usov, M.A., Izv. SPb. politekhn. inst., No. 19, 1913, p. 542.
2. Cameron, D.J., Trans. Metal. Soc. AIME, 224, No. 6, 1285, 1962.
3. Carter, P.T., A.B. Murad, R. Hay, J. West. Scotl. Iron a. Steel Inst., 60, No. 450, 123, 1953.
4. Dukelow, D.A., G. Derge, Trans. Metal. Soc. AIME, 218, No. 1, 136, 1960.
5. Hay, R., J. White, A.B. McIntosh, Iron Coal Trade Rev., 1, 200, 1935; J. West. Scotl. Iron a. Steel Inst., 42, 99, 1934-1935.
6. Maddocks, W.R., Iron a. Steel Inst., Carnegie Scholarship Memoirs, 24, No. 1, 51, 1935.
7. Riboud, P.V., A. Muan, Trans. Metal. Soc. AJME, 224, No. 2, 26, 1962.
8. Schwerdtfeger, K., A. Muan, Trans. Metal. Soc. AIME, 236, No. 2, 201 1956.
9. Scimar, R., Rev. Univ. Mines de la Metal., Mecanique d. Travaux Publics, 18, No. 9, 602, 1962.
10. White, J., J. Iron a. Steel Inst., 148, No. 11, 579, 1943.

COBALT SILICATE SYSTEMS



The presence of three series of solid solutions is characteristic of the system: $(\text{Mn}, \text{Co})\text{O}$, $(\text{Mn}, \text{Co})_2\text{SiO}_4$ and $(\text{Mn}, \text{Co})\text{SiO}_3$. Biggers and Muan [1] have investigated the "activity-composition" for the orthosilicate and metasilicate solid solutions at 1200 and 1250° (study of equilibria in the presence of metallic cobalt and a gas phase of a known oxygen potential¹). The authors present a schematic phase diagram for 1200° (Fig. 119).

A partial Mn_2SiO_4 -- Co_2SiO_4 section is characterized by a continuous series of solid solutions. The solid solutions in the MnSiO_3 -- CoSiO_3 section are limited, since CoSiO_3 is unstable at normal pressure.

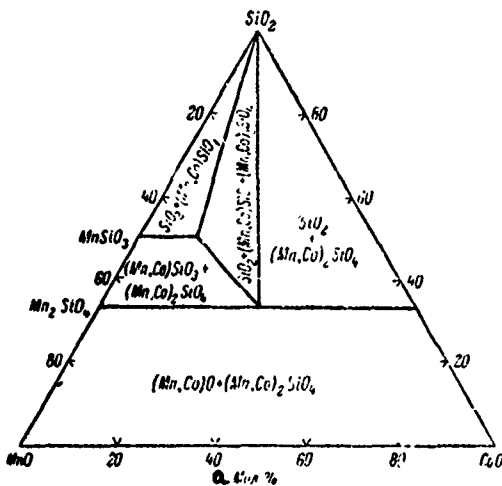


Fig. 119. Diagram of phase relationships of MnO -- CoO -- SiO_2 system in the sub-solidus region at 1200° (from Biggers and Muan).

Key:

a. Mole %

BIBLIOGRAPHY

1. Biggers, J. V., A. Muan, J. Amer. Ceram. Soc., 50, No. 5, 230, 1967.

NICKEL SILICATE SYSTEMS



The system has been partially studied by Grigor'yev [1, 2], Dilaktorskiy [3, 4] and Ringwood [7]. According to Grigor'yev, forsterite (Mg_2SiO_4) dissolves 8.52 weight % Ni_2SiO_4 , and enstatite (MgSiO_3) dissolves 11.8 weight % NiSiO_3 . According to Dilaktorskiy, NiSiO_3 is included in the solid solution of clinoenstatite (MgSiO_3) in the amount of 12-15 weight % and of diopside ($\text{CaMgSi}_2\text{O}_6$), up to 15-18 weight %, and Mg and Ni olivines form a continuous series of solid solutions.

An approximate diagram of the Ni_2SiO_4 -- Mg_2SiO_4 partial system obtained by Ringwood is depicted in Fig. 120; the components form a continuous series of solid solutions. Between 50 weight % Ni_2SiO_4 + 50 weight % Mg_2SiO_4 and 100 weight % Mg_2SiO_4 , the system is truly binary, with type I Roseboom melting. Between 50 weight % Ni_2SiO_4 + 50 weight % Mg_2SiO_4 and 100 weight % Ni_2SiO_4 , the olivine solid solutions melt incongruently, with release of NiO. Within these limits, the three-phase field exists above the solidus, in which NiO and solid solutions of Ni_2SiO_4 -- Mg_2SiO_4 are in equilibrium with the liquid. Within these limits, the composition of the liquid

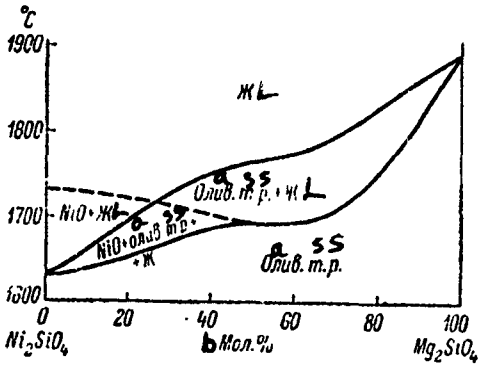


Fig. 120. Phase diagram of partial system
 Ni_2SiO_4 -- Mg_2SiO_4 (from Ringwood).

Key:

- a. Olivine
- b. Mole %

phase is not determined from the diagram. The upper boundary of the NiO field is determined only provisionally (dashed line), as a consequence of absorption of nickel by the platinum-rhodium heater at high temperatures.

The indices of refraction (Ng and Np) change linearly, as a function of the composition of the Ni_2SiO_4 -- Mg_2SiO_4 solid solutions (mole %). Some small deviations from the rectilinear curve is explained by sample nonuniformity.

Hayashi and Naka [6], studying the $\text{MgO} \text{-- CoO} \text{-- NiO} \text{-- SiO}_2$ system, note limited solubility of NiSiO_3 in MgSiO_3 , reaching up to 15-20 mole % NiSiO_3 .

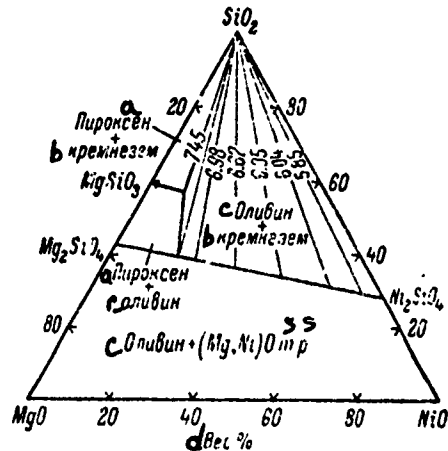


Fig. 121. Diagram of phase relationships of $MgO - NiO - SiO_2$ system in the sub-solidus region at 1400° (from Campbell and Roedder): The figures are values of $\log f_{O_2}$ for equilibrium between nickel and the condensed phase.

Key:

- a. Pyroxene
- b. Silica
- c. Olivine
- d. Weight %

Campbell and Roedder [5], annealing a mixture of MgO , NiO and SiO_2 at 1400° , observed (besides silica) three types of solid solutions: between MgO and NiO , between Mg_2SiO_4 and Ni_2SiO_4 and a pyroxene solid solution (Fig. 121).

Schwab [8] showed that, by means of rapid quenching of a melt from a temperature of $1600-1650^\circ$, pyroxene of a yellow color can be obtained,

containing 50 mole % NiSiO_3 . Crystals of $\text{MgNiSi}_2\text{O}_6$, of the monoclinic crystal system, had $\text{Ng} = 1.731$, $\text{Nm} = 1.728$, $\text{Np} = 1.719$, $2V = 39^\circ$. The $\text{Mg}_2\text{Si}_2\text{O}_6$ -- $\text{MgNiSi}_2\text{O}_6$ partial system, according to Schwab, is presented in Fig. 122. The stability temperature of rhombic mangesium-nickel enstatite increases in increase in NiSiO_3 content, i.e., the Ni^{2+} ion favors the rhombic structure: the maximum thermal stability is achieved at a 12.5 mole % NiSiO_3 content. Below this, a quantity of rhombic enstatite changes to β clinoenstatite, and dissociation into olivine and cristobalite takes place above. For conversion of pure, rhombic MgSiO_3 into β clinoenstatite, a temperature of 1140° is obtained by extrapolation. The protoenstatite region of the solid solutions, expanding somewhat with increase in temperature, is limited to a content of 5 mole % NiSiO_3 over all, above which this modification is not found.

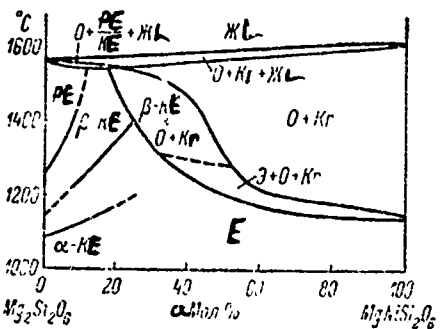


Fig. 122. Phase diagram of partial system $\text{Mg}_2\text{Si}_2\text{O}_6$ -- $\text{MgNiSi}_2\text{O}_6$ (from Schwab):
PE protoenstatite, KE clinoenstatite, E
enstatite, O olivine, Kr cristobalite.

Key:

a. Mole %

Schwab notes a considerable region of coexistence of pyroxene and amphibole; the distribution factor of Ni^{2+} and Mg^{2+} in the coexisting pyroxene -- olivine association depends on the temperature and oxygen partial pressure (the corresponding data are introduced).

BIBLIOGRAPHY

1. Grigor'yev, D. P., Byull. Mosk. obshch. ispyt. prir., otd. geol., 15, 2, 1937, p. 145.
2. Grigor'yev, D. F., Zap. Min. obshch., 67, 1, 1938, p. 63.
3. Dilaktorskiy, N. L., Ibid., 69, 1, 1940, p. 450.
4. Dilaktorskiy, N. L., Trudy 3-go soveshch. po eksper. mineral. i petrogr. [Proceedings, 3d Conference on Experimental Mineralogy and Petrography], AN SSSR Press, Moscow, 1940, p. 79.
5. Campbell, F. E., P. Roedder, Amer. Mineralogist, 53, No. 1-2, 257, 1968.
6. Hayashi, H., S. Naka, J. Mineral. Soc. Japan, 6, 277, 1963.
7. Ringwood, A. E., Geochim. cosmochim. acta, 10, No. 5-6, 297, 1956.
8. Schwab, R. G., Neues Jahrb. Mineral., Monatshefte, No. 10, 337, 1968.



In study of the system, Biggar [1] used coagel, precipitated from a mixed solution of calcium and magnesium nitrates and ammonium tetractyl silicate. Samples were annealed at 1340, 1390, 1475 and 1550°, in platinum capsules, and they were quenched in water. The phase diagram presented in Fig. 123 was obtained by extrapolation from data for the four temperatures indicated. The phase relationships for 1340 and 1475° are shown in Fig. 124.

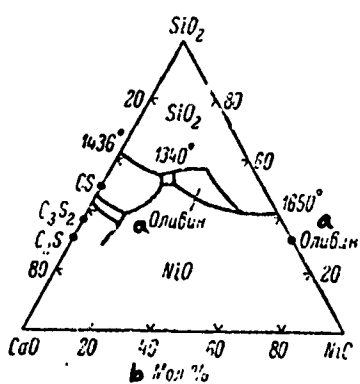


Fig. 123. Approximate phase diagram of
CaO -- NiO -- SiO₂ system (from Biggar).

Key:

- a. Olivine
- b. Mole %

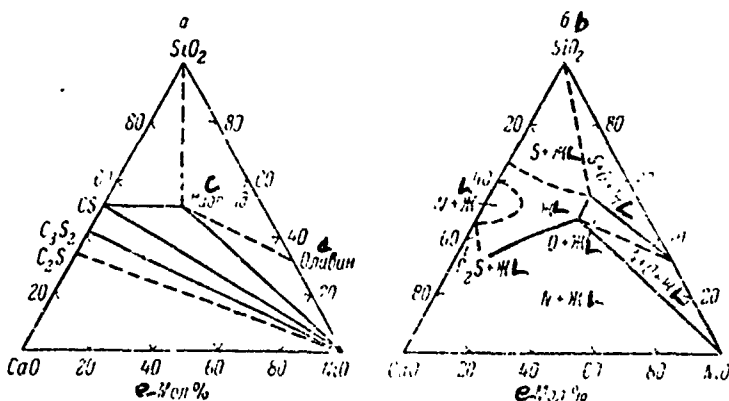


Fig. 124. Diagram of phase relationships in
CaO -- NiO -- SiO₂ system (from Biggar):
a. 1340°, b. 1475°; O. nickel olivine.
N. pseudowollastonite.

Key:

- c. Niopside
- d. Olivine
- e. Mole %

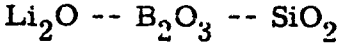
The existence of the ternary compound $\text{CaNiSi}_2\text{O}_6$, first described by Gjessing [2], has been confirmed. Biggar considers this compound to be an analog of diopside, and he calls it niopside. The compound CaNiSiO_4 (monticellite analog), as Santoro and Newnham have already pointed out [3], does not exist in the system.

Biggar introduces a small niopside field in the figure, noting that the four ternary melting reactions observed here take place in the 1340-1360° range. Niopside $\text{CaNiSi}_2\text{O}_6$ coexists with SiO_2 , CaSiO_3 , Ni_2SiO_4 and NiO . Nickel monoxide coexists in the subsolidus region with CaSiO_3 , $\text{Ca}_3\text{Si}_2\text{O}_7$ and Ca_2SiO_4 .

BIBLIOGRAPHY

1. Biggar, G. M., J. Amer. Ceram. Soc., 52, No. 6, 316, 1969.
2. Gjessing, L., Norsk. Geol. Tidskr., 20, No. 3-4, 265, 1940.
3. Santoro, R. P., R. E. Newnham, Acta crystallogr., 22, No. 3, 344, 1967.

BOROSILICATE SYSTEMS



The system has been studied by Sastry and Hummel [1, 2], by the quenching method and by means of carrying out solid state reactions. Three partial eutectic systems are presented, with indication of the composition and melting temperature of the eutectics: $\text{Li}_2\text{O}\cdot\text{SiO}_2 \text{-- } \text{Li}_2\text{O}\cdot\text{B}_2\text{O}_3$ (~ 20 weight % $\text{Li}_2\text{O}\cdot\text{SiO}_2$, $810 \pm 4^\circ$), $\text{Li}_2\text{O}\cdot\text{SiO}_2 \text{-- } \text{Li}_2\text{O}\cdot 2\text{B}_2\text{O}_3$ (~ 40 weight % $\text{Li}_2\text{O}\cdot\text{SiO}_2$, $787 \pm 4^\circ$), $\text{Li}_2\text{O}\cdot 2\text{SiO}_2 \text{-- } \text{Li}_2\text{O}\cdot 2\text{B}_2\text{O}_3$ (~ 50 weight % $\text{Li}_2\text{O}\cdot 2\text{SiO}_2$, $770 \pm 4^\circ$) and the $\text{SiO}_2 \text{-- } \text{Li}_2\text{O}\cdot 2\text{B}_2\text{O}_3$ system (Fig. 125). The existing phases are presented in the triple diagram (Fig. 126), but the fields of the separate compounds are only partially and approximately outlined. Ternary compounds are not noted. A quite extensive region of immiscible liquids, studied by Sastry and Hummel [2], is observed.

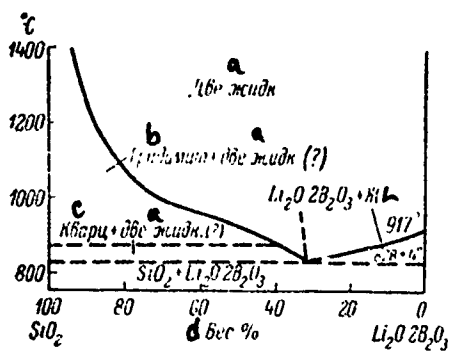


Fig. 125. Phase diagram of partial system
 SiO_2 -- $\text{Li}_2\text{O} \cdot 2\text{B}_2\text{O}_3$ (from Sastry and Hummel).

Key:

- a. Two liquids
- b. Tridymite
- c. Quartz
- d. Weight %

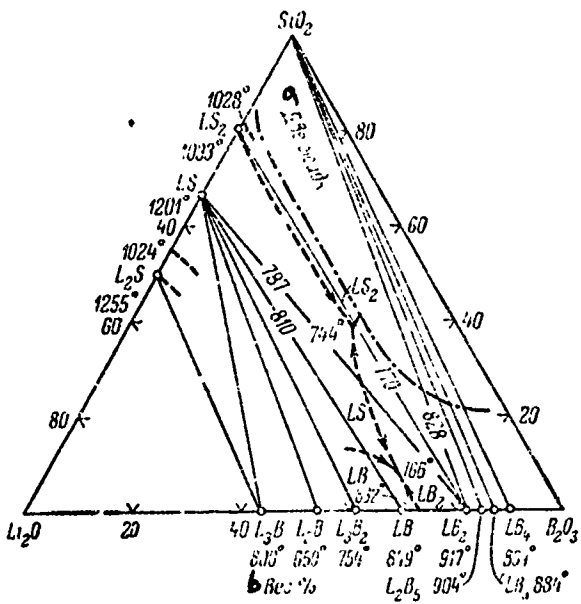


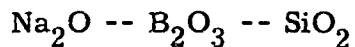
Fig. 126. Diagram of phase relationships of $\text{Li}_2\text{O} - \text{B}_2\text{O}_3 - \text{SiO}_2$ system (from Sastry and Hummel).

Key:

- a. Two liquids
 - b. Weight %

BIBLIOGRAPHY

1. Sastry, B. S. R., F. A. Hummel, J. Amer. Ceram. Soc., 42, No. 2, 81, 1959.
 2. Sastry, B. S. R., F. A. Hummel, J. Amer. Ceram. Soc., 43, No. 1, 23, 1960.



The system has been studied by Morey [2] by the quenching method. He encompassed the region with a Na_2O content below 50 weight %. The existence of one ternary compound, the composition $\text{Na}_2\text{O} \cdot \text{B}_2\text{O}_3 \cdot 2\text{SiO}_2$, melting at 766°,

like danburite ($\text{CaO} \cdot \text{B}_2\text{O}_3 \cdot 2\text{SiO}_2$), has been established. The field of the ternary compound is not plotted in Fig. 127; it is possible that it is located, in the form of a narrow strip, along the boundary separating the $\text{Na}_2\text{O} \cdot \text{B}_2\text{O}_3$ and SiO_2 phases. This compound could be obtained hydrothermally, by heating glass of a composition $\text{Na}_2\text{O} \cdot 2\text{SiO}_2$ with boric acid in a bomb at 500°.

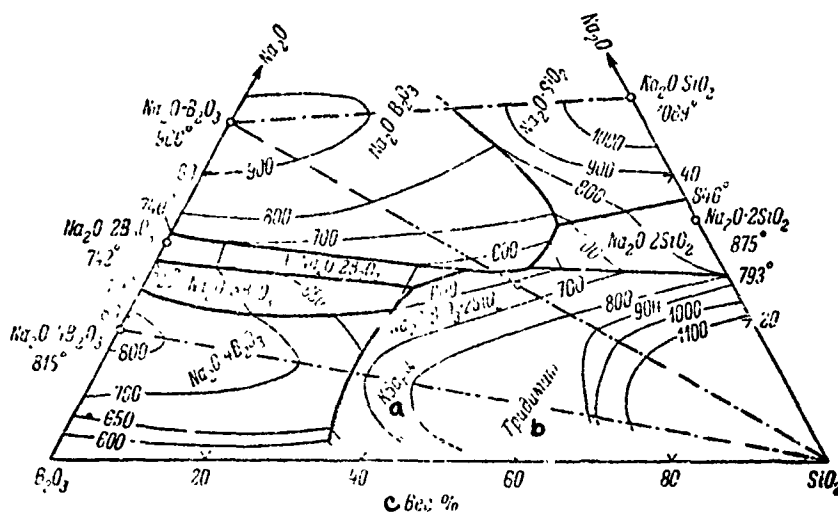


Fig. 127. Phase diagram of $\text{Na}_2\text{O} - \text{B}_2\text{O}_3 - \text{SiO}_2$ system (from Morey).

Key:

- a. Quartz
- b. Tridymite
- c. Weight %

The partial system $\text{Na}_2\text{O} \cdot 4\text{B}_2\text{O}_3 - \text{SiO}_2$ also was studied by Rockett and colleagues [3]; the data for it are presented in Fig. 128. According to the latter authors, the eutectic in this binary system is at 730°, instead of 675° according to Morey.

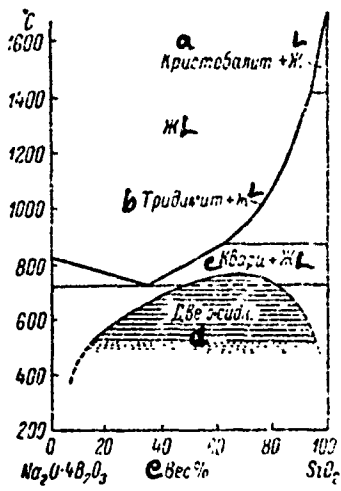


Fig. 128. Phase diagram of partial system $\text{Na}_2\text{O} \cdot 4\text{B}_2\text{O}_3$ -- SiO_2 (from Rockett and colleagues).

Key:

- a Cristobalite
- b. Tridymite
- c. Quartz
- d. Two liquids
- e. Weight %

Morey did not find separation of the liquid phases in the system.

Rockett and colleagues found a metastable liquation in examination of glass of the $\text{Na}_2\text{O} \cdot 4\text{B}_2\text{O}_3$ -- SiO_2 profile. The glasses were kept for a long time (up to 50 hours) at a temperature a little below the liquidus curve, then they were quenched and examined under the electron microscope. The metastable liquation region is shown in Fig. 128. At the maximum, the SiO_2 content is 60-70 weight %, temperature 755°.

Tishura [1], as a result of thermodynamic calculations of the isobaric potentials of formation of the compound in the system, obtained a coexisting phase triangle in the subsolidus region. All eight fields in the diagram are three-phase.

INVARIANT POINTS OF $\text{Na}_2\text{O} - \text{B}_2\text{O}_3 - \text{SiO}_2$ SYSTEM

a Фазы	b Процес	c Состав, вес. %			d Темпера- тура, °C
		Na ₂ O	B ₂ O ₃	SiO ₂	
Двойные инвариантные точки					
Na ₂ O·B ₂ O ₃ + Na ₂ O·2B ₂ O ₃ + жидкость f	Эвтектика	32	68	—	740
Na ₂ O·2B ₂ O ₃ + Na ₂ O·3B ₂ O ₃ + жидкость f	»	27.7	72.3	—	722
Na ₂ O·3B ₂ O ₃ + Na ₂ O·4B ₂ O ₃ + жидкость f	Реакция	24	76	—	766
Na ₂ O·B ₂ O ₃ + Na ₂ O·SiO ₂ + жидкость f	Эвтектика	18.9	23.6	27.5	833
Na ₂ O·B ₂ O ₃ + SiO ₂ + жидкость f	»	26.9	31.1	42.0	530
Na ₂ O·SiO ₂ + SiO ₂ + жидкость f	»	42.2	55.3	32.5	675
Тройные инвариантные точки					
Na ₂ O·B ₂ O ₃ + Na ₂ O·2SiO ₂ + Na ₂ O·SiO ₂ + жидкость f	Реакция	33.0	18.0	49.0	640
Na ₂ O·B ₂ O ₃ + Na ₂ O·2SiO ₂ + SiO ₂ + жидкость f	Эвтектика	27.0	25.0	48.0	520
Na ₂ O·B ₂ O ₃ + Na ₂ O·2B ₂ O ₃ + SiO ₂ + жидкость f	»	27.0	33.0	40.0	520
Na ₂ O·3B ₂ O ₃ + SiO ₂ + Na ₂ O·4B ₂ O ₃ + жидкость f	Реакция	21.0	45.0	34.0	600

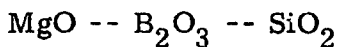
Key:

- a. Phases
- b. Process
- c. Composition, weight %
- d. Temperature, °C
- e. Double invariant points
- f. Liquid
- g. Eutectic
- h. Reaction
- i. Triple invariant point.

Sasaki and colleagues [4] studied the effect of pressures up to 1000 kgf/cm² on phase separation of the glasses (metastable liquation under nonequilibrium conditions), containing 60 and 70 mole % SiO₂ and from 2.5 to 10.0 mole % Na₂O. A decrease in immiscibility temperature always was observed with increase in temperature.

BIBLIOGRAPHY

1. Tishura, T.A., Ukransk. khim. zhurn., 34, 5, 1968, p. 469.
2. Morey, G.W., J. Soc. Glass Techn., 35, No. 167, 270, 1951.
3. Rockett, T.J., W.R. Foster, R.J. Ferguson, J. Amer. Ceram. Soc., 48, No. 6, 329, 1965.
4. Sasaki, T., A. Makishima, T. Sakaino, J. Ceram Assoc. Japan, 77, No. 881, 31, 1969.



The system has been studied by Kuzel [1] by the quenching method. Ternary compounds were not found. A broad region of immiscibility of the liquids is characteristic. The fields of cristobalite, protoenstatite and magnesium pyroborate are overlaid by the region of immiscibility of the melts. There also should be a B₂O₃ crystallization field. The phase diagram of the system is presented in Fig. 129. Kuzel determined compositions of the separating liquids. As two examples, we present the composition of the coexisting liquids for two initial mixtures, one rich in boron oxide and the other rich in silica. With the initial composition MgO -- 18.0, B₂O₃ -- 77.0 and SiO₂ -- 5.0 weight %, the heavy melt has the composition MgO -- 34.5, B₂O₃ -- 63.2, SiO₂ -- 2.3 weight %; the light melt MgO -- 0.6, B₂O₃ -- 91.9, SiO₂ -- 7.5 weight %; the temperature of the coexisting liquids is 1180°. With the initial composition

$\text{MgO} \sim 18.0$, $\text{B}_2\text{O}_3 \sim 13.0$, $\text{SiO}_2 \sim 69.0$ weight %, the heavy melt has the composition $\text{MgO} \sim 37.6$, $\text{B}_2\text{O}_3 \sim 20.2$, $\text{SiO}_2 \sim 42.2$ weight %; the light melt, $\text{MgO} \sim 8.5$, $\text{B}_2\text{O}_3 \sim 9.0$, $\text{SiO}_2 \sim 82.5$ weight %; the temperature of the coexisting liquids is 1300° .

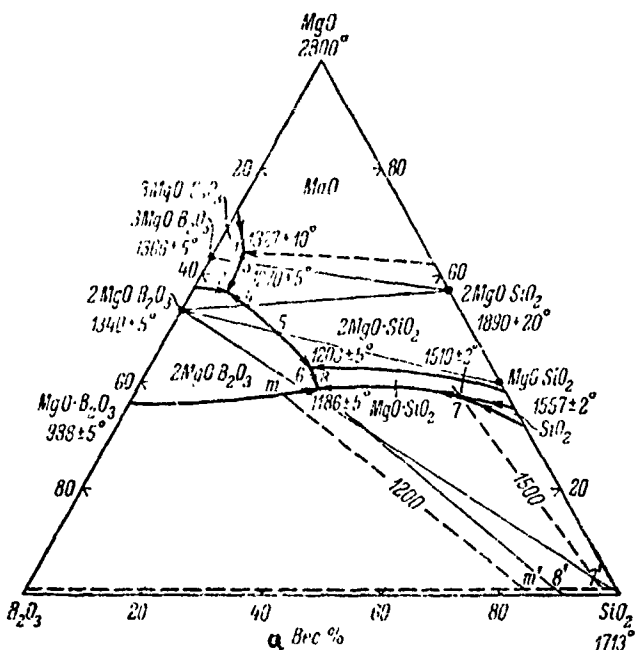


Fig. 129. Phase diagram of $\text{MgO} - \text{B}_2\text{O}_3 - \text{SiO}_2$ system (from Kuzel).

Key:

a. Weight %

INVARIANT POINTS OF MgO -- B₂O₃ -- SiO₂ SYSTEM

Точки (рис. 129)	Фазы	Процесс	Состав, вес. %			Темпера- тура, °C
			MgO	B ₂ O ₃	SiO ₂	
f В равновесии с одной жидкостью						
1	MgO + 3MgO·B ₂ O ₃ + 2MgO·SiO ₂	г. Эвтектика	64	31	5	1327 ± 10
2	3MgO·B ₂ O ₃ + 2MgO·B ₂ O ₃ + 2MgO·SiO ₂	»	56.7	37.3	6.0	1270 ± 5
6	2MgO·B ₂ O ₃ + 2MgO·SiO ₂ + MgO·SiO ₂	д. Перитек- тика	42.4	30.6	27.0	1203 ± 5
g В равновесии с двумя жидкостями						
7	MgO·SiO ₂ + SiO ₂	е. Монотек- тика	37	8	55	1510 ± 20
7'	MgO·SiO ₂ + SiO ₃	ж. То же	~1	~3	~96	1510 ± 20
8	2MgO·B ₂ O ₃ + MgO·SiO ₂	»	38.8	31.0	30.2	1186 ± 5
8'	2MgO·B ₂ O ₃ + MgO·SiO ₂	»	~1	10	89	1186 ± 5
m	2MgO·B ₂ O ₃	—	38	37	25	1200 ± 5
m'	2MgO·B ₂ O ₃	—	~1	~15	~84	1200 ± 5
h В равновесии с одной жидкостью в точках температурного максимума						
3	2MgO·SiO ₂ + 3MgO·B ₂ O ₃ + Жидкость m	—	62.8	31.8	5.4	1331 ± 5
4	2MgO·SiO ₂ + 2MgO·B ₂ O ₃ + Жидкость m	—	54.4	35.6	10.0	1283 ± 5

Key:

- a. Points (Fig. 129)
- b. Phases
- c. Process
- d. Composition, weight %
- e. Temperature, °C
- f. In equilibrium with 1 liquid
- g. Eutectic
- h. Peritectic
- i. In equilibrium with 2 liquids
- j. Monotectic
- k. Same
- l. In equilibrium with 1 liquid at temperature maximum points
- m. Liquid

BIBLIOGRAPHY

1. Kuzel, H.J., Neues Jahrb. Mineral., Abh., 100, No. 3, 322, 1963.

$\text{CaO} - \text{B}_2\text{O}_3 - \text{SiO}_2$

The system has been studied by Flint and Wells [2]. A phase diagram of the system is presented in Fig. 130. Two ternary compounds were found: $\text{CaO} \cdot \text{B}_2\text{O}_3 \cdot 2\text{SiO}_2$ and $5\text{CaO} \cdot \text{B}_2\text{O}_3 \cdot \text{SiO}_2$. The first of them corresponds to the natural mineral danburite; synthesis of this compound from dry melts is unsuccessful, but it can be obtained hydrothermally. Upon heating to 1002° , it melts, with formation of two immiscible liquids.

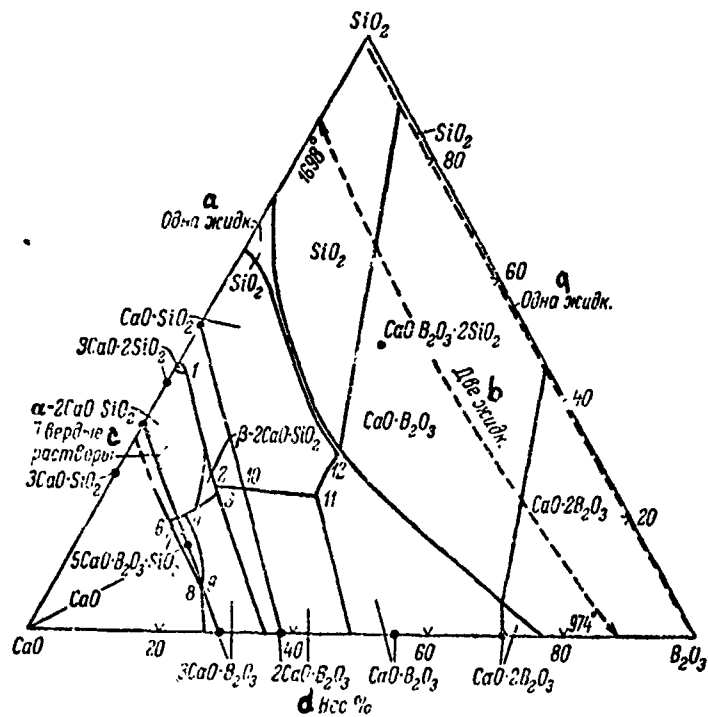


Fig. 130. Phase diagram of $\text{CaO} - \text{B}_2\text{O}_3 - \text{SiO}_2$ system (from Flint and Wells).

Key:

- a. 1 liquid
- b. 2 liquids
- c. Solid solutions
- d. Weight %

Of a large number of partial binary systems between various calcium borates and silicates studied, only the $2\text{CaO} \cdot \text{B}_2\text{O}_3$ -- $\text{CaO} \cdot \text{SiO}_2$ system is truly binary, i. e., it does not contain compounds other than those specified. Morey and Ingerson [4] studied the region of the system in which phase separation of the liquids is observed. In the phase separation region in Fig. 131, tie lines are plotted on the basis of experimental determinations of the overall composition (points 1) and the composition of the separated layers (points 2).

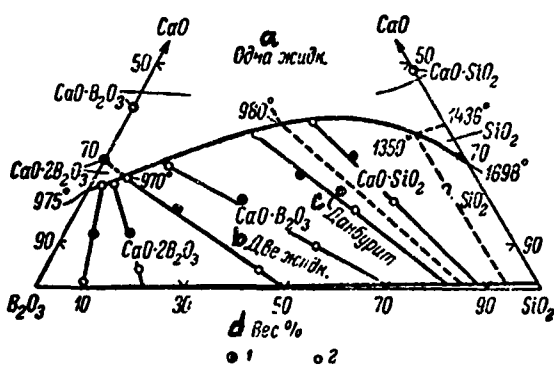


Fig. 131. Liquid phase separation region in $\text{CaO} \text{--} \text{B}_2\text{O}_3 \text{--} \text{SiO}_2$ system (from Morey and Ingerson):
 1. composition by synthesis (for initial mixtures);
 2. composition by analysis of separated liquid layers.

Key:

- a. 1 liquid
- b. 2 liquids
- c. Danburite
- d. Weight %

The compound α - $2\text{CaO} \cdot \text{SiO}_2$ dissolves considerable quantities of $\text{CaO} \cdot \text{B}_2\text{O}_3$, $2\text{CaO} \cdot \text{B}_2\text{O}_3$ and $5\text{CaO} \cdot \text{B}_2\text{O}_3 \cdot \text{SiO}_2$. The $\alpha \rightarrow \beta$ conversion temperature

of dicalcium silicate (an actual solid solution) decreases in this case, from 1420° for pure $2\text{CaO} \cdot \text{SiO}_2$ to 1230° .

Tishura [1] introduces a diagram of phase coexistence triangles, in plotting which he used thermodynamic data.

TABLE 1
CRYSTALLINE PHASES OF $\text{CaO} - \text{B}_2\text{O}_3 - \text{SiO}_2$ SYSTEM

a Соединение	b Габитус	<i>N_g</i>	<i>N_p</i>	$2V^\circ$	c Оптический знак
$5\text{CaO} \cdot \text{B}_2\text{O}_3 \cdot \text{SiO}_2$	d Полисинтетиче- ские двойники, зерна	1.690	1.666	e Варьирует	—
$\text{CaO} \cdot \text{B}_2\text{O}_3 \cdot 2\text{SiO}_2$ (дан- бурит)	f Ромбические зирацы	1.636	1.630	86—90	(—)

Key:

- a. Compound
- b. Appearance
- c. Optical sign
- d. Polysynthetic twins, grains
- e. Varies
- f. Danburite
- g. Rhombic prisms

Mircea [3] has studied the partial system $3\text{CaO} \cdot \text{SiO}_2 - \text{B}_2\text{O}_3$, heating the corresponding mixtures in the 1000–1600° temperature range. The B_2O_3 content reached 4%. Separation of free CaO and formation of a solid solution in the $2\text{CaO} \cdot \text{SiO}_2 - 5\text{CaO} \cdot \text{B}_2\text{O}_3 \cdot \text{SiO}_2$ series, the limiting composition of which depends on temperature, was observed.

TABLE 2
INVARIANT POINTS OF CaO -- B₂O₃ -- SiO₂ SYSTEM

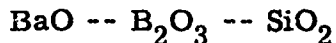
Точки (рис. 130)	b Фазы	c Процесс	d Состав, вес. %			e Темпера- тура, °C
			CaO	B ₂ O ₃	SiO ₂	
2	CaO · SiO ₂ + 2CaO · SiO ₂ + 2CaO · B ₂ O ₃ + жидкость f	Эвтектика	59.2	16.0	24.8	1118
6	2CaO · SiO ₂ + CaO + 5CaO · B ₂ O ₃ · SiO ₂ + жидкость f	»	69.2	12.6	18.2	1398
8	CaC + 5CaO · B ₂ O ₃ · SiO ₂ + 3CaO · B ₂ O ₃ + жидкость f	»	70.0	23.2	6.8	1404
12	CaO · SiO ₂ + CaO · B ₂ O ₃ + SiO ₂ + жидкость f	»	38.3	31.5	30.2	977
1.	CaO · SiO ₂ + 3CaO · 2SiO ₂ + 2CaO · SiO ₂ + жидкость f	Реакция	54.6	1.5	43.9	1436
3	2CaO · SiO ₂ + 3CaO · B ₂ O ₃ + 2CaO · B ₂ O ₃ + жидкость f	»	59.4	16.6	24.0	1128
4	2CaO · SiO ₂ + 5CaO · B ₂ O ₃ · SiO ₂ + 3CaO · B ₂ O ₃ + жидкость f	»	66.2	14.1	19.7	1266
11	CaO · SiO ₂ + 2CaO · B ₂ O ₃ + CaO · B ₂ O ₃ + жидкость f	»	45.0	31.7	23.3	1017
7	5CaO · B ₂ O ₃ · SiO ₂ + жидкость f	Мягкое плавление	—	—	—	1419
5	α-2CaO · SiO ₂ твердый раствор + 5CaO · B ₂ O ₃ · SiO ₂ + жидкость f	Эвтектика	67.7	13.3	19.0	1400
9	3CaO · B ₂ O ₃ + 5CaO · B ₂ O ₃ · SiO ₂ + жидкость f	»	69.4	22.8	7.8	1415
10	2CaO · B ₂ O ₃ + CaO · SiO ₂ + жидкость f	»	55.4	20.4	24.2	1150

Key:

- a. Points (Fig. 130)
- b. Phases
- c. Process
- d. Composition, weight %
- e. Temperature, °C
- f. Liquid
- g. Eutectic
- h. Reaction
- i. Melting
- j. Solid solution

BIBLIOGRAPHY

1. Tishura, T.A., Ukransk. khim. zhurn., 34, No. 5, 468, 1968.
2. Flint, E.P., L.S. Wells, J. Res. Nat. Bur. Stand., 17, 745, 1936.
3. Mircea, S., Silikaty, 9, No. 1, 34, 1965.
4. Morey, G.W., E. Ingerson, Amer. Mineralogist, 22, No. 1, 38, 1937.



The system has been studied by Levin and Ugr'nic [5] by the quenching method. A phase diagram with isotherms applied is presented in Fig. 132. Coexisting phase triangles are plotted in Fig. 133. The ternary compound $3\text{BaO} \cdot 3\text{B}_2\text{O}_3 \cdot 2\text{SiO}_3$, melting without decomposition at 1009° , has been determined in the system. Solid solutions forming between $2\text{BaO} \cdot 3\text{SiO}_2$ and $\text{BaO} \cdot 2\text{SiO}_2$ extend into the three-component portion of the diagram. The region shown by crosshatching in Fig. 132 should be considered to be a solid solution of silicates ($3\text{BaO} \cdot 3\text{SiO}_2$ and $\text{BaO} \cdot 2\text{SiO}_2$) with barium borosilicate $3\text{BaO} \cdot 3\text{B}_2\text{O}_3 \cdot 2\text{SiO}_2$.

Immiscibility (liquation) in the $\text{BaO} \text{ -- } \text{B}_2\text{O}_3 \text{ -- } \text{SiO}_2$ system has been studied in greater detail by Levin and Cleek [4]. The critical liquation line is the peak of the oblong "hill," represented in Fig. 134. This line passes approximately parallel to the $\text{B}_2\text{O}_3 \text{ -- } \text{SiO}_2$ side, and the coordinates of the extreme points are 1225° on the $\text{BaO} \text{ -- } \text{B}_2\text{O}_3$ side (15 weight % BaO) and 1405° at a content of $\text{BaO} \text{ -- } 18$ weight %, $\text{B}_2\text{O}_3 \text{ -- } 10.5$ weight % and $\text{SiO}_2 \text{ -- } 71.5$ weight %. A vertical profile through the critical immiscibility line is represented in Fig. 134a. Extrapolation of this line in the direction of the $\text{BaO} \text{ -- } \text{SiO}_2$ system permits the metastable liquation position in this binary system to be

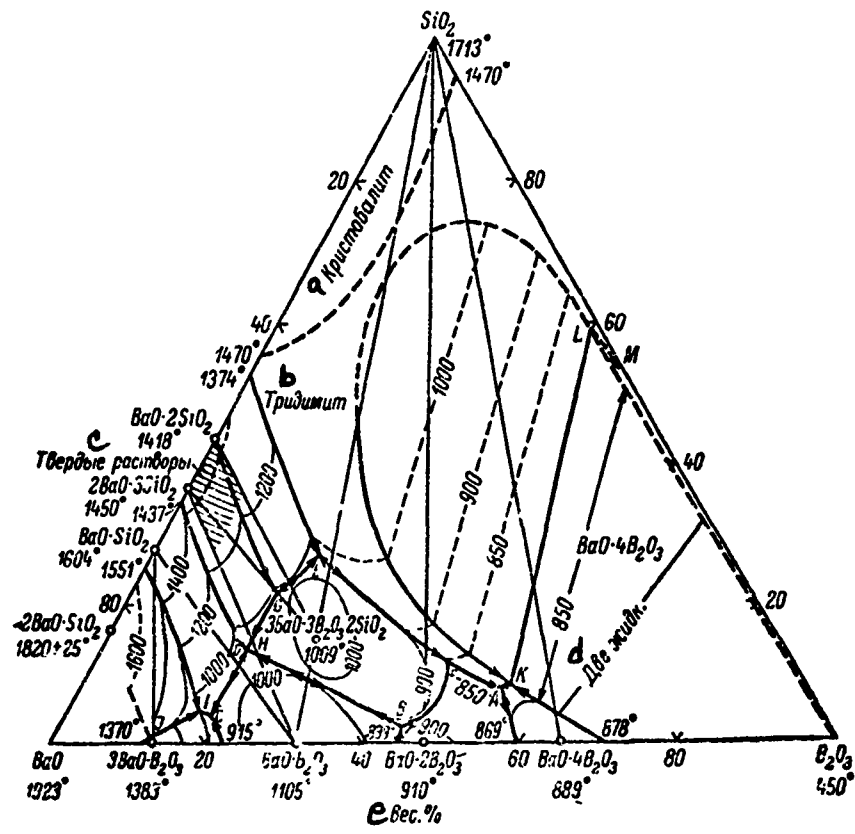


Fig. 132. Phase diagram of BaO -- B₂O₃ -- SiO₂ system (from Levin and Ugrinic); melting temperatures of invariant points: A. 810 ± 10°; B. 875 ± 5°; C. 875 ± 5°; D. 920 ± 10°; E. 950 ± 20°; F. 825 ± 10°; G. 980 ± 5°; H. 925 ± 10°; I. 962 ± 10°; J. 1370°; K, L. 815 ± 10°; M. 450°.

Key:

- a. Cristobalite
 - b. Tridymite
 - c. Solid solutions
 - d. Two liquids
 - e. Weight %

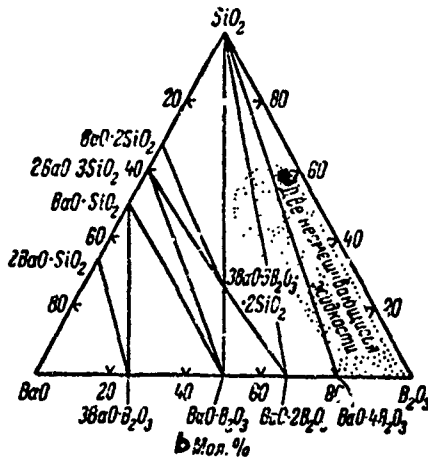


Fig. 133. Phase coexistence triangles of BaO -- B₂O₃ -- SiO₂ system (from Levin and Ugrinic).

Key:

- a. Two immiscible liquids
- b. Mole %

found (see Fig. 134b). Lines characterizing immiscibility for isopleths with a 22.5 weight % BaO content are presented in Fig. 134c. The primary crystallization field of silica is intersected by these lines at 1395° and a content of 68 weight % SiO₂.

Phase separation of the liquids in the system has been studied by Gerth and Rehfeld [2]. At a certain low concentration, a section has been found in which several liquation regions in a row exist. The number of these regions is equal to the number of phases in the system. This interesting phenomenon requires further checking.

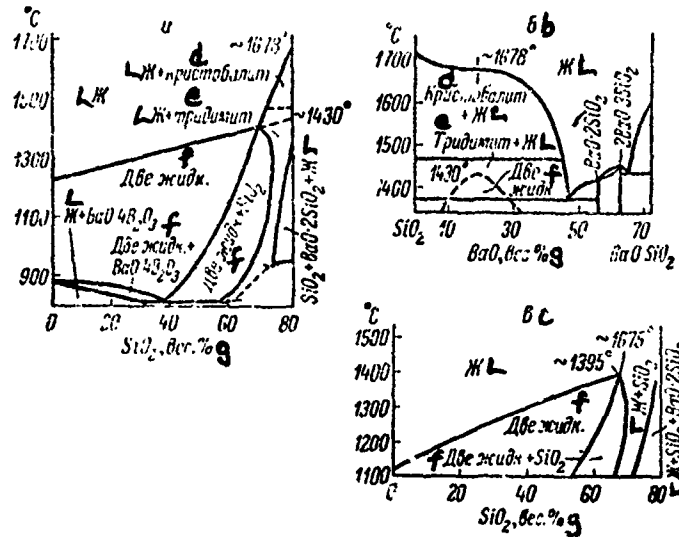


Fig. 134. Some binary profiles of the $\text{BaO} - \text{B}_2\text{O}_3 - \text{SiO}_2$ system, passing through the liquid immiscibility region (from Levin and Cleek'; see text for explanation).

Key:

- d. Cristobalite
- e. Tridymite
- f. Two liquids
- g. Weight %

Glasses form easily over an extensive region of the system, and they have been studied by Hamilton and colleagues [3].

INVARIANT POINTS OF BaO -- B₂O₃ -- SiO₂ SYSTEM

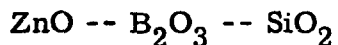
a точка (рис. 132)	b Фазы	c Процесс	d Состав, вес. %			e Темпера- тура, °C
			BaO	B ₂ O ₃	SiO ₂	
A	BaO·2B ₂ O ₃ +BaO·4B ₂ O ₃ ·f+SiO ₂ +жидкость f	g Эвтектика	38.7	53.8	7.5	810
B	BaO·B ₂ O ₃ +BaO·2B ₂ O ₃ ++3BaO·3B ₂ O ₃ ·2SiO ₂ +жидкость f	•	51.2	44.0	1.8	875
C	3BaO·B ₂ O ₃ +BaO·B ₂ O ₃ +BaO··SiO ₂ +жидкость f	•	77.4	19.0	3.6	875
D	BaO·B ₂ O ₃ +BaO·SiO ₂ +2BaO··3SiO ₂ +жидкость f	•	68.0	18.6	13.4	920
E	3BaO·3B ₂ O ₃ ·2SiO ₂ +BaO··2SiO ₂ +SiO ₂ +жидкость f	•	51.8	21.2	27.0	950
F	3BaO·3B ₂ O ₃ ·2SiO ₂ +BaO··2B ₂ O ₃ +SiO ₂ +жидкость f	h Реакция	43.4	45.4	11.2	825
G	3BaO·3B ₂ O ₃ ·2SiO ₂ +BaO··2SiO ₂ +2BaO·3SiO ₂ +жидкость f	•	60.2	18.4	21.4	930
H	BaO·B ₂ O ₃ +BaO·SiO ₂ +2BaO··3SiO ₂ +жидкость f	•	67.5	18.5	14.0	925
I	3BaO·B ₂ O ₃ +BaO·SiO ₂ ++2BaO·SiO ₂ +жидкость f	•	78.3	17.3	4.4	962
J	BaO+3BaO·B ₂ O ₃ ·2BaO··SiO ₂ +жидкость f	•	87	12	1	<1370
M	BaO·4B ₂ O ₃ +3B ₂ O ₃ +SiO ₂ +жидкость f	g Эвтектика	<2	>30	<30	<450
i	Фазы в равновесии с двумя жидкостями					
K	BaO·4B ₂ O ₃ +SiO ₂ +две ; жидкости	—	37.4	54.6	8.0	815
L	BaO·4B ₂ O ₃ +SiO ₂ +две ; жидкости	—	1	40	59	815

Key:

- a. Points (Fig. 132)
- b. Phases
- c. Process
- d. Composition, weight %
- e. Temperature, °C
- f. Liquid
- g. Eutectic
- h. Reactions
- i. Phases in equilibrium with two liquids
- j. Two liquids

BIBLIOGRAPHY

1. Toropov, N. A., F. Ya. Galakhov, I. A. Bondar', DAN SSSR, 89, 1, 1958, p. 89.
2. Gerth, K., A. Rehfeld, Silikattechnik, 20, No. 7, 227, 1969.
3. Hamilton, E. H., G. W. Cleek, O. H. Crauer, J. Amer. Ceram. Soc., 41, No. 6, 209, 1958.
4. Levin, E. M., C. W. Cleek, J. Amer. Ceram. Soc., 41, No. 5, 177, 1958.
5. Levin, E. M., G. Ugrinic, J. Res. Nat. Bur. Stand., 51, No. 1, 37, 1953.



An approximate phase diagram of the system, according to Ingerson and colleagues [1], is presented in Fig. 135. An extensive region of separation of two immiscible liquids is characteristic. A curve representing the composition of the lighter liquid (curve L_2) actually should be located closer to the $\text{B}_2\text{O}_3 \text{ -- } \text{SiO}_2$ line (ZnO content should be less than 1 weight %).

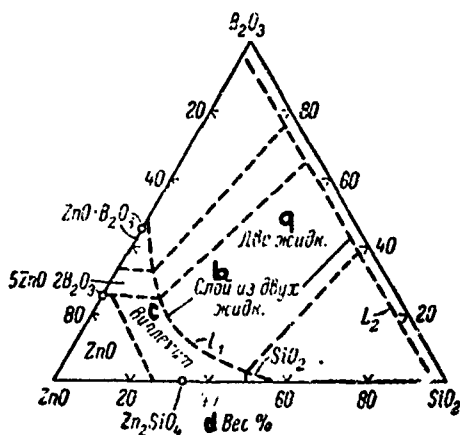


Fig. 135. Phase diagram of $\text{ZnO} \text{ -- } \text{B}_2\text{O}_3 \text{ -- } \text{SiO}_2$ system (from Ingerson and colleagues).

Key:

- | | |
|-------------------------|--------------|
| a. Two liquids | c. Willemite |
| b. Layer of two liquids | d. Weight % |

BIBLIOGRAPHY

1. Ingerson, E., G.W. Morey, O.F. Tuttle, Amer. J. Sci., 246, No. 1, 37, 1948.



The system has been studied roughly by Gielisse and Foster [2]. Ternary compounds have not been found (Fig. 136). A continuous series of solid solutions, also studied by Kim and Hummel [3] (Fig. 137), apparently exists between the binary compounds $3\text{Al}_2\text{C}_3 \cdot 2\text{SiO}_2$ and $9\text{Al}_2\text{O}_3 \cdot 2\text{B}_2\text{O}_3$. The Al_2O_3 , $3\text{Al}_2\text{O}_3 \cdot 2\text{SiO}_2$, $2\text{Al}_2\text{O}_3 \cdot \text{B}_2\text{O}_3$ and SiO_2 fields are indicated approximately in the diagram of Gielisse and Foster (Fig. 136), but a solid solution field was not noted.

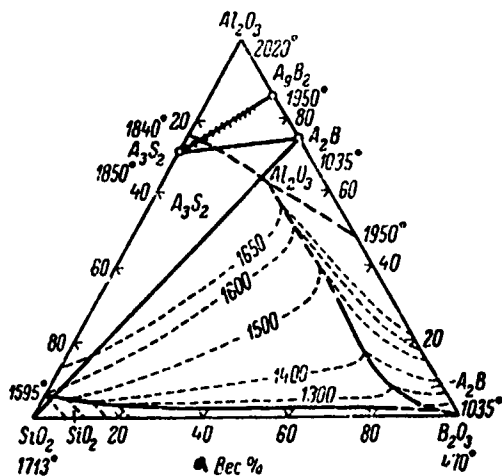


Fig. 136. Approximate diagram of phase relationships of Al_2O_3 -- B_2O_3 -- SiO_2 system (from Gielisse and Foster).

Key:

a. Weight %

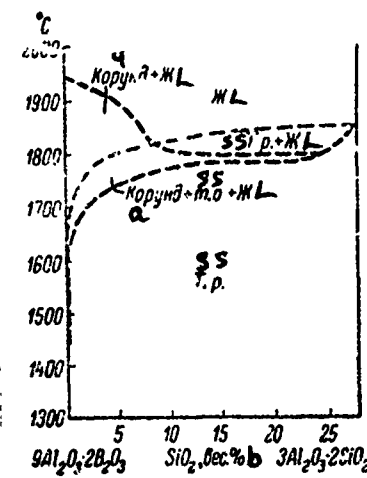


Fig. 137. Approximate phase diagram of partial system $9\text{Al}_2\text{O}_3 \cdot 2\text{B}_2\text{O}_3$ -- $3\text{Al}_2\text{O}_3 \cdot 2\text{SiO}_2$ (from Kim and Hummel).

Key:

- a. Corundum
- b. Weight %

Dietzel and Scholze [1] have determined the index of refraction of the silica-rich glasses of the system.

BIBLIOGRAPHY

1. Dietzel, A., H. Scholze, Glastech. Ber., **28**, No. 2, 48, 1955.
2. Gielisse, P.J., W.R. Foster, in: E.M. Levin, C.R. Robbins, H.F. McMurdie, Phase diagrams for ceramists, USA, Columbus, fig. 763, 1964.
3. Kim, K.H., F.A. Hummel, in: E.M. Levin, C.R. Robbins, H.F. McMurdie, Phase diagrams for ceramists, USA, Columbus, fig. 764, 1964.

$\text{PbO} \text{ -- } \text{B}_2\text{O}_3 \text{ -- } \text{SiO}_2$

The system has been studied by Geller and Bunting [1] and by Johnson and Hummel [2]. One ternary compound $5\text{PbO} \cdot \text{B}_2\text{O}_3 \cdot \text{SiO}_2$, melting with decomposition at 551° and formation of $2\text{PbO} \cdot \text{SiO}_2$ and liquid, has been established.

Geller and Bunting found a region of solid solutions between $5\text{PbO} \cdot \text{B}_2\text{O}_3 \cdot \text{SiO}_2$ and $4\text{PbO} \cdot \text{B}_2\text{O}_3$ (or PbO). Crystals of $5\text{PbO} \cdot \text{B}_2\text{O}_3 \cdot \text{SiO}_2$ are prismatic in shape, in the rhombic crystal system; $2V$ is practically equal to 0; the optical sign is negative, $\text{Ng} = 2.085 \pm 0.005$, $\text{Np} = 2.04 \pm 0.005$. In formation of a solid solution, the index of refraction increases, reaching up to 2.12.

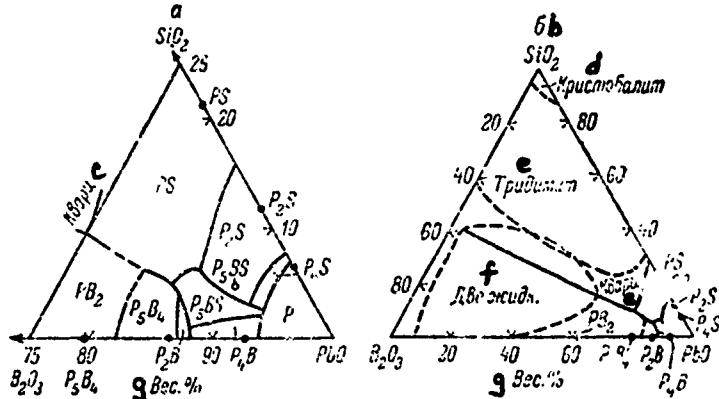


Fig. 138. Phase diagram of $\text{PbO} \text{ -- } \text{B}_2\text{O}_3 \text{ -- } \text{SiO}_2$ system (from Johnson and Hummel); a. PbO -rich region, b. general characteristics of the system.

Key:

- | | |
|-----------------|----------------|
| c. Quartz | f. Two liquids |
| d. Cristobalite | g. Weight % |
| e. Tridymite | |

Johnson and Hummel [2] have studied the portion of the system which is rich in PbO, and also have studied phase separation (liquation) of the liquid phase. The region adjacent to the PbO apex is presented in Fig. 138a. An extensive region of phase separation of the melt is shown in Fig. 138b, which encompasses the entire system. The region adjacent to the silica apex encompasses metastable liquation. The authors accomplished mechanical separation of the immiscible liquids (in the region poor in silica, where stable liquation is present), with the aid of a high-temperature centrifuge, and they determined the composition of the lead-rich and lead-poor liquids. With an overall content of 30 weight % PbO, there was 35-40 weight % PbO in the lead-rich layer and 15-20 weight % PbO in the lead-poor layer.

INVARIANT POINTS OF PbO -- B₂O₃ -- SiO₂ SYSTEM (from Geller and Bunting)

a Фазы	b Процесс	c Состав, вес. %			d Температура, °C
		PbO	B ₂ O ₃	SiO ₂	
SiO ₂ +PbO·SiO ₂ +PbO·2B ₂ O ₃ +жидкость	g Реакция	75	15	10	540±10
PbO·SiO ₂ +PbO·2B ₂ O ₃ +5PbO·4B ₂ O ₃ +жидкость	•	81	13	6	527±5
5PbO·B ₂ O ₃ ·SiO ₂ +PbO·SiO ₂ +5PbO·4B ₂ O ₃ +жидкость	h Эвтектика	84.5	11.0	4.5	484±2
5PbO·B ₂ O ₃ ·SiO ₂ +2PbO·SiO ₂ +2PbO·SiO ₂ +4PbO·SiO ₂ +жидкость	g Реакция	86.3	7.0	6.1	530±3
5PbO·B ₂ O ₃ ·SiO ₂ +2PbO·SiO ₂ +4PbO·SiO ₂ +жидкость	•	91.5	5.3	3.2	538±2
5PbO·B ₂ O ₃ ·SiO ₂ +4PbO·SiO ₂ +PbO+жидкость	•	92.7	4.5	2.8	531±2
5PbO·B ₂ O ₃ ·SiO ₂ +4PbO·B ₂ O ₃ +PbO+жидкость	h Эвтектика	92.7	4.8	2.5	532±2
5PbO·B ₂ O ₃ ·SiO ₂ +4PbO·B ₂ O ₃ +2PbO·B ₂ O ₃ +жидкость	•	87.5	11.4	1.1	488±2
5PbO·B ₂ O ₃ ·SiO ₂ +2PbO·B ₂ O ₃ +5PbO·4B ₂ O ₃ +жидкость	g Реакция	86.0	10.6	3.4	486±2

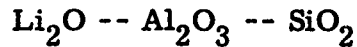
Key:

- | | |
|--------------------------|--------------|
| a. Phases | f. Liquid |
| b. Process | g. Reactions |
| c. Composition, weight % | h. Eutectic |
| d. Temperature, °C | |

BIBLIOGRAPHY

1. Geller, R.F., E.N. Bunting, J. Res., Nat. Bur. Stand., 23, No. 2, 275, 1939.
2. Johnson, D.W., F.A. Hummel, J. Amer. Ceram. Soc., 51, No. 4, 196, 1968.

ALUMINOSILICATE SYSTEMS



The system has been studied by Hatch [10], R. Roy and Osborn [21], R. Roy, D. Roy and Osborn [22], Murthy and Hummel [19], Galakhov [1], Eppler [8] and others. Hatch studied the partial system $\text{Li}_2\text{O} \cdot \text{Al}_2\text{O}_3 \text{ -- SiO}_2$, within which the figurative points of the ternary compounds petalite $\text{Li}_2\text{O} \cdot \text{Al}_2\text{O}_3 \cdot 8\text{SiO}_2$, spodumene $\text{Li}_2\text{O} \cdot \text{Al}_2\text{O}_3 \cdot 4\text{SiO}_2$ and eucryptite $\text{Li}_2\text{O} \cdot \text{Al}_2\text{O}_3 \cdot 2\text{SiO}_2$ are located. However, crystallization of petalite (just like the compound $\text{Li}_2\text{O} \cdot \text{Al}_2\text{O}_3 \cdot 6\text{SiO}_2$) from the melt does not take place, and the following phases are indicated in Fig. 139: 1. silica (in the tridymite form); 2. β spodumene¹ (and the solid solutions based on it); 3. β eucryptite (and the solid solutions based on it); 4. lithium aluminate $\text{Li}_2\text{O} \cdot \text{Al}_2\text{O}_3$ (and the solid solutions based on it); and 5. $\gamma\text{Al}_2\text{O}_3$. From pure SiO_2 to 64.6 weight % SiO_2 (the composition of β spodumene), the system has a binary character, and it consists of fields of silica and solid solutions of the β spodumene type, with a eutectic between them at 84.5 weight % SiO_2 , melting at 135° .

1

Here, β spodumene (just like β eucryptite) is the high-temperature form.

β spodumene has a distinctly expressed temperature maximum at 1423°.

Between 64.6 and 47.7 weight % SiO_2 (the eucryptite composition), the system also is of a binary nature above the solidus line, and it is divided into β spodumene and β eucryptite solid solution fields. With a lower silica content the system completely loses its binary nature, and γ alumina and eucryptite solid solutions are observed as the crystallization products.

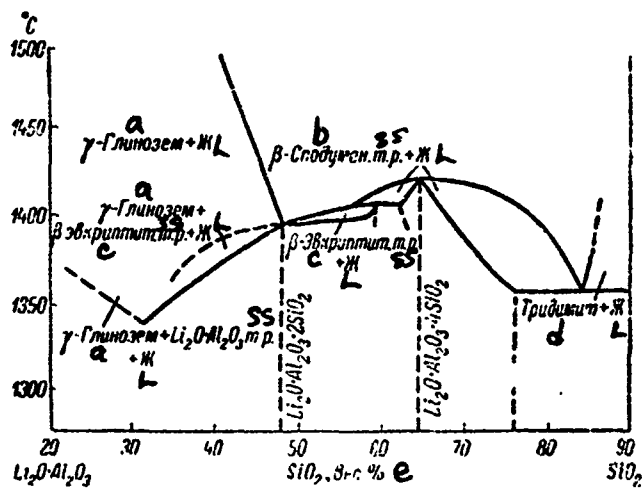


Fig. 139. Phase diagram of partial system $\text{Li}_2\text{O}\cdot\text{Al}_2\text{O}_3$ -- SiO_2 (from Hatch).

Key:

- a. Alumina
- b. Spodumene
- c. Eucryptite
- d. Tridymite
- e. Weight %

The alumina apex of the system has been studied by Galakhov [1]. A large field of high-alumina lithium aluminate $\text{Li}_2\text{O}\cdot 5\text{Al}_2\text{O}_3$, called γ alumina ($\gamma\text{Al}_2\text{O}_3$), has been determined here. The corundum field is a narrow strip,

and its boundary with the γ alumina field has been determined approximately (dashed line). The boundary between the γ alumina and lithium aluminate $\text{Li}_2\text{O} \cdot \text{Al}_2\text{O}_3$ fields begins at the eutectic point of the binary system $\text{Li}_2\text{O} \cdot \text{Al}_2\text{O}_3$ -- Al_2O_3 (Fig. 140). Galakhov, just like Hatch, notes the existence of $\text{Li}_2\text{O} \cdot \text{Al}_2\text{O}_3$ base solid solutions. In proportion to entry of alumina into the $\text{Li}_2\text{O} \cdot \text{Al}_2\text{O}_3$ lattice, the index of refraction decreases.

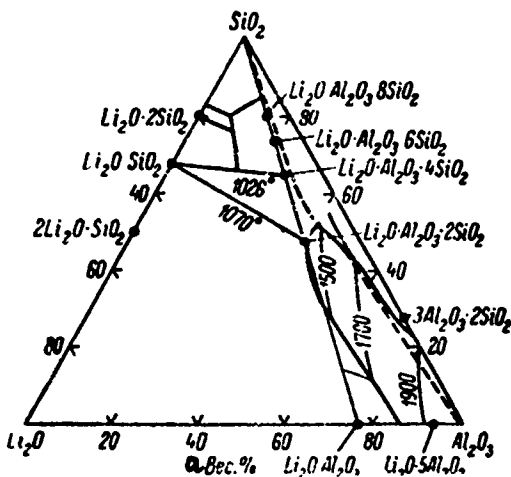


Fig. 140. Phase diagram of $\text{Li}_2\text{O} \text{--} \text{Al}_2\text{O}_3 \text{--} \text{SiO}_2$ system; apex adjacent to alumina (from Galakhov).

Key: a. Weight %

Murthy and Hummel [19] have investigated the partial system lithium metasilicate (Li_2SiO_3) -- β eucryptite, using the quenching method. The system is a simple binary, with a eutectic containing 57 weight % eucryptite and melting at 1070° (Fig. 141).

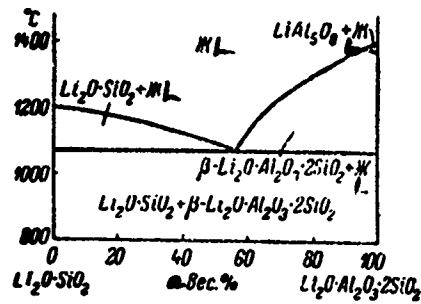


Fig. 141. Phase diagram of partial system $\text{Li}_2\text{O}\cdot\text{SiO}_2$ -- $\text{Li}_2\text{O}\cdot\text{Al}_2\text{O}_3\cdot 2\text{SiO}_2$ (from Murthy and Hummel).

Key:

a. Weight %

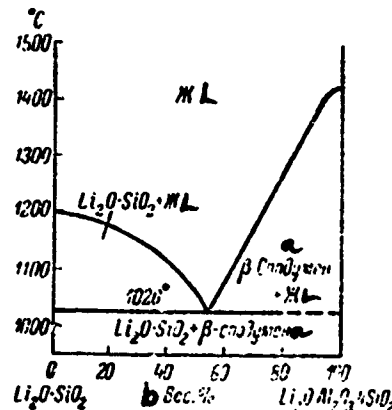


Fig. 142. Phase diagram of partial system $\text{Li}_2\text{O}\cdot\text{SiO}_2$ -- $\text{Li}_2\text{O}\cdot\text{Al}_2\text{O}_3\cdot 4\text{SiO}_2$ (from Roy and Osborn).

Key:

a. Spodumene
b. Weight %

Roy and Osborn [21] have studied the partial system lithium metasilicate -- β -spodumene ($\text{Li}_2\text{O} \cdot \text{Al}_2\text{O}_3 \cdot 4\text{SiO}_2$). This system turned out to be a simple eutectic. The eutectic with 45.4 weight % Li_2SiO_3 melts at 1026° (Fig. 142).

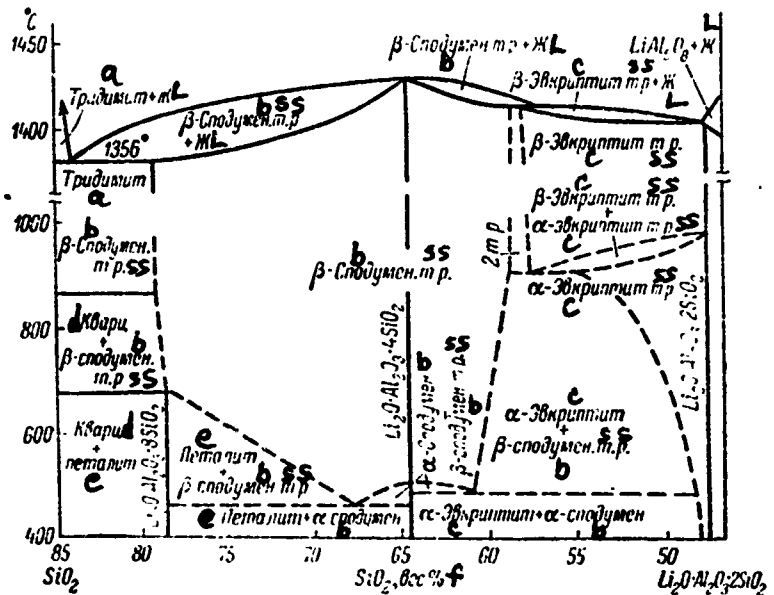


Fig. 143. Phase diagram of portion of partial system $\text{Li}_2\text{O} \cdot \text{Al}_2\text{O}_3 \cdot 2\text{SiO}_2$ -- SiO_2 (high temperature portion from Hatch, low temperature, from Roy, Roy and Osborn).

Key:

- a. Tridynite
- b. Spodumene
- c. Eucryptite
- d. Quartz
- e. Petalite
- f. Weight %

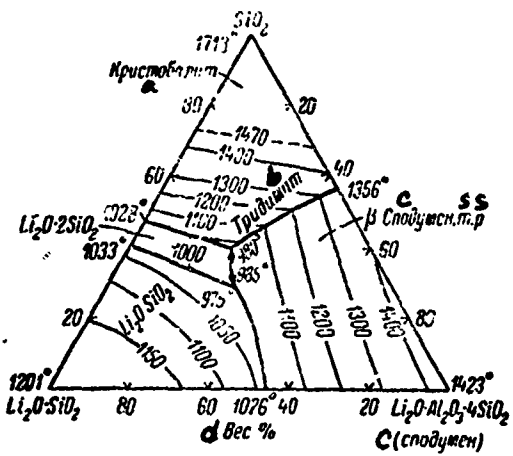


Fig. 144. Phase diagram of partial system $\text{Li}_2\text{O}\cdot\text{SiO}_2$ -- $\text{Li}_2\text{O}\cdot\text{Al}_2\text{O}_3\cdot 4\text{SiO}_2$ -- SiO_2 (from Roy and Osborn).

Key:

- a. Cristobalite
- b. Tridymite
- c. Spodumene
- d. Weight %

R. Roy, D. Roy and Osborn [22] have described a section of the $\text{Li}_2\text{O}\cdot\text{Al}_2\text{O}_3\cdot\text{SiO}_2$ system (from $\text{Li}_2\text{O}\cdot\text{Al}_2\text{O}_3\cdot 2\text{SiO}_2$ on the SiO_2 side) in the sub-solidus region. The minerals were synthesized under hydrothermal conditions, at a pressure of about 700 kgf/cm^2 . Petalite, which is stable below 680° , was synthesized under these conditions. The transition temperature of high-temperature spodumene to the low-temperature turned out to be $\sim 500^\circ$ (Fig. 143).

Roy and Osborn have plotted a phase diagram of the ternary system $\text{Li}_2\text{O}\cdot\text{SiO}_2$ -- $\text{Li}_2\text{O}\cdot\text{Al}_2\text{O}_3\cdot 4\text{SiO}_2$ -- SiO_2 (Fig. 144). The following are presented for the two eutectic points: 1. melting temperature 980° , composition SiO_2 39.2 weight %, spodumene 26 weight % and lithium metasilicate 34.8

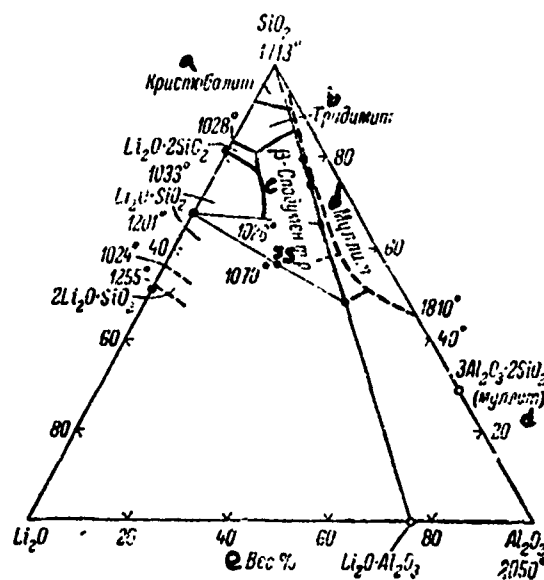


Fig. 145. Schematic phase diagram of $\text{Li}_2\text{O} - \text{Al}_2\text{O}_3 - \text{SiO}_2$ system (from Roy and Osborn).

Key:

- a. Cristobalite
- b. Tridymite
- c. Spodumene
- d. Mullite
- e. Weight %

weight %; 2. 975° , composition lithium metasilicate 39.2 weight %, SiO_2 28.2 weight % and spodumene 32.6 weight %. The complete $\text{Li}_2\text{O} - \text{Al}_2\text{O}_3 - \text{SiO}_2$ diagram is presented schematically in Fig. 145.

In examining the series of solid solutions in the $\text{Li}_2\text{O} \cdot \text{Al}_2\text{O}_3 - \text{SiO}_2$ system, Roy [20] distinguishes an O series ("silica O"), a K series, an " $\alpha \text{LiAlSi}_2\text{O}_6$ " series and a " $\beta \text{LiAlSiO}_2$ " series, which are presented *

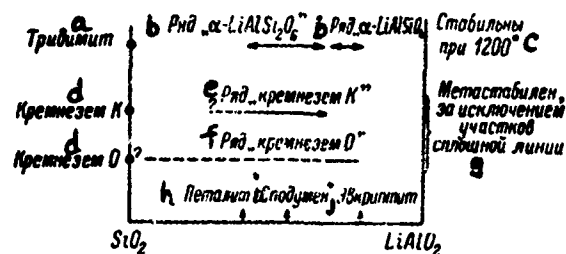


Fig. 146. Schematic phase diagram, showing types of solid solutions in LiAlO_2 -- SiO_2 system (from Roy).

Key:

- a. Tridymite
- b. Series
- c. Stable at 1200°
- d. Alumina
- e. "Alumina K" series
- f. "Alumina O" series
- g. Metastable, with exception of solid line sections
- h. Petalite
- i. Spodumene
- j. Eucryptite

schematically in Fig. 146. The "silica O" series extends from eucryptite (LiAlSiO_4) in the direction of silica, and it is characterized by a α quartz type structure. Henglein [11] has demonstrated that the quartz-like type of structure can be brought into being over a wide range, from pure quartz to eucryptite proper.

The "K series," i.e., spodumene solid solutions, are characterized by the tetragonal structure inherent in kitite, and it extends from $\text{Li}_2\text{O} \cdot \text{Al}_2\text{O}_3 \cdot 4\text{SiO}_2$ in the direction of silica.

The transformation of α eucryptite to β eucryptite (from Winkler) [26, 27] is observed at $972 \pm 10^\circ$.

Behruzi and Hahn [7] demonstrate that, under appropriate conditions of crystallization of eucryptite glass, besides known modifications, two more modifications can be obtained, monoclinic and triclinic.

Skinner and Evans [24, 25] have carried out a monocrystal X-ray investigation of β spodumene and its solid solutions.

Urazov and colleagues [6] have studied the $\alpha \rightleftharpoons \beta$ transformation of spodumene, using the natural mineral.

Kolesova [4], just like Ignat'yeva [2], on the basis of study of the infrared spectra of α and β spodumene, assert that a change in the coordination number of aluminum takes place during the transition of α spodumene to β spodumene: a transition from six-fold coordination (in α spodumene) to four-fold.

Kondrat'yev [5] explains the difference in high-temperature and low-temperature eucryptite by the hypothesis of change in degree of disorder in substitution of the $[SiO_4]$ and $[AlO_4]$ tetrahedra. He gives a similar interpretation to explain the existence of three forms of spodumene of different properties. Some properties of high-temperature lithium aluminosilicates are reported in Table 1.

Saalfeld [23] has studied the thermal conversions of natural petalite. Slow heating of natural petalite to 1200° leads to formation of the $\alpha\text{-Li}_2O \cdot Al_2O_3 \cdot 6SiO_2$ phase.

Kalinina and Filipovich [3] and Eppler [8] have shown that, depending on the crystallization temperature of aluminosilicate glasses, metastable solutions can be distinguished.

Isaacs and Roy [13] have studied the $\alpha \rightleftharpoons \beta$ inversion of eucryptite as a function of pressure.

Munoz [17] has studied polymorphism of lithium aluminosilicate, with the general formula $\text{Li}_2\text{O} \cdot \text{Al}_2\text{O}_3 \cdot 4\text{SiO}_2$, under high pressure conditions, taking his investigation up to 40 kbar, and he has observed three phases, which are variable, but apparently close to the formula indicated: 1. normal high-temperature β spodumene, melting at $1429 \pm 1^\circ$, according to new data; 2. a mineral of the pyroxene group, forming at high pressures, called simply "spodumene" by Munoz; 3. in the intermediate region between the two compounds mentioned, a phase was observed which Munoz calls " β eucryptite solid solution," but he ascribes the chemical formula to it characteristic of spodumene; this phase has a structure which is characteristic of high-temperature quartz.

A phase diagram of lithium aluminosilicate $\text{Li}_2\text{O} \cdot \text{Al}_2\text{O}_3 \cdot 4\text{SiO}_2$ is presented in Fig. 147. The possibility of obtaining the " β eucryptite solid solution" at pressures above 10 kbar, both from crystalline β spodumene and from the "spodumene" stable at high pressure, was tested experimentally. In accordance with the molar volume values of the " β eucryptite solid solution" and β spodumene, 77.32 and $78.31 \text{ cm}^3/\text{mole}$, respectively, an increase in pressure facilitates stabilization of β eucryptite, at the expense of β spodumene.

β spodumene melts congruently at a pressure of 8.5 ± 0.5 kbar and a temperature of 1400° ; at higher pressures, incongruent melting takes place, with formation of the " β eucryptite solid solution" and liquid. The presence of a two-phase region was demonstrated by special tests, in which the initial materials were β spodumene or " β eucryptite solid solution." The two-phase region was not

TABLE I
PROPERTIES OF POLYMORPHIC MODIFICATIONS OF
EUCRYPTITE AND SPODUMENE (from Kondrat'yev)

Modification	Formula	Nature of Substitution	Symmetry	Unit cell parameters, Å		C_p ritical sign	Shell bands in reflection spectrum, 1/cm	Method of obtaining
				a	c			
"Highly symmetrical" eucryptite ꝝ eucryptite	LiAlSiO ₄	Disordered	Hexagonal	5.24	5.48	(-)	1025, broad	Eucryptite glass crystallization
	"	Ordered	Same	5.24	5.55	(-)	1005, 1055, narrow	Slow growth from melt
"Highly symmetrical" hexagonal spodumene "Highly symmetrical" tetragonal spodumene ꝝ spodumene	LiAlSi ₂ O ₆	Disordered	"	5.24	5.46	(-)	1025, 1086, 1190, broad	Spodumene glass crystallization below 830°
	"	Same	Tetragonal	7.53	9.15	(+)	1040, 1180, broad	Spodumene glass crystallization above 830°
	"	Ordered	Same	7.53	9.15	(+)	1025, 1170, narrow	Slow growth from melt

TABLE 2
OPTICAL PROPERTIES OF CRYSTALLINE PHASES OF
 $\text{Li}_2\text{O} - \text{Al}_2\text{O}_3 - \text{SiO}_2$
SYSTEM

Compound	N_e	N_o	N_g	Optical Nature	Crystal Habit	Extinction Angles
α Eucryptite: Synthetic	1.587 ± 0.002	1.572 ± 0.002	—	Uniaxial positive	Quartz-like, trigonal pyramids Hexagonal forms	—
Natural	$1.587 (?)$	1.572	—	Same	—	—
β Eucryptite, synthetic: from [22]	1.520 ± 0.003	1.524 ± 0.003	—	Uniaxial negative	—	—
from [10]	1.523	1.531	—	Same	—	—
α Spodumene: Synthetic	—	—	1.75 1.68	Biaxial positive	Flakes Pyroxene-like	30° $23-27^\circ$
Natural	—	—	1.65	—	—	—
β Spodumene synthetic: from [22]	—	—	1.522 1.516	Uniaxial positive	Ditetragonal dipyramids	—
from [10]	—	—	1.523 1.516	Same Biaxial positive	Same Needles and wide flakes (in the synthetic)	0°
Petalite, syn- thetic and natural are identical	—	—	1.504	—	—	—

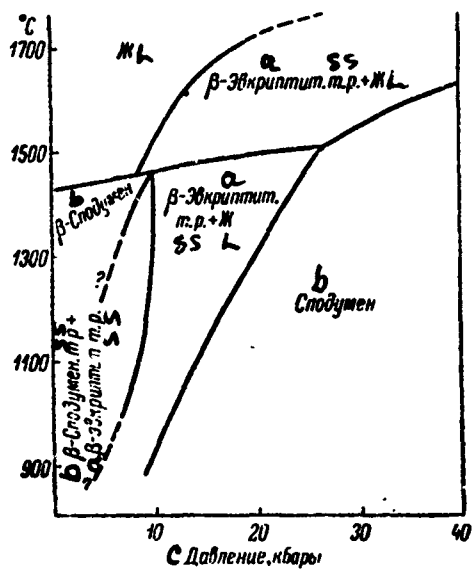


Fig. 147. Phase relationships for lithium aluminosilicate $\text{Li}_2\text{O} \cdot \text{Al}_2\text{O}_3 \cdot 4\text{SiO}_2$ (from Munoz).

Key:

- a. Eucryptite
- b. Spodumene
- c. Pressure, kbar

precisely outlined, but it extends to low temperatures and to pressures less than 5 kbar. Munoz conducted special tests, to precisely define the location of the boundary between "β eucryptite solid solution" and "spodumene" which, by extrapolating this boundary to one atmosphere, permitted the stability temperature of spodumene under normal conditions to be found. This temperature, depending on the apparatus used, was between 520 and 395°.

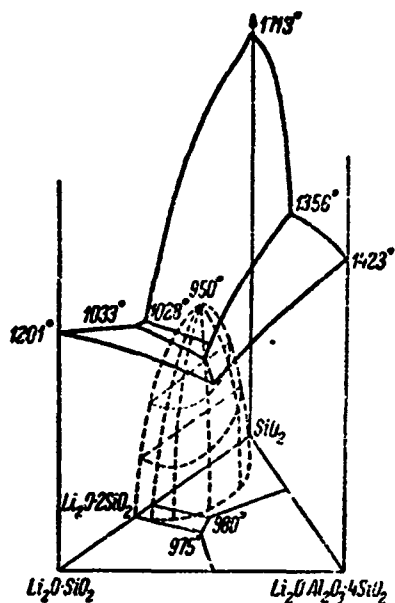


Fig. 148. Metastable liquation (phase separation) of $\text{Li}_2\text{O}\cdot\text{SiO}_2$ -- $\text{Li}_2\text{O}\cdot\text{Al}_2\text{O}_5\cdot 4\text{SiO}_2$ system glasses (from Marinov and Radenkova-Janeva).

Munoz [18] has synthesized hexagonal solid solutions (called β quartz) of the $\text{LiAlSi}_2\text{O}_6$ -- SiO_2 series, at a pressure of 15 kbar and a temperature of 1350° , which turned out to be stable up to 1500° and pressures of 10-20 kbar.

Li Chi-tang and Peacor [15] discuss three polymorphic forms of spodumene: a low-temperature, monoclinic α form (natural spodumene), a high-temperature, tetragonal β form and a hexagonal γ form, similar in structure to high-temperature quartz. The authors propose designating these modifications in the following manner: $\text{LiAlSi}_2\text{O}_6\text{-I}$, $\text{LiAlSi}_2\text{O}_6\text{-II}$ and $\text{LiAlSi}_2\text{O}_6\text{-III}$. In a detailed structural study, Li Chi-tang and Peacor demonstrated that $\text{LiAlSi}_2\text{O}_6\text{-II}$

is a derivative of kitite. The structure of $\text{LiAlSi}_2\text{O}_6$ -III was studied by Li Chi-tang [14], who, noting a very small (Si, Al)-Li distance, gave an explanation of the small coefficient of thermal expansion of spodumene.

TABLE 3
INVARIANT POINTS OF ALUMINA-RICH REGION
OF $\text{Li}_2\text{O} - \text{Al}_2\text{O}_3 - \text{SiO}_2$ SYSTEM
(from Galakhov)

a Фазы	b Процесс	c Состав, вес. %			d Темпера- турса, °C
		Li ₂ O	Al ₂ O ₃	SiO ₂	
$\alpha\text{-Al}_2\text{O}_3 + \gamma\text{-Al}_2\text{O}_3 + 3\text{Al}_2\text{O}_3 \cdot 2\text{SiO}_2 +$ жидкость	f Реакция	7	43	50	1500
$\gamma\text{-Al}_2\text{O}_3 + \beta\text{-Li}_2\text{O} \cdot \text{Al}_2\text{O}_3 \cdot 2\text{SiO}_2$ твердый раствор + $3\text{Al}_2\text{O}_3 \cdot 2\text{SiO}_2 +$ жидкость	»	8	41	51	1490
$\gamma\text{-Al}_2\text{O}_3 + \text{Li}_2\text{O} \cdot \text{Al}_2\text{O}_3$ твердый раствор + $\beta\text{-Li}_2\text{O} \cdot \text{Al}_2\text{O}_3 \cdot 2\text{SiO}_2$ твердый раствор + жидкость	»	15	43	42	1400

Key:

- | | |
|--------------------------|-------------------|
| a. Phases | e. Liquid |
| b. Process | f. Reactions |
| c. Composition, weight % | g. Solid solution |
| d. Temperature, °C | |

Gillary and Bush [9] measured the thermal expansion and contraction of pure high-temperature β eucryptite. The coefficient of thermal expansion parallel to the C axis turned out to be $\alpha = 17.6 \cdot 10^{-6}$ and perpendicular to the C axis $\alpha = 8.21 \cdot 10^{-6}$.

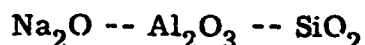
For glasses of the partial system $\text{Li}_2\text{O} \cdot \text{SiO}_2 - \text{Li}_2\text{O} \cdot \text{Al}_2\text{O}_3 \cdot 4\text{SiO}_2 - \text{SiO}_2$, metastable liquation (phase separation) is characteristic. Marinov and Radenkova-Janeva [16] subjected glass to heat treatment (they varied the

holding temperature and time), and they observed the phase separation phenomenon by electron microscope. The liquation region, in the form of a dome cross section, is presented in Fig. 148. A critical point on the surface of the phase separation space is a temperature of 950° and composition $\text{Li}_2\text{O} -- 12.45$ mole %, $\text{SiO}_2 -- 87.55$ mole %.

BIBLIOGRAPHY

1. Galakhov, F. Ya., Izv. DAN SSSR, OKhN, 5, 1959, p. 575.
2. Ignat'yeva, L. A., Optika i spektroskopiya, 6, 6, 1959, p. 807.
3. Kalinina, A. M., V. N. Filipovich, in the collection Strukturnyye prevrashcheniya steklakh pri povyshennykh temperaturakh [Structural Transformation of Glass at Elevated Temperatures], Nauka Press, Moscow-Leningrad, 1965, p. 124.
4. Kolesova, V. A., Izv. AN SSSR, OKhN, 1, 1963, p. 187.
5. Kondrat'yev, Yu. N., Izv. AN SSSR, Neorg. mater., 1, 8, 1965, p. 1395.
6. Urazov, G. G., V. Ye. Plyushchev, I. V. Shakhno, DAN SSSR, 113, 2, 1959, p. 361.
7. Behruzi, M., Th. Hahn, Naturwissenschaften, 54, 24, 643, 1967.
8. Eppler, R. A., J. Amer. Ceram. Soc., 46, 2, 97, 1963.
9. Gillery, F. H., E. A. Bush, J. Amer. Ceram. Soc., 42, 4, 175, 1959.
10. Hatch, R. A., Amer. Mineralogist, 28, 9-10, 471, 1943.
11. Henglein, E., Fortschritte Mineral., 34, 1, 40, 1956.
12. Hummel, F. A., J. Amer. Ceram. Soc., 34, 7, 235, 1951.
13. Isaacs, Th., R. Roy, Geochim. cosmochim. acta, 15, 3, 213, 1958.
14. Li Chi-tang, Zs. Kristallogr., 127, 5-6, 327, 1968.
15. Li Chi-tang, D. R. Peacor, Zs. Kristallogr., 126, 1-3, 46, 1968.
16. Marinov, M. R., M. S. Radenkova-Janeva, Proc. 9th Conf. Silicate Ind., Budapest, 119, 1968.

17. Munoz, J. L., Carnegie Inst. Washington Year Book, 66, 370, 1966-1967.
18. Munoz, J. L., Carnegie Inst. Washington Year Book, 67, 137, 1967-1968.
19. Murthy, K. M., F.A. Hummel, J. Amer. Ceram. Soc., 37, 1, 14, 1954.
20. Roy, R., Zs. Kristallogr., 111, 3, 185, 1959.
21. Roy, R., E.F. Osborn, J. Amer. Chem. Soc., 71, 6, 2086, 1949.
22. Roy, R., D.M. Roy, E.F. Osborn, J. Amer. Ceram. Soc., 33, 5, 156, 1950.
23. Saalfeld, H., Ber. Dtsch. keram. Ges., 38, 7, 281, 1961
24. Skinner, B.J., H.T. Evans, Amer. J. Sci., 258A, Bradley vol., 312, 1960.
25. Skinner, B.J., H.T. Evans, Zs. Kristallogr., 117, 2/3, 227, 1962.
26. Winkler, H.G.F., Acta crystallogr., 1, 1, 27, 1948.
27. Winkler, H.G.F., Acta crystallogr., 6, 1, 99, 1953.



The ternary compounds in the system are the common natural aluminosilicates $\text{Na}_2\text{O} \cdot \text{Al}_2\text{O}_3 \cdot 2\text{SiO}_2$ (nephelite, carnegieite), $\text{Na}_2\text{O} \cdot \text{Al}_2\text{O}_3 \cdot 4\text{SiO}_2$ (jadeite) and $\text{Na}_2\text{O} \cdot \text{Al}_2\text{O}_3 \cdot 6\text{SiO}_2$ (albite). Aluminosilicates richer in alkalis have been obtained synthetically.

Two ternary compounds result from crystallization of melts, $\text{Na}_2\text{O} \cdot \text{Al}_2\text{O}_3 \cdot 6\text{SiO}_2$ (albite) and $\text{Na}_2\text{O} \cdot \text{Al}_2\text{O}_3 \cdot 2\text{SiO}_2$ (carnegieite). Jadeite is not obtained from the melt by crystallization.

The first studies of the system were limited to study of certain partial profiles. Tilley [36] studied the partial system $\text{Na}_2\text{O} \cdot \text{SiO}_2 \text{ -- Na}_2\text{O} \cdot \text{Al}_2\text{O}_3 \cdot 2\text{SiO}_2$ (Fig. 149) and $\text{Na}_2\text{O} \cdot 2\text{SiO}_2 \text{ -- Na}_2\text{O} \cdot \text{Al}_2\text{O}_3 \cdot 2\text{SiO}_2$ (simple eutectic) and the partial ternary system $\text{Na}_2\text{O} \cdot \text{SiO}_2 \text{ -- Na}_2\text{O} \cdot 2\text{SiO}_2 \text{ -- Na}_2\text{O} \cdot \text{Al}_2\text{O}_3 \cdot 2\text{SiO}_2$; Greig and Barth [15] plotted a phase diagram of the nephelite-albite system

(Fig. 150). The sodium metasilicate -- nephelite pseudobinary eutectic system, according to refined data of Spivak[35], has a eutectic containing 46.75 weight % $\text{Na}_2\text{O} \cdot \text{Al}_2\text{O}_3 \cdot 2\text{SiO}_2$, melting at 902°. The phases in this system are $\text{Na}_2\text{O} \cdot \text{SiO}_2$ and nephelite; solid solutions were not found. As a result of entry of $\text{Na}_2\text{O} \cdot \text{SiO}_2$ into the carnegieite lattice, the temperature of transformation of nephelite to carnegieite is reduced from 1250 to 1163°. Galakhov [2] has precisely determined the location of the boundary between the mullite and corundum fields on the triple diagram.

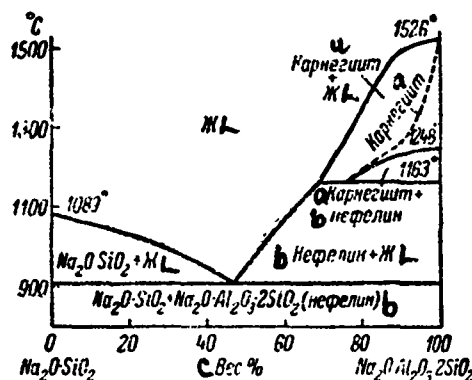


Fig. 149. Phase diagram of partial system $\text{Na}_2\text{O} \cdot \text{SiO}_2$ -- $\text{Na}_2\text{O} \cdot \text{Al}_2\text{O}_3 \cdot \text{SiO}_2$ (from Tilley).

Key:

- a. Carnegieite
- b. Nephelite
- c. Weight %

Schairer and Bowen [32] proposed the first variant of the system in 1947 and, in 1956, gave a refined, detailed phase diagram [33]. Osborn and Muan [23], based on the data of Bowen and Schairer and introducing several more additions, gave a more complete diagram in 1960 (Fig. 151).

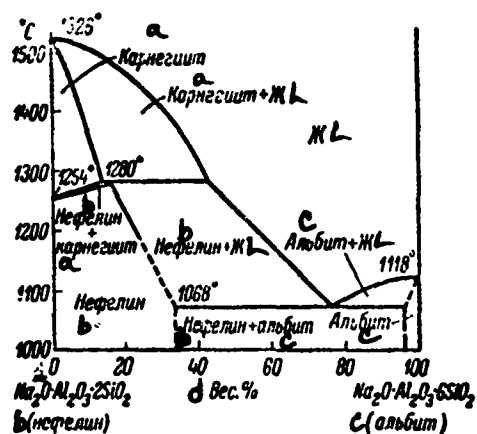


Fig. 150. Phase diagram of partial system nephelite ($\text{Na}_2\text{O} \cdot \text{Al}_2\text{O}_3 \cdot \text{SiO}_2$) -- albite ($\text{Na}_2\text{O} \cdot \text{Al}_2\text{O}_3 \cdot 6\text{SiO}_2$) (from Greig and Barth).

Key:

- a. Carnegieite
- b. Nephelite
- c. Albite
- d. Weight %

Up to the present time, the position on the diagram of the high-alumina compound "β alumina," of composition $\text{Na}_2\text{O} \cdot 11\text{Al}_2\text{O}_3$ (according to the data of some authors, $\text{Na}_2\text{O} \cdot 12\text{ Al}_2\text{O}_3$), has not been ascertained. Schairer and Bowen do not present this compound on their diagram. Pablo-Galan and Foster [24] propose that the "β alumina" field should be located along the "corundum -- carnegieite" boundary line. The point at which the corundum, β alumina and carnegieite fields meet should then be not a eutectic, but a reaction point.

The partial system $\text{Na}_2\text{O} \cdot \text{Al}_2\text{O}_3 \cdot 6\text{SiO}_2$ -- SiO_2 is a simple eutectic, with a eutectic containing 68.5 weight % $\text{Na}_2\text{O} \cdot \text{Al}_2\text{O}_3 \cdot 6\text{SiO}_2$ and melting at $1062 \pm 3^\circ$.

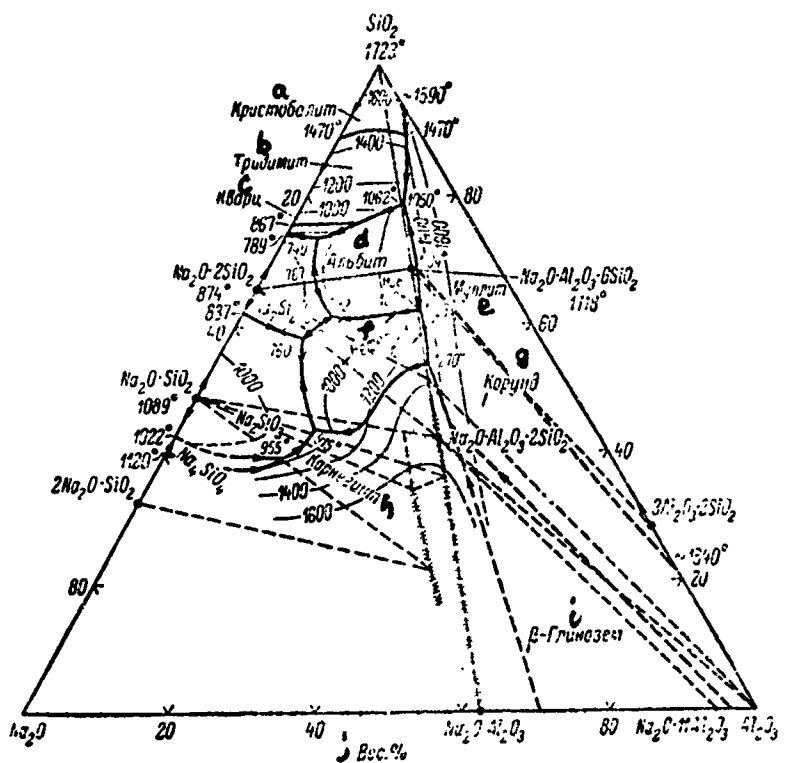


Fig. 151. Phase diagram of $\text{Na}_2\text{O} - \text{Al}_2\text{O}_3 - \text{SiO}_2$ system (from Osborn and Muan).

Key:

- | | |
|-----------------|----------------|
| a. Cristobalite | f. Nephelite |
| b. Tridymite | g. Corundum |
| c. Quartz | h. Carnegieite |
| d. Albite | i. Alumina |
| e. Mullite | j. Weight % |

Formation of solid solutions, the structures of which have been studied by Donnay and colleagues [13], is characteristic of the $\text{Na}_2\text{O} \cdot \text{Al}_2\text{O}_3 \cdot 2\text{SiO}_2$ -- SiO_2 system. Roy and colleagues [30], under increased pressure conditions, obtained a solid solution at 550° , with the structure of tridymite at a 10 mole % SiO_2 content.

The partial system $\text{Na}_2\text{O} \cdot \text{Al}_2\text{O}_3 \cdot 6\text{SiO}_2$ -- $\text{Na}_2\text{O} \cdot 2\text{SiO}_2$ also is a simple eutectic; the melting temperature of the eutectic is $767 \pm 3^\circ$, and the composition, $\text{Na}_2\text{O} \cdot \text{Al}_2\text{O}_3 \cdot 6\text{SiO}_2$, 38 weight %. This system is not binary, since the connecting line intersects the $\text{Na}_2\text{O} \cdot 2\text{SiO}_2$ and $\text{Na}_2\text{O} \cdot \text{Al}_2\text{O}_3 \cdot 6\text{SiO}_2$ fields. The $\text{Na}_2\text{O} \cdot \text{SiO}_2$ and albite phases are incompatible.

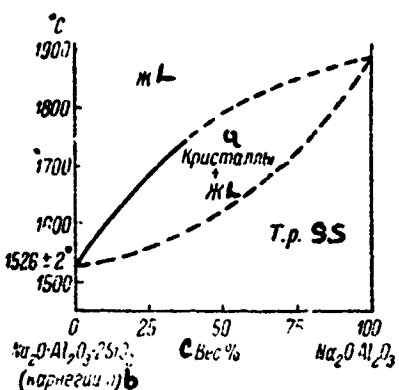


Fig. 152. Phase diagram of partial system $\text{Na}_2\text{O} \cdot \text{Al}_2\text{O}_3 \cdot \text{SiO}_2$ -- $\text{Na}_2\text{O} \cdot \text{Al}_2\text{O}_3$ (from Schairer and Bowen).

Key:

- a. Crystals
- b. Carnegieite
- c. Weight %

In the partial system $\text{Na}_2\text{O} \cdot \text{Al}_2\text{O}_3 \cdot 6\text{SiO}_2$ -- corundum, there is a eutectic, with final members differing strongly in melting temperature, containing 1.5 weight % Al_2O_3 in all and melting at $1103 \pm 3^\circ$.

The partial system $\text{Na}_2\text{O} \cdot \text{Al}_2\text{O}_3 \cdot 2\text{SiO}_2$ -- corundum is a eutectic, with a eutectic containing 7 weight % Al_2O_3 and melting at $1475 \pm 10^\circ$. Unstable

crystallization of " γ alumina" from glasses of any composition also is observed here.

The partial system $\text{Na}_2\text{O} \cdot \text{Al}_2\text{O}_3 \cdot 2\text{SiO}_2$ -- $\text{Na}_2\text{O} \cdot \text{Al}_2\text{O}_3$ is characterized by formation of the continuous series of carnegieite type solid solutions (Fig. 152). Because of volatilization of Na_2O , the presence of small quantities of corundum and " β alumina" usually is observed. The formerly assumed compound $\text{Na}_2\text{O} \cdot \text{Al}_2\text{O}_3 \cdot \text{SiO}_2$ apparently does not exist, and the composition corresponding to it is one of the members of the continuous series of solid solutions with a melting temperature of 1725° . According to Schairer and Bowen, $\text{Na}_2\text{O} \cdot \text{Al}_2\text{O}_3$ melts at 1850° .

In the partial system albite -- nephelite (carnegieite), Schairer and Bowen observed $\text{NaAlSi}_3\text{O}_8$ solid solutions in both nephelite and carnegieite, with the solubility of the albite being greater in the low-temperature modification, in connection with which, the carnegieite-nephelite inversion point is increased from 1248 to 1280° .

Robertson and colleagues [29] plotted a phase diagram of the $\text{Na}_2\text{O} \cdot \text{Al}_2\text{O}_3 \cdot 2\text{SiO}_2$ -- $\text{Na}_2\text{O} \cdot \text{Al}_2\text{O}_3 \cdot 6\text{SiO}_2$ system, at pressures of 15 and 30 kbar (Fig. 153). The liquidus line is plotted hypothetically. The authors think that nephelite will change to the high-density, polymorphic modification designated nephelite II at high pressures. It is evident from Fig. 153 that the stability regions of albite and nephelite are preserved in proportion to the increase in pressure. At a pressure of 30 kbar, the albite + nephelite association is unstable; however, in the presence of jadeite or liquid, these minerals may be stable.

At the present time, four modifications of the compound corresponding to the formula $\text{Na}_2\text{O} \cdot \text{Al}_2\text{O}_3 \cdot 2\text{SiO}_2 = \text{NaAlSiO}_4$, are accepted. Cubic, high-temperature

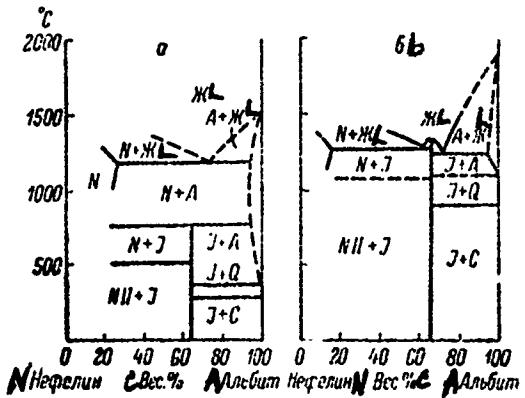


Fig. 153. Phase diagram of $\text{Na}_2\text{O} \cdot \text{Al}_2\text{O}_3 \cdot 2\text{SiO}_2$ -- $\text{Na}_2\text{O} \cdot \text{Al}_2\text{O}_3 \cdot 6\text{SiO}_2$ system at various pressures (from Robertson and colleagues); a. 15 kbar; b. 30 kbar; A. albite; C. coesite; J. jadeite; N. nephelite, Q. quartz.

Key:

c. Weight %

α carnegieite is stable from the melting temperature to 1250°, when a slow transformation into the stable, rhombic nephelite phase (high-temperature α nephelite) takes place. With reduction in temperature, α nephelite quickly changes to β nephelite, with crystals in the hexagonal system (from Tuttle and Smith [37] at 850°). For the α - β carnegieite transformation, as D. Roy and R. Roy [31] demonstrated, it is stretched out over several tens of degrees: from 669 to 694 upon heating and from 698 to 686° upon cooling.

A phase diagram of the compound NaAlSiO_4 , in "pressure-temperature" coordinates, has been studied by Boyd and England [9] and Tuttle and Smith [38],

the results of which are presented in Fig. 154a and b, respectively. According to the data of the first authors, pure NaAlSiO_4 is subjected to decomposition into two phases N (1) and N (2), the nature of which has not been established precisely, at high pressures. The N (2) phase apparently is similar to jadeite and is of the pyroxene type. Tuttle and Smith accept three modifications of carnegieite and two of nephelite.

Jadeite $\text{Na}_2\text{O} \cdot \text{Al}_2\text{O}_3 \cdot 4\text{SiO}_2$ crystallizes in the monoclinic system; the indices of refraction are $\text{Ng} = 1.667$, $\text{Nm} = 1.659$, $\text{Np} = 1.654$; the density is $3.3-3.4 \text{ g/cm}^3$. It melts at $1000-1060^\circ$. Artificial production of crystalline jadeite involves great difficulties. Boyd and England [10] succeeded in synthesizing jadeite under hydrothermal conditions. Rigby and Hutton [26] observed jadeite crystals when carrying out crystallization of glass in the presence of sodium vanadate at 800° . However, heating to 900° led to disappearance of the jadeite and to the appearance of nephelite. Jadeite can be obtained under high pressure conditions. Robertson and colleagues [29] studied the reaction albite + nephelite = jadeite at pressures between 10,000 and 25,000 kgf/cm^2 and temperatures between 600 and 1200° . Birch and LeCompte [7] studied the reaction albite = jadeite + quartz, at pressures from 15 to 25 kbar and temperatures from 600 to 1000° . The position of the reaction equilibrium line is expressed by the ratio $P(\text{bars}) = 6000 (\pm 500) + 20 (\pm 2)t(\text{°C})$. This expression is in good agreement with the curve plotted by Kelley and colleagues [16], on the basis of thermochemical data.

Albite $\text{Na}_2\text{O} \cdot \text{Al}_2\text{O}_3 \cdot 6\text{SiO}_2$ is very difficult to crystallize, without fail in the presence of mineralizers (sodium tungstate, magnetite, etc.). Barrer and White [1] synthesized albite by the hydrothermal method, from a gel of the

composition $\text{Na}_2\text{O} \cdot \text{Al}_2\text{O}_3 \cdot n\text{SiO}_2$ ($n = 4$). The best results were achieved at 410° and $\text{pH} = 10$.

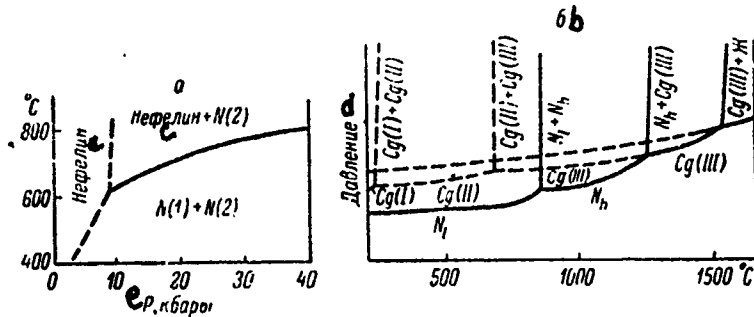


Fig. 154. P-t diagram for NaAlSiO_4 system (compounds);
a. from Boyd and England; b. from Tuttle and Smith;
Cg. carnegieite, N_h . high nephelite; N_l . low nephelite.

Key:

- c. Nephelite
- d. Pressure
- e. P , kbar

It has been established recently that albite changes to the high-temperature modification, which Laves [18] calls analbite, at a temperature of $700 \pm 25^\circ$. Laves and Chaisson [19] demonstrated that analbite has a lower index of refraction and a higher specific volume than albite.

The careful structural studies showed that "dimorphism" of $\text{NaAlSi}_3\text{O}_8$ is a typical example of "order-disorder" transformation. The problem of order in the feldspar group has been studied in detail by Marfunin [4]. Mackenzie [22] demonstrated the special, continuous nature of the transformation being discussed.

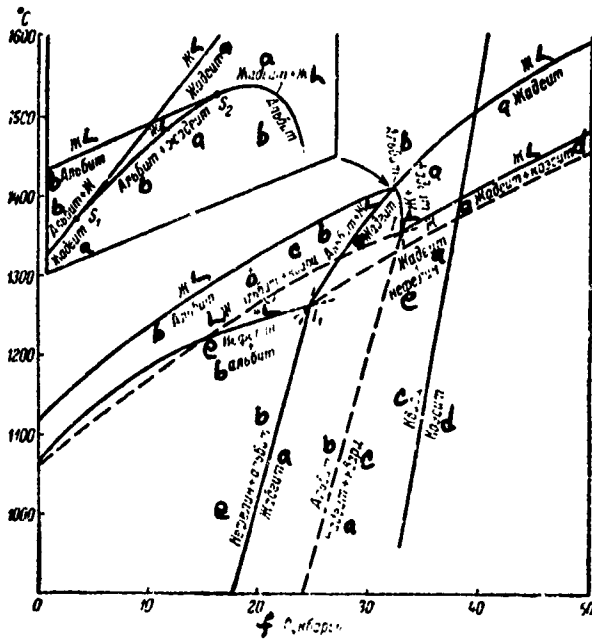


Fig. 155. Diagram characterizing interrelationships of jadeite, albite, nephelite, quartz and coesite under high pressure conditions (from Bell and Roseboom); I. invariant points; S. singular points.

Key:

- | | |
|------------|--------------|
| a. Jadeite | d. Coesite |
| b. Albite | e. Nephelite |
| c. Quartz | f. P, kbar |

The effect of pressure on melting temperature of albite has been studied by Boyd and England [10] and Roberts and colleagues.

Bell and Roseboom [6] have plotted a complete diagram of albite-jadeite-nephelite transitions, in "pressure-temperature" coordinates. The complete phase diagram of the nephelite-quartz system, up to a pressure of 50 kbar, is presented in Fig. 155. In plotting this diagram, data of earlier investigations

were used (Robertson and colleagues [29], Schairer and Yoder [34], Birch and Le Compte [7] and still older works). The most interesting section of the diagram is depicted on a large scale in the upper left corner. The incongruent melting curves of jadeite and albite begin at points I_1 and I_2 , and they end at points S_1 and S_2 . Melting of jadeite proceeds by the same path as that of albite. Both albite and jadeite have a certain section of incongruent melting. At a pressure of 32 kbar, the albite composition of the liquid is exchanged for a jadeite composition.

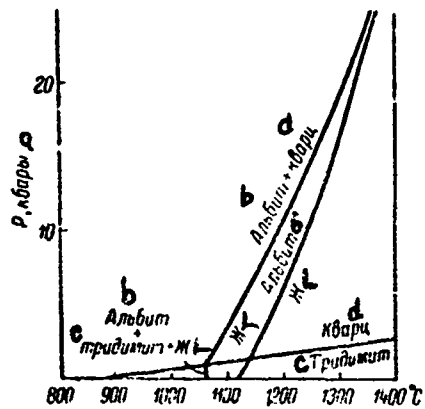


Fig. 156. Phase diagram of partial system albite -- silica at various pressures (from Tsch).

Key:

- a. P, kbar
- b. Albite
- c. Tridymite
- d. Quartz

According to Newton and Kennedy [21], the line dividing the albite and jadeite-quartz mixture fields is defined by the equation P (bars) = $6800 + 18.6 t$ ($^{\circ}$ C), and the corresponding line, characterizing the reaction albite + nephelite = jadeite, by the equation P (bars) = $25 t$ ($^{\circ}$ C) - 4000.

Luth [20] has studied the system $\text{Na}_2\text{O} \cdot \text{Al}_2\text{O}_3 \cdot 6\text{SiO}_2 - \text{SiO}_2$ under various pressure conditions, bringing it up to 20 kbar. The eutectic temperature was increased in this case, and the composition changed according to a complex function: At the beginning, some increase in silica content was exchanged for an increase in feldspar concentration. In Fig. 156, the phase ratios in the system are presented in "temperature-pressure" coordinates. The line characterizing the quartz-tridymite inversion was borrowed from the work of Kennedy and colleagues [17]. The curve characterizing the albite-liquid equilibrium was plotted from Boyd and England [11].

Ringwood and Major [27, 28] showed that jadeite is stable at least up to the pressure of 180 kbar (900 $^{\circ}$). The authors propose that, by analogy with germanium jadeite, the reaction $\text{NaAlSi}_2\text{O}_6$ (jadeite) = NaAlSiO_4 (new phase) + SiO_2 (stishovite) takes place at higher pressures. To clear up this question, it is desirable to study the behavior of germanium silicate jadeite solid solutions $\text{NaAl}(\text{GeSi})\text{O}_4$. Reid and colleagues [25] propose that the NaAlSiO_4 modification existing at high pressure has the structure of calcium ferrite CaFe_2O_4 , and that the transition of nephelite into this modification is accompanied by an increase in density by 46.6%.

Sodium aluminosilicates, which are richer in alkali than nephelite, are known. Dominikiewicz [12] obtained disodium aluminosilicate $2\text{Na}_2\text{O} \cdot \text{Al}_2\text{O}_3 \cdot 2\text{SiO}_2$ synthetically, by annealing nephelite with soda. Borchert and Keidel [8]

CRYSTALLINE PHASES OF $\text{Na}_2\text{O} - \text{Al}_2\text{O}_3 - \text{SiO}_2$ SYSTEM

Compound	Crystal System	Appearance	Cleavage	N_g	N_m	N_p	$2V^\circ$	Optical Sign	Density g/cm ³	Notes
$\text{Na}_2\text{O} \cdot \text{Al}_2\text{O}_3 \cdot 2\text{SiO}_2$ (c. _r rhögelite)	Cubic	—	—	—	1.51	—	—	—	—	Stable above 1248°
$\text{Na}_2\text{O} \cdot \text{Al}_2\text{O}_3 \cdot 2\text{SiO}_2$ (carnegieite)	Triclinic	Complex poly synthetic cleavages	—	1.514	1.514	1.509	12-15	(-)	2.51	Forms from Q form at 687°
$\text{Na}_2\text{O} \cdot \text{Al}_2\text{O}_3 \cdot 2\text{SiO}_2$ (nephelite)	Hexagonal	Short prisms	Weak along (1010) and along (0001)	1.537	—	1.533	0	(-)	2.619	Glass, N = 1.510
$\text{Na}_2\text{O} \cdot \text{Al}_2\text{O}_3 \cdot 6\text{SiO}_2$ (albite)	Triclinic	Plates along (001)	Perfect along (001), distinct along (010) at < 88°	1.5386	1.5323	1.5282	70	(+)	2.605	Plane of optical axis almost \perp (010), $\frac{Z}{(010)} = 75^\circ$, 2V =

consider disodium aluminosilicate as the final member of a series of solid solutions of the NaAlSiO_4 -- Na_2O series. The formation of such a solid solution takes place by means of introduction of sodium oxide into lattice vacancies of α carnegieite, which stabilizes the structure and prevents its transition to the β form.

Yakovlev [5] has described the compound $2\text{Na}_2\text{O} \cdot \text{Al}_2\text{O}_3 \cdot 2\text{SiO}_2$, which is a weakly anisotropic substance, with an index of refraction of 1.531 and density of 2.58 g/cm^3 . It reacts with aluminum oxide, forming β carnegieite and sodium aluminate.

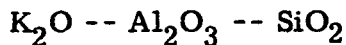
Manvelyan [3], by annealing a complex aluminosilicate mixture containing soda, obtained a uniform product, to which he ascribed the formula $\text{Na}_2\text{O} \cdot \text{Al}_2\text{O}_3 \cdot \text{SiO}_2$. The indices of refraction of this compound are $N = 1.519-1.524$.

BIBLIOGRAPHY

1. Barrer, R., Ye. White, in the collection Fizicheskaya khimiya silikatov [Physical Chemistry of Silicates], Foreign Literature Publishing House, Moscow, 1956, p. 156.
2. Galakhov, F. Ya., Izv. AN SSSR, OKhN, 5, 1959, p. 770.
3. Manvelyan, M. G., in the collection Mater. Vsegoysuzn. soveshch. po khimiya i tekhnologii glinozema [Materials, All-Union Conference on Chemistry and Technology of Alumina], Novosibirsk, 59, 1960.
4. Marfunin, A. S., Trudy Inst. geologii rudnykh mestorozhdeniy, petrografii, mineralogii i geokhimii AN SSSR, No. 78, Moscow, 1962.
5. Yakovlev, L. K., in the collection Khimiya i tekhnologiya glinozema, Trudy Vsegoysuzn. soveshch. (6-9 X 1959) [Chemistry and Technology of Alumina: Proceedings of All-Union Conference (6-9 Oct 1959)], Alma-Ata, 1961, p. 62.
6. Bell, P. M., E. H. Roseboom, Carnegie Inst. Washington Year Book, 64, 139, 1964-1965.
7. Birch, F., P. Le Compte, Amer. J. Sci., 258, No. 3, 209, 1960.

8. Borchert, W., J. Keidel, Heidelberger Beitr. Mineral. u. Petrogr., 1, 1-3, 17, 1947.
9. Boyd, F.R., J.L. England, Carnegie Inst. Washington Year Book, 55, 154, 1955-1956.
10. Boyd, F.R., J.L. England, Carnegie Inst. Washington Year Book, 60, 119, 1961.
11. Boyd, F.R., J.L. England, J. Geophys. Res., 68, 2, 311, 1963.
12. Dominikiewicz, M., Roczniki Chem., 12, 836, 1932.
13. Donnay, G., J.F. Schairer, J.D.H. Donnay, Mineral Magaz., 32, No. 245, 93, 1959.
14. Ferguson, R.B., R.J. Traill, W.H. Taylor, Acta crystallogr., 11, No. 5, 331, 1958.
15. Greig, J.W., T.F.W. Barth, Amer. J. Sci., (5), 35, 206, 93, 1938.
16. Kelley, K.K., S.S. Todd, K.L. Orr, E.G. King, K.R. Bonnickson, U.S. Bur. Mines Rept. Invest., 4955, 1953.
17. Kennedy, G.C., G.J. Wasserburg, H.C. Heard, R.C. Newton, Amer. J. Sci., 260, 7, 501, 1962.
18. Laves, F., J. Geol., 60, 5, 436, 1952.
19. Laves, F., U. Chaisson, J. Geol., 58, 5, 584, 1950.
20. Luth, W.C., Carnegie Inst. Washington Year Book, 66, 480, 1966-1967.
21. Newton, M.S., G.C. Kennedy, Amer. J. Sci., 266, 3, 728, 1968.
22. Mackenzie, W.S., Amer. J. Sci., 255, 7, 481, 1957.
23. Osborn E.F., A. Muan, in: E.M. Levin, C.R. Robbins, H.F. McMurdie, Phase diagrams for ceramists. USA, Columbus, fig. 501, 1964.
24. Pablo-Galan de L., W.R. Foster, J. Amer. Ceram. Soc., 42, 10, 491, 1959.
25. Reid, A.F., A.D. Wadsley, A.E. Ringwood, Acta crystallogr., 23, 5, 736, 1959.
26. Rigby, G.R., R. Hutton, J. Amer. Ceram. Soc., 45, 2, 68, 1962.
27. Ringwood, A.E., A. Major, Earth a. Planetary Sci., Lett., 2, 3, 255, 1967.

28. Ringwood, A. E., A. Major, Earth a. Planetary Sci. Lett., 2, 2, 106, 1967.
29. Robertson, E.C., F. Birch, G.J.F. MacDonald, Amer. J. Sci., 255, 2, 115, 1957.
30. Roy, R., Th. Isaacs, E.C. Shafer, Bull. Geol. Soc. Amer., 68, 2, 1789, 1957.
31. Roy, D.M., R. Roy, Bull. Geol. Soc. Amer., 69, 12, 1637, 1958.
32. Schairer, J.F., N.L. Bowen, Amer. J. Sci., (5), 245, 4, 193, 1947.
33. Schairer, J.F., N.L. Bowen, Amer. J. Sci., 254, 3, 129, 1956.
34. Schairer, J.F., H.S. Yoder, Amer. J. Sci., 258A, Bradley vol., 273, 1960.
35. Spivak, J., J. Geol., 52, 1, 24, 1944.
36. Tilley, C.E., Mineral. Petrogr. Mitteilungen, 43, 406, 1933.
37. Tuttle, O.F., J.V. Smith, Carnegie Inst. Washington Year Book, 52, 54, 1952-1953.
38. Tuttle, O.F., J.V. Smith, Amer. J. Sci., 256, 8, 583, 1958.



The system has been studied by Bowen and Schairer [2, 3, 15, 21, 22]. A phase diagram of the $K_2O -- Al_2O_3 -- SiO_2$ system is presented in Fig. 157, according to Osborn and Muan [17].

There are the following ternary compounds in the system: $K_2O \cdot Al_2O_3 \cdot 2SiO_2$, calcilite; $K_2O \cdot Al_2O_3 \cdot 4SiO_2$, leucite; $K_2O \cdot Al_2O_3 \cdot 6SiO_2$, calcium feldspar (microcline, orthoclase and sanidine). The following partial binary systems have been studied: 1. leucite -- SiO_2 (Fig. 158), incongruent melting of calcium feldspar takes place at $1150 \pm 20^\circ$, and the composition of the liquid phase forming here corresponds to 57.8 weight % leucite component and 42.4 weight %

silicic acid; 2. leucite -- corundum, eutectic composition ($1588 \pm 5^\circ$) K_2O -- 19.9, Al_2O_3 -- 29.3, SiO_2 -- 50.8 weight %; 3. calcium disilicate -- leucite, eutectic composition ($918 \pm 5^\circ$) K_2O -- 36.9, Al_2O_3 -- 7.4, SiO_2 -- 55.7 weight %; 4. rhombic $KAlSiO_4$ -- leucite, eutectic composition ($1615 \pm 10^\circ$) K_2O -- 24.8, Al_2O_3 -- 27.0, SiO_2 -- 48.2 weight %; 5. calcium disilicate -- $KAlSiO_4$, eutectic composition ($923 \pm 5^\circ$) K_2O -- 40.6, Al_2O_3 -- 7.7, SiO_2 -- 51.7 weight %; 6. calcium tetrasilicate -- calcium feldspar (Fig. 159), eutectic composition ($725 \pm 5^\circ$) K_2O -- 26.1, Al_2O_3 -- 3.3, SiO_2 -- 70.6 weight %; 7. $KAlSiO_4$ -- corundum, with the eutectic melting at 1680° .

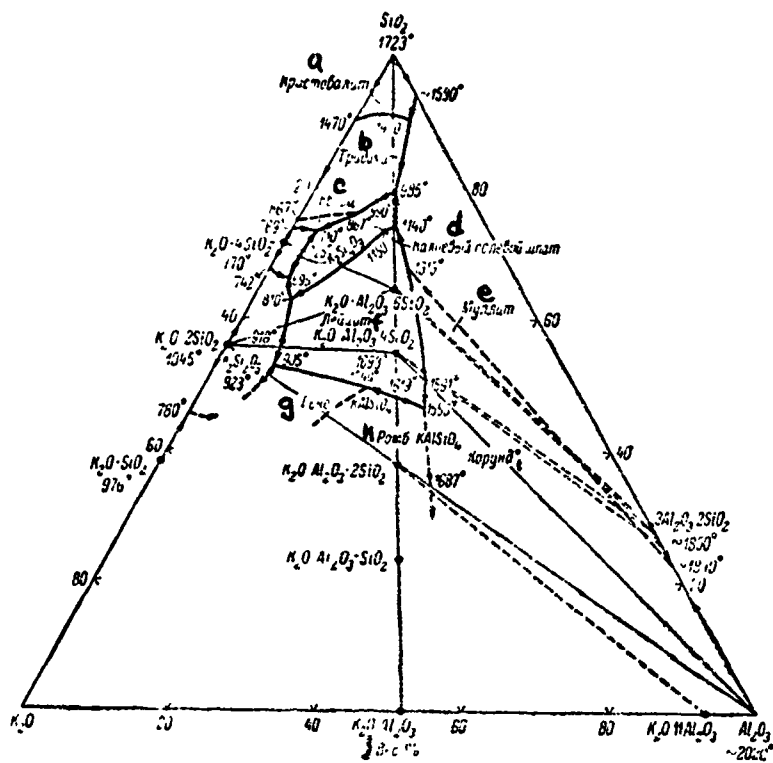
Calcium feldspar can exist in various structural states. The structure of high-temperature sanidine and the nature of the Si and Al distribution in the tetrahedral positions in it have been studied by Cole and colleagues [6]. Determination of the structure of orthoclase by Jones and Taylor [9] showed that partial ordering of the silicon and aluminum atoms takes place in it; the symmetry is monoclinic, or negligible deviations from monoclinic are observed.

According to Laves [11], orthoclase is submicroscopically paired triclinic domains.

Microcline is the lowest temperature form of calcium feldspar. Goldsmith and Laves [7] have shown that the lattice of microcline changes within broad limits, from monoclinic to triclinic.

The order-disorder processes in calcium feldspars have been studied by infrared spectroscopy [8] and nuclear magnetic resonance [4]. These methods make it possible to detect the differences between high and low sanidine.

Calcsilite $KAlSiO_4$, according to Rigby and Richardson [18], is produced only in the presence of Na_2O at $650-1200^\circ$; however, Tuttle and Smith [25]



Reproduced from
best available copy.

Fig. 157. Phase diagram of K_2O -- Al_2O_3 -- SiO_2 system (from Osborn and Muan).

- | | |
|---------------------|-------------------------|
| a. Cristobalite | f. Leucite |
| b. Tridymite | g. Hexagonal $KAlSiO_4$ |
| c. Quartz | h. Rhombic $KAlSiO_4$ |
| d. Calcium feldspar | i. Corundum |
| e. Mullite | j. Weight % |

obtained calcilite hydrothermally, from a mixture of sodium disilicate and aluminum oxide, at a temperature below 840°. A diagram characterizing the polymorphic transformations of $KAlSiO_4$ is shown in Fig. 160. The structure of calcilite has not been studied in detail; it is based on a tridymite-like

skeleton. The structure of hexagonal calcilite has been studied by Claringbull and Bannister [5]. Sahama and Smith [20] indicate the existence of ordered ($a = 5.15$ Å) and disordered ($a = 8.9$ Å) forms of calcilite. Beside hexagonal calcilite, there is a high-temperature form O_1 , rhombic calcilite. The hexagonal calcilite \rightleftharpoons rhombic calcilite (O_1) inversion takes place slowly, and the high-temperature phase (O_1) can be obtained by rapid cooling. Kunz [10] gives a summary of the literature on rhombic calcilite. Tuttle and Smith [25] have detected a second rhombic form of calcilite (O_2).

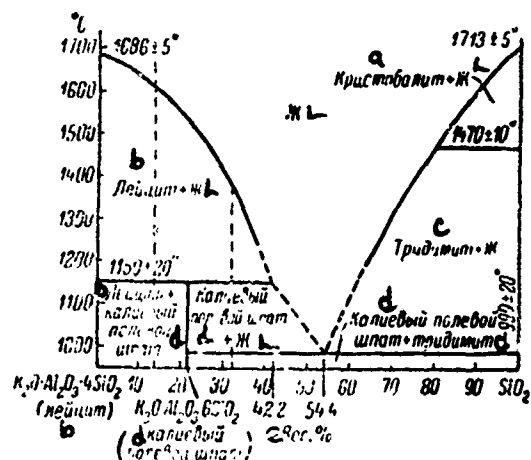


Fig. 158. Phase diagram of partial system leucite ($K_2O \cdot Al_2O_3 \cdot 4SiO_2$) -- SiO_2 (from Schairer and Bowen).

Key:

- a. Cristobalite
- b. Leucite
- c. Tridymite
- d. Calcium feldspar
- e. Weight %

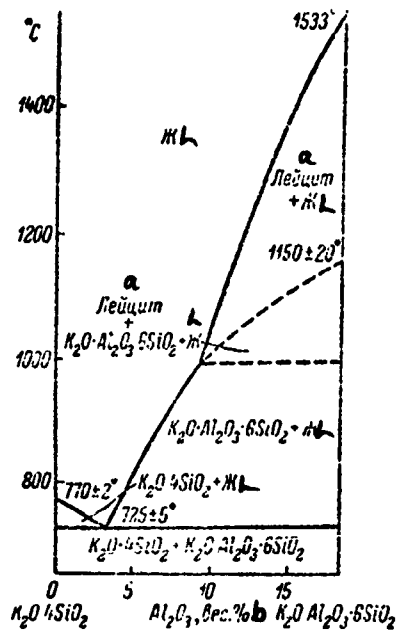


Fig. 159. Phase diagram of partial system
 $K_2O \cdot 4SiO_2$ -- $K_2O \cdot Al_2O_3 \cdot 6SiO_2$ (from Schairer
 and Bowen).

Key:

- a. Leucite
- b. Weight %

Synthetic caliophyllite [25] is not identical to natural caliophyllite, but it is a disordered form of natural caliophyllite.

Leucite $KAlSi_2O_6$ is encountered in two modifications [16]: low-temperature (tetragonal crystal system) and high-temperature (cubic crystal system).

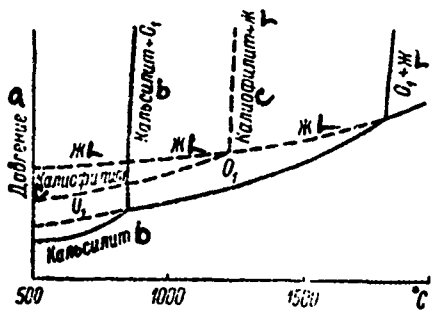


Fig. 160. Phase diagram of KalSiO_4 compounds
(from Tuttle and Smith); O_1 rhombic KAlSiO_4

Key:

- a. Pressure
- b. Calcilite
- c. Caliophyllite

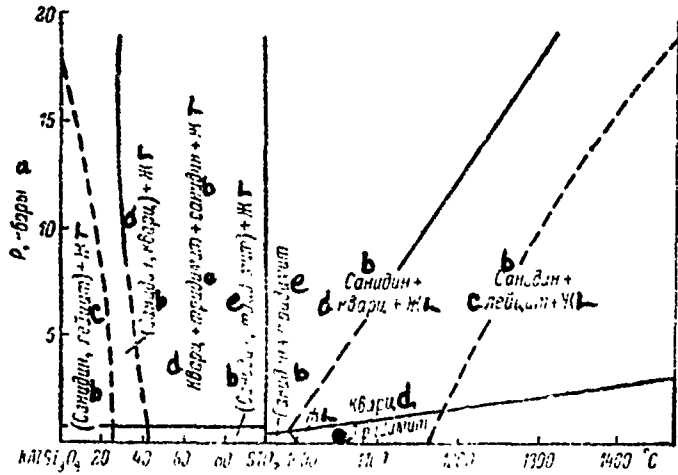


Fig. 161. Phase diagram of $\text{KAlSi}_3\text{O}_8 - \text{SiO}_2$ system, in "P-t" and "pressure-composition" coordinates (from Luth).

Key:

- | | |
|-------------|--------------|
| a. P, kbar | d. Quartz |
| b. Sanidine | e. Tridymite |
| c. Leucite | |

TABLE 1
BINARY INVARIANT POINTS OF
 K_2O -- Al_2O_3 -- SiO_2 SYSTEM

Phases	Process	Composition, weight %			Tempera-ture, °C
		K_2O	Al_2O_3	SiO_2	
Calcium feldspar + tridymite + liquid	Eutectic	9.8	10.7	79.5	990 ± 20
Tridymite + cristobalite + liquid	Polymorphic transformation	4.3	4.7	91	1470 ± 10
Leucite + calcium feldspar + liquid	Reactions	12.5	13.5	74.0	1150 ± 20
Calcium tetrasilicate + calcium feldspar + liquid	Eutectic	26.1	3.3	70.6	725 ± 5
Calcium disilicate + leucite + liquid	"	36.9	7.4	55.7	918 ± 5
Calcium disilicate + hexagonal $KAlSiO_4$ + liquid	"	40.6	7.7	51.7	923 ± 5
Hexagonal $KAlSiO_4$ + rhombic $KAlSiO_4$ + liquid	Polymorphic transformation	35.6	19.0	45.4	about 1540
Leucite + corundum + liquid	Eutectic	19.9	29.3	50.8	1588 ± 5
Rhombic $KAlSiO_4$ + corundum + liquid	"	27.4	37.7	34.9	1680 ± 10
Leucite + rhombic $KAlSiO_4$ + liquid	"	24.8	27.0	48.2	1615 ± 10

Luth [13] has plotted a phase diagram for the $KAlSi_3O_8$ -- SiO_2 system, in "pressure-temperature-composition" coordinates (Fig. 161). The system was studied up to a pressure of 20 kbar. At a pressure of 20 kbar, leucite is not found and only sanidine is present. Curves characterizing the equilibrium sanidine + quartz + liquid and sanidine + leucite + liquid are presented on the right of the figure in "pressure-temperature" coordinates, and on the left, in "pressure-composition" coordinates, curves characterizing the change in composition of the nonvariant liquids, which coexist with the following phases: sanidine + leucite, sanidine + quartz or sanidine + tridymite.

Seki and Kennedy [23] have shown that sanidine ($KAlSi_3O_8$) and hexagonal calcilite ($KAlSiO_4$) can coexist at high pressures. The authors have studied the

TABLE 2
TRIPLE INVARIANT POINTS OF K_2O -- Al_2O_3 -- SiO_2 SYSTEM

Phases	Process	Composition, weight %			Tempera-ture, °C
		K_2O	Al_2O_3	SiO_2	
Calcium feldspar + quartz + calcium tetrasilicate + liquid	Eutectic	22.8	3.7	73.5	710 ± 20
Quartz + tridymite + calcium feldspar + liquid	Polymorphic transformation	17.0	6.8	76.2	867 ± 3
Calcium feldspar + tridymite + mullite + liquid	Eutectic	9.5	10.9	79.6	985 ± 20
Tridymite + cristobalite + mullite + liquid	Polymorphic transformation	2.4	7.3	90.3	1470 ± 15
Calcium feldspar + leucite + mullite + liquid	Reactions	12.2	13.7	74.1	1140 ± 20
Leucite + mullite + corundum + liquid	"	12.2	13.7	74.1	1315 ± 10
Calcium feldspar + leucite + calcium disilicate + liquid	"	32.1	5.3	62.6	810 ± 5
Calcium feldspar + calcium tetrasilicate + calcium disilicate + liquid	Eutectic	30.4	3.2	66.4	695 ± 5
Leucite + hexagonal $KAlSiO_4$ + calcium disilicate + liquid	"	39.3	7.8	52.9	905 ± 10
Hexagonal $KAlSiO_4$ + rhombic $KAlSiO_4$ + leucite + liquid	Polymorphic trans-formation	28.5	22.0	49.5	about 1540
Leucite + rhombic $KAlSiO_4$ + corundum + liquid	Eutectic	22.1	31.3	46.6	1553 ± 5

reaction $2KAlSi_2O_6$ (leucite) = $KAlSi_3O_8$ (sanidine) + $KAlSiO_4$ (hexagonal cal-cilite), using pressures up to 20 kbar, in the presence of water as a flux. The index of refraction of hexagonal cacilite is 1.537-1.542, density 2.59 g/cm^3 . For sanidine, the index of refraction is 1.520-1.53, density 2.57 g/cm^3 .

Lindsley [12] has studied the melting of calcium feldspar under high pressure conditions; the triple point at which leucite + liquid, "high sanidine" and liquid are in equilibrium, has the coordinates: temperature $1445 \pm 10^\circ$, pressure $19 \pm 1 \text{ kbar}$.

Seki and Kennedy [23] have shown that, under dry conditions, calcium feldspar is stable even up to 1000°, at a pressure of 60 kbar. Under hydrothermal conditions, formation of the hexagonal phase $KAlSi_3O_8 \cdot H_2O$ takes place, at 300-400° and pressures of 15-20 kbar.

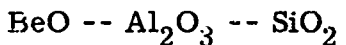
Ringwood and colleagues [19] have demonstrated experimentally that synthetic calcium feldspar $KAlSi_3O_8$ (sanidine), at a pressure of 120 kbar and a temperature of 900°, undergoes a polymorphic transformation, changing to a hollandite structure (space group I4/m, $a = 9.38$, $c = 2.74 \pm 0.01$ Å), with an average index of refraction of 1.745. In the transition of sanidine to the new modification with the hollandite structure, the density increases from 2.55 to 3.48 g/cm^3 , i.e., by 50%. The authors propose that leucite at high pressure disproportionates into hollandite and $KAlO_2$.

For summary data on the mineralogy of calcium aluminosilicates, see the book of Dir and colleagues [1].

BIBLIOGRAPHY

1. Dir, U.A., R.A. Howie, G. Zusman, Porodoobrazuyushchiye mineraly [Ore-Forming Minerals], Vol. 4, Mir Press, Moscow, 1966, pp. 14, 268, 304.
2. Bowen, N.L., J. Amer. Ceram. Soc., 26, 9, 285, 1943.
3. Bowen, N.L., J.F. Schairer, Amer. J. Sci., (5), 245, 193, 1947.
4. Brun, E., St. Hafner, P. Hartmann, F. Laves, H.H. Staub. Zs. Kristallogr., 113, 65, 1960.
5. Claringbull, C.F., F.A. Bannister, Acta crystallogr., 1, 1, 42, 1948.
6. Cole, W.F., H. Sörum, O. Kenard, Acta crystallogr., 2, 5, 280, 1949.
7. Goldsmith, J.R., F. Laves, Geochim. cosmochim. acta, 5, 1, 1, 1954.
8. Hafner, St., F. Laves, Zs. Kristallorg., 109, 3/4, 204, 1957.

9. Jones, J. B., W.H. Taylor, Acta crystallogr., 14, 4, 443, 1961.
10. Kunz, G., Heidelberg. Beitr. z. Mineral., 4, 1/2, 99, 1954.
11. Laves, F., J. Geol., 60, 5, 436, 1952.
12. Lindsley, D.H., Amer. Mineralogist, 51, 11-12, 1703, 1966.
13. Luth, W.C., Amer. J. Sci., 267A, Schairer vol., 325, 1969.
14. MacKerzie, W.S., Mineral. Magaz., 30, 225, 354, 1954.
15. Morey, G.W., N.L. Bowen, Amer. J. Sci., (5), 4, 1, 1922.
16. Naray-Szabo, St., Zs. Kristallogr., 104, 1, 39, 1942.
17. Osborn, E.F., A. Muan, in: E.M. Levin, C.R. Robbins, H.F. McMurdie, Phase Diagrams for Ceramists, USA, Columbus, fig. 407, 1964.
18. Rigby, G.R., H.M. Richardson, Mineral. Magaz., 28, 197, 75, 1947.
19. Ringwood, A.E., A.F. Reid, A.D. Wadsley, Acta crystallogr., 23, 6, 1093, 1967.
20. Sahama, Th. G., J.V. Smith, Amer. Mineralogist, 42, 3-4, 286, 1957.
21. Schairer, J.F., J. Geol., 58, 5, 512, 1950.
22. Schairer, J.F., N.L. Bowen, Amer. J. Sci., 253, 12, 681, 1955.
23. Seki, Y., G.C. Kennedy, Amer. Mineralogist, 49, 9-10, 1267; 11-12, 1688, 1964.
24. Smith, J.V., O.F. Tuttle, Amer. J. Sci., 255, 4, 282, 1957.
25. Tuttle, O.F., J.V. Smith, Amer. J. Sci., 256, 8, 571, 1958.



The system has been studied by Galakhov [2] and Ganguli and Saha [6]. Galakhov studied the region adjacent to the alumina apex (Fig. 162). In the region studied, there are two invariant reaction points: between the fields of corundum, mullite and $\text{BeO} \cdot 3\text{Al}_2\text{O}_3$, of the composition 6 weight % BeO, 74 weight % Al_2O_3 and 20 weight % SiO_2 , with a melting temperature of 1780° and

between the fields of $\text{BeO} \cdot 3\text{Al}_2\text{O}_3$, $\text{BeO} \cdot \text{Al}_2\text{O}_3$ and mullite, of the composition 13 weight % BeO, 58 weight % Al_2O_3 and 29 weight % SiO_2 , with a melting temperature of 1630° . The boundary between BeO and $3\text{BeO} \cdot \text{Al}_2\text{O}_3$ is a reaction one.

Ganguli and Saha [6] studied the region of the system adjacent to the silica apex by the quenching method (Fig. 163). There is a eutectic (E_1) between the chrysoberyl, phenacite and cristobalite fields, of the composition: 6.0 weight % BeO, 11.3 weight % Al_2O_3 and 82.7 weight % SiO_2 , with a melting temperature of $1515 \pm 5^\circ$. Points P_1 and P_2 are paratetic (reaction), and they have the respective compositions: 3.5 and 5.0 weight % BeO, 12 and 4 weight % Al_2O_3 and 84.5 and 91 weight % SiO_2 , with melting temperatures of 1548 ± 5 and $1640 \pm 15^\circ$. Beryl $3\text{BeO} \cdot \text{Al}_2\text{O}_3 \cdot 6\text{SiO}_2$ ($\text{Be}_3\text{Al}_2\text{Si}_6\text{O}_{18}$) was obtained at temperatures just below the eutectic, but the authors admit the presence of a small beryl field on the diagram, close to the eutectic point. Combining their results with the data of other authors, mainly of Galakhov, the authors plotted a phase diagram of the system (Fig. 164).

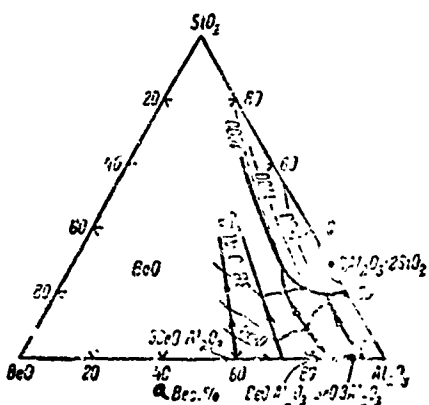


Fig. 162. Phase diagram of high-alumina portion of $\text{BeO} \cdots \text{Al}_2\text{O}_3 \cdots \text{SiO}_2$ (from Galakhov).

Key: a. Weight %

TABLE 3
CRYSTALLINE PHASES OF K_2O -- Al_2O_3 -- SiO_2 SYSTEM

Compound	Crystal system	Crystal appearance	Unit cell parameters	Indices of refraction	Density, g/cm ³
Sanidine $KAlSi_3O_8$ high-temperature (stable above 900°) [6]	Monoclinic, C2/m	Flakes along (010)	$a = 8.564$, $b = 13.00$, $c = 7.174$ Å, $\beta = 115^{\circ}39'$	$N_g = 1.523$, $N_m = 1.522$, $N_p = 1.517$, $N_g - N_p = 0.006$	2.57-- 2.58
Orthoclase $KAlSi_3O_8$ [6]	Same	Lamellar	$a = 8.561$, $b = 12.996$, $c = 7.193$ Å, $\alpha = 116^{\circ}09'$	$N_g = 1.5236$, $N_m = 1.5230$, $N_p = 1.5188$, $N_g - N_p = 0.005$	2.56
Microcline $KAlSi_3O_8$ low-temperature [14]	Triclinic, C1	"	$a = 8.574$, $b = 12.981$, $c = 7.222$ Å, $\alpha = 90^{\circ}41'$, $\beta = 115^{\circ}59'$, $\gamma = 87^{\circ}30'$	$N_g = 1.525$, $N_m = 1.522$, $N_p = 1.518$	2.54
Adular $K_2O \cdot Al_2O_3 \cdot 6SiO_2$ (stable at low temperatures)	Monoclinic	Short prisms	—	$N_g = 1.525$, $N_m = 1.523$, $N_p = 1.519$, $N_g - N_p = 0.006$	2.55
Leucite $KAlSi_2O_6$ low-temperature [16]	Tetragonal (pseudo-cubic), $I4_1/a$	Complex poly synthetic cleavage	$a = 13.1$, $c = 13.82$ Å	$N_g = 1.510$	2.48
Leucite $KAlSi_2O_6$ high-temperature (stable above 620°) [16]	Cubic, Ia3d	Isometric crystals	$a = 13.4$ Å	$N_g = 1.485$	2.47
Calcilite $KAlSiO_4$ [24]	Hexagonal, $P6_3^{22}$	—	$a = 5.2$, $c = 3.7$ Å	$N_g = 1.538$, $N_c = 1.532$, $N_g - N_c = 0.006$	3.59
Calcilite rhombic O ₁ [24]	Rhombic	—	$a = 9.1$, $b = 15.7$, $c = 8.6$ Å	—	—
Calcilite rhombic O ₂ [24]	"	—	$a = 8.9$, $b = 10.5$, $c = 8.5$ Å	—	—
Tricalcilitite [20]	Hexagonal, $P6_3(?)$	—	$a = 15.4$, $c = 8.6$ Å	—	—
Tetracalcilitite $K_3NaAl_4Si_4O_{16}$ [24]	Hexagonal, $P6_3^{22}$	Needle-shaped	$a = 20.5$, $c = 8.5$ Å	$N_g - N_p$ very low	—
Caliophyllite synthetic (glass has $N = 1.508$) [24]	Same	Prismatic	$a = 5.2$, $c = 8.6$ Å	$N_g = 1.532$, $N_p = 1.527$, $N_g - N_p = 0.005$	2.61

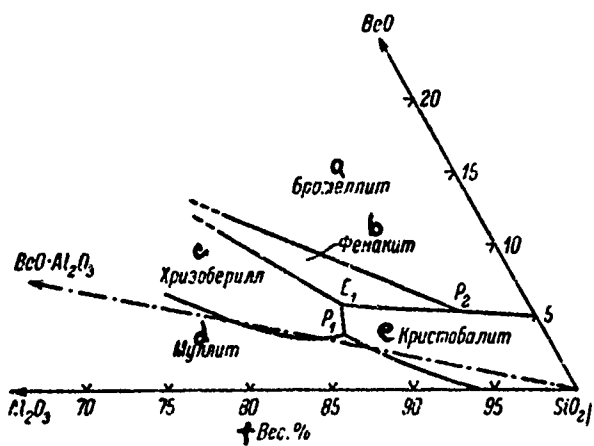


Fig. 163. Phase diagram of high-silica portion of $\text{BeO} - \text{Al}_2\text{O}_3 - \text{SiO}_2$ system (from Ganguli an. Saha).

Key:

- | | |
|----------------|-----------------|
| a. Bromellite | d. Mullite |
| b. Phenacite | e. Cristobalite |
| c. Chrysoberyl | f. Weight % |

Van Valkenburg [9] determined that beryl melts incongruently at 1450° , dissociating into phenacite and liquid.

Miller and Mercer [7], using a heating microscope, have studied the thermal decomposition of beryl in greater detail. The phenacite and liquid, forming as a result of dissociation of beryl at 1450° , forms chrysoberyl and liquid upon subsequent heating. Both crystalline phases coexist in the $1450 - 1475^\circ$ range. In the $1475 - 1490^\circ$ temperature range, chrysoberyl gradually decomposes to formation of BeO . After holding for 6 hours at 1490° , only one crystalline phase, beryllium oxide, is found.

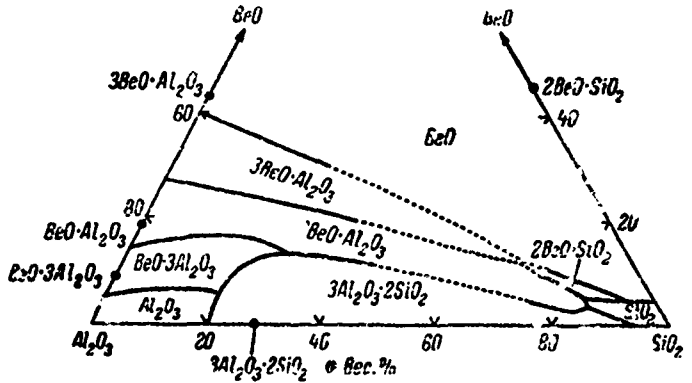


Fig. 164. Phase diagram of BeO -- Al₂O₃ -- SiO₂ system (from Ganguli and Saha, taking account of data of Galakhov).

Key:

a. Weight %

As a result of crystallization of beryllium glass, Miller and Mercer obtained a new compound, which they call the hybrid beryllium aluminosilicate phase. The new compound can be considered either as a beryllium-containing mullite, with the formula Be₅Al₃SiAl₃O₁₆, or as a compound formed as a result of substitution of aluminum for beryllium in beryl, with the formula Be₄Al₄Si₃O₁₆.

Ganguli and Saha [5] have studied the thermal breakdown of beryl, using the natural mineral, containing impurities of Fe₂O₃ (0.65 weight %), TiO₂ (0.24 weight %), CaO (0.25 weight %) and MgO (0.13 weight %). The total alkali content was 0.87 weight %, Ne = 1.574 and No = 1.578, density 2.66 g/cm³. At 1507 ± 2°, beryl melts incongruently, with decomposition into

phenacite, chrysoberyl and liquid. Phenacite is present up to 1523°. Complete melting begins at 1627°. The primary phase in crystallization of the melt is chrysoberyl. Glass of beryllium composition has an index of refraction of 1.525. The authors propose the presence of liquation of the beryllium glass. Crystallization of beryl from glass takes place only in the presence of nuclei, added small crystals of beryl.

Riebling and Duke [8] observed phase separation of the melt, corresponding to the beryl composition (or close to it) at temperatures over 1600°. The authors think that, during incongruent melting of beryl, dissociation of the Si_6O_{18} ring and appearance of discrete BeO_4 tetrahedra and AlO_6 octahedra takes place.

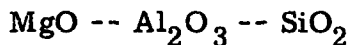
Ebelmen [3], and then other investigators, have accomplished numerous syntheses of artificial beryl, emerald $\text{Be}_3\text{Al}_2\text{Si}_6\text{O}_{18}$. Large, high-quality monocrystals of emerald have been obtained by the hydrothermal method by Flanigen and colleagues [4]. The indices of refraction of these crystals: $\text{No} = 1.569$, $\text{Ne} = 1.563$; density 2.56 g/cm^3 .

Bakakin and Belov [1], as a result of study of large number of natural beryls, have determined the limits of possible replacement of beryllium, aluminum and silicon by other elements.

BIBLIOGRAPHY

1. Bakakin, V. V., N. V. Belov, Geokhimiya, 5, 1962, p. 420.
2. Galakhov, F. Ya., Izv. AN SSSR, OKhN, 9, 1957, p. 1032.
3. Ebelmen, J. J., Ann. Chim. Phys., 22, (3), 237, 1848.
4. Flanigen, E. M., D. W. Breck, N. R. Mumbach, A. M. Taylor, Amer. Mineralogist, 52, No. 5-6, 744, 1967.
5. Ganguli, D., P. Saha, Bull. Centr. Glass Ceram. Res. Inst., 12, No. 1, 24, 1965.

6. Ganguli, D., P. Saha, Trans. Indian Ceram. Soc., 24, No. 4, 134, 1965.
7. Miller, R.P., R.A. Mercer, Mineral. Magaz., 35, No. 270, 250, 1965.
8. Riebling, E.F., D.A. Duke, J. Materials Sci., 2, No. 1, 33, 1967.
9. Van Valkenburg, A., C.E. Weir, Bull. Geol. Soc. Amer., 68, No. 12, 1808, 1957.



The first studies of the system were done by Rankin and Merwin [32] and Bowen and Greig [11]. According to their data, the only ternary compound in the system is cordierite. Foster [22] also established the presence of sapphirine in the system, together with cordierite, and conjecturally plotted the field of its crystallization in the diagram. The presence of a small sapphirine stability field was confirmed by Keith and Schairer [28, 35], according to whom the temperatures of the three invariant triple points: 1. spinel + sapphirine + mullite + liquid; 2. sapphirine + mullite + cordierite + liquid; 3. sapphirine + spinel + cordierite + liquid, are 1482 ± 3 , 1460 ± 5 and $1453 \pm 5^\circ$, respectively. Still another compound, pyrope, was obtained subsequently. The most complete triple diagram, in which all preceding studies were correlated, was offered by Osborn and Muan [31] in 1960 (Fig. 165).

Cordierite $2\text{MgO} \cdot 2\text{Al}_2\text{O}_3 \cdot 5\text{SiO}_2$ has an incongruent melting character, forms a series of stable and metastable solid solutions and has a number of polymorphic modifications (see below). Dittler and Kohler [20] and Schreyer and Yoder [44] detected spinel $\text{MgO} \cdot \text{Al}_2\text{O}_3$ in the decomposition products of cordierite when melting.

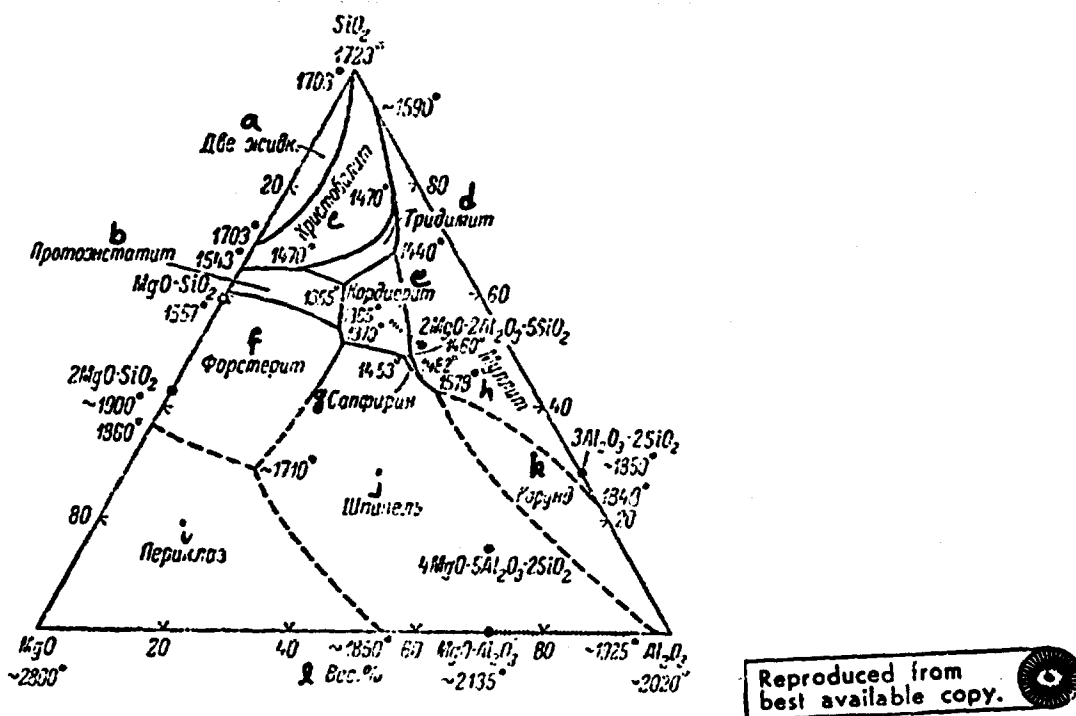


Fig. 165. Phase diagram of $\text{MgO} - \text{Al}_2\text{O}_3 - \text{SiO}_2$ system (from Osborn and Muan).

Key:

- | | |
|-------------------|---------------|
| a. Two liquids | g. Sapphirine |
| b. Protoenstatite | h. Mullite |
| c. Cristobalite | i. Periclase |
| d. Tridymite | j. Spinel |
| e. Cordierite | k. Corundum |
| f. Forsterite | l. Weight % |

The composition of sapphirine has not been conclusively established up to now; Foster proposes the formula $4\text{MgO} \cdot 5\text{Al}_2\text{O}_3 \cdot 2\text{SiO}_2 = \text{Mg}_4\text{Al}_{10}\text{Si}_2\text{O}_{23}$. There must be 80 atoms of oxygen in the unit cell of sapphirine; therefore, the average Si content will be 7.00 and Al, 33.98. The number of silicon atoms in the cells varies between 5.96 and 8.07, and of Al, from 31.30 to 35.99. The

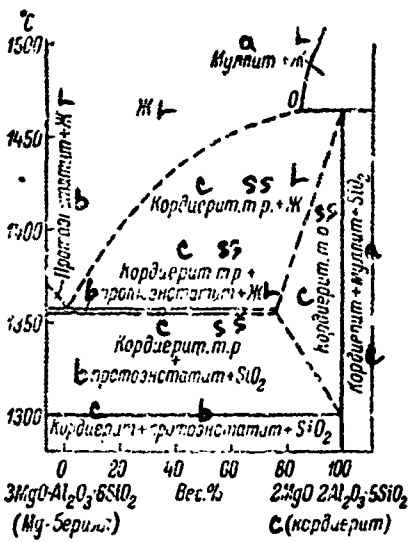


Fig. 166. Phase diagram of binary profile cordierite -- Mg beryl (from Miyama).

Key:

- a. Mullite
- b. Pötkenstatite
- c. Cordierite
- d. Mg beryl
- e. Weight %

formula (in which the charges are not balanced) can be represented in the form

$Mg_{14}Al_{35}Si_7O_{80}$. At 1475° , monoclinic synthetic sapphirine [23] melts incongruently into spinel and liquid. Below this temperature, sapphirine is compatible with cordierite, spinel and mullite. Sapphirine may not be encountered with forsterite, periclase or clinoenstatite. Schreyer and Seifert [43] introduced the formula $2MgO \cdot 2Al_2O_3 \cdot SiO_2$, for sapphirine synthesized under hydrothermal conditions (13 kbar, 900°); the average index of refraction is 1.699 ± 0.003 .

A limited series of solid solutions, beginning with cordierite and proceeding in the direction of the hypothetical magnesium beryl $3\text{MgO} \cdot \text{Al}_2\text{O}_3 \cdot 6\text{SiO}_2$ is shown in Fig. 166. In formation of the solid solutions, heterovalent isomorphism, according to the scheme $\text{Mg}^{2+} + \text{Si}^{4+} = 2\text{Al}^{3+}$, appears. The maximum solubility of Mg beryl in cordierite is found at 1350° , and it is over 20 weight %.

Schreyer and Schairer [42] have found a small region of solid solutions in study of the cordierite- MgSiO_3 profile (Fig. 167). Solubility, limited to a value of less than 1 weight % MgSiO_3 , also is at a maximum at a temperature a little above 1350° .

In study of the cordierite - $\text{MgO} \cdot \text{Al}_2\text{O}_3$ profile (Fig. 168), solid solutions were not found. Figs. 166 and 167 permit representation of equilibrium conditions in crystallization of cordierite close to the liquidus temperatures and variations in its composition.

Budnikov and Zlochevskaya [2], occupied with synthesis of a spinel-mullite ceramic, investigated the fusibility diagram of the binary partial system spinel - mullite. The minimum fusibility, at approximately 1800° , was found with equimolecular ratios of mullite and spinel.

Schlaudt and D. Roy [37] have studied two profiles: MgAl_2O_4 - Mg_2SiO_4 (Fig. 169) and MgO - Mg_2SiO_4 . Solid solutions were found in these partial systems. The maximum solubility of MgAl_2O_4 in the forsterite structure is 0.5 mole % overall at 1720° (double eutectic temperature). Somewhat over 5 mole % Mg_2SiO_4 can enter the spinel structure at this temperature. The solubility of MgO in forsterite is limited to 0.5 mole % at the eutectic temperature 1860° . Up to 11 mole % Mg_2SiO_4 can enter the periclase structure at this temperature.

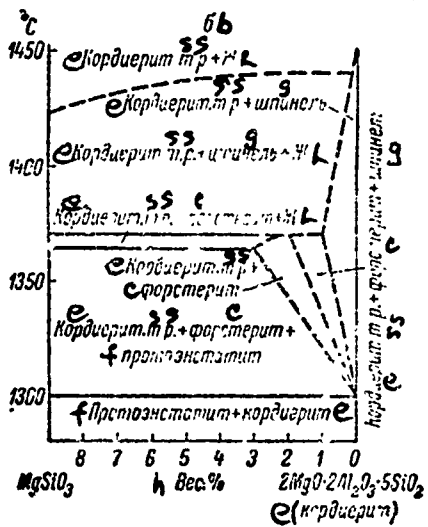
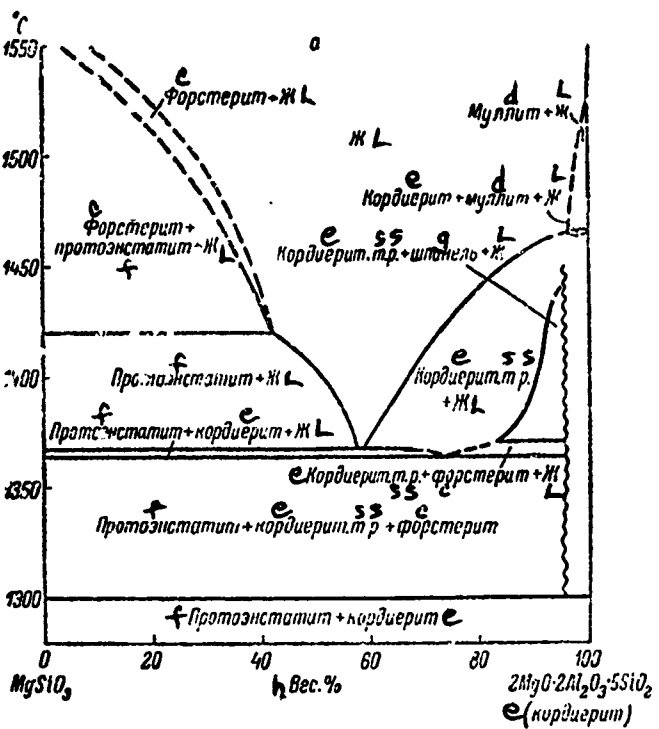


Fig. 167. Phase diagram of binary profile cordierite -- enstatite (from Schreyer and Schairer); a. cordierite -- enstatite profile; b. section adjacent to cordierite.

Key:

- | | |
|---------------|-------------------|
| c. Forsterite | f. Protoenstatite |
| d. Mullite | g. Spinel |
| e. Cordierite | h. Weight % |

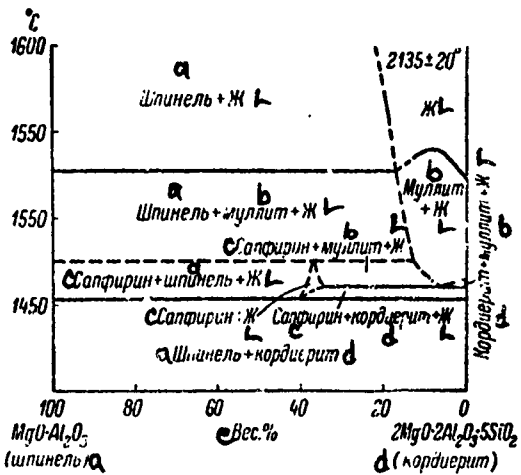


Fig. 165. Phase diagram of binary profile cordierite -- magnesium spinel (from Schreyer and Schairer).

Key:

- a. Spinel
- b. Mullite
- c. Sapphirine
- d. Cordierite
- e. Weight %

Schlaudt and D. Roy have established the existence of ternary periclase solid solutions in the MgO -- $MgAl_2O_4$ -- Mg_2SiO_4 system, extending up to a composition of $Mg_{0.853}Al_{0.063}Si_{0.026}O$, at a temperature of 1710° (eutectic among MgO , $MgAl_2O_4$ and Mg_2SiO_4).

Under certain conditions, the ternary compound $3MgO \cdot Al_2O_3 \cdot 3SiO_2$, pyrope, belonging to the garnet group, can be found in the system.

Medvedeva and Popova [3] have synthesized pyrope $Mg_3Al_2(SiO_4)_3$ from a mixture of MgO , $Mg(NO_3)_2 \cdot 6H_2O$, $Al(OH)_3$ and SiO_2 , at pressures of 60-120

kbar and a temperature of $1500 \pm 150^\circ$. The resulting crystals have a zonal structure. The index of refraction on the periphery of the grains was 1.720-1.725 and, in the central part, 1.735 and higher. Skinner [45] and Ford [21] present lower indices of refraction: 1.714 and 1.705. At the liquidus temperature, this compound is unstable and it decomposes upon heating into a mixture of forsterite, spinel and cordierite. However, at elevated pressures, the temperature region of stability of pyrope is considerably enlarged. Boyd and England [13] have plotted a preliminary, incomplete diagram of the stability field of pyrope.

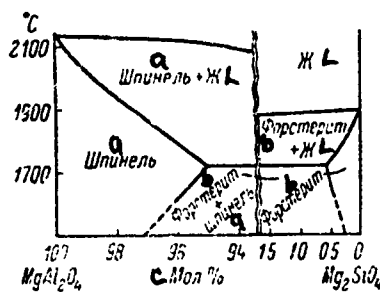


Fig. 169. Phase diagram of partial system $\text{Mg}_2\text{SiO}_4 \rightarrow \text{MgAl}_2\text{O}_4$ (from Schlaudt and D. Roy).

Key:

- a. Spinel
- b. Forsterite
- c. Mole %

Berezhnoy and Karyakin [1] and Pavlushkin and colleagues [4], studying solid phase reactions, found that, at any oxide ratios in the $\text{MgO} \rightarrow \text{Al}_2\text{O}_3 \rightarrow \text{SiO}_2$ system, the initial reaction product is magnesium spinel MgAl_2O_4 , the

reaction of which with silica leads to formation of sapphirine or cordierite, depending on the composition of the initial mixture. Rasch and colleagues [33] have studied the solid phase reactions in the $MgSiO_3$ -- $MgAl_2O_4$ system, and they have found that, at 1000° , forsterite and spinel appear, at 1100° , magnesium metasilicate and, only at 1200 - 1300° , cordierite; decomposition of cordierite was observed at 1400° .

Boyd and England [17] have studied the phase ratios in the MgO -- Al_2O_3 -- SiO_2 system at high pressures. Taking account of their previous work [12, 14-16], as well as the research of Schreyer and Yoder [44] and Clark [19], the authors were able to show what phases coexist up to a pressure of 40 kbar. At atmospheric pressure, cordierite coexists with many phases of the system: mullite, tridymite, protoenstatite, forsterite, spinel and sapphirine. At elevated pressures, the number of phases with which cordierite can coexist decreases. At a pressure of 8 kbar and 1100° , when cordierite still is stable, it can crystallize in equilibrium with only three phases: alumina-containing enstatite, sillimanite and quartz. At 21 kbar and 1400° , when pyrope is stable, it coexists only with alumina-containing enstatite, sapphirine and sillimanite. At elevated pressures, pyrope can crystallize in equilibrium with many phases.

Ringwood and Major [34] have studied the partial system $MgSiO_3$ -- Al_2O_3 under high pressure conditions. Glasses containing Al_2O_3 from 5 weight % to the composition of pyrope, i.e., 25.3 weight % Al_2O_3 , were subjected to pressures of from 110 to 200 kbar at 900° . The reaction products were garnet and clinoenstatite. $MgSiO_3$ (up to 50 weight %) was included in the garnet structure. The unit cell parameter increases appreciably in this case.

Cordierite is distinguished by complex polymorphism. Besides the formation of metastable modifications and intermediate phases, the presence

of regions of uniformity (solid solutions) is characteristic of cordierite. Therefore, it is more nearly correct to speak of cordierite-like phases.

The following four cordierite (cordierite-like) phases can be encountered in the literature at the present time:

1. α cordierite, "high" cordierite, indialite phase; this modification is obtained by rapid, high-temperature ($1000\text{--}1300^\circ$) crystallization of glass of composition 2:2:5 or close to it. The crystals are characterized by hexagonal symmetry. The structure is disordered at a constant composition. The rarely-encountered natural cordierites are similar in structure to artificial α cordierite. Miyashiro [30], finding this variety of cordierite in Vaccaro clay shales in India, called them indialite and proposed calling artificial α cordierite by this name. The unit cell parameters: $a = 9.7698$, $c = 9.3517 \text{ \AA}$ (according to Schreyer and Schairer [42]) and $a = 9.782$, $c = 9.365 \text{ \AA}$ (according to Miyashiro). According to Toropov and Sirazhiddinov [8], crystals of α cordierite are uniaxial, with indices of refraction $N_g = 1.523$, $N_p = 1.520$; the density is 2.513 g/cm^3 ;

2. β cordierite, "low" cordierite, rhombic cordierite; it is obtained by low-temperature (below 950°) prolonged crystallization of glass. It is stable, and it is characterized by rhombic symmetry with an ordered structure. It exists stably up to the solidus temperature. In the presence of the liquid phase, it changes into α cordierite [9];

For the natural mineral, Schreyer and Schairer present indices of refraction $N_g = 1.520$, $N_p = 1.517$ and density 2.507 g/cm^3 ; the unit cell parameters are $a = 17.0621$, $b = 9.7208$ and $c = 9.3389 \text{ \AA}$; the crystals are biaxial, negative, with a large optical axis angle;

Toropov and colleagues [6, 7] have determined the conditions for the mutual transition $\alpha \rightleftharpoons \beta$ cordierite; hexagonal cordierite, after prolonged holding at 1400°, changes into "low" rhombic, stable up to 1440°; at 1460°, the reverse transition to the high-temperature α modification takes place;

3. Osumilite phase; this cordierite-like metastable phase was obtained by Schreyer and Schairer [41], by crystallization of glass containing more silica than in cordierite, at a temperature of 1050-1250°; there is a similarity with the mineral osumilite (earlier taken to be cordierite); the osumilite structure is based on hexagonal double rings $(\text{Si}, \text{Al})_{12}\text{O}_{30}$; the indices of refraction are $N_o = 1.545-1.547$, $N_e = 1.549-1.551$; (+)2V usually is 0°;

4. "Petalite" phase; this cordierite-like metastable phase was obtained by crystallization of glass rich in magnesium oxide and silica [41]; structurally, it is similar to lithium aluminosilicate $\text{Li}_2\text{O} \cdot \text{Al}_2\text{O}_3 \cdot 8\text{SiO}_2$, petalite; the composition of the synthetic "petalite" phase probably lies in the triangle $\text{MgO} \cdot 2\text{SiO}_2 \sim \text{MgO} \cdot \text{Al}_2\text{O}_3 \cdot 8\text{SiO}_2 \sim \text{MgO} \cdot \text{Al}_2\text{O}_3 \cdot 3\text{SiO}_2$.

Data on the polymorphic differences in the compound $2\text{MgO} \cdot 2\text{Al}_2\text{O}_3 \cdot 5\text{SiO}_2$, according to Eitel, are presented in Table 1.

A whole series of intermediate structural states exists between α and β cordierites, which are evaluated, according to Miyashiro [29, 30] and Iiyama [26], by the so called orderliness index (see [5]).

The coefficient of thermal expansion of cordierite, according to Hummel and Reid [25], is $20 \cdot 10^{-7}$ degrees in the 25-1000° range. Sugiura and Kuroda [46] show that cordierite undergoes a certain decrease in volume in the 20-500° range.

TABLE 1
CRYSTALLINE PHASES OF $MgO - Al_2O_3 - SiO_2$ SYSTEM

a Соединение	b Система кристаллов	c Габитус	d Спайность	Ng	Nm	Np	Ng - Np	2V°	e Оптическая ориентировка	f Плотность, g/cm^3
$\alpha\text{-}2MgO \cdot 2Al_2O_3 \cdot 5SiO_2$, (кордierит)	Гексагональная	Прямы	—	1.528	—	1.524	0.004	Очень мал	(—)	2.57—2.65
$\mu\text{-}2MgO \cdot 2Al_2O_3 \cdot 5SiO_2$, (кристаллизуется из стекла ниже 925°)	?	Волокна	—	1.535	—	—	—	—	—	—
$3MgO \cdot Al_2O_3 \cdot 3SiO_2$, (природный пироп)	Кубическая	—	—	1.705	—	—	—	—	—	3.5—3.8
$5MgO \cdot 6Al_2O_3 \cdot 2SiO_2$, (природный сапфирин)	Моноклинная	Таблицы	Нет	1.703—1.734	1.707—1.733	1.704—1.729	0.003—0.006	69	(+)	3.3—3.5

Key:

- | | |
|---------------------------------------|-----------------------|
| a. Compound | j. Natural sapphirine |
| b. Crystal system | k. Hexagonal |
| c. Appearance | l. Cubic |
| d. Cleavage | m. Monoclinic |
| e. Optical orientation | n. Prisms |
| f. Density, g/cm^3 | o. Fibers |
| g. Cordierite | p. Sheets |
| h. Crystallizes from glass below 925° | q. None |
| i. Natural pyrope | r. Very small |

The cordierite structure has been studied by Bystrom [18], Zoltai [47] and Gibbs [24].

The majority of the cordierites are optically positive. The change in indices of refraction are independent of the structural state of the cordierite [44].

Rankin and Merwin [32] have found a metastable phase, the composition of which varied from $MgO \cdot Al_2O_3 \cdot 2.5SiO_2$ to $MgO \cdot Al_2O_3 \cdot 3SiO_2$. Karkhanavala and Hummel [27] called this phase μ cordierite and assumed it to be isostructural with high-temperature spodumene $LiAlSi_2O_6$.

Schreyer and Schairer [40], studying the partial system $MgAl_2O_4$ -- SiO_2 , found metastable solid solutions with a high-temperature quartz structure. The authors assume that 58.7 weight % SiO_2 can be replaced by the sum of the oxides $Al_2O_3 + MgO$. The indices of refraction of quartz-like solid solutions are presented in Fig. 176. The composition 73.25 weight % SiO_2 , 7.58 weight % MgO and 19.17 weight % Al_2O_3 corresponds to an isotropic phase, which is not birefringent ($N_o = N_e$). Here, the optical indicatrix changes its optical sign from minus to plus.

Toropov and Sirazhiddinov [8], by low-temperature (about 800°) crystallization of glass containing over 35% SiO_2 , obtained metastable solid solutions with the high-temperature quartz structure and indices of refraction $N_g = 1.540$ and $N_p = 1.537$.

Structural conversions of metastable quartz-like solid solutions have been studied by Khedakovskaya and Pavlushkin [10] in sialls. A sharp increase in the maximum (102) is observed on the diffractograms of the quartz-like phases at 1050°, which is interpreted as an approach of the solid solution structure to that of low-temperature quartz.

Scheel [36] has shown that crystals (1-2 mm long) of metastable, quartz-like solid solutions can be grown in a matrix of glass, of the composition $MgO \cdot Al_2O_3 \cdot 3SiO_2$, subjected to three months of heat treatment, with gradual increase in temperature from 600 to 800°. The crystals grew on the walls of a narrow, cylindrical channel drilled in the glass and filled with flux of the composition $Li_2O \cdot 4WO_3$.

Schreyer [38, 39] demonstrates the possibility of isomorphic replacements in cordierite by two systems: $Mg^{2+} + Si^{4+} \rightleftharpoons 2Al^{3+}$ and $2Al^{3+} + Mg^{2+} \rightleftharpoons 2Si^{4+}$. As a result of such replacements, four types of cordierite can form:

TABLE 2
 POLYMORPHIC FORMS OF THE COMPOUND $2\text{MgO} \cdot 2\text{Al}_2\text{O}_3 \cdot 5\text{SiO}_2$
 (from Eitel: W. Eitel, *Silicate Science*, vol. III, New York-London, 1965, 297)

Compound	Crystal System	Space Group	Structural Type	Unit Cell Parameter A	Optical Angle	Indices of Refraction	Formation & Occurrence
High-temperature indialite $\#2\text{MgO} \cdot 2\text{Al}_2\text{O}_3 \cdot 5\text{SiO}_2$	Hexagonal	C6/mcc	Discrete rings (beryl type)	$a_0 = 9.782$, $c_0 = 9.365$	Uniaxial, negative	$N_o = 1.528$, $N_e = 1.524$	Synthetic form is formed over 830° , natural, in lavas
Low-temperature indialite $\#2\text{MgO} \cdot 2\text{Al}_2\text{O}_3 \cdot 5\text{SiO}_2$	Same	"	Same	$a_0 = 9.792$, $c_0 = 9.349$	Uniaxial (?), negative	$N_o = 1.541$, $N_e = 1.537$	Synthetic form is formed below 830°
265 High-temperature cordierite	Pseudo-hexagonal (rhombic?)	Cmm1	"	$a_0 = 17.1$, $b_0 = 9.7$, $c_0 = 9.3$	Biaxial, 2V $N_g = 80^\circ$ (to 110°)	$N_g = 1.541.55$, $N_p = 1.531.54$	In volcanic rocks
Low-temperature cordierite	Same	"	"	$a_0 = 17.1$, $b_0 = 9.7$, $c_0 = 9.3$	Biaxial, 2V $N_g = 75^\circ$ (up to 140°)	$N_g = 1.531.57$, $N_p = 1.521.56$	In metamorphic and igneous rocks
$\mu\text{-Mg}_2\text{Al}_4\text{Si}_5\text{O}_{18}$	Unknown	Unknown	Probably $\alpha\text{LiAlSiO}_4$ type	Unknown	Unknown	$N = 1.531.56$	Produced synthetically at 850-900°
Osumilite	Hexagonal	C6/mcc	Double rings (milarite type)	$a_0 = 10.17$, $c_0 = 14.34$	Uniaxial, positive	$N_o = 1.5451.547$, $N_e = 1.5491.551$	In volcanic rocks

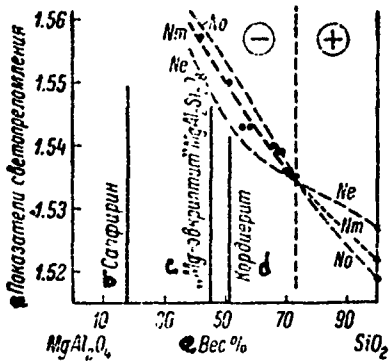


Fig. 170. Indices of refraction of metastable, quartz-like, α -quartz structure solid solutions (from Schreyer and Schairer): Dots, composition of initial glasses, from which solid solutions were obtained by means of crystallization.

Key:

- | | |
|--------------------------|---------------|
| a. Indices of refraction | d. Cordierite |
| b. Sapphirine | e. Weight % |
| c. Mg-eucryptite | |

1. cordierite, "supersaturated with silica," i.e., containing an excess of silicon, as a result of isomorphic substitution;
2. cordierite, "incompletely saturated with silica";
3. cordierite, "supersaturated with alumina (aluminum)";
4. cordierite, "incompletely saturated with alumina (aluminum)."

For the cordierite -- silica profile (Fig. 171), the solid solution is considered to be cordierite, "supersaturated with silica," "Si cordierite." It is evident here that the transition of "high" cordierite to "low" is accomplished through the stage of structurally intermediate cordierite. The cordierite solid solution forming in the binary cordierite -- "Mg beryl" profile, is not saturated

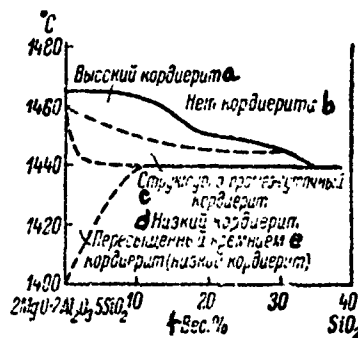


Fig. 171. Portion of phase diagram of cordierite -- silica binary profile in region adjacent to cordierite (from Schreyer).

Key:

- | | |
|------------------------|-------------------------|
| a. High cordierite | e. Cordierite super- |
| b. Nc cordierite | saturated with |
| c. Structurally inter- | silica (low cordierite) |
| mediate cordierite | f. Weight % |
| d. Low cordierite | |

with aluminum (alumina). The region of existence of "low" and "high" cordierite in this profile is shown in Fig. 172. In the conversion region, a change takes place in the orderliness indices. A region with variable silicon and aluminum content in the triple diagram according to Schreyer is represented schematically in Fig. 173. Stable solid solutions are represented here, in the form of two heavy lines, proceeding from theoretical cordierite 2:2:5. One of these solid solutions is "silicon (silica) supersaturated" cordierite and the second, "incompletely aluminum (alumina) saturated." Continuation of the heavy lines, just like the dotted field, is a region of metastable cordierite solid solutions, which should be considered as ternary solid solutions. Schreyer admits the

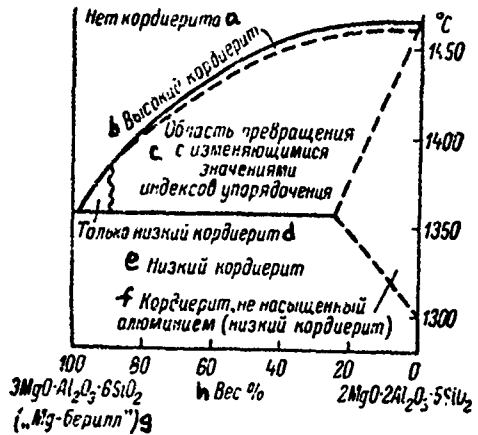


Fig. 172. Portion of phase diagram of cordierite -- Mg-beryl ($3\text{MgO} \cdot \text{Al}_2\text{O}_3 \cdot 6\text{SiO}_2$) binary profile in region adjacent to cordierite (from Schreyer).

Key:

- a. Nc cordierite
- b. High cordierite
- c. Conversion region with changing values of orderliness indices
- d. Only low cordierite
- e. Low cordierite
- f. Cordierite not saturated with aluminum (low cordierite)
- g. Mg-beryll
- h. Weight %

existence of metastable solid solutions, going from cordierite approximately in the direction of mullite. At 1320, 1355 and 1400°, binary cordierite solid solutions are observed. Beginning at 1420°, ternary solid solutions, existing up to 1460°, appear.

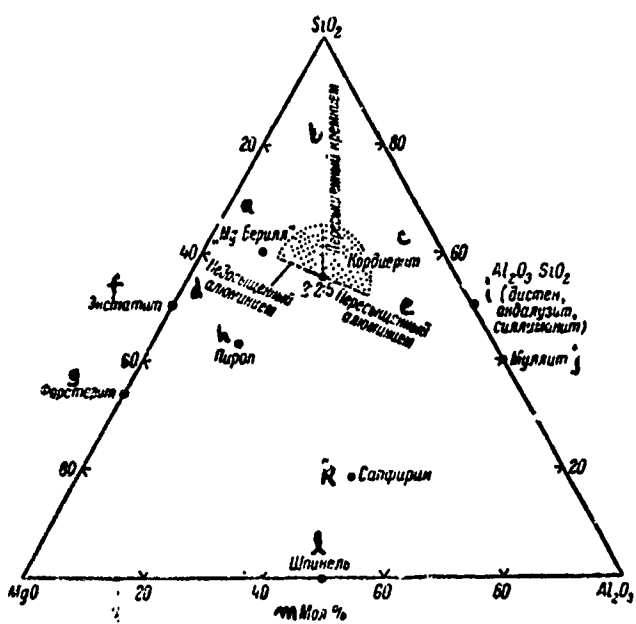


Fig. 173. Schematic triple diagram of $\text{MgO} - \text{Al}_2\text{O}_3 - \text{SiO}_2$ system. indicating principles of formation of cordierite solid solutions (from Schreyer).

Key:

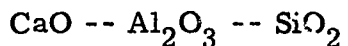
- | | |
|--|---|
| a. Mg-beryl | g. Forsterite |
| b. Supersaturated with
silica | h. Pyrope |
| c. Cordierite | i. Disthene, andalusite,
sillimanite |
| d. Incompletely saturated
with aluminum | j. Mullite |
| e. Supersaturated with
aluminum | k. Sapphirine |
| f. Enstatite | l. Spinel |
| | m. Mole % |

BIBLIOGRAPHY

1. Berezhnoy, A. S., L. I. Karyakin, DAN SSSR, 75, 3, 1950, p. 423.
2. Budnikov, P. P., K. M. Zlochevskaya, DAN SSSR, 156, 1, 1964, p. 158.
3. Medvedeva, M. S., S. V. Popova, Geokhimiya, 11, 1969, p. 1408.
4. Pavlushkin, N. M., R. L. Khodakovskaya, V. I. Zuyeva, V. A. Zuyev, DAN SSSR, 182, 3, 1968, p. 630.
5. Toropov, N. A., V. P. Barzakovskiy, Vysokotemperaturnaya khimiya silikatnykh i drugikh okisnykh sistem [High-Temperature Chemistry of Silicate and Other Oxide Systems], AN SSSR Press, Moscow-Leningrad, 1963, p. 34.
6. Toropov, N. A., R. - S. M. Zhukauskas, F. K. Aleynikov, Izv. AN SSSR, Neorg. mater., 2, 2, 1966, p. 357.
7. Toropov, N. A., R. - S. M. Zhukauskas, F. K. Aleynikov, Ibid., 3, p. 524.
8. Toropov, N. A., N. A. Sirazhiddinov, in the collection Strukturnye prevrashcheniya v steklakh pri povyshennykh temperaturakh [Structural Transformations in Glasses at Elevated Temperatures], Nauka Press, Moscow-Leningrad, 1965, p. 193.
9. Toropov, N. A., N. A. Sirazhiddinov, Ibid., p. 201.
10. Khodakovskaya, R. Ya., N. M. Pavlushkin, Izv. AN SSSR, Neorg. mater., 3, 10, 1967. p. 1908.
11. Bowen, N., J. Greig, Amer. J. Sci., 7, (5), No. 29, 238, 1924.
12. Boyd, F. R., J. L. England, Carnegie Inst. Washington Year Book, 57, 1957-1958.
13. Boyd, F. R., J. L. England, Carnegie Inst. Washington Year Book, 58, 1958-1959.
14. Boyd, F. R., J. L. England, Carnegie Inst. Washington Year Book, 59, 1959-1960.
15. Boyd, F. R., J. L. England, J. Geophys. Res., 65, No. 2, 749, 1960.
16. Boyd, F. R., J. L. England, Carnegie Inst. Washington Year Book, 61, 109, 1961-1962.
17. Boyd, F. R., J. L. England, Carnegie Inst. Washington Year Book, 62, 121, 1962-1963.

18. Byström, A., Arkiv Kemi, Miner. u. Geol., 15R, No. 12, 1, 1941.
19. Clark, S.P., E.C. Robertson, F. Birch, Amer. J. Sci., 255, No. 9, 628, 1957.
20. Dittler, E., A. Köhler, Zbl. Mineral., Geol., Palaeontol., Abt. A. Mineral. u. Petrogr., 149, 1938.
21. Ford, W.E., Amer. J. Sci., 40, (4), No. 235, 33, 1915.
22. Foster, W.F., J. Amer. Ceram. Soc., 33, No. 3, 73, 1950.
23. Foster, W.F., J. Geol., 58, No. 2, 135, 1950.
24. Gibbs, C.V., Amer. Mineralogist, 51, No. 7, 1068, 1966.
25. Hummel, F.A., H.W. Reid, J. Amer. Ceram. Soc., 34, No. 10, 319, 1951.
26. Iiyama, T., Proc. Japan Acad., 31, No. 3, 166, 1955.
27. Karkhanavala, M.D., F.A. Hummel, J. Amer. Ceram. Soc., 36, No. 12, 389, 1953.
28. Keith, M.L., J.F. Schairer, J. Geol., 60, No. 2, 181, 1952.
29. Miyashiro, A., Amer. Mineralogist, 41, No. 1-2, 104, 1956.
30. Miyashiro, A., Amer. J. Sci., 255, No. 1, 43, 1957.
31. Osborn, E.F., A. Muan, in E.M. Levin, C.R. Robbins, H.F. McMurdie, Phase diagrams for ceramists, USA, Columbus, fig. 712, 1964.
32. Rankin, G.A., W.E. Merwin, Amer. J. Sci., 45, (4), No. 268, 301, 1918.
33. Rasch, H., P. Bock, M. Kolterman, Tonindustrie Ztg., 88, No. 17-18, 430, 1964.
34. Ringwood, A.E., A. Major, Earth a. Planetary Sci. Lett., No. 5, 351, 1961.
35. Schairer, J.F., J. Amer. Ceram. Soc., 37, No. 11, 501, 1964.
36. Scheel, H.-J., J. Crystal. Growth, 2, No. 6, 411, 1963.
37. Schlaudt, Ch. M., D.M. Roy, J. Amer. Ceram. Soc., 48, No. 5, 248, 1965.
38. Schreyer, W., Neues Jahrbuch Mineral., Abh., 102, No. 1, 39, 1964.

39. Schreyer, W., Neues Jahrbuch Mineral., Abh., 105, No. 5, 211, 1966.
40. Schreyer, W., J.F. Schairer, Zs. Kristallogr., 116, No. 1-2, 60, 1961.
41. Schreyer, W., J.F. Schairer, J. Petrologie, 2, No. 3, 324, 1961.
42. Schreyer, W., J.F. Schairer, Amer. Mineralogist, 47, No. 1-2, 90, 1962.
43. Schreyer, W., F. Seifert, Amer. J. Sci., 267A, Schairer vol., 407, 1969.
44. Schreyer, W., H.S. Yoder, Neues Jahrbuch Mineral., Abh., 101, No. 3, 271, 1964.
45. Skinner, B.J., Amer. Mineralogist, 41, No. 5-6, 423, 1956.
46. Sugiura, K., J. Kuroda, Bull. Tokyo Inst. Technol., ser. B, No. 1, 1, 1955.
47. Zoltai, T., Amer. Mineralogist, 45, No. 9-10, 980, 1960.



The study of this system, carried out by Rankin and Wright [18] at the beginning of the twentieth century, was thought to be the start of development of a major section of silicate chemistry, the study of heterogeneous phase equilibria in complex silicate systems.

A phase diagram of the system, according to Osborn and Muan [17], reflecting the state of the principal studies in 1960, is presented in Fig. 174. Osborn and Muan introduced changes and refinements into the Rankin and Wright diagram, in accordance with the works of Greig (liquation, [11]), Filonenko and Lavrov (plotting the $\text{CaO} \cdot 6\text{Al}_2\text{O}_3$ field [4]), Toropov and Galakhov (congruent melting of mullite [2]), Langenberg and Chipman (refinement of the isotherm positions [14]) and others.

Gentile and Foster [9] think that calcium hexaaluminate $\text{CaO} \cdot 6\text{Al}_2\text{O}_3$ has its field in the diagram, but the area of this field is somewhat smaller than

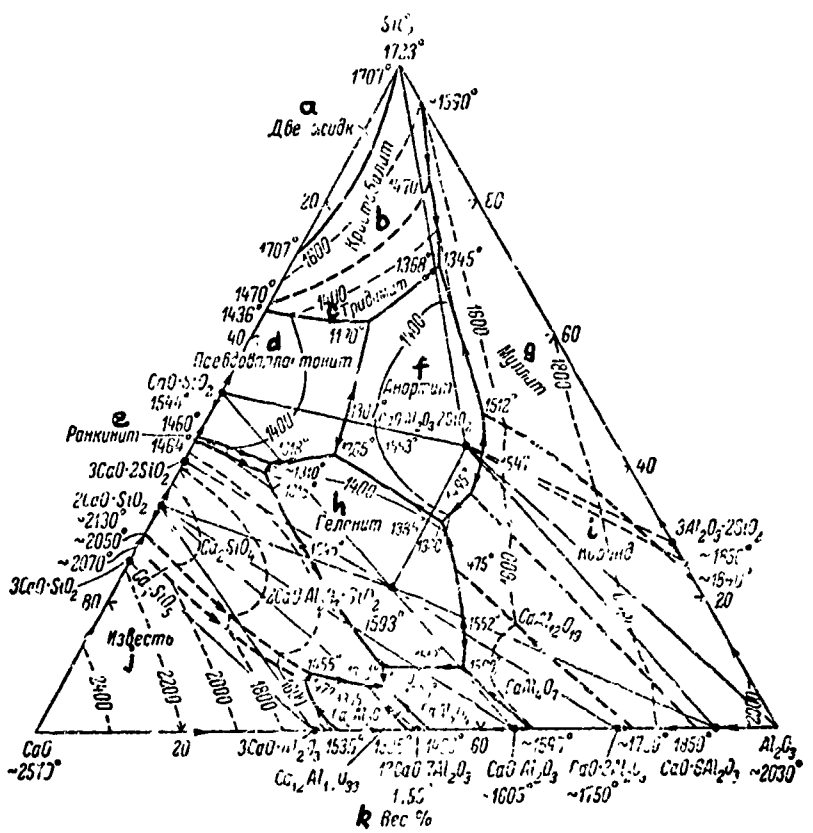


Fig. 174. Phase diagram of $\text{CaO} - \text{SiO}_2 - \text{Al}_2\text{O}_3$ system (from Osborn and Muñan).

Key:

- Two liquids
- Cristobalite
- Tridymite
- Pseudowollastonite
- Rankinitite
- Anorthite
- Mullite
- Gehlenite
- Corundum
- Lime
- Weight %

in Filonenko and Lavrov. The triple invariant point anorthite -- corundum -- calcium hexaaluminate, according to Gentile and Foster, has the composition: $\text{CaO} \sim 28.0$, $\text{Al}_2\text{O}_3 \sim 39.7$, $\text{SiO}_2 \sim 32.3$ weight % (melting temperature $1405 \pm 5^\circ$), and according to Filonenko: $\text{CaO} \sim 23.0$, $\text{Al}_2\text{O}_3 \sim 41.0$, $\text{SiO}_2 \sim 36.0$ weight % (melting temperature $1495 \pm 5^\circ$). The version of the diagram proposed by Gentile and Foster is presented in Fig. 175.

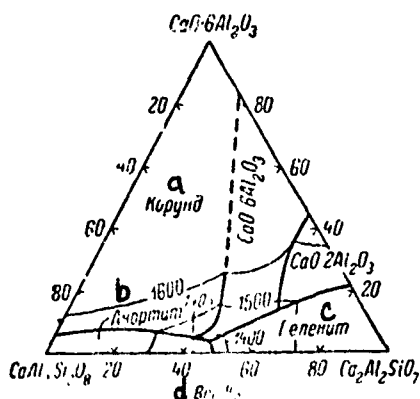


Fig. 175. Phase diagram of partial system $\text{CaO} - \text{Al}_2\text{O}_3 - \text{SiO}_2$, bounded by compounds $\text{CaO} \cdot \text{Al}_2\text{O}_3 \cdot 2\text{SiO}_2$, $2\text{CaO} \cdot \text{Al}_2\text{O}_3 \cdot \text{SiO}_2$ and $\text{CaO} \cdot 6\text{Al}_2\text{O}_3$ (from Gentile and Foster).

Key:

- a. Corundum
- b. Anorthite
- c. Gehlenite
- d. Weight %

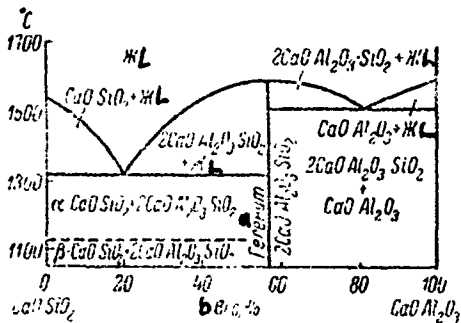


Fig. 176. Phase diagram of partial system $\text{CaO} \cdot \text{SiO}_2 \rightarrow \text{CaO} \cdot \text{Al}_2\text{O}_3$ (from Rankin and Wright).

Key:

- a Gehlenite
- b Weight %

The systems $\text{CaO} \cdot \text{Al}_2\text{O}_3 \cdot 2\text{SiO}_2$ -- silica, according to Schairer and Bowen [21], $\text{CaO} \cdot \text{Al}_2\text{O}_3 \cdot 2\text{SiO}_2$ -- $\text{CaO} \cdot \text{SiO}_2$, according to Osborn [16], $\text{CaO} \cdot \text{Al}_2\text{O}_3 \cdot 2\text{SiO}_2$ -- Al_2O_3 , anorthite $2\text{CaO} \cdot \text{Al}_2\text{O}_3 \cdot \text{SiO}_2$, $2\text{CaO} \cdot \text{Al}_2\text{O}_3 \cdot \text{SiO}_2$ -- $\text{CaO} \cdot \text{SiO}_2$ and $2\text{CaO} \cdot \text{Al}_2\text{O}_3 \cdot \text{SiO}_2$ -- $2\text{CaO} \cdot \text{SiO}_2$, according to Rankin and Wright [19], are simple eutectics. The system $\text{CaO} \cdot \text{SiO}_2 \rightarrow \text{CaO} \cdot \text{Al}_2\text{O}_3$, in which gehlenite comes into being, is presented in Fig. 176, according to the data of Rankin and Wright. The profile connecting CaSiO_3 and the eutectic between anorthite and gehlenite, studied by Yoder [22], in which there is grossularite $3\text{CaO} \cdot \text{Al}_2\text{O}_3 \cdot 3\text{SiO}_2$ in the low-temperature region encompassed (up to 400°), is shown in Fig. 177. The part of the $3\text{CaO} \cdot \text{SiO}_2 \rightarrow \text{Al}_2\text{O}_3$

profile up to 1.2 weight % Al_2O_3 has been studied by Bigaré and colleagues [5], in connection with study of the polymorphism of solid solutions of tricalcium silicate.

Toropov and Tigonen [3] have studied the metastable crystallization of glasses of the anorthite -- wollastonite system, beginning at temperatures of 400° below the eutectic.

Toropov [1] and Goggi [10] have examined the crystallization sequence for various portions of the system.

According to recent data, anorthite, $\text{CaO} \cdot \text{Al}_2\text{O}_3 \cdot 2\text{SiO}_2$ exists in three modifications: The common triclinic and the recently discovered rhombic and hexagonal, which are not analogs of the corresponding modifications of $\text{BaO} \cdot \text{Al}_2\text{O}_3 \cdot 2\text{SiO}_2$. Production of the two latter modifications is described by Davis and Tuttle [7]. It is interesting that the rhombic phase was not separated out by crystallization of pure anorthite glass, but was obtained from a melt containing 20 mole % plagioclase (the remainder was anorthite), by crystallization at 950° for a period of four days. The hexagonal modification of anorthite has been studied in detail by J. Donnay and G. Donnay [8], who demonstrated the complexity of its structure.

At high temperatures, the hexagonal and rhombic anorthite change to the common triclinic, but in the presence of water, 700° is sufficient for this transition. The latter circumstance forces the new anorthite modifications to be considered metastable. However, Yoshiki and colleagues [23], on the basis of dilatometric measurements, think that hexagonal anorthite is a stable modification up to 300°, changing to triclinic above this temperature, the stability limit of which extends to the melting temperature 1550°. In accordance with

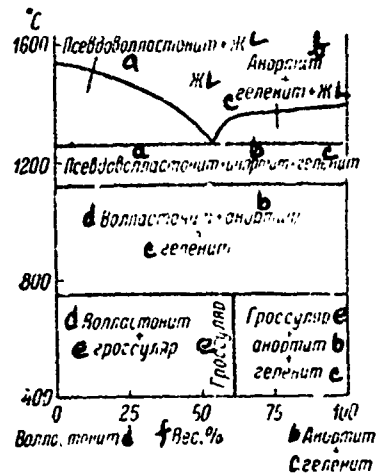


Fig. 177. Phase diagram of partial system wollastonite -- anorthite + gehlenite (eutectic) (from Yoder).

Key:

- | | |
|-----------------------|-----------------|
| a. Pseudowollastonite | d. Wollastonite |
| b. Anorthite | e. Grossularite |
| c. Gehlenite | f. Weight % |

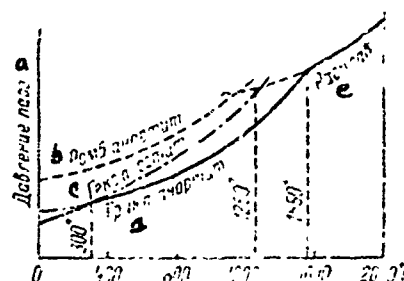


Fig. 178. Hypothetical phase diagram of $\text{CaAl}_2\text{Si}_2\text{O}_8$ system (compounds) (from Yoshiki).

Key:

- Vapor pressure
- Rhombic anorthite
- Hexagonal anorthite
- Triclinic anorthite
- Melt

TABLE 1
INVARIANT POINTS OF $\text{CaO} - 2\text{CaO}\cdot\text{SiO}_2 - 5\text{CaO}\cdot 3\text{Al}_2\text{O}_3$ SYSTEM
(from Goggi)

a Фазы	b Процес	c Состав, вес. %			d Темпера- тура, °C
		CaO	Al ₂ O ₃	SiO ₂	
3CaO·SiO ₂	диссоциация	73.59	—	26.41	1900 ± 20
2CaO·SiO ₂	литиение	65.00	—	35.00	2130 ± 20
3CaO·Al ₂ O ₃	диссоциация	62.22	37.78	—	1535 ± 2
5CaO·3Al ₂ O ₃	литиение	47.78	52.22	—	1455 ± 5
CaO - 3CaO·SiO ₂ - 2CaO·SiO ₂	треугольная реакционная точка	68.4	9.2	22.4	1900 ± 20
CaO - 3CaO·SiO ₂ - 3CaO·Al ₂ O ₃	т. же	49.7	32.8	7.5	1470 ± 5
3CaO·SiO ₂ - 2CaO·SiO ₂ - 3CaO·Al ₂ O ₃	»	58.3	33.0	8.7	1455 ± 5
2CaO·SiO ₂ - 3CaO·Al ₂ O ₃ - 5CaO·3Al ₂ O ₃	эвтектика	52.0	41.2	6.8	1335 ± 5

Key:

- | | |
|--------------------------|--------------------------|
| a. Phases | f. Melting |
| b. Process | g. Triple reaction point |
| c. Composition, weight % | h. Same |
| d. Temperature, °C | i. Eutectic |
| e. Dissociation | |

the hypothetical phase diagram of the $\text{CaAl}_2\text{Si}_2\text{O}_3$ system in "pressure-temperature" coordinates (Fig. 178), rhombic anorthite is metastable at all temperatures.

Under high pressure conditions, two compounds appear on the phase diagram of the system: grossularite $3\text{CaO}\cdot\text{Al}_2\text{O}_3\cdot 3\text{SiO}_2$ and pyroxene, of the composition $\text{CaO}\cdot\text{Al}_2\text{O}_3\cdot\text{SiO}_2 = \text{CaAl}_2\text{SiO}_6$ (see the works of Yoder [22] and Clark and colleagues [6]).

Hays [12] has studied the reaction $\text{CaAl}_2\text{Si}_2\text{O}_8$ (anorthite) + $\text{Ca}_2\text{Al}_2\text{SiO}_7$ (gehlenite) + $\text{Al}_2\text{O}_3 = 3\text{CaAl}_2\text{SiO}_6$ (pyroxene) under high pressure conditions.

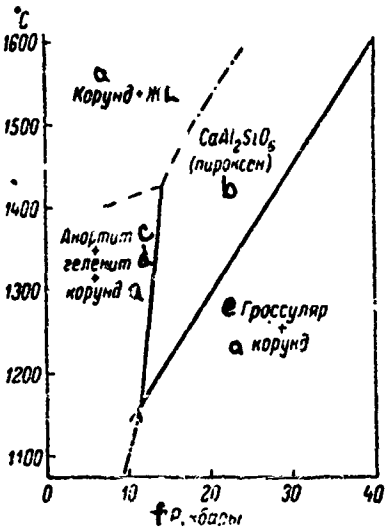


Fig. 179. Stability region of $\text{CaAl}_2\text{SiO}_6$ (pyroxene) vs. temperature and pressure (from Hays).

Key:

- | | |
|--------------|-----------------|
| a. Corundum | d. Gehlenite |
| b. Pyroxene | e. Grossularite |
| c. Anorthite | f. P, kbar |

The boundary line between the three-phase field of anorthite + gehlenite + corundum and the pyroxene field is shown in Fig. 179. Dissociation of pyroxene takes place with further increase in pressure: $3\text{CaAl}_2\text{SiO}_6 = \text{Ca}_3\text{Al}_2\text{Si}_3\text{O}_{12} + 2\text{Al}_2\text{O}_3$. Correlating existing data in the literature [15, 18] and adding the results of his own experiments, Hays determined the position of the boundary lines (straight lines) between the three-phase field of anorthite + gehlenite + wollastonite and the grossularite field, and between the two-phase fields of anorthite + wollastonite and grossularite + quartz (Fig. 180). The reaction $3\text{CaAl}_2\text{Si}_2\text{O}_8 = \text{Ca}_3\text{Al}_2\text{Si}_3\text{O}_{12} + 2\text{Al}_2\text{SiO}_5 + \text{SiO}_2$, taking place at pressures over 20 kbar, also has been studied by Hays.

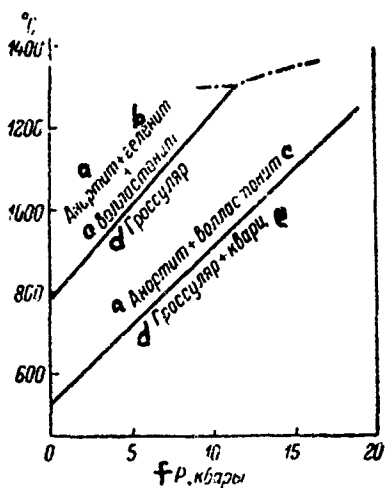


Fig. 180. Stability region of anorthite, gehlenite, wollastonite vs. temperature and pressure (from Hays).

Key:

- a. Anorthite
- b. Gehlenite
- c. Wollastonite
- d. Grossularite
- e. Quartz
- f. P, kbar

Clinopyroxene $\text{CaAl}_2\text{SiO}_6$, synthesized by Hays [13] (pressure over 12 kbar, 1050°), had indices of refraction: $\text{Ng} = 1.730 \pm 0.02$, $\text{Nm} = 1.714 \pm 0.002$, $\text{Np} = 1.709 \pm 0.002$; 2V (calculated) $59 \pm 15^\circ$, density $3.431 \pm 0.002 \text{ g/cm}^3$. Clark and colleagues [6] consider this compound as a calcium "Chermak molecule."

Ringwood and Major [20] have showed that, by subjecting a mixture of 90 weight % CaSiO_3 and 10 weight % Al_2O_3 to a pressure of 150 kbar (100°

TABLE 2
CRYSTALLINE PHASES OF $\text{CaO} - \text{Al}_2\text{O}_3 - \text{SiO}_2$ SYSTEM

a Соединение	b Система кристаллов	c Габитус	d Спайность	e Плотность, g/cm^3	Ng	Np	2V°	f Оптический знак	g Оптическая ориентировка
$\text{CaO} \cdot \text{Al}_2\text{O}_3 \cdot 2\text{SiO}_2$ (анортит)	k Триклини- ная	o Бруски, таблицы	r Спер- шенная по (001) и по (010)	2.765	1.589	1.576	t Большой	(-)	u Угол погасания по (001) 35° , полисинтети- ческое двой- шки —
$2\text{CaO} \cdot \text{Al}_2\text{O}_3 \cdot \text{SiO}_2$ (гелен- ит)	l Тетраго- нальная	p Зерна, таблицы, призмы	s Испаян по (001)	3.04	1.669	1.658	—	(-)	v —
$\text{CaO} \cdot \text{Al}_2\text{O}_3 \cdot \text{SiO}_2$	m Ромбиче- ская (?)	q Волокна	—	—	1.685	1.675	t Большой	(+)	z волокнам
$3\text{CaO} \cdot \text{Al}_2\text{O}_3 \cdot 3\text{SiO}_2$ (изо- сумарный продукт)	n Кубическая	—	(110)	—	1.735	—	—	—	w Иногда аномаль- ное двупрелом- ление

Key:

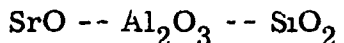
- | | |
|-----------------------------|--|
| a. Compound | l. Tetragonal |
| b. Crystal system | m. Rhombic |
| c. Appearance | n. Cubic |
| d. Cleavage | o. Blocks, sheets |
| e. Density, g/cm^3 | p. Grains, sheets, prisms |
| f. Optical sign | q. Fibers |
| g. Optical orientation | r. Perfect along (001) and along (010) |
| h. Anorthite | s. Distinct along (001) |
| i. Gehlenite | t. Large |
| j. Natural grossularite | u. Extinction angle along (001) 35° , poly- synthetic twins |
| k. Triclinic | v. Sometimes anomalous birefringence |

a garnet phase can be obtained, which is a mutual solid solution between grossularite $3\text{CaO} \cdot \text{Al}_2\text{O}_3 \cdot 3\text{SiO}_2$ and CaSiO_3 . The unit cell parameter of the phase discovered is 11.87 Å (11.851 Å for grossularite).

BIBLIOGRAPHY

1. Toropov, N. A., Khimiya tsementov [Cement Chemistry], Stroymaterialov State Publishing House, Moscow, 1956, p. 108.
2. Toropov, N. A., F. Ya. Galakhov, Voprosy petrografii i mineralogii [Problems of Petrography and Mineralogy] vol. 2, AN SSSR Press, Moscow, 1953, p. 245.
3. Toropov, N. A., G. V. Tigonen, Izv. AN SSSR, Neorg. mater., 1, 5, 1965, p. 763.
4. Filonenko, N. Ye., I. V. Lavrov, Zhurn. prikl. khim., 23, 10, 1950, p. 1040.
5. Bigaré, M., A. Guinier, C. Mazières, M. Regourd, N. Yannaquis, W. Eysel, Th. Hahn, E. Woermann, J. Amer. Ceram. Soc., 50, No. 11, 609, 1967.
6. Clark, L. A., J. F. Schairer, J. De Neufville, Carnegie Inst. Washington Year Book, 61, 59, 1961-1962.
7. Davis, G. L., O. F. Tuttle, Amer. J. Sci., Bowen vol., 107, 1952.
8. Donnay, J. D. H., G. Donnay, Acta crystallogr., 5, No. 1, 153, 1952, 12, No. 6, 465, 1959.
9. Gentile, A. L., W. R. Foster, J. Amer. Ceram. Soc., 46, No. 2, 74, 1963.
10. Goggi, G., Silicat. Industriels, 25, No. 7-8, 347, 1960, 26, No. 1, 17, 1961.
11. Greig, J. W., Amer. J. Sci., 13, (5), No. 1, 133, 1927.
12. Hays, J. F., Carnegie Inst. Washington Year Book, 65, 234, 1965-1966.
13. Hays, J. F., Amer. Mineralogist, 51, No. 9-10, 1524, 1966.
14. Langenberg, F. C., J. Chipman, J. Amer. Ceram. Soc., 39, No. 12, 432, 1956.
15. Newton, R. C., Amer. J. Sci., 264, No. 3, 204, 1966.
16. Osborn, E. F., Amer. J. Sci., 240, No. 11, 75, 1942.
17. Osborn, E. F., A. Muan, in E. M. Levin, C. R. Robbins, H. F. McMurdie, Phase diagrams for ceramists, USA, Columbus, fig. 630, 1964.
18. Pistorius, C. W. F. T., G. C. Kennedy, Amer. J. Sci., 258, No. 4, 247, 1960.
19. Rankin, G. A., F. E. Wright, Amer. J. Sci., 39, (4), No. 299, 1, 1915.

20. Ringwood, A. E., A. Major, Earth a. Planetary Sci. Lett., 1, No. 5, 351, 1966.
21. Schairer, J. F., N. L. Bowen, Bull. Soc. Geol. Finlande, 20, No. 140, 71, 1947.
22. Yoder, H. S., Jr., J. Geol., 58, No. 3, 221, 225, 1950.
23. Yostiki, B., Sh. Koide, M. Waki, Rep. Res. Lab. Asahi Glass Co., 3, No. 1, 137, 1953.



The system has been studied by Dear [2, 3], who determined the subsolidus phase ratios (annealing at 1350°). Three ternary compounds were found: strontium anorthite $\text{SrO} \cdot \text{Al}_2\text{O}_3 \cdot 2\text{SiO}_2$ and the compounds discovered by Dear $2\text{SrO} \cdot \text{Al}_2\text{O}_3 \cdot \text{SiO}_2$ (strontium gehlenite) and $6\text{SrO} \cdot 9\text{Al}_2\text{O}_3 \cdot 2\text{SiO}_2$. The phase relationships in the system and the coexisting phase triangles for 1350° are presented in Fig. 181. In subsequent studies, Dear [4] synthesized strontium ockermanite $2\text{SrO} \cdot \text{Al}_2\text{O}_3 \cdot 2\text{SiO}_2$, with crystals in the tetragonal system, optically positive, and unit cell parameters $a_0 = 5.181$ and $c_0 = 8.025$ Å.

Starczewski [6] has determined the melting temperatures of mixtures of the oxides by visual observations, identifying the phases by the X-ray method. He observed two ternary compounds: $\text{SrO} \cdot \text{Al}_2\text{O}_3 \cdot 2\text{SiO}_2$, melting congruently at 1765°, and $2\text{SrO} \cdot \text{Al}_2\text{O}_3 \cdot \text{SiO}_2$, melting incongruently at 1795°. The fusibility diagram of the system is presented in Fig. 182.

The compound $\text{SrO} \cdot \text{Al}_2\text{O}_3 \cdot 2\text{SiO}_2$ can be referred to the feldspar group of minerals. Crystals of this compound apparently belong to the triclinic system [5], with indices of refraction: $\text{Ng} = 1.586$, $\text{Nm} = 1.582$ and $\text{Np} = 1.574$; density is 3.12 g/cm^3 , $(-) 2V = 70^\circ$.

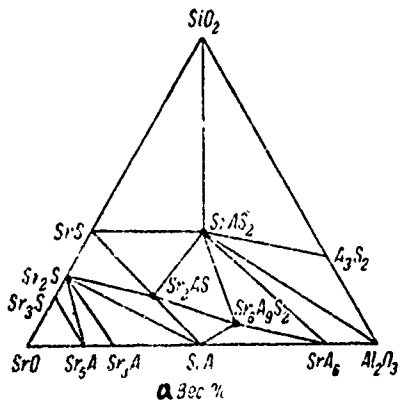


Fig. 181. Diagram of coexisting phase triangles of $\text{SrO} \text{ -- } \text{Al}_2\text{O}_3 \text{ -- } \text{SiO}_2$ system in subsolidus region at 1350° (from Dear).

Key:

a. Weight %

Sirazhiddinov and Arifov [1] have studied solid-phase synthesis of the compounds $\text{SrO} \cdot \text{Al}_2\text{O}_3 \cdot 2\text{SiO}_2$ and $2\text{SrO} \cdot \text{Al}_2\text{O}_3 \cdot \text{SiO}_2$. The initial substances were SrCO_3 or SrSO_4 , alumina and rock crystal or kaolin. Annealing was carried out at 1500° (5 hours). The initial products of the reaction were $3\text{SrO} \cdot \text{SiO}_2$ (it formed at 1000°) and $2\text{SrO} \cdot \text{SiO}_2$ (it formed at 800°), which, reacting with Al_2O_3 (over 1100°), gives the corresponding aluminosilicates.

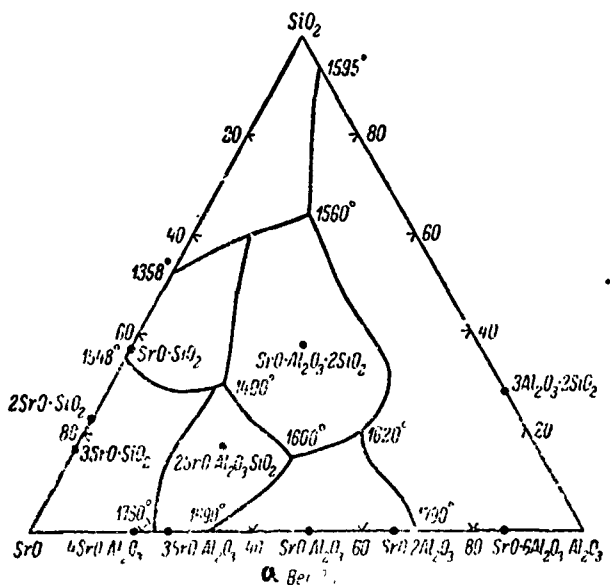


Fig. 182. Fusibility diagram of SrO -- Al₂O₃ -- SiO₂ system (from Starczewski).

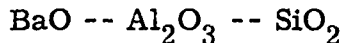
Key:

a. Weight %

BIBLIOGRAPHY

1. Sirazhiddinov, N. A., F. A. Arifov, in the collection Vysokotemperaturnaya khimiya silikatov i okislov [High-Temperature Chemistry of Silicates and Oxides], Nauka Press, Leningrad, 1972, p. 180.
2. Dear, P. S., Bull. Virginia Polytechn. Inst., 50, No. 6, Eng. Expt. Sta. Ser., No. 117, 1957.
3. Dear, P. S., Bull. Virginia Polytechn. Inst., 50, No. 11, Eng. Expt. Sta. Ser., No. 121, 1957.
4. Dear, P. S., Bull. Virginia Polytechn. Inst., 56, No. 10, Eng. Expt. Sta. Ser., No. 154, 1963.

5. Sorrell, C.A., Amer. Mineralogist, **47**, No. 3-4, 291, 1962.
6. Starczewski, M., Zeszyty Naukowe Politechn. Śląskiej, No. 106, 1964, p. 5.



The system has been studied by Toropov and colleagues [5, 6], Thomas [17] and Foster and colleagues [7, 10, 11, 15], by the quenching method.

The general form of the phase diagram of the $\text{BaO} \text{ -- } \text{Al}_2\text{O}_3 \text{ -- } \text{SiO}_2$ system is presented in Fig. 183a. Besides the binary compounds, the ternary compound celsian $\text{BaO} \cdot \text{Al}_2\text{O}_3 \cdot 2\text{SiO}_2$ is shown on the diagram, as well as two types of solid solutions: 1. a ternary solid solution in the section $2\text{BaO} \cdot 3\text{SiO}_2 \text{ -- } \text{BaO} \cdot 2\text{SiO}_2 \text{ -- } \text{BaO} \cdot \text{Al}_2\text{O}_3 \cdot 2\text{SiO}_2$; 2. a solid solution based on the incongruously melting compound $3\text{BaO} \cdot 3\text{Al}_2\text{O}_3 \cdot 2\text{SiO}_2$ (the second component is barium metasilicate). This solid solution crystallizes in the form of elongated prismatic crystals with direct extinction. The refraction changes within the following limits. $\text{Ng} = 1.924-1.644$, $\text{Np} = 1.615-1.632$, $\text{Ng-Np} = 0.009$. The compound $3\text{BaO} \cdot 3\text{Al}_2\text{O}_3 \cdot 2\text{SiO}_2$ melts at 1550° , with decomposition into barium monoaluminate and liquid. Planz and Mueller-Hesse [12] obtained the compound 3:3:2 by means of a solid-phase reaction, starting with barium carbonate and mullite (or sillimanite).

The region of ternary solid solutions formed by celsian, dibarium trisilicate and barium disilicate (sanbornite), established by Toropov and colleagues, extends from the line connecting $\text{BaO} \cdot 2\text{SiO}_2$ and $2\text{BaO} \cdot 3\text{SiO}_2$, on the alumina side, reaching up to 10 weight % Al_2O_3 (Fig. 183b). With a higher alumina content, a field of primary crystallization of celsian is reached. The points P and O designated on the diagram are invariant, in

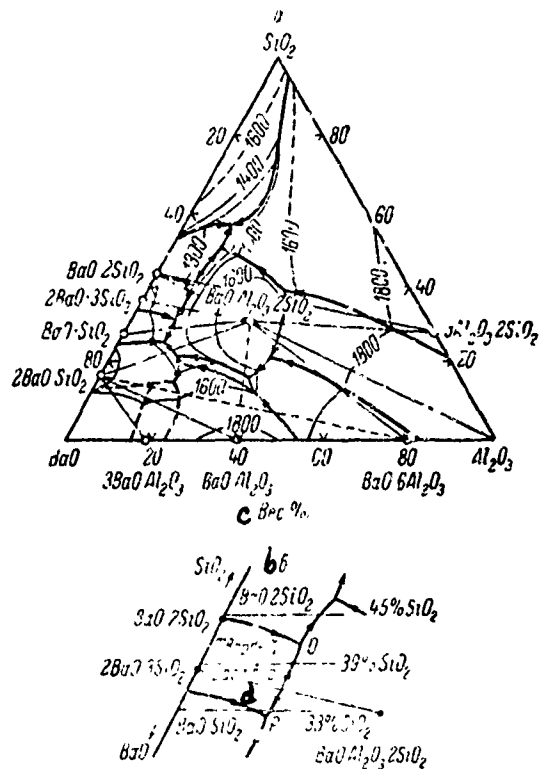


Fig. 183. Phase diagram of $\text{BaO} - \text{Al}_2\text{O}_3 - \text{SiO}_2$ system (from Toropov and colleagues).
 a. complete diagram; b. region of ternary solid solution formed by celsian ($\text{BaO} \cdot \text{Al}_2\text{O}_3 \cdot 2\text{SiO}_2$), sanbornite ($\text{BaO} \cdot \text{SiO}_2$) and dibarium trisilicate ($2\text{BaO} \cdot 3\text{SiO}_2$).

Key:

- c. Weight %
- d. Solid solution

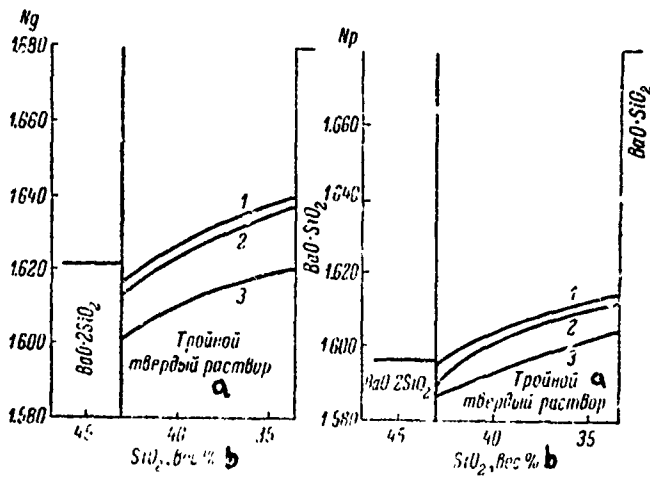


Fig. 184. Indices of refraction of ternary solid solution for three profiles with differing constant alumina content (from Toropcev and colleagues):
1. 3 weight % Al_2O_3 ; 2. 6%; 3 9%.

Key:

- a. Ternary solid solution
- b. Weight %

which point P is a eutectic with a melting temperature of 1320° , and point O is a reaction point with a melting temperature of 1280° .

The index of refraction of crystals of the ternary solid solution for the three profiles with constant alumina content of 3, 6 and 9 weight % is presented in Fig. 184. The change in optical properties takes place in two directions: along the lines parallel to the $\text{BaO} - \text{SiO}_2$ side and along lines going from this side to the central portion of the triangle. This change in optical properties of the crystals separated out can only be explained by the

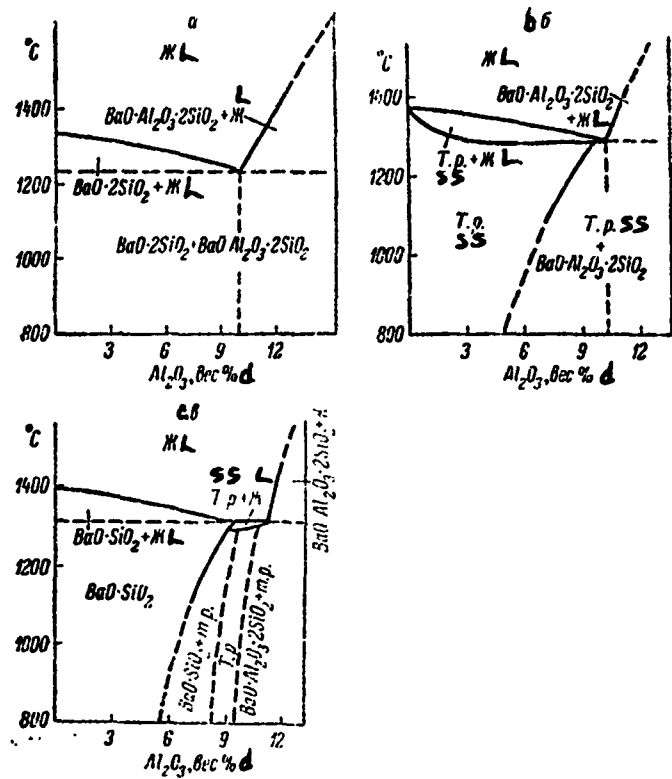


Fig. 185. Sections of $\text{BaO} - \text{Al}_2\text{O}_3 - \text{SiO}_2$ triple diagram proceeding from $\text{BaO} - \text{SiO}_2$ side: Constant SiO_2 content: a. 45, b. 39, c. 33 weight %.

Key:

d. Weight %

fact that they are formed from three components. The changes in the indices N_g and N_p vs. composition are shown in Fig. 184. The indices of refraction for $\text{BaO} \cdot 2\text{SiO}_2$ and $\text{BaO} \cdot \text{SiO}_2$ are constant and are represented by horizontal lines.

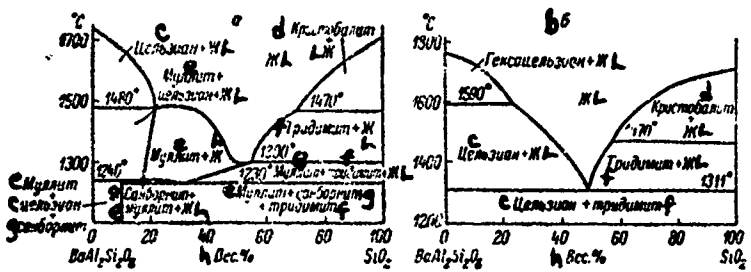


Fig. 186. Phase diagram of partial system $\text{BaAl}_2\text{Si}_2\text{O}_8$ -- SiO_2 : a. from Toropov and colleagues; b. from Foster and Lin.

Key:

- | | |
|-----------------|---------------|
| c. Celsian | f. Tridymite |
| d. Cristobalite | g. Sanbornite |
| e. Mullite | h. Weight % |

Vertical profiles parallel to the $\text{BaO} -- \text{Al}_2\text{O}_3$ side, with constant silica content of 45, 39 and 33 weight %, are shown in Fig. 185a-c. The figure presented makes it possible to characterize the equilibrium ratios in the region studied.

Foster and Lin [7] have shown that, if the data of Toropov and colleagues are used, the phase relationship diagram of the partial profile of celsian ($\text{BaAl}_2\text{Si}_2\text{O}_8$) -- silica is represented by Fig. 186a, i.e., the combined presence of celsian and silica is not observed, since a mullite field is located between the tridymite and celsian fields. Foster and Lin have done experimental studies of the partial system $\text{BaAl}_2\text{Si}_2\text{O}_8$ -- SiO_2 and, in distinction from Toropov and

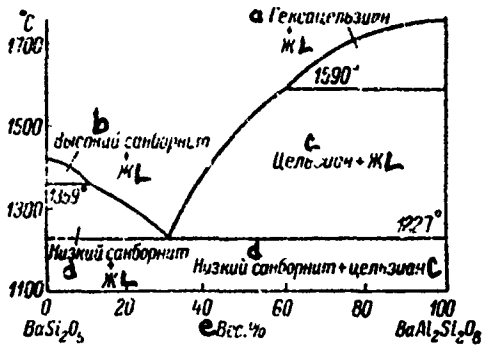


Fig. 187. Phase diagram of partial system BaSi_2O_5 -- $\text{BaAl}_2\text{Si}_2\text{O}_8$ (from Lin and Foster).

Key:

- a. Hexacelsian
- b. High sanbornite
- c. Celsian
- d. Low sanbornite
- e. Weight %

colleagues, they found that only one eutectic is observed here, of composition 51 weight % $\text{BaAl}_2\text{Si}_2\text{O}_8$ and 49 weight % SiO_2 , with a melting temperature of $1311 \pm 4^\circ$ (Fig. 186b). Carrying out prolonged crystallization of glass, the authors obtained only crystals of $\text{BaAl}_2\text{Si}_2\text{O}_8$ and silica, and did not find sanbornite or mullite.

Lin and Foster [11], in study of the partial profile sanbornite (BaSi_2O_5) -- celsian ($\text{BaAl}_2\text{Si}_2\text{O}_8$), did not find the ternary solid solutions indicated by Toropov and colleagues. In accordance with Fig. 187, the system is a simple

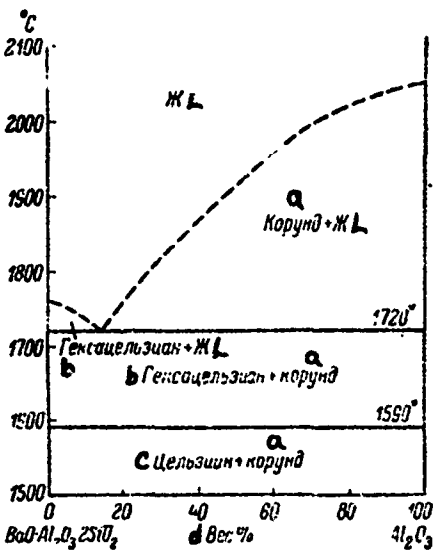


Fig. 188. Phase diagram of partial system $\text{BaAl}_2\text{Si}_2\text{O}_8$ -- Al_2O_3 (from Semler and Foster).

Key:

- a. Corundum
- b. Hexacelsian
- c. Celsian
- d. Weight %

eutectic, with a eutectic melting temperature of 1227° , at a content of 69 weight % sanbornite and 31 weight % celsian. In samples obtained by fusing the corresponding mixtures in an electric arc, as was done by Toropov and colleagues, i. e., under very low thermal exposure conditions, metastable solid solutions can be obtained. By carrying out the prolonged (up to 270 hours) exposure at 1200° , Lin and Foster did not find solid solutions.

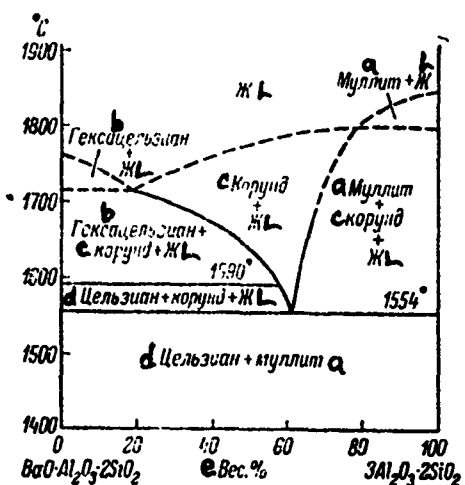


Fig. 189. Phase diagram of partial system $\text{BaAl}_2\text{Si}_2\text{O}_8$ -- $3\text{Al}_2\text{O}_3 \cdot 2\text{SiO}_2$ (from Semler and Foster).

Key:

- a. Mullite
- b. Hexacelsian
- c. Corundum
- d. Celsian
- e. Weight %

Semler and Foster [15] have studied the partial binary systems celsian -- alumina (Fig. 188) and celsian -- mullite (Fig. 189). The first of them is a simple eutectic, with a eutectic containing 86 weight % celsian and melting at $1720 \pm 10^\circ$. On the phase diagram of the pseudobinary celsian -- mullite system, a special phase is corundum. The lowest temperature of appearance of corundum (with a content of 38.5 weight % celsian), is 1554° (reaction point).

Schwiete and colleagues [13] have studied solid-phase reactions in the system.

A complex polymorphism, which is completely unstudied to this time, is characteristic of the compound $\text{BaAl}_2\text{Si}_2\text{O}_8$. Two polymorphic forms are formed artificially, a monoclinic (celsian proper, β form) and a hexagonal (ϵ form). The paracelsian found in nature, in the monoclinic system, usually is considered to be a special modification (δ form). There is evidence of a rhombic form.

Celsian proper belongs to the feldspar group, and it forms a continuous series of solid solutions with orthoclase. The monoclinic crystal system is assumed for celsian, and not the triclinic, as Taylor and colleagues thought [16].

Some physical properties of three polymorphic varieties of $\text{BaAl}_2\text{Si}_2\text{O}_8$ are presented in Table 1. The monoclinic celsian and paracelsian modifications are encountered in the form of minerals.

The hexagonal form, with a lamellar lattice and perfect cleavage along (0001), was first obtained by Ginzberg [1]. Especially pure initial materials are required for synthesis of this form, and the annealing must be carried out no lower than 1500° , with subsequent quenching.

The hexagonal modification synthesized by Yoshiki and Matsumoto [18] melted congruently at 1915° , and it had a reversible transformation in the metastable region at 300° . The crystals were very similar to mica, had very good basal cleavage, were optically positive, with the following unit cell parameters: $a_0 = 5.25 \pm 0.003$, $c_0 = 7.84 \pm 0.01$ Å.

TABLE 1
SOME PHYSICAL PROPERTIES OF POLYMORPHIC
VARIETIES OF $\text{BaAl}_2\text{Si}_2\text{O}_8$ (from R. G. Grebenshchikov)

Polymorphic Form	Symmetry	Unit Cell Parameters	Density g/cm ³	Optical Characteristics
Celsian (β form)	Monoclinic	$a = 8.627$, $b = 13.045$, $c = 7.202 \times 2\text{A}$ $\beta = 115^\circ 13'$, $Z = 8$	3.37	Short prismatic crystals, optical sign (+), $\text{Ng} = 1.594$, $\text{Np} = 1.583$, cleavage perfect along (001)
Faracelsian (δ form)	Monoclinic (pseudo-rhombic)	$a = 9.08$, $b = 9.58$, $c = 8.58 \text{ A}$, $\beta \sim 90^\circ$, $Z = 4$	3.31	Prismatic crystals, optical sign (-), $\text{Ng} \sim 1.587$, $\text{Np} = 1.570$
Hexagonal form (α or high-temperature celsian)	Hexagonal	$a = 5.25$ $c = 7.64\text{A}$, $c/a = 1.494$ $Z = 1$	3.299	Hexagonal plates, optical sign (+), cleavage perfect along (000!), $\text{No} = 1.573$

Yoshiki and colleagues [19], synthesizing the hexagonal modification ("hexacelsian") of kaolinite and barium carbonate, by means of carrying out the reaction in the solid state at 1000°, demonstrated its transition at 1200° into celsian proper (Fig. 190a). Hexacelsian exists in two enantiotropic modifications, with an inversion point of 300°. Above 1200°, "hexacelsian" is metastable with respect to celsian.

Seki and Kennedy [14] found that, at atmospheric pressure, hexagonal celsian changes to monoclinic at 700°.

Grebenshchikov [2,3] accepts only celsian proper (β form), melting equiponderantly at 740°, as a stable form. Hexacelsian is considered to be

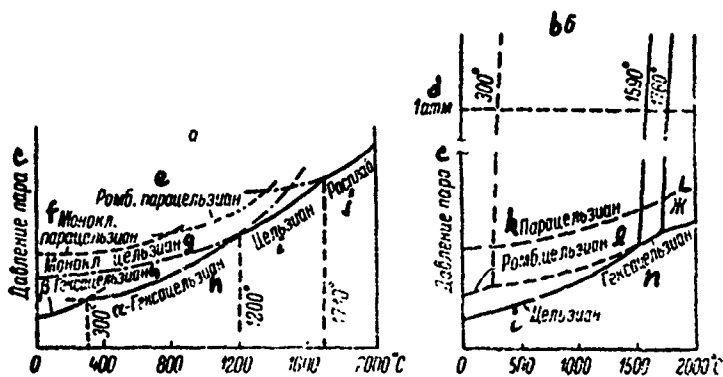


Fig. 190. Schematic phase diagram characterizing polymorphism of celsian: a. from Yoshiki and colleagues; b. from Lin and Foster.

Key:

- | | |
|---------------------------|--------------------|
| c. Vapor pressure | h. Hexacelsian |
| d. One atmosphere | i. Celsian |
| e. Rhombic paracelsian | j. Melt |
| f. Monoclinic paracelsian | k. Paracelsian |
| g. Monoclinic celsian | l. Rhombic celsian |

a metastable modification, transforming to the celsian form at 295°, at all temperatures.

Ivukina and Panova [4], by growing monocrystals by the method of Verneil, obtained a hexagonal modification, which thus is the highest temperature form. The monocrystals obtained were uniaxial, positive, negative elongation, direct extinction.

Lin and Foster [10] carried out long tests under hydrothermal and "dry" conditions. It was determined that monoclinic celsian is stable from room temperature to 1590°, when it slowly and reversibly changes to the hexagonal

TABLE 2
INVARIANT POINTS OF BaO -- Al₂O₃ -- SiO₂ SYSTEM

a Фазы	b Процесс	c Состав						f _{ра} Температура, °C	
		d вес. %			e мол. %				
		BaO	Al ₂ O ₃	SiO ₂	BaO	Al ₂ O ₃	SiO ₂		
Al ₂ O ₃ + 3Al ₂ O ₃ · 2SiO ₂ + BaO · Al ₂ O ₃ · 2SiO ₂ + жидкость g	Реакция	29	32	40	15.7	27	57.3	1590	
Al ₂ O ₃ + BaO · Al ₂ O ₃ · 2SiO ₂ + жидкость g	"	41	37	22	26.9	36.4	36.7	1610	
Твердый раствор + BaO · 6Al ₂ O ₃ + BaO · Al ₂ O ₃ · 2SiO ₂ + жидкость g	"	48.5	35	16.5	33.8	36.8	29.4	1580	
Твердый раствор + 2BaO · SiO ₂ + BaO · Al ₂ O ₃ · 2SiO ₂ + жидкость g	Эвтектика	63	14.5	22.5	44.3	15.3	40.4	1330	
2BaO · SiO ₂ + BaO · SiO ₂ + BaO · Al ₂ O ₃ · 2SiO ₂ + жидкость g	"	64	10	26	44	10.3	45.7	1360	
BaO · SiO ₂ + твердый раствор + BaO · Al ₂ O ₃ · 2SiO ₂ + жидкость g	"	53	10	32	37.5	9.8	52.7	1320	
Твердый раствор + BaO · 2SiO ₂ + BaO · Al ₂ O ₃ · 2SiO ₂ + жидкость g	Реакция	49	10	41	29	8.9	62.1	1280	
BaO · 2SiO ₂ + 3Al ₂ O ₃ · 2SiO ₂ + BaO · Al ₂ O ₃ · 2SiO ₂ + жидкость g	"	37	11	52	19.8	9	71.2	1240	
BaO · 2SiO ₂ + SiO ₂ + 3Al ₂ O ₃ · 2SiO ₂ + жидкость g	Эвтектика	32	11	57	16.4	8.6	75	1230	
Твердый раствор + BaO · 6Al ₂ O ₃ + BaO · Al ₂ O ₃ · 2SiO ₂ + жидкость g	Реакция	49	37	11	34.8	39.7	25.5	1610	
Твердый раствор + BaO · Al ₂ O ₃ · 2SiO ₂ + 2BaO · SiO ₂ + жидкость g	"	63	16.5	20.5	45	17.7	37.3	1340	
BaO · Al ₂ O ₃ · 2BaO · Al ₂ O ₃ · 2SiO ₂ + жидкость g	"	66	18	16	49.3	20.2	30.5	1490	
3BaO · Al ₂ O ₃ + BaO · 2BaO · SiO ₂ + жидкость g	"	72	13	15	55.3	15.1	29.6	1520	
BaO · Al ₂ O ₃ · 2SiO ₂ + жидкость g	Плавление	41.1	27.2	31.7	25	25	50	1740	

Key

Key:

- a. Phases
- b. Process
- c. Composition
- d. Weight %
- e. Mole %
- f. Temperature, °C
- g. Liquid
- h. Solid solution
- i. Reactions
- j. Eutectic
- k. Melting

form (hexacelsian). The latter is stable up to the melting temperature of 1760° (Fig. 190b). Hexacelsian is easily supercooled and, in the metastable state, it quickly and reversible changes to the rhombic form at 300°. Paracelsian (the authors used the natural metal) is metastable at all temperatures; it changes monotropically into celsian proper through the hexacelsian stage. These transitions are observed at 500° and perhaps at still lower temperatures.

As we see, there are three points of view on polymorphism of $\text{BaAl}_2\text{Si}_2\text{O}_8$, which are reduced to different interpretation of the position of the hexagonal form in the system: 1. The hexagonal form is always metastable (Grebenshchikov); 2. The hexagonal form is stable in a lower temperature region than monoclinic celsian (Yoshiki and colleagues, Seki and Kennedy); 3. The hexagonal form is the highest temperature form, melting equiponderantly (Ivukina and Panova, Lin and Foster).

Gebert [8] and Kockel and Oehlschlegel [9] have obtained a new barium aluminosilicate, $\text{BaO} \cdot \text{Al}_2\text{O}_3 \cdot \text{SiO}_2$. Gebert heated a mixture of the composition $4\text{BaO} + 3\text{Al}_2\text{O}_3 + 3\text{SiO}_2$ in a platinum crucible, at temperatures between 1380 and 1450°, from 1 to 14 days. The formula of the new compound was determined by means of an electron microanalyzer. Having hexagonal symmetry, the crystals had unit cell parameters $a_0 = 9.9$ and $c_0 = 18.59$ Å.

Kockel and Oehlschlegel [9] obtained $\text{BaO} \cdot \text{Al}_2\text{O}_3 \cdot \text{SiO}_2$ by means of a solid-phase reaction at 1380-1400°. The space group of the crystals is $P6_3$, indices of refraction $N_g = 1.636$, $N_p = 1.628$, the crystals are colorless, there is insignificant cleavage parallel to (0001), and a strong anomaly of the optical axis is characteristic: $2V = 0-30^\circ$. The incongruent melting temperature is 1400°.

The authors did not find solid solutions between the compound $\text{BaO} \cdot \text{Al}_2\text{O}_3 \cdot \text{SiO}_2$ and the compounds $3\text{BaO} \cdot 3\text{Al}_2\text{O}_3 \cdot 2\text{SiO}_2$ and $\text{BaO} \cdot \text{SiO}_2$, or for the concentration region from 55 mole % $\text{AlO}_{1.5}$, 27 mole % BaO , 18 mole % SiO_2 to 30 mole % $\text{AlO}_{1.5}$, 38 mole % BaO and 32 mole % SiO_2 , and only one compound, the unit cell parameters of which were practically constant, was found together with celsian and the binary compounds.

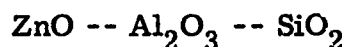
Planz and Mueller-Hesse [12] apparently obtained the compound $\text{BaO} \cdot \text{Al}_2\text{O}_3 \cdot \text{SiO}_2$, since the values of the interplane distances and intensities which they presented coincide with those obtained by Kockel and Oehlschlegel. According to the data of these authors, the compound being discussed melts incongruently above 1550° , forming $\text{BaO} \cdot \text{Al}_2\text{O}_3$, hexagonal $\text{BaO} \cdot \text{Al}_2\text{O}_3 \cdot 2\text{SiO}_2$ and liquid.

Toropov and colleagues determined the concentration region of the system in which glass can be obtained.

BIBLIOGRAPHY

1. Ginzberg, A. S., Izv. Pertogr. politekhn. inst., 23, 1, 1915, p. 207.
2. Grebenschikov, R. G., Izv. AN SSSR, OKhN, 2, 1963, p. 205.
3. Grebenschikov, R. G., "Structural analogy and interrelation of physico-chemical properties in silicate and model systems," Author's abstract, doctoral dissertation, Leningrad, 1967.
4. Ivukina, A. K., Ya. I. Panova, Kristallografiya, 9, 4, 1964, p. 560.
5. Toropov, N. A., F. Ya. Galakhov, I. A. Bondar', DAN SSSR, 89, 1, 1953, p. 89.
6. Toropov, N. A., F. Ya. Galakhov, I. A. Bondar', Izv. AN SSSR, OKhN, 1, 1955, p. 3.
7. Foster, W. R., H. C. Lin, Amer. J. Sci., 267A, Schairer vol., 134, 1969.
8. Gebert, W., Naturwissenschaften, 55, No. 8, 387, 1968.

9. Kockel, A., G. Oehlschlegel, Neues Jahrb. Mineral., Monatshefte, No. 15, 1969.
10. Lin, H.C., W.R. Foster, Amer. Mineralogist, 53, No. 1-2, 134, 1968.
11. Lin, H.C., W.R. Foster, Mineral. Magaz., 57, No. 288, 459, 1969.
12. Planz, J.E., H. Mueller-Hesse, Ber. Dtsch. keram. Ges., 40, No. 3, 191, 1963.
13. Schwiete, H.E., H. Mueller-Hesse, J.E. Planz, Forschungsber. Land. Nord. Westfal., No. 998, 170, 1961.
14. Seki, Y., G.C. Kennedy, Amer. Mineralogist, 49, No. 9-10, 1467, 1964.
15. Semler, C.E., W.R. Foster, J. Amer. Ceram. Soc., 52, No. 12, 579, 1969.
16. Taylor, W.H., I.A. Darbyshire, M. Strunz, Zs. Kristallogr., 87, No. 4, 464, 1934.
17. Thomas, R.H., J. Amer. Ceram. Soc., 33, No. 2, 36, 1950.
18. Yoshiki, B., K. Matsumoto, J. Amer. Ceram. Soc., 34, No. 9, 283, 1951.
19. Yoshiki, B., Sh. Koide, M. Waki, Rep. Res. Lab. Asahi Glass Co., 3, 135, 1954.



The system has been studied by Bunting [2]. Ternary compounds were not found. Incoherent melting of mullite is indicated in the diagram introduced by Bunting (Fig. 191). In connection with the work of Toropov and Galakhov [1], demonstrating the congruent nature of melting of mullite, the direction of the lines fixing the boundaries of the corundum and mullite fields must be changed.

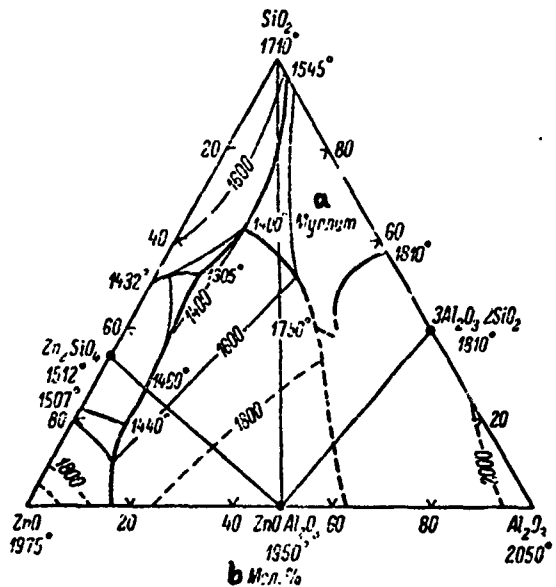


Fig. 191. Phase diagram of $\text{ZnO} - \text{Al}_2\text{O}_3 - \text{SiO}_2$ system (from Bunting).

Key:

- a. Mullite
- b. Mole %

BIBLIOGRAPHY

1. Toropov, N.A., F.Ya. Galakhov, DAN SSSR, **78**, 2, 1951, p. 299.
2. Bunting, E.N., J. Res. Nat. Bur. Stand., **8**, No. 2, 279, 1932.

$\text{Y}_2\text{O}_3 - \text{Al}_2\text{O}_3 - \text{SiO}_2$

The system has been studied by Bondar' and Galakhov [1], by the quenching method. Ternary compounds were not found. A phase diagram of the system, with isotherms plotted, is presented in Fig. 192. The diagram consists of 11

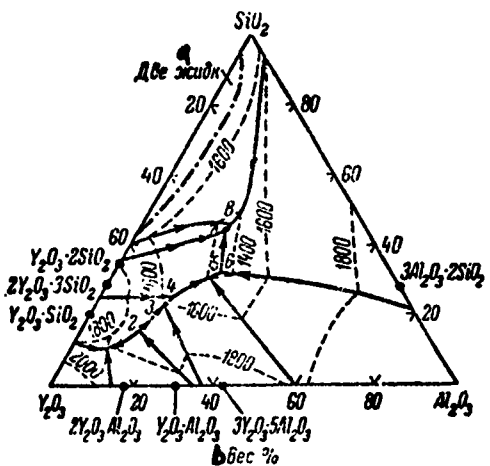


Fig. 192. Phase diagram of Y_2O_3 -- Al_2O_3 -- SiO_2 system (from Bondar' and Galakhov).

Key:

- a. Two liquids
- b. Weight %

fields of stability of the corresponding phases. The phase separation region extends up to 5 weight % Al_2O_3 in the ternary system. Addition of alumina to a mixture of oxides in the Y_2O_3 -- SiO_2 system shrinks the phase separation region. While considerable phase separation regions form and the production of transparent glass is hampered in binary silicate systems with rare earth element oxides, with addition of Al_2O_3 , a region of opalescent glass (Al_2O_3 content 8 weight %) exists, together with a liquation region. At a higher Al_2O_3 content, the glass is transparent.

INVARIANT POINTS OF Y_2O_3 -- Al_2O_3 -- SiO_2 SYSTEM

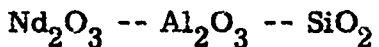
a Точка (рис. 192)	b Фазы	c Процесс	d Состав, вес. %			e Темп- ература, °C
			Y_2O_3	Al_2O_3	SiO_2	
1	$\text{Y}_2\text{O}_3 + 2\text{Y}_2\text{O}_3 \cdot \text{Al}_2\text{O}_3 + \text{Y}_2\text{O}_3 \cdot \text{SiO}_2 +$ жидкость f	Эвтектика	80.5	8.5	11.0	1840
2	$2\text{Y}_2\text{O}_3 \cdot \text{Al}_2\text{O}_3 + \text{Y}_2\text{O}_3 \cdot \text{SiO}_2 +$ $+ \text{Y}_2\text{O}_3 \cdot \text{Al}_2\text{O}_3 +$ жидкость f	Реакция	70	14	16	1680
3	$\text{Y}_2\text{O}_3 \cdot \text{Al}_2\text{O}_3 + 3\text{Y}_2\text{O}_3 \cdot \text{Al}_2\text{O}_3 +$ $+ \text{Y}_2\text{O}_3 \cdot \text{SiO}_2 +$ жидкость f	*	60	16.6	23.4	1600
4	$\text{Y}_2\text{O}_3 \cdot \text{SiO}_2 + 2\text{Y}_2\text{O}_3 \cdot 3\text{SiO}_2 +$ $+ 3\text{Y}_2\text{O}_3 \cdot 5\text{Al}_2\text{O}_3 +$ жидкость f	*	56.5	18.2	25.3	1585
5	$3\text{Y}_2\text{O}_3 \cdot 5\text{Al}_2\text{O}_3 + 2\text{Y}_2\text{O}_3 \cdot 3\text{SiO}_2 +$ $+ \text{Al}_2\text{O}_3 +$ жидкость f	*	45	24.5	30.5	1400
6	$\text{Al}_2\text{O}_3 + 3\text{Al}_2\text{O}_3 \cdot 2\text{SiO}_2 + 2\text{Y}_2\text{O}_3 \cdot$ $+ 3\text{SiO}_2 +$ жидкость f	*	41.4	25.8	32.8	1385
7	$3\text{Al}_2\text{O}_3 \cdot 2\text{SiO}_2 + \text{Y}_2\text{O}_3 \cdot 2\text{SiO}_2 +$ $+ 2\text{Y}_2\text{O}_3 \cdot 3\text{SiO}_2 +$ жидкость f	*	34.5	21.5	44.0	1360
8	$3\text{Al}_2\text{O}_3 \cdot 2\text{SiO}_2 + \text{Y}_2\text{O}_3 \cdot 2\text{SiO}_2 +$ $+ \text{SiO}_2 +$ жидкость f	Эвтектика	32	22	46	1345

Key:

- a. Points (Fig. 192)
- b. Phases
- c. Process
- d. Composition, weight %
- e. Temperature, °C
- f. Liquid
- g. Eutectic
- h. Reaction

BIBLIOGRAPHY

1. Bondar', I. A., F. Ya. Galakhov, Izv. AN SSSR, ser. khim., 7, 1964, p. 1325.

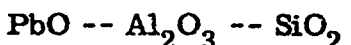


The system has not been studied. For the purpose of ascertaining the effect of alumina on liquation processes in the Nd_2O_3 -- SiO_2 system, Toropov

and Kiseleva [1] added Al_2O_3 to mixtures containing 80-90 mole % SiO_2 . Aluminum oxide does not eliminate phase separation of the liquids, but it changes the mutual distribution of the liquids in the mass: in place of separate, considerable regions, very fine drops form.

BIBLIOGRAPHY

1. Toropov, N. A., T. P. Kiseleva, Zhurn. neorg. khim., 6, 10, 1961, p. 2353.



The system has been studied by Geller and Bunting [1] (Fig. 193). Three ternary compounds have been distinguished: $8\text{PbO} \cdot \text{Al}_2\text{O}_3 \cdot 4\text{SiO}_2$, $4\text{PbO} \cdot \text{Al}_2\text{O}_3 \cdot 2\text{SiO}_2$ and $6\text{PbO} \cdot \text{Al}_2\text{O}_3 \cdot 6\text{SiO}_2$, melting below 1000° .

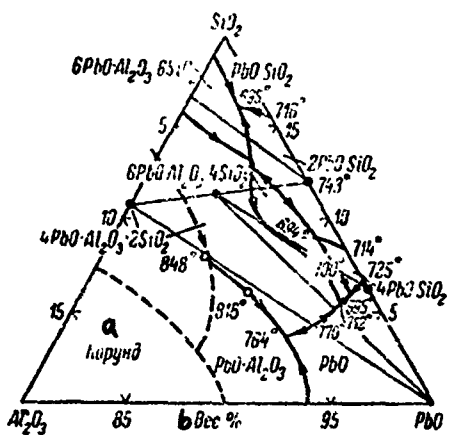


Fig. 193. Part of phase diagram of $\text{PbO} \text{ -- } \text{Al}_2\text{O}_3 \text{ -- } \text{SiO}_2$ system in region adjacent to lead oxide (from Geller and Bunting).

Key:

- a. Corundum
- b. Weight %

TABLE 1
INVARIANT POINTS OF PbO -- Al₂O₃ -- SiO₂ SYSTEM

a Фазы	b Процесс	c Состав, вт.-%			d Темпера- тура, °C
		PbO	Al ₂ O ₃	SiO ₂	
2PbO·SiO ₂ +8PbO·Al ₂ O ₃ ·4SiO ₂ + +4PbO·Al ₂ O ₃ ·2SiO ₂ +жидкость e	f Реакция	85.1	2.3	12.6	705
PbO+8PbO·Al ₂ O ₃ ·4SiO ₂ +PbO ·Al ₂ O ₃ ·2SiO ₂ +жидкость e	g	92.9	1.6	5.5	712
PbO·Al ₂ O ₃ ·4PbO·Al ₂ O ₃ ·2SiO ₂ +? + +жидкость e	g	85.7	6.8	7.5	827
PbO·Al ₂ O ₃ +Al ₂ O ₃ ? +жидкость e	g	87.0	10.0	3.0	Около 765
PbO·SiO ₂ +SiO ₂ ? +жидкость e	g Эвтектика	70.7	1.0	28.3	Около 725
PbO·SiO ₂ +2PbO·SiO ₂ +4PbO·Al ₂ O ₃ · ·6SiO ₂ +жидкость e	g	82.6	1.4	16.0	695
2PbO·SiO ₂ +6PbO·Al ₂ O ₃ ·6SiO ₂ + +4PbO·Al ₂ O ₃ ·2SiO ₂ +жидкость e	g	84.6	2.2	13.2	701
2PbO·SiO ₂ +4PbO·SiO ₂ +8PbO· ·Al ₂ O ₃ ·SiO ₂ +жидкость e	g	89.8	1.2	9.0	694
4PbO·SiO ₂ +PbO+8PbO·Al ₂ O ₃ · ·4SiO ₂ +жидкость e	g	93.1	1.1	5.8	695
PbO+4PbO·Al ₂ O ₃ ·2SiO ₂ +PbO· ·Al ₂ O ₃ +жидкость e	g	91.2	5.2	3.6	764
8PbO·Al ₂ O ₃ ·4SiO ₂ +жидкость e	h. плавление с разло- жением	83.92	4.79	11.29	735 ± 5
4PbO·Al ₂ O ₃ ·2SiO ₂ +жидкость e	i. То же	80.08	9.14	10.78	837
6PbO·Al ₂ O ₃ ·(SiO ₂ +жидкость e)	j. Плавление	74.34	5.36	20.00	811

Key:

- a. Phases
- b. Process
- c. Composition, weight %
- d. Temperature, °C
- e. Liquid
- f. Reaction
- g. Eutectic
- h. Melting with decomposition
- i. Same
- j. Melting
- k. About

TABLE 2
CRYSTALLINE PHASES OF PbO -- Al₂O₃ -- SiO₂ SYSTEM

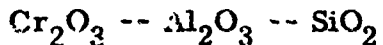
a Соединение	b Габитус	<i>N_g</i>	<i>N_p</i>	c Оптический знак	d Оптические характеристики
8PbO · Al ₂ O ₃ · 4SiO ₂	Бруски	2.08	2.04	—	—
4PbO · Al ₂ O ₃ · 2SiO ₂	f. Пла- стинки	1.91	1.93	(+) $2V^{\circ}=0$	—
6PbO · Al ₂ O ₃ · 6SiO ₂	g. Прямоугольные	1.89	1.79	—	h. Прямоугольные, поглощают свет, узкое отражательное

Key:

- a. Compound
- b. Appearance
- c. Optical sign
- d. Optical characteristics
- e. Rods
- f. Sheets
- g. Prisms
- h. Direct extinction, negative elongation

BIBLIOGRAPHY

1. Geller, R.F., E.N. Bunting, J. Res. Nat. Bur. Stand., 31, No. 5, 1943, p. 255.



A fusibility diagram of the system has been plotted by Bron [1], and solid solutions of chromium oxide in mullite have been studied by Ford and Rees [3] and Murthy and Hummel [4].

Bron studied the fusibility of mixtures in the Al₂O₃ -- Cr₂O₃ -- SiO₂ system by aggregation of cones. The refractoriness of mixtures adjacent to

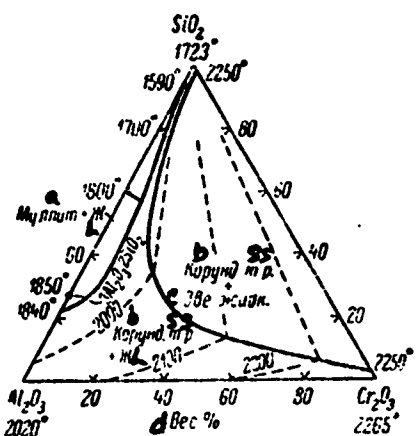


Fig. 194. Phase diagram of Cr_2O_3 -- Al_2O_3 -- SiO_2 system (from Roeder and colleagues).

Key:

- a. Mullite
- b. Corundum
- c. Two liquids
- d. Weigh%.

the Al_2O_3 -- SiO_2 side in composition, with chromium oxide content from 0 to 30 weight %, was studied. By introduction of chromium oxide in quantities up to 10 weight % to aluminosilicate masses with variable Al_2O_3 content (from 20 to 80%), reduction in refractoriness of the mixtures does not occur. This is connected with the formation of solid solutions of Cr_2O_3 in mullite and corundum. Upon adding more than 10% chromium oxide to a mixture of Al_2O_3 and SiO_2 , dissociation of mullite occurs.

According to the data of Ford and Rees [3], under equilibrium conditions at 1600°, mullite can accept about 2 weight % chromium oxide in a solid solution,

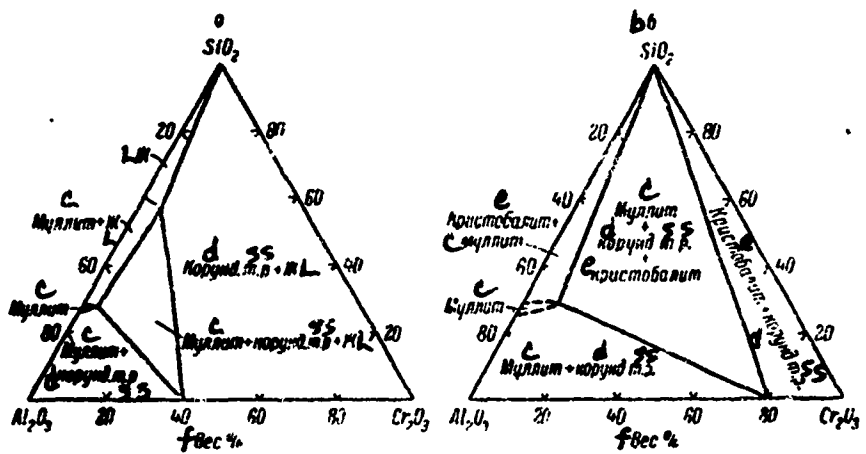


Fig. 195. Diagram of phase relationships of Cr_2O_3 -- Al_2O_3 -- SiO_2 system (from Roeder and colleagues):
a. 1800°; b. 1575°.

Key:

- c. Mullite
- d. Corundum
- e. Cristobalite
- f. Weight %

with small expansion of the mullite unit cell parameters in this case. Further (over 8%) addition of chromium oxide leads to dissociation of the mullite, in which the alumina freed forms a solid solution with chromium oxide, and the remaining alumina gives a melt, with silica separating out upon decomposition of the mullite. At a composition of 53% mullite + 47% Cr_2O_3 , mullite was completely dissociated and, at room temperature, the product contained a solid solution of "alumina -- chromium oxide" and about 20% glass.

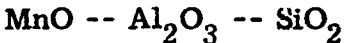
Murthy and Himmel [4] have determined that from 8 to 10 weight % of chromium oxide can enter the mullite structure. Reaction of mullite with Cr_2O_3 begins at 1400° and, at 1700° , dissociation of a small quantity of mullite takes place, with formation of corundum.

The system has been studied in detail by Roeder and colleagues [5], using the quenching method. The phase diagram presented in Fig. 194 is characterized by a very large field of corundum solid solutions and a long, narrow field of mullite. The cristobalite field is extremely small. Cristobalite, a mullite solid solution of the composition 61 weight % Al_2O_3 , 10 weight % Cr_2O_3 and 29 weight % SiO_2 , and a corundum solid solution of the composition 19 weight % Al_2O_3 and 81 weight % Cr_2O_3 , coexist in a triple eutectic, with a liquid of a composition 6 weight % Al_2O_3 , 1 weight % Cr_2O_3 and 93 weight % SiO_2 , at a temperature of 1580° .

A large region of two immiscible liquids covers the primary phase field of corundum solid solutions. The region of immiscible liquids on the SiO_2 -- Cr_2O_3 boundary is in equilibrium with the solid phase at a temperature of 2250° , and the minimum temperature of existence of the liquation region is approximately 1950° . The phase ratios at 1800 and 1575° are presented in Fig. 195. The authors determined the parameters of the mullite solid solutions, which can be considered to be an $\text{Al}_6\text{Si}_2\text{O}_{13}$ -- $\text{Cr}_6\text{Si}_2\text{O}_{13}$ series. Diagrams are presented in the article, which show the pathways of split (fractional) and equilibrium crystallization. According to Chadeyron and Rees [2], addition of 15% chromium oxide to a sillimanite refractory increases its resistance to the action of iron slags.

BIBLIOGRAPHY

1. Bron, V. A., Trudy 5-go soveshch. po eksper. i tekhn. mineral. i petrogr. [Proceedings, 5th Conference on Experimental-Engineering Mineralogy and Petrography], AN SSSR Press, Moscow, 1958, p. 479.
2. Chadeyron, A., W. Rees, Trans. Brit. Ceram. Soc., 42, No. 8, 163, 1942.
3. Ford, W.F., W.J. Rees, Trans. Brit. Ceram. Soc., 45, No. 3, 125, 1946.
4. Murthy, M. K., F.A. Hummel, J. Amer. Ceram. Soc., 43, No. 5, 267, 1960.
5. Roeder, P.L., F.P. Glasser, E.F. Osborn, J. Amer. Ceram. Soc., 51, 585, 1968.



The system has been studied by Glaser [2], Snow [3] and Galakhov [1].

Glaser established the formation of only two ternary compounds.

Snow, conducting a study by the quenching method, showed (Fig. 196), by heating samples in a nitrogen atmosphere (the Mn_2O_3 content was negligible in this case), that there are the following three ternary compounds in the system: spessartite or manganese garnet ($3\text{MnO} \cdot \text{Al}_2\text{O}_3 \cdot 3\text{SiO}_2$), melting at 1200° , "manganese cordierite" ($2\text{MnO} \cdot 2\text{Al}_2\text{O}_3 \cdot 5\text{SiO}_2$), melting with decomposition, forming mullite and liquid, and "manganese anorthite" ($\text{MnO} \cdot \text{Al}_2\text{O}_3 \cdot 2\text{SiO}_2$). "Manganese anorthite" decomposes at 1055° , with formation of mullite and glass and, with repeated, prolonged heating at $1120-1150^\circ$ and intermediate cooling, it is replaced by "manganese cordierite." "Manganese cordierite" is similar in structure to common cordierite ($2\text{MgO} \cdot 2\text{Al}_2\text{O}_3 \cdot 5\text{SiO}_2$). "Manganese anorthite" can only hypothetically be compared with common anorthite.

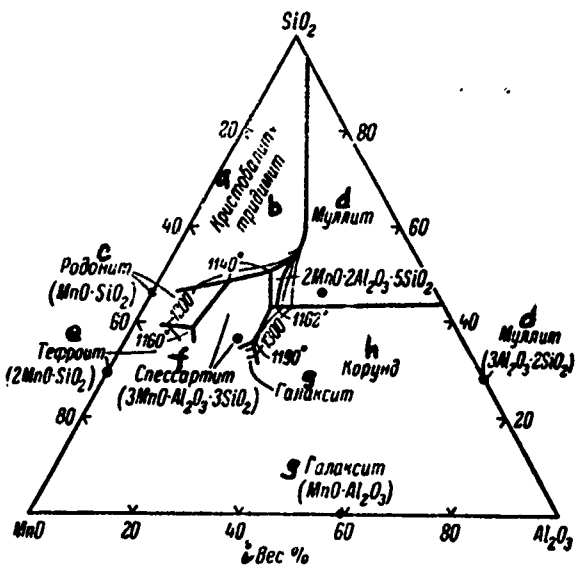


Fig. 196. Phase diagram of $\text{MnO} - \text{Al}_2\text{O}_3 - \text{SiO}_2$ system (from Snow).

Key:

- | | |
|-----------------|----------------|
| a. Cristobalite | f. Spessartite |
| b. Tridymite | g. Galaxite |
| c. Rhodonite | h. Corundum |
| d. Mullite | i. Weight % |
| e. Tephroite | |

Galakhov, studying the region adjacent to alumina, established the boundary between the mullite and corundum fields. On the diagram, which combines the data of Snow and Galakhov (Fig. 197), the position of the mullite -- corundum boundary is in conformance with the invariant reaction point of the mullite, corundum and "manganese cordierite" fields and the corresponding eutectic point of the alumina -- silica system. In a large concentration region of the system, glass can be obtained.

TABLE 1
INVARIANT POINTS IN $\text{MnO} - \text{Al}_2\text{O}_3 - \text{SiO}_2$ SYSTEM

a. Фазы	b. Процесс	c. Состав, вес. %			d. Темп- ратура, °C
		MnO	Al ₂ O ₃	SiO ₂	
3MnO·Al ₂ O ₃ ·3SiO ₂ + тридимит + e + 2MnO·2Al ₂ O ₃ ·5SiO ₂ + жидкость f	Эвтектика	30	19	51	1140
Тридимит + 3Al ₂ O ₃ ·2SiO ₂ + 2MnO· ·2Al ₂ O ₃ ·5SiO ₂ + жидкость f	Реакция	24	23	53	1200
3MnO·Al ₂ O ₃ ·3SiO ₂ + Al ₂ O ₃ + 2MnO· ·2Al ₂ O ₃ ·5SiO ₂ + жидкость f	*	33	24	43	1162
2MnO·2Al ₂ O ₃ ·5SiO ₂ + 3Al ₂ O ₃ ·2SiO ₂ + + Al ₂ O ₃ + жидкость f	*	32	25	43	1168
3MnO·Al ₂ O ₃ ·3SiO ₂ + Al ₂ O ₃ + MnO· ·Al ₂ O ₃ + жидкость f	*	40	24	36	1190
MnO·SiO ₂ + тридимит + 3MnO·Al ₂ O ₃ · ·3SiO ₂ + жидкость f	Эвтектика	38	13	49	1140
MnO·SiO ₂ + 3MnO·Al ₂ O ₃ ·3SiO ₂ + + 2MnO·SiO ₂ + жидкость f	*	50	11	39	1160
3MnO·Al ₂ O ₃ ·3SiO ₂ + тридимит + «Mn- гапортит» + жидкость f	-	29	20	51	1120
Тридимит + «Mn-анортит» + 3Al ₂ O ₃ · ·2SiO ₂ + жидкость f	-	27	22	51	1145
3MnO·Al ₂ O ₃ ·3SiO ₂ + «Mn-анортит» + + 3Al ₂ O ₃ ·2SiO ₂ + жидкость f	-	31	23	46	1145
3MnO·Al ₂ O ₃ ·3SiO ₂ + 3Al ₂ O ₃ ·2SiO ₂ + + Al ₂ O ₃ + жидкость f	-	33	24	43	1160
3MnO·Al ₂ O ₃ ·3SiO ₂ + расплав h	Нагревание	-	-	-	1200

Key:

- | | |
|--------------------------|-----------------|
| a. Phases | g. Mn anorthite |
| b. Process | h. Melt |
| c. Composition, weight % | i. Eutectic |
| d. Temperature, °C | j. Reaction |
| e. Tridymite | k. Melting |
| f. Liquid | |

TABLE 2
CRYSTALLINE PHASES OF $MnO - Al_2O_3 - SiO_2$ SYSTEM

a Соединение	b Система кристаллов	c Габитус	d N_g	d N_p	d $2V^\circ$	d Оптическая ориентировка
$MnO \cdot Al_2O_3$ (галаксит) • $MnO \cdot Al_2O_3 \cdot 2SiO_2$ ("Мн-анортит")	Изкубическая Триклиническая	1 Октаэдры Двойниковые плстины	1.823	—	—	—
$2MnO \cdot 2Al_2O_3 \cdot 5SiO_2$ ("Мн-кордиерит")	Ромбическая	II Псевдоокта- гональный	1.558	1.537	—	—
$3MnO \cdot Al_2O_3 \cdot 3SiO_2$ ("спессартит")	Изкубическая	III Додека- гра	1.810	—	—	—

Key:

- | | |
|------------------------|------------------------------|
| a. Compound | i. Cubic |
| b. Crystal system | j. Triclinic |
| c. Appearance | k. Rhombic |
| d. Optical orientation | l. Octahedra |
| e. Galaxite | m. Twinned sheets |
| f. Mn anorthite | n. Pseudohexagonal |
| g. Mn cordierite | o. Dodecahedra |
| h. Spessartite | p. Extinction of sheets 4-3° |

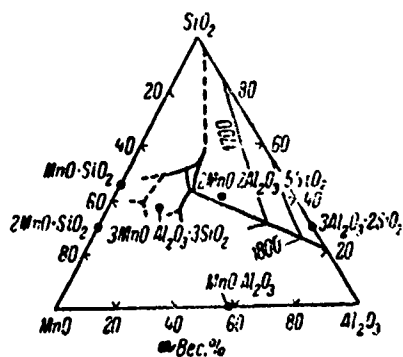
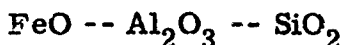


Fig. 197. Phase diagram of $MnO - Al_2O_3 - SiO_2$ system (from Snow, with additions by Галакхов).

Key: a. Weight %

BIBLIOGRAPHY

1. Galakhov, F. Ya., Izv. AN SSSR. OKhN, 5, 1957, p. 625.
2. Glaser, O., Zbl. Mineral., A, 81, 1926.
3. Snow, R. B., J. Amer. Ceram. Soc., 26, No. 1, 11, 1943.



The system has been studied by Schairer and Yagi [7] and by Galakhov [1]. In study of this system (as in all systems with FeO), the possibility of forming ferric oxide (Fe_2O_3) must be taken into account [7]. In fusing mixtures of FeO, Al_2O_3 and SiO_2 in an electric arc, Fe_2O_3 (up to 3.5 weight %, according to Galakhov, at a 23 weight % FeO content) forms in the melts. Schairer and Yagi have investigated the region adjacent to the $\text{FeO} -- \text{SiO}_2$ side. Galakhov has studied the alumina apex of the diagram. Osborn and Muan [6], taking account of the data of Schairer and Yagi and Galakhov, have plotted a phase diagram of the $\text{FeO} -- \text{Al}_2\text{O}_3 -- \text{SiO}_2$ system (Fig. 198), using the data of Toropov and Galakhov [2] and Fischer and Hoffmann [5] on the $\text{Al}_2\text{O}_3 -- \text{SiO}_2$ and $\text{FeO} -- \text{Al}_2\text{O}_3$ systems. A single ternary compound $2\text{FeO} \cdot 2\text{Al}_2\text{O}_3 \cdot 5\text{SiO}_2$, iron cordierite, stable in the presence of a melt, exists in the system. At 1210° , iron cordierite undergoes decomposition into mullite, tridymite and melt. Iron cordierite forms feathery and fibrous aggregates of crystals, having a negative principal zone and indices of refraction $\text{Ng} = 1.574$, $\text{Nm} = 1.564$ and $\text{Np} = 1.551$. The crystals are in the rhombic system; $(-)2V$ is large. As a consequence of the low crystallization rate of iron cordierite, the formation of metastable invariant points in the system is possible: fayalite + tridymite + spinel + liquid at $1073 \pm 5^\circ$ and mullite + hercynite + tridymite +

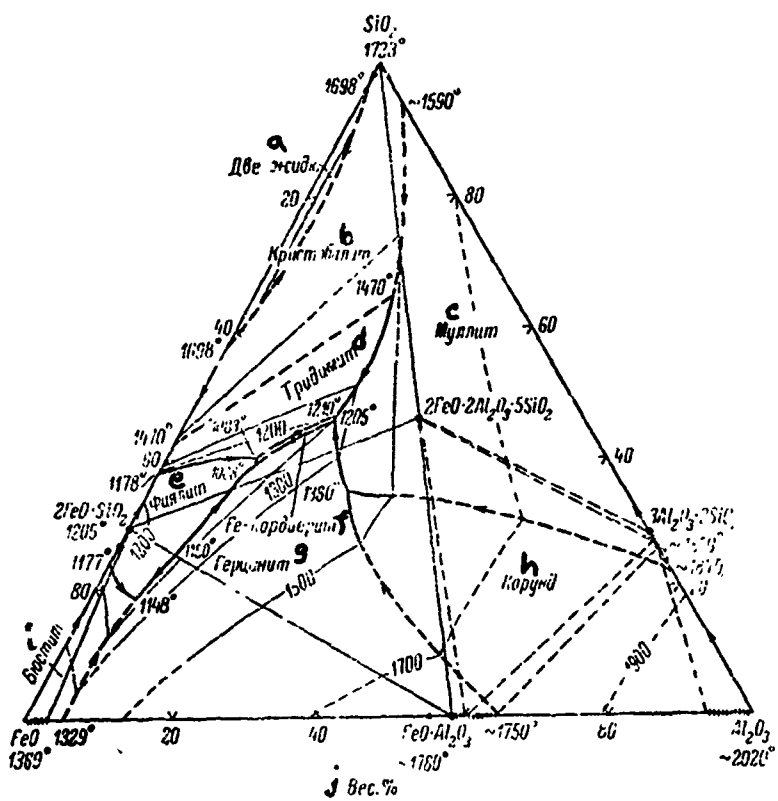


Fig. 198. Phase diagram of FeO -- Al₂O₃ -- SiO₂ system (from Osborn and Muan).

Key:

- | | |
|-----------------|------------------|
| a. Two liquids | f. Fe cordierite |
| b. Cristobalite | g. Hercynite |
| c. Mullite | h. Corundum |
| d. Tridymite | i. Wüstite |
| e. Fayalite | j. Weight % |

liquid at $1205 \pm 10^\circ$. Brownell [3], heating a mixture of FeO and mullite at 1000° for a period of 44 hours, did not detect the formation of solid solutions.

At 1192° , i. e., in the subsolidus region, FeO reacts with mullite, with formation

INVARIANT POINTS OF FeO -- Al₂O₃ -- SiO₂ SYSTEM

a Фазы	b Процесс	c Состав, вес. %			d Темпера- тура, °C
		FeO	Al ₂ O ₃	SiO ₂	
Фаялит + герцинит + жидкость	l. Реакция	Фаялита 89.3,			1150 ± 5
Корунд + муллит + герцинит + жидкость	m. Эвтектика	75.8	5.9	18.3	1148 ± 5
Корунд + муллит + герцинит + жидкость	l. Реакция	38	27	35	1380 ± 5
Кордиерит + тридимит + муллит + жидкость	•	33.3	20	46.7	1210 ± 5
Кордиерит + тридимит + муллит + жидкость	•	33.9	20.1	46.0	1205 ± 10
Кордиерит + герцинит + фаялит + жидкость	•	47.7	12.6	39.7	1088 ± 5
Кордиерит + фаялит + тридимит + жидкость	m. Эвтектика	47.5	12.0	40.5	1083 ± 5

Key:

- | | |
|--------------------------|---------------|
| a. Phases | h. Corundum |
| b. Process | i. Mullite |
| c. Composition, weight % | j. Cordierite |
| d. Temperature, °C | k. Tridymite |
| e. Fayalite | l. Reaction |
| f. Hercynite | m. Eutectic |
| g. Liquid | |

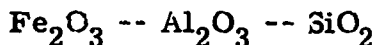
of FeAl₂O₄ and Fe₂SiO₄. Schrairer and Yagi obtained glass in the FeO -- Al₂O₃ -- SiO₂ system.

Schreyer and Schairer [9] have shown that silica-base, quartz-like solid solutions form in the partial section FeAl₂O₄ -- SiO₂, but their concentration region is smaller than in the MgO -- Al₂O₃ -- SiO₂ system. According to Schreyer [8], iron cordierite is stable under hydrothermal conditions only above 400-600° (correspondingly, below 6-10 kbar).

Coes [4] synthesized almandine garnet at a pressure of 10 kbar and a temperature of 800-900°. At normal pressure and a temperature of 900°, almandine decomposes in the solid state, with formation of hercynite, iron cordierite and fayalite. The index of refraction of almandine glass is 1.662.

BIBLIOGRAPHY

1. Galakhov, F. Ya., Izv. AN SSSR, OKhN, 5, 1957, p. 525.
2. Toropov, N. A., F. Ya. Galakhov, in the collection Voprosy petrografii i mineralogii [Problems in Petrography and Mineralogy], issue 2, AN SSSR Press, Moscow, 1953, p. 254.
3. Brownell, W. E., J. Amer. Ceram. Soc., 41, No. 6, 226, 1958.
4. Coes, L., J. Amer. Ceram. Soc., 38, No. 2, 98, 1955.
5. Fischer, W. A., A. Hoffmann, Arch. Eisenhüttenw., 27, No. 5, 343, 1956.
6. Osborn, E. F. A. Muan, in E. M. Levin, C. R. Robbins, H. F. McMurdie, Phase Diagrams for Ceramists, USA, Columbus, fig. 696, 1964.
7. Schairer, J. F., K. Yagi, Amer. J. Sci., Bowen vol., pt. 2, 471, 1952.
8. Schreyer, W., Beitr. Mineral., Petrogr., 11, No. 3, 297, 1965.
9. Schreyer, W., J. F. Schairer, Zs. Kristallogr., 116, No. 1-2, 60, 1961.



The system has been studied roughly by Nowotny and Funk [6]. Mixtures of the oxides were melted in an oxygen atmosphere (pressure 110 atm). Ternary compounds were not found. In the fusibility diagram, represented by dashed lines (Fig. 199), a triple eutectic is recorded, located close to the silica apex, has been recorded, as well as a reaction point, at which the following process takes place: corundum (solid solution) + liquid = mullite ($3\text{Al}_2\text{O}_3 \cdot 2\text{SiO}_2$) + hematite (solid solution). The authors did not observe

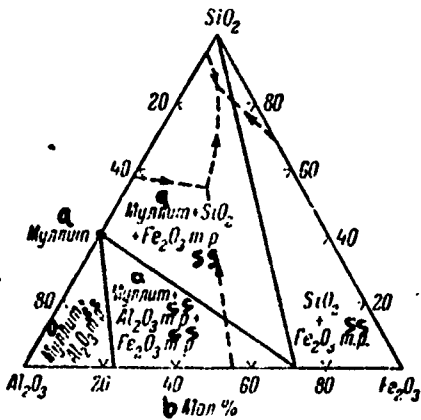


Fig. 199. Approximate fusibility diagram of Fe_2O_3 -- Al_2O_3 -- SiO_2 system and coexisting phase triangles for 1000° (from Nowotny and Funk).

Key:

a. Mullite

b. Mole %

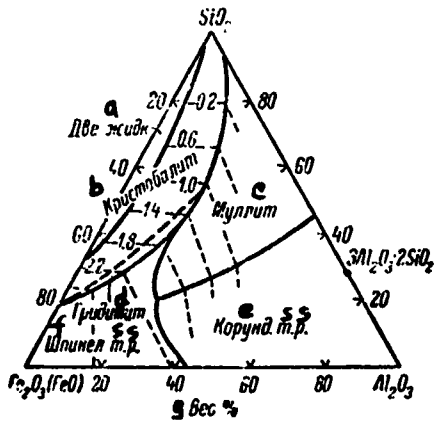


Fig. 200. Diagram of phase relationships of $\text{Fe}_2\text{O}_3(\text{FeO})$ -- Al_2O_3 -- SiO_2 system (from Muan).

Key:

a. Two liquids
b. Cristobalite
c. Mullite

d. Tridymite
e. Corundum
f. Spinel
g. Weight %

solubility of Fe_2O_3 in cristobalite. Compounds were not found (at 1400°) in the binary system Fe_2O_3 -- SiO_2 ; Fe_2O_3 melts at 1730°.

The phase equilibria in the system at the liquidus temperatures in air have been studied by Muan [4] (Fig. 200). The dashed lines correspond to the equilibrium ratio of Fe_2O_3 -- FeO on the liquidus surface, and they show the location of points on the 0.21 atm O_2 isobaric surface, relative to the Fe_2O_3 (FeO) -- Al_2O_3 -- SiO_2 plane. The presence of two quadruple "penetrating (piercing) points" is characteristic of the system.

Brownell [3] has studied the solid solutions of mullite and iron oxide (hematite). A mixture of these substances was annealed in air at temperatures from 1000 to 1300°. With the increase in temperature, the amount of Fe_2O_3 dissolving in mullite increased, amounting to 1 mole % at 1000°, 3 mole % at 1100°, 10 mole % at 1200° and 18 mole % at 1300°. Inclusion of Fe_2O_3 in the mullite lattice caused its expansion. The index of refraction increased in this case.

Thermal soaking of the solid solution caused its decomposition, with separation of ferric oxide; the solid solution obtained at 1300° disclosed decomposition at 1200°, progressing with decrease in temperature to 900°. Ferrous oxide (FeO) does not dissolve in mullite and, at 1192°, the formation of ferrous aluminate and silicate is observed.

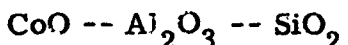
According to Murthy and Hummel [5], the maximum Fe_2O_3 content in mullite is 10-12 weight % at a temperature of 1450°.

Plekhanova and colleagues [2] obtained solid solutions of mullite with ferric oxide by annealing (1300°) a mixture of kaolinite and Fe_2O_3 , with subsequent treatment with hydrofluoric acid. The maximum concentration of Fe_2O_3 in the solid solution at 1300° is 10 weight %.

Berezhnay [1] carried out triangulation of the system, showing that mullite coexists with Fe_2O_3 and FeAlO_3 .

BIBLIOGRAPHY

1. Berezhnay, A. S., Mnogokomponentnye sistemy okislov [Multicomponent Oxide Systems], Naukova dumka Press, Kiev, 1970, p. 233.
2. Plekhanova, Ye. A., G. A. Golubova, N. I. Zyuzin, Izv. Sibirsk. otd. AN SSSR, [3], ser. khim. nauk., 1, 1965, p. 48.
3. Brownell, W. E., J. Amer. Ceram. Soc., 41, No. 6, 226, 1958.
4. Muan, A., J. Amer. Ceram. Soc., 40, No. 4, 121, 1957.
5. Murthy, M. K., F. A. Hummel, J. Amer. Ceram. Soc., 43, No. 5, 267, 1960.
6. Nowotny, H., R. Funk, Radex-Rundschau, No. 8, 337, 1951.



The system has been studied by Dayal and colleagues [1] by the quenching method. Crystalline phases are shown in Fig. 201, which occur in equilibrium with liquid: mullite (approximate composition $\text{Al}_6\text{Si}_2\text{O}_{13}$), spinel (CoAl_2O_4), cobalt orthosilicate (Co_2SiO_4), cobalt monoxide (CoO), corundum and silica (tridymite or cristobalite). It was shown by special tests that change in oxygen pressure does not have an effect on the position of the invariant points, i. e., all of the cobalt is in the divalent state. The coexisting phase triangles, as well as the invariant point temperatures, are presented in Fig. 202.

Noda and Ushio [2] produced crystallization of glass at pressures of 20-40 kbar and temperatures of 600-1900° and cobalt garnet $3\text{CoO} \cdot \text{Al}_2\text{O}_3 \cdot 3\text{SiO}_2$, stable at temperatures of 1200 (pressure 23 kbar) and 1500° (24 kbar). At

INVARIANT POINTS OF CoO -- Al₂O₃ -- SiO₂ SYSTEM

α Фазы	б Состав, вес. %			с Температура, °C
	CoO	Al ₂ O ₃	SiO ₂	
Корунд + муллит + спинель + жидк. + кость	25	41	34	1615
Шпинель + муллит + SiO ₂ + жидк. - + кость	21	22	57	1425
Шпинель + SiO ₂ + Co ₂ SiO ₄ + жидк. - + кость	47	12	41	1268
Шпинель + Co ₂ SiO ₄ + CoO + жидк. - + кость	61	10	29	1340

Key:

Reproduced from
best available copy.

- a. Phases
- b. Composition, weight %
- c. Temperature, °C
- d. Corundum
- e. Mullite
- f. Spinel
- g. Liquid

lower P and t, dissociation takes place, with formation of CoO·Al₂O₃, 2CoO·SiO₂ and quartz. The bright red crystals have N(D) = 1.82 ± 0.01 (25°) and unit cell parameter a = 14.473 ± 0.008 Å.

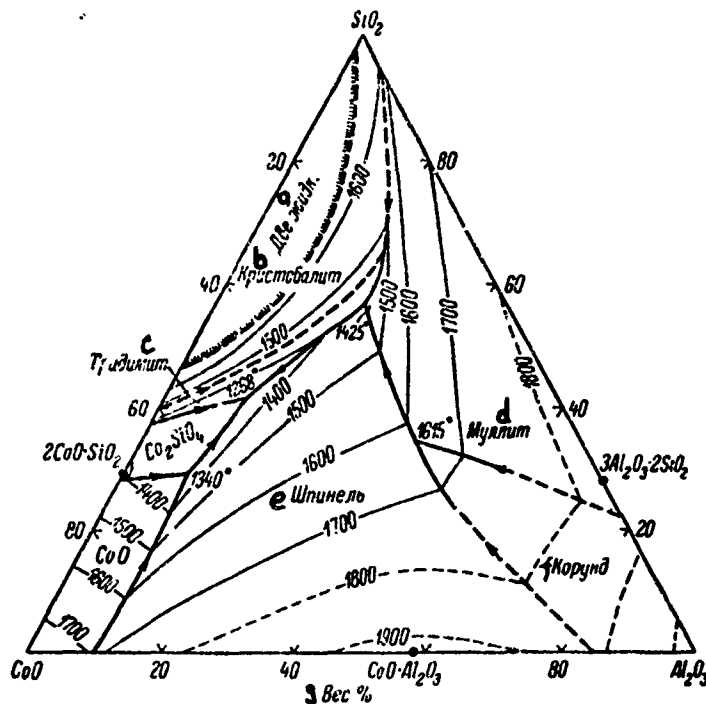


Fig. 201. Phase diagram of $\text{CoO} - \text{Al}_2\text{O}_3 - \text{SiO}_2$ system (from Dayal and colleagues).

Key:

- a. Two liquids
- b. Cristobalite
- c. Tridymite
- d. Mullite
- e. Spinel
- f. Corundum
- g. Weight %

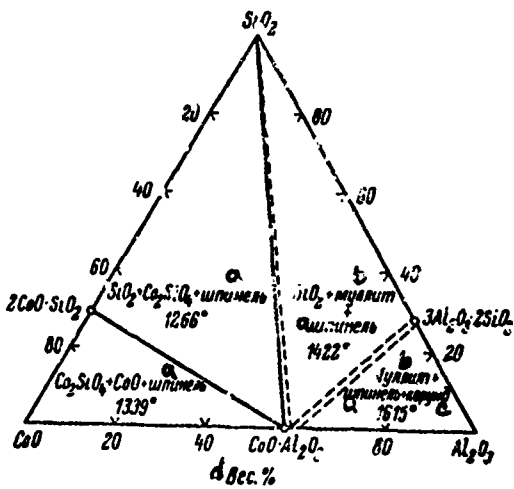


Fig. 202. Coexisting phase triangles of
CoO -- Al₂O₃ -- SiO₂ system (from
Dayal and colleagues).

Key:

- a. Spinel
- b. Mullite
- c. Corundum
- d. Weight %

BIBLIOGRAPHY

1. Dayal, R. R., R. E. Johnson, A. Muan, J. Amer. Ceram. Soc., 50, No. 10, 537, 1967.
2. Noda, T., M. Ushio, J. Ceram. Assoc. Japan, 75, No. 5, 125, 1967.

NiO -- Al₂O₃ -- SiO₂

The system has been studied by Phillips and colleagues [1] by the quenching method. The phases were identified microscopically, and the X-ray method was used sometimes. The authors gave a phase diagram of ternary system

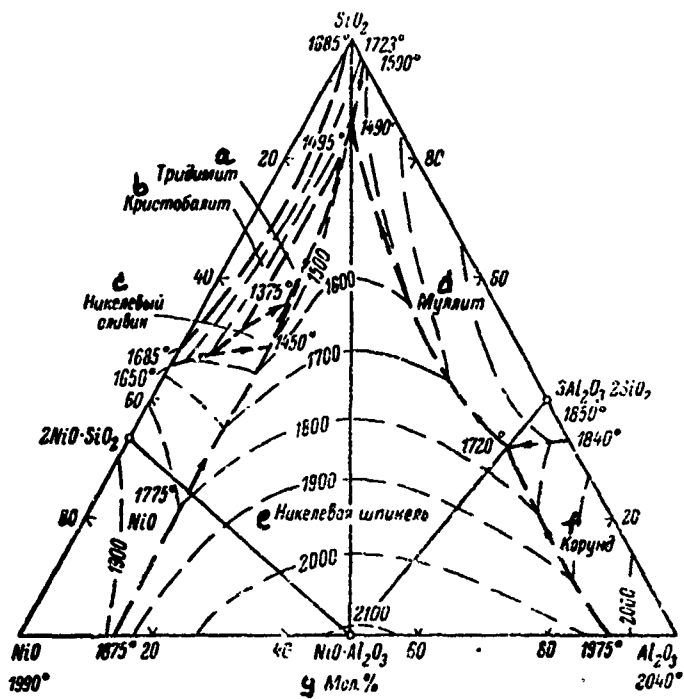


Fig. 203. Phase diagram of NiO -- Al₂O₃ -- SiO₂ system (from Phillips and colleagues).

Key:

- a. Tridymite
- b. Cristobalite
- c. Nickel olivine
- d. Mullite
- e. Nickel spinel
- f. Corundum
- g. Mole %

(Fig. 203). Ternary compounds were not noted. The partial binary systems NiO·Al₂O₃ -- SiO₂ and NiO·Al₂O₃ -- 3Al₂O₃·2SiO₂ are binary eutectics, and no other crystalline phases were observed, apart from the extremes. The

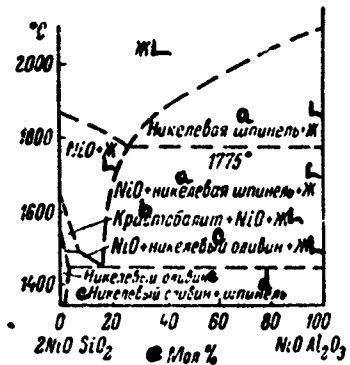


Fig. 204. Phase diagram of partial system $2\text{NiO}\cdot\text{SiO}_2$ -- $\text{NiO}\cdot\text{Al}_2\text{O}_3$ (from Phillips and colleagues).

Key:

- a. Nickel spinel
- b. Cristobalite
- c. Nickel olivine
- d. Spinel
- e. Mole %

partial system $2\text{NiO}\cdot\text{SiO}_2$ -- $\text{NiO}\cdot\text{Al}_2\text{O}_3$ (Fig. 204) is binary only below 1450° .

Above 1450° , a liquid phase appears and two three-phase regions are formed: a region where Ni_2SiO_4 (nickel olivine), NiO and liquid coexist and a region of coexistence of NiAl_2O_4 (nickel spinel), NiO and liquid. The dissociation temperature of nickel olivine decreases from 1545 to 1490° in the presence of NiAl_2O_4 , which is a consequence of the solubility of NiAl_2O_4 in Ni_2SiO_4 . The phase separation region of the melt adjoins the SiO_2 -- NiO boundary line.

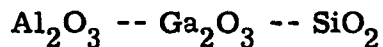
The authors draw attention to the presence of a Ni_2SiO_4 field in the triple diagram, in which this compound is in equilibrium with the liquid, although

nickel olivine is unstable at the liquidus temperature in the binary system NiO -- SiO₂. In the opinion of the authors, this situation is the only example found up to now in a system of refractory oxides.

BIBLIOGRAPHY

1. Phillips, B., J.J. Hutta, I. Warshaw, J. Amer. Ceram. Soc., 46, No. 12, 579, 1963.

GALLIUM SILICATE SYSTEMS



Orlov [1] has studied the partial profile $3\text{Al}_2\text{O}_3 \cdot 2\text{SiO}_2$ (mullite) -- Ga_2O_3 , by the quenching method.

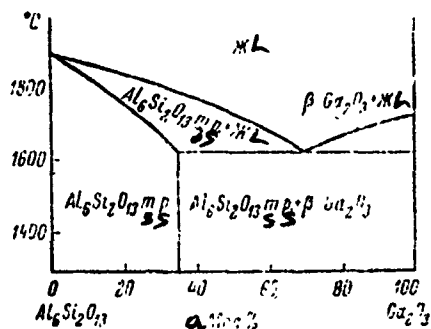


Fig. 205. Phase diagram of partial system
 $3\text{Al}_2\text{O}_3 \cdot 2\text{SiO}_2$ -- Ga_2O_3 (from Orlov).

Key:

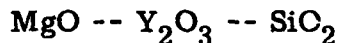
a. Mole %

As a result of X-ray and IR spectroscopic studies, it has been determined that the maximum solubility of gallium oxide in mullite is 35 mole % Ga_2O_3 . A phase diagram of the profile being discussed is presented in Fig. 205. A eutectic containing 70 mole % Ga_2O_3 melts at 1620° . The limiting solid solution has indices of refraction $\text{Ng} = 1.677$ and $\text{Np} = 1.664$; pycnometric density is 3.69 g/cm^3 ; unit cell parameters are $a = 7.632$, $b = 7.749$ and $c = 2.909 \text{ \AA}$.

BIBLIOGRAPHY

1. Orlov, V. A., "Physicochemical study of mullite-like compounds and solid solutions based on them in aluminum-gallium-germanium silicate systems," Author's abstract, candidate's dissertation, Leningrad, 1970.

YTTRIUM SILICATE SYSTEMS

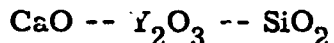


Suwa and colleagues [1] have shown that a region of solid solutions with the apatite structure exists in the system. Synthesis was conducted by repeated annealing (with intermediate grinding) of the appropriate mixtures at a temperature of about 1500° in air. The composition of the solid solution varied from $(\text{Y}_4\text{Mg})\text{Si}_2\text{O}_{13}$ to $(\text{Y}_{3.3}\text{Mg}_{1.3})\text{Si}_{3.4}\text{O}_{13}$.

The hexagonal unit cell of $(\text{Y}_4\text{Mg})\text{Si}_3\text{O}_{13}$ had the parameters $a_0 = 9.298 \pm 0.002$ and $c_0 = 6.635 \pm 0.001$ Å. The indices of refraction of this compound are $\text{Ne} = 1.810 \pm 0.005$ and $\text{No} = 1.820 \pm 0.005$.

BIBLIOGRAPHY

1. Suwa, Y., Sh. Naka, T. Noda, Mater. Res. Bull., 3, No. 2, 139, 1968.



The system has not been studied fully. Toropov and Fedorov [3, 4] have investigated the partial system $\text{Ca}_2\text{SiO}_4 \text{ -- } \text{Y}_4(\text{SiO}_4)_3$ in the range from 1650° to the melting temperature, using the quenching method. Below 1650°, $\text{Y}_4(\text{SiO}_4)_3$

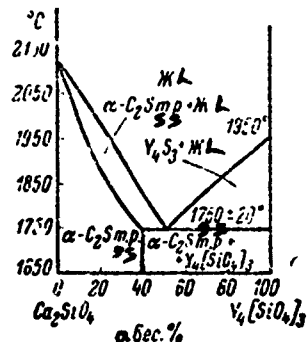


Fig. 206. Phase diagram of partial system
 Ca_2SiO_4 -- $\text{Y}_4(\text{SiO}_4)_3$ (from Toropov and
Fedorov)

Key:

a. Weight %

) undergoes thermal decomposition. The formation of limited Ca_2SiO_4 -base solid solutions was established. The maximum concentration of $\text{Y}_4(\text{SiO}_4)_3$ is 42.5 ± 2.5 weight %. For the limiting solid solution, the indices of refraction are $\text{Ng} = 1.721$ and $\text{Np} = 1.717$; density is 3.52 g/cm^3 .

The phase diagram of the Ca_2SiO_4 -- $\text{Y}_4(\text{SiO}_4)_3$ system presented in Fig. 206 is characterized by a eutectic of the solid solution and yttrium orthosilicate, having a composition of 51 weight % $\text{Y}_4(\text{SiO}_4)_3 + 49$ weight % Ca_2SiO_4 , melting at $1750 \pm 20^\circ$. Compounds of the anorthite type $\text{CaY}_2(\text{SiO}_4)_2$ were not found.

Depending on the composition, the solid solution takes on the structure of one of the three-temperature modifications of dicalcium silicate, α , α'

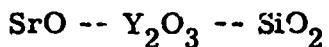
or β . With an yttrium orthosilicate content of up to 5 weight %, the structure of the solid solution corresponds to $\beta\text{Ca}_2\text{SiO}_4$, at a $\text{Y}_4(\text{SiO}_4)_3$ content between 10 and 20 weight %, the X-ray photo corresponds to $\alpha'\text{Ca}_2\text{SiO}_4$ and, finally, the higher content of the dissolved substance, the $\alpha\text{Ca}_2\text{SiO}_4$ structure is present.

Boykova and colleagues [1] have studied solid solutions in the series $3\text{CaO}\cdot\text{SiO}_2$ -- $\text{Y}_2\text{O}_3\cdot\text{SiO}_2$. The maximum concentration of yttrium silicate was 5 weight %.

Sokolov and colleagues obtained the compound $\text{Ca}_{1.5}\text{Y}_3(\text{SiO}_4)_3$, with the apatite structure, and having luminescence properties [2]. This compound, with a melting temperature of 1680° , has indices of refraction $\text{Ng} = 1.809$ and $\text{Np} = 1.806$; the pycnometric density is 3.82 g/cm^3 , the calculated is 3.86 g/cm^3 ; the hexagonal unit cell parameters are $a = 9.39 \pm 0.03$ and $c = 6.79 \pm 0.02 \text{ \AA}$.

BIBLIOGRAPHY

1. Boykova, A. I., N. A. Toropov, V. T. Timofeyeva, G. N. Samsonkina, Yu. G. Sokolov, in the collection Khimiya vysokotemperurnykh materialov [Chemistry of High-Temperature Materials], Nauka Press, Leningrad, 1967, p. 188.
2. Sokolov, A. N., A. A. Kolpakova, L. Ye. Tarasova, N. A. Toropov, Sb. referatov po khimii i tekhnologii lyuminoforov [Collection of Papers on Luminophore Chemistry and Technology], Leningrad, 1969, p. 39.
3. Toropov, N. A., N. F. Fedorov, Zhurn. prikl. khim., 35, 10, 1962, p. 2156.
4. Toropov, N. A., N. F. Fedorov, Zhurn. neorg. khim., 10, 3, 1965, p. 666.



Toropov and Mao Chzhi-tsyun [1, 2] have studied two partial profiles: $\text{Sr}_2(\text{SiO}_4)$ -- $\text{Y}_4(\text{SiO}_4)_3$ and Sr_3SiO_5 -- Y_2SiO_5 . The first pseudobinary system

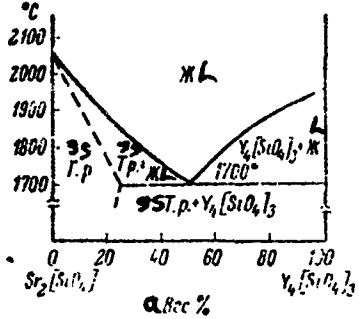


Fig. 207. Phase diagram of partial system $\text{Sr}_2(\text{SiO}_4)$ -- $\text{Y}_4(\text{SiO}_4)_3$ (from Toropov and Mao Chzhi-tsyun).

Key:

a. Weight %

was studied in the 1650-2100° temperature range by the quenching method.

The formation of Sr_2SiO_4 -base solid solutions was established. The limiting solid solution contains 25 weight % $\text{Y}_4(\text{SiO}_4)_3$. The eutectic of these solid solutions and yttrium orthosilicate contains 50.3 weight % (30 mole %) $\text{Y}_4(\text{SiO}_4)_3$, and it melts at 1700° (Fig. 207).

Strontium orthosilicate melts without decomposition at $2060 \pm 50^\circ$.

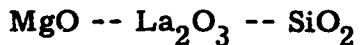
The indices of refraction of pure Sr_2SiO_4 are $\text{Ng} = 1.756 \pm 0.002$ and $\text{Np} = 0.727 \pm 0.002$. With increase in yttrium orthosilicate content in the solid solution, the indices of refraction of the latter increase and reach up to $\text{Ng} = 1.761 \pm 0.002$ and $\text{Np} = 1.737 \pm 0.002$; on the other hand, the density decreases from 4.51 to 4.40 g/cm³.

The pseudobinary system Sr_3SiO_5 -- Y_2SiO_5 has been studied in the region adjacent to strontium silicate, where solid solutions were found. Annealing of compressed samples was carried out at 1400° . The solubility limit of Y_2SiO_5 in Sr_3SiO_5 is 3 weight %. Ternary chemical compounds were not found.

BIBLIOGRAPHY

1. Toropov, N.A., Mao Chzhi-tsuyu, Zhurn. neorg. khim., 7, 7, 1962, p. 1632.
2. Toropov, N.A., Mao Chzhi-tsyun, Izv. AN SSSR, ser. khim., 12, 1963, p. 2079.

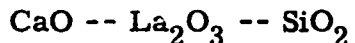
LANTHANIDE-SILICATE SYSTEMS



Toropov and Mao Chzhi-tsyun [1] limited themselves to study of the $\text{Mg}_2(\text{SiO}_4)$ -- $\text{La}_4(\text{SiO}_4)_3$ profile. In this partial system, formation of solid solutions and ternary chemical compounds does not take place. The system is a simple eutectic (the eutectic contains approximately 17 mole % $\text{La}_4(\text{SiO}_4)_3$, and it melts at a little over 1500°).

BIBLIOGRAPHY

1. Toropov, N.A., Mao Chzhi-tsyun, Izv. AN SSSR, ser. khim., 12, 1963, p. 2079.



The system has not been studied. Toropov and Fedorov [2] studied the binary profile Ca_2SiO_4 -- $\text{La}_4(\text{SiO}_4)_3$ by the quenching method, in the range from 1650° to the melting temperature (at 1650°, lanthanum orthosilicate dissociates thermally). One region of solid solutions has been established in the system, with concentrations from 0 to 35 weight % $\text{La}_4(\text{SiO}_4)_3$. The eutectic of the solid

solution and $\text{La}_4(\text{SiO}_4)_3$ contains 57 weight % of the latter, and it melts at $1770 \pm 25^\circ$ (Fig. 208).

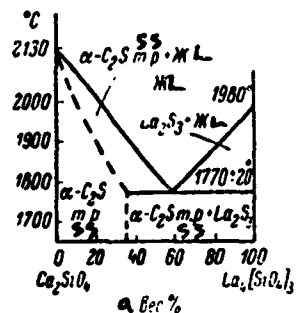


Fig. 208. Phase diagram of partial system Ca_2SiO_4 -- $\text{La}_4(\text{SiO}_4)_3$ (from Toropov and Fedorov).

Key:

a. Weight %

Toropov and Fedorov [3] have shown that, in samples of the solid solution quenched from $1800-1850^\circ$, depending on the lanthanum silicate concentration, various high-temperature forms of dicalcium silicate are stabilized: from 1 to 10 weight % $\text{La}_4(\text{SiO}_4)_3$, the solid solution structure corresponds to the $\beta\text{-Ca}_2\text{SiO}_4$, from 10 to 15 weight % lanthanum silicate, together with lines characteristic of $\beta\text{-Ca}_2\text{SiO}_4$, there are lines corresponding to $\alpha'\text{-Ca}_2\text{SiO}_4$, becoming single ones at 20% lanthanum silicate content. With further concentration increase of the latter, a diffraction image is recorded corresponding to the α modification of Ca_2SiO_4 .

Boykova and colleagues [1] studied a portion of the binary profile $3\text{CaO}\cdot\text{SiO}_2$ -- $\text{La}_2\text{O}_3\cdot\text{SiO}_2$. Annealing of the appropriate mixtures was carried out at 1400-1450°, and fusibility of the system was not studied. $\text{La}_2\text{O}_3\cdot\text{SiO}_2$ forms a solid solution with tricalcium silicate; however, it is difficult to determine the maximum concentration. It apparently is over 5%, since a solid solution with a higher index of refraction was obtained, than that for the solid solution containing 5 weight % $\text{La}_2\text{O}_3\cdot\text{SiO}_2$, namely, 1.732 vs. 1.72.

The authors note that, in formation of the solid solutions, an increase in amount of CaO above the stoichiometric 3:1 also takes place. The excess CaO in the solid solution reaches 3-4 weight %. Formation of Ca_2SiO_4 (in the β and γ forms) was observed simultaneously.

BIBLIOGRAPHY

1. Boykova, A. I., N. A. Toropov, A. K. Kuznetsov, DAN SSSR, 156, 4, 1964, p. 865.
2. Toropov, N. A., N. F. Fedorov, Zhurn. prikl. khim., 35, 11, 1962, p. 2548.
3. Toropov, N. A., N. F. Fedorov, Izv. AN SSSR, Neorg. mater., 1, 1, 1965, p. 126.

$\text{SrO} \text{ -- } \text{La}_2\text{O}_3 \text{ -- } \text{SiO}_2$

Toropov and Mao Chzhi-tsyun [1, 2] have studied two binary profiles: Sr_2SiO_4 -- $\text{La}_4(\text{SiO}_4)_3$ and Sr_3SiO_5 -- La_2SiO_5 . The first partial system was studied by the quenching method in the 1600-2100° range, i.e., in the stability region of $\text{La}_4(\text{SiO}_4)_3$. Solid solutions form only on the strontium orthosilicate side, in which the solubility limit of $\text{La}_4(\text{SiO}_4)_3$ is 20 weight %. The partial system studied is of the eutectic type, with limited solid solutions. The eutectic

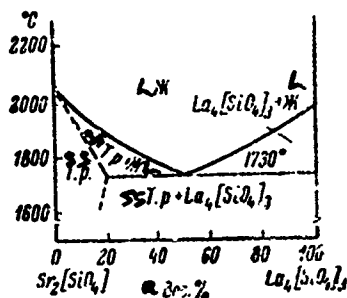


Fig. 209. Phase diagram of partial system $\text{Sr}_2(\text{SiO}_4)$ -- $\text{La}_4(\text{SiO}_4)_3$ (from Toropov and Mao Chzhi-tsyun).

Key:

a. Weight %

contains 50.9 weight % (25 mole %) $\text{La}_4(\text{SiO}_4)_3$, and it melts at a temperature of 1730° (Fig. 209). The indices of refraction of the solid solution increase with increase in $\text{La}_4(\text{SiO}_4)_3$ content, reaching up to $N_g = 1.765 \pm 0.002$ and $N_p = 1.737 \pm 0.002$ at a 15 weight % lanthanum silicate content, solid solution densities increase to 4.57 g/cm^3 , in this case. A solid solution can be obtained, not only by crystallization from a melt, but as a result of solid-phase reactions, by means of annealing at 1400° for a period of 5 hours.

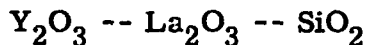
The partial system Sr_3SiO_5 -- La_2SiO_5 has been studied in the concentration range from 0 to 50 weight %, in samples annealed at 1400°. The limiting solid solution contains 10 weight % La_2SiO_5 .

Schwarz [3] synthesized ternary compounds with apatite structure, having some regions of homogeneity.

For the compound $\text{Sr}_{3-y}\text{La}_6 + 2y/3(\text{SiO}_4)_6$, y can change from +1 to -1; for $\text{Sr}_{4-y}\text{La}_6 + 2y/3(\text{SiO}_4)_6\text{O}$, $4 \geq y \geq 0$ and, for $\text{Sr}_{2-y}\text{La}_8 + 2y/3(\text{SiO}_4)_6\text{O}$, $2 \geq y \geq 0$.

BIBLIOGRAPHY

1. Toropov, N. A., Mao Chzhi-tsyun, Zhurn. neorg. khim., 7, 7, 1962, p. 1632.
2. Toropov, N. A., Mao Chzhi-tsyun, Izv. AN SSSR, ser. khim., 12, 1963, p. 2079.
3. Schwarz, H., Angewand. Chem., 79, No. 12, 584, 1967.



Toropov and Gurudas Mandal [1] have studied the $\text{Y}_2\text{O}_3 \cdot 2\text{SiO}_2 \text{ -- } \text{La}_2\text{O}_3 \cdot 2\text{SiO}_2$ diorthosilicate profile by the quenching method. The corresponding phase diagram is presented in Fig. 210. The diagram is of the type characterized by the presence of only limited mutual solubility in the system, which apparently is connected with difference in structures of the yttrium and lanthanum diorthosilicates. The region of coexistence of mixtures of the two solid solutions occupies a considerable portion of the diagram.

The compounds $\text{Y}_2\text{O}_3 \cdot 2\text{SiO}_2$ and $\text{La}_2\text{O}_3 \cdot 2\text{SiO}_2$ melt incongruently at 1775 and 1750°, respectively, with decomposition into liquid and $2\text{Y}_2\text{O}_3 \cdot 3\text{SiO}_2$ and $2\text{La}_2\text{O}_3 \cdot 3\text{SiO}_2$ orthosilicates, the presence of which is noted on the diagram.

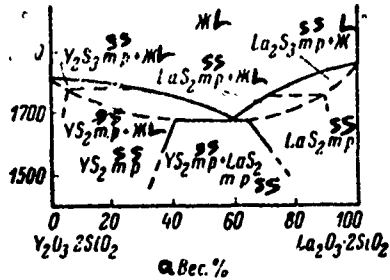


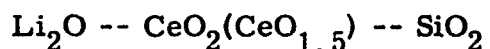
Fig. 210. Phase diagram of partial system $\text{Y}_2\text{Si}_2\text{O}_7$ -- $\text{La}_2\text{Si}_2\text{O}_7$ (from Toropov and Gurudas Mandal).

Key:

a. Weight %

BIBLIOGRAPHY

1. Toropov, N.A., Gurudas Mandal, DAN SSSR, 156, 5, 1964, p. 1127.

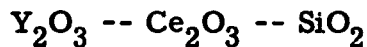


Bayer and colleagues [1] have studied the crystallization of glasses, the content of which included 10-40 mole % Li_2O , 5-15 mole % CeO_2 and 55-80 mole % SiO_2 , in an atmosphere of air. They also have studied the solid-phase reactions in inert, reducing and oxidizing atmospheres. Trivalent cerium, in the presence of SiO_2 , appeared even in an oxidizing atmosphere at 1400°. Ternary compounds (in particular, the conjectural LiCeSiO_4) were not found.

Besides SiO_2 , CeO_2 and lithium silicates, there was only the disilicate of trivalent cerium $\text{Ce}_2\text{Si}_2\text{O}_7$, with a large crystallization field, in the crystalline phases. Liquation was discovered with increase in CeO_2 and SiO_2 content.

BIBLIOGRAPHY

1. Bayer, G., J. Felsche, H. Hirsiger, Glastechn. Ber., 42, No. 8, 317, 1969.



Toropov and colleagues [2] have studied the partial system $\text{Y}_2\text{Si}_2\text{O}_7$ -- $\text{Ce}_2\text{Si}_2\text{O}_7$, using the quenching method and solid-phase syntheses from high temperatures in an argon environment. Four regions of homogeneity were found (Fig. 211): α and β solid solutions, based on the high-temperature and low-temperature modifications of $\text{Y}_2\text{Si}_2\text{O}_7$, solid solutions with the structure of $\text{Ce}_2\text{Si}_2\text{O}_7$ and the δ solid solution with a structure characteristic of di-orthosilicates of the rare earth elements of the first subgroup.

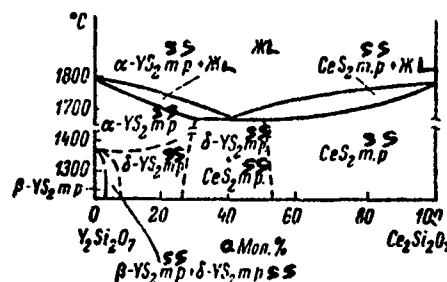


Fig. 211. Phase diagram of partial system $\text{Y}_2\text{Si}_2\text{O}_7$ -- $\text{Ce}_2\text{Si}_2\text{O}_7$ (from Toropov and colleagues).

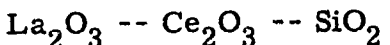
Key:

a. Mole %

Ito [3], under certain conditions (at increased temperatures), obtained four modifications of $Y_2Si_2O_7$, with transformation temperatures of 1225, 1445 and 1525°, which may be connected with hysteresis and differing degrees of purity of the materials used. Bondar' and colleagues [1] have studied the luminescence properties of the solid solutions described above.

BIBLIOGRAPHY

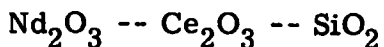
1. Bondar', I. A., A. A. Kolpakova, L. Ya. Markovskiy, A. N. Sokolov, N. A. Toropov, Izv. AN SSSR ser. fiz., 33, 6, 1969, p. 1057.
2. Toropov, N. A., I. F. Andreyev, A. N. Sokolov, L. N. Sanzharevskaya, Izv. AN SSSR, Neorg. mater., 6, 4, 1970, p. 427.
3. Ito, J., Amer. Mineralogist, 53, No. 11-12, 1968.



Leonov [1, 2] has studied the partial profile $La_2Si_2O_7$ -- $Ce_2Si_2O_7$, in which a continuous series of solid solutions is observed in a reducing atmosphere. In air, upon heating in the temperature range from 1000 to 1300°, solid solutions containing over 50 mole % $Ce_2Si_2O_7$ decompose: oxidation of cerium and formation of CeO_2 and SiO_2 take place. However, at higher temperatures, from 1400 to 1500°, regeneration of these solid solutions takes place, since cerium is reduced here to the trivalent state. By heating the initial solid solutions (obtained under reducing conditions), containing 75, 80 and 90 mole % $Ce_2Si_2O_7$, up to a temperature of about 1300° in air, 16, 25 and 58 mole % of the Ce_2SiO_7 , respectively, decomposes. With a 50 mole % $Ce_2Si_2O_7$ content and less, the solid solution is stable in air at all temperatures (up to 1600°).

BIBLIOGRAPHY

1. Leonov, A.I., Izv. AN SSSR, ser. khim., 12, 1963, p. 2084.
2. Leonov, A.I., in the collection Silikaty i okisly v khimii vysokikh temperatur [Silicates and Oxides in High-Temperature Chemistry], Vses. khim. obshch. im. D.I. Mendeleyeva Press, Moscow, 1963, p. 95.

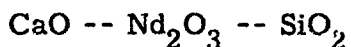


Leonov [1] has studied the partial profile $\text{Nd}_2\text{Si}_2\text{O}_7 \text{ -- Ce}_2\text{Si}_2\text{O}_7$. Under a reducing atmosphere, a continuous series of solid solutions is observed and the color of the samples changes from white ($\text{Ce}_2\text{Si}_2\text{O}_7$) to light lilac ($\text{Nd}_2\text{Si}_2\text{O}_7$). In an atmosphere of air, these solid solutions are stable only in the high temperature region (above 1300-1400°). With a $\text{Ce}_2\text{Si}_2\text{O}_7$ content of less than 25 mole %, the solid solution is stable at all temperatures (up to 1600°).

In decomposition of the solid solutions, oxidation of cerium and formation of free CeO_2 and SiO_2 take place. The solid solution corresponding to the composition $\text{Ce}_{0.75}\text{Nd}_{0.25}\text{Si}_2\text{O}_7$ undergoes the maximum decomposition at 1250-1300° (38 mole % $\text{Ce}_2\text{Si}_2\text{O}_7$ decomposes). In the solid solution of equimolecular content, under the conditions specified, 3% of the cerium diorthosilicate overall decomposes.

BIBLIOGRAPHY

1. Leonov., A.I., Izv. AN SSSR, ser. khim., 12, 1963, p. 2084.



The system has not been studied. Toropov and Fedorov [1] have investigated the binary profile $\text{Ca}_2\text{SiO}_4 \text{ -- Nd}_4(\text{SiO}_4)_3$, using the quenching method, in the range from 1650° to the melting temperature (below 1650°, neodymium

orthosilicate is unstable). A solid solution forms only on a base of Ca_2SiO_4 , and the diagram corresponds to a system of the simple eutectic type, with a eutectic of the solid solutions and neodymium orthosilicate (Fig. 212). The maximum concentration of the solid solution is 40 ± 2.5 weight % $\text{Nd}_4(\text{SiO}_4)_3$. The eutectic corresponds to a composition of 55 weight % neodymium silicate. The ternary compound $\text{CaNd}_2(\text{SiO}_4)_2$, indicated by Tromel [4], was not found by the authors.

Toropov and Fedorov [2] have shown that three different phases are found in the solid solution studied, corresponding to the β , α' and α Ca_2SiO_4 , according to their X-ray photos. With from 0 to 5 weight % $\text{Nd}_4(\text{SiO}_4)_3$ content, the solid solution has the β Ca_2SiO_4 structure, at concentrations from 17 to 25 weight % neodymium orthosilicate, the structure corresponds to α' Ca_2SiO_4 and, in the range from 30 to 40 weight % $\text{Nd}_4(\text{SiO}_4)_3$, the structure corresponds to α Ca_2SiO_4 . A mixture of structures is found in some concentration sections. The density and indices of refraction of the solid solutions also reflect their structural changes. In the transition of the solid solution from the β Ca_2SiO_4 structure to the structure of the α' form, an increase in density and a sharp decrease in birefringence are observed. The transformation of the α' solid solution to the α modification structure is accompanied by a decrease in both density and refraction.

Refraction, density, molecular refraction and melting temperatures of solid solutions of $\text{Nd}_4(\text{SiO}_4)_3$ in calcium orthosilicate are presented in the Table.

Tunik [3] has shown that, in the partial sys. m CaSiO_3 -- Nd_2SiO_5 , there is a chemical compound with the apatite structure, having a certain region of

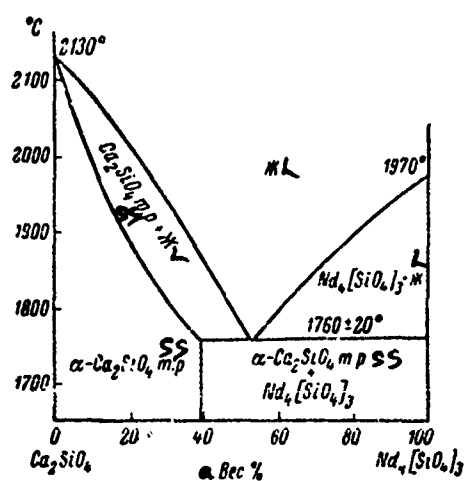


Fig. 212. Phase diagram of partial system Ca_2SiO_4 -- $\text{Nd}_4(\text{SiO}_4)_3$ (from Toropov and Fedorov).

Key: a. Weight %

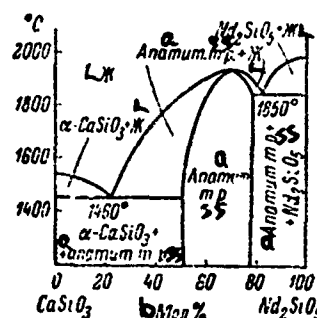


Fig. 213. Phase diagram of partial system CaSiO_3 -- Nd_2SiO_5 (from Tunik).

Key:

- a. Apatite
- b. Mole %

INDICES OF REFRACTION, DENSITY, MOLECULAR
REFRACTION (R) AND MELTING TEMPERATURES
OF SOLID SOLUTIONS OF NEODYMIUM ORTHOSILICATE
IN CALCIUM SILICATE

a Состав, вес. %		b Температура плавления, °C	c Плотность, g/cm³	Ng	Np	R, cm³
Ca ₂ SiO ₅	Nd ₂ SiO ₅					
95	5	2100±50	3.29±0.01	1.734±0.002	1.720±0.002	20.83
90	10	2070	3.31	1.736	1.722	20.72
85	15	2050	3.36	1.738	1.726	20.52
80	20	2000	3.48	1.736	1.731	19.91
75	25	1960	3.51	1.736	1.730	19.64
70	30	1920	3.56	1.731	1.728	19.33
65	35	1870	3.55	1.731	1.727	19.26
60	40	1830	3.70	1.736	1.730	18.59
55	45	1800	—	—	—	—

Key:

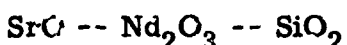
- a. Composition, weight %
- b. Melting temperature, °C
- c. Density, g/cm³

uniformity: CaNd₄(SiO₄)₃O (Fig. 213). The uniformity region extends from 50 to 78 mole % Nd₂SiO₅. The index of refraction in this case changes from Ne = 1.851 and N₂ = 1.861 to Ne = 1.866 and N₂ = 1.885. The maximum melting temperature is located at a certain concentration distance from the formula presented above, which is typical of oxyapatite.

BIBLIOGRAPHY

1. Toropov, N.A., N.F. Fedorov, Zhurn. neorg. khim., 9, 1, 1964, p. 156.
2. Toropov, N.A., N.F. Fedorov, Izv. AN SSSR, Neorg. mater., 1, 1, 1965, p. 126.

3. Tunik, T.A., "Study of phase equilibrium in silicate systems containing oxides of neodymium and alkali earth elements (Mg, Ca, Sr, Ba)," author's abstract, candidate's dissertation, Leningrad, 1970.
4. Trömel, G., Verh. K. Wilhelm Inst. Silikatforschung, 3, Berlin, 103, 1930.



Toropov and Mac Chzhi-tsyun [1, 2] have studied two binary profiles of the system: $\text{Sr}_2\text{SiO}_4 \text{ -- Nd}_4(\text{SiO}_4)_3$ and $\text{Sr}_3\text{SiO}_5 \text{ -- Nd}_2\text{SiO}_5$. The first system was studied by the quenching method in the 1650-2100° range, i.e., in the $\text{Nd}_2(\text{SiO}_4)_3$ stability region. A limited region of Sr_2SiO_4 -base solid solutions was found, with a limiting concentration of 20 weight % $\text{Nd}_4(\text{SiO}_4)_3$. The eutectic melted at 1750° and contained 51 weight % (24.2 mole %) $\text{Nd}_4(\text{SiO}_4)_3$. The indices of refraction and density increased with increase in $\text{Nd}_4(\text{SiO}_4)_3$ content in the solid solution. At a concentration of 15 weight % $\text{Nd}_4(\text{SiO}_4)_3$, $\text{Ng} = 1.66 \pm 0.002$ and $\text{Np} = 1.739 \pm 0.002$; the density is 4.58 g/cm^3 . The solid solutions described can be obtained as a result of solid-phase reactions, by means of annealing the appropriate mixtures at 1400°, with 5-hour exposure.

The partial system $\text{Sr}_3\text{SiO}_5 \text{ -- Nd}_2\text{SiO}_5$ has been studied only in the subsolidus region (annealing at 1400°, 5 hours), with Nd_2SiO_5 concentrations from 0 to 50 weight %. The maximum content of the Sr_3SiO_5 -base solid solution formed is 10 weight % Nd_2SiO_5 .

Tunik [3] has studied the partial binary system $\text{SrSiO}_3 \text{ -- Nd}_2\text{SiO}_5$. Here, a compound with the apatite structure $(\text{SrNd}_4(\text{SiO}_4)_3)\text{O}$ has been found, having a considerable region of uniformity (Fig. 214). The apatite-like phase extends from a composition containing 50 mole % Nd_2SiO_5 (the remainder is SrSiO_3)

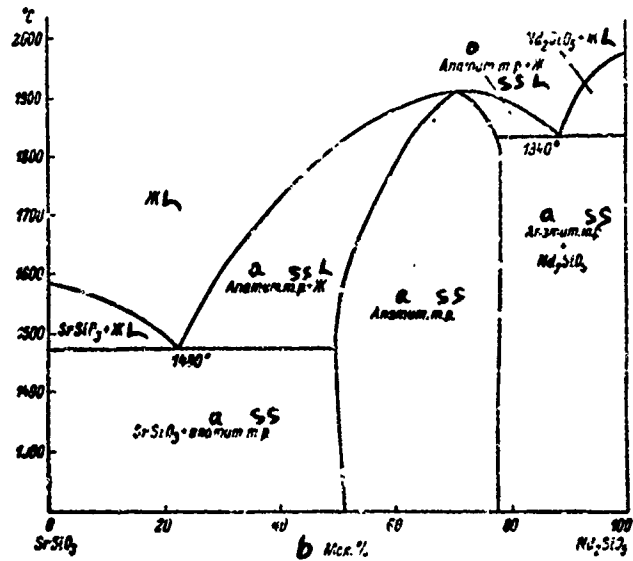


Fig. 214. Phase diagram of partial system SrSiO_3 -- Nd_2SiO_5 (from Tunik).

Key:

- a. Apatite
- b. Mole %

to 78 mole % Nd_2SiO_5 . The indices of refraction in this case change from $\text{No} = 1.854$ and $\text{Ne} = 1.844$ to $\text{No} = 1.883$ and $\text{Ne} = 1.864$. The maximum melting temperature is located at a certain concentration distance from the formula presented above, which is typical of oxyapatite. The region of apatite solid solutions is evident from Fig. 215.

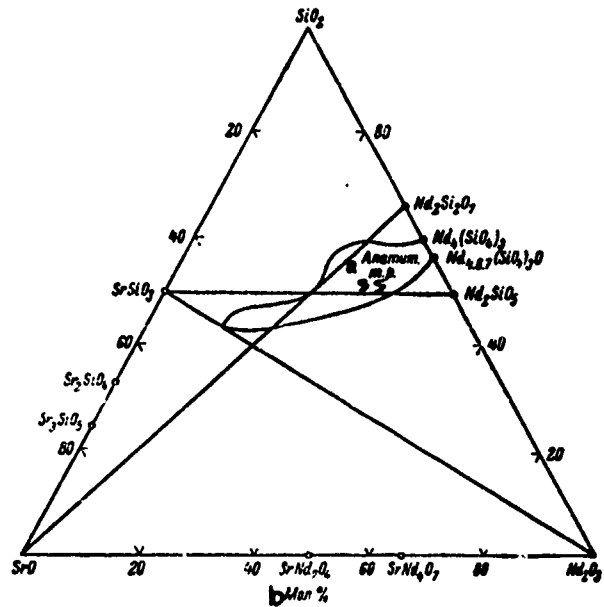


Fig. 215. Region of apatite solid solutions in $\text{SrO} - \text{Nd}_2\text{O}_3 - \text{SiO}_2$ system (from Tunik).

Key:

- a. Apatite
- b. Mole %

BIBLIOGRAPHY

1. Toropov, N.A., *Mao Chzhi-tsyn*, *Zhurn. neorg. khim.*, 7, 7, 1962, p. 1632.
2. Toropov, N.A., *Mao Chzhi-tsyn*, *Izv. AN SSSR, ser. khim.*, 12, 1963, p. 2079.
3. Tunik, T.A., "Study of phase equilibria in silicate systems containing oxides of neodymium and alkali earth elements (Mg, Ca, Sr, Ba)," author's abstract, candidates dissertation, Leningrad, 1970.

La_2O_3 -- Sm_2O_3 -- SiO_2

The system has been studied by Bondar' and colleagues [1, 2], for the purpose of ascertaining the formation of solid solutions in the systems La_2O_3 -- 2SiO_2 -- $\text{Sm}_2\text{O}_3 \cdot 2\text{SiO}_2$, $2\text{La}_2\text{O}_3 \cdot 3\text{SiO}_2$ -- $2\text{Sm}_2\text{O}_3 \cdot 3\text{SiO}_2$ and $\text{La}_2\text{O}_3 \cdot \text{SiO}_2$ -- $\text{Sm}_2\text{O}_3 \cdot \text{SiO}_2$. Phase diagrams of the systems formed by lanthanum and samarium silicates, characterized by the formation of continuous solid solutions, are presented in Figs 216 and 217. The appearance of solid solutions of the 2:3 series in Fig. 216 is connected with the fact that lanthanum and samarium diorthosilicates melt, with decomposition into the orthosilicates ($2\text{Ln}_2\text{O}_3 \cdot 3\text{SiO}_2$) and liquid, and that an invariant line dividing the 2:3 and 1:2 crystallization fields should exist on the polythermic profile.

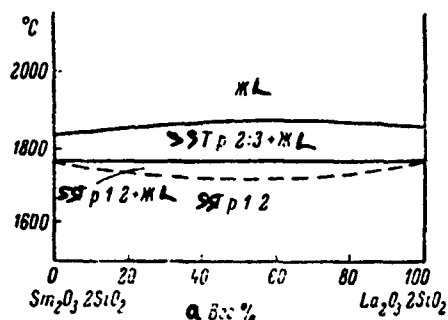


Fig. 216. Phase diagram of partial system $\text{Sm}_2\text{O}_3 \cdot 2\text{SiO}_2$ -- $\text{La}_2\text{O}_3 \cdot 2\text{SiO}_2$ (from Bondar' and colleagues).

Key:

a. Weight %

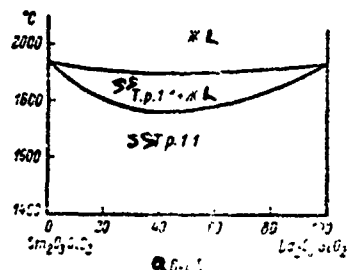


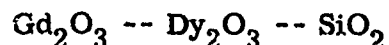
Fig. 217. Phase diagram of partial system $\text{Sm}_2\text{O}_3 \cdot \text{SiO}_2$ -- $\text{La}_2\text{O}_3 \cdot \text{SiO}_2$ (from Bondar' and colleagues)

Key:

a. Weight %

BIBLIOGRAPHY

1. Bondar', I. A., F. Ya. Gaiakhov, N. A. Toropov, Izv. AN SSSR, OKhN, 3, 1962, p. 377.
2. Bondar', I. A., N. A. Toropov, L. N. Koroleva, in the collection Khimiya vysokotemperaturnykh materialov [Chemistry of High-Temperature Materials], Nauka Press, Leningrad, 1967, p. 25.



Bondar' and colleagues [1] have studied the phase diagram of three binary profiles: $\text{Gd}_2\text{O}_3 \cdot 2\text{SiO}_2 \text{ -- } \text{Dy}_2\text{O}_3 \cdot 2\text{SiO}_2$, $2\text{Gd}_2\text{O}_3 \cdot 3\text{SiO}_2 \text{ -- } 2\text{Dy}_2\text{O}_3 \cdot 3\text{SiO}_2$ and $\text{Gd}_2\text{O}_3 \cdot \text{SiO}_2 \text{ -- } \text{Dy}_2\text{O}_3 \cdot \text{SiO}_2$. The formation of continuous solid solutions is characteristic of these three partial systems.

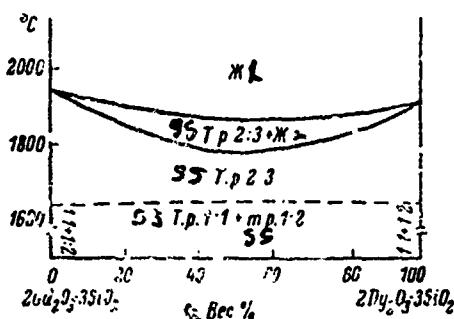


Fig. 218. Phase diagram of partial system $2\text{Gd}_2\text{O}_3 \cdot 3\text{SiO}_2 \text{ -- } 2\text{Dy}_2\text{O}_3 \cdot 3\text{SiO}_2$ (from Bondar' and colleagues).

Key:

a. Weight %

A phase diagram of the pseudobinary system $2\text{Gd}_2\text{O}_3 \cdot 3\text{SiO}_2$ -- $2\text{Dy}_2\text{O}_3 \cdot 3\text{SiO}_2$ is presented in Fig. 218. The compounds $2\text{Gd}_2\text{O}_3 \cdot 3\text{SiO}_2$ and $2\text{Dy}_2\text{O}_3 \cdot 3\text{SiO}_2$ are stable above 1630 and 1650° , respectively, decomposing into a mixture of orthosilicates (1:1) and diorthosilicates (1:2) below these temperatures. This is reflected in the diagram.

PUBLIOGRAPHY

1. Bondar', I. A., F. Ya. Galakhov, N. A. Toropov, Izv. AN SSSR, OKhN, 3, 1952, p. 377.

Y_2O_3 -- Er_2O_3 -- SiO_2

Galakhov and colleagues [1] have plotted a phase diagram of the three binary profiles: $\text{Y}_2\text{O}_3 \cdot \text{SiO}_2$ -- $\text{Er}_2\text{O}_3 \cdot \text{SiO}_2$, $\text{Y}_2\text{O}_3 \cdot 2\text{SiO}_2$ -- $\text{Er}_2\text{O}_3 \cdot 2\text{SiO}_2$, $2\text{Y}_2\text{O}_3 \cdot 3\text{SiO}_2$ -- $2\text{Er}_2\text{O}_3 \cdot 3\text{SiO}_2$. The formation of limited solid solutions is characteristic of the $\text{Y}_2\text{O}_3 \cdot 2\text{SiO}_2$ -- $\text{Er}_2\text{O}_3 \cdot 2\text{SiO}_2$ and $2\text{Y}_2\text{O}_3 \cdot 3\text{SiO}_2$ -- $2\text{Er}_2\text{O}_3 \cdot 3\text{SiO}_2$ systems (Figs. 219, 220). Continuous solid solutions form in the $\text{Y}_2\text{O}_3 \cdot \text{SiO}_2$ -- $\text{Er}_2\text{O}_3 \cdot \text{SiO}_2$ system (Fig. 221). The compound $\text{Y}_2\text{O}_3 \cdot 2\text{SiO}_2$ melts at 1775° , with decomposition, forming $2\text{Y}_2\text{O}_3 \cdot 3\text{SiO}_2$ and liquid, which is reflected in the appearance of the $2\text{Y}_2\text{O}_3 \cdot 3\text{SiO}_2$ solid solution field (mixed with liquid) in Fig. 219.

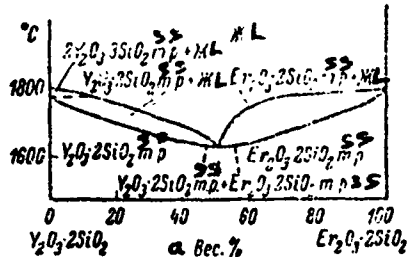


Fig. 219. Phase diagram of partial system $\text{Y}_2\text{O}_3 \cdot 2\text{SiO}_2$ -- $\text{Er}_2\text{O}_3 \cdot 2\text{SiO}_2$ (from Galakov and colleagues).
Key: a. weight %

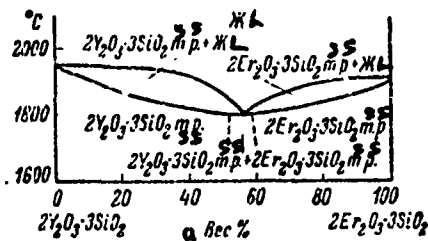


Fig. 220. Phase diagram of partial system
 $2\text{Y}_2\text{O}_3 \cdot 3\text{SiO}_2$ -- $2\text{Er}_2\text{O}_3 \cdot 3\text{SiO}_2$ (from Galakhov and colleagues).

Key:

a. Weight %

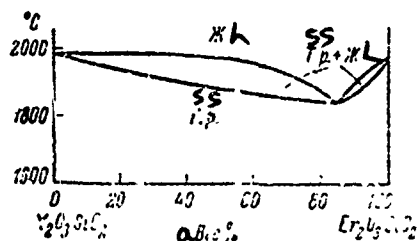


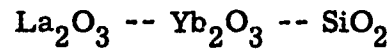
Fig. 221. Phase diagram of partial system
 $\text{Y}_2\text{O}_3 \cdot \text{SiO}_2$ -- $\text{Er}_2\text{O}_3 \cdot \text{SiO}_2$ (from Galakhov and colleagues).

Key:

a. Weight %

BIBLIOGRAPHY

1. Galakhov, F. Ya., N. A. Toropov, S. F. Konovalova, Izv. AN SSSR, OKhN, 5, 1962, p. 738.



Bondar' [1] has studied the system, for the purpose of ascertaining the formation of solid solutions in the systems: $\text{La}_2\text{O}_3 \cdot 2\text{SiO}_2$ -- $\text{Yb}_2\text{O}_3 \cdot 2\text{SiO}_2$, $2\text{La}_2\text{O}_3 \cdot 3\text{SiO}_2$ -- $2\text{Yb}_2\text{O}_3 \cdot 3\text{SiO}_2$, $\text{La}_2\text{O}_3 \cdot \text{SiO}_2$ -- $\text{Yb}_2\text{O}_3 \cdot \text{SiO}_2$. Phase diagrams of the $\text{La}_2\text{O}_3 \cdot 2\text{SiO}_2$ -- $\text{Yb}_2\text{O}_3 \cdot 2\text{SiO}_2$ and $\text{La}_2\text{O}_3 \cdot \text{SiO}_2$ -- $\text{Yb}_2\text{O}_3 \cdot \text{SiO}_2$ systems are presented in Figs. 222 and 223. Lanthanum and ytterbium are in different subgroups, and they form solid solutions of limited concentrations. These systems belong to the fifth type of solid solutions according to Roseboom. $\text{La}_2\text{O}_3 \cdot 2\text{SiO}_2$ melts at 1750° , with decomposition into $2\text{La}_2\text{O}_3 \cdot 3\text{SiO}_2$ and liquid.

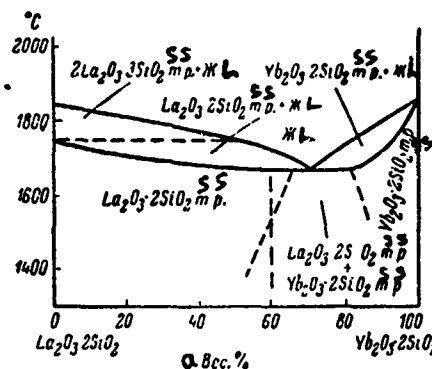


Fig. 222. Phase diagram of partial system
 $\text{La}_2\text{O}_3 \cdot 2\text{SiO}_2$ -- $\text{Yb}_2\text{O}_3 \cdot 2\text{SiO}_2$ (from Bondar').

Key:

a. Weight %

Bondar' has examined the process of dispersion hardening, which takes place during decomposition of supersaturated solid solutions formed by lanthanum and ytterbium silicates [2].

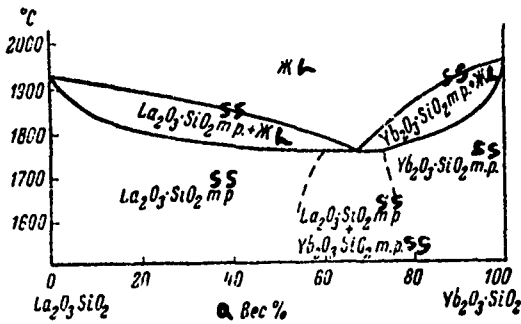


Fig. 223. Phase diagram of partial system $\text{La}_2\text{O}_3 \cdot \text{SiO}_2$ -- $\text{Yb}_2\text{O}_3 \cdot \text{SiO}_2$ (from Bondar').

Key:

a. Weight %

1. Bondar', I. A., Izv. AN SSSR, OKhN, 3, 1962, p. 383.
2. Bondar', I. A., Izv. AN USSR, ser. khim, 11, 1964, p. 2110.

$\text{CoO} \text{ -- } \text{Yb}_2\text{O}_3 \text{ -- } \text{SiO}_2$

The system has been partially studied by Babayev [1, 2], limited to determination of the phase ratios of the Co_2SiO_4 -- $\text{Yb}_4(\text{SiO}_4)_3$ profile. The complex appearance of the diagram presented in Fig. 224 is due to two reasons: 1. a restricted region of stability of ytterbium orthosilicate $\text{Yb}_4(\text{SiO}_4)_3$ (above 1675°); 2. occurrence of the reaction $\text{Co}_2\text{SiO}_4 + \text{Yb}_4(\text{SiO}_4)_3 = 2\text{CoO} + 2\text{Yb}_2\text{Si}_2\text{O}_7$.

Ternary compounds (of the garnet type, for example) have not been found in the system. Ytterbium occurs in the subsolidus region only in the form of $\text{Yb}_2\text{Si}_2\text{O}_7$ (region with Co_2SiO_4 content over 20 weight %) or in the form of a mixture of $\text{Yb}_2\text{Si}_2\text{O}_7$ and $\text{Yb}_4(\text{SiO}_4)_3$ (with a Co_2SiO_4 content less than 20 weight %). The existence of $\text{Yb}_4(\text{SiO}_4)_3$ in this region apparently is connected

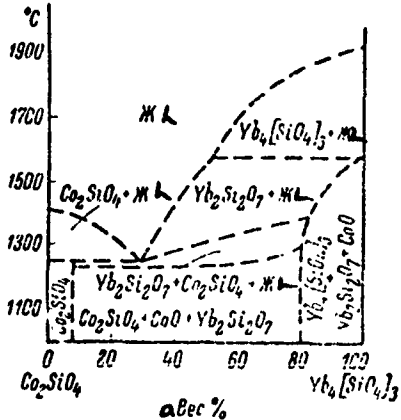


Fig. 224. Phase diagram of partial system
 Co_2SiO_4 -- $\text{Yb}_4(\text{SiO}_4)_3$ (from Babayan).

Key:

a. Weight %

with a stabilizing effect of Co_2SiO_4 , possibly forming a solid solution of low concentration.

In the presence of cobalt silicate, the stability boundary of $\text{Yb}_4(\text{SiO}_4)_3$ is shifted to a temperature of 1600° (for pure $\text{Yb}_4(\text{SiO}_4)_3$, this temperature equals 1675°). Some Co_2SiO_4 -base solid solution region is formed, with a concentration of $\text{Yb}_4(\text{SiO}_4)_3$ of somewhat over 6 weight %.

Cobalt orthosilicate forms dark violet crystals, in the rhombic crystal system, with a melting temperature of $1400 \pm 20^\circ$ and density of 4.7 g/cm^3 [2].

BIBLIOGRAPHY

1. Babayan, S.A., Izv. AN Arm. SSR, OKhN, 18, 5, 1965, p. 529.
2. Toropov, N.A., S.A. Babayan, Zhurn. neorg. khim., 11, 2, 1966, p. 28.

$\text{NiO} \text{ -- } \text{Yb}_2\text{O}_3 \text{ -- } \text{SiO}_2$

Babayan [1, 2] has studied the phase ratios of the Ni_2SiO_4 -- $\text{Yb}_4(\text{SiO}_4)_3$ orthosilicate profile. Because of dissociation of Ni_2SiO_4 at 1550° (even before melting) and the limited stability of $\text{Yb}_4(\text{SiO}_4)_3$ from 1675° to the melting point 1920° , in addition to the initial orthosilicates, NiO and $\text{Yb}_2\text{Si}_2\text{O}_7$ figure in the diagram presented (Fig. 225). The latter substance is formed by the reaction $\text{Yb}_4(\text{SiO}_4)_3 + \text{Ni}_2\text{SiO}_4 = 2\text{NiO} + 2\text{Yb}_2\text{Si}_2\text{O}_7$.

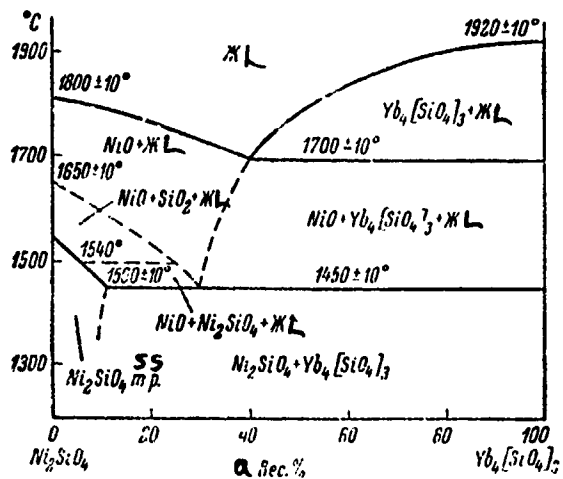


Fig. 225. Phase diagram of partial system
 $\text{Ni}_2\text{SiO}_4 \text{ -- } \text{Yb}_4(\text{SiO}_4)_3$ (from Babayan).
 Key: a. Weight %

Depending on the Ni_2SiO_4 content, either only $\text{Yb}_2\text{Si}_2\text{O}_7$ (with greater than 20 weight % Ni_2SiO_4 content) or $\text{Yb}_2\text{Si}_2\text{O}_7$, together with $\text{Yb}_4(\text{SiO}_4)_3$ (with a content of less than 20 weight % Ni_2SiO_4) is present in the subsolidus region. The existence of $\text{Yb}_4(\text{SiO}_4)_3$ in this temperature region probably is connected with a stabilizing effect of Ni_2SiO_4 , forming a solid solution with

$\text{Yb}_4(\text{SiO}_4)_3$ at low concentration. The thermal decomposition temperature of ytterbium orthosilicate decreases to 1600° in the presence of Ni_2SiO_4 . A small region of Ni_2SiO_4 -base solid solutions forms (somewhat over 6 weight % $\text{Yb}_4(\text{SiO}_4)_3$).

Nickel orthosilicate, obtained by sintering at 1400°, forms light green crystals in the rhombic crystal system, with indices of refraction $\text{Ng} = 1.99$ and $\text{Np} = 1.94$, unit cell parameters $a = 4.724$, $b = 10.105$ and $c = 5.928 \text{ \AA}$ and density 4.72 g/cm^3 . At a temperature somewhat exceeding 1500°, nickel silicate in the solid state dissociates into NiO and SiO_2 .

BIBLIOGRAPHY

1. Babayan, S.A., Izv. AN Arin. SSR, OKhN, 18, 6, 1966, p. 612.
2. Toropov, N.A., S. A. Babayan, Zhurn. neorg. khim., 11, 1, 1966, p. 28.

GERMANIUM SILICATE SYSTEMS



Lazarev and Tenisheva [1] have shown that there is continuous series of solid solutions in the Li_2SiO_3 -- Li_2GeO_3 partial profile. Synthesis of uniform solid solutions was carried out at 1250-1350°. The indices of refraction of the solid solutions change linearly with composition.

Völlenkle and colleagues [2] have studied the $\text{Li}_2\text{Si}_2\text{O}_5$ -- $\text{Si}_2\text{Ge}_2\text{O}_5$ partial profile, demonstrating the presence of a continuous series of solid solutions. The unit cell parameters change from $a = 5.81$, $b = 14.66$ and $c = 4.79$ Å (for $\text{Li}_2\text{Si}_2\text{O}_5$) to $a = 5.97$, $b = 15.30$ and $c = 4.95$ Å (for $\text{Li}_2\text{Ge}_2\text{O}_5$).

At temperatures above the region of existence of continuous solid solutions, the compound $\text{Li}_2(\text{Si}_{0.25}\text{Ge}_{0.75})_2\text{O}_5$ was obtained, with a broad region of homogeneity and unit cell parameters, differing from the corresponding values for the solid solution of the same composition.

BIBLIOGRAPHY

1. Lazarev, A. N., T. F. Tenisheva, Optika i spektroskopiya, 13, 5, 1962, p. 708.
2. Völlenkle, H., A. Wittmann, H. Nowotny, Zs. Kristallogr., 126, 1-5, 37, 1968.

$\text{MgO} \text{-- } \text{GeO}_2 \text{-- } \text{SiO}_2$

Dachille and Roy [1] have studied the partial system $\text{Mg}_2\text{GeO} \text{-- } \text{Mg}_2\text{SiO}_4$ at various pressures up to 580,000 psi.

Magnesium orthogermanate exists in the form of spinel and olivine modifications, with the inversion temperature at atmospheric pressure of 810° . With increase in pressure, the inversion temperature increases rectilinearly. Olivine and spinel solid solutions form in the $\text{Mg}_2\text{GeO}_4 \text{-- } \text{Mg}_2\text{SiO}_4$ system. Above the inversion temperature, Mg_2GeO_4 forms a continuous series of olivine solid solutions. The limiting silicate content in the spinel solid solution, amounting to 10 mole % overall at 542° and a pressure of 700 bars, increases to 50 mole % at a pressure of 60,000 bar. The phase equilibrium in the system at 542° is presented in Fig. 226. A diagram characterizing the system in three-dimensional coordinates "pressure-temperature-composition (X)," is presented in Fig. 227. It was found by extrapolation that the olivine-spinel conversion takes place at a pressure of 100 ± 15 kbar for pure Mg_2SiO_4 , in which the unit cell parameter of the spinel phase of Mg_2SiO_4 is 8.22 Å.

Sarver and Hummel [2] have accomplished a more complete study of the $\text{MgO} \text{-- } \text{GeO}_2 \text{-- } \text{SiO}_2$ system. It is evident from Fig. 228 that, at normal pressure, besides forsterite (olivine) solid solutions, enstatite solid solutions exist. A phase diagram of the section adjacent to MgSiO_3 in the subsolidus region is presented in Fig. 229. In accordance with the polymorphism of MgSiO_3 , three types of solid solutions are formed: enstatite, clinoenstatite and protoenstatite.

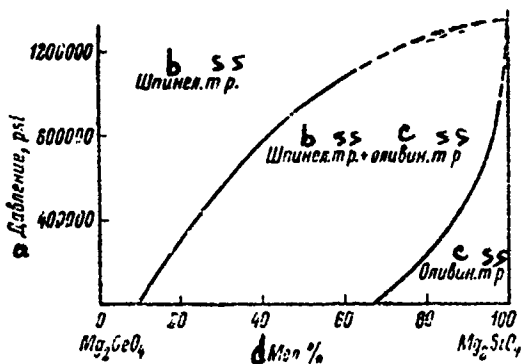


Fig. 226. Region of existence of spinel and olivine solid solutions at temperature of 542° and various pressures (from Dachille and Roy).

Key:

- a. Pressure, psi
- b. Spinel
- c. Olivine
- d. Mole %

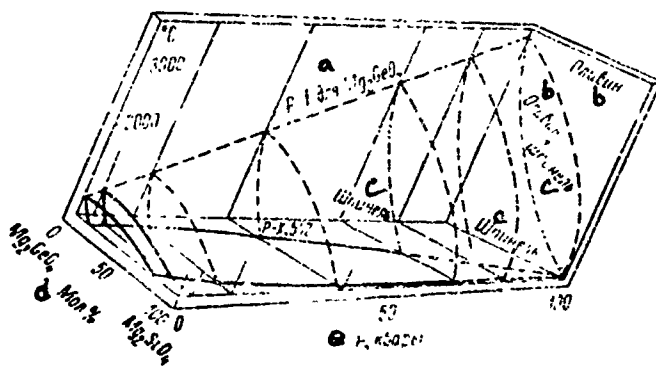


Fig. 227. Diagram characterizing $\text{MgO} - \text{GeO}_2 - \text{SiO}_2$ system in "pressure-temperature-composition" coordinates (from Dachille and Roy).

Key:

- | | |
|--------------------------------------|------------|
| a. F-t for Mg_2GeO_4 | d. Mole % |
| b. Olivine | e. P, kbar |
| c. Spinel | |

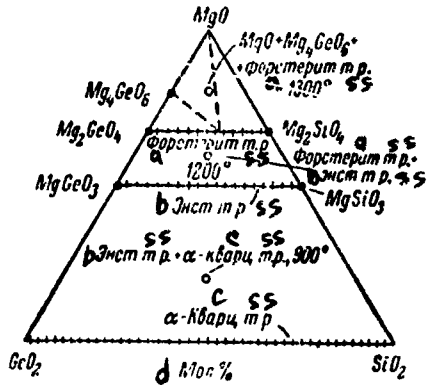


Fig. 228. Diagram of phase relationships of $\text{MgO} - \text{GeO}_2 - \text{SiO}_2$ system in subsolidus region (from Sarver and Hummel).

Key:

- a. Forsterite
- b. Enstatite
- c. Quartz
- d. Mole %

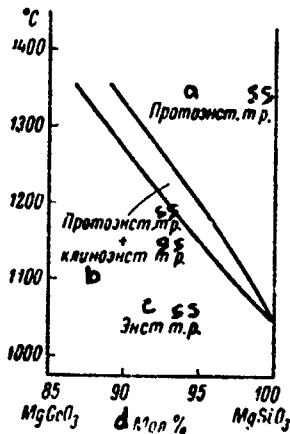


Fig. 229. Diagram of phase relationships of partial system $\text{MgGeO}_3 - \text{MgSiO}_3$ in subsolidus region (from Sarver and Hummel).

Key:

- | | |
|-------------------|--------------|
| a. Protoenstatite | c. Enstatite |
| b. Clinoenstatite | d. Mole % |

Ringwood and colleagues [3, 4] have studied the transformations of the MgSiO_3 -- MgGeO_3 series of solid solutions under high pressure conditions. Fusions rich in MgGeO_3 undergo the following transformation at pressures of about 50 kbar: $2\text{Mg}(\text{GeSi})\text{O}_3 \rightarrow \text{Mg}_2(\text{GeSi})\text{O}_4$ (spinel) + $(\text{GeSi})\text{O}_2$ (rutile). At a pressure of 180 kbar, fusions from $0.75 \text{MgGeO}_3 \cdot 0.25\text{MgSiO}_3$ to $0.2\text{MgGeO}_3 \cdot 0.8\text{MgSiO}_3$, taken in the form of glass, change into the ilmenite modification.

BIBLIOGRAPHY

1. Dachille, F., R. Roy, Amer. J. Sci., 258, No. 4, 225, 1960.
2. Sarver, J.F., F.A. Hummel, J. Electrochem. Soc., 110, No. 7, 726, 1963.
3. Ringwood, A.E., A. Major, Earth a. Planetary Sci. Lett., 1, No. 5, 351, 1966.
4. Ringwood, A.E., M. Seabrook, J. Geophys. Res., 68, 4601, 1963.

$\text{CaO} - \text{GeO}_2 - \text{SiO}_2$

The system has not been completely studied. Grebenshchikov and Toropov and colleagues [2, 3] have studied the Ca_2SiO_4 -- Ca_2GeO_4 profile, in which a continuous series of solid solutions, complicated by the polymorphism of both compounds, exists. The phase composition was determined by means of microscopic, X-ray and differential thermal analyses. The results of the study are presented in Fig. 230. In the low-temperature region, solid solutions form between $\gamma \text{Ca}_2\text{SiO}_4$ and the olivine variety of Ca_2GeO_4 . The existence of two types of solid solutions has been established here: 1. based on $\gamma \text{Ca}_2\text{SiO}_4$, containing from 0 to 52.5 mole % Ca_2GeO_4 ; 2. based on Ca_2GeO_4 , containing from 0 to 46.25 mole % Ca_2SiO_4 . The indices of refraction of the solid solutions increase monotonically from $\text{Ng} = 1.652$ and $\text{Np} = 1.644$ to $\text{Ng} = 1.680$ and

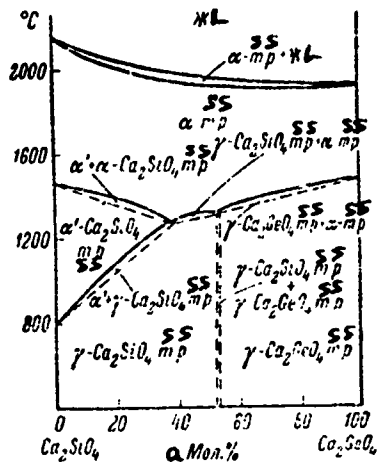


Fig. 230. Phase diagram of partial system Ca_2SiO_4 -- Ca_2GeO_4 (from Toropov and Shirvinskaya).

Key:

a. Mole %

$N_p = 1.676$, then, after a sharp increase in birefringence (at somewhat over 40 mole % Ca_2GeO_4 content), a uniform increase of N_g and N_p is observed, from the values 1.692 and 1.674 to 1.734 and 1.700, respectively. The authors could not precisely determine the boundary of the two-phase region and, by drawing them with dashed lines, note that this region exists in a very narrow concentration range. In the high-temperature region, two types of solid solutions were found: limited solid solutions based on α' Ca_2SiO_4 and a continuous series of solid solutions between α Ca_2SiO_4 and α Ca_2GeO_4 (α -SS in Fig. 230). The maximum solubility of Ca_2GeO_4 in α' Ca_2SiO_4 is approximately 37 mole %. The positions of the lower boundary curves are drawn conjecturally (dashed lines). The possibility of the formation of a metastable solid solution based on β Ca_2SiO_4 , with up to 15 mole % Ca_2GeO_4 content, is noted.

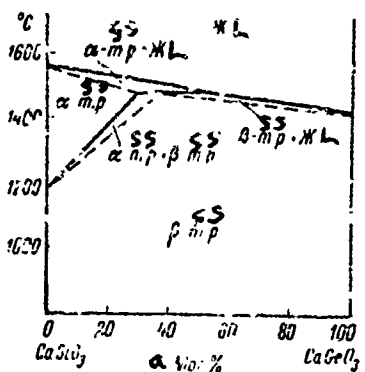


Fig. 231. Phase diagram in partial system
 CaSiO_3 -- CaGeO_3 (from Toropov and Shirvinskaya).

Key:

a. Mole %

Shirvinskaya and colleagues [4] have studied the pseudobinary system CaSiO_3 -- CaGeO_3 . The nature of the solid solutions formed here is determined by the polymorphism of the extreme members. Calcium metasilicate exists below 1160° in the form of the wollastonite modification, with a chain structure and a triclinic unit cell. A transition to the pseudowollastonite modification, the principal structural reason for which is the three-member ring $(\text{Si}_3\text{O}_9)^{6-}$, takes place at 1160°. Only the wollastonite structure is characteristic of calcium metagermanate. Two types of solid solutions are found in the system, in accordance with the modifications enumerated: continuous, with a wollastonite structure (β SS) and limited, with a pseudowollastonite structure (α SS), based on calcium metasilicate (Fig. 231). The peritectic melting of the solid solution indicated in the diagram takes place at 1480°. The limiting

pseudowollastonite solid solution contains approximately 30 mole % CaGeO_3 . As we see, the polymorphic transformation temperature of CaSiO_3 increases sharply with increase in GeO_2 content in the solid solution. The authors note the possibility of obtaining (by means of quenching) metastable pseudowollastonite solid solutions with a high GeO_2 content.

The solid solutions in the Ca_2GeO_4 -- Ca_2SiO_4 system have been studied by Eysel and Hahn [5]. In the low-temperature region, the authors found only one type of solid solution, based on $\gamma \text{Ca}_2\text{GeO}_4$, with an approximate maximum concentration of 40 mole % Ca_2SiO_4 . The $\gamma \text{Ca}_2\text{SiO}_4$ -base solid solution was not found. Solubility of Ca_2GeO_4 in $\alpha' \text{Ca}_2\text{SiO}_4$ is 25 mole %. Besides, metastable $\beta \text{Ca}_2\text{SiO}_4$ -base solid solutions were found, with a content of up to 10 mole % of the germanate component.

Boykova and colleagues [1] have studied the partial system $3\text{CaO}\cdot\text{SiO}_2$ -- $3\text{CaO}\cdot\text{GeO}_2$ in the subsolidus region, by the differential thermal analysis method. $3\text{CaO}\cdot\text{SiO}_2$ and $3\text{CaO}\cdot\text{GeO}_2$ have similar polymorphism, taking place according to the following schemes: $3\text{CaO}\cdot\text{SiO}_2$ -- triclinic I $\xrightarrow{620^\circ}$ triclinic II $\xrightarrow{920^\circ}$ triclinic III $\xrightarrow{970^\circ}$ monoclinic $\xrightarrow{990^\circ}$ rhombic $\xrightarrow{1050^\circ}$ hexagonal; $3\text{CaO}\cdot\text{GeO}_2$ -- triclinic I $\xrightarrow{750^\circ}$ triclinic II $\xrightarrow{1020^\circ}$ triclinic III $\xrightarrow{1160^\circ}$ monoclinic. There actually are four types of solid solutions on the phase diagram (Fig. 232): triclinic I, triclinic II, triclinic III and monoclinic. The region of higher temperatures and the liquidus curve were not investigated by the authors.

Ringwood and Major [6] have shown that a homogeneous sample corresponding to the composition $\text{Ca}(\text{Ge}_{0.5}\text{Si}_{0.5})\text{O}_3$, obtained by annealing a mixture of oxides at 1400° , when subjected to a pressure of 170 kbar (900°), changes into a mixture of two phases, one of which (primary) has a slightly deformed

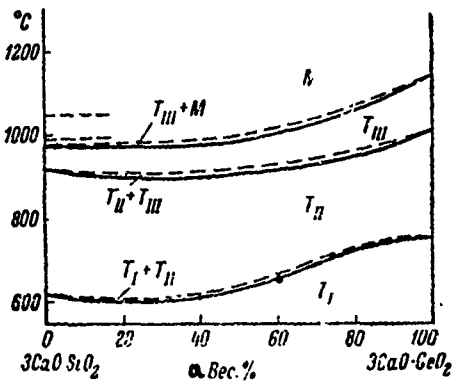


Fig. 232. Diagram of phase ratios of solid solutions of the $3\text{CaO}\cdot\text{SiO}_2$ -- $3\text{CaO}\cdot\text{GeO}_2$ system in the sub-solidus region (from Boykova and colleagues).

Key:

a. Weight %

perovskite structure, with a pseudocubic lattice (parameter 3.969 Å). The authors conclude from this that the CaSiO_3 included in the solid solution should exist in the perovskite structure.

Calcium metacarbonate changes completely into the perovskite modification, with a density of 5.17 g/cm^3 , at a pressure of 120 kbar and 900° . Even at 250 kbar, CaSiO_3 (in the form of glass) did not succeed in changing into the perovskite structure, but the perovskite solid solution obtained indicates the possibility of existence of CaSiO_3 in the form of a perovskite modification at higher pressures.

BIBLIOGRAPHY

1. Boykova, A.I., N.A. Toropov, V.T. Vavilonova, DAN SSSR, 175, 3, 1967, p. 654.

2. Grebenschikov, R. G., A. K. Shirvinskaya, V. I. Shitova, N. A. Toropov, in the collection Khimiya vysokotemperaturnykh materialov [Chemistry of High-Temperature Materials], Nauka Press, Leningrad, 1967, p. 109.
3. Toropov, N. A., A. K. Shirvinskaya, DAN SSSR, 153, 5, 1963, p. 1081.
4. Shirvinskaya, A. K., R. G. Grebenschikov, V. I. Shitova, N. A. Toropov, Izv. AN SSSR, neorg. mater., 2, 10, 1966, p. 1900.
5. Eysel, W., Th. Hahn, Neues Jahrb. Mineral., Abh., No. 6, 737, 1963.
6. Ringwood, A. E., A. Major, Earth a. Planetary Sci. Lett., 2, No. 2, 106, 1967.



The system has been partially studied by Grebenschikov and colleagues [1, 2], limited to plotting a phase diagram of the partial systems Sr_2SiO_4 -- Sr_2GeO_4 and SrSiO_3 -- SrGeO_3 .

Continuous solid solutions of the structural type β K_2SO_4 have been found in the partial system Sr_2SiO_4 -- Sr_2GeO_4 , which is characteristic of both extreme members. The linear change in index of refraction and monotonic change in interplane distances on the X-ray photos also confirm complete miscibility.

The liquidus curve decreases uniformly from the melting temperature of Sr_2SiO_4 (2160°) to the melting temperature of Sr_2GeO_4 (1880°). Thus, the solid solution corresponding to the composition $\text{Sr}_{2-\delta}\text{Si}_{0.4}\text{Ge}_{0.6}\text{O}_4$ has a liquidus temperature of 2030° .

The formation of solid solutions also has been found in the partial system SrSiO_3 -- SrGeO_3 , complicated by the existence of two polymorphic forms of SrGeO_3 , a pseudowollastonite ring form, thermodynamically stable above 990° , and a pyroxenoid chain form, below 990° . In conformance with this, two types

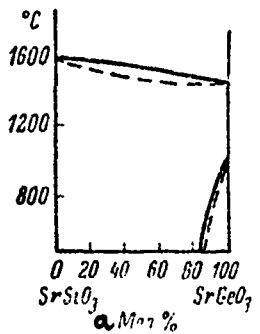


Fig. 233. Phase diagram of partial system SrSiO_3 -- SrGeO_3 (from Grebenschchikov and colleagues).

Key:

a. Mole %

of solid solutions are observed in the system: a continuous pseudowollastonite (α SS) and a limited SrGeO_3 -base pyroxenoid chain form (Fig. 233). The maximum solubility of SrSiO_3 in strontium metagermanate is approximately 15 mole % (at 500°).

BIBLIOGRAPHY

1. Grebenschchikov, R.G., A.K. Shirvinskaya, V.I. Shitova, Zhurn. neorg. khim., 12, 12, 1967, p. 3399.
2. Grebenschchikov, R.G., A.K. Shirvinskaya, V.I. Shitova, Izv. AN SSSR, Neorg. mater., 4, 8, 1968, p. 1376.



Grebenschchikov and colleagues [1-3] have studied the partial systems Ba_2SiO_4 -- Ba_2GeO_4 and BaSiO_3 -- BaGeO_3 . Solid solutions were obtained

here by sintering mixtures of the previously synthesized ortho and meta compounds. A Galakhov microfurnace was used for determination of the melting temperatures.

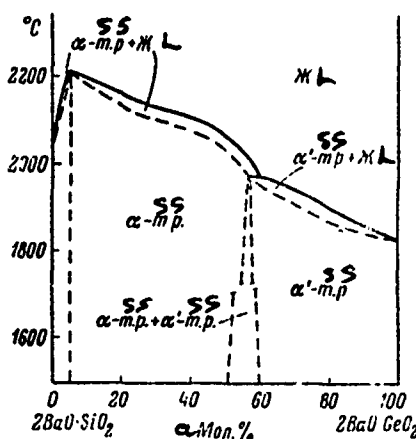


Fig. 234. Phase diagram of partial system
 $2\text{BaO}\cdot\text{SiO}_2$ -- $2\text{BaO}\cdot\text{GeO}_2$ (from Grebenschchikov
 and colleagues).

Key:

a. Mole %

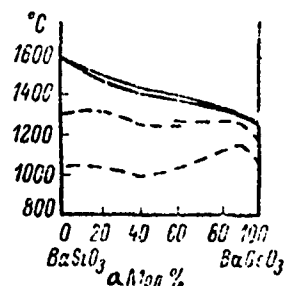


Fig. 235. Phase diagram of partial system
 BaSiO_3 -- BaGeO_3 (from Grebenschchikov
 and colleagues).

Key: a. Mole %

A phase diagram of the partial system Ba_2SiO_4 -- Ba_2GeO_4 is presented in Fig. 234; the maximum on the liquidus curve, with a temperature of 2210° , corresponds to a composition of 95 mole % Ba_2SiO_4 . The existence of two solid solutions has been established: based on Ba_2SiO_4 (α SS) and based on Ba_2GeO_4 (α' SS). The characteristic bend in the liquidus curve in the region of 50-60 mole % Ba_2GeO_4 is connected by the authors with a discontinuity in miscibility of the solid solutions and their peritectic decomposition, taking place at 1970° . The existence of a region of immiscibility is confirmed by the concentration dependence of refraction and density. A discontinuity in the curves occurs in the region of 50-60 mole % Ba_2GeO_4 . The phase diagram of the partial system BaSiO_3 -- BaGeO_3 is characterized by a continuous series of solid solutions (Fig. 235). In conformance with the polymorphism of BaSiO_3 and BaGeO_3 , according to subsequent refined data, the subsolidus section consists of three regions: a low-temperature region of pseudowollastonite solid solutions and two regions with solid solutions of pyroxenoid structure. The polymorphic transition of pure BaSiO_3 takes place at temperatures of ~ 1040 and 1300° and, of pure BaGeO_3 , at 1225° .

The authors have found new solid solutions based on BaSi_2O_5 and BaGe_4O_9 , with the hypothetical compounds " BaGe_2O_5 " and " BaSi_4O_9 ".

BIBLIOGRAPHY

1. Grebenshchikov, R.G., in the collection Eksperiment v tekhnicheskoy mineralogii i petrografii [Experiment in Technical Mineralogy and Petrography], Nauka Press, Moscow, 1966, p. 30.
2. Grebenshchikov, R.G., N.A. Toropov, V.I. Shitova, Izv. AN SSSR, Neorg. mater., 1, 1, 1965, p. 121.
3. Grebenshchikov, R.G., V.I. Shitova, N.A. Toropov, DAN SSSR, 175, 4, 1967, p. 840.

$\text{ZnO} - \text{GeO}_2 - \text{SiO}_2$

Investigation of the system has been limited to study of the Zn_2SiO_4 -- Zn_2GeO_4 profile. Ingerson and colleagues [3], carrying out annealing at 1200°, obtained a continuous series of solid solutions, the index of refraction of which changed linearly with composition. Brown and Hummel [2], annealing appropriate mixtures of oxides at 1000°, did not obtain solid solutions, and observed only the formation of pure zinc silicate and germanate. Several signs of formation of solid solutions were found in mixtures subjected to prolonged (1 month) soaking at 1000°, in the presence of a mineralizer. Meanwhile, if a solid solution is obtained at 1200° (48 hours) and it is held for a long time at 1000°, no decomposition whatever takes place. For an explanation of the facts observed, further investigation of the subsolidus processes in the Zn_2SiO_4 -- Zn_2GeO_4 system is necessary.

Merkulov and Khristoforov [1] obtained a continuous series of solid solutions of Zn_2SiO_4 -- Zn_2GeO_4 , as they think, at 100°, precipitating coagels from the corresponding solutions containing ZnCl_2 , Na_2SiO_3 and Na_2GeO_3 .

BIBLIOGRAPHY

1. Merkulov, A. G., B. S. Khristoforov, Izv. Sibirsk. otd. AN SSSR, ser. khim. nauk., 1, 1970, p. 36.
2. Brown, J. J., F. A. Hummel, Trans. Brit. Ceram. Soc., 64, No. 9, 419, 1965.
3. Ingerson, E., G. W. Morey, O. F. Tuttle, Amer. J. Sci., 246, No. 1, 31, 1943.



Toropov and colleagues [1] have studied the partial "mullite" profile $3\text{Al}_2\text{O}_3 \cdot 2\text{SiO}_2 \text{ -- } 3\text{Al}_2\text{O}_3 \cdot 2\text{GeO}_2$, by annealing appropriate mixtures of oxides at up to 1500° , as well as by determining the melting temperatures in a vacuum microfurnace. A continuous series of solid solutions has been established. The melting temperature (liquidus line) decreases smoothly from 1900° (for $3\text{Al}_2\text{O}_3 \cdot 2\text{SiO}_2$) to 1785° (for $3\text{Al}_2\text{O}_3 \cdot 2\text{GeO}_2$).

A practically linear nature of change in the indices of refraction has been established, from $\text{Ng} = 1.654$ and $\text{Np} = 1.642$ for $3\text{Al}_2\text{O}_3 \cdot 2\text{SiO}_2$ to $\text{Ng} = 1.758$ and $\text{Np} = 1.712$ for $3\text{Al}_2\text{O}_3 \cdot 2\text{GeO}_2$. The density changes regularly from 3.160 for $3\text{Al}_2\text{O}_3 \cdot 2\text{SiO}_2$ to 3.662 for $3\text{Al}_2\text{O}_3 \cdot 2\text{GeO}_2$. The solid solution studied may be referred to as ideal.

BIBLIOGRAPHY

1. Toropov, N.A., I.F. Andreev, V.A. Orlov, S.P. Shmitt-Fogelovich, Izv. AN SSSR, Neorg. mater., 6, 6, 1970, p. 1136.



Lazarev and colleagues [1] have studied the partial profile $\text{Sc}_2\text{Si}_2\text{O}_7 \text{ -- Sc}_2\text{Ge}_2\text{O}_7$ by the quenching method. A continuous series of solid solutions was found, with a minimum melting temperature (at 50 mole % $\text{Sc}_2\text{Ge}_2\text{O}_7$) of 1766° . Scandium diorthogermanate melts at 1850° , and it has unit cell parameters $a = 6.47 \pm 0.02$, $b = 8.47 \pm 0.03$, $c = 4.90 \pm 0.02 \text{ \AA}$, $\beta = 103^\circ 30'$, $Z = 2$.

The indices of refraction of the solid solutions change regularly from $\text{Ng} = 1.804$ and $\text{Np} = 1.754$ for $\text{Sc}_2\text{Si}_2\text{O}_7$ to $\text{Ng} = 1.847$ and $\text{Np} = 1.797$ for $\text{Sc}_2\text{Ge}_2\text{O}_7$. The density changes correspondingly from 3.39 to 4.46 g/cm^3 .

For solid solutions of this series, discrete radicals of three types are noted simultaneously; $(\text{Si}_2\text{O}_7)^{6-}$, $(\text{Ge}_2\text{O}_7)^{6-}$ and $(\text{SiGeO}_7)^{6-}$.

BIBLIOGRAPHY

1. Lazarev, A. N., T. F. Tenisheva, A. N. Sokolov, A. N. Mitropol'skiy, N. A. Toropov, DAN SSSR, 183, 2, 1968, p. 352.



Toropov and colleagues [1, 2], using the quenching method and solid-phase synthesis, have studied two partial profiles of the system: $\text{Y}_2\text{SiO}_5 \text{ -- Y}_2\text{GeO}_5$ and $\text{Y}_2\text{Si}_2\text{O}_7 \text{ -- Y}_2\text{Ge}_2\text{O}_7$, for which continuous series of solid solutions with a melting temperature minimum is characteristic.

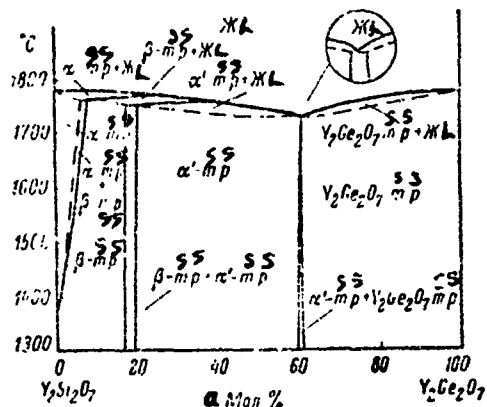


Fig. 236. Phase diagram of partial system $\text{Y}_2\text{Si}_2\text{O}_7 \text{ -- Y}_2\text{Ge}_2\text{O}_7$ (from Toropov and colleagues).

Key:

a. Mole %

For the partial system Y_2SiO_5 -- Y_2GeO_5 , the minimum melting temperature is 1910° (with approximately a 50 mole % Y_2GeO_5 content). The melting temperature of Y_2GeO_5 , according to new determinations, is 1950° (Y_2SiO_5 -- 1980°). Crystals of the solid solution belong to the monoclinic crystal system, with indices of refraction changing smoothly from $\text{Ng} = 1.848$ and $\text{Np} = 1.832$ for Y_2GeO_5 to $\text{Ng} = 1.825$ and $\text{Np} = 1.816$ for Y_2SiO_5 . The density changes from 4.83 (Y_2GeO_5) to 4.45 g/cm^3 (Y_2SiO_5). The following values of the unit cell parameters were obtained for Y_2GeO_5 : $a = 10.42 \pm 0.02$, $b = 6.77 \pm 0.015$, $c = 12.820 \pm 0.03 \text{ \AA}$, $\beta = 102^\circ 50'$, $Z = 8$ [3].

A phase diagram of the partial system $\text{Y}_2\text{Si}_2\text{O}_7$ -- $\text{Y}_2\text{Ge}_2\text{O}_7$ is presented in Fig. 236. In connection with the existence of several polymorphic modifications of $\text{Y}_2\text{Si}_2\text{O}_7$, three types of solid solutions based on this compound are observed: α , β and γ .

BIBLIOGRAPHY

1. Sokolov, A.N., R.G. Grebenschikov, N.A. Toropov, DAN SSSR, 185, 1, 1969, p. 107.
2. Toropov, N.A., R.G. Grebenschikov, A.N. Sokolov, Izv. AN SSSR, Neorg. mater., 5, 2, 1969, p. 321.
3. Harris, L.A., C.B. Finch, Amer. Mineralogist, 50, No. 9, 1493, 1965.

Nd_2O_3 -- GeO_2 -- SiO_2

Toropov and Kougiya [1] have studied the partial profile Nd_2SiO_5 -- Nd_2GeO_5 , in which a continuous series of solid solutions is formed. Uniform samples were obtained by multiple, multistage annealing (1000 , 1200 , 1500°), with intermediate pulverization. The authors present a fusibility curve, in the form of a straight line between the melting temperatures of Nd_2SiO_5 (1980°)

and Nd_2GeO_5 (1900°), noting that they did not succeed in defining the solidus curve, as a consequence of the high crystallization rate of the germanates. The rectilinear relationship $d = 5.93 \pm 0.053 K$, where K is the volumetric fraction of Nd_2GeO_5 , was obtained for the densities of the solid solutions, with the composition expressed in volumetric fractions. The indices of refraction change linearly from $\text{Ng} = 1.948$ and $\text{Np} = 1.939$ for Nd_2GeO_5 to $\text{Ng} = 1.888$ and $\text{Np} = 1.871$ for Nd_2SiO_5 . The crystals are biaxial and optically positive.

BIBLIOGRAPHY

1. Toropov, N.A., M.V. Kougiya, Izv. AN SSSR, Neorg. mater., 5, 2, 1969, p. 398.



The system has not been studied. Mydlar and colleagues [2] have shown that the germanium in the germanate can be replaced by silicon, but silicon is not replaced by germanium in the silicates. Replacement by silicon in germanium-rich germanates (for example, $\text{PbO} \cdot 2\text{GeO}_2$), does not take place.

The authors obtained uniform solid solutions, proceeding from $3\text{PbO} \cdot \text{GeO}_2$ (this compound, discovered by Gooju and colleagues [1], was confirmed by Mydlar and colleagues), $3\text{PbO} \cdot 2\text{GeO}_2$ and $\text{PbO} \cdot \text{GeO}_2$. The corresponding mixtures of oxides were initially annealed at about 1000° , and then for a long time (up to 50 hours) at 600° . The following uniform phases were obtained: $3\text{PbO} \cdot x\text{GeO}_2 \cdot (1-x)\text{SiO}_2$ ($x = 0.0, 0.33, 0.5, 0.67$), $3\text{PbO} \cdot 2x\text{GeO}_2 \cdot 2(1-x)\text{SiO}_2$ ($x = 0.0, 0.17, 0.25, 0.33, 0.5, 0.66, 0.83$), $\text{PbO} \cdot x\text{GeO}_2 \cdot (1-x)\text{SiO}_2$ ($x = 0.0, 0.25, 0.5, 0.75$).

BIBLIOGRAPHY

1. Gooju, D., J. Fournier, R. Kohlmuller, Compt. rend., 266, ser. C, No. 14, 1063, 1968.
2. Mydlar, M., H. Nowotny, K.J. Seifert, Monatshefte Chem., 100, No. 1, 191, 1969.



Ringwood [1-3] has studied the partial system $\text{Ni}_2\text{GeO}_4 \text{ -- } \text{Ni}_2\text{SiO}_4$. The subsolidus phase equilibria in this system at atmospheric pressure, according to [3], are presented in Fig. 237. Conducting tests under a pressure of 30 kbar at 650° for a period of three hours (initial mixture Ni(OH)_2 , SiO_2 and the hydrated form of germanium dioxide), Ringwood obtained a complete series of homogeneous spinel solid solutions between Ni_2GeO_4 and Ni_2SiO_4 . The unit cell parameters of these solid solutions are subject to the rule of Begard.

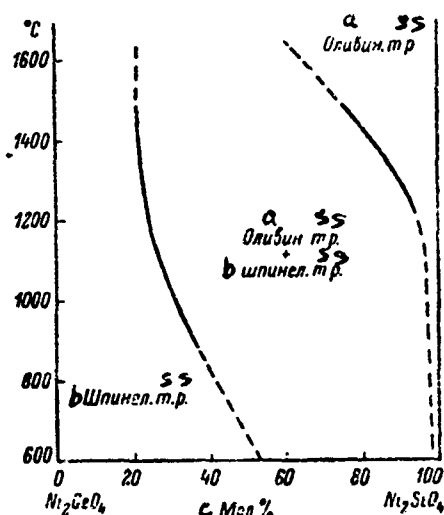


Fig. 237. Subsolidus phase equilibria in $\text{Ni}_2\text{GeO}_4 \text{ -- } \text{Ni}_2\text{SiO}_4$ system (from Ringwood).

Key:

- a. Olivine
- b. Spinel
- c. Mole %

BIBLIOGRAPHY

- O 1. Ringwood, A. E., Geochim. cosmochim. acta, 15, No. 1/2, 18, 1958.
2. Ringwood, A. E., Nature, 187, No. 4742, 1019, 1960.
3. Ringwood, A. E., Geochim. cosmochim. acta, 26, No. 4, 457, 1962.

TITANOSILICATE SYSTEMS



The system has been investigated by Kim and Hummel [2], by means of study of reactions in the solid state and by the quenching method. The region studied was limited to compositions of not over 50 mole % Li_2O . The phase relationships in the system are presented in Fig. 238. One ternary compound $\text{Li}_2\text{O} \cdot \text{TiO}_2 \cdot \text{SiO}_2$ has been found, which melts at $1207 \pm 3^\circ$, with formation of two immiscible liquids. The immiscible liquid region is very widespread in the system, from 0 to 20 weight % Li_2O . Galakhov and Konovalova [1] showed that, in fact, the equilibrium immiscibility of the liquids is limited to a content of only one-two weight % Li_2O , and that the extensive immiscibility indicated by Kim and Hummel is a metastable, nonequilibrium microliquation.

The compound $\text{Li}_2\text{O} \cdot \text{TiO} \cdot \text{SiO}_2$ forms crystals in the tetragonal crystal system, which are uniaxial, negative and with indices of refraction $N_e = 1.81 - 1.82$ and $N_o = 1.83 - 1.84$.

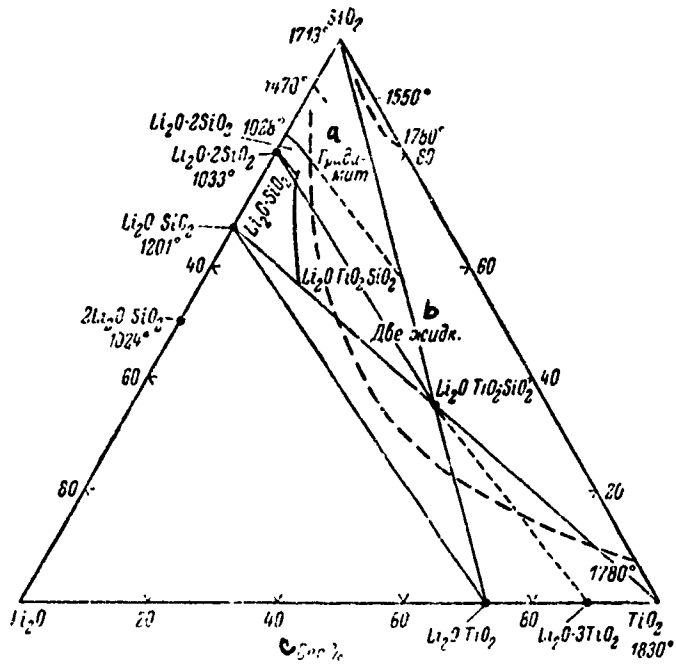


Fig. 238. Phase diagram of $\text{Li}_2\text{O} - \text{TiO}_2 - \text{SiO}_2$ system (from Kim and Hummel).

Key:

- a. Tridymite
- b. Two liquids
- c. Weight %

BIBLIOGRAPHY

1. Galakhov, F. Ya., S. F. Konovalova, Izv. AN SSSR. Neorg. mater., **1**, 8, 1965, p. 1399.
2. Kim, K. H., F. A. Hummel, J. Amer. Ceram. Soc., **42**, No. 6, 286, 1959.

$\text{Na}_2\text{O} \text{-- } \text{TiO}_2 \text{-- } \text{SiO}_2$

Hamilton and Cleek [1], in connection with study of glasses, indicate a field of initially separating crystals on the triple diagram (Fig. 239). Beside the ternary compound $\text{Na}_2\text{O} \cdot \text{TiO}_2 \cdot \text{SiO}_2$ (phase E), three fields of ternary compounds of unknown composition are introduced: D, F_1 and F_2 . The boundary separating fields F_1 and F_2 have not been established. Phase E is represented by rod-shaped crystals, with low birefringence, negative elongation and $\text{Ng} \sim 1.77$, $\text{Np} \sim 1.73$. Phase D forms crystals with high birefringence: $\text{Ng} \sim 1.70$ and $\text{Np} \sim 1.60$. Phase F_1 forms needle-shaped crystals with moderate birefringence, positive elongation and $\text{Ng} \sim 2.00$, $\text{Np} < 2.00$.

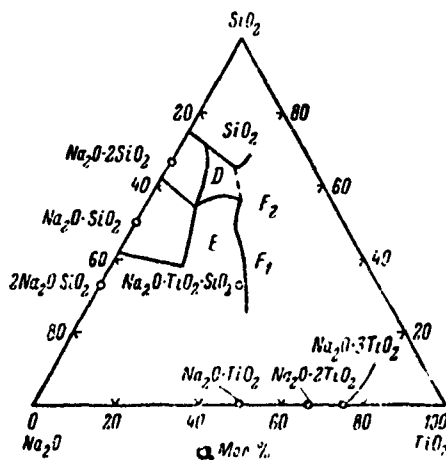


Fig. 239. Schematic diagram of phase relationships of $\text{Na}_2\text{O} \text{-- } \text{TiO}_2 \text{-- } \text{SiO}_2$ system (from Hamilton and Cleek).

Key:

a. Mole %

BIBLIOGRAPHY

1. Hamilton, E. H., G. W. Cleek, J. Res. Nat. Bur. Stand., 61, No. 2, 89, 1958.

MgO -- TiO₂ -- SiO₂

The first investigation of the system was made by Berezhnoy [1]. He heated mixtures of previously synthesized binary compounds at a temperature of 1400-1500°. Magnesium titanosilicates were not found. They are unknown in nature. Forsterite ($2\text{MgO} \cdot \text{SiO}_2$) does not react with $\text{MgO} \cdot 2\text{TiO}_2$ or $2\text{MgO} \cdot \text{TiO}_2$, right up to melting, but solution of the latter in forsterite is possible. In triple mixtures of $\text{MgO} + \text{TiO}_2 + \text{SiO}_2$, the initial product of solid-phase reactions is $\text{MgO} \cdot \text{TiO}_2$, then forsterite forms and, only after this, magnesium orthotitanate. Berezhnoy has plotted an approximate fusibility diagram of the system and coexisting phase triangles (Fig. 240), which does not differ from those presented by Sarver and Hummel [11].

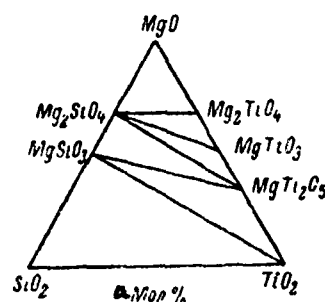


Fig. 240. Coexisting phase triangles of
MgO -- TiO₂ -- SiO₂ system (from
Berezhnoy).

Key:

a. Mole %

The reaction relationships in mixtures of $2\text{MgO} \cdot \text{SiO}_2 + 2\text{MgO} \cdot \text{TiO}_2$ has been studied by Ramakrishna [10], according to whom, magnesium orthotitanate has a melting temperature of $1770 \pm 75^\circ$. Forsterite and magnesium orthotitanate do not form a simple binary system, but are a part of the $\text{MgO} - \text{TiO}_2 - \text{SiO}_2$ triple system.

Berezhnay and Gul'ko [2] found that Mg_2TiO_4 forms a solid solution in forsterite, with up to 4 weight % Mg_2TiO_4 content, and a pseudobinary eutectic in the $\text{Mg}_2\text{SiO}_4 - \text{Mg}_2\text{TiO}_4$ section melts at 1637° . Orthosilicate solutions are common in the magnesium metasilicate region, but their boundaries still have not been established precisely. The lowest melting eutectic in the system, with a melting temperature of 1415° , occurs at the intersection of the MgSiO_3 , TiO_2 and SiO_2 fields, and not of MgSiO_3 , MgTi_2O_5 and TiO_2 , as Massazza and Sircchia think [9].

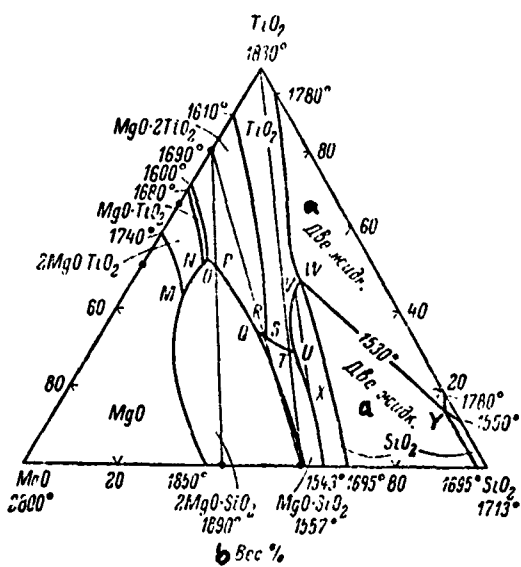


Fig. 241. Phase diagram of $\text{MgO} - \text{TiO}_2 - \text{SiO}_2$ system (from Massazza and Sircchia).

Key:

- a. Two liquids
- b. Weight %

A phase diagram of the triple system, according to Massazza and Sircchia [9], is presented in Fig. 241. The liquid phase separation region is very extensive. Upon cooling the liquid richer in silica, glass forms, and a liquid richer in TiO_2 , depending on composition, forms glass + cristobalite, glass + cristobalite + rutile or glass + rutile. The results of the investigations indicated the absence of the substitution $Si^{4+} \rightarrow Ti^{4+}$.

MacGregor [7] ascertained the phase ratios in the system under high pressure conditions. He studied the binary profiles $MgSiO_3 - TiO_2$, $Mg_2SiO_4 - TiO_2$ and $MgSiO_3 - MgTi_2O_5$. The $MgSiO_3 - TiO_2$ profile is a simple eutectic over the entire range of pressures investigated, from 1 to 40 kbar. The eutectic temperature at 1 atm turned out to be somewhat lower (by approximately 10°) than Massazza and Sircchia indicate. The TiO_2 content in the eutectic increases with increase in pressure: by 10 weight % TiO_2 in the transition from 1 atm to 10 kbar. The author proposes the possibility of solution of TiO_2 in enstatite. A small TiO_2 content (less than 1 weight %) has been found in natural enstatites. The binary profiles $Mg_2SiO_4 - TiO_2$ and $MgSiO_3 - MgTi_2O_5$ are presented in Figs. 242 and 243, for a pressure of 10 kbar.

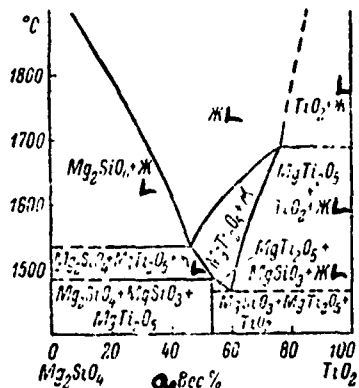


Fig. 242. Fusibility diagram of partial system $Mg_2SiO_4 - TiO_2$ for pressure of 10 kbar (from MacGregor).

Key: a. Weight %

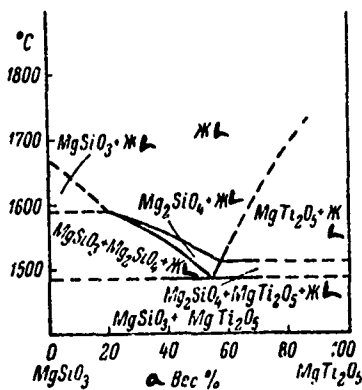


Fig. 243. Fusibility diagram of partial system MgSiO_3 -- MgTi_2O_5 for pressure of 10 kbar (from MacGregor).

Key:

a. Weight %

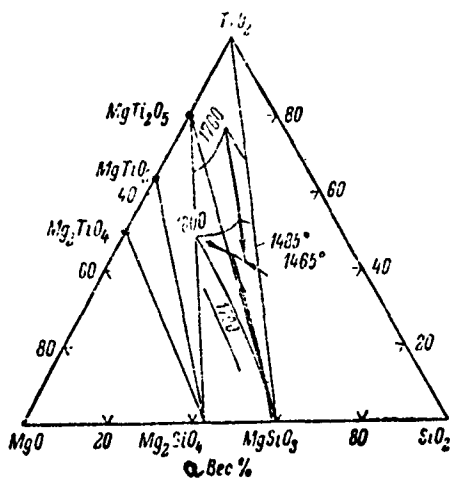


Fig. 244. Diagram indicating position of triple eutectics in MgO -- TiO_2 -- SiO_2 system for pressure of 10 kbar (from MacGregor).

Key:

a. Weight %

A small section of the system is presented in Fig. 244, the region in which triple eutectics occur. In place of two triple eutectics at 1 atm, only one triple eutectic is observed at 10 and 20 kbar, with the respective compositions: 26.0 MgO, 42.0 TiO₂ and 32.0 weight % SiO₂ and 25.2 MgO, 50.0 TiO₂ and 24.8 weight % SiO₂.

INVARIANT POINTS OF MgO -- TiO₂ -- SiO₂ SYSTEM
(from Massazza and Sirchia)

a Точка (рас. зл.)	b Фазы	c Состав, вес. %			d Темп- ература, °C
		MgO	TiO ₂	SiO ₂	
M	MgO + 2MgO · TiO ₂ + 2MgO · SiO ₂ + жидкость e	43.8	43.6	12.6	1580
N	2MgO · TiO ₂ + MgO · TiO ₂ + 2MgO · SiO ₂ + жидкость e	35.8	51.6	12.6	1540
O	MgO · TiO ₂ + MgO · 2TiO ₂ + 2MgO · SiO ₂ + жидкость e	34.4	52.6	13.0	1520
P	MgO · 2TiO ₂ + 2MgO · SiO ₂ + жидкость e	33.4	51.6	15.0	1540
Q	MgO · 2TiO ₂ + 2MgO · SiO ₂ + MgO · SiO ₂ + жидкость e	32.2	34.6	33.2	1440
R	MgO · 2TiO ₂ + MgO · SiO ₂ + жидкость e	31.8	34.0	34.2	1425
S	MgO · 2TiO ₂ + TiO ₂ + MgO · SiO ₂ + жидкость e	31.4	33.4	35.2	1390
T	кость				
TiO ₂ + MgO · SiO ₂ + жидкость e		28.0	30.0	42.0	1420
U	TiO ₂ + MgO · SiO ₂ + тридимит + жидкость e	27.4	29.2	43.4	1400
V	TiO ₂ + тридимит + кристобалит + жидкость e	20.6	43.4	36.0	1470
W	кость				
TiO ₂ + кристобалит + жидкость A + жидкость B		16.8	47.4	35.8	1530
X	MgO · SiO ₂ + тридимит + кристобалит + жидкость e	29.0	20.0	51.0	1470
Y	TiO ₂ + кристобалит + жидкость A + жидкость B	1.8	44.8	53.4	1530

Key:

- | | |
|--------------------------|-----------------|
| a. Points (Fig. 241) | e. Liquid |
| b. Phases | f. Tridymite |
| c. Composition, weight % | g. Cristobalite |
| d. Temperature, °C | |

In the concentration region studied (pressure up to 20 kbar), only one subsolidus reaction takes place: $MgSiO_3 + MgTi_2O_5 \rightleftharpoons Mg_2SiO_4 + 2TiO_2$.

MacGregor [8] subsequently showed that the following invariant reactions take place in the range from 1 atm to 40 kbar: $En + M = Fo + 2R$ (1), $Fo + En + M = L_2$ (2), $M + En = Fo + L_3$ (3), $M + En + R = L_4$ (4), $Fo + R = M + L_5$ (5), $Fo + En + R = L_6$ (6) and $M + Fo + R = L_7$ (7). Here, $En = MgSiO_3$, $M = MgTi_2O_5$, $Fo = Mg_2SiO_4$ and $R = TiO_2$.

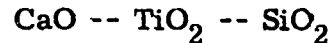
The composition of the liquids is enriched in titanium dioxide and depleted of magnesium oxide and silica with increase in pressure. Presenting the equilibrium positions of the reactions enumerated above on a graph in "temperature-pressure" coordinates, MacGregor showed that the corresponding curves for reactions (1), (3)-(6) intersect at a single point, at a temperature of 1489° and a pressure of 15.2 kbar. The line dividing the $MgSiO_3 + MgTi_2O_5$ and $Mg_2SiO_4 + TiO_2$ fields on the graph in "temperature-pressure" coordinates is expressed by the equation $t = 32.46 P + 996$ (t is in °C and P in kilobars).

The crystalline phases of the system have the following structural parameters: 1. $2MgO \cdot TiO_2$ (magnesium orthotitanate), cubic crystal system, $a = 8.44 \text{ \AA}$ [6]; 2. $MgO \cdot TiO_2$ (geikielite), rhombohedral crystal system, $a = 5.54 \text{ \AA}$, $\alpha = 54^\circ 39'$ [4]; $MgO \cdot 2TiO_2$ (magnesium dititanate), rhombic crystal system, $a = 3.7$, $b = 9.8$, $c = 10.0 \text{ \AA}$ [3]; indices of refraction [5]: $N_{av} = 1.959$ for $2MgO \cdot TiO_2$, $N_{av} = 1.95-2.28$ for $MgO \cdot TiO_2$ and $N_{av} = 2.11-2.23$ for $MgO \cdot 2TiO_2$.

BIBLIOGRAPHY

1. Berezhnoy, A. S., Ogneupory, 15, 10, 1950, p. 446.
2. Berezhnoy, A. S., Mnogokomponentnye sistemy okislov, [Multicomponent Oxide Systems], Naukova dumka Press, Kiev, 1970, p. 218.

3. Zhdanov, G.S., A.A. Rusakov, Trudy Inst. kristallogr. AN SSSR, 9, 1954, p. 165.
4. Ormont, B.F., Struktury neorganicheskikh veshchestv (Structure of Inorganic Substances], Moscow-Leningrad, 1950.
5. Coughanour, L.W., V.A. DeProsse, J. Res. Nat. Bur. Stand., 51, No. 2, 85, 1953.
6. Cumulative alphabetical index of X-ray diffraction data, ASTM, Philadelphia, 1953.
7. MacGregor, I.D., Carnegie Inst. Washington Year Book, 64, 135, 1964-1965.
8. MacGregor, I.D., Amer. J. Sci., 267A, Schairer vol., 342, 1969.
9. Massazza, F., E. Sirchia, Chim. e l'Industr. (Milano), 40, No. 6, 460, 1958.
10. Ramakrishna, R.M., J. Sci. Industr. Res., 16B, 10, 444, 1957.
11. Sarver, J.F., F.A. Hummel, J. Electrochem. Soc., 110, No. 7, 726, 1963.



Berezhnoy [1], in connection with study of the $\text{MgO} \text{ -- } \text{CaO} \text{ -- } \text{TiO}_2 \text{ -- } \text{SiO}_2$ system, determined the fusibility (by fusing of cones) of the $\text{CaO} \text{ -- } \text{TiO}_2 \text{ -- } \text{SiO}_2$ system. Some information can be found in the extensive works of Agamavi and White [8], who studied the $\text{CaO} \text{ -- } \text{Al}_2\text{O}_3 \text{ -- } \text{TiO}_2 \text{ -- } \text{SiO}_2$ system. The ternary compound CaTiSiO_5 , sphene, was found in the system long ago. Ginzberg and Nikogosyan [4] have described the ternary compound $\text{CaO} \cdot 2\text{TiO}_2 \cdot 2\text{SiO}_2$, called calcium ramsayite.

In 1911, Smolensky [6], studying the $\text{CaSiO}_3 \text{ -- } \text{CaTiO}_3$ profile, discovered solid solutions. Feodot'yev [7] showed that there is a simple eutectic here, containing 20 weight % CaTiO_3 and 80 weight % CaSiO_3 . Iwase and Fukushima [10] have studied the two partial profiles $\text{CaO} \cdot \text{TiO}_2 \text{ -- } \text{SiO}_2$ and $\text{CaO} \cdot \text{SiO}_2 \text{ -- } \text{TiO}_2$, where the compound $\text{CaO} \cdot \text{SiO}_2 \cdot \text{TiO}_2$ is formed.

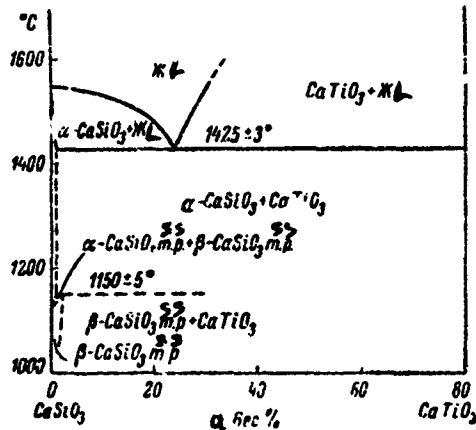


Fig. 245. Phase diagram of partial system
 $\text{CaO} \cdot \text{SiO}_2$ -- $\text{CaO} \cdot \text{TiO}_2$ (from DeVries and
 colleagues).

Key:

a. Weight %

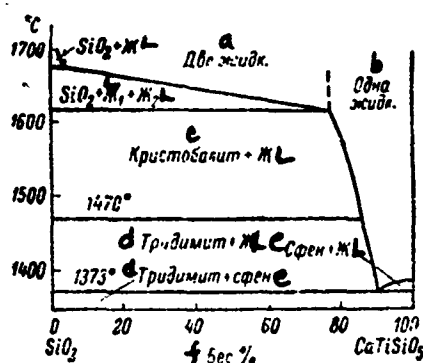
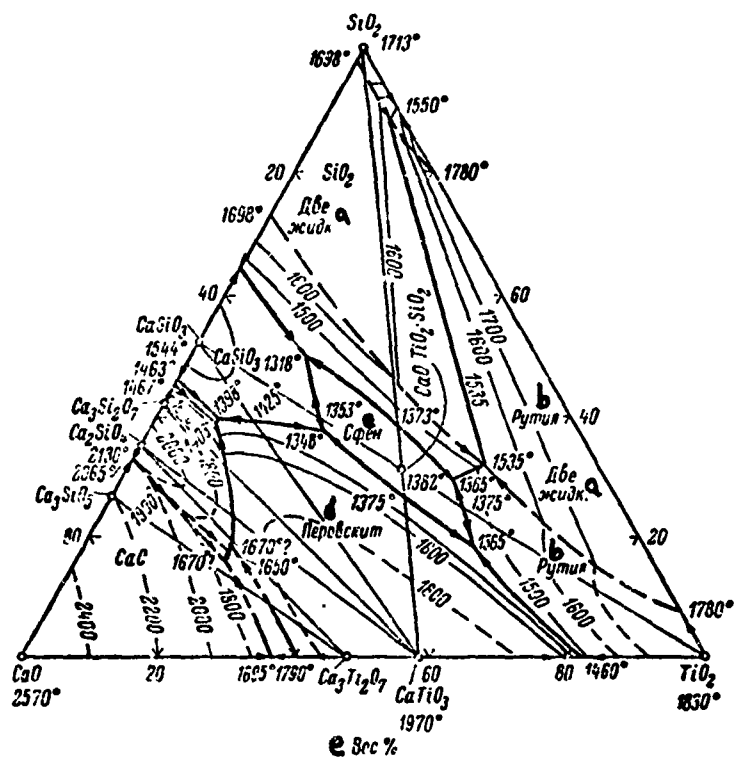


Fig. 246. Phase diagram of partial system
 CaTiSiO_5 -- SiO_2 (from DeVries and colleagues).

Key:

- | | |
|-----------------|--------------|
| a. Two liquids | d. Tridymite |
| b. One liquid | e. Sphene |
| c. Cristobalite | f. Weight % |

A detailed study of the system was carried out by DeVries and colleagues [9]. They studied the partial binary systems CaSiO_3 -- CaTiO_3 (Fig. 245) and CaTiSiO_5 -- SiO_2 (Fig. 246), and they plotted a complete triple diagram (Fig. 247). A considerable region of two immiscible liquids is located at the apex of the triangle adjacent to SiO_2 . Phase separation is characteristic of both binary systems: $\text{CaO} -- \text{SiO}_2$ and $\text{TiO}_2 -- \text{SiO}_2$.



Yeremin and colleagues [5], carrying out annealing at 1400°, showed that 0.75% TiO_2 dissolves in $\beta 2CaO \cdot SiO_2$ and that titanium dioxide is practically insoluble in the γ modification of dicalcium silicate. Thus, TiO_2 facilitates the process of transition of $\beta 2CaO \cdot SiO_2$ into $\gamma 2CaO \cdot SiO_2$.

Berezhnay and colleagues [3], on the basis of the thermodynamic properties of $CaTiSiO_5$, allowing for the partial density of oxygen in it, came to the conclusion that this compound should be stable at very high pressures. Berezhnay [2] made a triangulation system, showing that sphene coexists with $CaSiO_3$, $CaTiO_3$, SiC_2 and TiO_2 .

TABLE 1
CRYSTALLINE PHASES OF $CaO - TiO_2 - SiO_2$ SYSTEM

a Соединение	b Система кристаллов	c Габитус	d Спайность	Ng	Np	2V°	e Плотность, g/cm^3	f Оптическая ориентировка
$CaO \cdot TiO_2 \cdot SiO_2$ (сфен) g	Моноклинная	Таблички	Ясная по (110)	2.003	1.893	+23	3.4-3.56	Плоскость оптической оси (010)
$CaO \cdot TiO_2$ (перовскит) h	Кубическая (?)	Кубы, октаэдры и пр.	Слабая по (100)	2.38	-	+90	4.0	-

Key:

- | | |
|------------------------|--------------------------------|
| a. Compound | i. Monoclinic |
| b. Crystal system | j. Cubic |
| c. Appearance | k. Plates |
| d. Cleavage | l. Cubes, octahedra and others |
| e. Density, g/cm^3 | m. Distinct along (110) |
| f. Optical orientation | n. Weak along (100) |
| g. Sphene | o. Plane of optical axis (010) |
| h. Perovskite | |

TABLE 2. INVARIANT POINTS OF CaO -- TiO₂ -- SiO₂ SYSTEM

a Фазы	б Состав, вес. %			c Темп- ература, °C
	CaO	TiO ₂	SiO ₂	
CaO + Ca ₂ SiO ₅ + Ca ₂ Ti ₂ O ₅ + жидкость d	62.0	22.0	16.0	1670(?)
Ca ₂ SiO ₅ + Ca ₂ Ti ₂ O ₅ + Ca ₂ SiO ₄ + жидкость d	61.0	21.5	17.5	1650
Ca ₂ Ti ₂ O ₅ + Ca ₂ SiO ₄ + CaTiO ₃ + жидкость d	60.0	22.0	18.0	1671(?)
Ca ₂ SiO ₅ + Ca ₂ Ti ₂ O ₅ + CaO + жидкость d	65.5	3.0	26.5	1900
Ca ₂ SiO ₄ + CaTiO ₃ + Ca ₂ Si ₂ O ₇ + жидкость d	52.3	9.1	38.6	1403
CaTiO ₃ + Ca ₂ Si ₂ O ₇ + CaSiO ₃ + жидкость d	51.5	9.3	39.2	1398
CaTiO ₃ + a-CaSiO ₃ + CaTiSiO ₆ + жидкость d	36.8	26.2	37.0	1318
a-CaSiO ₃ + CaTiSiO ₆ + SiO ₂ (тринит) + жидкость d	33.1	17.5	49.4	1318
жидкость				
CaTiSiO ₆ + SiO ₂ (тринит) + TiO ₂ + жидкость d	22.2	48.8	29.0	1365
SiO ₂ (тринит) + SiO ₂ (кристобалит) + TiO ₂ + + жидкость d	19.0	50.7	30.3	1470
SiO ₂ (кристобалит) + TiO ₂ + жидкость d.	15.5	53.0	31.5	1535
TiO ₂ + CaTiSiO ₆ + CaTiO ₃ + жидкость d	1.5	10.5	88.0	1535
	24.5	57.5	18.0	1365

Key:

- | | |
|--------------------------|-----------------|
| a. Phases | d. Liquid |
| b. Composition, weight % | e. Tridymite |
| c. Temperature, °C | f. Cristobalite |

BIBLIOGRAPHY

1. Berezhnoy, A. S., Ogneupory, 15, 1950, 8, p. 350; 10, p. 446.
2. Berezhnoy, A. S., Mnogokomponentnye sistemy okislov, [Multicomponent Oxide Systems], Naukova dumka Press, Kiev, 1970, p. 193.
3. Berezhnoy, A. S., R. A. Kordyuk, N. V. Gul'ko, Trudy Ukrainsk. inst. ogneuporov, 7, 1963, p. 173.
4. Ginzberg, A. S., Kh. S. Nikogosyan, Izv. Geol. kom., 43, 1924, p. 397.
5. Yeremin, N. I., A. I. Yegereva, A. M. Dmitrievya, I. B. Firfarova, Zhurn. prikl. khim., 43, 1, 1970, p. 18.
6. Smolensky, S., Izv. SPb. politekhn. inst., 15, 1911, p. 245; Zs. anorgan. allgem. Chem., 73, 3, 1912, p. 293.
7. Feodot'yev, K. M., Zap. Vse oss. mineral obshch., [2], 68, 3, 1939, p. 425.
8. Agamavi, Y. M., J. White, Trans Brit. Ceram. Soc., 53, 1, 1954, p. 3.
9. DeVries, R. C., R. Roy, E. F. Osborn, J. Amer. Ceram. Soc., 38, 5, 1955, p. 158.
10. Iwase, K., M. Fukushima, Sci. Rep. Tokoku Imp. Univ., Honda vol., 25, 3, 1936, p. 504.

SrO -- TiO₂ -- SiO₂

The system has not been studied. Robbins [1] observed crystallization of the partial profile SrTiO₃ -- SiO₂ (between 1:1 and 1:9), by means of a high-temperature microscope. The liquidus temperature is over 1450° for the 1:1 mixture. The formation of only large (up to 2.5 mm long) crystals of SrTiO₃ was observed. Solid solutions were not found.

BIBLIOGRAPHY

1. Robbins, C.R., J. Crystal Growth, 2, No. 6, 402, 1968.

BaO -- TiO₂ -- SiO₂

Study of the system initially was limited to investigation of the BaTiO₃ -- SiO₂ profile, carried out by Rase and Roy [3], who used the quenching method (Fig. 248). Three barium titanosilicates were found in the system: BaTiSiO₅, BaTiSi₂O₇ and BaTiSi₃O₉. The first two compounds melt without decomposition, at 1400 and 1250°, respectively. The compound BaTiSi₃O₉, synthetic bentonite, was synthesized hydrothermally. It is stable under hydrothermal conditions up to only 965° and, under "dry" conditions, it dissociates into BaTiSi₂O₇ and SiO₂ at 1050°. The three eutectics have the respective compositions and melting temperatures: SiO₂ and BaTiSi₂O₇, 70 mole % SiO₂, 1245°; BaTiSi₂O₇ and BaTiSiO₅, 63 mole % SiO₂, 1246°; BaTiSiO₅ and BaTiO₃, 29 mole % SiO₂, 1260°. Barium titanate forms a solid solution with silica, with a small limiting concentration of the latter. The transition temperature of the cubic form of barium titanate to the hexagonal increases sharply, as a result of incorporation of SiO₂ into the BaTiO₃ lattice. Thus, while the temperature of this transition

for pure BaTiO_3 is 1460° , with a low SiO_2 content, the transition temperature is 1575° . The maximum concentration of silica in the cubic form is 8 mole % and, in the hexagonal, 4 mole %.

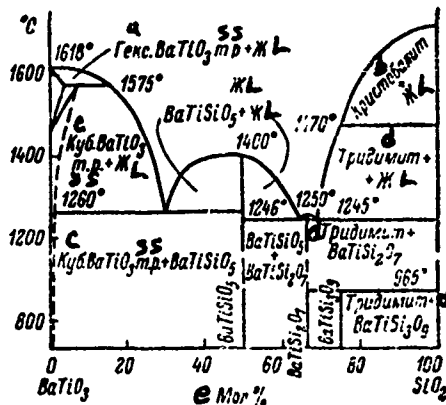


Fig. 248. Phase diagram of partial system $\text{BaTiO}_3 \text{ -- } \text{SiO}_2$ (from Rase and Roy).

Key:

- Hexagonal
- Cristobalite
- Cubic
- Tridymite
- Mole %

Berberova and colleagues [1] studied some sections of the system, using the noncrucible melting method. Solid solutions were not found in the partial system $\text{BaTiO}_3 \text{ -- } \text{BaSiO}_3$ or $\text{BaTiO}_3 \text{ -- } \text{SiO}_2$.

The $\text{BaTiO}_3 \text{ -- } \text{BaTiSiO}_5$ section is a simple eutectic. The $\text{BaTiO}_3 \text{ -- } \text{BaSiO}_3$ partial profile is distinguished by great complexity: the BaTiO_3 and BaSiO_3 fields do not coexist, and they are separated by fields of crystallization of barium orthotitanate, barium orthosilicate and bentonite.

Köppen and Dietzel [2] describe three barium titanosilicates: $2\text{BaO} \cdot \text{TiO}_2 \cdot 2\text{SiO}_2$, $\text{BaO} \cdot \text{TiO}_2 \cdot 2\text{SiO}_2$ and a third compound, with the formula not precisely established, approximately $\text{BaO} \cdot \text{TiO}_2 \cdot 3\text{SiO}_2$. The compound $\text{BaO} \cdot \text{TiO}_2 \cdot 2\text{SiO}_2$ melts congruently at approximately 1450° , and it does not disclose polymorphism. The elongated prismatic crystals are in the tetragonal crystal system. $\text{BaO} \cdot \text{TiO}_2 \cdot 2\text{SiO}_2$ melts incongruently at 1245° , with formation of $2\text{BaO} \cdot \text{TiO}_2 \cdot 2\text{SiO}_2$ and a melt, it exists in two forms, high-temperature tetragonal and low-temperature monoclinic or triclinic, with indices of refraction $\text{Ng} = 1.800$ and $\text{Np} = 1.742$. The third compound has indices of refraction $\text{Ng} = 1.693$ and $\text{Np} = 1.676$, which indicates a higher SiO_2 content than in $\text{BaO} \cdot \text{TiO}_2 \cdot 2\text{SiO}_2$. The compound with the conjectural formula $\text{BaO} \cdot \text{TiO}_2 \cdot 3\text{SiO}_2$ occurs in the SiO_2 field in the phase diagram, and it melts incongruently in the 1240 - 1250° range. The authors express the hypothesis that the new titanosilicate is a high-temperature modification of the mineral bentonite, having the formula $\text{BaO} \cdot \text{TiO}_2 \cdot 3\text{SiO}_2$.

BIBLIOGRAPHY

1. Berberova, L. M., M. I. Molokhovich, O. P. Kramarov, I. N. Belyayev, in the collection Mekhanizm i kinetika kristallizatsiya. Tezisy dokladov coveshchaniya 30 IX-6 X 1968 [Mechanism and Kinetics of Crystallization: Summaries of Reports to Conference 30 Sept. - 6 Oct. 1968], Minsk, 1968, p. 134.
2. Köppen, N., A. Dietzel, Naturwissenschaften, 56, No. 9, 460, 1969.
3. Rase, D. E., R. Roy, J. Amer. Ceram. Soc., 38, No. 11, 389, 1955.



The system has been studied by Agamawi and White [2], Galakhov [1], Murthy and Hummel [4] and others. A phase diagram for the high-silica part of the system, plotted by Agamawi and White, is presented in Fig. 249. Point

E is a triple eutectic, in which cristobalite, $\text{TiO}_2 \cdot \text{Al}_2\text{O}_3$, rutile and liquid are in equilibrium; the composition is 7.5 weight % Al_2O_3 , 13.5 TiO_2 and 79.0 SiO_2 ; temperature 1470°. The composition of point **R** is 8.2 weight % Al_2O_3 , 12.4 TiO_2 and 79.4 SiO_2 ; temperature 1430°. The partial system $\text{Al}_2\text{O}_3 \text{-- SiO}_2$ is presented in Fig. 250.

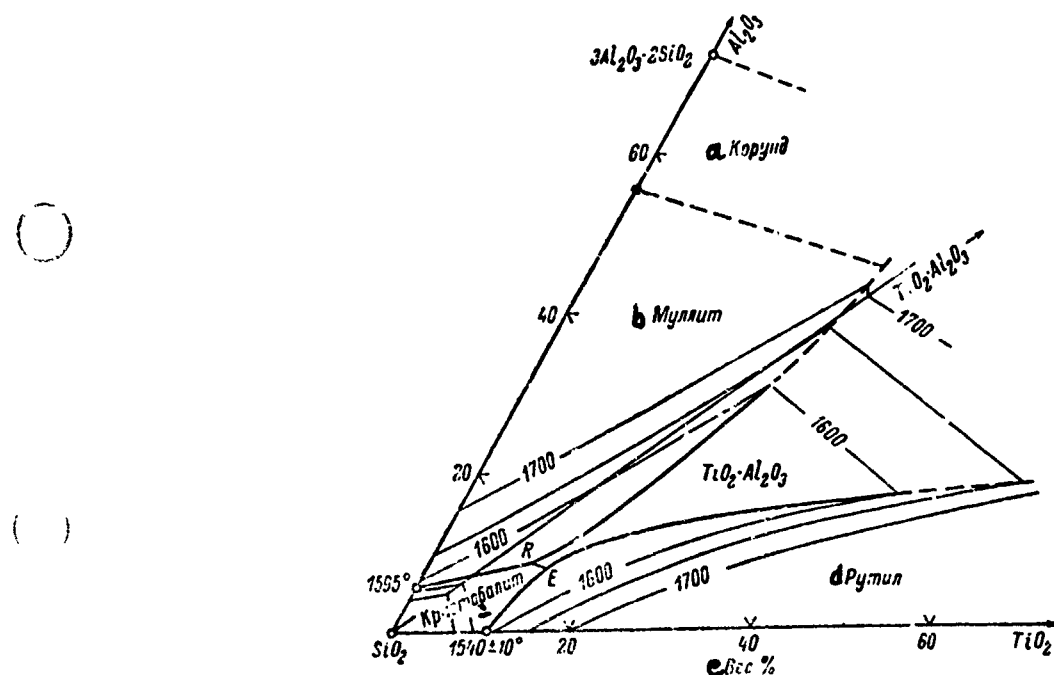


Fig. 249. Diagram of phase relationships of a $\text{Al}_2\text{O}_3 \text{-- TiO}_2 \text{ -- SiO}_2$ system in the region rich in silica (from Agamawi and White).

Key:

- a. Corundum
- b. Mullite
- c. Cristobalite
- d. Rutile
- e. Weight %

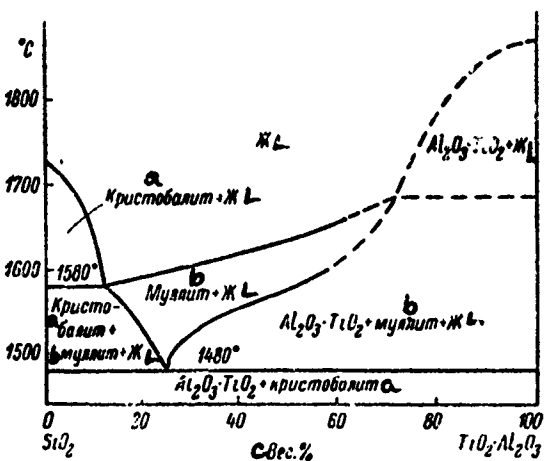


Fig. 250. Phase diagram of partial system
 SiO_2 -- $\text{Al}_2\text{O}_3 \cdot \text{TiO}_2$ (from Agamawi and White).

Key:

- a. Cristobalite
- b. Mullite
- c. Weight %

Galakhov [1] introduced a correction to the diagram of the system in the alumina region of it. He has refined the position of several boundary lines. A complete phase diagram of the Al_2O_3 -- TiO_2 -- SiO_2 system, according to the data of Agamawi and White, with additions by Galakhov, is given in Fig. 251. An invariant point having the composition 32 weight % TiO_2 , 52 Al_2O_3 and 16 SiO_2 , and a melting temperature of 1710° , which is common to the corundum, mullite and aluminum titanate ($\text{TiO}_2 \cdot \text{Al}_2\text{O}_3$) fields, is of a reaction nature, since it lies outside the fields of the phase triangle of the three compounds named.

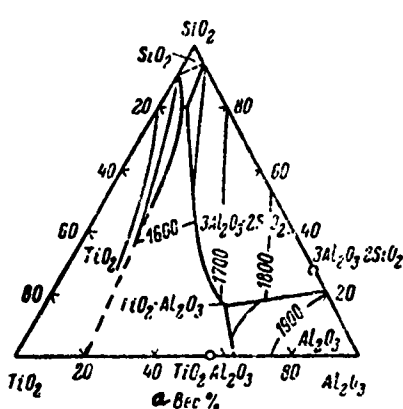


Fig. 251. Phase diagram of Al_2O_3 -- TiO_2 -- SiO_2 system (from Aginawi and White, with additions by Galakhov).

Key:

a. Weight %

Murthy and Hummel [4] have studied the solid solutions of titanium dioxide in mullite ($3\text{Al}_2\text{O}_3 \cdot 2\text{SiO}_2$). It was shown that, at 1000 and 1200°, no significant changes in the parameters were observed and, consequently, Ti^{4+} is not included in the mullite structure at these temperatures. With incorporation of Ti^{4+} into the mullite structure (1400° and higher), not only an enlargement of the unit cell, but distortion of it, takes place. Based on petrographic data, it can be considered that the solubility of TiO_2 in mullite at the temperatures studied is between 2 and 4%, which is in agreement with the data of Agrell and Smith [3], on the presence of TiO_2 in natural mullites. The authors noted a discrepancy between the petrographic and X-ray data.

BIBLIOGRAPHY

1. Galakhov, F. Ya., Izv. AN SSSR, OKhN, 5, 1958, p. 529.
2. Agamawi, Y. M., J. White, Trans. Brit. Ceram. Soc., 51, No. 5, 293, 1952.
3. Agrell, S. O., J. W. Smith, J. Amer. Ceram. Soc., 43, No. 2, 69, 1960.
4. Murthy, M. K., F. A. Hummel, J. Amer. Ceram. Soc., 43, No. 5, 267, 1960.



A possible phase diagram for the Ti_2O_3 -- TiO_2 -- SiO_2 system is introduced in Fig. 252, from the data of Roy and colleagues [1]. Ternary compounds are absent. Among the binary compounds, $Ti_2O_3 \cdot TiO_2$ (= Ti_3O_5 , anosovite) and the sesquisilicate of trivalent titanium ($3Ti_2O_3 \cdot 2SiO_2$) have been distinguished, as well as in extensive region of immiscibility of two liquid phases in the TiO_2 -- SiO_2 system boundary, extending within the ternary system to approximately a 10% Ti_2O_3 content.

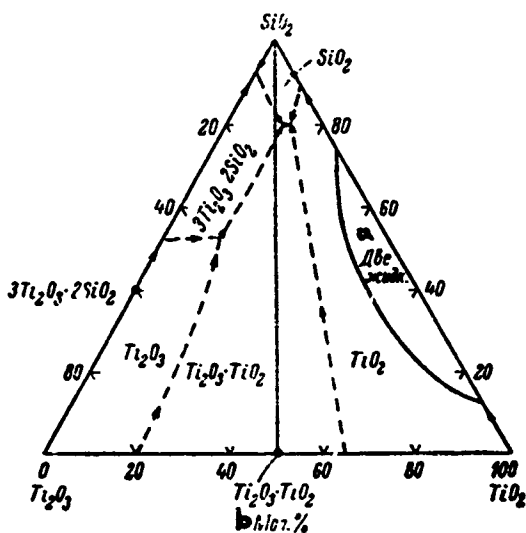


Fig. 252. Hypothetical phase diagram of Ti_2O_3 -- TiO_2 -- SiO_2 system (from Roy and colleagues).

Key: a. Two liquids b. Mole %

BIBLIOGRAPHY

1. Roy, R., R.C. DeVries, D.E. Rase, M.W. Shafer, E.F. Osborn, in: Levin, E.M., C.R. Robbins, H.F. McMurdie, Phase diagrams for ceramists, USA, Columbus, fig. 115, 1964.



The initial rough study of the system was carried out by Sowman and Andrews [4]. Ternary compounds were not found; a triple eutectic with a melting temperature of 1500° has the composition 2 weight % ZrO_2 , 10 TiO_2 and 88 SiO_2 (Fig. 253). McTaggart and Andrews [3] have distinguished the presence of immiscibility of the liquid phases, and they have shown a ZrTiO_4 field and excluded a ZrSiO_4 field in the hypothetical diagram (Fig. 254). Some information on the system was introduced in the work of Cocco and Schromek [2].

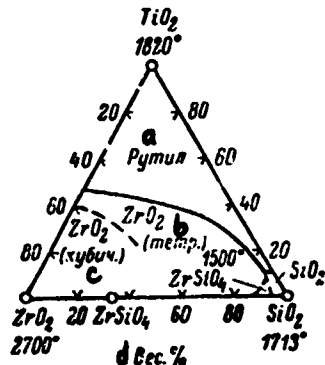


Fig. 253. Approximate phase diagram of ZrO_2 -- TiO_2 -- SiO_2 system (from Sowman and Andrews).

Key:

- a. Rutile
- b. Tetragonal
- c. Cubic
- d. Weight %

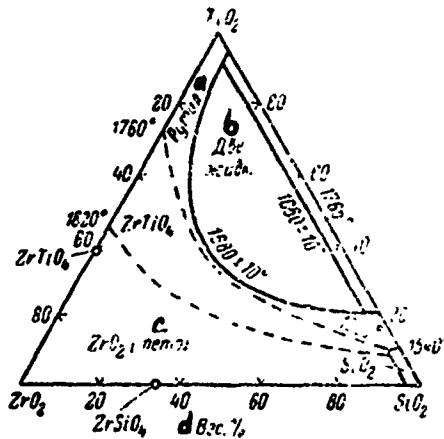


Fig. 254. Approximate phase diagram of ZrO_2 -- TiO_2 -- SiO_2 system (from McTaggart and Andrews).

Key:

- a. Rutile
- b. Two liquids
- c. Tetragonal
- d. Weight %

Berezhnay [1] has shown that ZrTiO_4 reacts with silica up to a temperature of 1500° and, therefore, the primary crystallization field of ZrTiO_4 in the work of McTaggart and Andrews was marked incorrectly. He also has shown that zircon and rutile coexist below the dissociation temperature of ZrSiO_4 at any pressure. In accordance with the triangulation carried out, ZrSiO_4 coexists with ZrTiO_4 .

BIBLIOGRAPHY

1. Berezhnay, A. S., Mnogokomponentnyye sistemy okislov (Multicomponent Oxide Systems], Naukov dumka Press, Kiev, 1970, p. 239.

2. Cocco, A., N. Schromek, Chim. e Industr. (Milano), 42, No. 5, 480, 1960.
3. McTaggart, G.D., A.I. Andrews, J. Amer. Ceram. Soc., 40, No. 5, 167, 1957.
4. Sowman, H.G., A.I. Andrews, J. Amer. Ceram. Soc., 34, No. 10, 298, 1951.



Smolensky [5] has studied the partial system $\text{MnO} \cdot \text{SiO}_2 \text{-- MnO} \cdot \text{TiO}_2$ (Fig. 255). Limiting solid solutions are formed with a content of from 0 to 61.7 mole % $\text{MnO} \cdot \text{SiO}_2$. Rhodonite $\text{MnO} \cdot \text{SiO}_2$ melts at 1218° , has a triclinic crystal system (Fedorov group $P\bar{1}$), and it belongs to the pyroxenoids, with five-fold repetition in location of the silicon-oxygen tetrahedra [4]. Liebau [3] distinguishes low and high-temperature forms of rhodonite; the latter is isostructural with bustamite or pseudowollastonite.

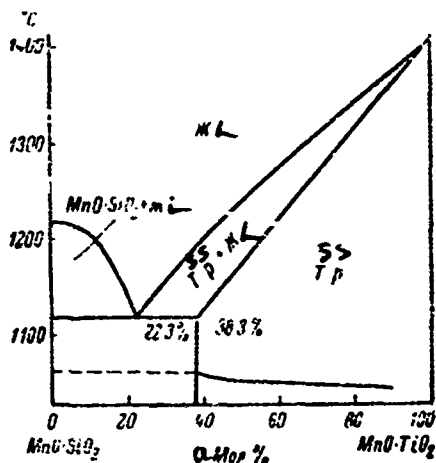


Fig. 255. Approximate phase diagram of partial system $\text{MnO} \cdot \text{SiO}_2 \text{-- MnO} \cdot \text{TiO}_2$ (from Smolensky).

Key:

a. Mole %

Pyrophanite $MnO \cdot TiO_2$, according to Smolensky, has a nonstoichiometric composition: 45.2 mole % SiO_2 and 54.8 mole % MnO ; its melting temperature is 1404° , density is 4.53 g/cm^3 , it is isostructural with ilmenite $FeTiO_3$ and geikielite $MgTiO_3$, trigonal crystal system, $R\bar{3}$. According to Portnov [2], for the natural mineral, $Ne = 2.07$, $No = 2.46$, $No-Ne = 0.39$.

BIBLIOGRAPHY

1. Dilaktorskiy, N. L., Trudy Petrogr. inst. AN SSSR, 6, 1934, p. 369.
2. Portnov, A. M., DAN SSSR, 153, 1, 1963, p. 187.
3. Liebau, F., W. Hilmer, J. Lindemann, Acta crystallogr., 12, No. 3, 182, 1959.
4. Liebau, F., M. Sprung, E. Thilo, Zs. anorgan. allgem. Chem., 297, No 3/4, 213, 1958.
5. Smolensky, S. S., Zs. anorgan. allgem. Chem., 73, No. 3, 299, 1912.

ZIRCONOSILICATE SYSTEMS



Schwarz and Haacke [4] have studied the fusibility diagram of the Li_4SiO_4 -- ZrSiO_4 profile (Fig. 256). The maximum found on the fusibility curve at 60 mole % ZrSiO_4 is connected with the hypothesis of the existence of a zirconosilicate of the composition $2\text{Li}_4\text{SiO}_4 \cdot 3\text{ZrSiO}_4$.

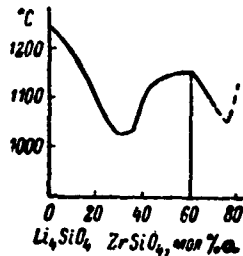


Fig. 256. Fusibility diagram of Li_4SiO_4 -- ZrSiO_4 system (from Schwarz and Haacke).

Key:

a. Mole %

Polezhayev and Chukhlantsev [1] have studied the structure of the subsolidus region of the system. They have studied the solid phase reactions between the following compounds: 1. $ZrSiO_4$ -- Li_2ZrO_3 , 2. $ZrSiO_4$ -- Li_2CO_3 , 3. $ZrSiO_4$ -- Li_4SiO_4 , 4. ZrO_2 -- Li_2SiO_3 , 5. Li_2ZrO_3 -- $Li_2Si_2O_5$, 6. Li_2ZrO_3 -- SiO_2 , 7. $ZrSiO_4$ -- Li_2SiO_3 , 8. ZrO_2 -- $Li_2Si_2O_5$, 9. ZrO_2 -- Li_4SiO_4 , 10. Li_2ZrO_3 -- Li_2SiO_3 , 11. Li_2ZrO_3 -- Li_4SiO_4 , 12. $ZrSiO_4$ -- $Li_2Si_2O_5$. Annealing of the corresponding mixtures was conducted at 30-50° below their melting temperatures (in the 900-1200° range), for periods of 100-140 hours.

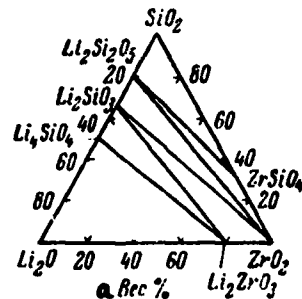


Fig. 257. Coexisting phase triangles of Li_2O -- ZrO_2 -- SiO_2 system (from Polezhayev and Chukhlantsev).

Key:

a. Weight %

Coexisting phase triangles are presented in Fig. 257, showing that, of the twelve binary profiles listed above, only profiles 4, 8, 10, 11 and 12 are true binary systems.

Polezhayev and Chukhlantsev did not find ternary compounds. Yet, Schenck indicates the compound $\text{Li}_2\text{ZrSiO}_5$ [3], and Fenton and Hyppert, the compound $2\text{Li}_2\text{O} \cdot \text{ZrO}_2 \cdot \text{SiO}_2$ [2], the existence of which is denied by Polezhayev and Chukhlantsev.

BIBLIOGRAPHY

1. Polezhayev, Yu. M., V. G. Chukhlantsev, Izv. AN SSSR, Neorg. mater., 1, 5, 1965, p. 784.
2. Fenton, W. M., P. A. Hyppert, Sheet Metal. Industr., 25, No. 259, 2255, 1948.
3. Schenck, J., Nucleonics, 10, No. 1, 54, 1952.
4. Schwarz, R., A. Haacke, Zs. anorgan. allgem. Chem., 115, No. 1, 87, 1921.



The system has been partially studied by D'Ans and Löffler [6], in the region adjacent to the $\text{Na}_2\text{O} -- \text{SiO}_2$ side (Fig. 258). Three ternary compounds have been found: $\text{Na}_2\text{O} \cdot \text{ZrO}_2 \cdot \text{SiO}_2$, melting with decomposition at 1473° ; $2\text{Na}_2\text{O} \cdot 2\text{ZrO}_2 \cdot 3\text{SiO}_2$, melting without decomposition at 1540° ; and $\text{Na}_2\text{O} \cdot \text{ZrO}_2 \cdot 2\text{SiO}_2$. In the binary system $\text{Na}_2\text{O} -- \text{ZrO}_2$, the compound $\text{Na}_2\text{O} \cdot \text{ZrO}_2$ melts with decomposition at 1800° . A phase diagram of the partial $\text{Na}_2\text{SiO}_3 -- \text{ZrO}_2$ is introduced in Fig. 259. Polezhayev and Chukhlantsev [4] have investigated the subsolidus portion of the system by X-ray phase and chemical phase analysis, and they obtained the same three ternary compounds. They plotted coexisting phase triangles (Fig. 260) which differ from those introduced by D'Ans and Löffler. Polezhayev and Chukhlantsev confirmed the existence of sodium pyrosilicate $\text{Na}_6\text{Si}_2\text{O}_7$, obtained by annealing Na_2ZrO_3 or ZrSiO_4 with soda or

sodium silicate. According to Zintl and Leverkus [8], sodium pyrosilicate is stable at temperatures above 402° and dissociates upon cooling according to the scheme $\text{Na}_6\text{Si}_2\text{O}_7 = \text{Na}_2\text{SiO}_3 + \text{Na}_4\text{SiO}_4$. In connection with this, the diagram in Fig. 260 holds true in the subsolidus region for temperatures over 402°.

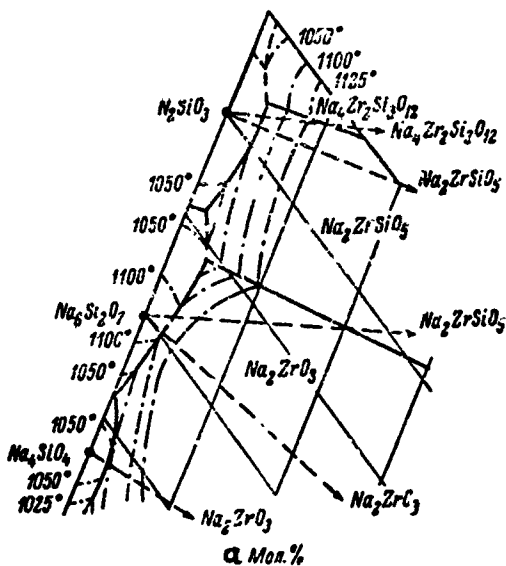


Fig. 258. Phase diagram of partial system $\text{Na}_2\text{O} \cdot \text{SiO}_2 \text{ -- } 2\text{Na}_2\text{O} \cdot \text{SiO}_2 \text{ -- } \text{ZrO}_2$ (from D'Ans and Löffler).

Key:

a. Mole %

The sequence of formation of sodium zirconosilicates, upon sintering a mixture of $2\text{ZrSiO}_4 + \text{Na}_2\text{CO}_3$ in the 900-1100° range, has been studied by Chukhlantsev and colleagues [5]. $\text{Na}_2\text{ZrSiO}_5$ forms first, together with other binary compounds. In proportion to further (in time) sintering, $\text{Na}_4\text{Zr}_2\text{Si}_3\text{O}_{12}$ forms initially and, finally, $\text{Na}_2\text{ZrSi}_2\text{O}_7$, which is the final product of the reaction, together with monoclinic ZrO_2 .

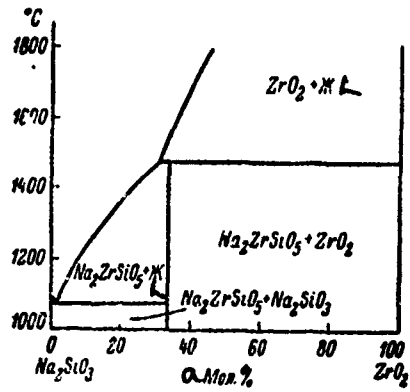


Fig. 259. Phase diagram of partial system $\text{Na}_2\text{O} \cdot \text{SiO}_2$ -- ZrO_2 (from D'Ans and Löffler).

Key:

a. Mole %

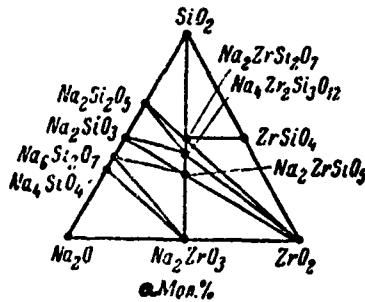


Fig. 260. Coexisting phase triangles of $\text{Na}_2\text{O} \text{--} \text{ZrO}_2 \text{--} \text{SiO}_2$ system (from Polezhayev and Chukhlantsev).

Key:

a. Mole %

Polezhayev and colleagues [3] have studied the decomposition of the zirconosilicate $\text{Na}_2\text{ZrSiO}_5$, upon heating over 1100° , showing that, in this case, $\text{Na}_4\text{Zr}_2\text{Si}_3\text{O}_{12}$, $\text{Na}_2\text{ZrSi}_2\text{O}_7$ and, finally, a melt form in sequence. The auto-catalytic nature of formation of the two latter zirconosilicates was demonstrated.

CRYSTALLINE PHASES OF $\text{Na}_2\text{O} - \text{ZrO}_2 - \text{SiO}_2$ SYSTEM

a Соединение	b Система кристаллов	c Габитус	<i>N_B</i>	<i>N_P</i>	<i>2V°</i>	Плот- ность, г/см ³
$2\text{Na}_2\text{O} + 2\text{ZrO}_2 + 3\text{SiO}_2$	e Гексагональ- ная	k Ромбоэдры	1.715	1.632	(—)	2.83
$\text{Na}_2\text{O} + \text{ZrO}_2 + \text{SiO}_2$	f Ромбическая	i Псевдооктаго- нальные двой- ники, призмы	1.790	1.741	Малый	3.00
$\text{Na}_2\text{O} + \text{ZrO}_2 + 2\text{SiO}_2$	g Вероятно, моноclinic	j Нити	1.710	1.633	—	—

Key:

- a. Compound
- b. Crystal system
- c. Appearance
- d. Density, g/cm³
- e. Hexagonal
- f. Rhombic
- g. Probably monoclinic
- h. Rhombohedra
- i. Pseudohexagonal twins, prisms
- j. Needles
- k. Small

Fukui and Ogawa [7], studying the effect of the vapors of salts (Na_2CO_3 , Na_2SO_4 , NaCl) on zircon refractories, observed formation of the same three zirconosilicates: $\text{Na}_2\text{ZrSiO}_5$, $\text{Na}_2\text{ZrSi}_2\text{O}_7$ and $\text{Na}_4\text{Zr}_2\text{Si}_3\text{O}_{12}$.

Vargin and Heifetz [2] and Botvinkin and Demichev [1] have studied glasses in the $\text{Na}_2\text{O} - \text{ZrO}_2 - \text{SiO}_2$ system.

BIBLIOGRAPHY

1. Botvinkin, O. R., S. A. Demichev, Steklo, 2, 1964, p. 1.
2. Vargin, V. V., Ye. M. Milyukov, V. S. Heifetz, Zhurn. prikl. khim., 40, 1, 1967, p. 183.
3. Polezhayev, Yu. M., K. V. Alyamovskaya, V. G. Chukhlantsev, Zhurn. neorg. khim., 14, 8, 1969, p. 2277.
4. Polezhayev, Yu. M., V. G. Chukhlantsev, Izv. AN SSSR. neorg. mater., 1, 11, 1965, p. 1990.
5. Chukhlantsev, V. G., Yu. M. Polezhayev, K. V. Alyamovskaya, Ibid., 4, 5, 1968, p. 745.
6. D'Ans, J., J. Löffler, Zs. anorgan. allgem. Chem., 191, No. 1, 1, 1930.
7. Fukui, T., H. Ogawa, Rep. Res. Lab. Asahi Glass Co., 17, No. 2, 77, 1967.
8. Zintl, E., H. Leverkus, Zs. anorgan. allgem. Chem., 243, 1, 1939, p. 1.

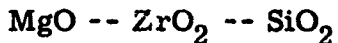


Chukhlantsev and Alyamovskaya [1] have shown that a ternary compound, rubidium zirconosilicate $\text{Rb}_2\text{ZrSi}_2\text{O}_7$ exists in the system; it was obtained by means of prolonged sintering (75-100 hours) of zircon with rubidium carbonate or silicate, at 870-950°. $\text{Rb}_2\text{ZrSi}_2\text{O}_7$ melts above 1350°, its density is $3.84 \pm 0.03 \text{ g/cm}^3$, it is easily broken down by diluting with solutions of strong acids, and it is completely soluble upon heating in hydrochloric acid (1:1). An equimolecular mixture of the resulting compound with silica begins to melt at 1000-1100°, with formation of a glass-like product.

Subsequently, Chukhlantsev and Alyamovskaya [2] showed that there is a more silica-rich zirconosilicate $\text{Rb}_2\text{ZrSi}_4\text{O}_{11}$, obtained by annealing appropriate mixtures of ZrSiO_4 , ZrO_2 , SiO_2 and rubidium carbonate, initially at 860° (10 hours), then at 1050° (150 hours). $\text{Rb}_2\text{ZrSi}_4\text{O}_{11}$ is more stable thermally than $\text{Rb}_2\text{ZrSi}_2\text{O}_7$, and it is produced from the latter at a temperature of 950°.

BIBLIOGRAPHY

1. Chukhlantsev, V.G., K.V. Alyamovskaya, Izv. AN SSSR. neorg. mater., 1, 11, 1965, p. 1994.
2. Chukhlantsev, V.G., K.V. Alyamovskaya, Ibid., 3, 10, 1967, p. 1892.



Foster [3] and Berezhnoy and Karyakin [2] have triangulated the system and plotted coexisting phase triangles (Fig. 261). These authors have not confirmed the existence of the ternary compounds $\text{MgO} \cdot \text{ZrO}_2 \cdot \text{SiO}_2$ and $4\text{MgO} \cdot \text{ZrO}_2 \cdot \text{SiO}_2$, which was indicated by Roussin and Chesters [5]. Berezhnoy and Karyakin have studied the fusibility diagram of the system. The most easily melted triple eutectic has the approximate composition 60 weight % SiO_2 , 15 weight % ZrO_2 and 25 weight % MgO , and a melting temperature of about 1500°. Solid solutions in the system being considered are limited only to a field adjacent to ZrO_2 . The latter does not form solid solutions with magnesium silicates. A limiting composition is introduced for the binary solid solution of MgO in ZrO_3 , corresponding to the formula $\text{Mg}_2\text{Zr}_3\text{O}_8 = 4(\text{Zr}_{0.75}\text{Mg}_{0.5})\text{O}_2$. In the partial section $\text{ZrO}_2 \text{ -- } \text{Mg}_2\text{SiO}_4$, a eutectic containing 15 weight % ZrO_2 melts at 1677°, and, in the section $\text{ZrSiO}_4 \text{ -- } \text{Mg}_2\text{SiO}_4$, at 1577° (30 weight % ZrSiO_4). As a result of a thermodynamic analysis and study of the kinetics of the reaction $3\text{ZrSiO}_4 + 8\text{MgO} = 3\text{Mg}_2\text{SiO}_4 + 4(\text{Zr}_{0.75}\text{Mg}_{0.5})\text{O}_2$, Berezhnoy [1] came to the conclusion that the reaction takes place only in the direction indicated, in the temperature range from 600 to 1500° and at pressures between 1 atm and 120 kbar.

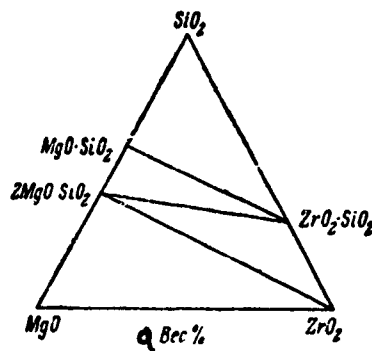


Fig. 261. Coexisting phase triangles of $\text{MgO} - \text{ZrO}_2 - \text{SiO}_2$ system (from Berezhnoy).

Key:

a. Weight %

Hossain and Brett [4] have studied the system by the quenching method, in the region adjacent to the $\text{MgO} - \text{SiO}_2$ side; the ZrO_2 content reached only 25 weight %. Some partial sections, laid out parallel to the $\text{MgO} - \text{SiO}_2$ side are introduced in Fig. 262. The liquidus curves in the triple system are shown in Fig. 263. The zircon field is defined by the invariant points introduced in the table.

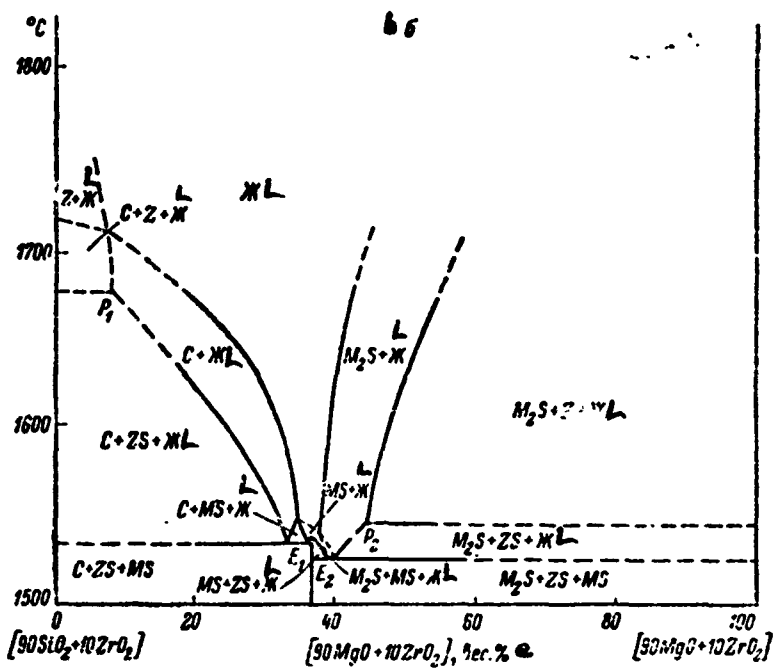
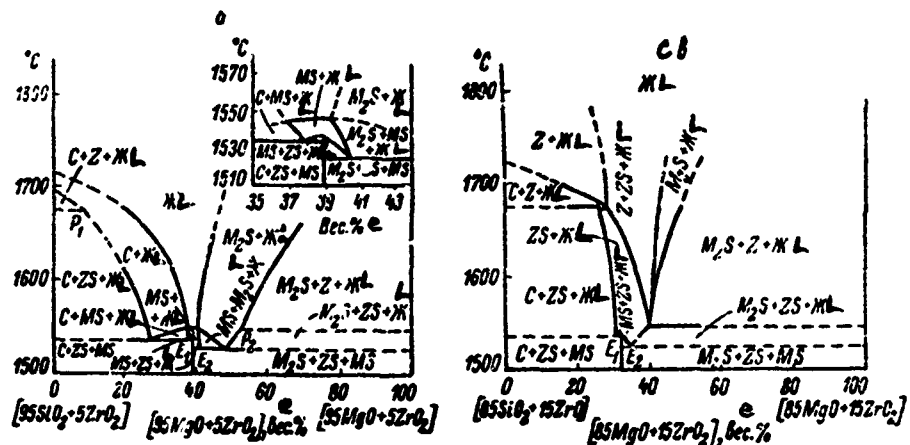


Fig. 262. Phase diagrams of various sections of $\text{MgO} - \text{ZrO}_2 - \text{SiO}_2$ system (from Hossain and Brett):
 Sections: a. $(95\text{SiO}_2 + 5\text{ZrO}_2) - (95\text{MgO} + 5\text{ZrO}_2)$;
 b. $(90\text{SiO}_2 + 10\text{ZrO}_2) - (90\text{MgO} + 10\text{ZrO}_2)$;
 c. $(85\text{SiO}_2 + 15\text{ZrO}_2) - (85\text{MgO} + 15\text{ZrO}_2)$;
 C Cristobalite

C. Cristobalite

Key:

e. Weight %

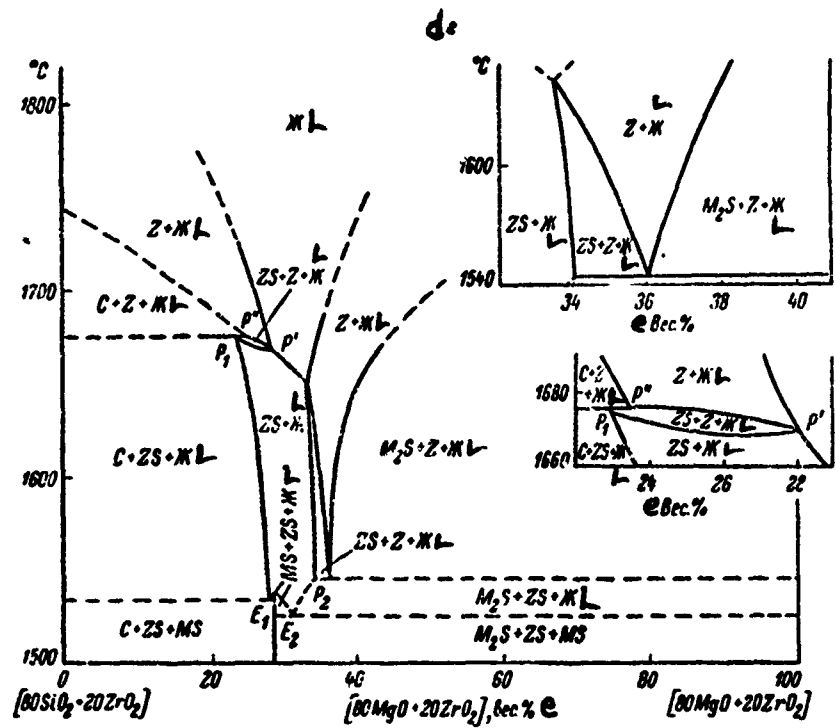


Fig. 262. (continued): d. $(80\text{SiO}_2 + 20\text{ZrO}_2)$ -- $(80\text{MgO} + 20\text{ZrO}_2)$; C. Cristobalite.

Key:

e. Weight %

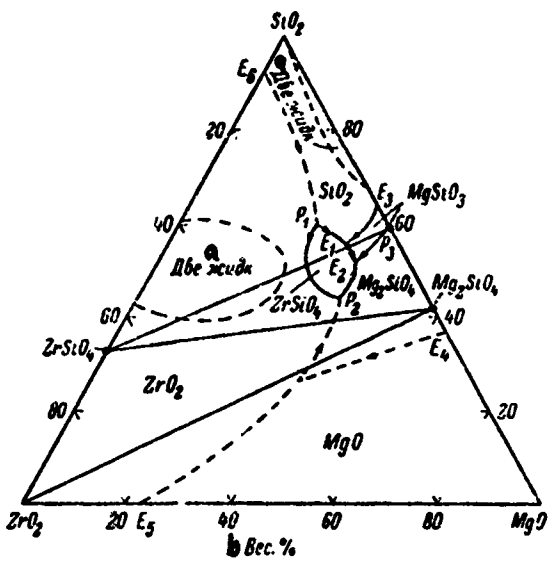


Fig. 263. Fusibility diagram of $\text{MgO} - \text{ZrO}_2 - \text{SiO}_2$ system (from Hossain and Brett).

Key:

a. Two liquids b. Weight %

INVARIANT POINTS OF PARTIAL TERNARY SYSTEM
 $\text{Mg}_2\text{SiO}_4 - \text{ZrSiO}_4 - \text{SiO}_2$ (from Hossain and Brett)

a Точка (Fig. 263)	b Процесс	c. Состав, вес.%			d Температура, °C
		MgO	ZrO ₂	SiO ₂	
P_1	Перитектика e	27	14	59	1675
E_1	Эвтектика f	35.5	10.5	54	1534
E_2	*	38	11	51	1525
P_2	Перитектика e	39	17	44	1515

Key:

- a. Points (Fig. 263)
- b. Process
- c. Composition, weight %
- d. Temperature, °C
- e. Peritectic
- f. Eutectic

BIBLIOGRAPHY

1. Berezhnoy, A. S., Mnogokomponentnye sistemy okislyv [Multicomponent Oxide Systems], Naukov dumka Press, Kiev, 1970, p. 217.
2. Berezhnoy, A. S., L. I. Karyakin, Ogneupory, 17, 1952, 3, p. 111; 5, p. 211.
3. Foster, W. R., J. Amer. Ceram. Soc., 34, No. 10, 301, 1951.
4. Hossain, D., M. H. Brett, Trans. Brit. Ceram. Soc., 68, No. 4, 145, 1969.
5. Roussin, A. L., J. H. Chesters, Trans. Brit. Ceram. Soc., 30, No. 6, 217, 1931.



The first investigation of the system was done by Matsumoto and colleagues [8], who, determining the composition of cast refractory blocks, plotted an approximate fusibility diagram (Fig. 264). The authors did not find a single ternary compound.

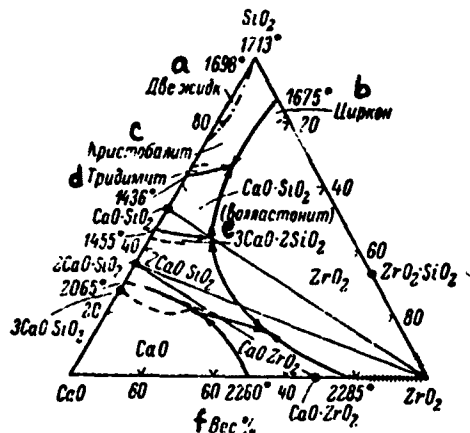


Fig. 264. Approximate fusibility diagram of $\text{CaO} - \text{ZrO}_2 - \text{SiO}_2$ system (from Matsumoto and Sawamoto).

Key:

- | | |
|-----------------|-----------------|
| a. Two liquids | d. Tridymite |
| b. Zircon | e. Wollastonite |
| c. Cristobalite | f. Weight % |

Berezhnay and Kordyuk [2] have studied the fusibility of the system, and they have found two ternary compounds: $3\text{CaO}\cdot\text{ZrO}_2\cdot 2\text{SiO}_2$ (I), melting incongruently at around 1600° , with formation of $2\text{CaO}\cdot\text{SiO}_4$ and ZrO_2 , and the compound $2\text{CaO}\cdot\text{ZrO}_4\cdot 4\text{SiO}_2$ (II), melting incongruently with formation of ZrSiO_4 . On the basis of optical studies, it is noted that ZrO_2 does not form solid solutions with Ca_2SiO_4 . The most easily melted eutectic, melting at around 1400° , is located close to the eutectic CaSiO_3 -- SiO_2 , and it contains about 3-5 weight % ZrO_2 . Crystals of $3\text{CaO}\cdot\text{ZrO}_2\cdot 2\text{SiO}_2$ belong conjecturally to the rhombic crystal system, with indices of refraction $\text{Ng} = 1.758$, $\text{Nm} = 1.737$ and $\text{Np} = 1.735$, density is 3.46 g/cm^3 ; crystals of $2\text{CaO}\cdot\text{ZrO}_4\cdot 4\text{SiO}_2$ belong to the rhombic crystal system, with indices of refraction $\text{Ng} = 1.658$ and $\text{Np} = 1.653$, density 3.06 g/cm^3 .

TABLE 1
CHARACTERISTICS OF TERNARY COMPOUNDS IN
 $\text{CaO} - \text{ZrO}_2 - \text{SiO}_2$ SYSTEM

	$\text{Ca}_2\text{ZrSi}_2\text{O}_9$	$\text{Ca}_2\text{ZrSi}_4\text{O}_{11}$
a Плавление, $^\circ\text{C}$	1600 ^e , с разложением на $\text{Ca}_2\text{SiO}_4 + \text{ZrO}_2 +$ + расплав	1400 ^f , с разложением на $\text{ZrSiO}_4 +$ + расплав
b Симметрия	g Ромбическая (?)	g Ромбическая (?)
Ng	1.758	1.658
Nm	1.735	1.653
$\text{Np} - \text{Ng}$	0.023	0.005
$2V^\circ$	292'	—
Плотность, g/cm^3 d	3.46	3.06
$\alpha \cdot 10^{-4}$	11.0	5.9

Key:

- a. Melting temperature, $^\circ\text{C}$
- b. Symmetry
- d. Density, g/cm^3
- e. With decomposition into $\text{Ca}_2\text{SiO}_4 + \text{ZrO}_2 +$ melt
- f. With decompositio' into $\text{ZrSiO}_4 +$ melt
- g. Rhombic (?)

Kordyuk and Gul'ko [4], studying the subsolidus region of the partial system CaSiO_3 -- ZrO_2 , did not confirm the presence of the ternary compound CaZrSiO_5 , which Estrada [7] mentioned. These authors found that ternary compound (I) does not react with ZrO_2 or calcium silicates, and that there is no reaction between (II) and ZrO_2 , ZrSiO_4 , SiO_2 or CaSiO_3 . The characteristics of the ternary compounds are presented in Table 1.

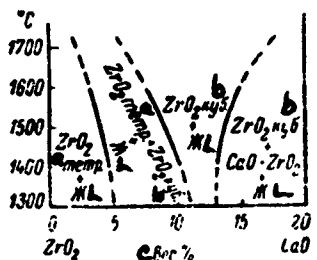


Fig. 265. Schematic diagram of phase relationships of $\text{CaO} - \text{ZrO}_2 - \text{SiO}_2$ system in region rich in ZrO_2 , with 4% SiO_2 content (from Cocco and Barbariol).

Key:

- a. Tetragonal
- b. Cubic
- c. Weight %

The effect of small additions of SiO_2 (4%) to the $\text{CaO} - \text{ZrO}_2$ system has been studied by Cocco and Barbariol [6]. The diagram is presented in Fig. 265.

Quereshi and Brett [9, 10], using the quenching method, with phase identification in a reflecting microscope and by the X-ray method, gave a more complete characterization of the phase relationships in the system. The authors confirmed the existence of the ternary compound $\text{Ca}_3\text{ZrSi}_2\text{O}_9$ ($3\text{CaO} \cdot \text{ZrO}_2 \cdot 2\text{SiO}_2$), which melts incongruently at 1635° . The composition of the compound was determined by means of electron microprobe analysis. Crystals of $\text{Ca}_3\text{ZrSi}_2\text{O}_9$ have low symmetry. Quereshi and Brett considered separately the data on three partial systems: 1. SiO_2 -- $\text{CaO} \cdot \text{SiO}_2$ -- ZrO_2 , 2. $\text{CaO} \cdot \text{SiO}_2$ -- $2\text{CaO} \cdot \text{SiO}_2$ -- ZrO_2 , 3. CaO -- $2\text{CaO} \cdot \text{SiO}_2$ -- ZrO_2 .

In the partial system SiO_2 -- $\text{CaO} \cdot \text{SiO}_2$ -- ZrO_2 , six double profiles have been studied, beginning with ZrO_2 and proceeding to the $\text{CaO} \cdot \text{SiO}_2$ side, to points corresponding to 15, 30, 35, 47, 60 and 90 weight % SiO_2 content. Two profiles are introduced in Figs. 266a and b. A fusibility diagram of this triple partial system is given in Fig. 267. Attention is drawn here to the presence of a small field of zircon ZrSiO_4 and a region of immiscibility of the liquids. The compounds of $2\text{CaO} \cdot \text{ZrO}_2 \cdot 4\text{SiO}_2$, to which Berezhnoy and Kordyuk referred, were not found by the authors and, using X-ray microprobe analysis, they determined that pure zircon is separated out as the initial phase in the region being considered and that the lowest temperature of coexistence of the two liquids is $1662 \pm 5^\circ$.

In study of the partial system $\text{CaO} \cdot \text{SiO}_2$ -- $2\text{CaO} \cdot \text{SiO}_2$ -- ZrO_2 , the authors studied twelve binary profiles, each of which proceeds from ZrO_2 . Four of the most typical phase diagrams are presented in Fig. 268. The partial system $\text{CaO} \cdot \text{SiO}_2$ -- ZrO_2 (Fig. 268a) has one eutectic (16 weight % ZrO_2), melting at 1460° . The fusibility diagram (the liquidus surface) of the system $\text{CaO} \cdot \text{SiO}_2$ -- $2\text{CaO} \cdot \text{SiO}_2$ -- ZrO_2 is represented in Fig. 269.

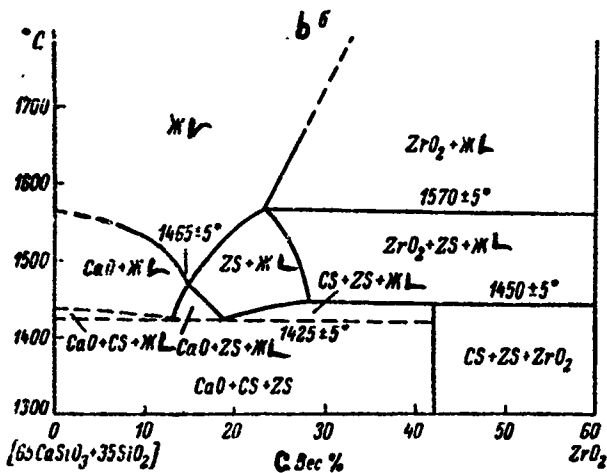
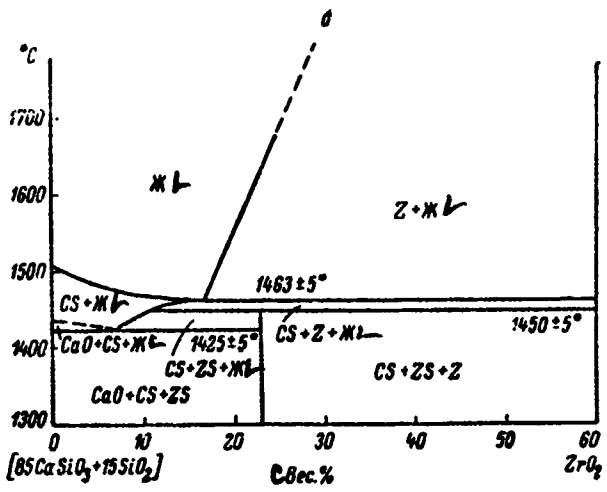


Fig. 266. Phase diagram of some sections of partial triple system ZrO_2 -- $\text{CaO} \cdot \text{SiO}_2$ -- SiO_2 (from Quereshi and Brett): a. section $(85\text{CaSiO}_3 + 15\text{SiO}_2)$ -- ZrO_2 ; b. section $(65\text{CaSiO}_3 + 35\text{SiO}_2)$ -- ZrO_2 .

Key:

c. Weight %

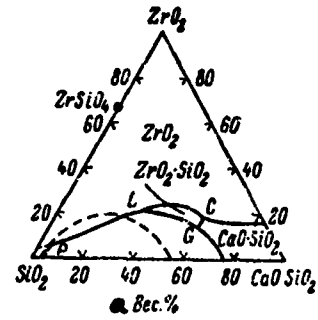


Fig. 267. Fusibility diagram of partial triple system $\text{CaO} \cdot \text{SiO}_2$ -- ZrO_2 -- SiO_2 (from Quereshi and Brett).

Key:

a. Weight %

TABLE 2
INVARIANT POINTS OF $\text{CaO} \cdot \text{ZrO}_2 \cdot \text{SiO}_2$ SYSTEM
(from Quereshi and Brett)

a Точка (рис. 267, 269, 270)	b Процесс	c Состав, вес. %			d T , темпера- тура, °C
		CaO	SiO ₂	ZrO ₂	
C	Перитектика e	28.1	53.9	18.0	1450
G	Эвтектика f	27.5	58.2	14.0	1425
L	Перитектика e	15.4	64.6	20.0	1650
P		2.0	93.0	5.0	1667
q		48.0	35.9	15.5	1635 ± 5
a	Эвтектика f	41.1	43.4	15.5	1460 ± 5
t	Перитектика e	53.5	44.0	2.5	1455 ± 5
w	Эвтектика f	53.0	44.5	2.5	1445 ± 5
z	Перитектика e	66.2	24.8	9.0	1950 ± 25
s	Эвтектика f	65.0	25.0	10.0	1925 ± 25
5		52.0	24.0	24.0	1970 ± 25

Key:

- | | |
|---------------------------------|--------------------|
| a. Points (Figs. 267, 269, 270) | d. Temperature, °C |
| b. Process | e. Peritectic |
| c. Composition, weight % | f. Eutectic |

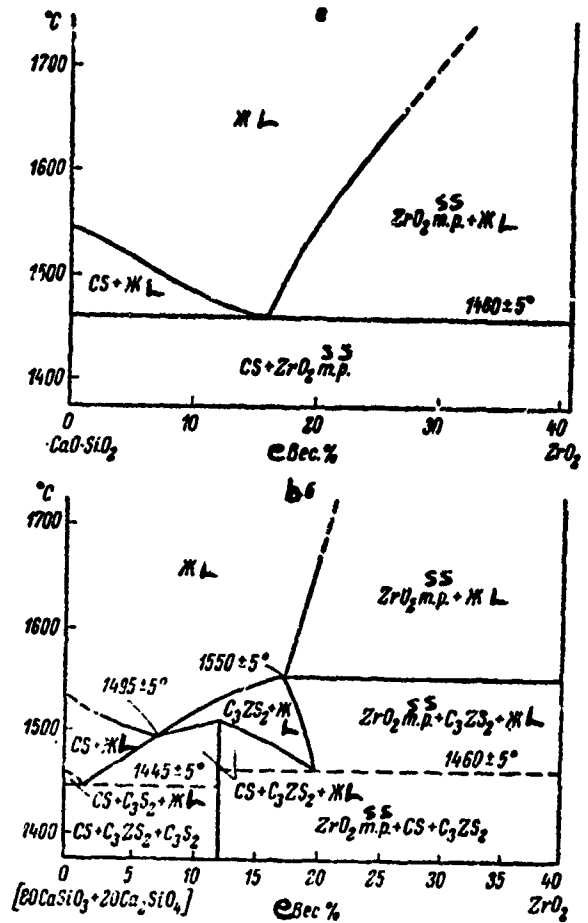


Fig. 268. Phase diagrams of some sections of partial triple system $\text{CaO} \cdot \text{SiO}_2$ -- $2\text{CaO} \cdot \text{SiO}_2$ -- ZrO_2 (from Qureshi and Brett): Sections: a. $\text{CaO} \cdot \text{SiO}_2$ -- ZrO_2 ; b. $(80\text{CaSiO}_3 + 20\text{Ca}_2\text{SiO}_4)$ -- ZrO_2 .

Key:

e. Weight %

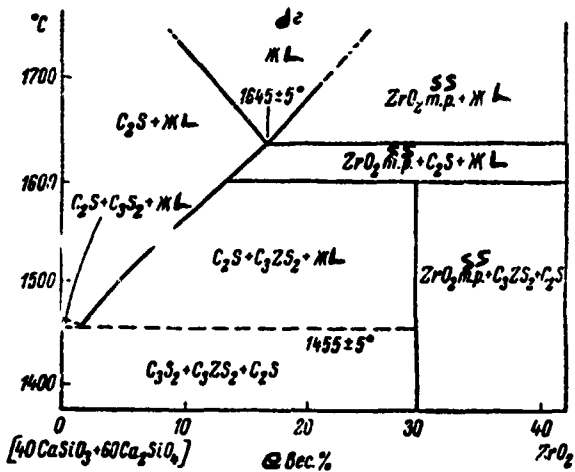
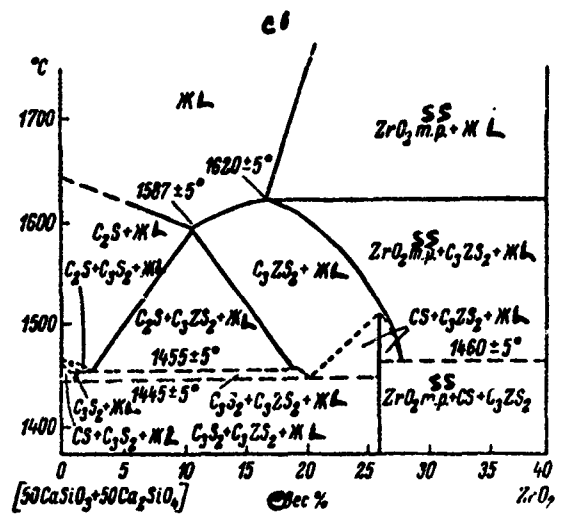


Fig. 268 (continued):

- c. $(50\text{CaSiO}_3 + 50\text{Ca}_2\text{SiO}_4) \text{ -- } \text{ZrO}_2$;
- d. $(40\text{CaSiO}_3 + 60\text{Ca}_2\text{SiO}_4) \text{ -- } \text{ZrO}_2$.

Key:

e. Weight %

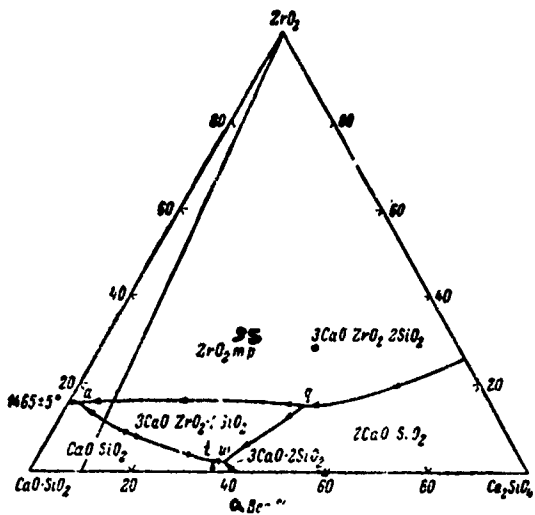


Fig. 269. Fusibility diagram of partial triple system $\text{CaO}\cdot\text{SiO}_2$ -- $2\text{CaO}\cdot\text{SiO}_2$ -- ZrO_2 (from Quereshi and Brett).

Key:

a. Weight %

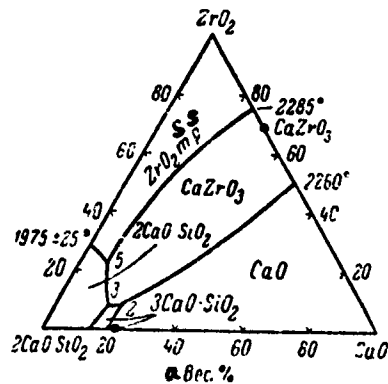


Fig. 270. Fusibility diagram of partial system $2\text{CaO}\cdot\text{SiO}_2$ -- CaO -- ZrO_2 (from Quereshi and Brett).

Key:

a. Weight %

High liquidus temperatures (over 2000°) are characteristic of the triple partial system $\text{CaO} \text{ -- } ?\text{CaO}\cdot\text{SiO}_2 \text{ -- } \text{ZrO}_2$. A fusibility diagram of the system is presented in Fig. 270, which was plotted on the basis of study of eight binary profiles, proceeding from ZrO_2 in the direction of $\text{CaO} \text{ -- } 2\text{CaO}\cdot\text{SiO}_2$. Two temperature maxima are noted: 1. in the partial system $\text{CaZrO}_3 \text{ -- } \text{Ca}_2\text{SiO}_4$, $2025 \pm 25^\circ$; 2. in the partial system $\text{Ca}_2\text{SiO}_4 \text{ -- } \text{ZrO}_2$, $1975 \pm 25^\circ$.

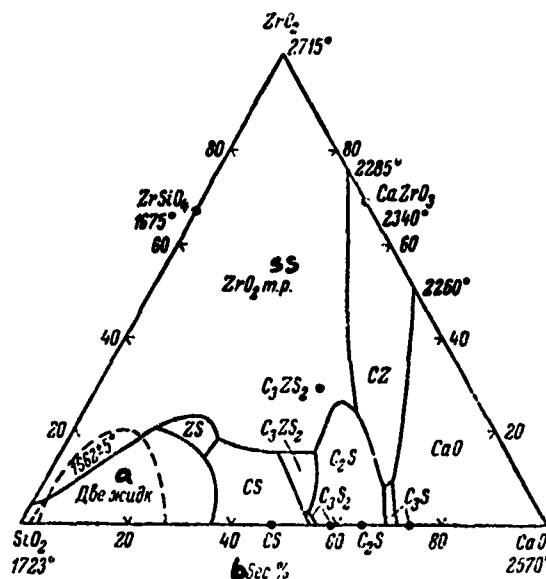


Fig. 271. Phase diagram of $\text{CaO} \text{ -- } \text{ZrO}_2 \text{ -- } \text{SiO}_2$ system (from Quereshi and Brett).

Key:

- Two liquids
- Weight %

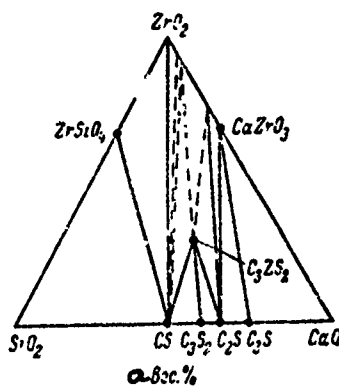


Fig. 272. Coexisting phase triangles of $\text{CaO} - \text{ZrO}_2 - \text{SiO}_2$ system (from Quereshi and Brett).

Key:

a. Weight %

Complete phase diagram of the $\text{CaO} - \text{ZrO}_2 - \text{SiO}_2$ system is represented in Fig. 271. The coexisting phase triangles (triangulation) of the triple system, showing the phases coexisting in the $1500-2000^\circ$ temperature range, are given in Fig. 272.

According to Kordyuk [3], the compound $\text{Ca}_3\text{ZrSi}_2\text{O}_9$ is formed easily from a mixture of calcium oxides or silicates and ZrO_2 at temperatures over 1200° , and the compound $\text{Ca}_2\text{ZrSi}_4\text{O}_{12}$, at 1400° and 15 hours exposure. The last compound possibly is identical with the mineral eucolite, the composition of which has not been precisely established.

Chukhlantsev and Galkin [5] annealed a mixture of CaO and ZrSiO_4 at 1100 , 1200 and 1350° , with subsequent chemical and X-ray analysis. Besides

CaZrO_3 and calcium silicates, $\text{Ca}_3\text{ZrSi}_2\text{O}_9$ and $\text{Ca}_2\text{ZrSi}_4\text{O}_{12}$ occurred in the reaction products. The compound CaZrSiO_5 was not found, which is in agreement with the data of Kordyuk and Gui'ko.

Belyavskaya and Kupriyanova [1] selected specific solvents for the $\text{CaO} - \text{ZrO}_2 - \text{SiO}_2$ system, which permitted determination, with sufficient accuracy, of the content in the mixture of the compounds CaC , ZrO_2 , SiO_2 , CaSiO_3 , Ca_2SiO_4 , CaZrC_3 , $\text{Ca}_3\text{ZrSi}_2\text{O}_9$ and ZrSiO_4 .

BIBLIOGRAPHY

1. Belyavskaya, V. A., L. A. Kupriyanova, Zavodsk. labor., 34, 8, 1968, p. 913.
2. Berezhnoy, A. S., R. A. Kordyuk, Ogneupory, 2, 1962, p. 85.
3. Kordyuk, R. A., Trudy Ukrainski inst. ogneuporov, 7, 1963, p. 213.
4. Kordyuk, R. A., N. V. Gui'ko, DAN SSSR, 142, 3, 1962, p. 639.
5. Chukhlantsev, V. G., Yu. M. Galkin, ibid 161, 2, 1965, p. 171.
6. Cocco, A., J. Barbariol, Chim. e Industr. (Milano), 41, 9, 886, 1959.
7. Estrada, D. A., Arxiv Kami, 7, 4, 33, 1954.
8. Matsumoto, K., T. Sawamoto, S. Koide, Rep. Res. Lab. Asahi Glass Co., 4, 2, 8, 1954.
9. Quereshi, M. H., N. H. Brett, Trans. Brit. Ceram. Soc., 57, 6, 205, 1968.
10. Quereshi, M. H., N. H. Brett, in: Science of Ceramics, 4, London-New York, 275, 1968.

$\text{SrO} - \text{ZrO}_2 - \text{SiO}_2$

Dear [2] limited himself to study of the subsolidus region of the system. He discovered the compound $6\text{SrO} \cdot \text{ZrO}_2 \cdot 5\text{SiO}_2$. Galkin and Chukhlantsev [1], studying the subsolidus region of the partial system $\text{SrO} - \text{ZrSiO}_4$ (annealing

at 1150 and 1350°), confirmed the existence of this ternary compound, which dissolves easily in hydrochloric acid. Summarizing existing data, the authors gave a diagram of the phase relationships in the system (Fig. 273).

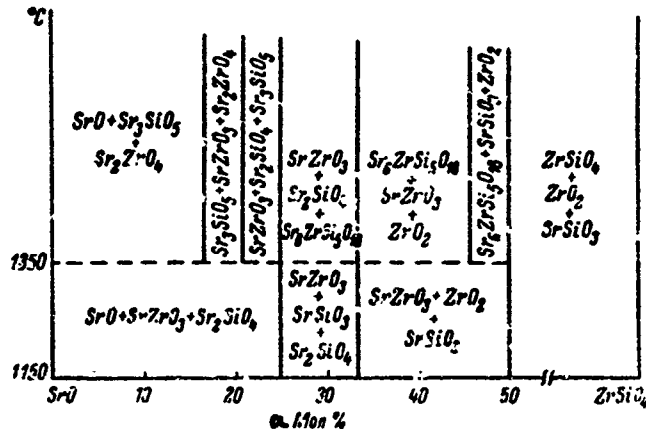


Fig. 273. Diagram of phase relationships of $\text{SrO} - \text{ZrO}_2 - \text{SiO}_2$ system in subsolidus region (from Galkin and Chukhlantsev).

Key:

a. Mole %

BIBLIOGRAPHY

1. Galkin, Yu. M., V. G. Chukhlantsev, Izv. AN SSSR, Neorg. mater., 11, 1955, p. 2000.
2. Dear, P. S., Bull. Virginia Polytechn. Inst., 51, 8, 3, 1958.

$\text{BaO} - \text{ZrO}_2 - \text{SiO}_2$

The system has been studied by Chukhlantsev and Galkin [1], in the subsolidus region. Annealing was carried out at temperatures which eliminated

melting of the mixtures. The phase composition was determined by chemical analysis. Under the annealing conditions adopted, the formation of two ternary compounds was established, the composition of which correspond best to the formulas $2\text{BaO} \cdot 2\text{ZrO}_2 \cdot 3\text{SiO}_2$ and $\text{BaO} \cdot \text{ZrO}_2 \cdot 3\text{SiO}_2$. The compound $\text{BaO} \cdot \text{ZrO}_2 \cdot \text{SiO}_2$, to which Jacobs referred [2, 3], was not found.

The coexisting phase triangles (triangulars) of the system is represented in Fig. 274. A verification study of annealing of mixtures of the two compatible phases did not demonstrate any new compounds at all. Pure zirconosilicates were obtained by sintering of the oxides at 1300° for a period of 24-30 hours. Crystals of $2\text{BaO} \cdot 2\text{ZrO}_2 \cdot 3\text{SiO}_2$ are weakly anisotropic, have an average index of refraction of 1.793, density of 4.38 g/cm^3 and they melt incongruently at about 1380° , with formation of $\text{BaO} \cdot \text{ZrO}_2 \cdot 3\text{SiO}_2$ and melt. Crystals of $\text{BaO}_2 \cdot \text{ZrO}_2 \cdot 3\text{SiO}_2$ have indices of refraction $\text{Ng} = 1.682$ and $\text{Np} = 1.678$, density of 3.74 g/cm^3 , and they melt without decomposition at approximately 1450° . Polymorphism was not found in these compounds. Compound 2:2:3 is easily broken down in cold, diluted hydrochloric acid, and compound 1:1:3 is decomposed by a mixture of hydrofluoric and sulphuric acids.

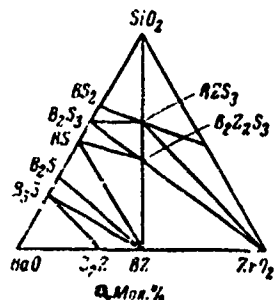


Fig. 274. Coexisting phase triangles of $\text{BaO} \cdots \text{ZrO}_2 \cdots \text{SiO}_2$ system (from Chukhlantsev and Galkin).

Key: a. Mole %

BIBLIOGRAPHY

1. Chukhlantsev, V.G., Yu.M. Galkin, DAN SSSR, 169, 3, 1966, p. 645.
2. Jacobs, C.W.F., J. Amer. Ceram. Soc., 37, 5, 216, 1954.
3. Jacobs, C.W.F., W.J. Baldwin, J. Amer. Ceram. Soc., 37, 6, 258, 1954.



It has been studied roughly by Budnikov and Litvakovskiy [1, 2] by the quenching method. The investigators limited themselves to the region adjacent to the Al_2O_3 apex. A detailed study was accomplished by Quereshi and Brett [4]. According to the data of the first authors, the system is characterized by the presence of one triple eutectic (Fig. 275), of the composition 53 weight % Al_2O_3 , 17 SiO_2 and 30 ZrO_2 . The melting temperature of the eutectic is about 1800°.

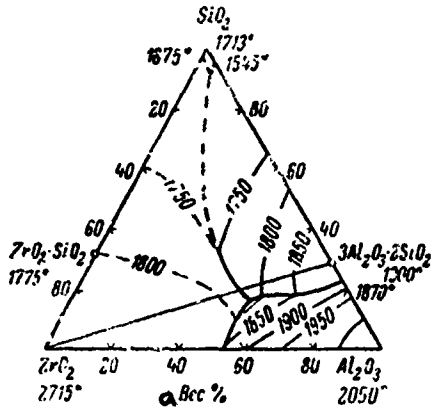


Fig. 275. Approximate phase diagram of Al_2O_3 -- ZrO_2 -- SiO_2 system (from Budnikov and Litvakovskiy).

Key:

a. Weight %

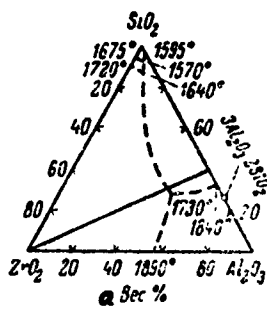


Fig. 276. Approximate diagram of phase relationships of Al_2O_3 -- ZrO_2 -- SiO_2 system (from Barbariol and Podda).

Key:

a. Weight %

Barbariol and Podda [3] have studied the system in the subsolidus region (1450-1700°), carrying out prolonged annealing (with intermediate pulverization of the samples). Ternary compounds and ternary solid solutions were not found. A triple eutectic between the ZrO_2 , Al_2O_3 and mullite fields melts at $1730 \pm 20^\circ$, and it has the composition 29 weight % ZrO_2 , 53 Al_2O_3 and 18 SiO_2 (Fig. 276).

The authors propose the existence of a second eutectic between the SiO_2 , zircon and mullite fields, with an SiO_2 content of 90-95 mole %, melting at $1570 \pm 20^\circ$. Up to 1630°, the triple phase diagram consists of three coexisting phase triangles: 1. SiO_2 -- ZrSiO_4 -- $3\text{Al}_2\text{O}_3 \cdot 2\text{SiO}_2$; 2. ZrSiO_4 -- $3\text{Al}_2\text{O}_3 \cdot 2\text{SiO}_2$ -- solid solution of ZrSiO_4 in ZrO_2 ; 3. ZrO_2 -- Al_2O_3 -- solid solution of Al_2O_3 in $3\text{Al}_2\text{O}_3 \cdot 2\text{SiO}_2$. Above 1700°, the position changes, and equilibrium between ZrSiO_4 and $3\text{Al}_2\text{O}_3 \cdot 2\text{SiO}_2$ cannot be spoken of.

INVARIANT POINTS OF Al_2O_3 -- ZrO_2 -- SiO_2 SYSTEM
(from Quereshi and Brett)

α Точка (пнс. 278)	β Процесс	Состав, вес. %			d _{тепе- ратура, °C}
		Al_2O_3	ZrO_2	SiO_2	
1	Родотектика	8	3	89	1550
2	Перитектика	5	5	90	1660
5	,	17	9	74	1645

Key:

- a. Points (Fig. 278)
- b. Process
- c. Composition, weight %
- d. Temperature, °C
- e. Eutectic
- f. Peritectic

Quereshi and Brett [4] have studied the region bounded by the compounds $3\text{Al}_2\text{O}_3 \cdot 2\text{SiO}_2$ -- ZrO_2 -- SiO_2 . Mixtures were annealed to 1740°, with from 1 to 5 hours exposure and quenching in air. The authors presented their results in the form of seven sections, two of which are introduced in Fig. 277. A schematic diagram of the phase regions of the triple system is represented in Fig. 278. The composition of the invariant points is given in the table.

The steep rise in the liquidus surface within the ZrO_2 field (close to the mullite-baddeleyite boundary) indicates a limited solubility of ZrO_2 in the melt. Ternary compositions containing more than 20-30 weight % ZrO_2 have high refractoriness (over 1750°).

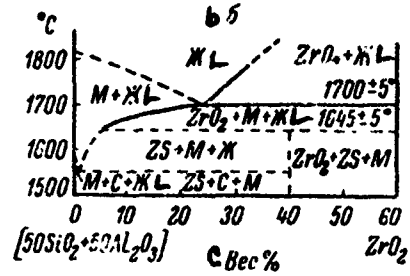
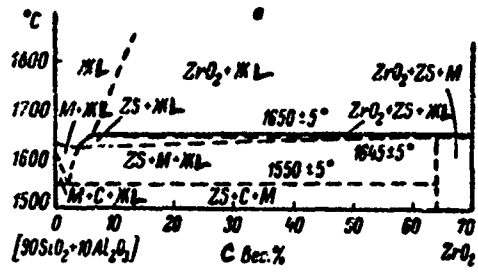


Fig. 277. Phase diagram of some sections of partial triple system $3\text{Al}_2\text{O}_3 \cdot 2\text{SiO}_2$ -- ZrO_2 -- SiO_2 (from Quereshi and Brett): a. section $(90\text{SiO}_2 + 10\text{Al}_2\text{O}_3)$ -- ZrO_2 ; b. section $(50\text{SiO}_2 + 50\text{Al}_2\text{O}_3)$ -- ZrO_2 ; C. cristobalite; M. mullite.
Key:
c. Weight %

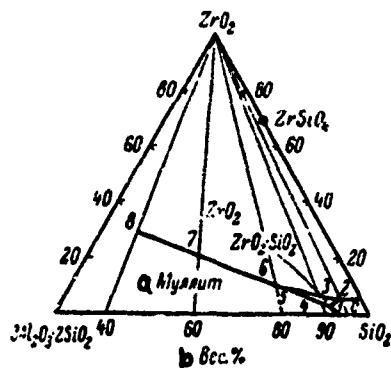


Fig. 278. Fusibility diagram of partial triple system $3\text{Al}_2\text{O}_3 \cdot 2\text{SiO}_2$ -- ZrO_2 -- SiO_2 (from Quercshi and Brett):
 1. $1550 \pm 5^\circ$; 2. $1580 \pm 5^\circ$;
 3. $1650 \pm 5^\circ$; 4. $1600 \pm 5^\circ$; 5. $1645 \pm 5^\circ$;
 6. $1655 \pm 5^\circ$; 7. $1695 \pm 5^\circ$; 8. $1705 \pm 5^\circ$
 C. cristobalite.

Key:

- a. Mullite
- b. Weight %

BIBLIOGRAPHY

1. Budnikov, P.P., A.A. Litvakovskiy, DAN SSSR, 106, 2, 1956, p. 267.
2. Litvakovskiy, A.A., Steklo i keramika, 11, 1956, p. 11.
3. Barbariol, L., L. Podda, Tecnica Italiana, 33, 7/8, 1968.
4. Quercshi, M.H., N.H. Brett, Trans. Brit. Ceram. Soc., 67, 11, 569, 1963.

HfO_2 -- ZrO_2 -- SiO_2

Ramakrishnan and colleagues [1], annealing finely-ground (up to 20 microns) mixtures of ZrO_2 , HfO_2 and quartz at 1450° , showed that ZrSiO_4 and HfSiO_4 form a continuous series of solid solutions. The unit cell parameters changed smoothly from $a = 6.603$, $c = 5.981 \text{ \AA}$ for ZrSiO_4 to $a = 6.569$, $c = 5.967 \text{ \AA}$ for HfSiO_4 .

BIBLIOGRAPHY

1. Ramakrishnan, S. S., K. V. Gokhale, E. C. Subbarao, Mater. Res. Bull., **4**, 5, 323, 1969.

ThO_2 -- ZrO_2 -- SiO_2

The system at subsolidus temperatures (300 - 1400°), according to the data of Mumpton and Roy [2], is represented in Fig. 279. Very limited solid solutions have been found between zircon and thorite, right up to 1175° . ThSiO_4 dissolves in ZrSiO_4 , up to 4 ± 2 mole %, and ZrSiO_4 in thorite, in an amount not greater than 6 ± 2 mole %. The limits of the solid solutions in Fig. 279 are somewhat exaggerated for clarity. Considerably greater solubility limits have been found in the metastable solid solutions obtained: the solubility of ThSiO_4 in zircon reached 35 mole % and of ZrSiO_4 in thorite, 25 mole %. See [1] for metastable solid solutions of ZrO_2 and ThO_2 .

Specific proofs of the compatibility of the phases on the connecting lines ThSiO_4 -- ZrO_2 and ZrSiO_4 -- ThO_2 were not obtained. Baddeleyite is never associated with thorite in nature; therefore, the coexistence of ZrSiO_4 and ThO_2 (at low temperatures) can be assumed. Zircon and ThC_2 react upon heating to 1400° , with formation of huttonite + ZrO_2 .

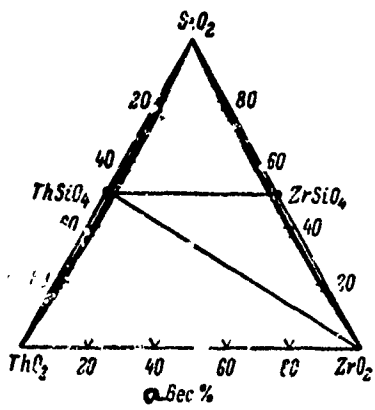


Fig. 279. Schematic diagram of phase relationships of ThO_2 -- ZrO_2 -- SiO_2 system (from Mumpton and Roy).

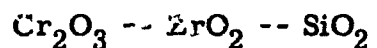
Key:

a. Weight %

Thorium silicate is encountered in the form of two polymorphic modifications, thorite (tetragonal crystal system) and huttonite (monoclinic crystal system), and ZrSiO_4 in one tetragonal modification.

BIBLIOGRAPHY

1. Mumpton, F.A., R. Roy, J. Amer. Ceram. Soc., 43, 5, 234, 1960.
2. Mumpton, F.A., R. Roy, Geochim. Cosmochim. acta, 21, 3/4, 217, 1961.



The system has been studied by Smachnaya [1, 2]. A fusibility diagram, in the form of a liquidus surface, is presented in Fig. 280. Ternary compounds

were not found. Two triple eutectics (E_5 and E_6) melt at 1700 and 1660°, and they have the compositions 15 mole % ZrO_2 , 30 Cr_2O_3 and 55 SiO_2 and 10 mole % ZrO_2 , 5 Cr_2O_3 and 85 SiO_2 ; the pseudobinary eutectic point E_7 , located on the ZrO_2 -- $Cr_2O_3 \cdot SiO_2$ connecting line, corresponds to the composition 15 mole % ZrO_2 , 21.25 Cr_2O_3 and 63.75 SiO_2 , and it has a temperature maximum of 1840° on the boundary line between E_5 and E_6 .

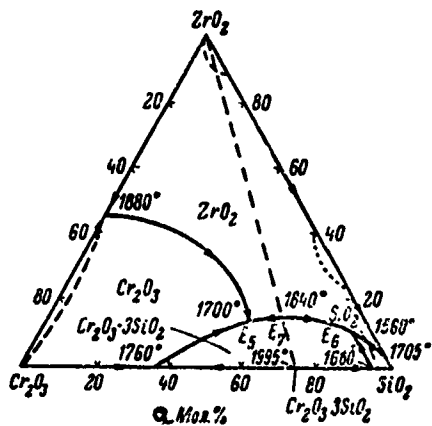


Fig. 280. Fusibility diagram of Cr_2O_3 -- ZrO_2 -- SiO_2 system (from Smachnaya).

Key:

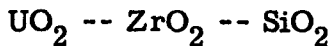
a. Mole %

Smachnaya established the existence of two triple solid solution regions:

1. adjacent to the ZrO_2 -- SiO_2 side (close to the ZrO_2 apex) with a limiting Cr_2O_3 content of not over 5 mole % and SiO_2 not over 10 mole %;
2. adjacent to the Cr_2O_3 -- ZrO_2 side (close to the Cr_2O_3 apex), with a limiting SiO_2 content of not over 3 mole % and ZrO_2 not over 45 mole %.

BIBLIOGRAPHY

1. Smachnaya, V. F., Izv. vyssh. uchebn. zaved., Chernaya metallurgiya, 11, 1962, p. 191.
2. Smachnaya, V. F., Zap. Len. gorn. inst., 42, 3, 1963, p. 41.



The system was studied briefly by Mumpton and Roy [1] in the subsolidus region. A diagram characterizing the solid solutions existing in the system in the 300-1350° temperature region is presented in Fig. 281. In an oxygen atmosphere at 1350°, not over 4 \pm 2 mole % of the hypothetical compound "USiO₄" dissolves in zircon (ZrSiO_4). This compound has not been obtained in pure form, and SiO_2 + UO_2 solid solution + ZrSiO_4 solid solution and ZrO_2 solid solution + UO_2 solid solution + ZrSiO_4 solid solution coexist in the three-phase regions. Up to 20 mole % "USiO₄" can dissolve in zircon, in the form of a metastable solid solution.

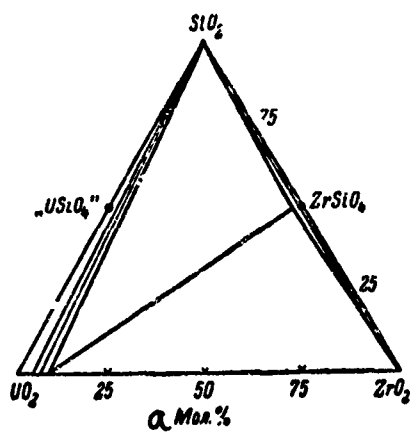


Fig. 281. Schematic diagram of phase relationships of UO_2 -- ZrO_2 -- SiO_2 system (from Mumpton and Roy).

Key: a. Mole %

BIBLIOGRAPHY

1. Mumpton, F.A., R. Roy, Geochim. cosmochim. acta, 21, 3-4, 217, 1961.



Muan [1], on the basis of thermodynamic data, triangulated the system for 1200°. It was shown that the free reaction energy of $2\text{CoO} + \text{ZrSiO}_4 = \text{Co}_2\text{SiO}_4 + \text{ZrO}_2$ is a value less than 0 and, therefore, the compounds $2\text{CoO} \cdot \text{SiO}_2 + \text{ZrO}_2$ and $2\text{CoO} \cdot \text{SiO}_2 + \text{ZrO}_2 \cdot \text{SiO}_2$ will coexist.

BIBLIOGRAPHY

1. Muan, A., Proc. Brit. Ceram. Soc., 8, 103, 1967.

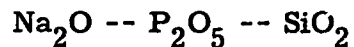


On the basis of thermodynamic data, Muan [1] triangulated the system for 1200°. He showed that ΔG of the reaction $2\text{NiO} + \text{ZrSiO}_4 = \text{Ni}_2\text{SiO}_4 + \text{ZrO}_2$ is a value greater than 0 and that the following compounds will coexist: $\text{Ni}_2\text{SiO}_4 + \text{ZrSiO}_4$ and $\text{NiO} + \text{ZrSiO}_4$.

BIBLIOGRAPHY

1. Muan, A., Proc. Brit. Ceram. Soc., 8, 103, 1967.

SILICOPHOSPHATE SYSTEMS



The system has been studied in detail by Turkdogan and Maddocks [1].

Important conclusions as to the phase composition were drawn, on the basis of density determinations. The existence of three ternary compounds was established: congruently melting $9\text{Na}_2\text{O} \cdot 2\text{P}_2\text{O}_5 \cdot 6\text{SiO}_2$ and incongruently melting $5\text{Na}_2\text{O} \cdot \text{P}_2\text{O}_5 \cdot 4\text{SiO}_2$ and $15\text{Na}_2\text{O} \cdot 5\text{P}_2\text{O}_5 \cdot 3\text{SiO}_2$. The authors give no indications as to the formation of solid solutions.

Four partial binary systems were studied: $3\text{Na}_2\text{O} \cdot \text{P}_2\text{O}_5 \text{ -- } \text{Na}_2\text{O} \cdot \text{SiO}_2$ (simple eutectic), $3\text{Na}_2\text{O} \cdot \text{P}_2\text{O}_5 \text{ -- } \text{Na}_2\text{O} \cdot 2\text{SiO}_2$ (Fig. 282), $2\text{Na}_2\text{O} \cdot \text{P}_2\text{O}_5 \text{ -- } 9\text{Na}_2\text{O} \cdot 2\text{P}_2\text{O}_5 \cdot 6\text{SiO}_2$ (Fig. 283), $2\text{Na}_2\text{O} \cdot \text{P}_2\text{O}_5 \text{ -- } \text{SiO}_2$ (simple eutectic) and two partial triple systems: $3\text{Na}_2\text{O} \cdot \text{P}_2\text{O}_5 \text{ -- } \text{Na}_2\text{O} \cdot \text{SiO}_2 \text{ -- } \text{Na}_2\text{O} \cdot 2\text{SiO}_2$ and $3\text{Na}_2\text{O} \cdot \text{P}_2\text{O}_5 \text{ -- } 2\text{Na}_2\text{O} \cdot \text{P}_2\text{O}_5 \text{ -- } 9\text{Na}_2\text{O} \cdot \text{P}_2\text{O}_5 \cdot 6\text{SiO}_2$. In addition, the pseudobinary profile $9\text{Na}_2\text{O} \cdot 2\text{P}_2\text{O}_5 \cdot 6\text{SiO}_2 \text{ -- } \text{Na}_2\text{O} \cdot \text{SiO}_2$ was studied (Fig. 284).

A complete phase diagram of the triple system is represented in Fig. 285.

Studies of the density confirmed the phase relationships established on the basis of thermodynamic data [Translator's note: Portion of text missing]

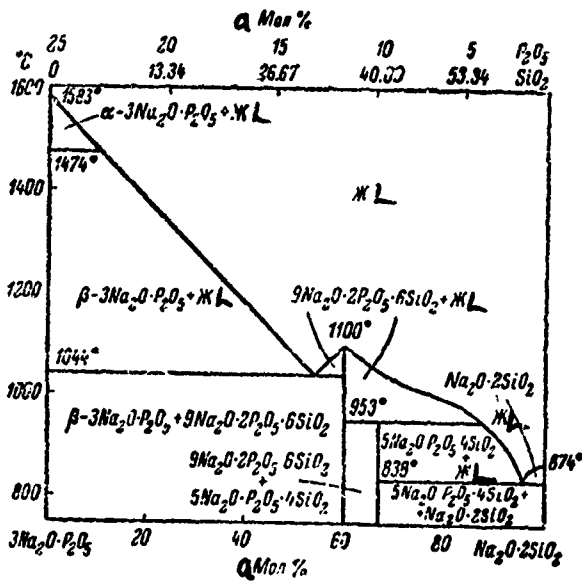


Fig. 282. Phase diagram of partial system
 $3\text{Na}_2\text{O}\cdot\text{P}_2\text{O}_5$ -- $\text{Na}_2\text{O}\cdot 2\text{SiO}_2$ (from Turkdogan
 and Maddocks).

Key: a. Mole %

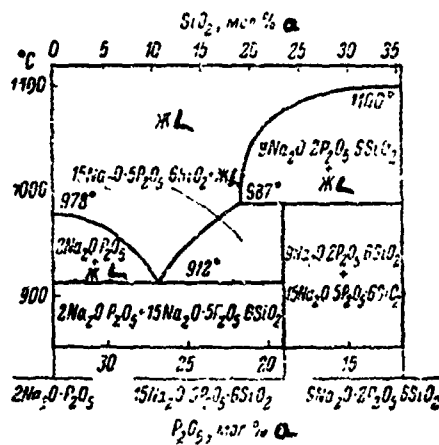


Fig. 283. Phase diagram of partial system $2\text{Na}_2\text{O}\cdot\text{P}_2\text{O}_5$ -- $9\text{Na}_2\text{O}\cdot\text{P}_2\text{O}_5\cdot 6\text{SiO}_2$ (from Turkdogan and Maddocks).

Key: a. Mole %

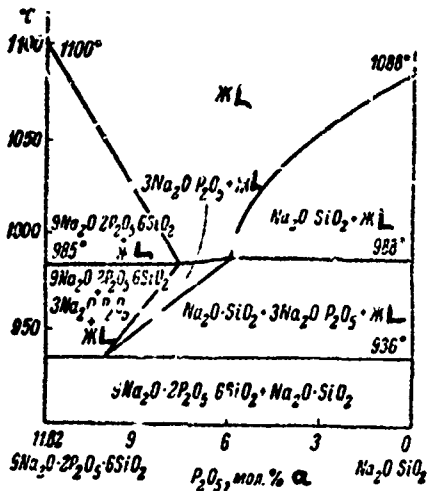


Fig. 284. Phase diagram of partial system $9\text{Na}_2\text{O} \cdot 2\text{P}_2\text{O}_5 \cdot 6\text{SiO}_2$ -- $\text{Na}_2\text{O} \cdot \text{SiO}_2$ (from Turkdogan and Maddocks).

Key: a. Mole %

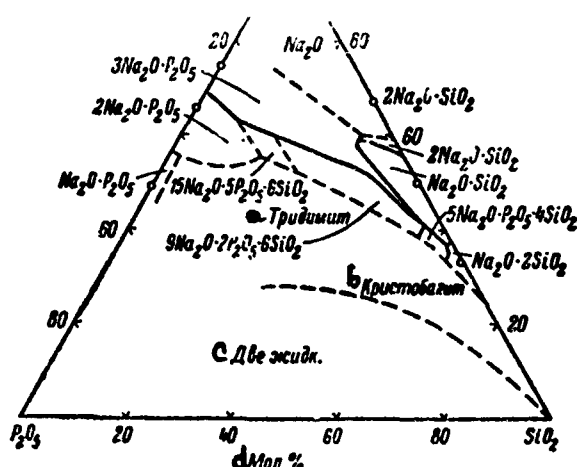


Fig. 285. Phase diagram of $\text{Na}_2\text{O} -- \text{P}_2\text{O}_5 -- \text{SiO}_2$ system (from Turkdogan and Maddocks).

Key:

- | | |
|-----------------|----------------|
| a. Tridymite | c. Two liquids |
| b. Cristobalite | d. Mole % |

$2\text{Na}_2\text{O}\cdot\text{P}_2\text{O}_5$ -- $\text{Na}_2\text{O}\cdot\text{SiO}_2$ and $2\text{Na}_2\text{O}\cdot\text{P}_2\text{O}_5$ -- SiO_2 , diagrams of the specific volume were obtained, with complete additivity. For binary systems, in which there are ternary compounds in the "specific volume-composition" diagrams, the corresponding discontinuities are observed.

The compound $9\text{Na}_2\text{O}\cdot 2\text{P}_2\text{O}_5\cdot 6\text{SiO}_2$ is isotropic, and it has an index of refraction of 1.520. For the anisotropic compound $5\text{Na}_2\text{O}\cdot\text{P}_2\text{O}_5\cdot 4\text{SiO}_2$, the average index of refraction is 1.515. A well expressed twinning is characteristic of the compound $15\text{Na}_2\text{O}\cdot 5\text{P}_2\text{O}_5\cdot 6\text{SiO}_2$, in which anisotropic crystals have an average index of refraction of 1.510.

On the basis of indirect considerations, the author concludes that a region of immiscibility of the liquids exists adjacent to the P_2O_5 -- SiO_2 side.

TABLE 1
INVARIANT POINTS OF $\text{Na}_2\text{O} - \text{P}_2\text{O}_5 - \text{SiC}_2$ SYSTEM

a. Фазы	b. Проведене	c. Состав, вес. %			d. Темп., °C
		1	2	3	
$9\text{Na}_2\text{O} \cdot \text{P}_2\text{O}_5 \cdot 4\text{SiO}_2 + \text{Na}_2\text{O} \cdot 2\text{SiO}_2 + 3\text{SiC}_2 +$ жидкость e	Изотермическое плавление	39.77	3.65	56.41	903
$5\text{Na}_2\text{O} \cdot \text{P}_2\text{O}_5 \cdot 4\text{SiO}_2 + 9\text{Na}_2\text{O} \cdot 2\text{SiO}_2 + 3\text{SiC}_2 +$ жидкость e	Электролиз	35.57	1.37	63.06	838
$5\text{Na}_2\text{O} \cdot \text{P}_2\text{O}_5 \cdot 4\text{SiO}_2 + \text{Na}_2\text{O} \cdot 2\text{SiO}_2 +$ жидкость e	*	62.92	26.92	10.16	912
$2\text{Na}_2\text{O} \cdot \text{P}_2\text{O}_5 + 15\text{Na}_2\text{O} \cdot 5\text{P}_2\text{O}_5 \cdot 6\text{SiO}_2 +$ жидкость e	Ликвидогрупповое плавление	59.90	21.98	18.12	957
$15\text{Na}_2\text{O} \cdot 5\text{P}_2\text{O}_5 \cdot 6\text{SiO}_2 + 9\text{Na}_2\text{O} \cdot 2\text{P}_2\text{O}_5 \cdot 6\text{SiO}_2 +$ жидкость e	Изотермическое плавление	53.04	11.82	35.14	1100
$9\text{Na}_2\text{O} \cdot 2\text{P}_2\text{O}_5 \cdot 6\text{SiO}_2 +$ жидкость e	Электролиз	51.41	27.20	18.39	961
$2\text{Na}_2\text{O} \cdot \text{P}_2\text{O}_5 + \text{Tridymite} +$ жидкость e	Реакция	43.40	3.50	53.10	936
$3\text{Na}_2\text{O} \cdot \text{P}_2\text{O}_5 + \text{Na}_2\text{O} \cdot \text{SiO}_2 = 9\text{Na}_2\text{O} \cdot 2\text{P}_2\text{O}_5 \cdot 6\text{SiO}_2 +$ жидкость e	*	41.50	2.70	55.70	920
$9\text{Na}_2\text{O} \cdot 2\text{P}_2\text{O}_5 \cdot 6\text{SiO}_2 + \text{Na}_2\text{O} \cdot \text{SiO}_2 =$ $= 5\text{Na}_2\text{O} \cdot \text{P}_2\text{O}_5 \cdot 4\text{SiO}_2 +$ жидкость e	Электролиз	36.80	1.09	62.20	816
$5\text{Na}_2\text{O} \cdot \text{P}_2\text{O}_5 \cdot 4\text{SiC}_2 + \text{Na}_2\text{O} \cdot \text{SiO}_2 +$ $+ \text{Na}_2\text{O} \cdot 2\text{SiO}_2 +$ жидкость e	Реакция	59.50	21.50	19.01	950
$3\text{Na}_2\text{O} \cdot \text{P}_2\text{O}_5 + 9\text{Na}_2\text{O} \cdot 2\text{P}_2\text{O}_5 \cdot 6\text{SiO}_2 =$ $= 15\text{Na}_2\text{O} \cdot 5\text{P}_2\text{O}_5 \cdot 6\text{SiO}_2 +$ жидкость e	Электролиз	62.70	26.80	10.50	900
$2\text{Na}_2\text{O} \cdot \text{P}_2\text{O}_5 + 15\text{Na}_2\text{O} \cdot 5\text{P}_2\text{O}_5 \cdot 6\text{SiO}_2 +$ $+ 2\text{Na}_2\text{O} \cdot \text{P}_2\text{O}_5 +$ жидкость e					

Key:

Reproduced from
best available copy.

- a. Phases
- b. Process
- c. Composition, weight %
- d. Temperature, °C
- e. Liquid
- f. Tridymite
- g. Melting
- h. Incongruent melting
- i. Eutectic
- j. Reaction

TABLE 2
CRYSTALLINE PHASES OF $\text{Na}_2\text{O} - \text{P}_2\text{O}_5 - \text{SiO}_2$ SYSTEM

α Соединение	Кристаллографическая характеристика	С Габитус	Nm
$9\text{Na}_2\text{O} \cdot 2\text{P}_2\text{O}_5 \cdot 6\text{SiO}_2$	Изогропная	—	1.520
$5\text{Na}_2\text{O} \cdot \text{P}_2\text{O}_5 \cdot 4\text{SiO}_2$	Анзотропная	—	1.515
$15\text{Na}_2\text{O} \cdot 5\text{P}_2\text{O}_5 \cdot 6\text{SiO}_2$	—	Двойниковые пластинки	1.510

Key:

- a. Compound
- b. Crystallographic characteristic
- c. Appearance
- d. Isotropic
- e. Anisotropic
- f. Twinned plates

BIBLIOGRAPHY

1. Turkdogan, E. T., W. R. Maddocks, J. Iron a. Steel Inst., 172, 1, 1, 1952.

$\text{MgO} - \text{P}_2\text{O}_5 - \text{SiO}_2$

The system has been studied by Wojciechowska and Berak [1], limited to the region $\text{MgO} - 3\text{MgO} \cdot \text{P}_2\text{O}_5 - \text{SiO}_2$ and using the methods of thermal, microstructural and X-ray analysis.

In the partial system $3\text{MgO} \cdot \text{P}_2\text{O}_5 - \text{SiO}_2$ (Fig. 286), a eutectic was observed with a SiO_2 content of 3.5 weight % and a melting temperature of 1330° . An extensive region of immiscibility of the two liquids extends from 24 to 99 weight % SiO_2 .

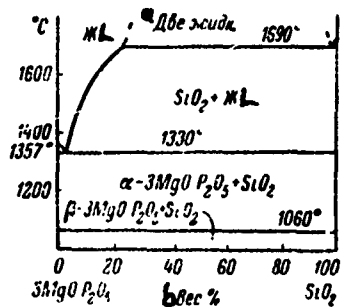


Fig. 286. Phase diagram of partial system $3\text{MgO}\cdot\text{P}_2\text{O}_5$ -- SiO_2 (from Wojciechowska and Berak).

Key:

- a. Two liquids
- b. Weight %

The partial system $3\text{MgO}\cdot\text{P}_2\text{O}_5$ -- $\text{MgO}\cdot\text{SiO}_2$ is a simple eutectic, with a eutectic melting temperature of 1290° , and containing 30 weight % $\text{MgO}\cdot\text{SiO}_2$. The $3\text{MgO}\cdot\text{P}_2\text{O}_5$ -- $2\text{MgO}\cdot\text{SiO}_2$ system is a simple eutectic, which contains 30 weight % $2\text{MgO}\cdot\text{SiO}_2$ and melts at 1315° .

In the partial ternary system bounded by the compounds MgO , SiO_2 and $3\text{MgO}\cdot\text{P}_2\text{O}_5$ (Fig. 287), there are three eutectics of the compositions 18 weight % SiO_2 , 39 weight % P_2O_5 and 43 weight % MgO , with a melting temperature of 1286° , and 15 weight % SiO_2 , 38 weight % P_2O_5 and 47 weight % MgO , 1287° , and 11 weight % SiO_2 , 38 weight % P_2O_5 and 51 weight % MgO , 1307° .

The authors note that, with a SiO_2 content of over 10 weight %, glass can easily be obtained in the region of binary and ternary eutectics.

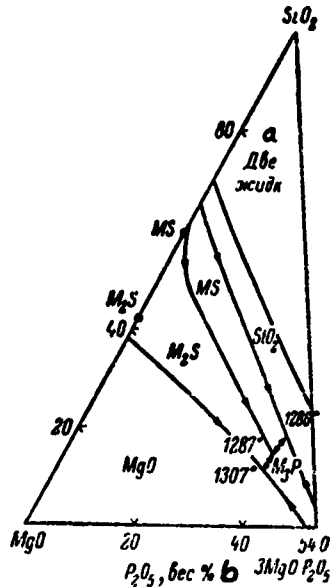


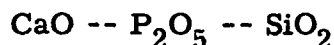
Fig. 287. Phase diagram of partial triple system $MgO - 3MgO \cdot P_2O_5 - SiO_2$ (from Wojciechowska and Berak).

Key:

- a. Two liquids
 - b. Weight %

BIBLIOGRAPHY

1. Wojciechowska, J., J. Berak, Roczn. Chem., 33, 1, 21, 1959.



The system has been studied by Barrett and McCaughey [7], Bredig [9, 10], Trömel and colleagues [22], Toropov and colleagues [5], Wojciechowska and colleagues [23], Berak and Wojciechowska [8], St. Pierre [21], Nurse and colleagues [18], Gutt [13] and others. Two ternary compounds have been

established: $5\text{CaO} \cdot \text{P}_2\text{O}_5 \cdot \text{SiO}_2$ (silicocarnotite) and $7\text{CaO} \cdot \text{P}_2\text{O}_5 \cdot 2\text{SiO}_2$ (nagelschmidtite). Several series of solid solutions have been found. In the region adjacent to the $\text{P}_2\text{O}_5 - \text{SiO}_2$ side, there is a region of immiscibility of the liquids. The general appearance of a phase diagram of the $\text{CaO} - \text{P}_2\text{O}_5 - \text{SiO}_2$ system, according to the data of Barrett and McCaughey [7], is presented in Fig. 288. A section of the system which is of interest from the practical viewpoint has been investigated by Wojciechowska and colleagues and Berak and Wojciechowska, the data from which is presented in Fig. 289a and b. The region adjacent to the CaO apex and bounded by the $\text{CaO} - 2\text{CaO} \cdot \text{SiO}_2 - 3\text{CaO} \cdot \text{P}_2\text{C}_5$ compositions has also been investigated by Trömel and colleagues (Fig. 289c). The partial system $3\text{CaO} \cdot \text{P}_2\text{O}_5 - 2\text{CaO} \cdot \text{SiO}_2$, in which silicocarnotite and nagelschmidtite occur, has been studied in the greatest detail. According to Barrett and McCaughey, for all four phases of this system, $3\text{CaO} \cdot \text{P}_2\text{O}_5$, $2\text{CaO} \cdot \text{SiO}_2$, $7\text{CaO} \cdot \text{P}_2\text{O}_5 \cdot 2\text{SiO}_2$ and $5\text{CaO} \cdot \text{P}_2\text{O}_5 \cdot \text{SiO}_2$, limited mutual solubility is characteristic, connected with the closeness of the ionic radii of Si (0.39 Å) and P (0.35 Å).

As early as 1939, Lapin [2] showed that there is an excess of $3\text{CaO} \cdot \text{P}_2\text{O}_5$, relative to the composition ascribed to this mineral, $3\text{CaO} \cdot \text{P}_2\text{O}_5 \cdot 2\text{CaO} \cdot \text{SiO}_2$, in silicocarnotite extracted from slag. Changes and complications were introduced in subsequent investigations. Trömel and colleagues found the following phases: 1. a solid solution based on $2\text{CaO} \cdot \text{SiO}_2$, containing 2 weight % P_2O_5 ; 2. solid solutions containing from 3.5 to 6 weight % P_2O_5 and isotropic K_2SO_4 ; 3. solid solutions with variable P_2O_5 content, from 12.5 to 36 weight %, with nagelschmidtite falling in this region; $4 \frac{1}{3}\text{CaO} \cdot \text{P}_2\text{O}_5$ based solid solutions, with fluctuations of the SiO_2 in them from 0 to 5 weight %.

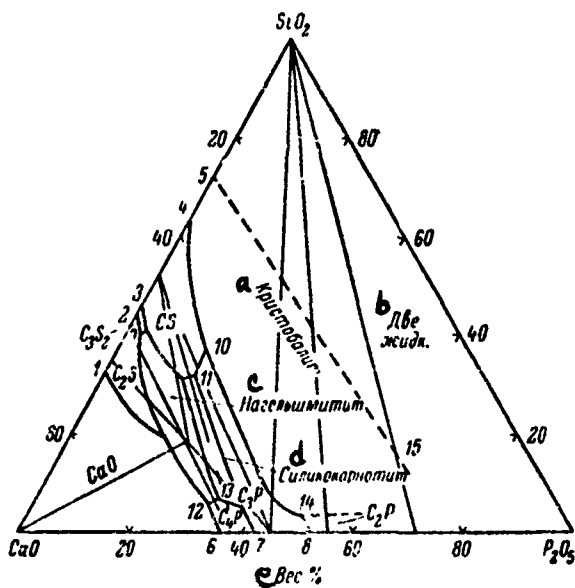


Fig. 288. Phase diagram of CaO -- P₂O₅ -- SiO₂ system (from Barrett and McCaughey): Temperatures are indicated approximately: 1. 2065°; 2. 1475°; 3. 1455°; 4. 1436°; 5. 1700°; 6. 1670°; 7. 1570°; 8. 1280°; 9. 1450°; 10. 1350°; 11. 1400°; 12. 1600°; 13. 1600°; 14. 1250°; 15. 1400°.

Key:

- | | |
|--------------------|--------------------|
| a. Cristobalite | d. Silicocarnotite |
| b. Two liquids | e. Weight % |
| c. Nagelschmidtite | |

The compound 5CaO · P₂O₅ · SiO₂ (silicocarnotite), according to Trömel, is stable at temperatures below 1300° and can occur in equilibrium with the melt. Silicocarnotite is formed as a result of a solid phase reaction, from compositions containing from 30 to 39 weight % P₂O₅. Klement and Erler [15],

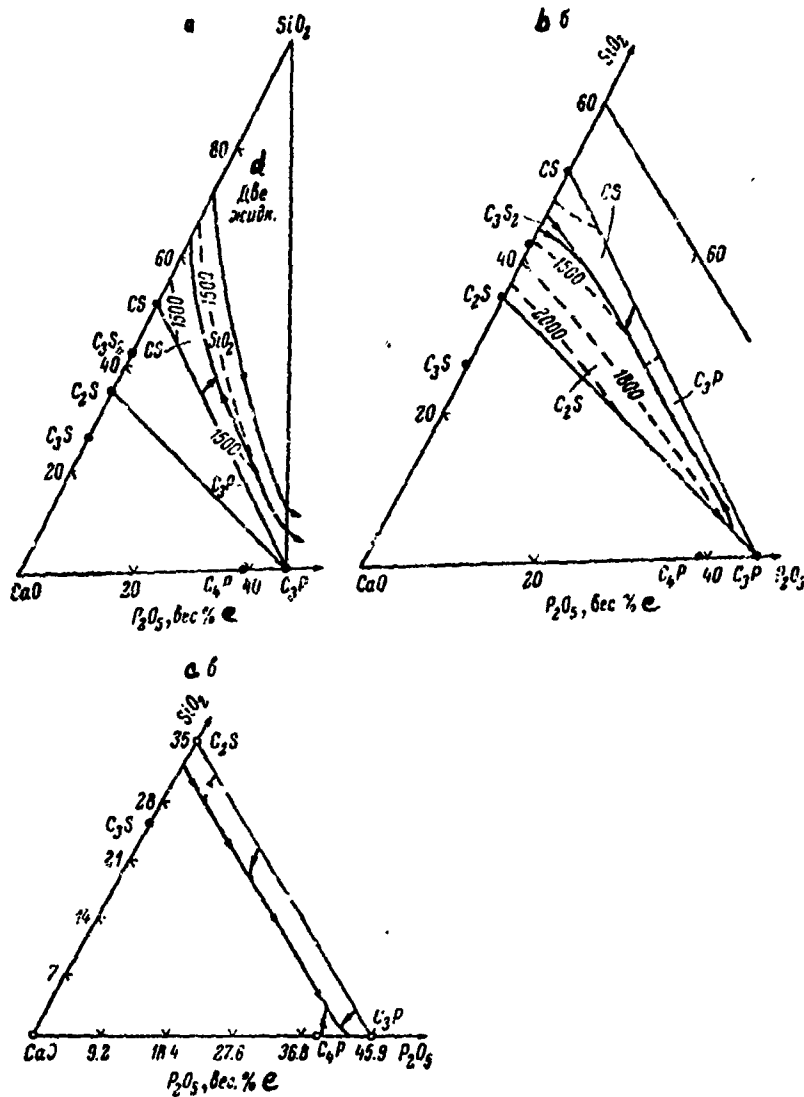


Fig. 289. Phase diagram of partial system $\text{CaO} \text{ -- } \text{SiO}_2 \text{ -- } 3\text{CaO}\cdot\text{P}_2\text{O}_5$: a. partial system $\text{CaO}\cdot\text{SiO}_2 \text{ -- } \text{SiO}_2 \text{ -- } 3\text{CaO}\cdot\text{P}_2\text{O}_5$ (from Wojciechowska and colleagues); b. partial system $\text{CaO}\cdot\text{SiO}_2 \text{ -- } 2\text{CaO}\cdot\text{SiO}_2 \text{ -- } 3\text{CaO}\cdot\text{P}_2\text{O}_5$ (from Berak and Wojciechowska); c. partial system $\text{CaO} \text{ -- } 2\text{CaO}\cdot\text{SiO}_2 \text{ -- } 3\text{CaO}\cdot\text{P}_2\text{O}_5$ (from Trömel and colleagues).

Key: d. Two liquids
 e. Weight %

heating silicocarnotite to 2000°, detected its decomposition into the high-temperature form of $3\text{CaO}\cdot\text{P}_2\text{O}_5$ and the high-temperature α form of $2\text{CaO}\cdot\text{SiO}_2$.

We find further versions of the $3\text{CaO}\cdot\text{P}_2\text{O}_5$ -- $2\text{CaO}\cdot\text{SiO}_2$ system in Bredig. Together with the hexagonal $\alpha'2\text{CaO}\cdot\text{SiO}_2$ and the lower temperature rhombic $\alpha'2\text{CaO}\cdot\text{SiO}_2$, corresponding to natural bredigite, he demonstrated extensive solid solutions between $\alpha'2\text{CaO}\cdot\text{SiO}_2$ and $\alpha'3\text{CaO}\cdot\text{P}_2\text{O}_5$, with the peritectic reaction point between them at approximately 1880°. In a 1950 work, Bredig gave a new, somewhat modified version of the diagram, eliminating the β modification of dicalcium silicate and outlining the silicocarnotite field somewhat differently.

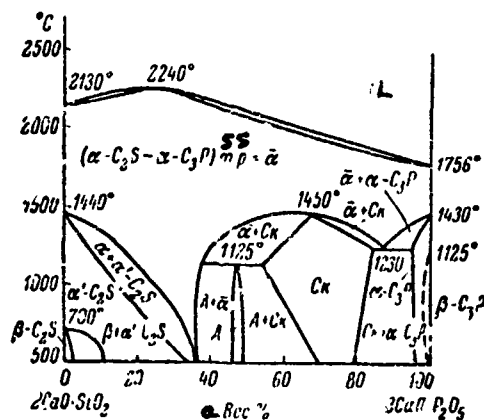


Fig. 290. Phase diagram of partial system $2\text{CaO}\cdot\text{SiO}_2$ -- $3\text{CaO}\cdot\text{P}_2\text{O}_5$ (from Nurse and colleagues): Ck silicocarnotite.

Key:

a. Weight %

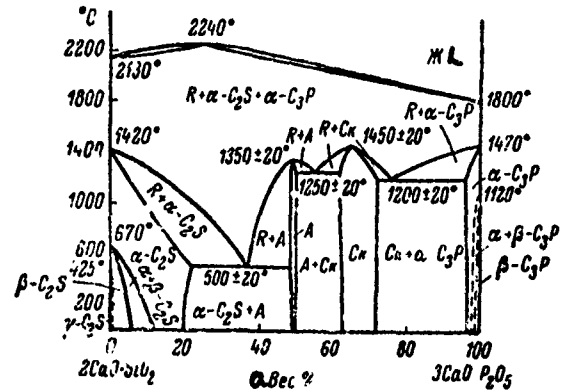


Fig. 291. Phase diagram of partial system
 $2\text{CaO}\cdot\text{SiO}_2$ -- $3\text{CaO}\cdot\text{P}_2\text{O}_5$ (from Fix and
 colleagues): Ch silic-carnotite.

Key:

a. Weight %

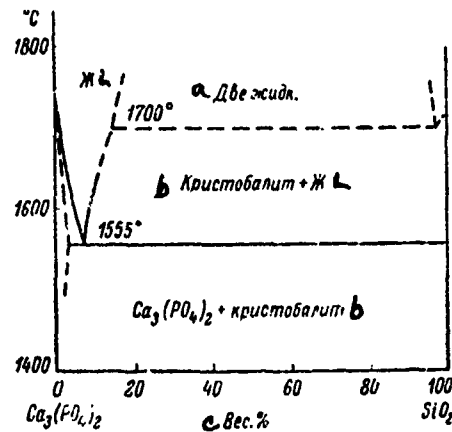


Fig. 292. Phase diagram of partial system
 $\text{Ca}_3(\text{PO}_4)_2$ -- SiO_2 (from St. Pierre).

Key:

- a. Two liquids
 - b. Cristobalite
 - c. Weight %

We find new data on the partial system $2\text{CaO}\cdot\text{SiO}_2$ - $3\text{CaO}\cdot\text{P}_2\text{O}_5$ in Nurse and colleagues [18], the results of which are presented in Fig. 290.

The nature of the new phase found (A) is not explained. The subsolidus ratios in the system being considered recently were studied carefully by Fix and colleagues [12], by means of high-temperature (up to 1900°) X-ray photography of samples, prepared by long (21 days) annealing at $1400-1450^\circ$. The region next to $3\text{CaO}\cdot\text{P}_2\text{O}_5$, where polymorphic transformations take place slowly, was studied especially carefully. The number of phases found was the same as in the work of Nurse and colleagues, but the positions of the boundary lines are significantly different. As is evident from Fig. 291, the silicocarnotite (Ck) field is considerably smaller, and the position of the stable temperature maximum was found at a $3\text{CaO}\cdot\text{P}_2\text{O}_5$ content of 64 weight %, which is close to the composition of silicocarnotite $5\text{CaO}\cdot\text{P}_2\text{O}_5\cdot\text{SiO}_2$. Phase A, corresponding to the stoichiometric compound $7\text{CaO}\cdot\text{P}_2\text{O}_5\cdot2\text{SiO}_2$, changes directly to phase R at 1350° . The field of solid solutions based on $\alpha' 2\text{CaO}\cdot\text{SiO}_2$ reaches a content of 20 weight % $3\text{CaO}\cdot\text{P}_2\text{O}_5$ at 500° .

Balajiva and colleagues [6] plotted a diagram of the dependence of average refraction on composition, in the $2\text{CaO}\cdot\text{SiO}_2$ -- $3\text{CaO}\cdot\text{P}_2\text{O}_5$ series of solid solutions (up to 15 mole % of the latter).

The partial system $\text{Ca}_3(\text{PO}_4)_2$ -- SiO_2 has been studied by St. Pierre [21], who determined the critical temperature of phase separation (Fig. 292). The partial system $\text{CaO}\cdot\text{SiO}_2$ -- $3\text{CaO}\cdot\text{P}_2\text{O}_5$, according to the data of Wojciechowska and colleagues [23], is represented in Fig. 293.

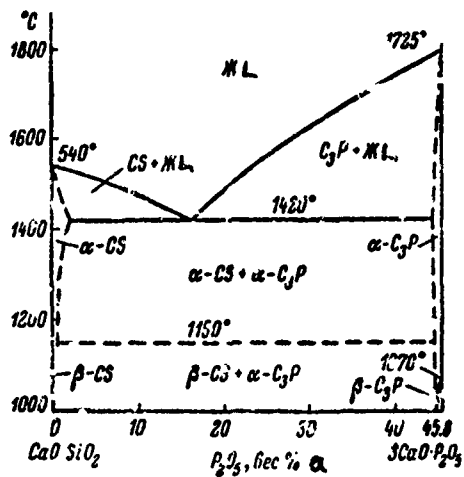


Fig. 293. Phase diagram of partial system $\text{CaO} \cdot \text{SiO}_2$ -- $3\text{CaO} \cdot \text{P}_2\text{O}_5$ (from Wojciechowska and colleagues).

Key:

a. Weight %

Toropov and colleagues [5] have studied the reactions taking place in the $3\text{CaO} \cdot \text{SiO}_2$ -- $3\text{CaO} \cdot \text{P}_2\text{O}_5$ system at 1450° . At this temperature, dissociation of tricalcium silicate takes place, caused by the presence of $3\text{CaO} \cdot \text{P}_2\text{O}_5$ and, with prolonged annealing, depending on composition of the initial mixture, $4\text{CaO} \cdot \text{P}_2\text{O}_5$, silicocarnotite and nagelschmidtite can be found in the reaction products.

Toropov and colleagues determined that silicocarnotite and nagelschmidtite dissolve calcium oxide. Thus, at 1450° , compounds (solid solutions) form, with the compositions $5.3\text{CaO} \cdot \text{P}_2\text{O}_5 \cdot \text{SiO}_2$ and $7.3\text{CaO} \cdot \text{P}_2\text{O}_5 \cdot \text{SiO}_2$, i. e., 0.3 mole of calcium oxide is incorporated in the silicophosphate structure.

Nagelschmidtite forms hexagonal crystals, with the α K_2SO_4 type structure; cleavage is good along (001) and perfect along (110). The indices of refraction: according to Nagelschmidt [17], $Ng = 1.661$, $Np = 1.652$, $(-) 2V^\circ$ very small; according to Segnit [20], Ng from 1.690 to 1.661 for different specimens, Np from 1.680 to 1.652, $(-) 2V^\circ = 0$.

Silicocarnotite crystallizes in the form of short, blue, rhombic prisms, and more rarely in the form of lamellar crystals, compressed along the C axis. According to the measurements of Lapir. [3], the crystallographic axis ratio is $a:b:c = 0.66105: 1:1.54380$. The plane of the optical axes is perpendicular to the basic pinacoid; $(+)$ $2V = 76^\circ$. The indices of refraction: according to Barrett and McCaughey, $Ng = 1.640$, $Nm = 1.636$, $Np = 1.632$; according to Riley and Segnit [19], $Ng = 1.657-1.677$, $Np = 1.630-1.660$; according to Lapin (for samples extracted from slag). $Ng = 1.652-1.656$, $Np = 1.638-1.642$. Cleavage is distinct along two mutually perpendicular directions: (100) and (010). Thus, silicocarnotite, in conformance with the measurements of Lapin, definitely belongs to the rhombic system, and not to the monoclinic, as was asserted by Bücking [11]. The density is 3.08 g/cm^3 (at 22°). Keppler [14] studied numerous monocrystals of silicocarnotite from technical Thomas phosphate and confirmed its formula $5CaO \cdot P_2O_5 \cdot SiO_2$ or $Ca_5(PO_4)_2SiO_4$. Structurally, this compound belongs to the apatite class, with crystals described as rhombic-pseudohexagonal [19].

CRYSTALLINE PHASES OF CaO -- P₂O₅ -- SiO₂ SYSTEM

Compound	System	Ng	Nm	Np	2V°	Notes
5CaO · P ₂ O ₅ · SiO ₂ (silico-carnotite)	Monoclinic (?)	1.640	1.636	1.632	(+) about 90°	Pleochroism in blue tones in microscopic section; density 3.084 g/cm ³
7CaO · P ₂ O ₅ · 2SiO ₂ (nagelschmidtite)	?	1.661	-	1.652	(+) about 20° and up to 0°	Density 3.035 g/cm ³

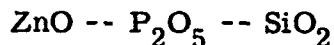
In addition to silicocarnotite and nagelschmidtite, two more silico-phosphates have been found in Thomasphosphates, steadite and thomasite [1]. These minerals, extracted from technical products, contain impurities, and they apparently do not figure in the CaO -- Al₂O₃ -- SiO₂ triple diagram. Thomasite forms blue-green hexagonal crystals, of the composition (6CaO · P₂O₅) · (2FeO · SiO₂). According to Kroll [16], the Fe content decreases right down to iron-free thomasite, of the composition (6CaO · P₂O₅) · (2CaO · SiO₂). Thomasite has not been characterized optically. Steadite has been studied in detail by Lapin [4]. Steadite apparently has a noticeable variability in composition, as a consequence of the formation of solid solutions. Lapin, to isolate steadite from Thomasphosphate, specifies the following oxide ratios: 13.87CaO · 3.32P₂O₅ · 1.00SiO₂ or 3.3(3CaO · P₂O₅) · (2CaO · SiO₂) · 2CaO. This composition should be considered as an average one, since the light refraction of various samples changed from 1.652 to 1.682. The birefringence of steadite is extremely narrow: 0.003-0.004; it forms hexagonal prisms with definite cleavage along the prism and along the base; it is slight pleochroic, from

colorless to yellowish brown. Lapin thinks that steatite is dimorphic and, upon cooling (from high temperatures), undergoes transformation (similar to, for example, leucite and becscite) from the high temperature hexagonal modification to a modification with lower symmetry (monoclinic or triclinic), which is stable at low temperatures. The density of the mineral, determined pycnometrically at 21°, is 3.163 g/cm³.

BIBLIOGRAPHY

1. Belyankin, D. S., B. V. Ivanov, V. V. Lapin, Petrografiya tekhnicheskogo kamnya [Petrography of Industrial Stone], AN SSSR Press, Moscow, 1952, p. 370.
2. Lapin, V. V., Trudy Inst. geol. nauk AN SSSR, issue 20, petrogr. ser., 6, 1939, p. 35.
3. Lapin, V. V., Ibid, issue 77, petrogr. ser., 25, 1945, p. 1.
4. Lapin, V. V., Trudy Inst. geol. rudnykh mestorozhd., petrografii, mineralogii i geokhim., Moscow, 1956, p. 61.
5. Toropov, N. A., A. I. Borisenko, P. V. Shirokova, DAN SSSR, 92, 5, 1953, p. 1015.
6. Balajiva, K., A. G. Quarrell, P. A. Vajragupta, J. Iron a. Steel Inst., 153, 1, 115, 1946.
7. Barrett, R. L., W. J. McCaughey, Amer. Mineralogist, 27, 10, 680, 1942.
8. Berak, J., J. Wojciechowska, Roczn. Chem., 30, 758, 1956.
9. Bredig, M. A., Amer. Mineralogist, 28, 11-12, 594, 1943.
10. Bredig, M. A., J. Amer. Ceram. Soc., 33, 6, 188, 1950.
11. Bücking, L., Stahl u. Eisen, 4, 245, 1887.
12. Fix, W., H. Heymann, R. Heink, J. Amer. Ceram. Soc., 52, 6, 346, 1969.
13. Gutt, W., Nature, 197, 4863, 142, 1963.
14. Keppler, U., Neues Jahrb. Mineral., Monatshefte, 9, 320, 1968.

15. Klement, R., K. Erler, Zs. anorgan. allgem. Chem., 257, 4, 173, 1948.
16. Kroll, V.A., J. Iron a. Steel Inst., 84, 11, 126, 1911.
17. Nagelschmidt, G.J., J. Chem. Soc., 5, 865, 1937.
18. Nurse, R.W., J.H. Welch, W. Gutt, J. Chem. Soc., 3, 1977, 1959.
19. Riley, D.P., E.R. Segnit, Mineral. Magaz., 28, 204, 496, 1949.
20. Segnit, E.R., Mineral. Magaz., 29, 210, 173, 1950.
21. St. Pierre, P.D.S., J. Amer. Ceram. Soc., 39, 4, 143, 1956.
22. Trömel, G., H.J. Harkort, W. Hotop, Zs. anorgan. allgem. Chem., 256, 5-6, 253, 1948.
23. Wojciechowska, J., J. Berak, W. Trzebiatowski, Roczn. Chem., 30, 750, 1956.



Brown and Hummel [1] have studied the subsolidus region of the system (annealing at 1400°). Ternary compounds were not found. The coexisting phase triangles on the triple diagram are given in Fig. 294. It was found that SiO_2 is soluble in the zinc phosphates $\beta \text{Zn}_3(\text{PO}_4)_2$ and $\beta \text{Zn}(\text{PO}_3)_2$, amounting to approximately 5 mole %. Solid solutions have not been found in other binary profiles.

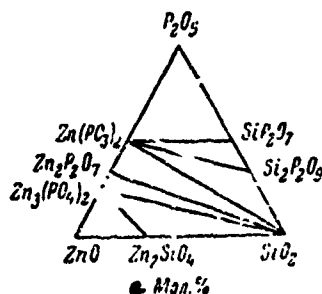
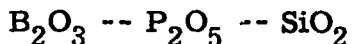


Fig . Coexisting phase triangles of $\text{ZnO} \text{ -- } \text{P}_2\text{O}_5 \text{ -- } \text{SiO}_2$ system (from Brown and Hummel).

Key: a. Mole %

BIBLIOGRAPHY

1. Brown, J.J., F.A. Hummel, Trans. Brit. Ceram. Soc., 64, 9, 419, 1965.



Study of the system is very difficult, because of the volatility of P_2O_5 and difficulties in crystallization. Approximate data are introduced by Horn and Hummel [2] and Englert and Hummel [1]. Horn and Hunmel studied the central section of the partial system BPO_4 -- SiO_2 , and they present the liquidus curve in the 30-70 weight % SiO_2 concentration region in Fig. 295. The mixture containing 62 weight % SiO_2 has the lowest melting temperature $975 \pm 25^\circ$. In the work of Englert and Hummel, an effort was made to plot a phase diagram of the triple system B_2O_3 -- P_2O_5 -- SiO_2 . It is noted that the samples contain water, even at a temperature of 1400° . Boron phosphate BPO_4 , the approximate crystallization field of which is shown in Fig. 296, separated out as the first phase in crystallization of glasses. Glasses rich in silica and boric oxide could not be crystallized, even after 240 hours of soaking at 900° . Glasses are easily obtained in the partial system BPO_4 - SiO_2 .

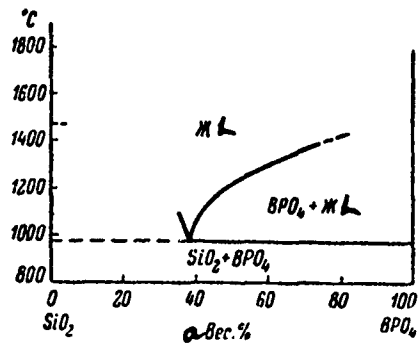


Fig. 295. Section of partial system SiO_2 -- BPO_4 (from Horn and Hummel).

Key:

a. Weight %.

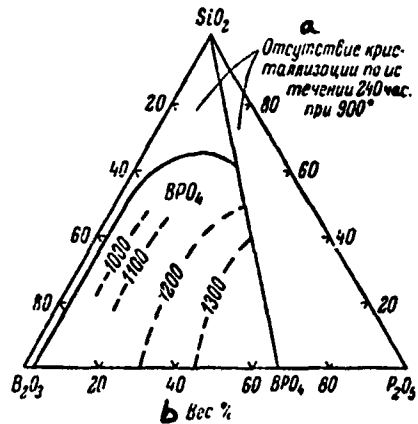


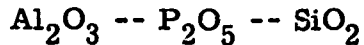
Fig. 296. Schematic phase diagram of B_2O_3 -- P_2O_5 -- SiO_2 system (from Englert and Hummel).

Key:

- a. Absence of crystallization after 240 hours at 900°
- b. Weight %.

BIBLIOGRAPHY

1. Englert, W.J., F.A. Hummel, J. Soc. Glass Technol., 39, 187, 121, 1955.
2. Horn, W.F., F.A. Hummel, J. Soc. Glass Technol., 39, 187, 113, 1955.



The subsolidus relationships in the portion of the $\text{Al}_2\text{O}_3 \text{ -- } \text{P}_2\text{O}_5 \text{ -- } \text{SiO}_2$ system containing less than 50 mole % P_2O_5 has been studied by Robinson and McCartney [4]. Ternary compounds have not been found. Solid solutions of silica and aluminum phosphate (AlPO_4), the formation of which can be expected on the basis of similarities of the unit cell dimensions, were not detected in using various methods, including the electron microprobe method.

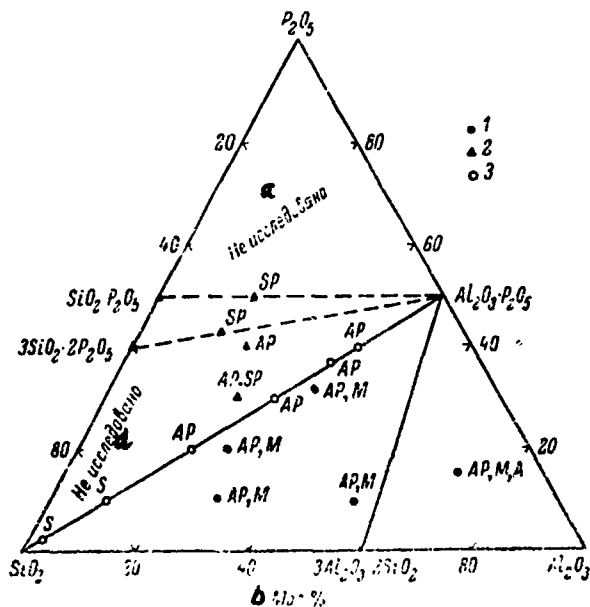


Fig. 297. Schematic phase diagram of $\text{Al}_2\text{O}_3 \text{ -- } \text{P}_2\text{O}_5 \text{ -- } \text{SiO}_2$ system (from Robinson and McCartney): 1. 800° ; 2. 1250° ; 3. 1400° ; M mullite.

Key:

- a. Not investigated
- b. Mole %

$\text{Al}_2\text{O}_3 \cdot \text{P}_2\text{O}_5$ was found in two polymorphic modifications in the temperature range studied (800-1400°): tridymite and cristobalite. At 1050° and 72 hour exposure, both forms crystallized. Upon heating to 1250°, cristobalite and the cristobalite form of AlPO_4 were recorded. Compositions with 80 mole % SiO_2 and above contained only cristobalite, and 60 % and below, only the cristobalite form of AlPO_4 . Low-temperature AlPO_4 , synthesized under hydrothermal conditions (350°, 1 month), had the low-temperature quartz structure, according to Strada [5].

Robinson and McCartney assert that two silicon phosphates exist, $\text{SiO}_2 \cdot \text{P}_2\text{O}_5$ and $3\text{SiO}_2 \cdot \text{P}_2\text{O}_5$, i.e., the data of Bouillé and Jary [1] and Jacoby [2] are confirmed, but not that of Tien and Hummel [6], who demonstrated the existence of $\text{SiO}_2 \cdot \text{P}_2\text{O}_5$ and $2\text{SiO}_2 \cdot \text{P}_2\text{O}_5$. For both phosphates, Robinson and McCartney present interplane distances and X ray line intensities. A coexisting phase diagram is presented in Fig. 299, from their data (coexisting phase triangles for 800, 1250 and 1400°).

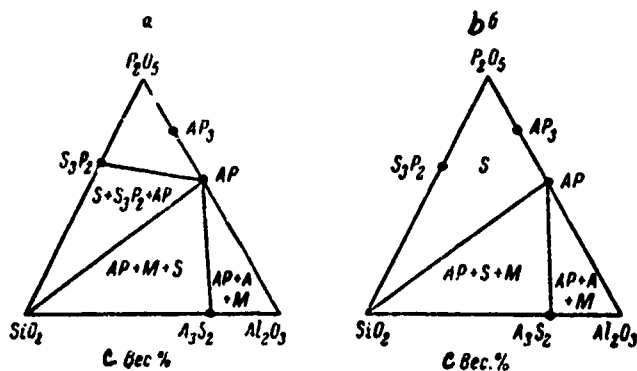


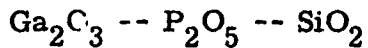
Fig. 298. Coexisting phase triangles of $\text{Al}_2\text{O}_3 \text{--} \text{P}_2\text{O}_5 \text{--} \text{SiO}_2$ system (from Lehmann): a. 900°; b. 900-1200°; M. mullite.

Key: c. Weight %

Lehmann [3] has studied the subsolidus region of the system and plotted coexisting phase triangles for 900° (Fig. 298a) and for the temperature range between 900 and 1200° (Fig. 298b). At the temperatures indicated, according to Lehmann, only one silicon phosphate $3\text{SiO}_2 \cdot 2\text{P}_2\text{O}_5$ exists.

BIBLIOGRAPHY

1. Bouillé, A., R. Jary, Compt. rend., 237, 4, 328, 1953.
2. Jacoby, W.H., Equilibrium relations in a portion of the system SiO_2 -- P_2O_5 . University Microfilms (Ann Arbor, Mich.), Publ. No. 22528, Dissertation Abstr., 17, 2233, 1957.
3. Lehmann, H., Siliconf 1967 (IX Silicon Industry Conference), 21-25 Nov, Budapest, 21-25 Nov, 91, 1967.
4. Robinson, P., E.R. McCartney, J. Amer. Ceram. Soc., 47, 11, 587, 1964.
5. Strada, M., Gazz. Chim. Ital., 64, 653, 1934.
6. Tien, T.Y., F.A. Hummel, J. Amer. Ceram. Soc., 45, 9, 422, 1962.



Study of the system has been limited to the work of Shaffer and Roy [1], who plotted an approximate diagram of the partial system GaPO_4 -- SiO_2 (Fig. 299), in which solid solutions based on both SiO_2 and GaPO_4 form. With increase in temperature, the region of solid solutions expands, and it increases to 25 mole % GaPO_4 close to the melting temperature of cristobalite.

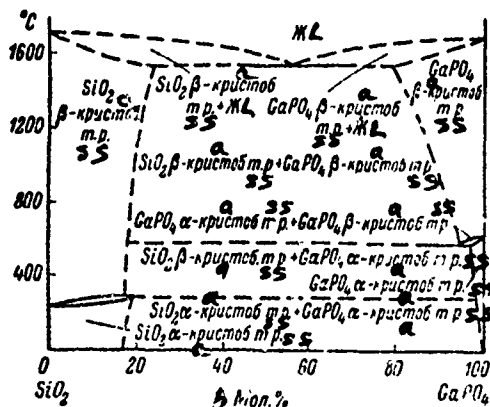


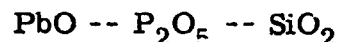
Fig. 299. Phase diagram of partial system
 SiO_2 -- GaPO_4 (from Shaffer and Roy).

Key:

- a. Cristobalite
- b. Mole %

BIBLIOGRAPHY

1. Shaffer, E. C., R. Roy, J. Amer. Ceram. Soc., 39, 10, 336, 1956.



The system has been studied in the region adjacent to lead oxide by Paetsch and Dietzel [1], using a heated microscope. The portion of the phase diagram studied is represented in Fig. 300. The formation of two ternary compounds is indicated: $5\text{PbO} \cdot \text{P}_2\text{O}_5 \cdot \text{SiO}_2$ and $16\text{PbO} \cdot \text{P}_2\text{O}_5 \cdot 2\text{SiO}_2$.

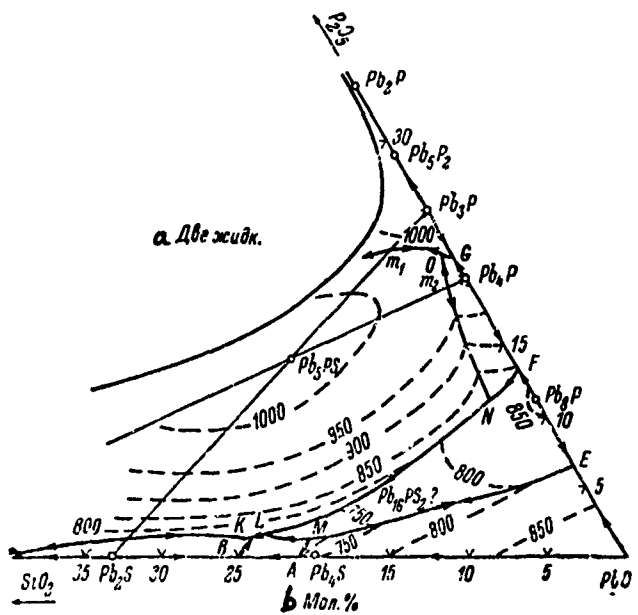


Fig. 300. Phase diagram of part of $\text{PbO} - \text{P}_2\text{O}_5 - \text{SiO}_2$ system; region rich in lead oxide (from Paetsch and Dietzel); invariant points: A. 725°, B. 710°, E. 815°, F. 838°, G. 954°, K. 695°, L. 700°, M. 710°, N. 828°, O. 948°, m_1 . 985°, m_2 . 973°.

Key:

- a. Two liquids
- b. Mole %

Wondratscek and Merker [2] obtained $5\text{PbO} \cdot \text{P}_2\text{O}_5 \cdot \text{SiO}_2$ from a melt, in the form of hexagonal needles or rod-like shapes. The crystals are optically uniaxial, the index of refraction is between 2.0 and 2.1 and extinction is direct. The compound does not disclose polymorphic transformations, and it melts congruently at a temperature of $1016 \pm 5^\circ$. The compound with the conjectural composition $16\text{PbO} \cdot \text{P}_2\text{O}_5 \cdot 2\text{SiO}_2$ is formed by a reaction in the

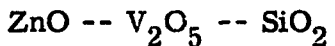
solid state at 600°. This compound exists in two modifications: the modification transformation is accompanied by disintegration of the crystals into powder.

The region of liquid phase separation extends up to 70 mole % PbO. Melts with greater than a 30 mole % SiO₂ content, with a low P₂O₅ content, give glass upon cooling. All other melts are easily crystallized.

BIBLIOGRAPHY

1. Paetsch, H.H., A. Dietzel, Glastech. Ber., 29, 9, 345, 1956.
2. Wondratscek, H., L. Merker, Naturwissenschaften, 43, 21, 494, 1959.

VANADATE-SILICATE SYSTEMS



The system has been studied by Brown and Hummel [1], in the subsolidus region. The coexisting phase triangles are shown in Fig. 301. Negligible solubility of zinc oxide and Zn_2SiO_4 in $\beta \text{Zn}_3(\text{VO}_4)_2$ was observed. Other solid solutions were not found.

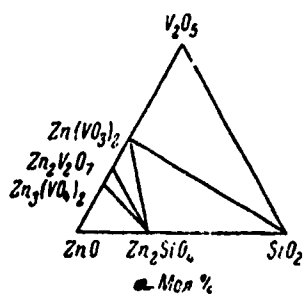


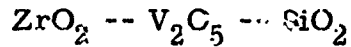
Fig. 301. Coexisting phase triangles of $\text{ZnO} \text{ -- } \text{V}_2\text{O}_5 \text{ -- } \text{SiO}_2$ system (from Brown and Hummel).

Key:

a. Mole %

BIBLIOGRAPHY

1. Brown, J.J., F.A. Hummel, Trans. Brit. Ceram. Soc., 64, 9, 419, 1965.



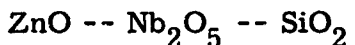
Investigation of the system has been limited to annealing of certain mixtures of oxides for the purpose of obtaining ceramic pigments. Some information on this question is contained in the works of Cini [4], Burdese and Borlera [3] and Matkovich and Corbett [5].

Bystrikov [1, 2] demonstrates that vanadium of various degrees of oxidation is incorporated in the zircon structure, with formation of the compounds: $\text{Zr}_{1-2x}\text{V}_{x+y}^{5+}\text{V}_{x+y}^{3+}\text{Si}_{1-2y}\text{O}_4^{2-}$ of a green color, $\text{Zr}_{1-x}\text{V}_{x+y}^{4+}\text{Si}_{1-y}\text{O}_4^{2-}$ of a blue color. Here, x and y are the respective fractions of substituted zirconium and silicon ions.

BIBLIOGRAPHY

1. Bystrikov, A.S., Trudy NIIstroykeramiki, 24, 1964, p. 189.
2. Bystrikov, A.S., Steklo i keramika, 6, 1965, p. 5.
3. Burdese, A., M.L. Borlera, Ann. Chim., (Roma), 50, 11, 15'0, 1960.
4. Cini, L., La ceramica, 16, 11, 60, 1961.
5. Matkovich, V.J., P.M. Corbett, J. Amer. Ceram. Soc., 44, 3, 128, 1961.

NIOBATE-SILICATE SYSTEMS



The system has been studied by Brown and Hummel [1], in the subsolidus region. The coexisting phase triangles are shown in Fig. 302. Solid solutions have not been found.

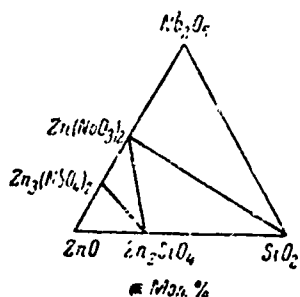


Fig. 302. Coexisting phase triangles of $\text{ZnO} \text{ -- } \text{Nb}_2\text{O}_5 \text{ -- } \text{SiO}_2$ (from Brown and Hummel).

Key:

a. Mole %

BIBLIOGRAPHY

1. Brown, J.J., F.A. Hummel, Trans. Brit. Ceram. Soc., 9, 419, 1965.

TANTALATE-SILICATE SYSTEMS



Reeve and Bright [3] have studied the system, using a high-temperature microscope and the quenching method. The authors introduce a phase diagram of the binary system Ta_2O_5 -- SiO_2 (Fig. 303). In plotting the diagram, the data of Bush [1] were used. The authors draw attention to the anomalous trend of the liquidus curve (a break at a SiO_2 content of somewhat over 10 weight %). In accordance with the data of Reeve [2], there are 5 compounds in the $\text{CaO} \text{ -- } \text{Ta}_2\text{O}_5$ system: $\text{CaO} \cdot 2\text{Ta}_2\text{O}_5$ (incongruent melting, 1730°), $\text{CaO} \cdot \text{Ta}_2\text{O}_5$ (congruent melting, 1958°), $2\text{CaO} \cdot \text{Ta}_2\text{O}_5$ (congruent melting, 1896°), $4\text{CaO} \cdot \text{Ta}_2\text{O}_5$ (incongruent melting, 1990°) and $5\text{CaO} \cdot \text{Ta}_2\text{O}_5$ (stable in the 1460 - 1590° range).

One compound, melting incongruently at 1478° , $10\text{CaO} \cdot \text{Ta}_2\text{O}_5 \cdot 6\text{SiO}_2$ (Ta kaiite) has been found in the triple system; it is isostructural with the mineral niokalite. A large region of liquid immiscibility is characteristic of the system; it extends from the $\text{CaO} \text{ -- } \text{SiO}_2$ side, but it does not intersect the $\text{Ta}_2\text{O}_5 \text{ -- } \text{SiO}_2$ side (the boundary line is at a distance of about 1 weight %).

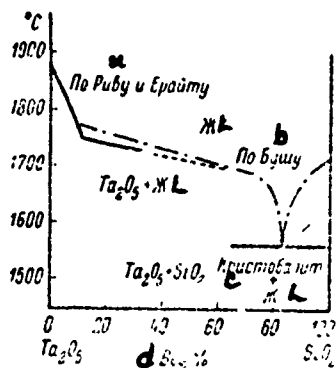


Fig. 303. Phase diagram of binary system Ta_2O_5 -- SiO_2 (from Bush).

Key:

- a. According to Reeve and Bright
 - b. According to Bush
 - c. Cristobalite
 - d. Weight %

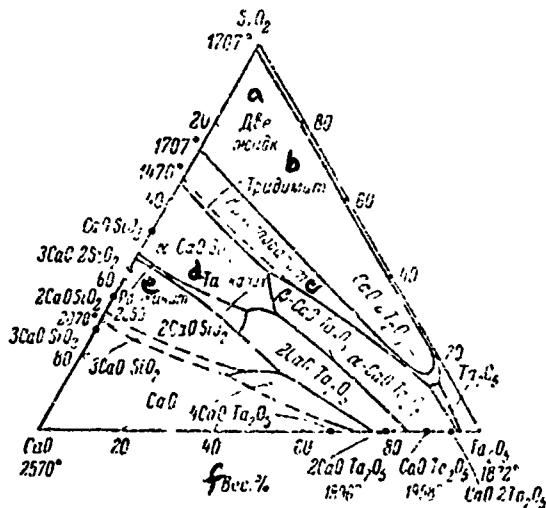


Fig. 304. Phase diagram of CaO -- Ta₂O₅ -- SiO₂ system (from Reeve and Bright).

Key: a. Two liquids d. Ta kalite
 b. Tridymite e. Rankinite
 c. Cristobalite f. Weight %

INVARIANT POINTS OF CaO -- Ta₂O₅ -- SiO₂ SYSTEM

a Фазы	b Процесс	c Состав, вес. %			d Темпера- тура, °C
		CaO	Ta ₂ O ₅	SiO ₂	
e Получено методом закалки					
α-CaO · SiO ₂ + β-CaO · Ta ₂ O ₅ + + SiO ₂ + жидкость f	г Эвтектика	27.2	31.5	41.3	1316
α-CaO · SiO ₂ + β-CaO · Ta ₂ O ₅ + + 2CaO · Ta ₂ O ₅ + жидкость f	г Перитектика	31.2	38.6	30.2	1376
α-CaO · SiO ₂ + 3CaO · 2SiO ₂ + + 10CaO · Ta ₂ O ₅ · 6SiO ₂ + жидкость f	г Эвтектика	50.2	10.0	39.8	1414
2CaO · SiO ₂ + 3CaO · 2SiO ₂ + + 10CaO · Ta ₂ O ₅ · 6SiO ₂ + жидкость f	г Перитектика	50.6	10.0	39.4	1418
α-CaO · SiO ₂ + 2CaO · Ta ₂ O ₅ + + 10CaO · Ta ₂ O ₅ · 6SiO ₂ + жидкость f	г Эвтектика	37.4	31.8	30.8	1429
2CaO · SiO ₂ + 2CaO · Ta ₂ O ₅ + + 10CaO · Ta ₂ O ₅ · 6SiO ₂ + жидкость f	»	42.2	32.8	25.0	
f Получено с нагревательным микроскопом					
2CaO · SiO ₂ + 2CaO · Ta ₂ O ₅ + + 4CaO · Ta ₂ O ₅ + жидкость f	г Перитектика	37.7	47.8	14.5	1610
CaO · 2Ta ₂ O ₅ · Ta ₂ O ₅ · SiO ₂ + + жидкость f	»	3.3	84.7	12.0	1640
CaO · 2Ta ₂ O ₅ + α-CaO · Ta ₂ O ₅ + + SiO ₂ + жидкость f	г Эвтектика	6.0	82.2	11.8	1650
2CaO · SiO ₂ + 3CaO · SiO ₂ + + 4CaO · Ta ₂ O ₅ + жидкость f	г Перитектика	46.5	38.0	15.5	1870
3CaO · SiO ₂ + 3CaO · Ta ₂ O ₅ + + CaO + жидкость f	»	50.0	36.0	14.0	1950

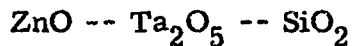
Key:

- | | |
|---------------------------------|------------------------------------|
| a. Phases | f. Liquid |
| b. Process | g. Eutectic |
| c. Composition, weight % | h. Peritectic |
| d. Temperature, °C | i. Obtained with heated microscope |
| e. Obtained by quenching method | |

A phase diagram of the system is represented in Fig. 304. Three partial profiles are simple eutectics: CaO · SiO₂ -- 10CaO · Ta₂O₅ · 6SiO₂, CaO · SiO₂ -- 2CaO · Ta₂O₅ and 2CaO · SiC₂ -- 10CaO · Ta₂O₅ · 6SiO₂. The authors present indices of refraction for several glasses of the system.

BIBLIOGRAPHY

1. Bush, E.A., Progress Rep., 1a, 2, Depart. Ceram. Technol., Pennsylvania State Univ., 1964.
2. Reeve, D.A., J. Less Common Metals, 17, 2, 215, 1969.
3. Reeve, D.A., N.F.H. Bright, J. Amer. Ceram. Soc., 52, 8, 405, 1969.



The system has been studied by Brown and Hummel [1], in the subsolidus region. Coexisting phase triangles are introduced in Fig. 305. Solid solutions have not been found.

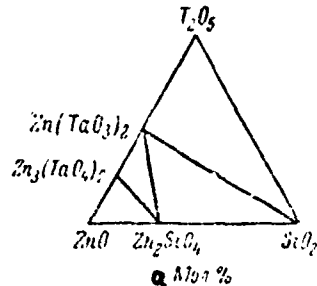


Fig. 305. Coexisting phase triangles of $\text{ZnO} \text{ -- } \text{Ta}_2\text{O}_5 \text{ -- } \text{SiO}_2$ system (from Brown and Hummel).

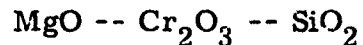
Key:

a. Mole %

BIBLIOGRAPHY

1. Brown, J.J., F.A. Hummel, Trans. Brit. Ceram. Soc., 64, 9, 419, 1965.

CHROMOSILICATE SYSTEMS



The system has been studied by the quenching method by Keith [3].

Extensive investigations in the subsolidus region have been carried out by Klyucharov and colleagues. Keith did not find ternary compounds. A large region of immiscibility of the liquids has been established, adjacent to the $\text{SiO}_2 \text{ -- } \text{Cr}_2\text{O}_3$ side (Fig. 306). It is interesting that, of the six compounds existing in this system -- MgO , SiO_2 , Cr_2O_3 , $2\text{MgO} \cdot \text{SiO}_2$, $\text{MgO} \cdot \text{SiO}_2$ and $\text{MgO} \cdot \text{Cr}_2\text{O}_3$ -- the triple diagram field is occupied predominantly by only 3 compounds, MgO , Cr_2O_3 and $\text{MgO} \cdot \text{Cr}_2\text{O}_3$ (magnesiochromite). The cristobalite field is especially small (see upper left in Fig. 306).

The immiscible liquids give glass upon cooling. The silica-rich liquid has an index of refraction of 1.462, which is close to the index of pure silica glass (1.458). Coexisting phase triangles of the system are introduced by Ford and Rees [2].

Klyucharov and Khlebnikova [1] have studied the reactions forming compounds in the subsolidus region (annealing in the 1000-1600° range).

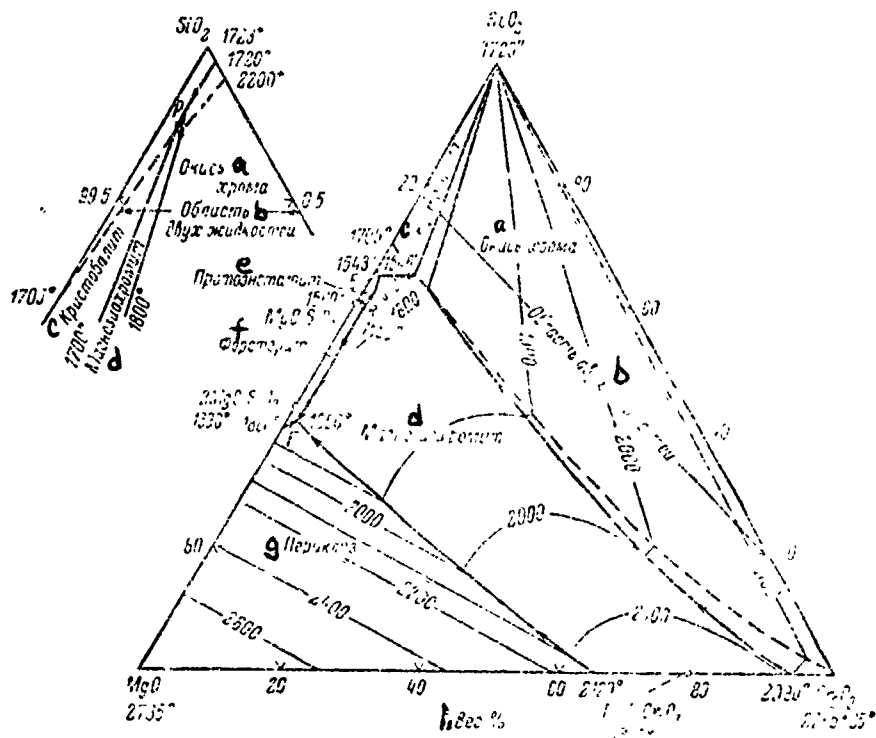


Fig. 306. Phase diagram of $\text{MgO} \text{ -- } \text{Cr}_2\text{O}_3 \text{ -- } \text{SiO}_2$ system (from Keith).

Key:

- | | |
|--------------------------|------------------|
| a. Chromic oxide | e. Protoenstaite |
| b. Region of two liquids | f. Forsterite |
| c. Cristobalite | g. Periclase |
| d. Magnesiochromite | h. Weight % |

Ternary compounds were not found. All of the chromic oxide reacts quickly with magnesium oxide below 1000° , with formation of $\text{MgO} \cdot \text{Cr}_2\text{O}_3$. Regardless of the ratio of the initial oxides, the first silicate compound is forsterite, which, in the case of the presence of an excess of silica, forms enstatite as a secondary phase. In the $\text{MgO} \text{ -- } 2\text{MgO} \cdot \text{SiO}_2 \text{ -- } \text{MgO} \cdot \text{Cr}_2\text{O}_3$ concentration

region, $2\text{MgO} \cdot \text{SiO}_2$ is present in samples annealed at 1400°, when equilibrium is reached rapidly. In the $\text{MgO} \cdot \text{Cr}_2\text{O}_3$ -- $2\text{MgO} \cdot \text{SiO}_2$ -- SiO_2 concentration region, when $2\text{MgO} \cdot \text{SiO}_2$ and $\text{MgO} \cdot \text{SiO}_2$ are present, equilibrium is reached over a long period of time.

INVARIANT POINTS OF $\text{MgO} \text{--} \text{Cr}_2\text{O}_3 \text{--} \text{SiO}_2$ SYSTEM

a Точка (рис. 306)	b Фазы	c Процесс	d Состав, вес. %			e Температура, °C
			MgO	Cr_2O_3	SiO_2	
F	Периклаз + форстерит + магнезиохромит + жидкость	Эвтектика	59	1	40	1950 ± 10
E	Протостатит + кристобаллит + магнезиохромит + жидкость	>	34.5	1	64.5	1516 ± 3
R	Форстерит + протозистатит + магнезиохромит + жидкость	Реакционная точка	39	2	59	1550 ± 5
P	Магнезиохромит + кристобаллит + олиев хромат + жидкость	o То же	~ 0.5	~ 0.5	99	1710 ± 10

Key:

- a. Points (Fig. 306)
- b. Phases
- c. Process
- d. Composition, weight %
- e. Temperature, °C
- f. Periclase
- g. Forsterite
- h. Magnesiochromite
- i. Liquid
- j. Protostatite
- k. Cristobalite
- l. Chromic oxide
- m. Eutectic
- n. Reaction point
- o. Same

BIBLIOGRAPHY

1. Klyucharov, Ya. F., I. Yu. Khlebnikova, Trudy Vsesoyuzn. gos. inst. ogneuporov, Issue 36, 1964, p. 119.
2. Ford, W. F., W. J. Rees, Trans. Brit. Ceram. Soc., 57, 5, 238, 1958.
3. Keith, M. L., J. Amer. Ceram. Soc., 37, 10, 490, 1954.

$\text{CaO} \text{-- } \text{Cr}_2\text{O}_3 \text{-- } \text{SiO}_2$

The system has been studied by Glasser and Gsborn [6] by the quenching method. The region adjacent to the CaO apex, where the appearance of chromium with high valence is possible under oxidizing conditions, was not studied. A phase diagram of the system is presented in Fig. 307. The characteristics of the cristobalite field are given at the upper right in this figure. The liquid phase separation region adjoins the $\text{Cr}_2\text{O}_3 \text{-- } \text{SiO}_2$ side. In the boundary section, where the Cr_2O_3 and cristobalite fields meet, two crystalline and two liquid phases coexist. One of these liquids is almost pure silica, and the second has the composition 27 weight % CaO, 1 Cr_2O_3 and 72 SiO_2 .

One ternary compound has been found in the system, $3\text{CaO} \cdot \text{Cr}_2\text{O}_3 \cdot 3\text{SiO}_2 = \text{Ca}_3\text{Cr}_2\text{Si}_3\text{O}_{12}$, which is found in nature in the form of the mineral uvarovite. This compound, existing at low temperatures, dissociates at 1370° into αCaSiO_3 and Cr_2O_3 . A diagram illustrating the phase equilibria along the $\text{CaSiO}_3 \text{-- } \text{Cr}_2\text{O}_3$ profile is presented in Fig. 308. The subsolidus phase relationships and coexisting phase triangles at 1350° are shown in Fig. 309.

The authors point out that the compound of calcium oxide and chromic oxide, to which Ford and Rees [4] ascribed the formula $9\text{CaO} \cdot 4\text{CrO}_3 \cdot \text{Cr}_2\text{O}_3$, actually is a compound with pentavalent chromium $\text{Ca}_3(\text{CrO}_4)_2$, which is structurally similar to $\text{Ca}_3(\text{PO}_4)_2$ and which forms a solid solution with Ca_2SiO_4 containing up to 20% chromate. The compound $\text{Ca}_3(\text{CrO}_4)_2$ can be obtained by heating (24 hours) a mixture of the composition $3\text{CaO} + \text{Cr}_2\text{O}_3$ in air at 900-1000°. It is stable in the low temperature range. At 800°, it is oxidized to CaCrO_4 , and it can be melted congruently at 1228°.

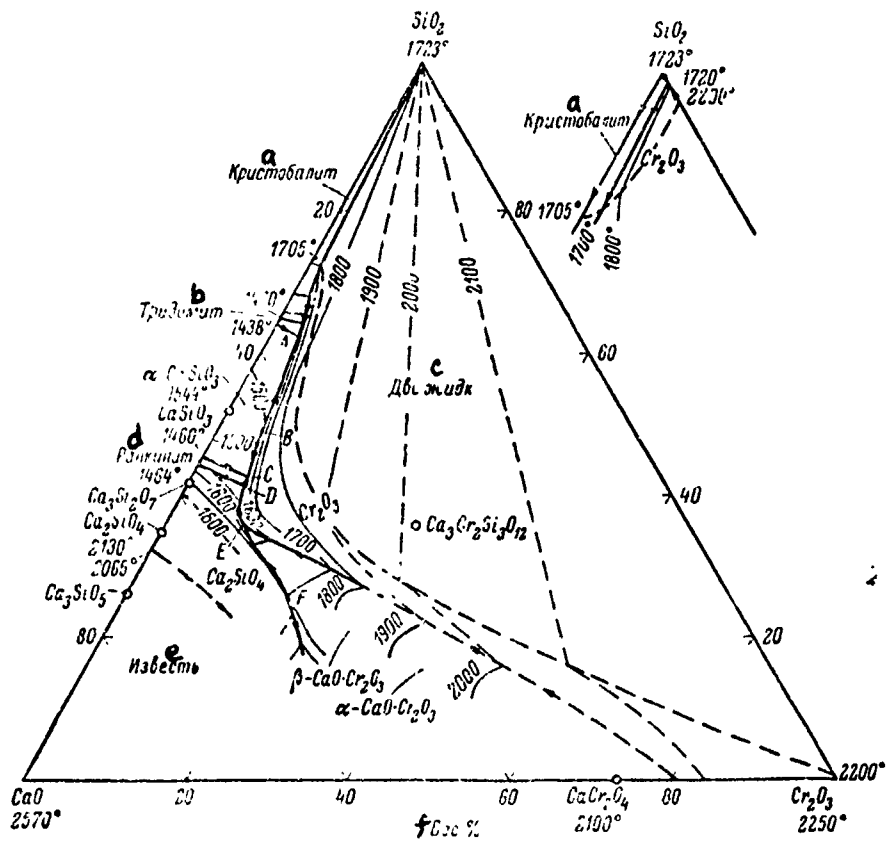


Fig. 307. Phase diagram of $\text{CaO} \text{ -- } \text{Cr}_2\text{O}_3 \text{ -- } \text{SiO}_2$ system (from Glasser and Osborn).

Key:

- a. Cristobalite
- b. Tridymite
- c. Two liquids
- d. Rankinite
- e. Lime
- f. Weight %

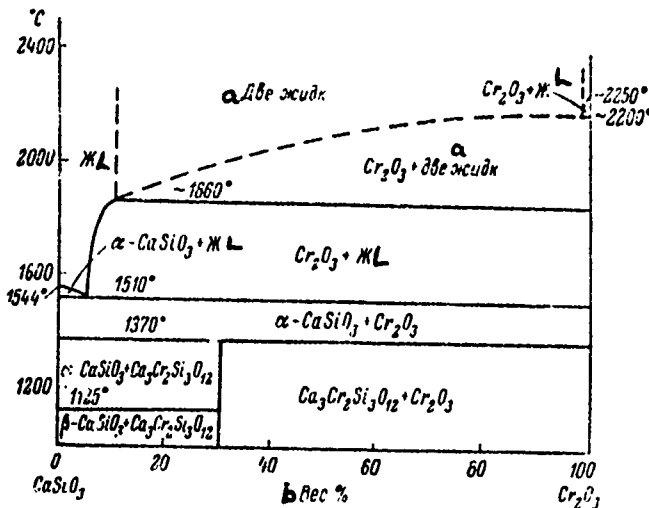


Fig. 308. Phase diagram of partial system CaSiO_3 -- Cr_2O_3 (from Glasser and Osborn).

Key:

- a. Two liquids
- b. Weight %

Swisher and McCabe [8] have studied the phase separation of melts.

They showed that phase separation is observed at 1600° . The authors proposed an original method for determination of the chemical composition of the liquid phases separating, which is especially suitable for liquids which easily give emulsions. A binary melt ($\text{CaO} + \text{SiO}_2$) is in a platinum crucible with holes in the sides, placed inside a large crucible. Cr_2O_3 powder is poured into the large crucible, above which a binary calcium silicate melt is built up. After prolonged controlled heating of the entire system and achievement of equilibrium, the inner crucible contains only lighter liquid A; two liquid layers

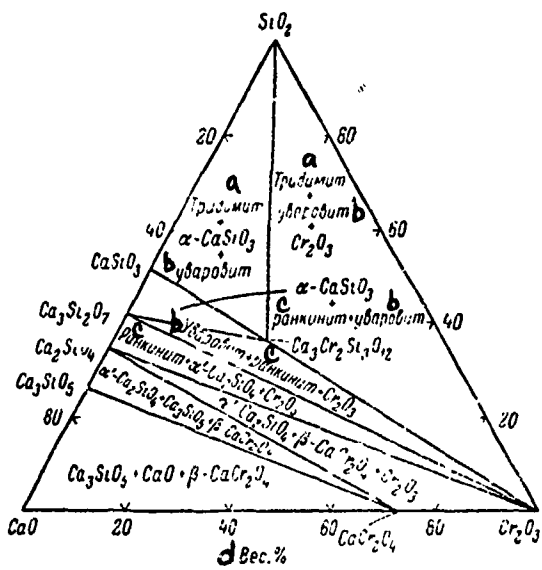


Fig. 309. Diagram of subsolidus phase relationships of CaC -- Cr₂O₃ -- SiO₂ system at 1350° (from Glasser and Osborn).

Key:

- a. Tridymite
 - b. Uvarovite
 - c. Rankinite
 - d. Weight %

are observed in the outer crucible, of which only the lower one, liquid B, is analyzed. The results of determination of the composition of both liquids, the chromic oxide-poor liquid A and the chromic oxide-rich liquid B, are presented in Fig. 310. The oval-shaped phase separation region extends from the $\text{CaO} - \text{SiO}_2$ side in the Cr_2O_3 direction. The tie lines are almost parallel to one another.

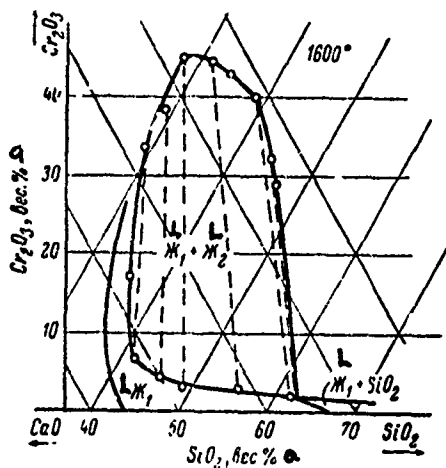


Fig. 310. Phase separation of melts in $\text{CaO} - \text{Cr}_2\text{O}_3 - \text{SiO}_2$ system (from Swisher and McCabe).

Key:

a. Weight %

Boykova and colleagues [2], annealing tricalcium silicate $3\text{CaO} \cdot \text{SiO}_2$ with Cr_2O_3 at $1450-1500^\circ$, showed that the solubility of Cr_2O_3 is 1.5 weight %. The resulting limiting solid solution has indices of refraction $\text{Ng} = 1.726 \pm 0.003$ and $\text{Np} = 1.722 \pm 0.003$. The authors observed an interesting process of breakdown of the solid solution, taking place at a temperature of about 1000° . As a result of the breakdown, calcium oxide and strongly birefringent, green crystals, with indices of refraction $\text{Ng} = 1.767 \pm 0.003$ and $\text{Np} = 1.754 \pm 0.003$, form. The nature of these crystals has not been precisely established, and the authors propose that they are a solid solution of Cr_2O_3 in $2\text{CaO} \cdot \text{SiO}_2$. It is interesting that incorporation of magnesium oxide into the solid solution prevents its breakdown.

INVARIANT POINTS OF CaO -- Cr₂O₃ -- SiO₂ SYSTEM

α Точка (рис. 307)	β Фазы	γ Процесс	δ Состав, вес.%			Темп- ратура, °C
			CaO	Cr ₂ O ₃	SiO ₂	
—	Кристобалит + тридимит + Cr ₂ O ₃ + жидкость	Превращение	32.5	3.0	64.5	1470
A	Гритинит + α-CaSiO ₃ + Cr ₂ O ₃ + жидкость	Эвтектика	34.5	3.0	62.5	1418
B	α-CaSiO ₃ + Cr ₂ O ₃ + жидкость	Листектическая	45.0	6.0	49.0	1514
C	Ранкинит + α-CaSiO ₃ + Cr ₂ O ₃ + жидкость	Эвтектика	51.0	7.0	42.0	1407
D	Ранкинит + Ca ₂ SiO ₄ + Cr ₂ O ₃ + жидкость	Перитектика	52.0	7.0	41.0	1430
E	Ca ₂ SiO ₄ + β-CaO·Cr ₂ O ₃ + Cr ₂ O ₃ + жидкость	То же	53.5	12.5	34.0	1566
F	Ca ₂ SiO ₄ + β-CaO·Cr ₂ O ₃ + Cr ₂ O ₃ + жидкость	Листектическая	54.0	20.5	25.5	1720

Key:

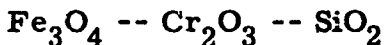
- | | |
|--------------------------|-------------------|
| a. Points (Fig. 307) | h. Liquid |
| b. Phases | i. Rankinite |
| c. Process | j. Transformation |
| d. Composition, weight % | k. Eutectic |
| e. Temperature, °C | l. Dystectic |
| f. Cristobalite | m. Peritectic |
| g. Tridymite | n. Same |

Sychev and Korneyev [3] have shown that the maximum solubility of Cr₂O₃ in 3CaO·SiO₂ at 1500° is approximately 2 weight %. With a higher Cr₂O₃ content, part of the SiO₂ is replaced by chromic oxide and 2CaO·SiO₂ and free calcium oxide form. The authors confirmed their conclusions by thermographic and IR spectroscopic examinations.

Berezhnay [1] notes the nonreproducibility of uvarovite synthesis by means of solid-phase reactions, from a mixture of CaSiO₃ and Cr₂O₃. Hummel [7] and Geller and Miller [5] were engaged in uvarovite synthesis.

BIBLIOGRAPHY

1. Berezhnoy, A. S., Mnogokomponentnyye sistemy okislov [Multicomponent Oxide Systems], Naukova dumka Press, Kiev, 1970, p. 154.
2. Boykova, A. I., N. A. Toropov, M. M. Piryutko, S. V. Grum-Grzhimaylo, Izv. AN SSSR, neorg. mater., 2, 10, 1966, p. 1796.
3. Sychev, M. M., V. I. Korneyev, N. F. Fedorov, Alit i belit v portland-tsementnom klinkere [Alite and Belite in Portland Cement Clinker], Stroyizdat Press, Leningrad-Moscow, 1965, p. 9.
4. Ford, W. F., W. J. Rees, Trans. Brit. Ceram. Soc., 47, 6, 207, 1948, 48, 8, 291, 1949.
5. Geller, S., C. E. Miller, Amer. Mineralogist, 44, 3-4, 445, 1959.
6. Glasser, F. P., E. F. Osborn, J. Amer. Ceram. Soc., 41, 9, 358, 1958.
7. Hummel, F. A., Amer. Mineralogist, 35, 3-4, 324, 1950.
8. Swisher, J. H., C. L. McCabe, Trans. Metal. Soc., AIME, 230, 1, 261, 1964.



Phase equilibria in the system have been studied in an atmosphere of air by the quenching method by Muan and Somiya [2]. A phase diagram for the liquidus temperature section, obtained by projecting the phase relationships on the $\text{Fe}_3\text{O}_4 \text{ -- Cr}_2\text{O}_3 \text{ -- SiO}_2$ plane, found along an uneven isobaric surface (O_2 pressure = 0.21 atm), passing through the tetrahedron of the Fe-Cr-Si-O system, is represented in Fig. 311. The section of the diagram adjacent to the silica apex is given to the right of the triangular diagram, in enlarged form.

The lowest liquidus temperature (in an atmosphere of air) in the $\text{Fe}_3\text{O}_4 \text{ -- SiO}_2$ system, i. e., the eutectic which is in equilibrium with tridymite, magnetite and liquid, according to Muan [1], is 1455° . In proportion to addition of Cr_2O_3 to the $\text{Fe}_3\text{O}_4 + \text{SiO}_2$ mixture, the liquidus temperature rapidly

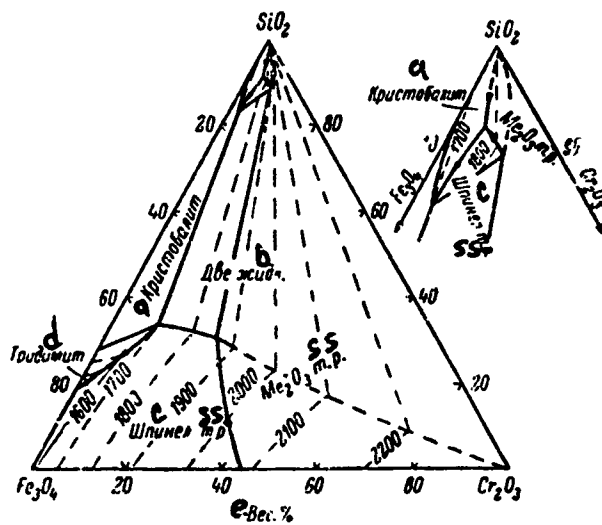


Fig. 311. Phase diagram of Fe_3O_4 -- Cr_2O_3 -- SiO_2 system (from Muan and Somiyc).

Key:

- | | |
|-----------------|--------------|
| a. Cristobalite | d. Tridymite |
| b. Two liquids | e. Weight % |
| c. Spinel | |

increases along the boundary curves on which tridymite (or cristobalite), spinel solid solutions and liquid are in equilibrium. With increase in amount of Cr_2O_3 , the liquidus temperature continues to increase, initially along the liquidus surface of the spinel solid solutions, through the region of two immiscible liquids and then along the liquidus surface of the sesquioxide solid solutions.

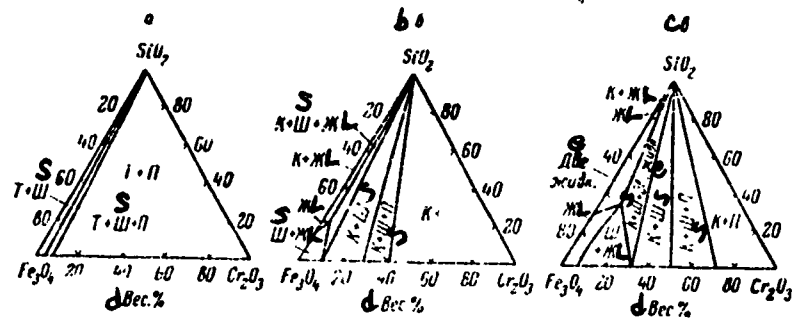


Fig. 312. Isothermal sections illustrating phase relationships during change in temperature from 1400 to 1700° in the Fe_3O_4 -- Cr_2O_3 -- SiO_2 system (from Muan and Somiya): a. 1400°; b. 1500°; c. 1700°; K. cristobalite; P. sesquioxide; S. spinel; T. tridymite.

Key:

- d. Weight %
- e. Two liquids

Three isobaric invariant reactions have been established in the system, in which the following phase associations are in equilibrium (weight %):

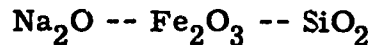
1. at 1710°, cristobalite, spinel solid solutions (50% Fe_3O_4 , 50% Cr_2O_3), sesquioxide solid solutions (29% Fe_3O_4 , 71% Cr_2O_3), liquid (91% SiO_2 , 6% Fe_3O_4 , 3% Cr_2O_3) and gas ($P_{\text{O}_2} = 0.21 \text{ atm}$); 2. at approximately 1850°, spinel solid solutions (43% Fe_3O_4 , 57% Cr_2O_3), sesquioxide solid solutions (18% Fe_3O_4 , 82% Cr_2O_3), two liquids (89% SiO_2 + 5% Fe_3O_4 + 6% Cr_2O_3 and 31% SiO_2 + 40% Fe_3O_4 + 23% Cr_2O_3) and gas ($P_{\text{O}_2} = 0.21 \text{ atm}$); 3. at 1700°, cristobalite, spinel solid solutions (69% Fe_3O_4 , 31% Cr_2O_3), two liquids (83% SiO_2 + 15% Fe_3O_4 + 2% Cr_2O_3 and 34% SiO_2 + 56% Fe_3O_4 + 10%

Cr_2O_3) and gas ($P_{\text{O}_2} = 0.21 \text{ atm}$). For a more detailed indication of the change in phase composition vs. change in temperature, a series of isothermal sections of the Fe_3O_4 -- Cr_2O_3 -- SiO_2 system in an atmosphere of air is presented in Fig. 312.

BIBLIOGRAPHY

1. Muan, A., J. Metals, 7, 9, 1955, (Trans. Amer. Inst. Mining Met. Engrs., 203, 965, 1955); J. Amer. Ceram. Soc., 40, 4, 121, 1957.
2. Muan, A., S. Somiya, J. Amer. Ceram. Soc., 43, 4, 204; 10, 531, 1960.

FERRISILICATE SYSTEMS



The system has been studied by Bowen and Schairer [3] and Bowen, Schairer and Willems [4]. At elevated temperatures, as a consequence of dissociation of ferric oxide, a small (on the order of 1%) quantity of ferrous oxide (FeO) appears, which can be disregarded. Four ternary compounds have been found: $\text{Na}_2\text{O} \cdot \text{Fe}_2\text{O}_3 \cdot 4\text{SiO}_2$ (acmite or aegirite), $5\text{Na}_2\text{O} \cdot \text{Fe}_2\text{O}_3 \cdot 8\text{SiO}_2$, $6\text{Na}_2\text{O} \cdot 4\text{Fe}_2\text{O}_3 \cdot 5\text{SiO}_2$ and $2\text{Na}_2\text{O} \cdot \text{Fe}_2\text{O}_3 \cdot \text{SiO}_2$. The fields of some ternary compounds are shown in Fig. 313. The direction of the tridymite-hematite boundary line indicates the small likelihood of existence of compounds between Fe_2O_3 and SiO_2 and, rather, is evidence that complete immiscibility should be observed between these oxides in the molten state.

Acmite $\text{Na}_2\text{O} \cdot \text{Fe}_2\text{O}_3 \cdot 4\text{SiO}_2$ melts incongruently, according to new data of Bailey and Schairer [2], at $988 \pm 5^\circ$, with separation of hematite and liquid, the composition of which becomes identical with the composition of acmite at 1310° .

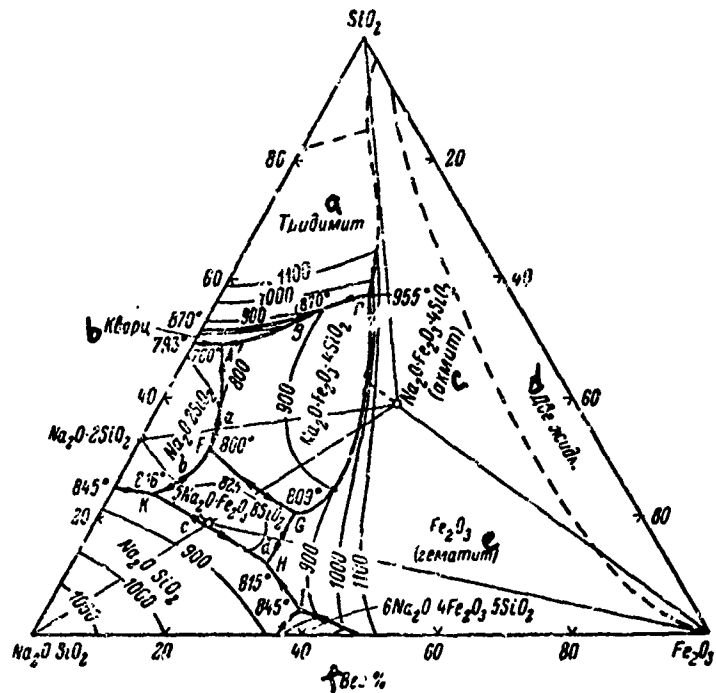


Fig. 313. Phase diagram of partial triple system Na_2O - SiO_2 - Fe_2O_3 - SiO_2 (from Bowen and colleagues).

Key:

- | | |
|--------------|----------------|
| a. Tridymite | d. Two liquids |
| b. Quartz | e. Hematite |
| c. Acmite | f. Weight % |

The compound $5\text{Na}_2\text{O} \cdot \text{Fe}_2\text{O}_3 \cdot 8\text{SiO}_2$ melts congruently at 838° . The strongly basic compound $6\text{Na}_2\text{O} \cdot 4\text{Fe}_2\text{O}_3 \cdot 5\text{SiO}_2$ has a small field, intersecting the line passing between $\text{Na}_2\text{O} \cdot \text{SiO}_2$ and Fe_2O_3 , and it melts congruently at 1091° . Doubts are expressed as to the existence of the compound $2\text{Na}_2\text{O} \cdot \text{Fe}_2\text{O}_3 \cdot \text{SiO}_2$.

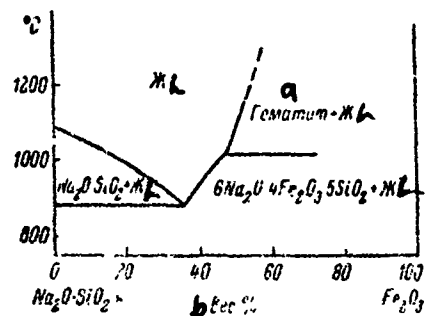


Fig. 314. Phase diagram of partial system $\text{Na}_2\text{O} \cdot \text{SiO}_2 \cdots \text{Fe}_2\text{O}_3$ (from Bowen and colleagues).

Key:

- a. Hematite
 - b. Weight %

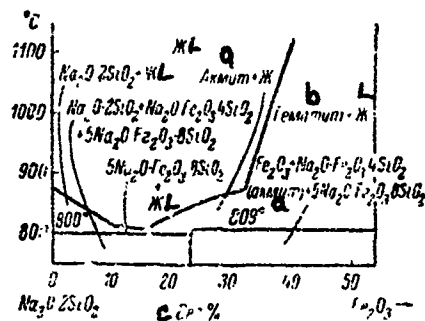
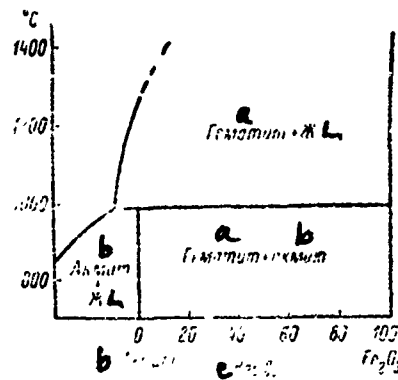


Fig. 315. Phase diagram of partial system $\text{Na}_2\text{O} \cdot 2\text{SiO}_2 \cdots \text{Fe}_2\text{C}_3$ (from Bowen and colleagues).

Key:

- a. Acmite
 - b. Hematite
 - c. Weight %



Key:

- a. Hematite
- b. Acmite
- c. Weight %

Fig. 316. Phase diagram of partial system $\text{Na}_2\text{O} \cdot \text{Fe}_2\text{O}_3 \cdot 4\text{SiO}_2$ -- Fe_2O_3 (from Eowen and colleagues).

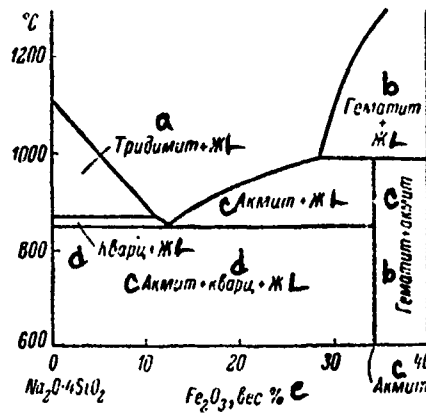


Fig. 317. Phase diagram of partial system $\text{Na}_2\text{O} \cdot 4\text{SiO}_2$ -- $\text{Na}_2\text{O} \cdot \text{Fe}_2\text{O}_3 \cdot 4\text{SiO}_2$ (from Bowen and colleagues).

Key:

- | | |
|--------------|-------------|
| a. Tridymite | d. Quartz |
| b. Hematite | e. Weight % |
| c. Acmite | |

Four partial binary profiles are given in Figs. 314-317.

Gilbert [5, 6] has studied the behavior of acmite at high pressures. With increase in pressure, the melting temperature of acmite increases, exceeding 1600° at a pressure of 50 kbar. A curve of the incongruent melting of acmite is shown in Fig. 318. This kind of melting of acmite has been followed to a pressure of 45 kbar, and it is expressed by the equation $t(^{\circ}\text{C}) = 988 + 20.87P$ (kbar) - $0.155 P^2$ (kbar). Attention is attracted to the extremely steep rise in the melting curve of acmite ($20^{\circ}/\text{kbar}$).

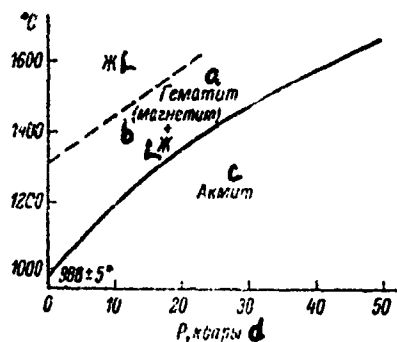


Fig. 318. Acmite melting temperature vs. pressure (from Gilbert).

Key:

- a. Hematite
- b. Magnetite
- c. Acmite
- d. P, kbar

TABLE 1
INVARIANT POINTS OF $\text{Na}_2\text{O} - \text{Fe}_2\text{O}_3 - \text{SiO}_2$ SYSTEM

a Точка (рис. 313)	b Фазы	c Состав, вес.%			d Темпера- тура, °C
		Na ₂ O	SiO ₂	Fe ₂ O ₃	
A	$\text{Na}_2\text{O} \cdot 2\text{SiO}_2 + \text{Na}_2\text{O} \cdot \text{Fe}_2\text{O}_3 \cdot 4\text{SiO}_2 + \text{SiO}_2$ e (кварц) + жидкость f	46.6	49.2	4.2	760
B	SiO_2 (кварц) $\geq \text{SiO}_2$ (тридимит) g	31.0	51.2	14.8	870
C	$\text{Na}_2\text{O} \cdot \text{Fe}_2\text{O}_3 \cdot 3\text{SiO}_2 + \text{Fe}_2\text{O}_3 + \text{SiO}_2$ (троллз) жидкость f	20.5	57.8	21.7	955
a	$\text{Na}_2\text{O} \cdot 2\text{SiO}_2 + \text{Na}_2\text{O} \cdot \text{Fe}_2\text{O}_3 \cdot 4\text{SiO}_2 +$ жидкость f	54.8	35.0	10.2	810
F	$\text{Na}_2\text{O} \cdot 2\text{SiO}_2 + \text{Na}_2\text{O} \cdot \text{Fe}_2\text{O}_3 \cdot 4\text{SiO}_2 +$ $+ 5\text{Na}_2\text{O} \cdot \text{Fe}_2\text{O}_3 \cdot 8\text{SiO}_2 +$ жидкость f	57.8	31.2	11.0	800
b	$\text{Na}_2\text{O} \cdot 2\text{SiO}_2 + 5\text{Na}_2\text{O} \cdot \text{Fe}_2\text{O}_3 \cdot 8\text{SiO}_2 +$ жидкость f	65.5	25.6	8.9	818
c	$\text{Na}_2\text{O} \cdot \text{SiO}_2 + 5\text{Na}_2\text{O} \cdot \text{Fe}_2\text{O}_3 \cdot 8\text{SiO}_2 +$ жидкость f	65.3	18.4	16.3	857
G	$5\text{Na}_2\text{O} \cdot \text{Fe}_2\text{O}_3 \cdot 8\text{SiO}_2 + \text{Na}_2\text{O} \cdot \text{Fe}_2\text{O}_3 \cdot$ $+ \text{SiO}_2 + \text{Fe}_2\text{O}_3 +$ жидкость f	50.7	20.5	28.8	809
d	$5\text{Na}_2\text{O} \cdot \text{Fe}_2\text{O}_3 \cdot 8\text{SiO}_2 + \text{Fe}_2\text{O}_3 +$ жидкость f	55.0	16.2	28.8	816
H	$\text{Na}_2\text{O} \cdot \text{SiO}_2 + \text{Fe}_2\text{O}_3 + 5\text{Na}_2\text{O} \cdot \text{Fe}_2\text{O}_3 \cdot$ $+ 8\text{SiO}_2 +$ жидкость f	59.2	11.9	28.9	815
I	$\text{Na}_2\text{O} \cdot \text{SiO}_2 + \text{Fe}_2\text{O}_3 + 6\text{Na}_2\text{O} \cdot 4\text{Fe}_2\text{O}_3 \cdot$ $+ 5\text{SiO}_2 +$ жидкость f	58.6	4.4	37.0	845
K	$\text{Na}_2\text{O} \cdot \text{SiO}_2 + \text{Na}_2\text{O} \cdot 2\text{SiO}_2 + 5\text{Na}_2\text{O} \cdot \text{Fe}_2\text{O}_3 \cdot$ $+ 8\text{SiO}_2 +$ жидкость f	70.1	23.9	6.0	816
-	$5\text{Na}_2\text{O} \cdot \text{Fe}_2\text{O}_3 \cdot 8\text{SiO}_2 +$ жидкость f	64.2	19.0	16.8	838

Key:

- a. Points (Fig. 313)
- e. Quartz
- b. Phases
- f. Liquid
- c. Composition, weight %
- g. Tridymite
- d. Temperature, °C

Reproduced from
best available copy.

Bailey [1] has studied the fusibility of acmite in the presence of water vapor, under conditions of controlled oxygen pressure. The melting of acmite is very sensitive to oxidizing conditions. Thus, at an oxygen pressure created by a buffer of hematite and magnetite, acmite melts at a total pressure of 2 kbar and temperature of 870° with decomposition into hematite, magnetite

TABLE 2
CRYSTALLINE PHASES OF $\text{Na}_2\text{O} - \text{Fe}_2\text{O}_3 - \text{SiO}_2$ SYSTEM

a Соединение	b Система кристаллов	c Габитус	d Спайность	Ng	Nn	Np	$\frac{Ng}{Np}$	$2V^\circ$	e Оптическая ориентировка	f Примечания
$5\text{Na}_2\text{O} \cdot \text{Fe}_2\text{O}_3 \cdot 8\text{SiO}_2$	Гексагональ- ный	Изометрические шары	—	1.625	—	1.630	0.916	(+)	—	Стекло, $N = 1.58$
$6\text{Na}_2\text{O} \cdot 4\text{Fe}_2\text{O}_3 \cdot 5\text{SiO}_2$	—	Структурные зерна, изометрические двойники	—	—	1.96	—	0.01	—	—	—
$\text{Na}_2\text{O} \cdot \text{Fe}_2\text{O}_3 \cdot 4\text{SiO}_2$ (сирингит, или акмит)	Моноклини- ческий	Тонкие плоскости по (100) под углом 88°	Совершенная по (110) под углом 88°	1.836	1.819	1.776	0.060	-60	Плоскость оптических осей (010) $X \Delta z = 1.7 \cdot 10^2$	Сланцевато- изометрические формы

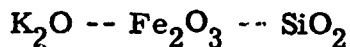
Key:

- a. Compound
- b. Crystal system
- c. Appearance
- d. Cleavage
- e. Optical orientation
- f. Notes
- g. Hexagonal
- h. Prisms
- i. Glass
- j. Rounded grains,
polysynthetic twins
- k. (aegirite or acmite)
- l. Monoclinic
- m. Thin plates along (100)
- n. Perfect along (110) at angle of 88°
- o. Optical axis plane (0.10)
- p. Elongation $\parallel c$; density 3.55 g/cm^3

and liquid; correspondingly, with a quartz, fayalite and magnetite buffer, the melting of acmite (at the same total pressure) takes place at 780°, with decomposition into magnetite and liquid.

BIBLIOGRAPHY

1. Bailey, D. K., Amer. J. Sci., 267A, Schairer vol., 1, 1969.
2. Bailey, D. K., J. F. Schairer, J. Petrol., 7, 1, 144, 1966.
3. Bowen, N. L., J. F. Schairer, Amer. J. Sci., (5), 18, 107, 365, 1929.
4. Bowen, N. L., J. F. Schairer, H. W. Willems, Amer. J. Sci., (5), 20, 120, 405, 1930.
5. Gilbert, M. C., Carnegie Inst. Washington Year Book, 65, 241, 1955-1966.
6. Gilbert, M. C., Amer. J. Sci., 267A, Schairer vol., 145, 1969.



The system has been studied partially by Faust [2], who presented the profile $\text{K}_2\text{O} \cdot 6\text{SiO}_2 \text{ -- } \text{K}_2\text{O} \cdot \text{Fe}_2\text{O}_3 \cdot 6\text{SiO}_2$ (Fig. 319), which should be considered to be pseudobinary. Compounds similar to the compounds in the $\text{K}_2\text{O} \text{ -- } \text{Al}_2\text{O}_3 \text{ -- } \text{SiO}_2$ system exist in the $\text{K}_2\text{O} \text{ -- } \text{Fe}_2\text{O}_3 \text{ -- } \text{SiO}_2$ system, namely: Fe orthoclase $\text{K}_2\text{O} \cdot \text{Fe}_2\text{O}_3 \cdot 6\text{SiO}_2$, Fe leucite $\text{K}_2\text{O} \cdot \text{Fe}_2\text{O}_3 \cdot 4\text{SiO}_2$ and Fe kaliophylite $\text{K}_2\text{O} \cdot \text{Fe}_2\text{O}_3 \cdot 2\text{SiO}_2$. These ternary compounds are shown in Fig. 320.

Wones and Appleman [4] have shown that iron feldspar exists in two polymorphic forms. The low-temperature form, similar to microcline, was synthesized from a mixture of crystallized glass having the composition $\text{K}_2\text{O} \cdot 6\text{SiO}_2$ and ferric oxide (Fe_2O_3), at a pressure of 1000-2000 bar and a temperature below 690°. The high-temperature form, similar to sanidine, was obtained by a synthesis carried out above 710°. Gaubert [3] synthesized Fe-sanidine

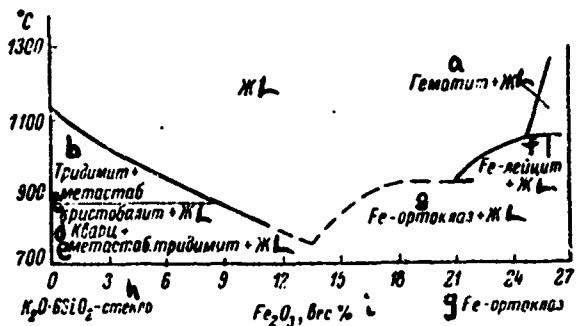


Fig. 319. Phase diagram of partial system
 $K_2O \cdot 6SiO_2$ -- $K_2O \cdot Fe_2O_3 \cdot 6SiO_2$ (from Faust).

Key:

- | | |
|----------------------------|------------------|
| a. Hematite | f. Fe-leucite |
| b. Tridymite | g. Fe-orthoclase |
| c. Metastable cristobalite | h. Glass |
| d. Quartz | i. Weight % |
| e. Metastable tridymite | |

by heating a mixture of SiO_2 and Fe_2O_3 in molten calcium vanadate. The transition of Fe-sanidine into Fe-microcline, according to Wones and Appleman, takes place at the pressure of 2000 bar and 60°C. At 770° and 1000 bar, Fe-microcline completely changes to Fe-sanidine.

Fe-sanidine melts with decomposition at 920°. Crystals of Fe-microcline are in the triclinic system. The optical orientation $X \sim B$, $Z \wedge c = 20 \pm 5^\circ$. The unit cell parameters: $a = 8.69$, $b = 13.11$, $c = 7.33$ Å, $\alpha = 90^\circ 36'$, $\beta = 116^\circ 02'$, $\gamma = 86^\circ 30'$. Fe-sanidine crystals belong to the monoclinic system, and they have indices of refraction (according to Gaubert): $Ng = 1.609$, $Nm = 1.605$, $Np = 1.601$. The optical orientation $Y = t$, $Z \wedge c = 16 \pm 4^\circ$. The unit cell parameters: $a = 8.69$, $b = 13.12$, $c = 7.32$ Å, $\beta = 116^\circ 06' \pm 0.5'$.

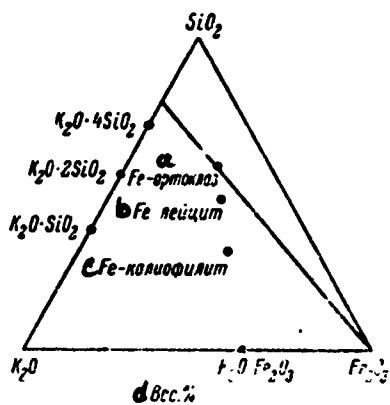


Fig. 320. Ternary compounds in K_2O -- Fe_2O_3 -- SiO_2 system (from Faust).

Key:

- a. Fe-orthoclase
- b. Fe-leucite
- c. Fe-kaliophylite
- d. Weight %

Faust and Beck [1, 2] measured the indices of refraction of glasses of the K_2O -- Fe_2O_3 -- SiO_2 system.

BIBLIOGRAPHY

1. Faust, G. T., Amer. Mineralogist, 21, 12, 751, 1936.
2. Faust, G. T., A. P. Beck, J. Amer. Ceram. Soc., 21, 9, 320, 1938.
3. Gaubert, P., Compt. rend., 180, 15, 1853, 1925.
4. Wones, D. R., D. E. Appleman, Amer. Mineralogist, 47, 1-2, 209, 1962.

$\text{MgO} \text{-- } \text{Fe}_2\text{O}_3 \text{-- } \text{SiO}_2$

The phase diagram of the system has not been determined. Berezhnoy [1, 2] showed that, in the partial section $\text{Mg}_2\text{SiO}_4 \text{-- MgFe}_2\text{O}_4$, there is a eutectic containing 75 weight % MgFe_2O_4 , melting at 1670° . A triple eutectic formed by the MgSiO_3 , Fe_2O_3 and SiO_2 fields, melts at 1340° .

Forsterite Mg_2SiO_4 reacts with hematite Fe_2O_3 at temperatures over 1000° , with formation of MgSiO_3 and MgFe_2O_4 . As a result of triangulation of the system, it was shown that MgFe_2O_4 coexists with MgSiO_3 and Mg_2SiO_4 and Fe_2O_3 with MgSiO_3 .

Coes [3], under high pressure conditions, obtained a garnet unknown in nature, kokharite $\text{Mg}_3\text{Fe}_2(\text{SiO}_4)_3$.

Koltermann [4] has studied thermal decomposition of olivines containing 11, 34 and 53 weight % Fe_2SiO_4 and 89, 66 and 47 weight %, respectively, Mg_2SiO_4 .

At 820° , oxidation of divalent iron to trivalent takes place. The silica freed in this case is X-ray-amorphous at this temperature. At elevated temperatures, part of it is transformed into cristobalite (1080°), and part reacts with Mg_2SiO_4 , forming enstatite. These reactions take place simultaneously and rapidly. With heating for many hours at 1100° , Fe_3O_4 is formed. Mg_2SiO_4 , cristobalite, MgSiO_3 , Fe_3O_4 and residual Fe_2O_3 are found at 1200° by X-ray radiography.

BIBLIOGRAPHY

1. Berezhnoy, A. S., in the collection Voprosy petrografii i mineralogii [Problems in Petrography and Mineralogy] 2d Ed., AN SSSR Press, Moscow, 1953, p. 281.

2. Berezhnoy, A. S., Sb. nauchn. trudov Vses. inst. ogneuporov [Collected Scientific Transactions, All-Union Institute of Refractories], issue 2, Metallurgizdat Press, Kharkov, 1958, p. 5.
3. Coes, L., J. Amer. Ceram. Soc., 38, 7, 298, 1955.
4. Koltermann, M., Neues Jahrb. Mineral., Monatshefte, 7/8, 181, 1962.



The system has been studied by Glasser [1], in the subsolidus region.

Annealings were carried out at 650-700°. Besides the known ternary compound melanotekite $2\text{PbO} \cdot \text{Fe}_2\text{O}_3 \cdot 2\text{SiO}_2$, phase X was obtained, with a probable composition $12\text{PbO} \cdot \text{Fe}_2\text{O}_3 \cdot 2\text{SiO}_2$ (Fig. 321). At 650°, melanotekite coexists with the following phases: alamosite (PbSiO_3), quartz, hematite (Fe_2O_3), magnetoplumbite ($\text{PbO} \cdot 6\text{Fe}_2\text{O}_3$) and plumboferrite ($\text{PbO} \cdot \text{Fe}_2\text{O}_3$).

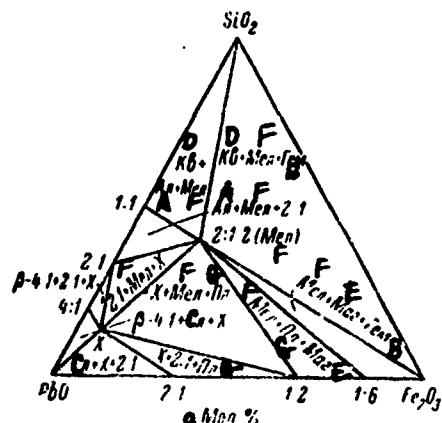


Fig. 321. Coexisting phase triangles of $\text{PbO} \text{ -- } \text{Fe}_2\text{O}_3 \text{ -- } \text{SiO}_2$ system at 650° (from Glasser):
A. alamosite; B. hematite; C. litharge; D. quartz;
E. Magnetoplumbite; F. melanotekite; G. plumboferrite.

Key: a. Mole %

Melanotekite has the following rhombic unit cell parameters: $a = 6.97$, $b = 11.0$, $c = 9.93$ Å. Melanotekite is isostructural with kentrolite ($2\text{PbO} \cdot \text{Mn}_2\text{O}_3 \cdot 2\text{SiO}_2$).

The new compound $12\text{PbO} \cdot \text{Fe}_2\text{O}_3 \cdot 2\text{SiO}_2$ with a density of 8.1 g/cm^3 , is slightly ferromagnetic. Upon heating to 740° , no signs of melting were found. Prolonged roasting at 700° does not lead to noticeable loss in weight, and it can be considered that there are no compounds of higher valence lead or iron in the compound being discussed.

BIBLIOGRAPHY

1. Glasser, F.P., Amer. Mineralogist, 52, 7-8, 1085, 1967.



The system has been studied by Masse and Muan [1-4], by the quenching method. The liquidus surface is presented in Fig. 322. There are two triple isobaric invariant points in the system: point a, with a temperature of $1328 \pm 5^\circ$ and composition 58 weight % CoO, 16 weight % Fe_3O_4 and 26 weight % SiO_2 , and point b, with a temperature of $1313 \pm 5^\circ$ and composition 55 weight % CoO, 14 weight % Fe_3O_4 and 31 weight % SiO_2 . The maximum on the silica -- spinel curve corresponds to a temperature of $1483 \pm 5^\circ$, and it has the composition 15 weight % CoO, 63 weight % Fe_3O_4 and 22 weight % SiO_2 .

The coexisting phase triangles are presented in Fig. 323. Points c and d indicate the compositions of spinel solid solutions occurring in equilibrium with liquids b and a, respectively, and point e, the composition of crystals of the $(\text{Co}, \text{Fe})\text{O}$ solid solution, occurring in equilibrium with liquid a.

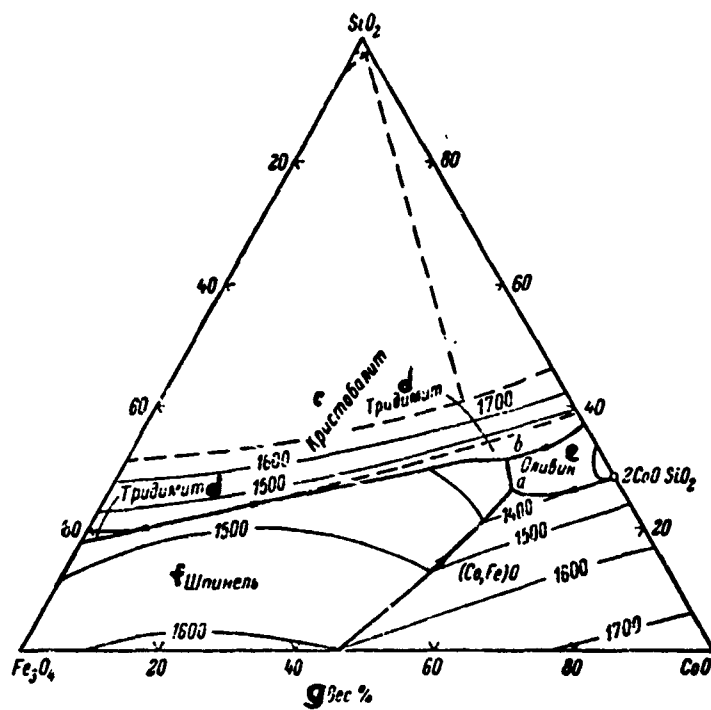


Fig. 322. Phase diagram of $\text{CoO} \text{ -- } \text{Fe}_3\text{O}_4 \text{ -- } \text{SiO}_2$ system (from Masse and Muan).

Key:

- | | |
|-----------------|-------------|
| c. Cristobalite | f. Spinel |
| d. Tridymite | g. Weight % |
| e. Olivine | |

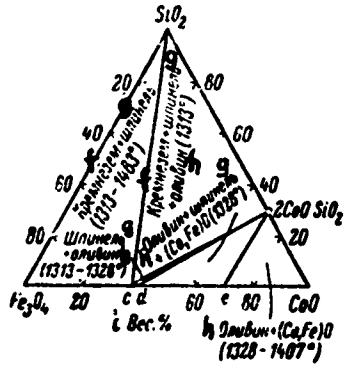


Fig. 323. Coexisting phase triangles of $\text{CoO} - \text{Fe}_3\text{O}_4 - \text{SiO}_2$ system (from Masse and Muan).

Key:

- f. Silica
- g. Spinel
- h. Olivine
- i. Weight %

BIBLIOGRAPHY

1. Masse, D. P., Rev. Escola Minas, **24**, 1, 21, 1965.
2. Masse, D. P., A. Muan, J. Amer. Ceram. Soc., **48**, 9, 466, 1965.
3. Masse, D. P., A. Muan, Trans. AIME, **233**, 7, 1448, 1965.
4. Muan, A., J. Metals, **7**, 965, 1955, (Trans. AIME, **203**, 9, 1955).

SYSTEMS CONTAINING FLUORINE



The partial profile $\text{NaF} \text{ -- Na}_2\text{SiO}_3$ has been studied by Booth and Starrs [1]. Booth, Starrs and Bahnson [2] found only a binary eutectic in the $\text{Na}_2\text{Si}_2\text{O}_5 \text{ -- NaF}$ system, corresponding to a temperature of 737° and a NaF content of 39.5 mole % (Fig. 324).

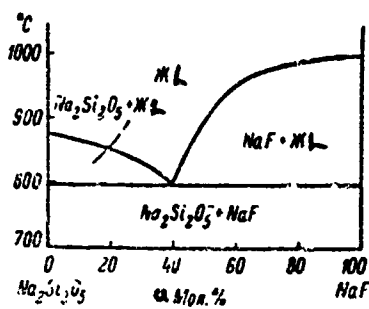


Fig. 324. Phase diagram of partial system $\text{Na}_2\text{Si}_2\text{O}_5 \text{ -- NaF}$ (from Booth and Starrs).

Key:

a. Mole %

BIBLIOGRAPHY

- Booth, H. S., B. A. Starrs, *J. Phys. Chem.*, **35**, 12, 3553, 1931.
- Booth, H. S., B. A. Starrs, M. J. Bahnsen, *J. Phys. Chem.*, **37**, 9, 1103, 1933.



The system has been studied by Fujii and Eitel [2], Hinz and Kunth [3] and MacCormick [4]. Phase separation of the melts has been studied by Ol'shanskiy [1]. According to [2], as a result of solid-phase reactions at 1200° , fluoronorbergite $2\text{MgO} \cdot \text{SiO}_2 \cdot \text{MgF}_2$ and fluorechondrodite $2(2\text{MgO} \cdot \text{SiO}_2) \cdot \text{MgF}_2$ (Fig. 325) are produced easily and quickly; fluoroclinohumite is produced by prolonged (42 hours) exposure of the samples. Hinz and Kunth also have obtained only two compounds, fluoronorbergite and fluorechondrodite.

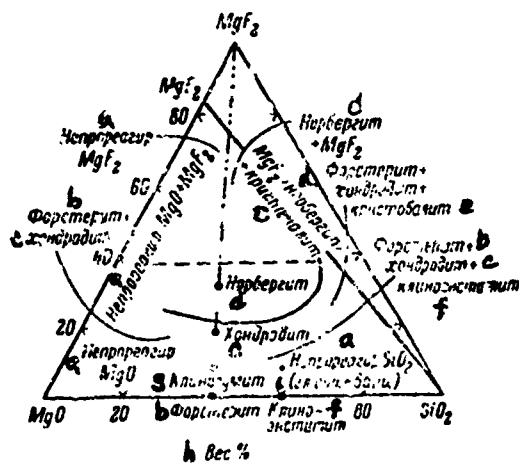


Fig. 325. Schematic diagram of phase relationships of $\text{MgO} - \text{MgF}_2 - \text{SiO}_2$ system (from Fujii and Eitel).

Key:

- | | |
|----------------|--------------------|
| a. Unreacted | e. Cristobalite |
| b. Forsterite | f. Clinoenstatite |
| c. Chondrodite | g. Clinohumite |
| d. Norbergite | h. Weight % |
| | i. (mainly quartz) |

MacCormick [4] conducted tests in closed platinum capsules at 1100-1300°.

The compositions were selected for the purpose of verifying all proposed compatibility lines (Fig. 326). The plotted diagram of the coexisting phase triangles consists of eleven partial triple systems, in which the existence in synthetic preparations of all four fluorosilicate compounds was established: fluoronorbergite, fluorochondrodite, fluorohumite ($3\text{Mg}_2\text{SiO}_4 \cdot \text{MgF}_2$) and fluoroclinohumite ($4\text{Mg}_2\text{SiO}_4 \cdot \text{MgF}_2$). Fluorohumite and fluoroclinohumite melt with decomposition; therefore, the number of partial triple systems for the liquidus region will be different (less than eleven). Fluorohumite can be synthesized at a temperature of about 1190° (no higher).

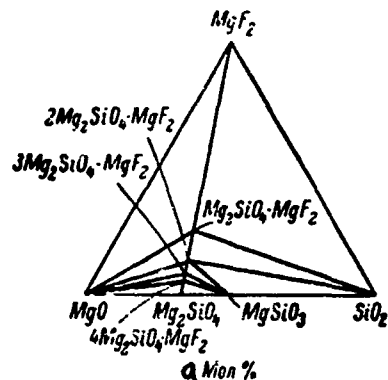


Fig. 326. Coexisting phase triangles of $\text{MgO} - \text{MgF}_2 - \text{SiO}_2$ system (from MacCormick).

Key:

a. Mole %

O'l'shanskiy [1] has studied the equilibrium of the immiscible liquids in the system. The investigations were carried out in riveted molybdenum crucibles (weighed batch 0.03-0.06 g), in a furnace with a molybdenum heater.

Evaporation of the SiF_4 formed by the reaction of the metal fluorides and SiO_2 practically did not take place from such crucibles. The presence of two liquid phases was determined microscopically in immersion preparations. Low-refraction glass (liquid rich in SiO_2), with round inclusions of the second liquid scattered in it usually was observed in the preparations; sometimes, formation of two layers, separated by a meniscus boundary, took place in the crucible.

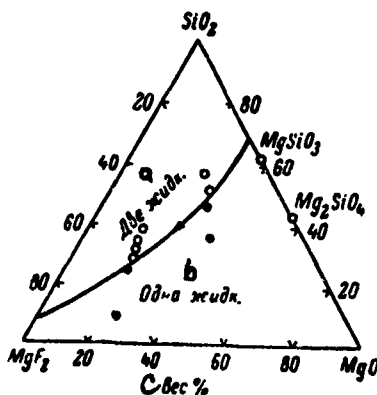


Fig. 327. Region of equilibrium of two liquid phases in the MgF_2 -- MgO -- SiO_2 system (from Ol'shanskiy).

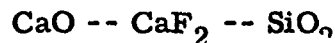
Key:

- a. Two liquids
- b. One liquid
- c. Weight %

The region of equilibrium of two liquid phases in the MgF_2 -- MgO -- SiO_2 system is shown in Fig. 327; the open circles designate samples containing two liquids and the solid ones, samples with one liquid. The index of refraction of the SiO_2 rich glass fluctuated from 1.446 to 1.456 (for different samples).

BIBLIOGRAPHY

1. Ol'shanskiy, Ya. I., DAN SSSR, 114, 6, 1957, p. 1246.
2. Fujii, T., W. Eitel, Radex-Rundschau, 1, 445, 1957.
3. Hinz, W., P.-O. Kunth, Amer. Mineralogist, 45, 6, 1198, 1960.
4. MacCormick, G. R., Radex-Rundschau, 6, 325, 1966.
5. Van Valkenburg, A., J. Res. Nat. Bur. Stand., 65A, 5, 415, 1961.



Karandeyev [2] and then Baak and Olander [7] have studied the partial system $\text{CaO} \cdot \text{SiO}_2 - \text{CaF}_2$ (Fig. 328). Eitel [10] has studied the partial triple system $\text{CaO} - \text{CaF}_2 - 2\text{CaO} \cdot \text{SiO}_2$. Lapin [4] refined the data of Eitel. One ternary compound $3\text{CaO} \cdot \text{CaF}_2 \cdot 2\text{SiO}_2$, corresponding to the natural mineral cuspidine, has been established.

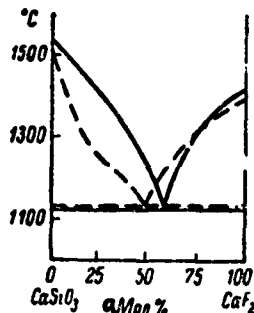


Fig. 328. Phase diagram of partial system $\text{CaSiO}_3 - \text{CaF}_2$ (from Karandeyev ... dashed lines and from Baak and Olander in solid lines).

Key:

a. Mole %

According to McCaughey and coileagues [13], cuspidine melts with decomposition. Brisi [9] indicates that cuspidine melts congruently a little above 1400° and has a density of 3.05 g/cm³.

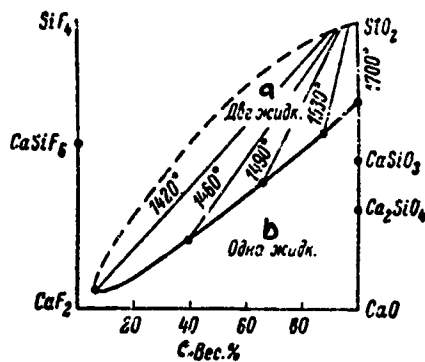


Fig. 329. Region of two liquid phases in CaO -- CaF₂ -- SiO₂(SiF₄) system (from Yershova and Ol'shanskiy).

Key:

- a. Two liquids
- b. One liquid
- c. Weight %

Separation of the liquid phases has been studied by Yershova and Olshanskiy [1]. The region of two liquid phases in the CaO -- CaF₂ -- SiO₂(SiF₄) system is shown in Fig. 329. In connection with formation of the SiO₂-rich liquid phase containing SiF₄ (appearing as a consequence of the reaction SiO₂ + 2CaF₂ → SiF₄ + 2CaO), the system is shown as reciprocal.

Mukerji [14], using hermetically sealed platinum tubes, has studied the CaO -- CaF₂ -- 2CaO · SiO₂ system more fully (Fig. 330). Cuspidine was not found. The two triple eutectics have the compositions: E₁ (1104°), 10 weight

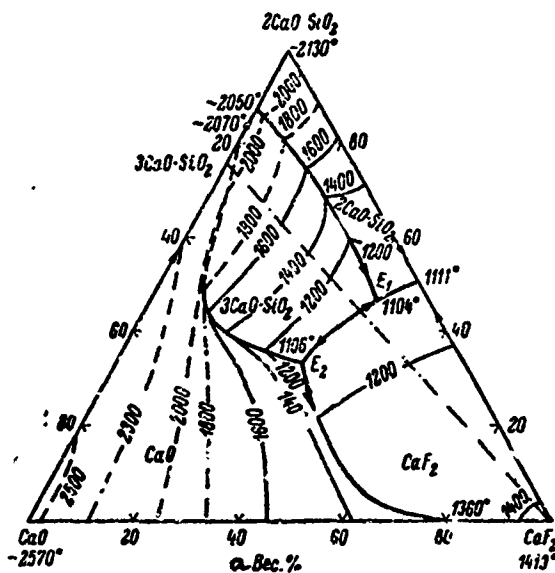


Fig. 330. Phase diagram of partial system $\text{CaO} \text{--} \text{CaF}_2 \text{--} 2\text{CaO} \cdot \text{SiO}_2$ (from Mukerji).

Key:

a. Weight %

% CaO , 46 weight % $2\text{CaO} \cdot \text{SiO}_2$ and 44 weight % CaF_2 ; E_2 (1100°), 31 weight % CaO , 33.5 weight % $2\text{CaO} \cdot \text{SiO}_2$ and 35.5 weight % CaF_2 . In the presence of a fluoride melt, tricalcium silicate can exist stably at 1104° , while pure Ca_3SiO_5 is stable only above 1300° . Mukerji plotted a complete phase diagram of the $\text{CaO} \text{--} \text{CaF}_2 \text{--} \text{SiO}_2$ system (Fig. 331).

Gutt and Osborne [11] have studied the partial profile $2\text{CaO} \cdot \text{SiO}_2 \text{--} \text{CaF}_2$, using sealed platinum tubes. The phases were determined on quenched samples, by means of differential thermal analysis. A new compound was

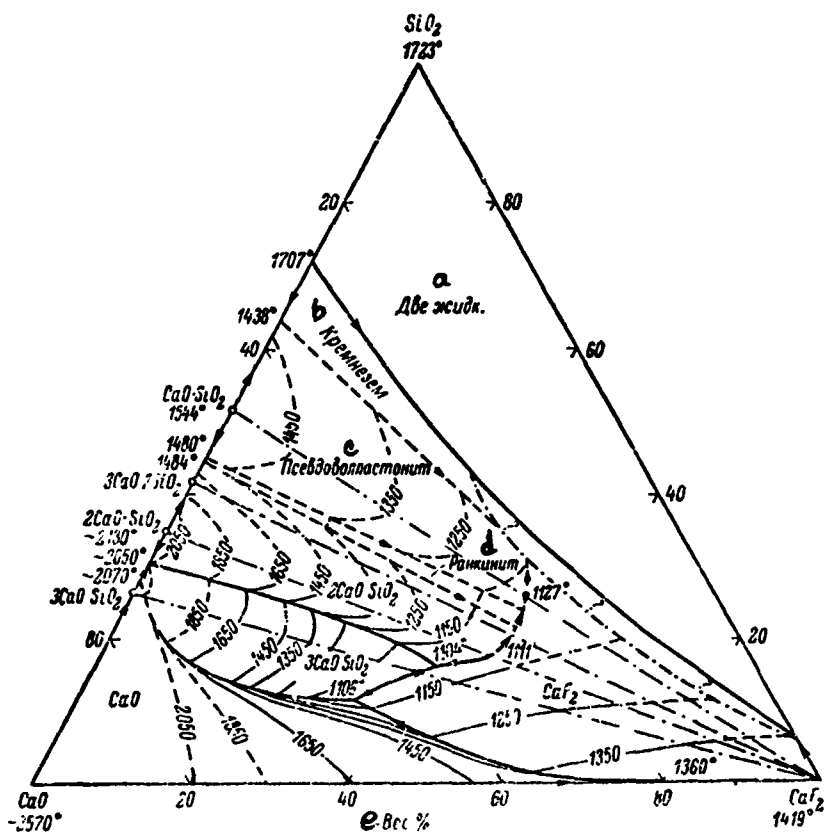


Fig. 331. Phase diagram of $\text{CaO} - \text{CaF}_2 - \text{SiO}_2$ system (from Mukerji).

Key:

- | | |
|-----------------------|--------------|
| a. Two liquids | d. Rankinite |
| b. Silica | e. Weight % |
| c. Pseudowollastonite | |

discovered, with the composition $(2\text{CaO} \cdot \text{SiO}_2)_2 \cdot \text{CaF}_2$ (an analog of calcio-chondrodite), with an average index of refraction of 1.60, biaxial negative crystals and a density of 2.91 g/cm^3 , which decomposes at 1040° into $2\text{CaO} \cdot \text{SiO}_2$ and CaF_2 (Fig. 332).

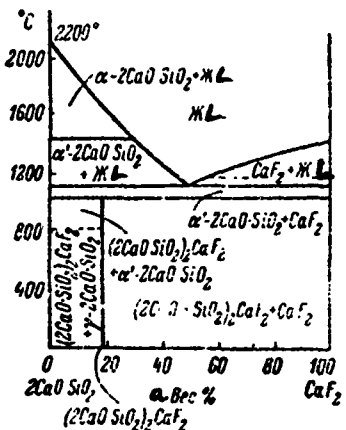


Fig. 332. Phase diagram of partial system $2\text{CaO}\cdot\text{SiO}_2$ -- CaF_2 (from Gutt and Osborne).

Key:

... Weight %

Later, Gutt and Osborne [12] obtained a new calcium silicofluoride, with the composition $(3\text{CaO}\cdot\text{SiO}_2)_3\cdot\text{CaF}_2$, for which the appropriate mixtures were heated in a sealed platinum tube for a period of 30 min at 1300° , and then 7 days at 1130° . The crystals are greenish, negative, $N_{av} \approx 1.690$, $2V < 15^\circ$.

The compound $(3\text{CaO}\cdot\text{SiO}_2)_3\cdot\text{CaF}_2$ is unstable below 1130° , and it dissociates, depending on temperature, into $2\text{CaO}\cdot\text{SiO}_2$, CaO and CaF_2 or $(2\text{CaO}\cdot\text{SiO}_2)_2\cdot\text{CaF}_2$ and a small amount of CaF_2 . The new silicofluoride melts incongruently, forming $3\text{CaO}\cdot\text{SiO}_2$ and liquid.

Akaiwa and colleagues [6], describing the compound $11\text{CaO} \cdot 4\text{SiO}_2 \cdot \text{CaF}_2$, which they obtained, apparently, as Gutt and Osborne confirm, was the compound $(3\text{CaO} \cdot \text{SiO}_2)_3 \cdot \text{CaF}_2$.

Judging from the similarity of the X-ray photos, Bereczky [8] obtained both calcium silicofluorides described, but he did not give their compositions.

The eutectic of dicalcium silicate and CaF_2 , according to Gutt and Osborne, contains 49.2 weight % of the latter, and it melts at 1110° . A two-phase region exists in the $1040-1110^\circ$ temperature range: $2\text{CaO} \cdot \text{SiO}_2$ and CaF_2 . Incorporation of fluorine ion into the Ca_2SiO_4 lattice was not detected.

CRYSTALLOOPTICAL CHARACTERISTICS OF NATURAL AND SLAG CUSPIDINE

а Кристаллографические и оптические свойства	б Куспидин природный	в Куспидин шлаковый
Система d	Моноклинная	Моноклинная
Габитус f	Конусвидные двойники по (100), полисинтетические по третьяму пинакоиду	Конусвидные двойники по (100), простые и полисинтетические
Координаты двойникового шва t	$N_g=6^\circ$, $N_m=90^\circ$, $N_p=84^\circ$ $Y=b$, $Z/c=5.5^\circ$ $62^\circ/63^\circ$	$N_g=6^\circ$, $N_m=90^\circ$, $N_p=84^\circ$ $Z/c=6^\circ$ 63°
Optическая ориентировка j		
$2V^\circ (+)$		
Свойство k	Ясная по (001)	Базальная и присматическая
N_g	1.602	1.605 ± 0.002
N_m	1.595	1.595 ± 0.002
N_p	1.590	1.592 ± 0.002
$N_g - N_p$	0.012 (0.010)	0.013

- Key:
- a. Crystallographic and optical properties
 - b. Natural cuspidine
 - c. Slag cuspidine
 - d. System
 - e. Monoclinic
 - f. Appearance
 - g. Spear-shaped twins along (100), polysynthetic along third pinacoid
 - h. Spear-shaped twins along (100), simple and polysynthetic
 - i. Twinning junction coordinates
 - j. Optical orientation $2V^\circ (+)$
 - k. Cleavage
 - l. Definite along (001)
 - m. Basal and prismatic

Lapin [3], studying cuspidine from electric welding slag, introduces the crystallooptical characteristics of natural and slag cuspidine (see table), which subsequently were confirmed by Van Valkenburg and Rynders [15]. Smirnova, Rumanova and Belov [5] gave a detailed interpretation of the structure of cuspidine. The monoclinic-prismatic crystals of cuspidine, with space group P_{2}/C , have unit cell parameters $a = 7.55$, $b = 10.43$, $c = 10.85 \text{ \AA}$, $\beta = 69^{\circ}56'$, $Z = 4$.

BIBLIOGRAPHY

1. Yershova, Z. P., Ya. I. Ol'shanskiy, Geokhimiya, 3, 1957, p. 220.
2. Karandeyev, B., Zs. anorgan. allgem. Chem., 68, 1-2, 1910, p. 188.
3. Lapin, V. V., DAN SSSR, 31, 7, 1941, p. 685.
4. Lapin, V. V., Trudy Inst. geol. rudn. mestorozhd., petrografii, mineralogii i geokhimiya AN SSSR [Proceedings, Institute of Geology of Ores, Petrography, Mineralogy and Geochemistry, USSR Academy of Sciences], 2d Ed., Moscow, 1956, p. 61.
5. Smirnova, R. F., I. M. Rumanova, N. V. Belov, Zap. Vsegoz. mineral. obshch., 84, 2, 1955, p. 159.
6. Akaiwa, S., G. Sucloh, M. Taraka, Rev. of 20th Meeting of Cement Ass. Japan, Tokyo, 1967.
7. Baak, T., A. Olander, Acta chem. Scand., 9, 8, 1351, 1955.
8. Bereczky, E., Epitöanyag, 16, 12, 441, 1964.
9. Bisi, C., J. Amer. Ceram. Soc., 40, 5, 174, 1957.
10. Eitel, W., Zs. angew. Mineral., 1, 3, 269, 1938; Zement, 27, 31, 469, 1938.
11. Gutt, W., G. J. Osborne, Trans. Brit. Ceram. Soc., 65, 9, 521, 1966.
12. Gutt, W., G. J. Osborne, Trans. Brit. Ceram. Soc., 67, 4, 125, 1968.
13. McCaughey, W. J., K. Kautz, R. G. Wells, Bull. Geol. Soc. Amer., 58, 12, 1204, 1947.

14. Mukerji, J., J. Amer. Ceram. Soc., 48, 4, 210, 1965.
15. Van Valkenburg, A., G.F. Rynders, Amer. Mineralogist, 43, 11-12, 1195, 1958.



Yershova and Ol'shanskiy [1, 2] have studied the phase separation of the liquid phases in the system (Fig. 333). For point A at 1495°, a separation into two layers was obtained; the lower limit of existence of the two liquid phases of this composition has a temperature of $\sim 1480^\circ$.

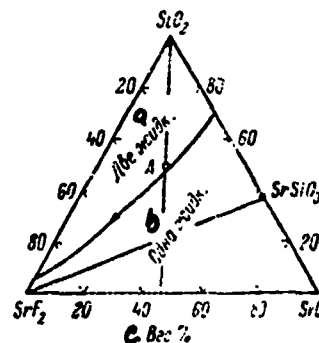


Fig. 333. Region of equilibrium (phase separation) of two liquid phases in $\text{SrO} -- \text{SrF}_2 -- \text{SiO}_2$ system (from Yershova and Ol'shanskiy).

Key:

- a. Two liquids
- b. One liquid
- c. Weight %

BIBLIOGRAPHY

1. Yershova, Z.R., Ya. I. Ol'shanskiy, Geokhimiya, 3, 1957, p. 214.
2. Ol'shanskiy, Ya.I., DAN SSSR, 114, 6, 1957, p. 1246.

$\text{BaO} - \text{BaF}_2 - \text{SiO}_2$

The region of equilibrium of two liquid phases in the system, according to Yershova and Ol'shanskiy [1, 2], is shown in Fig. 334. In the binary system $\text{BaO} - \text{SiO}_2$, formation of two immiscible liquids was not observed, but the liquidus curve has a characteristic break, indicating a "tendency" of the melt towards phase separation. The lower temperature limits of the phase separation regions in four profiles: profile I (composition 5) $\sim 1550^\circ$; profile II (composition 2) $\sim 1440^\circ$; profile III (composition 2) $\sim 1440^\circ$; profile IV (composition 1) $\sim 1575^\circ$. The upper temperature limits of the phase separation: profile I (composition 5) $\sim 1575^\circ$; profile IV (composition 1) $\sim 1615^\circ$.

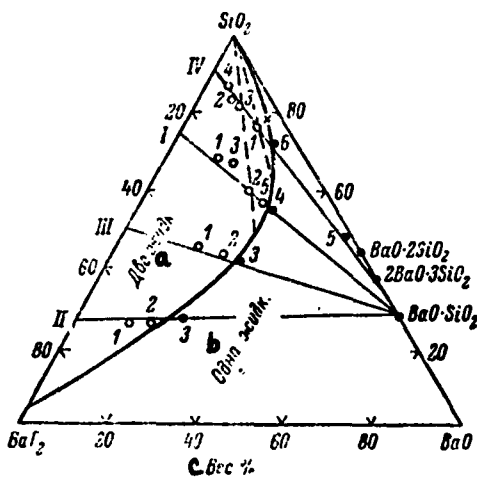


Fig. 334. Region of equilibrium (phase separation) of two liquid phases in $\text{BaO} - \text{BaF}_2 - \text{SiO}_2$ system (from Yershova and Ol'shanskiy): I-IV. profiles; 1-6. number of compositions studied.

Key:

- a. Two liquids
- b. One liquid
- c. Weight %

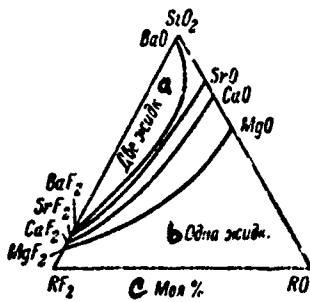


Fig. 335. Region of equilibrium of two liquid phases in fluorosilicate systems of alkali earth metals (from Yershova and Ol'shanskiy).

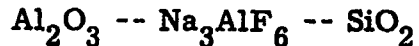
Key:

- a. Two liquids
- b. One liquid
- c. Mole %

Data on the regions of equilibrium of two liquid phases in fluorosilicate systems of alkali earth metals, according to the data of Yershova and Ol'shanskiy [1, 2], are reported in Fig. 335. Just as for normal silicate systems, the region of two liquid phases in fluosilicate systems of alkali earth metals decreases with increase in cation radius.

BIBLIOGRAPHY

1. Yershova, Z. R., Ya. I. Ol'shanskiy, Geokhimiya, 3, 1957, p. 214.
2. Ol'shanskiy, Ya. I., DAN SSSR, 114, 6, 1957, p. 1246.



Isothermal profiles at 1010 and 800° have been studied by Weil and Fyfe [1], and they are presented in Fig. 336. The invariant point contains 69 weight % SiO_2 and 14 weight % Al_2O_3 at 1010° and 50 weight % SiO_2 and 17 weight % Al_2O_3 at 800°. Phase separation of the liquids (liquation) was not observed in the temperature range studied.

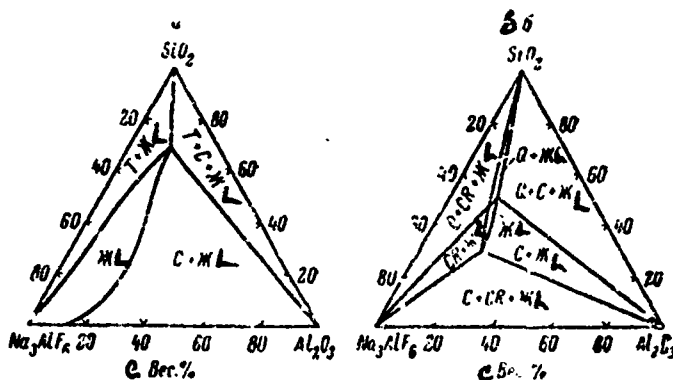


Fig. 336. Isothermal sections of Na_3AlF_6 -- Al_2O_3 -- SiO_2 system (from Weil and Fyfe): a. 110°; b. 800°; C. corundum; CR. cryolite; Q. quartz; T. tridymite.

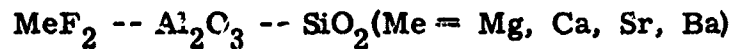
Key:

c. Weight %

Cryolite is encountered in two modifications: α , low-temperature and β , high-temperature. The $\beta \rightarrow \alpha$ transition is rapid and, therefore, the β form is not successfully recorded in quenched samples.

BIBLIOGRAPHY

1. Weil, D.F., W.S. Fyfe, J. Electrochem. Soc., 111, 5, 583, 1964.



Inasmuch as fluosilicate systems simulate aqueous silicate systems to a great extent, the study of liquation phenomena in the former is of interest for knowledge of liquation in natural magmas.

Yershova [1] has studied the equilibrium of two immiscible liquid phases in the $MgF_2 - Al_2O_3 - SiO_2$, $CaF_2 - Al_2O_3 - SiO_2$, $SrF_2 - Al_2O_3 - SiO_2$ and $BaF_2 - Al_2O_3 - SiO_2$ systems.

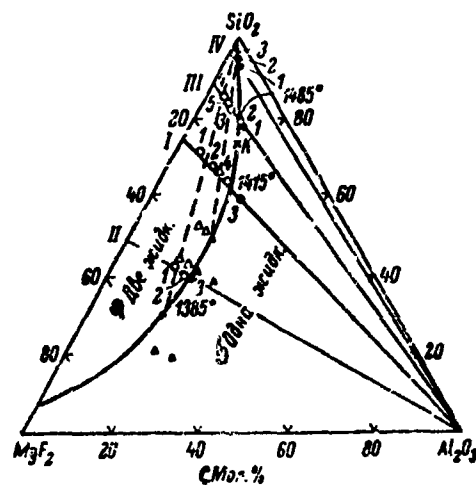


Fig. 337. Region of equilibrium of two liquid phases in $MgF_2 - Al_2O_3 - SiO_2$ system (from Yershova): Open circles, two liquids according to [1]; solid circles, one liquid according to [1]; open triangles, two liquids according to [2]; solid, one liquid according to [2]; dashed lines are tie lines.

Key:

- a Two liquids
 - b. One liquid
 - c. Mole %

The region of equilibrium of two liquid phases in the MgF_2 -- Al_2O_3 -- SiO_2 system is shown in Fig. 337. The boundary of the phase separation region in the limited MgF_2 -- SiO_2 system is plotted from [2]. At three limiting points, 4 (I), 2 (II) and 3 (III), the lower temperature limits of phase separation have been established: ~ 1415 , 1385 and 1485° , respectively. An increase in temperature for 2 (II) from 1385 to 1475° and for 4 (I) from 1415 to 1490° , did not lead to closing the immiscibility dome.

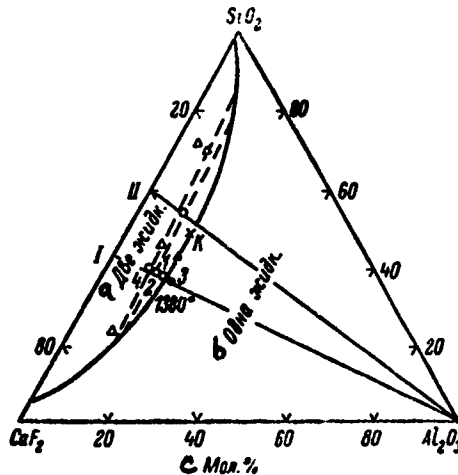


Fig. 332. Region of equilibrium of two liquid phases in CaF_2 -- Al_2O_3 -- SiO_2 system (from Yershova): designations same as in Fig. 337.
[Key: Same as in Fig. 337].

The region of equilibrium of two liquids in the CaF_2 -- Al_2O_3 -- SiO_2 system is shown in Fig. 338. The boundary of the region of phase separation in the CaF_2 -- SiO_2 system is given according to [2]. The weight ratios of

the liquids: for composition 4 (I), 30% liquid enriched in SiO_2 + 70% liquid depleted of SiO_2 ; for composition 1 (II), 50% liquid enriched in SiO_2 + 50% liquid depleted in SiO_2 . The position of the critical point K was determined from this: its position, according to microscope data, apparently is still further from the SiO_2 apex than is shown in Fig. 338. A similar point K in the MgF_2 -- Al_2O_3 -- SiO_2 system (Fig. 337) occurs considerably closer to the SiO_2 apex. For limiting point 2 (I), the lower temperature limit of formation of two liquid phases is $\sim 1380^\circ$.

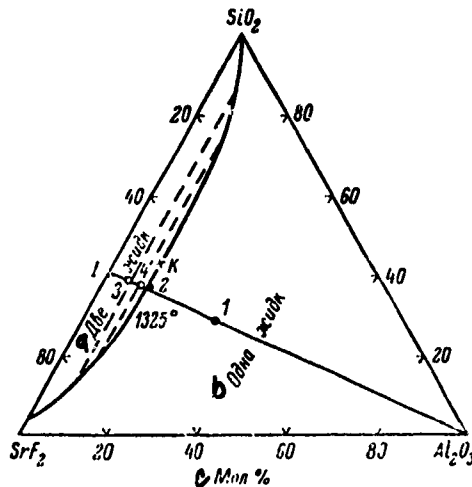


Fig. 339. Region of equilibrium of two liquid phases in the SrF_2 -- Al_2O_3 -- SiO_2 system (from Yershova): designations same as in Fig. 337. [Key: Same as in Fig. 337].

The region of equilibrium of two liquid phases in the SrF_2 -- Al_2O_3 -- SiO_2 system is presented in Fig. 339 and, for the BaF_2 -- Al_2O_3 -- SiO_2 system, in Fig. 340. The boundaries of the phase separation regions for the SrF_2 -- SiO_2 and BaF_2 -- SiO_2 systems are given according to [2].

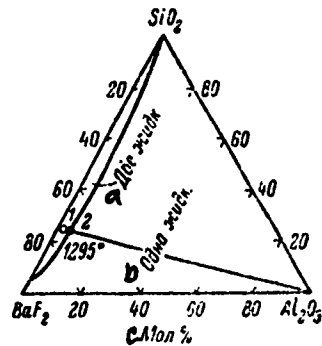


Fig. 340. Region of equilibrium of two liquid phases in BaF_2 -- Al_2O_3 -- SiO_2 system (from Yershova): designations same as in Fig. 337. [Key: Same as in Fig. 337].

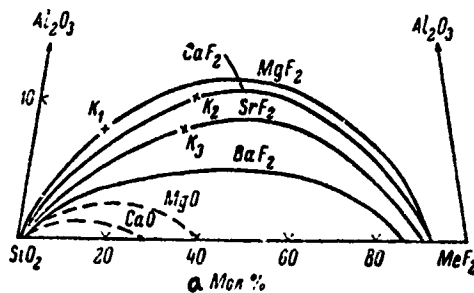


Fig. 341. Region of equilibrium of two liquid phases in MeF_2 -- Al_2O_3 -- SiO_2 systems (from Yershova): K_1 - K_3 , critical points in MgF_2 -- Al_2O_3 -- SiO_2 , CaF_2 -- Al_2O_3 -- SiO_2 and SrF_2 -- Al_2O_3 -- SiO_2 systems, respectively; boundaries of regions of two liquid phases in MgO -- Al_2O_3 -- SiO_2 and CaO -- Al_2O_3 -- SiO_2 systems also are shown, from data of Grieg (dashed lines).
Key: a. Mole %

Data characterizing the regions of immiscibility of the four systems presented above and, for comparison, according to Grieg [3], for the $\text{MgO} - \text{Al}_2\text{O}_3 - \text{SiO}_2$ and $\text{CaO} - \text{Al}_2\text{O}_3 - \text{SiO}_2$ systems, are reported in Fig. 341. The width of the phase separation regions, just as in $\text{MeO} - \text{MeF}_2 - \text{SiO}_2$ systems, where $\text{Me} = \text{Mg}, \text{Ca}, \text{Sr}$ and Ba (see description of these systems), decreases with increase in the ratio of the cation radius to valence.

The presence of Al_2O_3 considerably decreases the region of equilibrium of two liquid phases from that in the $\text{MeF}_2 - \text{MeO} - \text{SiO}_2$ systems, but, nevertheless, they are broader than in the $\text{MeO} - \text{Al}_2\text{O}_3 - \text{SiO}_2$ systems studied by Grieg [3].

BIBLIOGRAPHY

1. Yershova, Z. P., Geokhimiya, 4, 1957, p. 296.
2. Ol'shanskiy, Ya. I., DAN SSSR, 114, 6, 1957, p. 1246.
3. Grieg, J., in the collection Klassicheskiye raboty po fiziko-khimii silikatov [Classical Work on Silicate Physical Chemistry], Khimizdat Press, Moscow, 1937.

$\text{Me}''\text{F}_2 - \text{Me}'\text{F} - \text{SiO}_2$ ($\text{Me}'' = \text{Ca}, \text{Mg}, \text{Sr}, \text{Ba}$ and $\text{Me}' = \text{Na}, \text{K}$)

Study of the equilibrium of two immiscible liquids in fluorosilicate systems containing alkali metals, like the analogs in similar aqueous silicate systems, are of importance for study of liquation phenomena in natural magmas.

Yershova and Ol'shanskiy [2] have studied the equilibrium of two liquid phases in 13 fluorosilicate systems containing alkali metals.

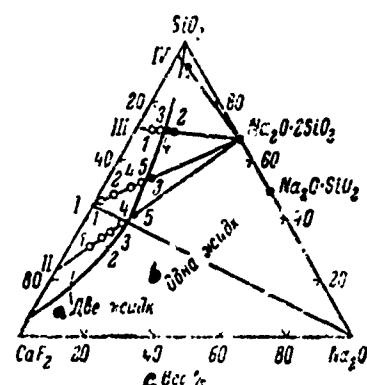


Fig. 342. Region of equilibrium of two liquid phases in CaF_2 -- Na_2O -- SiO_2 system (from Yershova and Ol'shanskiy): Open circles, two liquids; solid circles, one liquid; roman numbers, profiles; arabic numbers, numbers of the compositions studied.

Key:

- a. Two liquids
- b. One liquid
- c. Weight %

The region of equilibrium of two liquid phases in the CaF_2 -- Na_2O -- SiO_2 system is shown in Fig. 342. It was plotted from data of three profiles passing through the points: I. 56.5 weight % CaF_2 + 43.5 weight % (SiO_2 -- $\text{Na}_2\text{Si}_2\text{O}_5$); II. 79.2 weight % CaF_2 + 20.8 weight % (SiO_2 -- $\text{Na}_2\text{Si}_2\text{O}_5$); III. 30.2 weight % CaF_2 + 69.8 weight % (SiO_2 -- $\text{Na}_2\text{Si}_2\text{O}_5$) (the charge, besides CaF_2 and SiO_2 , included glass of the composition $\text{Na}_2\text{Si}_2\text{O}_5$). The following approximate lower temperature limits of formation of two liquids were determined for three points: 5 (I) 1440° , 4 (II) 1450° , 3 (III) 1440° . The indices of refraction of SiO_2 -rich glasses fluctuated between 1.444 and 1.451.

The presence of Na_2O sharply decreases the phase separation region (Fig. 342) from that in the CaF_2 -- CaO -- SiO_2 and CaF_2 -- Al_2O_3 -- SiO_2 systems. However, the region of immiscible liquids in the CaF_2 -- Na_2O -- SiO_2 system occupies an area which is greater than the corresponding area in the CaO -- Na_2O -- SiO_2 oxide system studied by Grieg [1].

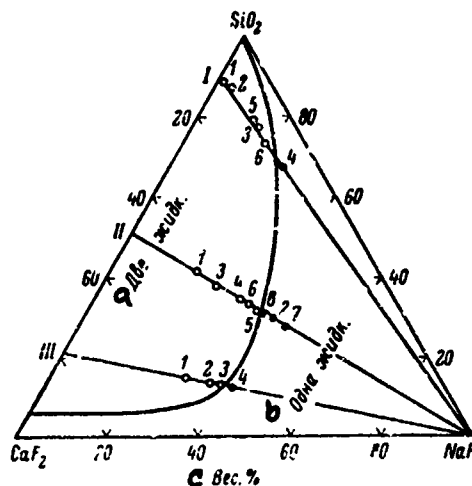


Fig. 343. Region of equilibrium of two liquid phases in the CaF_2 -- NaF -- SiO_2 system (from Yershova and Ol'shanskiy): designations same as in Fig. 342. [Key: same as in Fig. 342.]

The regions of equilibrium of two liquid phases in the CaF_2 -- NaF -- SiO_2 and MgF_2 -- NaF -- SiO_2 systems are presented in Figs. 343 and 344, respectively.

The lower temperature limits of the two liquid phases formed in the CaF_2 -- NaF -- SiO_2 system were determined for boundary points (Fig. 343) 6 (I), 1290°, and 5 (II), 1260°, and the upper limits, 5 (I), 1400°, and 5 (II), 1330°.

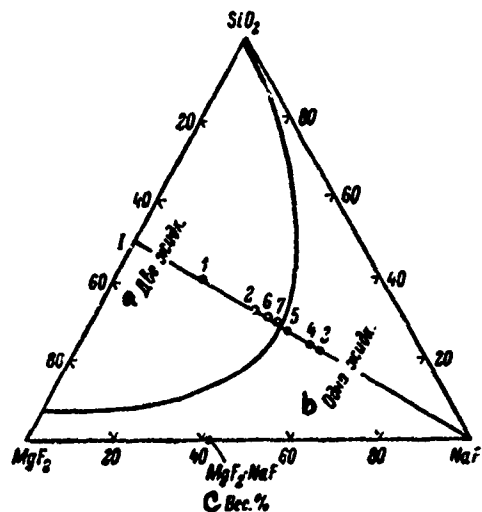


Fig. 344. Region of equilibrium of two liquid phases in MgF_2 -- NaF -- SiO_2 system (from Yershova and Ol'shanskiy): designations same as in Fig. 342. [Key: same as in Fig. 342.]

For the MgF_2 -- NaF -- SiO_2 system, the corresponding data for points 7 (I) (Fig. 344) are the lower limits 1280° , upper 1320° . The indices of refraction of the SiO_2 -rich glasses in the CaF_2 -- NaF -- SiO_2 system are from 1.444 to 1.451 and, in the MgF_2 -- NaF -- SiO_2 system, from 1.437 to 1.451.

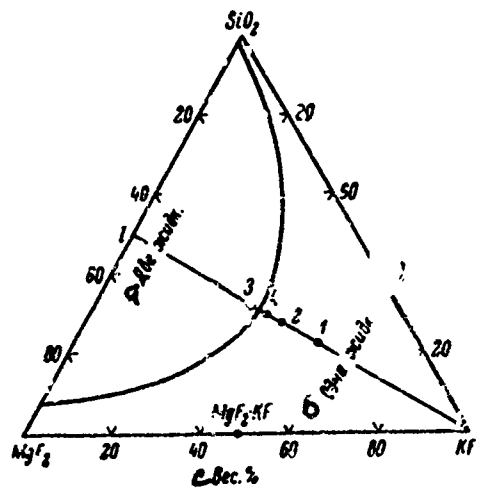


Fig. 345. Region of equilibrium of two liquid phases in MgF_2 -- KF -- SiO_2 system (from Yershova and Ol'shanskiy): designations same as in Fig. 342. [Key: same as in Fig. 342.]

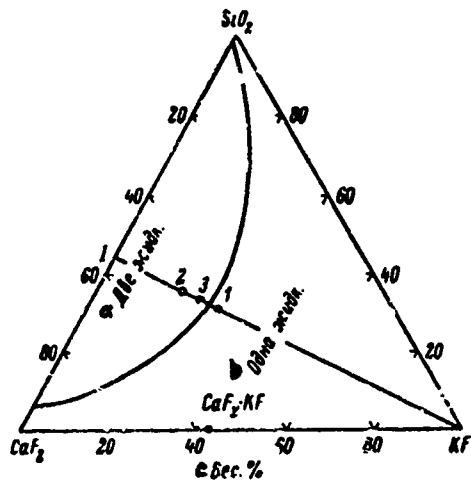


Fig. 346. Region of equilibrium of two liquid phases in CaF_2 -- KF -- SiO_2 system (from Yershova and Ol'shanskiy): designations same as in Fig. 342. [Key: same as in Fig. 342.]

The regions of equilibrium of two liquid phases for the MgF_2 -- KF -- SiO_2 and CaF_2 -- KF -- SiO_2 systems are shown in Figs. 345 and 346, respectively. The lower temperature limit in the CaF_2 -- KF -- SiO_2 system is $\sim 1265^\circ$.

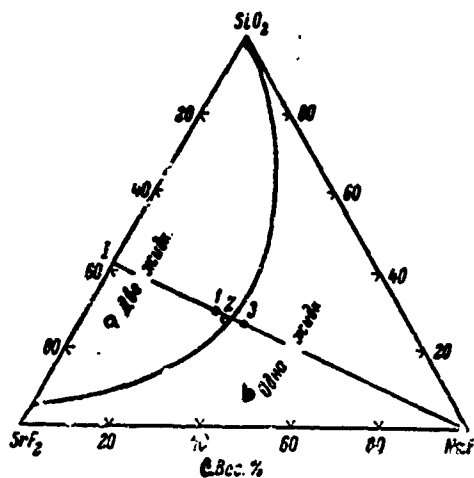


Fig. 347. Region of equilibrium of two liquid phases in SrF_2 -- NaF -- SiO_2 system (from Yershova and Ol'shanskiy): designations same as in Fig. 342. [Key: same as in Fig. 342.]

The boundaries of the phase separation regions in the SrF_2 -- NaF -- SiO_2 and BaF_2 -- NaF -- SiO_2 systems are plotted in Figs. 347 and 348, respectively. At boundary points 1 (I) in the SrF_2 -- NaF -- SiO_2 system and 4 (I) in the BaF_2 -- NaF -- SiO_2 system, the temperature limits have been established, with the upper one of them in the BaF_2 -- NaF -- SiO_2 system determined for composition 3 (I): the lower temperature limits --

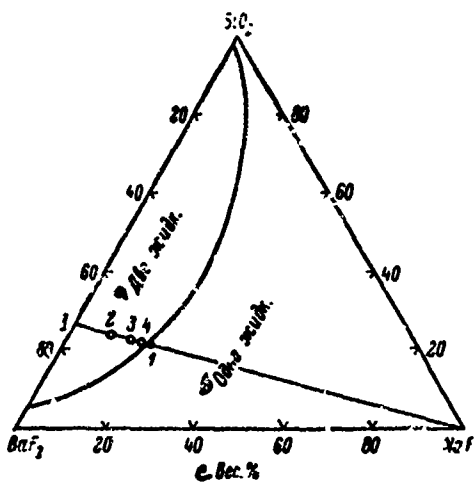


Fig. 348. Region of equilibrium of two liquid phases in BaF_2 -- NaF -- SiO_2 system (from Yershova and Ol'shanskiy): designations same as in Fig. 342. [Key: same as in Fig. 342.]

$1(\text{J}) \sim 1260^\circ$, $4(\text{I}) \sim 1250^\circ$; upper -- $1(\text{I}) \sim 1315^\circ$, $4(\text{I}) \sim 1310^\circ$. The indices of refraction of the SiO_2 -rich glasses in the SrF_2 -- NaF -- SiO_2 system are from 1.437 to 1.446 and, in the BaF_2 -- NaF -- SiO_2 system, from 1.444 to 1.451.

The region width of 2 liquid phases depends on the radius and charge of the cation. In all systems of the MeF_2 -- MeO -- SiO_2 , MeF_2 -- Al_2O_3 -- SiO_2 and $\text{Me}''\text{F}_2$ -- $\text{Me}'_2\text{F}_2$ -- SiO_2 types, the region of immiscibility of the liquids decreases with decrease in the ratio of the cation radius to valence [2, 3].

BIBLIOGRAPHY

1. Grieg, J., in the collection Klassicheskiye raboty po fiziko-khimii silikatov [Classical Work on Silicate Physical Chemistry], Khimizdat Press, Moscow, 1937.
2. Yershova, Z.P., Ya.I. Ol'shanskiy, Geokhimiya, 2, 1958, p. 144.
3. Yershova, Z.P., Trudy 6-go soveshch. po eksper. i tekhn. mineral. i petrograf. [Proceedings, 6th Conference on Experimental and Engineering Mineralogy and Petrography], AN SSSR Press, Moscow, 1962, p. 176.

SYSTEMS CONTAINING SULFIDES



Ol'shanskiy [1] has studied the phase separation region in this system, and he has compiled the diagram depicted in Fig. 349. As in the CaO -- CaS -- SiO_2 system, the boundary of the region next to $\text{MgS} \text{ -- SiO}_2$ could not be determined experimentally, and it is indicated by the dashed lines, on the basis of a number of considerations reported in work [1].

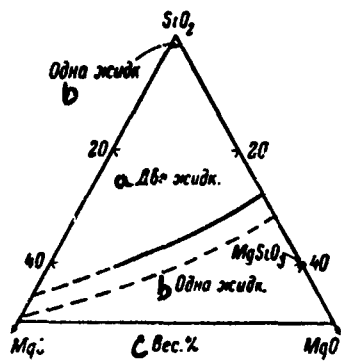


Fig. 349. Phase separation region in $\text{MgS} \text{ -- MgO -- SiO}_2$ system (from Ol'shanskiy): thick line, continued with dashes, phase separation boundary at 1800° ; thin dashed line, conjectural boundary of equilibrium region of two liquids + SiO_2 at 1700° . [Key: same as in Fig. 342.]

BIBLIOGRAPHY

1. Ol'shanskiy, Ya. I., Trudy 4-go soveshch. po eksper. mineral. i petrograf. [Proceedings, 4th Conference on Experimental Mineralogy and Petrography], 1st Ed., AN SSSR Press, Moscow, 1951, p. 55.



Ol'shanskiy [1] has determined the phase separation region in the system (Fig. 350).

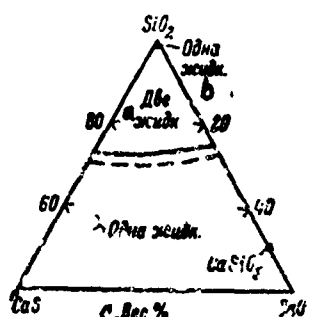


Fig. 350. Phase separation region in $\text{CaS} \text{ -- } \text{CaO} \text{ -- } \text{SiO}_2$ system (from Ol'shanskiy): designations same as in Fig. 349. [Key: same as in Fig. 342.]

Spherical inclusions of strongly refracting glass, usually partially crystallized, in low-refraction ($N = 1.468 \text{ -- } 1.476$), almost pure silica glass, were observed under the microscope.

BIBLIOGRAPHY

1. Ol'shanskiy, Ya. I., Trudy 4-go soveshch. po eksper. mineral. i petrograf. [Proceedings, 4th Conference on Experimental Mineralogy and Petrography], 1st Ed., AN SSSR Press, Moscow, 1951, p. 55.

FeS -- FeO -- SiO₂

The FeS -- FeO -- SiO₂ or pyrrhotine -- wüstite -- SiO₂ system is not strictly speaking ternary, since wüstite and pyrrhotine are phases of variable composition. The Fe content in them usually is lower than in the formulas presented (< 1). The pseudoternary FeS -- FeO -- SiO₂ system has been partially studied by Ol'shanskiy [1]. On the basis of his own and literature data, he has plotted a diagram (Fig. 351), in which the boundary of the FeS -- SiO₂ system is characterized by practically complete immiscibility of the FeS and SiO₂ components in the liquid state at the melting temperature of cristobalite. The second boundary of the pyrrhotine (FeS) -- wüstite (FeO) system is a pseudobinary, and its principal features can be understood only by examination of the Fe -- FeS -- FeO ternary system. A section of this triple diagram passing through the wüstite-pyrrhotine points does not intersect the region of heterogeneous equilibrium of the two liquid phases anywhere. Therefore, by depicting the FeS -- FeO system as a binary one, we obtain a fusibility diagram characterizing a simple eutectic.

The double elevation points and ternary eutectics determined by Ol'shanskiy [2], are depicted separately in the upper part of Fig. 351. The triple eutectic temperature, depending on composition of the wüstite participating in the equilibrium, has different values, from 920 to 1000°. The temperature of 920° corresponds to an equilibrium with wüstite saturated with iron (23.2% oxygen) and 1000°, to wüstite containing the greatest amount (24.6%) of oxygen.

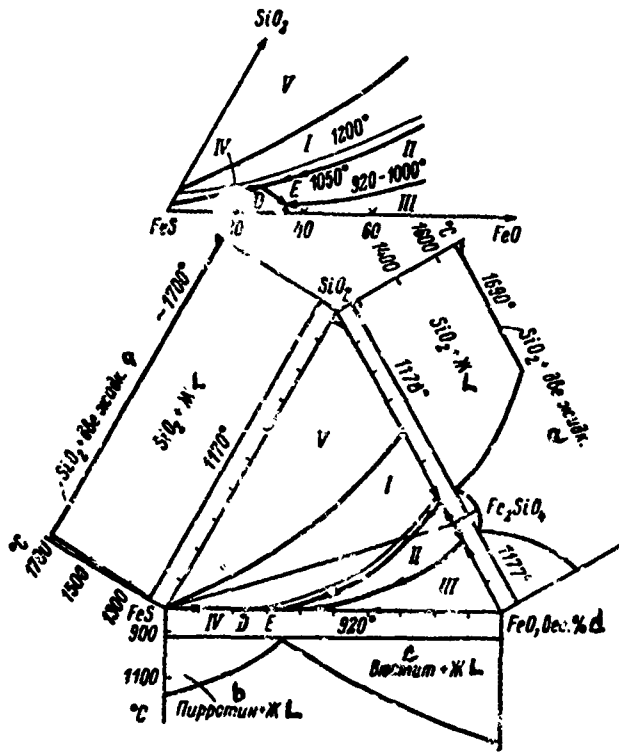


Fig. 351. Phase diagram of FeS -- FeO -- SiO₂ system (from Oi'shanskiy): I. SiO₂ + liquid; II. Fayalite + liquid; III. Wüstite + liquid; IV. Pyrrhotine + liquid; V. SiO₂ + two liquids.

Key:

- a. Two liquids
- b. Pyrrhotine
- c. Wüstite
- d. Weight %.

INVARIANT POINTS OF FeS -- SeO -- SiO₂ SYSTEM

a Точка (рис. 351)	b Фазы	c Процесс	d Состав, вес. %			e Тем- пература, °C
			FeS	FeO	SiO ₂	
E	Fe ₂ SiO ₄ + FeO + FeS + жидкое коство	g Эвтектика	65	35	< 1	920
D	Fe ₂ SiO ₄ + FeS + SiO ₂ + жидкое коство	h Точка двой- ного подъема	70	30	< 1	1050

Key:

- | | |
|--------------------------|---------------------------|
| a. Points (Fig. 351) | e. Temperature, °C |
| b. Phases | f. Liquid |
| c. Process | g. Eutectic |
| d. Composition, weight % | h. Double elevation point |

BIBLIOGRAPHY

1. Ol'shanskiy, Ya. I., DAN SSSR, 59, 3, 1948, p. 513.
2. Ol'shanskiy, Ya. I., DAN SSSR, 70, 2, 1950, p. 245.

SYSTEMS CONTAINING WATER



The system has been studied by Baker and Jue [2], at temperatures of 10 and 31° (Fig. 352), and by Baker, Jue and Willis [3], at temperatures of 50, 70 and 90° (Fig. 353). Morey and Hesselgesser [7] have studied the equilibrium saturation curves of SiO_2 , $\text{Na}_2\text{O}\cdot\text{SiO}_2$ and $\text{Na}_2\text{O}\cdot 2\text{SiO}_2$ in water solutions at 40°. The phase relationships in the system, at temperatures of 250, 300 and 350°, have been studied by Tuttle and Friedman [11] (Fig. 354), and at 400 and 450°, by Friedman [4] (Figs. 355, 356). Tuttle and Friedman have reported that, at 250°, the compound sodium disilicate-water does not form a binary system, since the field of two immiscible liquids intersects the line connecting $2\text{Na}_2\text{O}\cdot\text{SiO}_2$ and H_2O . The results of Tuttle and Friedman do not agree with the data of Morey and Hesselgesser [7] (Fig. 357). In the opinion of Rowe and colleagues [9], the studies of Morey and Hesselgesser are incomplete and unfinished.

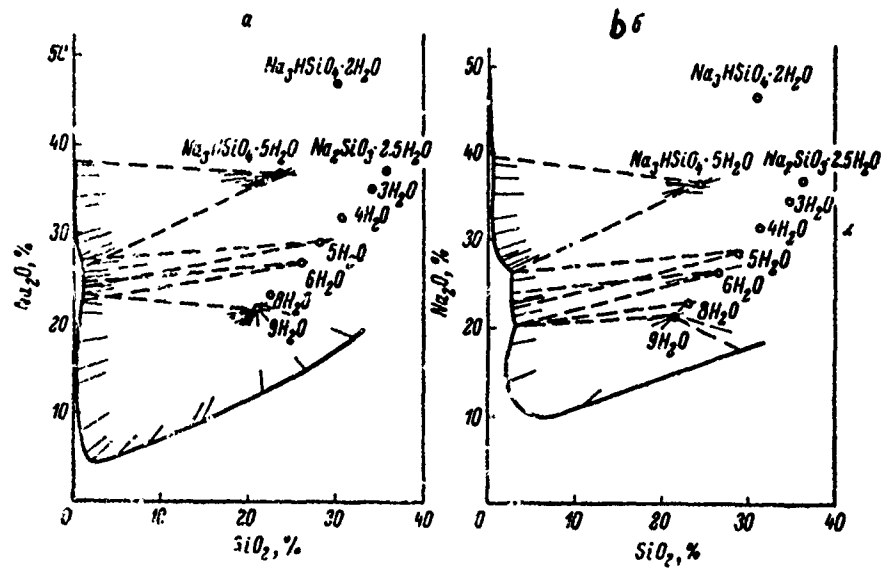


Fig. 352. Diagram of phase relationships of $\text{Na}_2\text{O} \text{-- SiO}_2 \text{-- H}_2\text{O}$ system (from Baker and Jue): a. 10° ; b. 31° .

Rowe, Fournier and Morey [9], studying the interrelationships of the phases in the system at 200 , 250 and 300° (Fig. 358), discovered three new phases: $\text{Na}_2\text{O} \cdot 3\text{SiO}_2 \cdot 11\text{H}_2\text{O}$, $\text{Na}_2\text{O} \cdot 3\text{SiO}_2 \cdot 6\text{H}_2\text{O}$, $\text{Na}_2\text{O} \cdot 3\text{SiO}_2 \cdot 5\text{H}_2\text{O}$.

A schematic diagram of the portion of the $\text{Na}_2\text{O} \text{-- SiO}_2 \text{-- H}_2\text{O}$ system bounded by the $\text{Na}_2\text{O} \cdot 2\text{SiO}_2 \text{-- SiO}_2 \text{-- H}_2\text{O}$ triangle (in P-t coordinates), at temperatures over 100° , according to Rowe, Fournier and Morey [9], is presented in Fig. 359.

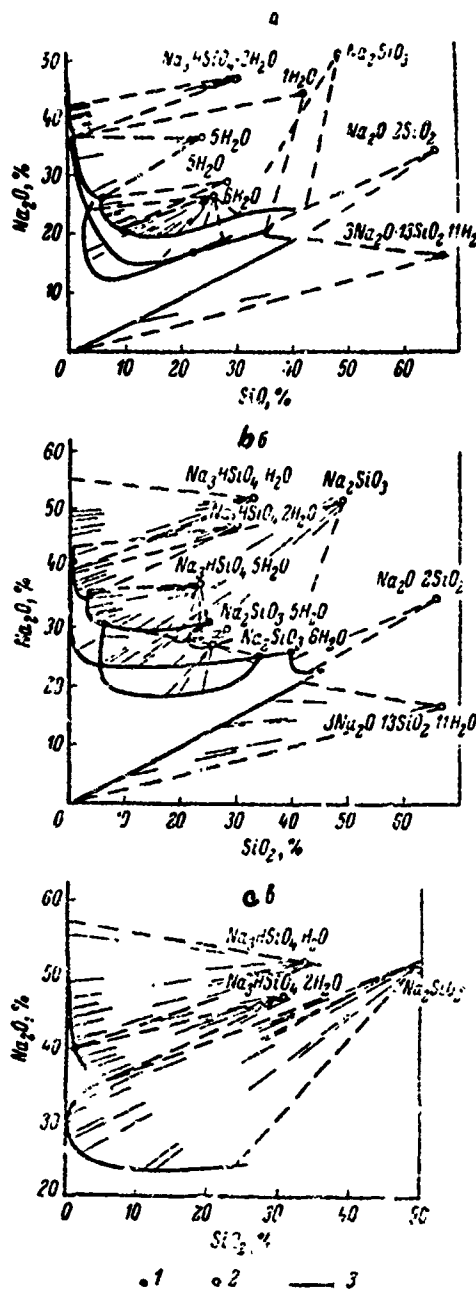


Fig. 353. Diagram of phase relationships of $\text{Na}_2\text{O} - \text{SiO}_2 - \text{H}_2\text{O}$ system (from Baker and colleagues):
 a. 50°; b. 70°, c. 90°; 1. isothermal invariant points;
 2. theoretical composition; 3. boundary curves.

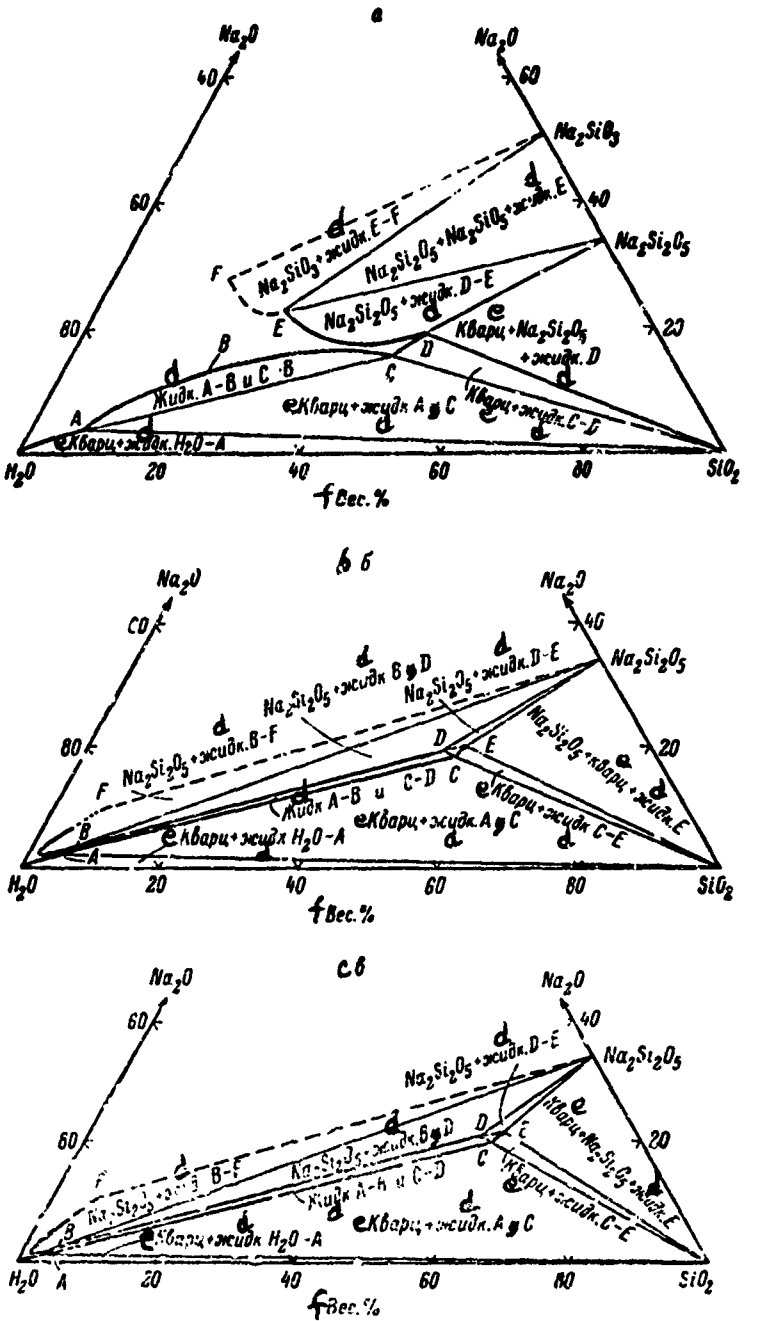


Fig. 354. Diagram of phase relationships in $\text{Na}_2\text{O} - \text{SiO}_2 - \text{H}_2\text{O}$ system (from Tuttle and Friedman): a. 250°; b. 300°; c. 350°.

Key:

- d. Liquid
- e. Quartz
- f. Weight %

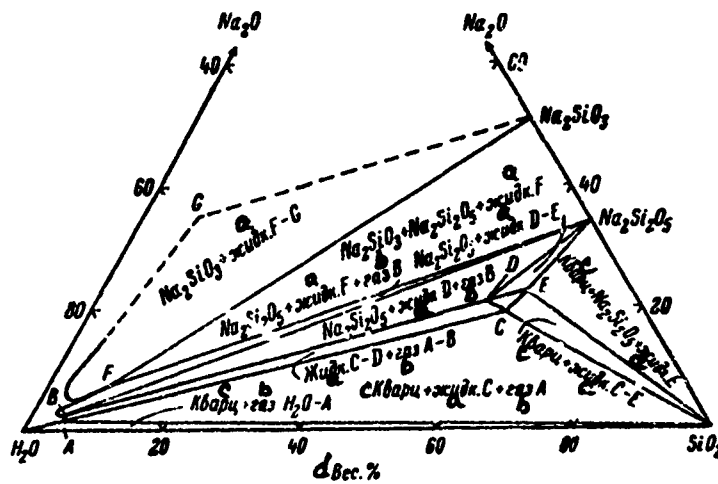


Fig. 355. Polybaric saturation curves at 400° in $\text{Na}_2\text{O} -- \text{SiO}_2 -- \text{H}_2\text{O}$ system (from Friedman).

Key:

- a. Liquid
- b. Gas
- c. Quartz
- d. Weight %

Possible invariant points in this system are represented by the authors in the following form: 1. GQDLH_{11} , 2. GQDLH_6 , 3. GQDLH_5 , 4. $\text{GQDH}_{11}\text{H}_6$, 5. $\text{GQH}_{11}\text{H}_5$, 6. GQDH_6H_5 , 7. $\text{GQLH}_{11}\text{H}_6$, 8. $\text{GQLH}_{11}\text{H}_5$, 9. GQLH_6H_5 , 10. $\text{GDLH}_{11}\text{H}_6$, 11. $\text{GDLH}_{11}\text{H}_5$, 12. GDLH_6H_5 , 13. $\text{GQH}_{11}\text{H}_6\text{H}_5$, 14. $\text{GDH}_{11}\text{H}_6\text{H}_5$, 15. $\text{GLH}_{11}\text{H}_6\text{H}_5$, 16. $\text{QDLH}_{11}\text{H}_6$, 17. $\text{QDLH}_{11}\text{H}_5$, 18. QDLH_6H_5 , 19. $\text{GDH}_{11}\text{H}_6\text{H}_5$, 20. $\text{QLH}_{11}\text{H}_6\text{H}_5$, 21. $\text{DLH}_{11}\text{H}_6\text{H}_5$ (G is gas, Q is quartz, D is $\text{Na}_2\text{O} \cdot 2\text{SiO}_2$, L is liquid, H_{11} is $\text{Na}_2\text{O} \cdot 3\text{SiO}_2 \cdot 11\text{H}_2\text{O}$, H_6 is $\text{Na}_2\text{O} \cdot 3\text{SiO}_2 \cdot 5\text{H}_2\text{O}$ and H_5 is $\text{Na}_2\text{O} \cdot 3\text{SiO}_2 \cdot 5\text{H}_2\text{O}$). The compositions of those invariant points which are designated in the figure correspond to those indicated above.

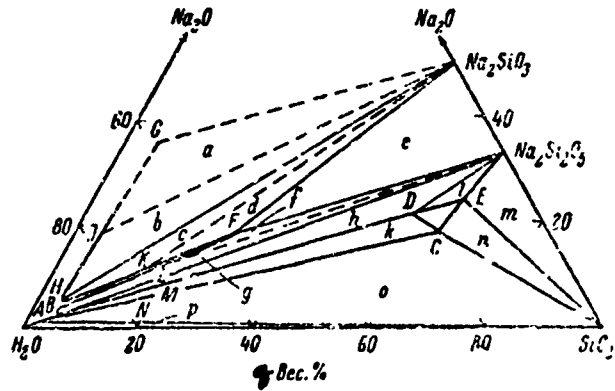


Fig. 356. Polybaric saturation curves at 450° in $\text{Na}_2\text{O} \text{-- } \text{SiO}_2 \text{ -- } \text{H}_2\text{O}$ system (from Friedman): a. Na_2SiO_3 + liquid G-J; b. Na_2SiO_3 + gas J-H; Na_2SiO_3 + gas H-K; d. Na_2SiO_3 + liquid K-F; e. Na_2SiO_3 + $\text{Na}_2\text{Si}_2\text{O}_5$ + liquid F; f. $\text{Na}_2\text{Si}_2\text{O}_5$ + liquid L-F; g. $\text{Na}_2\text{Si}_2\text{O}_5$ + gas L-B; h. $\text{Na}_2\text{Si}_2\text{O}_5$ + liquid D + gas B; k. liquid C-D + gas A-B; l. $\text{Na}_2\text{Si}_2\text{O}_5$ + liquid D-E; m. quartz + $\text{Na}_2\text{Si}_2\text{O}_5$ + liquid E; n. quartz + liquid C-E; o. quartz + liquid C + gas A; p. quartz + gas H₂O-A.

Key:

q. Weight %

The system also has been studied by Morey [6], Morey and Irgenson [8] and Witte and colleagues [12].

The characteristics of the hydrate phases of the system, sodium hydrosilicates, are presented in the table. For hydrosilicates of the compositions $\text{Na}_2\text{O} \cdot 2\text{SiO}_2 \cdot 3\text{H}_2\text{O}$, $\text{Na}_2\text{O} \cdot 3\text{SiO}_2 \cdot 5\text{H}_2\text{O}$, $\text{Na}_2\text{O} \cdot 3\text{SiO}_2 \cdot 6\text{H}_2\text{O}$ and $\text{Na}_2\text{O} \cdot 3\text{SiO}_2 \cdot 11\text{H}_2\text{O}$, data characterizing their features were not obtained.

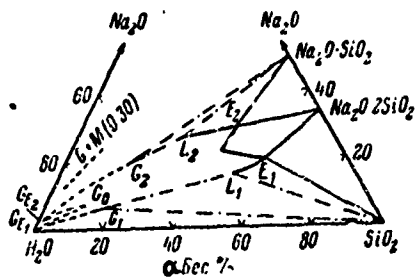


Fig. 357. Isothermal polybaric saturation curves at 400° in $\text{Na}_2\text{O} - \text{SiO}_2 - \text{H}_2\text{O}$ system (from Morey and Hesselgesser): E_1L_1 , saturation curve of quartz in liquid; GE_1G_1 , co-existing saturation curve; $G_1L_1\text{SiO}_2$, three-phase triangle at pressure of 2500 bar; E_1E_2 and G_1G_2 saturation curves of $\text{Na}_2\text{O}\cdot 2\text{SiO}_2$ with gas and liquid with $\text{Na}_2\text{O}\cdot 2\text{SiO}_2$; E_2L_2 and GE_2 , saturation curves of $\text{Na}_2\text{O}\cdot \text{SiO}_2$; $G_2L_2\text{Na}_2\text{O}\cdot \text{SiO}_2$, three-phase triangle at pressure of 2500 bar; $G + M (0.30)$, equilibrium line between gas phase and metasilicate at pressure of 2000 bar and $\text{SiO}_2:\text{Na}_2\text{O}$ ratio = 0.3.

Key:

a. Weight %

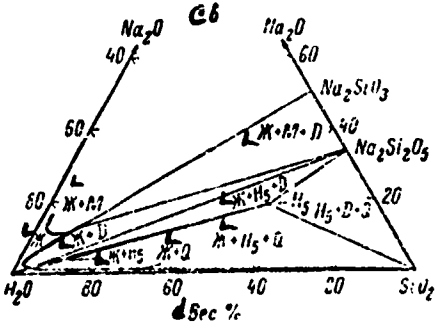
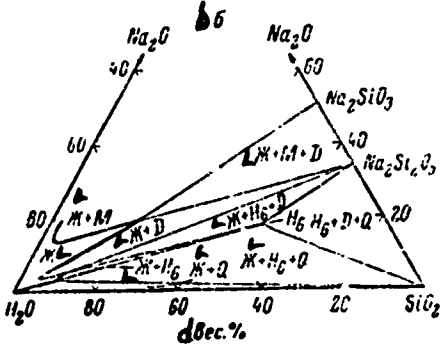
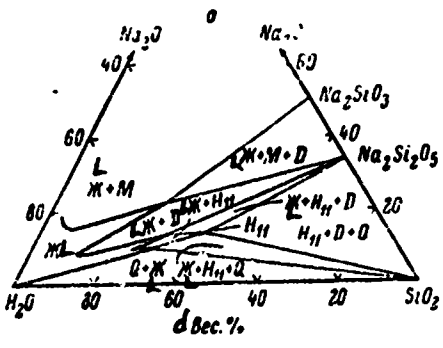


Fig. 358. Isothermal polybaric saturation curves in $\text{Na}_2\text{O} - \text{SiO}_2 - \text{H}_2\text{O}$ system (from Rowe, Fournier and Morey): a. 200°; b. 250°; c. 300°; the thin lines fix the limits of the phase stability field; thick lines are isothermal saturation curves; Q. quartz; D. sodium disilicate; M. sodium metasilicate; H_{11} . sodium trisilicate hendecahydrate; H_5 . sodium trisilicate pentahydrate; H_6 . sodium trisilicate hexahydrate.

Key:

d. Weight %

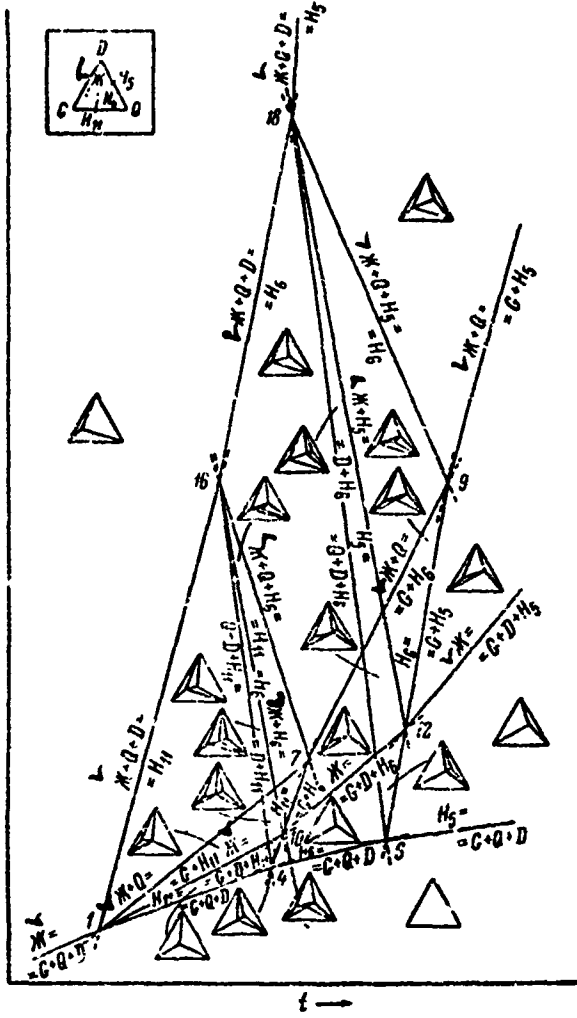


Fig. 359. Schematic, hypothetical P-t diagram of part of $\text{Na}_2\text{O} \text{-- } \text{SiO}_2 \text{-- } \text{H}_2\text{O}$ system, bounded by $\text{H}_2\text{O} \text{-- } \text{Na}_2\text{Si}_2\text{O}_5 \text{-- } \text{SiO}_2$ (from Rowe and colleagues): see explanation in text.

SODIUM HYDROSILICATE CHARACTERISTICS

a Состав	b Структурная формула	Ng	Nr	Nm	c Плот- ность, г/см ³	d Сингония	e Параметры элементарной ячейки			
							e:b:c	a	b	c
3Na ₂ O · 2SiO ₂ · 11H ₂ O (одинадцатигидрат диортосиликата)	Na ₂ [HSiO ₃] · 5H ₂ O	1.524	1.504	1.510	—	Ромбическая	0.884 : 1 : 1.10	—	—	—
Na ₂ O · SiO ₂ · 9H ₂ O	Na ₂ [H ₂ SiO ₃] · 8H ₂ O	1.460	1.451	1.455	1.646	»	0.692 : 1 : 0.342	—	—	—
Na ₂ O · SiO ₂ · 6H ₂ O (две модификации)	Na ₂ [H ₂ SiO ₃] · 5H ₂ O	1.485	1.465	1.473	1.507	Моноклинная	1.921 : 1 : 1.073	—	102°39'	—
Na ₂ O · SiO ₂ · 5H ₂ O	Na ₂ [H ₂ SiO ₃] · 4H ₂ O	1.407	1.447	1.454	1.75	Триclinная	0.736 : 1 : 0.901	128°8'	38°13'	102°50'
Na ₂ O · SiO ₂ · 8H ₂ O	Na ₂ [H ₂ SiO ₃] · 7H ₂ O	1.465	1.457	1.463	1.67	Моноклинная	0.864 : 1 : 0.715	—	111°37'	—

Key:

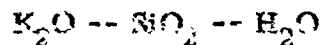
- | | |
|-------------------------------|-----------------------------------|
| a. Composition | f. Diorthosilicate hendecahydrate |
| b. Structural formula | g. Two modifications |
| c. Density, g/cm ³ | h. Rhombic |
| d. Crystal system | i. Monoclinic |
| e. Unit cell parameters | j. Triclinic |

Thilo and Miedreich [10] and Lange and Stakelberg [5] consider sodium hydrosilicates to be acid salts of monosilicic acid.

BIBLIOGRAPHY

1. Thilo, E., G. Funk, E.-M. Vickman, in the collection Fizicheskaya khimiya silikatov [Physical Chemistry of Silicates], Foreign Literature Publishing House, Moscow, 1956, p. 5.
2. Baker, C.L., L.R. Jue, J. Phys. Colloid Chem., 54, 3, 301, 1950.
3. Baker, C.L., L.R. Jue, J.H. Willis, J. Amer. Chem. Soc., 72, 12, 5373, 1950.
4. Friedman, I., J. Amer. Chem. Soc., 72, 10, 4573, 1950.
5. Lange, H., M. Stakelberg, Zs. anorgan. allgem. Chem. 256, 5-6, 273, 1948.

6. Morey, G.W., J. Amer. Ceram. Soc., 36, 9, 279, 1953.
7. Morey, G.W., J. Hesselgesser, Amer. J. Sci., Bowen vol., 361, 1952.
8. Morey, G.W., E. Irgenson, Amer. J. Sci., (5), 35A, 225, 1938.
9. Rowe, J.J., R.O. Fournier, G.W. Morey, Inorg. Chem., 6, 6, 1183, 1967.
10. Thilo, E., W. Miedreich, Zs. anorgan. allgem. Chem., 267, 1, 76, 1951.
11. Tuttle, D.F., J. Friedman, J. Amer. Chem. Soc., 70, 3, 923, 1948.
12. Witte, P., K. Langer, F. Seifert, W. Schreyer, Naturwissenschaften, 56, 8, 414, 1968.



The system has been studied by Morey [4] (Fig. 360). Compounds of the system have been synthesized by Morey [3] and Fukall [5]. Later, Funk and Stade [1] obtained potassium hydrosilicates of the following compositions: $(KHSiO_3)_x$, $KKH_2Si_2O_5$ (I) and $KHSi_2O_5$ (II). The authors present X-ray photos of these substances.

POTASSIUM HYDROSILICATE CHARACTERISTICS

Соединение	Структурная формула	N_d	N_m	N_p	Плотность, г/см ³	Сингония
$K_2O \cdot SiO_2 \cdot H_2O$	$KHSiO_3$	$N_{ep} = 1.50$ (вычисл.)	N_{ep}	—	f	Ромбическая
$K_2O \cdot SiO_2 \cdot H_2O$	$KHSi_2O_5$	$N_{ep} = 1.50$	N_{ep}	—	—	—
$2K_2O \cdot 2SiO_2 \cdot H_2O$	$K_2O \cdot 4SiO_3 \cdot H_2O$	$N_{ep} = 1.50$	$N_{ep} = 1.50$	—	—	Ромбическая
$2K_2O \cdot 4SiO_3 \cdot H_2O$	$K_4(HSiO_3)_4$	1.555	1.501	1.435	2.417	Monoclinic

Key.

- | | |
|-------------------------------|---------------|
| a. Compound | e. Calculated |
| b. Structural formula | f. Rhombic |
| c. Density, g/cm ³ | g. Monoclinic |
| d. Crystal system | |

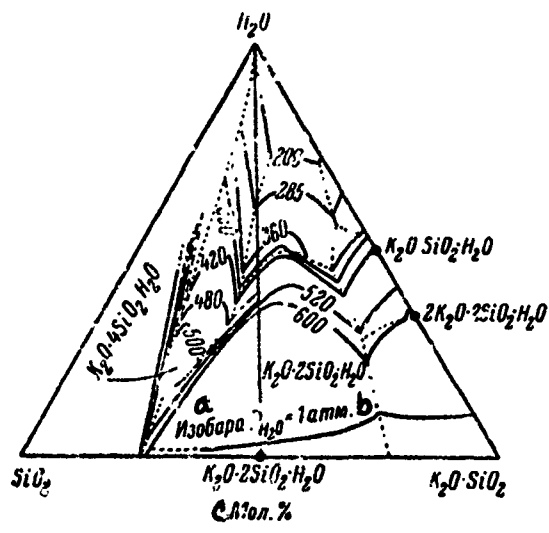


Fig. 360. Phase diagram of $K_2O - SiO_2 - H_2O$ system, isothermal saturation curves for partial system $SiO_2 - K_2O \cdot SiO_2 - H_2O$ (from Morey).

Key:

- a. Isobar
 - b. Atmosphere, atm
 - c. Mole %

Hilmer [2] has studied the structure of $K_4(HSiO_3)_4$. The unit cell parameters of this compound are $a = 7.51$, $b = 11.25$, $c = 7.50 \text{ \AA}$, $\beta = 100^\circ$; monoclinic crystal system.

The characteristics of the compounds in the system studied are presented in the table.

BIBLIOGRAPHY

1. Furuk., H., Stade. Zs. Morgan. allgem Chem., 315, 1-2, 79, 1962.
 2. Hilmer, W., Acta crystallogr., 17, 8, 1063, 1964.

3. Morey, G.W., Zs. anorgan. allgem. Chem., 86, 3, 314, 1914. J. Amer. Chem. Soc., 39, 6, 1190, 1917.
4. Morey, G.W., J. Soc. Glass. Technol., 6, Trans., 25, 1922.
5. Pukall, W., Ber. Dtsch. chem. Ges., 49, 2/3, 405, 1916.



The system has been studied thoroughly by Bowen and Tuttle [24] and supplemented by D. Roy and R. Roy [55-57], Osborn [53, 58], Jang [38], Ostrovskiy [17], Noil [52], Kitahara and Kennedy [44, 45], Pistorius [54], Kalousek [40], Yoder [10], and Butt and Rashkovich [5-7].

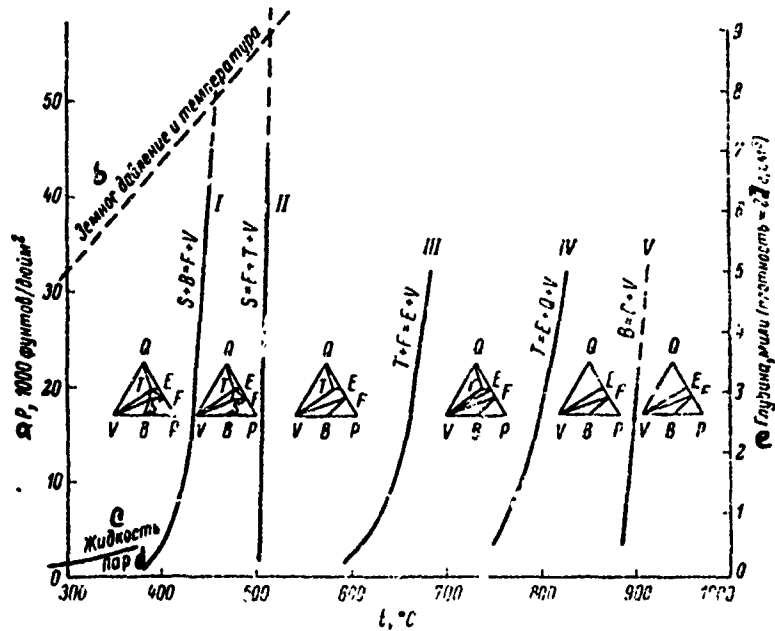


Fig. 361. P-t curves of monovariant equilibrium (I-V) of the $\text{MgO} \text{ -- } \text{SiO}_2 \text{ -- } \text{H}_2\text{O}$ system (from Bowen and Tuttle):
B. brucite; E. enstatite; F. forsterite; P. periclase;
Q. quartz; S. serpentine; T. talc; U. water vapor.

Key:

- | | |
|------------------------|---|
| a. Pressure P, 1000psi | c. Liquid |
| b. Ground pressure and | d. Vapor |
| temperature | e. Depth, miles (density = 2.7 g/cm^3) |

Investigation of the equilibrium states in the system was carried out by Bowen and Tuttle [24], at the following water vapor temperatures and pressures: 100°, ~ 1040 kgf/cm²; 600-900°, 2109 kgf/cm²; 600-300°, 2812 kgf/cm²; 300-100°, ~ 1400 kgf/cm². As a result, the monovariant equilibrium curves have been plotted in P-t coordinates (Fig. 361). The equation for the reaction to which the curves relate is presented beside each curve. The triangular diagrams in the divariant regions between the curves show the equilibrium combinations of phases at the corresponding pressures and temperatures. The vapor tension curve is at the lower left of the figure and, at the upper left, the curve of increase in temperature with depth of the rock (temperature gradient 34.2°/km, density of rock 2.7 g/cm³).

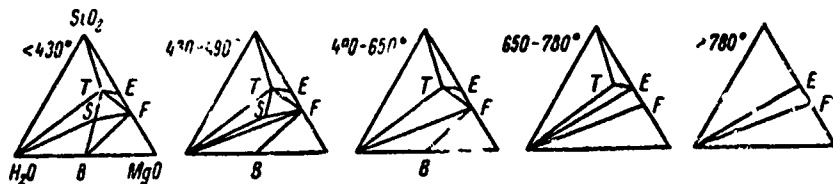


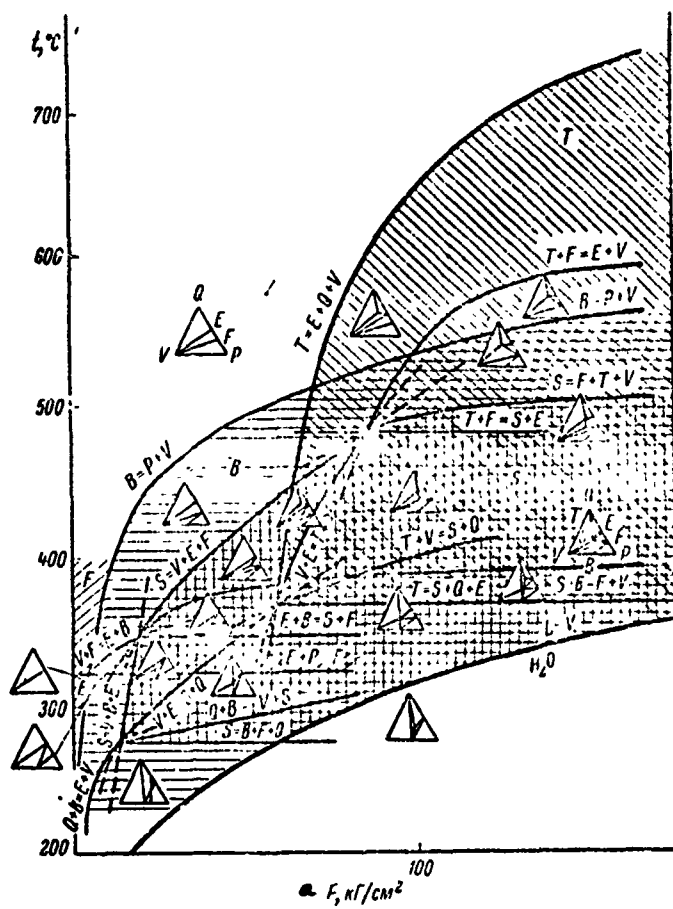
Fig. 362. Coexisting phase triangles of $MgO - SiO_2 - H_2O$ system (from D. Roy and R. Roy): T. talc; E. enstatite; F. forsterite; S. serpentine; B. brucite.

Coexisting phase triangles of the $MgO - SiO_2 - H_2O$ system, according to D. Roy and R. Roy [55], are presented in Fig. 362.

Yoder [10] has refined the position of the three-phase monovariant curve $Mg(OH)_2 \rightleftharpoons MgO + H_2O$.

Ostrovskiy [17] has correlated experimental data of various authors, and he has attempted to carry out an extrapolation to the region of lower

temperatures and pressures. The author introduces three different P-t diagrams of the $\text{MgO} - \text{SiO}_2 - \text{H}_2\text{O}$ system, for the cases when the following converge at one invariant point: 1. curves II and III (Fig. 363); 2. curves I and V (Fig. 364); 3. curves I and II (Fig. 365).



Reproduced from
best available copy.

Fig. 363. P-t diagram of $\text{MgO} - \text{SiO}_2 - \text{H}_2\text{O}$ system; curves II and III converge at one invariant point (from Ostrovskiy):
B. brucite; E. enstatite; F. forsterite; P. periclase; Q. quartz;
S. serpentine; T. talc; V. water vapor.

Key:

a. Pressure P, kgf/cm^2

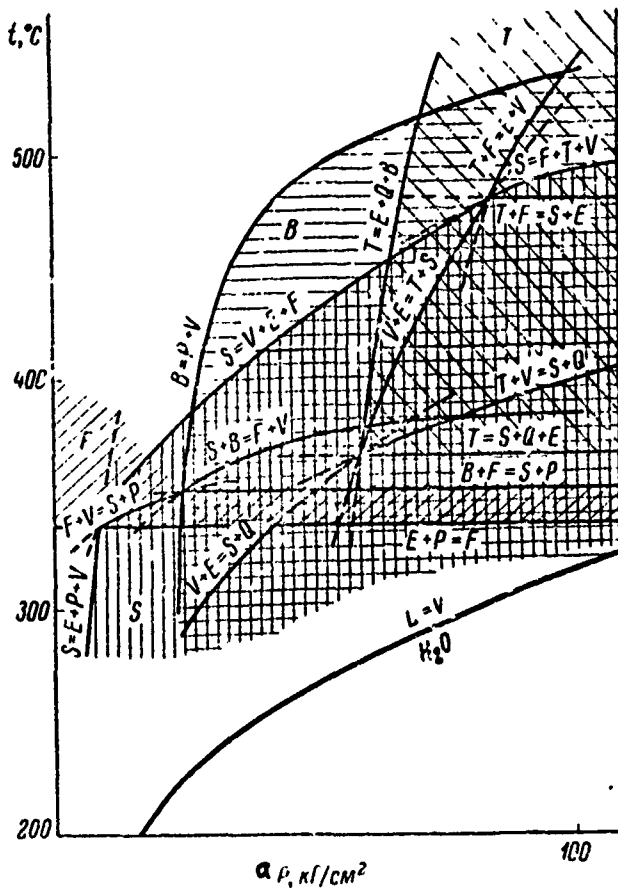


Fig. 364. P-t diagram of $\text{MgO} - \text{SiO}_2 - \text{H}_2\text{O}$ system:
Curves I and V converge at one invariant point (from
Ostrovskiy): designations same as in Fig. 363.

Key:

a. $P, \text{kgr/cm}^2$

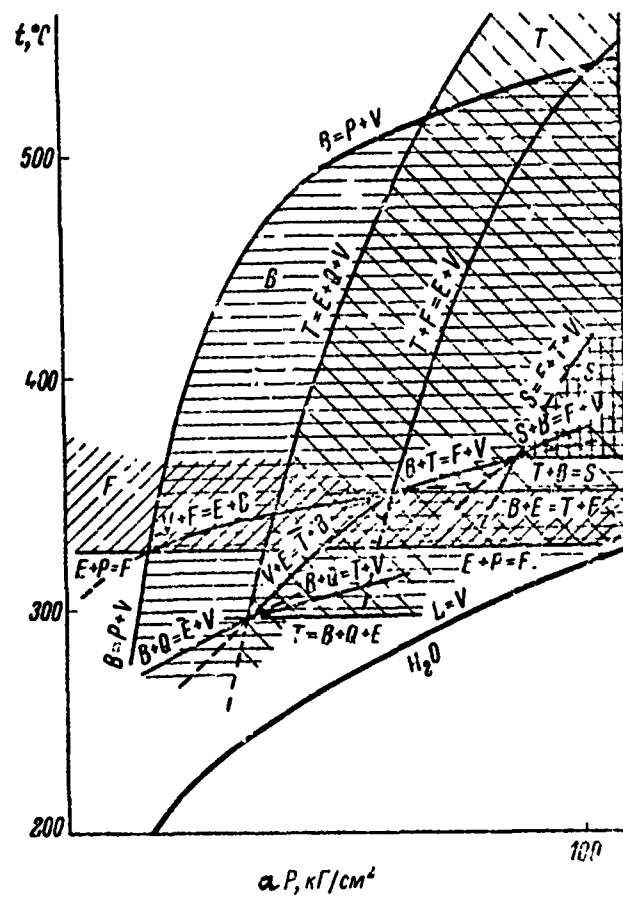


Fig. 365. P-t diagram of MgO -- SiO₂ -- H₂O system:
 Curves I and II converge at one invariant point (from
 Ostrovskiy). designations same as in Fig. 363.

Key:

a. $P, \text{kgr/cm}^2$

Some properties of hydrated and anhydrous magnesium compounds, formed as equilibrium phases in the MgO -- SiO_2 -- H_2O system, as well as of those magnesium hydrosilicates which are encountered in nature or are formed synthetically as metastable products, are presented in the table. Bowen and Tuttle consider that such a phase as attapulgite is a metastable phase, formed by decomposition of talc.

A number of investigators have studied the process of dehydration of magnesium hydrosilicates [2, 7, 16, 18-21, 25, 27, 31, 34, 37, 43, 48, 51, 53].

Many studies have been devoted to synthesis of magnesium hydrosilicates [5-11, 14, 15, 24, 29, 36-38, 40, 52, 59, 64, 67].

Study of the equilibria in the three-component system would be incomplete without data on the two-component system MgO -- H_2O .

MgO -- H_2O . The MgO -- H_2O system has been studied by many authors, who have obtained noncoinciding results, mainly as a consequence of failure to observe identity of experimental conditions.

Equilibrium curves of the reaction $Mg(OH)_2 \rightleftharpoons MgO + H_2O$, according to the data of various investigators, are presented in Fig. 366. As is evident from the curve, the $Mg(OH)_2 \rightleftharpoons MgO + H_2O$ equilibrium curve (curve 2) obtained by Bowen and Tuttle [24] differs considerably from the group of equilibrium curves in the left portion of the figure. Equilibrium curves 1, 4 and 6, obtained by Korzhinskiy [12], MacDonald [47] and Kennedy [42], respectively, agree well with one another. Equilibrium curve 4 was obtained by MacDonald by calculation. MacDonald theoretically calculated free energy for the reactions which correspond to curves 4 (equilibrium between natural brucite and

CHARACTERISTICS OF PHASES OF MgO -- SiO_2 -- H_2O SYSTEM

α Соединение	Габитус кристаллов	с Плотность, г/см ³	Ng	Nm	Np	Параметры элементарной ячейки				e Сингония
						a, Å	b, Å	c, Å	β	
α-MgSiO ₃ (энстатит) f	Призмы ψ	3.10	1.671	1.664	1.671	18.23	8.814	5.178	—	ff Ромбическая
β-MgSiO ₃ (клиноэнстатит) g	Кристаллические агрегаты, полисинтетические двойники	3.19	1.660	1.654	1.651	5.618	8.828	5.190	108°30'	gg Моноклинная
MgSiO ₃ (протоэнстатит) h	Брусковидные кристаллы, псевдоморфозы по энстатиту	—	ee Отличаются от энстатитовых не более чем на ± 0.002		9.25	8.74	5.32	—	ff	Ромбическая
Mg ₃ SiO ₄ (форстерит) i	Призмы ψ	3.22	1.668	—	1.636	4.752	10.226	5.977	—	hh Тексагональная
Mg(OH) ₂ (брюцит) j	Гексагональные пластины	—	1.53	—	1.559	3.125	4.73 kX	—	—	ii Тригональная
SiO ₂ (β -кварц) k	Зерна ψ	2.63	1.55	—	1.54	4.993	5.393	—	—	jj Кубическая
MgO (периклаз) l	Кубы, октаэдры z	3.58	N = 1.736		.203 kX		—	—	—	—
Mg ₂ Si ₂ O ₅ (OH) ₂ (тальк) m	Чешуйки α	2.7–2.8	1.585	1.582	1.545	5.29	9.16	29.0	101°39'	mm Моноклинная
Mg ₂ Si ₂ O ₅ (OH) ₂ (серпентин) n	Тонкие волокна bb	—	1.545	—	1.532–1.552	14.46	18.5	5.33	93°16'	nn
Mg ₂ Si ₂ O ₅ (OH) ₂ (хризотил) o	Волокна cc	2.96–2.5	1.555	—	1.547	11.75	18.26	5.16	93°16'	—
Mg ₂ Si ₂ O ₅ (OH) ₂ (антигорит) p	Чешуйки aa	2.53–2.58	1.571	1.570	1.560	5.3	9.25	13.52	91°4'	—
Mg ₂ (H ₂ O) ₂ (OH) ₂ [Si ₂ O ₅] ₂ ·2H ₂ O (аттепулгит) q	Волокна cc	—	1.54	—	1.508	—	—	—	—	—
Mg ₂ (H ₂ O) ₂ (OH) ₂ [Si ₂ O ₅] ₂ ·nH ₂ O (α -серпентин) r	—	2.4	1.505–1.526	—	1.490–1.519	23.2	15.7	5.32	90–93°	ff Ромбическая
Mg ₂ (Fe ₂ O ₃) ₂ (OH) ₂ (куппферит или антофиллит) s	Изоморфные dd	2.85–3.2	1.657	1.642	1.633	18.5	17.9	5.27	—	gg Моноклинная
α-MgO · SiO ₂ · H ₂ O (α -керосит)	—	2.3–2.4	1.579–1.557	—	—	14.68	8.24	5.16	93°	—
β-MgO · SiO ₂ · H ₂ O (β -керосит)	Чешуйки gg	—	N = 1.513–1.516		—	—	—	—	—	—

Key:

- a. Compound
- b. Appearance of crystals
- c. Density, g/cm³
- d. Unit cell parameters
- e. Crystal system
- f. Enstatite
- g. Clinoenstatite
- h. Protoenstatite
- i. Forsterite
- j. Brucite
- k. β -quartz
- l. Periclaste
- m. Talc
- n. Serpentine
- o. Chrysotile
- p. Antigorite
- q. Attapulgite
- r. α -sepiolite
- s. Kupfferite or anthophyllite
- t. Kerolite
- u. Prisms
- v. Crystalline aggregates, polysynthetic twins
- w. brick-shaped crystals, pseudomorphosis to enstatite
- x. Hexagonal plates
- y. Grains
- z. Cubes, octahedra
- aa. Lamella
- bb. Thin fibers
- cc. Fibers
- dd. Needles
- ee. Differ from those of enstatite by not over ± 0.002
- ff. Rhombic
- gg. Monoclinic
- hh. Hexagonal
- ii. Trigonal
- jj. Cubic

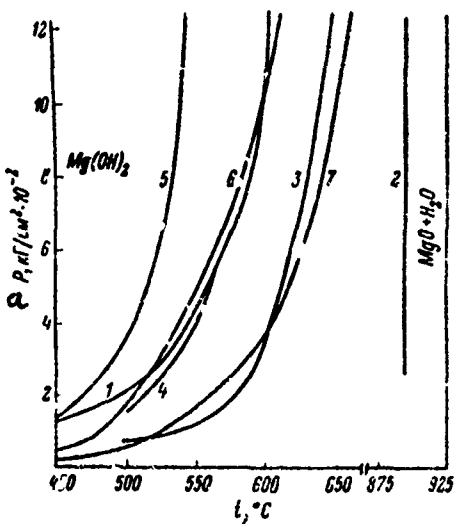


Fig. 366. Equilibrium curves for reaction $\text{Mg}(\text{OH})_2 \rightleftharpoons \text{MgO} + \text{H}_2\text{O}$: 1. from Korzhinskiy; 2. from Bowen and Tuttle; 3. from D. Roy and R. Roy and Osborn; 4, 5. from MacDonald; 6. from Kennedy; 7. from D. Roy and R. Roy.

Key:

a. Pressure P , $\text{kgf}/\text{cm}^2 \cdot 10^{-2}$

magnesium oxide, obtained at low temperature) and 5 (equilibrium between synthetic $\text{Mg}(\text{OH})_2$ and magnesium oxide, are obtained at high temperature). At constant temperature, the first reaction corresponds to a considerably lower equilibrium pressure than the second one.

The system also has been studied by D. Roy, R. Roy and Osborn [58] (curve 3) and subsequently refined by D. Roy and R. Roy [57] (curve 7). The

equilibrium conditions in the system have been studied by Fyfe [30], Fyfe and Goodwin [32], and by Meyer and Chi-Sun Jang [49].

The equilibrium curve according to Barnes and Ernst [22, 23] passes through the points 547°-245 atm, 572°-490 atm, 607°-980 atm, 634°-1470 atm and 657°-1960 atm.

The system also has been studied by Boreskov and colleagues [1], Johnston [39], Lebedev [13], Butt and Rashkovich [3-6] and Anderson and Horlock [20]. Chown and Deacon [28] have studied the mechanism of the magnesium oxide + steam reaction.

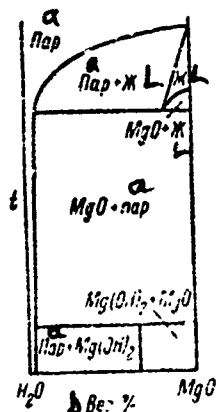


Fig. 367. Schematic isobaric "temperature-composition" profile of $\text{MgO} - \text{H}_2\text{O}$ system, studied at pressures up to 4000 kbar and showing region of high temperature melting (from Walter, Wyllie and Tuttle).

Key:

- a. Steam
- b. Weight %

Data on hydration of MgO, obtained by annealing at various temperatures, is presented by Wells and Taylor [62, 66], Layden and Brindley [46] and Walter, Wyllie and Tuttle [65]. A schematic profile of the "temperature-composition" diagram of the MgO -- H₂O system, according to the data of [65], is represented in Fig. 367.

Karlson and colleagues [41] have studied the solubility of magnesium oxide in water at high temperatures and pressures. The solubility curves of MgO in water are depicted in Fig. 368.

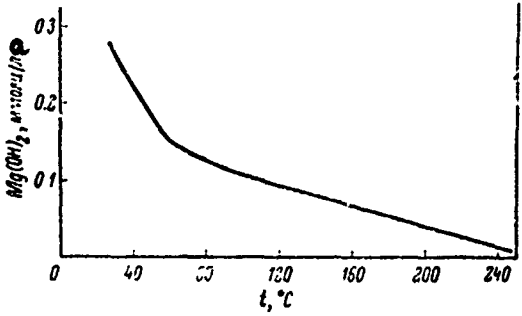


Fig. 368. Solubility of magnesium oxide in water at various temperatures (from Karlson and colleagues).

Key:

a. mmole/l

The brucite -- water system has been studied at 25° by Hostetler [35]. Brindley [26] obtained and studied brucite monocrystals. A number of investigators, Gjaldback [33], Murotani and colleagues [50], Butt and Rashkovich [6], Shirasaki [60] and others, have obtained Mg(OH)₂ in metastable form. Tagai and Saito [61] have studied the formation of large crystals of Mg(OH)₂, the sizes of which depended on the pH of the medium.

Mg(OH)_2 is encountered in nature in the form of brucite ($\text{Ne} = 1.580$, $\text{No} = 1.559$, as well as $\text{Ne} = 1.585$, $\text{No} = 1.566$, hexagonal, unit cell parameters $a = 3.125$, $c = 4.75 \text{ kX}$), the crystals of which have the form of regular hexagonal plates, and nemalite, a matted fiber variety. A colloidal variety of encrusted shapes also is encountered.

BIBLIOGRAPHY

1. Boreskov, K. G., V. A. Dzis'ko. M. S. Borisova, ZhFKh, 27, 8, 1953, p. 1172.
2. Budnikov, P. P., A. S. Berezhnoy, Reaktsii v tverdykh fazakh [Solid Phase Reactions], Promstroyizdat Press, Moscow, 1949.
3. Butt, Yu. M., Sb. trudov ROSNIIMS, 6, 1954, p. 115.
4. Butt, Yu. M., L. N. Rashkovich, Ibid., 13, 1957, p. 3.
5. Butt, Yu. M., L. N. Rashkovich, Trudy 5-go soveshch. po eksper. i tekhn. mineral. i petrograf. [Proceedings, 5th Conference on Experimental and Engineering Mineralogy and Petrography], AN SSSR Press, Moscow, 1958, p. 322.
6. Butt, Yu. M., L. N. Rashkovich, Tverdeniye vyazhushchikh pri povyshennykh temperaturakh [Hardening of Binders at Elevated Temperatures], Stroyizdat Press, Moscow, 1965.
7. Butt, Yu. M., L. N. Rashkovich, V. V. Volkov, Izv. vuzov, 'Khimika i khimicheskaya tekhnologiya', 3, 1958, p. 130.
8. Vektaris, B., I. Yanitskiy, I. Mituzas, Trudy Kaunassk. politekhn. inst., 5, 1957, p. 147.
9. Dement'yev, K. G., Nauchnyye osnovy tekhniki stroitel'nykh tsementov [Scientific Foundations of Structural Cement Technology], Kiev, 1905.
10. Yoder, H. S., Eksperimental'nyye issledovaniya v oblasti petrografii i rudoobrazovaniya [Experimental Studies in the Fields of Petrography and Ore Production], Foreign Literature Publishing House, Moscow, 1954.
11. Kantsepol'skiy, I. S., M. S. Zhabitskiy, Trudy Inst. khimii AN UzSSR, Issue 2, "General and Inorganic Chemistry," Tashkent, 1949, p. 27.

12. Korzhinskiy, D. S., Zap. Vseros. mineral. obshch., ya ser., 64, 1, 1935, p. 1.
13. Lebedev, V. I., Trudy 5-go soveshch. po eksper. i tekhn. mineral. i petrograf. [Proceedings 5th Conference on Experimental and Engineering Mineralogy and Petrography], AN SSSR Press, Moscow, 1958, p. 129.
14. Mchedlov-Petrosyan, O. P., DAN SSSR, 78, 3, 1951, p. 557.
15. Mchedlov-Petrosyan, C. P., Trudy 4-go Soveshch. po eksper. mineral. i petrograf. [Proceedings, 4th Conference on Experimental Mineralogy and Petrography], 1st Ed, AN SSSR Press, Moscow, 1951, p. 177.
16. Nagornyy, A. I., Ye. L. Soboleva, Ogneupory, 2, 1953, p. 81.
17. Ostrovskiy, I. A., Izv. AN SSSR, ser. geol., 1, 1957, p. 116.
18. Strelov, K. K., P. S. Mamykin, Trudy 4-go Soveshch. po eksper. mineral i petrograf. [Proceedings, 4th Conference on Experimental Mineralogy and Petrography], 2d Ed, AN SSSR Press, Moscow, 1953, p. 237.
19. Syromyatnikov, F. V., Byull. Mosk. obshch. ispyt. prirody, otd. geol., 42, 1, 1934, p. 137.
20. Anderson, P. J., R. F. Horlock, Trans. Farad. Soc., 58, 10, 1962, p. 1993.
21. Ball, M. C., H. F. W. Taylor, Mineral. Magaz., 33, 261, 1963, p. 467.
22. Barnes, H. Z., W. G. Ernst, Carnegie Inst. Washington Year Book, 59, 1959-1960, p. 63.
23. Barnes, H. Z., W. G. Ernst, Amer. J. Sci., 261, 2, 1963, p. 129.
24. Bowen, N. L., O. F. Tuttle, Bull. Geol. Soc. Amer., 60, 3, 1949, p. 439.
25. Brauner, K., A. Preisinger, Tschermaks mineral. u. petrogr. Mitt., 6, 1/2, 1956, p. 120.
26. Brindley, G. W., G. J. Ogilvie, Acta crystallogr., 5, 4, 1952, p. 412.
27. Brindley, G. W., J. Zussman, Amer. Mineralogist, 42, 7-8, 1957, p. 461.
28. Chown, J., R. F. Deacon, Trans. Brit. Ceram. Soc., 63, 2, 1964, p. 91.
29. Cole, W. F., H. V. Hueber, Silicates Industr., 22, 2, 1957, p. 75.
30. Fyfe, W. S., Amer. J. Sci., 256, 10, 1958, p. 729.
31. Fyfe, W. S., Amer. J. Sci., 260, 6, 1962, p. 460.

32. Fyfe, W.S., L. H. Godwin, Amer. J. Sci., 260, 4, 1962, p. 389.
33. Gjelback, J.K., Zs. anorgan. allgem. Chem., 144, 3, 1925, p. 269.
34. Hey, M.H., F.A. Bannister, Mineral. Magaz., 23, 201, 1948, p. 333.
35. Hostetler, P.B., Amer. J. Sci., 261, 3, 1963, p. 238.
36. Jander, W., R. Fett, Zs. anorgan. allgem. Chem., 242, 2, 1939, p. 143.
37. Jander, W., J. Wührer, Zs. anorgan. allgem. Chem., 235, 4, 1938, p. 273.
38. Jang, J.C., J. Amer. Ceram. Soc., 43, 10, 1960, p. 542.
39. Johnston, J., Zs. phys. Chem., 62, 3, 1908, p. 330.
40. Kalousek, G.L., D. Mui, J. Amer. Ceram. Soc., 37, 2, 1954, p. 38.
41. Karlson, E.T., R.B. Peppier, L.S. Wells, J. Res. Nat. Bur. Stand., 51, 4, 1953, p. 179.
42. Kennedy, G.C., Amer. J. Sci., 254, 9, 1956, p. 967.
43. Kiefer, M.C., Compt. rend., 230, 10, 1950, p. 977.
44. Kitahara, S., G.C. Kennedy, Amer. J. Sci., 265, 3, 1967, p. 211.
45. Kitahara, S., S. Takenouchi, G.C. Kennedy, Amer. J. Sci., 264, 3, 1966, p. 223.
46. Layden, G.K., G.W. Birdley, J. Amer. Ceram. Soc., 46, 11, 1963, p. 518.
47. MacDonald, G.J.F., J. Geol., 53, 3, 1955, p. 244.
48. Martin-Vivaldi, J.L., J. Cano-Ruiz, Anales de la Real Sociedad española de física y química, B52, 7/8, 1956, p. 499.
49. Meyer, J.W., J. Chi-Sun Jang, Amer. J. Sci., 260, 9, 1952, p. 707.
50. Murotani, H., T. Shiroasaki, H. Kodaira, Bull. Soc. Salt Sci. Japan, 11, 4, 1957.
51. Nagy, B., W.F. Bradley, Amer. Mineralogist, 40, 9-10, 1955, p. 885.
52. Noll, W., Zs. anorgan. allgem. Chem., 261, 1/2, 1950, p. 1.
53. Osborn, E.F., USA Pat. No. 2590566, 25 Mar 1952.
54. Pistorius, C.W.F.T., Neues Jahrb. Mineral., 11, 1963, p. 283.

55. Roy, D.M., R. Roy, Amer. Mineralogist, 39, 11/12, 1954, p. 972.
56. Roy, D.M., R. Roy, Amer. Mineralogist, 40, 3/4, 1955, p. 147.
57. Roy, D.M., R. Roy, Amer. J. Sci., 255, 3, 1957, p. 374.
58. Roy, D., R. Roy, E.F. Osborn, Amer. J. Sci., 251, 5, 1953, p. 337.
59. Sclar, C.B., L.C. Garrison, J.W. Stewart, Trans. Amer. Geophys. Union, 48, 1, 1967, p. 266.
60. Sudaiki, T., J. Electrochem. Soc. Japan, 29, 3, 202; 4, E248, 1961.
61. Tagai, H., K. Saito, J. Ceram. Assoc. Japan, 76, 3 (871), 1968, p. 80.
62. Taylor, K., L.S. Wells, J. Res. Nat. Bur. Stand., 21, 2, 1938, p. 133.
63. Thilo, E., G. Rogge, Ber. Dtsch. chem. Ges., 72, 2, 1939, p. 341.
64. Vournazos, A.C., Zs. anorgan. allgem. Chem., 200, 3, 1931, p. 237.
65. Walter, L.S., R.J. Wyllie, O.F. Tuttle, J. Petrol., 3, 1, 1962, p. 49.
66. Wells, L.S., K. Taylor, J. Res. Nat. Bur. Stand., 19, 2, 1937, p. 215.
67. Wiegmann, J., C.H. Horte, Silikattechnik, 11, 8, 1960, p. 380.



There is no complete phase diagram of the system. Investigation of it is complicated by a number of factors: difficulty in achieving equilibrium, the fineness of grain of neogenes and their poor crystallization, variable composition and metastability of many phases, by the effect of reaction conditions on the nature of the phases formed (nature of the initial material, reaction temperature, pressure, duration of test, number of liquid phases, method of mixing). Many tests are difficult to reproduce.

Synthesis of calcium hydrosilicates is most easily accomplished under hydrothermal conditions. The initial materials may be amorphous and

crystalline varieties of SiO_2 and calcium hydroxide, mono, di- and tricalcium silicates, low-alkalinity calcium hydrosilicates. The time necessary for formation of stable compounds is from several hours to several months.

One feature of the system is the difficulty in identification of the phases formed, as a consequence of the fine crystallinity and great similarity of many of their parameters (similar X-ray photos, close limits of refraction and endothermic transformation temperature regions, etc.). As a rule, identification can be accomplished only by use of a set of methods: crystallooptical, X-ray phase, differential-thermal, and, in case of necessity, chemical, infrared spectroscopy and electron microscopy as well.

Many compounds in the system are known as natural minerals, predominantly of contact-metamorphic origin. At the present time, there are about 30 natural and synthetic compounds in the system, calcium hydrosilicates.

Their basic characteristics are presented in Table 1. There is an extensive literature (about 600 works) on investigation of the system and separate phases. References are made in this handbook only to individual works containing extensive bibliographies and permitting sufficiently complete and detailed information to be had on the major results obtained in the $\text{CaO} - \text{SiO}_2 - \text{H}_2\text{O}$ system: structure, crystallooptical properties, X-ray radiography, differential-thermal analysis, infrared spectroscopy, electron microscopy, and chemical analysis of these compounds, as well as thermochemistry, thermodynamics, kinetics and mechanisms of reaction. For the most complete data, see works [2, 4, 6-8, 15, 26, 39, 43, 50, 51, 67, 69-72]. Infrared absorption spectra are presented in works [3, 5, 21-24, 34, 35, 46, 62]. Infrared absorption spectra, according to Ryskin [21-24], are given in Table 2.

TABLE 1
CHARACTERISTICS OF CALCIUM HYDROSILICATES

a Соединение	b Структурная формула	c Габитус кристал- лов	d Показатели светопре- ломления	e Плот- ность, г/см ³	f Сингония	g Параметры элементарной ячейки	h Темпера- туры дегидра- ции, °C	i Кристалличес- кие фазы, обраску- ющие при разложении
j Гидросиликаты, сходные по структуре с волластонитом								
2CaO · 6SiO ₂ · 8H ₂ O l (неконит)	Ca ₂ Si ₄ O ₁₀ · 2H ₂ O · 4H ₂ O	[Волокна]	N _{uv} = 1.533	2.24	Триклини- ческая	a = 3.86, b = 7.32, c = 7.60 Å, α = 111°48', β = 86°12', γ = 103°54'	800	Ориентированный волластонит и кристобаллит
3CaO · 6SiO ₂ · 6H ₂ O o (окенит)	3[Ca ₂ Si ₄ O ₁₀ · 2H ₂ O · 4H ₂ O]	"	N _g = 1.541, N _p = 1.530	2.33	"	a = 9.84, b = 7.20, c = 21.33 Å, α = 90°, β = 103.9°, γ = 111.5°	-	Ориентированный волластонит и неориентиро- ванный кристо- баллит
6CaO · 6SiO ₂ · H ₂ O q (хонотлит)	Ca ₆ [Si ₄ O ₁₀](OH) ₂	"	N _g = 1.595, N _m = 1.583, N _p = 1.583	2.70	Моно- клиническая	a = 16.5, b = 7.33, c = 7.03 Å	775	Ориентирован- ный β -CS
4CaO · 3SiO ₂ · H ₂ O t (Фосагит)	Ca ₄ Si ₃ O ₈ (OH) ₂	"	N _g = 1.605, N _m = 1.603, N _p = 1.597	2.96–2.73	"	a = 10.32, b = 7.35, c = 14.07 Å, β = 106°	650–750	-
2CaO · SiO ₂ · H ₂ O u (гильбрэндит)	Ca ₂ Si ₄ O ₁₀ (OH) ₂	"	N _g = 1.612, N _p = 1.605	2.66–2.69	"	a = 16.6, b = 7.26, c = 11.85 Å, α = 90°, β = 90°, γ = 90°	520–540	β -CS и некоторое количество γ -CS
w Тоберморитовая группа								
5CaO · 5SiO ₂ · 9H ₂ O (14 Å-тоберморит, K пломбировит) bb	Ca ₅ Si ₄ O ₁₀ H ₂ · 9H ₂ O	-	-	2.2	Ортого- ромбическая	a = 11.28, b = 7.32, c = 28.06 Å	55±5 200–220 250–450 450–650 Больше 700	11.3 Å-тоберморит X 11.3 Å- и 9.3 Å-то- берморит X 9.3 Å-тоберморит X 9.7 Å-тоберморит X Водные опилки X

- Key:
- a. Compound
 - b. Structural formula
 - c. Crystal appearance
 - d. Indices of refraction
 - e. Density, g/cm³
 - f. Crystal system
 - g. Unit cell parameters
 - h. Dehydration temperatures, °C
 - i. Crystalline phases formed by decomposition
 - j. Hydrosilicates similar in structure to wollastonite
 - k. Nekoite
 - l. Fibers
 - m. Triclinic
 - n. Oriented wollastonite and cristobalite
 - o. Okenite
 - p. Oriented wollastonite and unoriented cristobalite
 - q. Xonotlite
 - r. Monoclinic
 - s. Oriented β CS
 - t. Foshagite
 - u. Hillebrandite
 - v. β C₂S and a certain amount of γ -C₂S
 - w. Tobermorite group
 - x. Tobermorite
 - y. Orthorhombic
 - z. Above
 - aa. Wollastonite
 - bb. Plumbierite

TABLE 1 (continued)

a Соединение	b Структурная формула	c Габитус кристал- лов	d Показатели светопре- ломления	e Плот- ность, г/см ³	f Сингония	g Параметры одиничной ячейки	h Темпера- туры дегидра- ции, °C	i Бригада факта, обнару- женная при изучении
5CaO · 6SiO ₂ · 5H ₂ O (11 Å-тоберморит, X) тоберморит	Ca ₅ (Si ₄ O ₉ H) ₂ Ca · · 4H ₂ O, Ca ₅ (Si ₄ O ₉ H) · · 4H ₂ O	gg Тонкие плоскости	N _g = 1.575, N _m = 1.571, N _p = 1.570	7.44	dd Тонк.	a = 11.3 b = 7.3, c = 22.6 Å	260 800–850 (изотер- мический спектр)	9.3 Å-тоберморит Wollastonit
5CaO · 6SiO ₂ · 0–2H ₂ O (9.3 Å-тоберморит, X) риверсидит	—	gg Пластинки	N _g = 1.605, N _m = 1.601, N _p = 1.600	2.6–2.7	» »	a = 11.12, b = 7.32, c = 18.6 Å	700	—
Точный состав неиз- вестен (12.6 Å-тобер- морит) hh	—	—	—	—	—	—	—	—
Хорошо окристали- зованная форма CSH (II), точный состав неизвестен (10.0 Å-тоберморит)	—	—	—	2.5–2.6	Orthorhom- bicak	a = 11.3, b = 7.32, c = 29.5 Å	—	9.3 Å-тоберморит Wollastonit
5CaO · 6SiO ₂ (9.7 Å- тоберморит, jj) kk	—	—	—	—	—	—	730–770 850–900	9.7 Å-тоберморит Wollastonit
II Слабозакристаллизованные тобермориты								
0.8–1.5CaO · SiO ₂ · · H ₂ O (тоберморит X) CSH (II)	—	gg Закручен- ные листочки	—	—	—	a = 5.6, b = 3.6 Å	890	gg Wollastonit
1.5–2CaO · SiO ₂ · H ₂ O (тоберморит CSH (III)) X	—	mm Волнистые или гофри- рованные листочки	—	—	—	—	—	—

Key:

- a. Compound
- b. Structural formula
- c. Crystal appearance
- d. Indices of refraction
- e. Density, g/cm³
- f. Crystal system
- g. Unit cell parameters
- h. Dehydration temperatures, °C
- i. Crystalline phases formed by decomposition
- x. Tobermorite
- y. Orthorhom.bic
- aa Wollastonite
- cc Thin plates
- dd Same
- ee Exothermic peak
- ff Riversidite
- gg Plates
- hh Precise composition unknown (12.6 Å tobermorite)
- ii Well crystallized form CSH (E), precise composition unknown (10.0 Å tobermorite)
- jj Wollastonite (incomplete crystallization)
- kk Well-crystallized wollastonite
- ll Slightly crystallized tobermorite
- mm Twisted leaflets
- nn Fibers and corrugated plates

TABLE 1 (continued)

a Соединение	b Структурная формула	c Габитус кристал- лов	d Показатели светопре- ломления	e Плот- ность, г/см ³	f Сингония	g Параметры элементарной ячейки	h Темпе- ратуры дегра- дации, °C	i Кристаллические фазы, образую- щиеся при разложении
OO Гиролитовая группа								
$\text{CaO} \cdot 2\text{SiO}_2 \cdot 2\text{H}_2\text{O}$ (Z-фаза Ассарссона) pp	$\text{Ca}_2\text{Si}_2\text{O}_7$	Пластинки gg	$N_{\text{QV}} = 1.52$	—	Гексаго- нальная или псев- доекса- гональная gg	$a = 9.73 \text{ \AA}$	—	—
$6\text{CaO} \cdot 10\text{SiO}_2 \cdot 3\text{H}_2\text{O}$ (трускоттит) rr	$4(\text{Ca}_2\text{Si}_2\text{O}_7 \cdot 2\text{H}_2\text{O})$	—	—	—	—	—	800	Псевдоволасто- ss нит
$\text{K}_2\text{O} \cdot 28\text{CaO} \cdot 48\text{SiO}_2 \cdot$ $15\text{H}_2\text{O}$ (рениерит) tt	—	—	$N_{\text{QV}} = 1.560$	2.47	Триго- нальная uu	$a = 9.72$ $b = 18.71 \text{ \AA}$	800	dd То же
$8\text{CaO} \cdot 12\text{SiO}_2 \cdot 9\text{H}_2\text{O}$ $\cdot 2\text{CaO} \cdot 3\text{SiO}_2 \cdot 2\text{H}_2\text{O}$ (гиролит) vv	$\text{Ca}_2\text{Si}_2\text{O}_7 \cdot (\text{OH})_2 \cdot$ $\cdot 1 \cdot \text{H}_2\text{O}$ $2(\text{Ca}_2\text{Si}_2\text{O}_7 \cdot (\text{OH})_2 \cdot$ $\cdot 4\text{H}_2\text{O})$	Чешуи ww	$N_{\text{QV}} = 1.545$, $N_{\text{D}} = 1.535$	2.39	Гексаго- нальная xx	$a = 9.72$ $c = 22.13 \text{ \AA}$	800	—
УСТРУКТУРНОСХОДНЫЕ с $\gamma\text{-}2\text{CaO} \cdot \text{SiO}_2$								
$5\text{CaO} \cdot 2\text{SiO}_2 \cdot \text{H}_2\text{O}$ (кальциевый хондродит, фаза X Роя) zz	$\text{Ca}_5(\text{SiO}_4)_2(\text{OH})_2$	Призмы a'	$N_{\text{QV}} = 1.630$	2.84	Моно- клиническая yy	$a = 8.94 \pm$ $\pm 0.1^{\circ}$, $b = 11.42 \pm$ ± 0.05 , $c = 5.05 \pm$ $\pm 0.05 \text{ \AA}$, $\gamma = 103^{\circ}18' \pm$ $\pm 15'$	650–750 750–870 870	— b' Газовый переход
$3\text{CaO} \cdot 2\text{SiO}_2(8\text{CaO} \cdot$ $\cdot 5\text{SiO}_2)$ (килчоанит, фаза Z Роя) c'	$\text{Ca}_2\text{Si}_2\text{O}_7$	Чешуйки ww	$N_{\text{QV}} = 1.650$, $N_{\text{D}} = 1.67$	2.992	Орто ромбическая uu	$a = 5.03$, $b = 11.12$, $c = 21.95 \text{ \AA}$	1000	d' Rankinit
$\text{CaO} \cdot \text{SiO}_2 \cdot \text{H}_2\text{O}$ (такарит) f'	—	Пластинки gg	$N_{\text{QV}} = 1.537$	2.36	Прочие e'	—	750, 850	Бозластонит aa

Key:

- a. Compound
- b. Structural formula
- c. Crystal appearance
- d. Indices of refraction
- e. Density, g/cm³
- f. Crystal system
- g. Unit cell parameters
- h. Dehydration temperatures, °C
- i. Crystalline phases formed by decomposition
- r. Monoclinic
- y. Orthorhombic
- aa Wollastonite
- oo Gyrolite group
- pp Assarsson Z-phase
- qq Hexagonal or pseudohexagonal
- rr Truscottite

- ss Pseudowollastonite
- tt Reyerite
- uu Trigonal
- vv Gyrolite
- ww Laniella
- xx Hexagonal
- yy Structurally similar to $\gamma\text{-}2\text{CaO} \cdot \text{SiO}_2$
- zz Calcium chondrodite, Roy phase X
- a' Prisms
- b' Phase transition
- c' Kilchoanite, Roy phase Z
- d' Rankinite
- e' Others
- f' Tacharonite

TABLE 1 (continued)

a Состави	b Структурна формула	c Табіус "окта" ноз	d Показатели светопогло- щения	e Плот- ность, г/см ³	f Система	g Параметры элементарной ячейки	h Темпера- туры дегидра- ции, °C	i Приставочные газы, образую- щиеся при разложении
$\text{CaO} \cdot \text{SiO}_2 \cdot \text{H}_2\text{O}$ (суолунит) <i>g'</i>	$\text{Ca}_2\text{H}_2(\text{Si}_2\text{O}_5) \cdot \text{H}_2\text{O}$	Брусково- видные кристал- лические клю- гуны	$N_g = 1.623$, $N_m = 1.620$, $N_p = 1.619$	2.683	Ортоором- бическая	$a = 11.15$, $b = 19.57$, $c = 6.03 \text{ \AA}$	440	<i>Wollastonite</i>
$3\text{CaO} \cdot 2\text{SiO}_2 \cdot \text{H}_2\text{O}$ (розенхайнит) <i>i'</i>	$(\text{CaSiO}_3)_3 \cdot \text{H}_2\text{O}$	Плитко- войкой в виде кристаллов	$N_g = 1.616$, $N_m = 1.610$, $N_p = 1.625$	2.90— 2.89	Триплит <i>T</i> или	$a = 6.942$, $b = 9.57$, $c = 5.89 \text{ \AA}$, $\alpha = 95.30^\circ$, $\beta = 95.37^\circ$, $\gamma = 95.43^\circ$	400—500	—
$3\text{CaO} \cdot 2\text{SiO}_2 \cdot 3\text{H}_2\text{O}$ (афвиллит) <i>j'</i>	$\text{Ca}_3\text{SiO}_5(\text{OH})_2 \cdot$ $\cdot 2\text{H}_2\text{O}$	Прямо- угольные призмы	$N_g = 1.634$, $N_m = 1.620$, $N_p = 1.617$	2.61	Моноклини- ческая	$a = 16.27$, $b = 5.1$, $c = 13.2 \text{ \AA}$, $\beta = 13.48^\circ$	350 650 1300	<i>Phase Z</i> <i>Rankinit</i>
$2\text{CaO} \cdot \text{SiO}_2 \cdot \text{H}_2\text{O}$ (гидрат двухкаль- цийного силиката) <i>k'</i>	$\text{Ca}_2(\text{HSiO}_4) \cdot \text{OH}$	Пластин- ичные призмы	$N_g = 1.633$, $N_m = 1.620$, $N_p = 1.614$	2.60	Ортоором- бическая	$a = 9.3$, $b = 9.22$, $c = 10.61 \text{ \AA}$	430—480	$\beta\text{-CaS}$, иногда $\gamma\text{-CaS}$
$4\text{CaO} \cdot ? \cdot \text{H}_2\text{O}$ (рутазит) <i>l'</i>	$\text{Ca}_4(\text{Si}_2\text{O}_7)(\text{OH})_2$	Пластини- ческие призмы	$N_g = 1.614$, $N_m = 1.640$	2.65	Моноклини- ческая	$a = 7.92$, $b = 13.35$, $c = 10.3 \text{ \AA}$, $\alpha = 102.22^\circ$	—	—
$3\text{CaO} \cdot \text{SiO}_2 \cdot \text{H}_2\text{O}$ (деляйт, фаза Y) <i>m'</i>	$\text{Ca}_3[\text{SiO}_4][\text{Si}_2\text{O}_7](\text{OH})_2$	Пластини- ческие призмы	$N_g = 1.631$, $N_m = 1.625$, $N_p = 1.639$	2.91— 2.95	Триплит <i>T</i> или	$a = 5.55$, $b = 10.5$, $c = 2.0 \text{ \AA}$, $\alpha = 102.22^\circ$, $\beta = 95.45^\circ$, $\gamma = 95.45^\circ$	700, 850	$\beta\text{-CaS}$
$6\text{CaO} \cdot 2\text{SiO}_2 \cdot 2\text{H}_2\text{O}$ (ортооромбический диросиликат) <i>n'</i>	$\text{Ca}_6\text{Si}_2\text{O}_7(\text{OH})_2 \cdot$ $\cdot 2[\text{Si}_2\text{O}_7](\text{OH})_2 \cdot \text{H}_2\text{O}$	Ортоором- бическая	$N_g = 1.597$, $N_m = 1.593$	2.51	Ромбиче- ская	$a = 10.2$, $b = 10.3$, $c = 7.03 \text{ \AA}$	420—550,	$\gamma\text{-CaS}$ и $\beta\text{-CaS}$

Key:

- a. Compound
- b. Structural formula
- c. Crystal appearance
- d. Indices of refraction
- e. Density, g/cm³
- f. Crystal system
- g. Unit cell parameters
- h. Dehydration temperatures, °C
- i. Crystalline phases formed by decomposition
- m. Triclinic
- r. Monoclinic
- y. Orthorhombic

- 1. Fibers
- gg Plates
- aa Wollastonite
- g' Sulcunite
- h' Bar-shaped crystalline granules
- i' Rosenhahnite
- j' Lath-shaped crystals
- k' Afwillite
- l' Phase Z rankinite
- m' Dicalcium silicate hydrate
- n' Sometimes
- c' Rustamite
- p' Dellaite, phase Y
- q' Tricalcium hydrosilicate
- r' Needles
- s' Rhombic

TABLE 2
INFRARED ABSORPTION SPECTRA
(FREQUENCY MAXIMA, cm^{-1})

Таблица 2						
Инфракрасные спектры поглощения (частоты максимумов, cm^{-1})						
a. Хонотлит	б. Гиллебрандит		в. 11 Å-тоберморит синтетический		f. Афвиллит синтетический	g. α -Гидрот синтетический
природный г. Южная Осетия)	синтети- ческий	e. природный (Мексика, Веларденса)	синтети- ческий	11 Å-тобер- морит синте- тический	Афвиллит синтети- ческий	α -Гидрот синтети- ческий
3608	3607	3638	3626	3365	3340	3532
1197	1198	3563	3534	1635	3150	2844
1138	1137	1150	1154	1206	2770	2580
1063	1078	1074	1076	1173	2412	2459
1000	1000	1031	1025	1140	1658	1278
971	973	1017	990	1075	1623	998
925	927	987	968	1027	1320	931
708	710	969	934	971	1280	940
670	571	930	903	930	1100	812
634	633	898	840	897	938	756
610	609	854	722	747	963	746
535	534	762	646	675	912	719
493	493	64	590	633	883	709
478	476	570	540	610	803	675
462	456	530	500	524	813	513
455	415	510	468	478	781	468
410		468		450	673	424
					632	400
					512	386
					481	

Key:

- a. Xonotlite
- b. Hillebrandite
- c. Natural (South Ossetiya)
- d. Synthetic
- e. Natural (Velardena, Mexico)
- f. 11 Å synthetic tobermorite
- g. Synthetic afwillite
- h. Synthetic α hydrate

Roy and Harker [20] presented a series of experimental phase diagrams of the system, describing a number of phases which were found by successive increase in temperature, for all values of $\text{CaO}:\text{SiO}_2$ ratio (Fig. 369). The authors, however, indicate that hardly all the diagrams presented reflect a stable equilibrium.

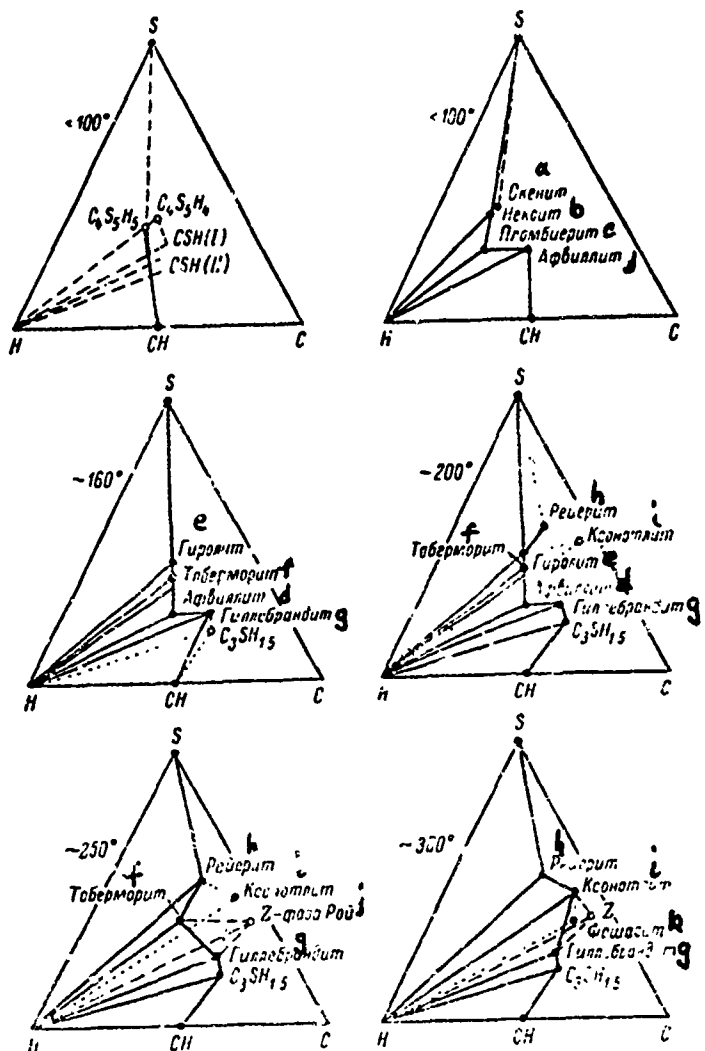


Fig. 369. $\text{CaO} - \text{SiO}_2 - \text{H}_2\text{O}$ system, represented in the form of coexisting phase triangles for various temperatures at the saturated vapor pressure (dotted lines) and at a pressure of about 1064 kgf/cm^2 (solid lines); dashed lines, conjectural equilibria (from Roy and Harker): CaC. calcium chondrodite.

Key:

- | | |
|----------------|------------------|
| a. Okenite | f. Tobermorite |
| b. Nekoite | g. Hillebrandite |
| c. Plumbierite | h. Reyerite |
| d. Afwillite | i. Xonotlite |
| e. Gyrolite | j. Rey Z phase |
| | k. Foshagite |

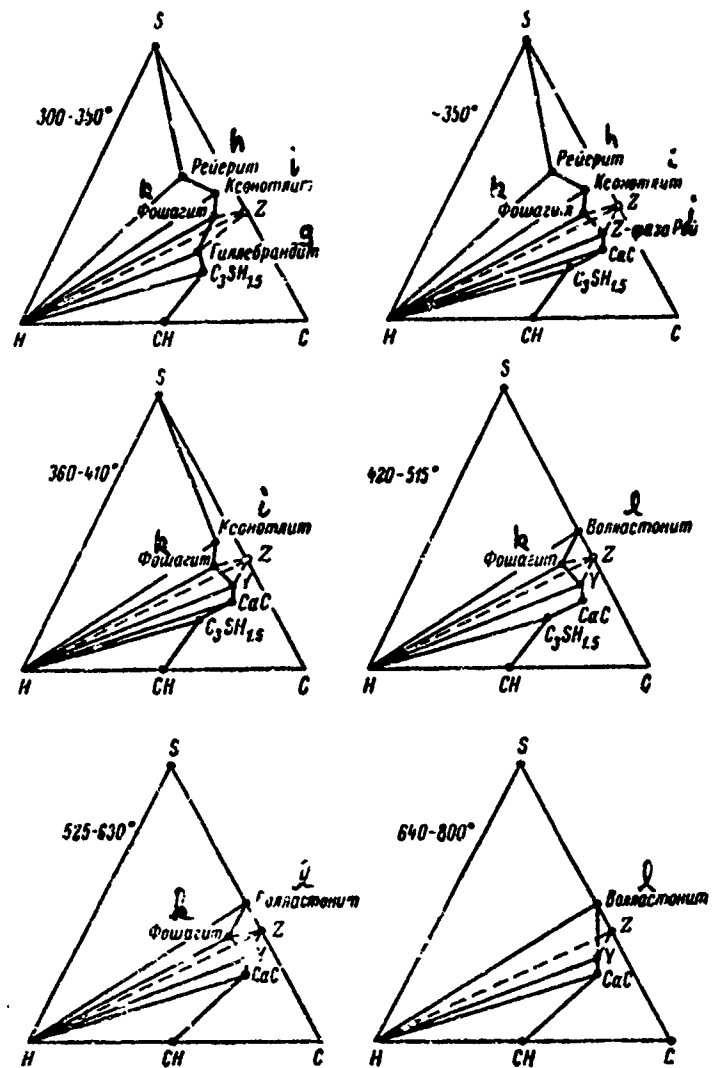


Fig. 369. (continued)

1. Wollastonite

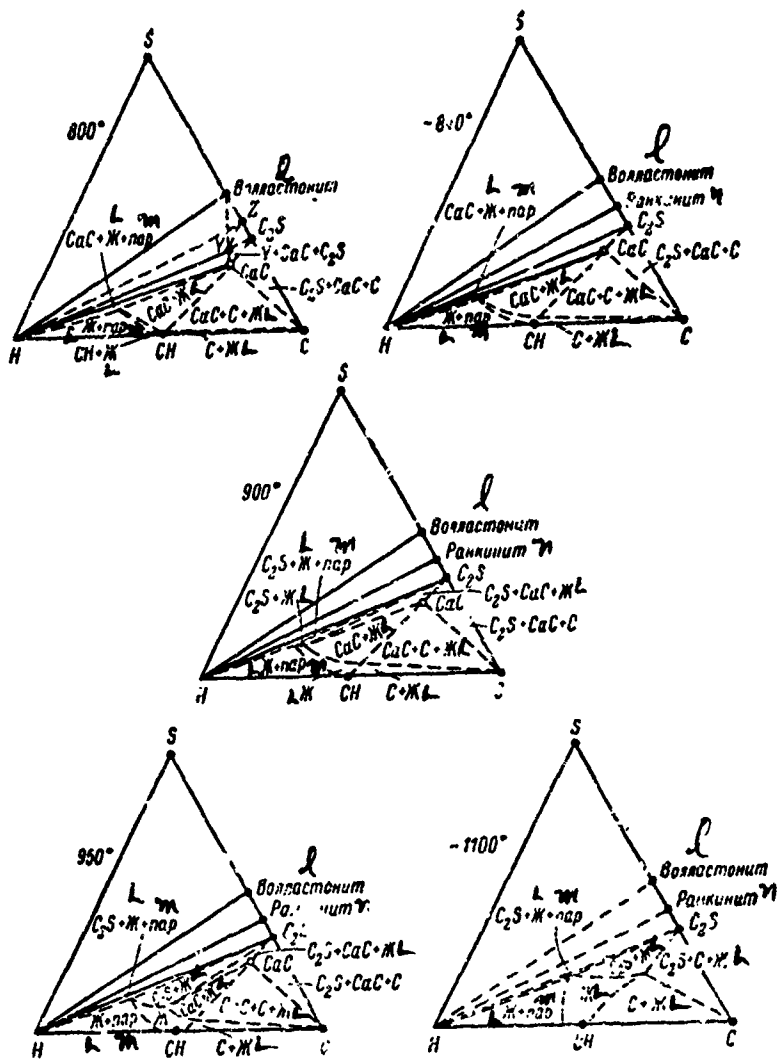


Fig. 369. (continued)

m. Vapor
n. Rankinite

Taylor [70] proposed a schematic diagram, on which the compounds of the system were plotted (Fig. 370). A diagram according to Taylor, showing the conditions for formation of the well-identified calcium hydrosilicates, is presented in Fig. 371. Anhydrous compounds form at temperatures above line ab; between line ab and cd, products form in which water is present, mainly in the form of hydroxyl ions; below line cd, the compounds formed contain H groups, characterizing the acid function; they can also contain molecular water and hydroxyl ions.

A composite phase diagram and their own data are presented by Butt and Timashev and colleagues [12] (Fig. 372). P-t equilibrium curves for certain phase transitions in the $\text{CaO} - \text{SiO}_2 - \text{H}_2\text{O}$ system, according to Buckner, D. Roy and R. Roy [32], are shown in Fig. 373.

Data from study of equilibria in the two-component system $\text{CaO} - \text{H}_2\text{O}$ and $\text{SiO}_2 - \text{H}_2\text{O}$ are necessary for study of the three-component system $\text{CaO} - \text{SiO}_2 - \text{H}_2\text{O}$.

$\text{CaO} - \text{H}_2\text{O}$. A phase diagram of the $\text{CaO} - \text{H}_2\text{O}$ system, at a pressure of 1000 bar, according to Wyllie and Tuttle [77], is presented in Fig. 374. Under these conditions, portlandite melts congruently at $835 \pm 5^\circ$. Two fields, representing the monovariant equilibria $\text{CaO} + \text{liquid} + \text{Ca}(\text{OH})_2$ and $\text{Ca}(\text{OH})_2 + \text{liquid} + \text{vapor}$, intersect the isobaric profile along invariant isobaric lines, at temperatures of 835 and 815° , respectively. The position of the $\text{CaO} - \text{Ca}(\text{OH})_2$ eutectic is very close to the composition of $\text{Ca}(\text{OH})_2$.

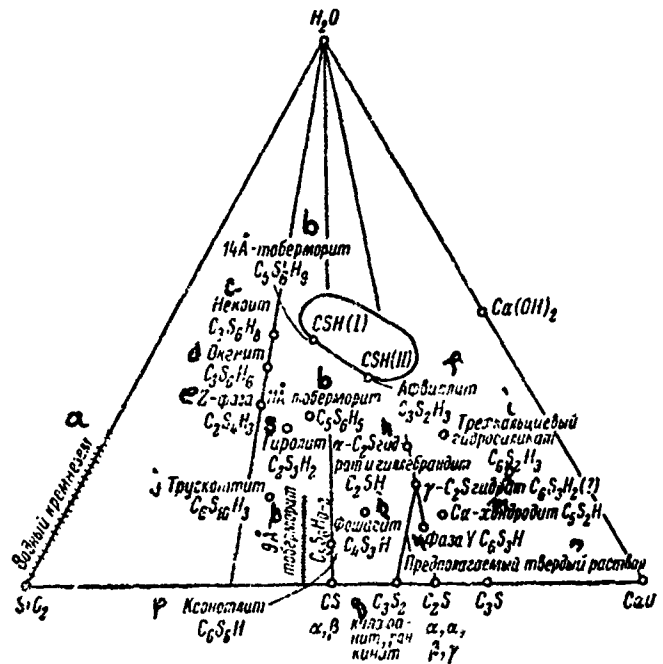


Fig. 370. Compounds in $\text{CaO} - \text{SiO}_2 - \text{H}_2\text{O}$ system (diagram from Taylor).

Key:

- | | |
|---|-------------------------------|
| a. Hydrated silica | j. Truscottite |
| b. Tobermorite | k. Foshagite |
| c. Nekoite | l. Hydrate |
| d. Okenite | m. Chondrodite |
| e. Z-phase | n. Phase Y |
| f. Afwillite | o. Conjectural solid solution |
| g. Hydrolite | p. Xonotlite |
| h. α - C_2S hydrate and
hillebrandite | q. Kilchoanite, rankinite |
| i. Tricalcium hydrosilicate | |

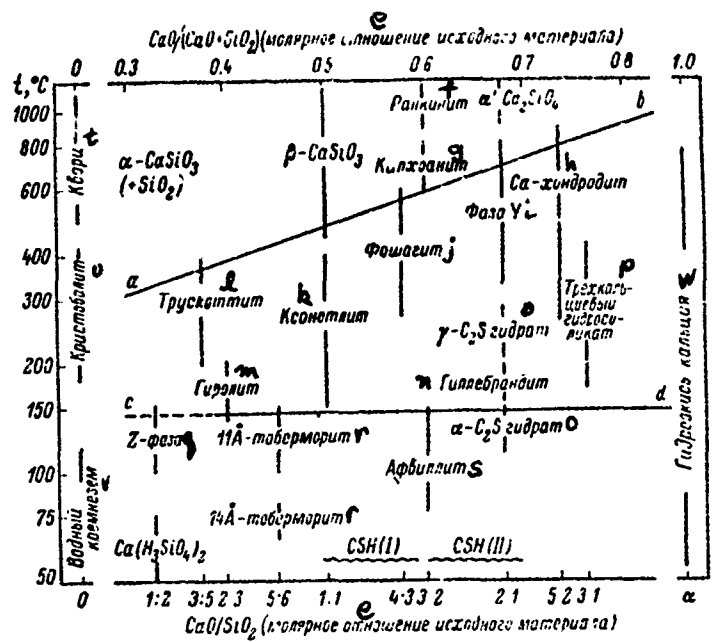


Fig. 371. Diagram indicating approximate conditions for formation of silicates and hydrosilicates of calcium under hydrothermal conditions (from Taylor): vertical lines Ca/Si molar ratio in compounds; extent of each line indicates the temperature region, in which a given compound forms; wavy lines, varying composition.

Key:

- | | |
|------------------------------------|-----------------------------|
| e. Molar ratio of initial material | n. Hillebrandite |
| f. Rankinite | o. Hydrate |
| g. Kilgoanite, rankinite | p. Tricalcium hydrosilicate |
| h. Chondrodite | q. Z-phase |
| i. Phase Y | r. Tobermorite |
| j. Foshagite | s. Afwillite |
| k. Xonotlite | t. Quartz |
| l. Truscottite | u. Cristobalite |
| m. Gyrolite | v. Hydrated silica |
| | w. Calcium hydroxide |

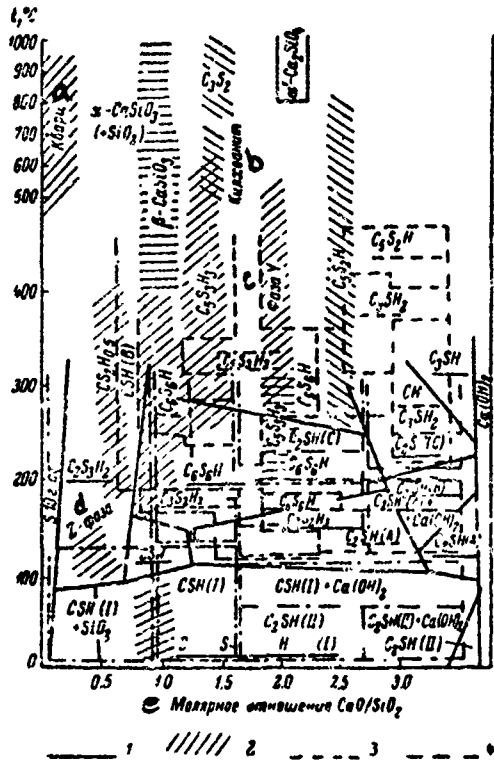


Fig. 372. Approximate crystallization stability regions in $\text{CaO} - \text{SiO}_2 - \text{H}_2\text{O}$ system; 1. from Bessey (see [15]); 2. from Taylor; 3. from Bernal; 4. from Grineva, Butt, Timashev and others.

Key:

- Quartz
- Kilchoanite
- Phase Y
- Phase Z
- $\text{CaO} / \text{SiO}_2$ molar ratio

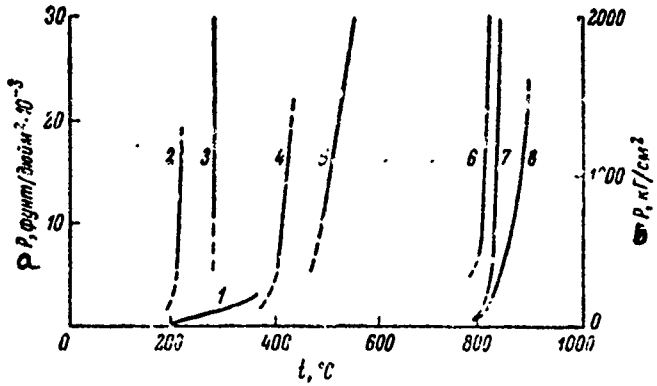


Fig. 373. P-t equilibrium curves for certain phase transitions in $\text{CaO} - \text{SiO}_2 - \text{H}_2\text{O}$ system (from Bunker, D. Roy and R. Roy); 1. saturated water vapor pressure curve; 2. afwillite = kilchoanite + H_2O ; 3. 11 A tobermorite = xonotlite + H_2O + truscottite; 4. xonotlite = wollastonite + H_2O ; 5. tricalcium hydrosilicate = calcium chondrotite + $\text{Ca(OH)}_2 + \text{H}_2\text{O}$; 6. Phase Y = α' $\text{C}_2\text{S} + \text{H}_2\text{O}$; 7. kilchoanite (hydrated) = rankinite + H_2O ; 8. calcium chondrotite = α' $\text{C}_2\text{S} + \text{CaO} + \text{H}_2\text{O}$.

Key:

- a. Pressure P , $\text{psi} \cdot 10^{-3}$
- b. Pressure, P , kgf/cm^2

A P-t projection of the monovariant equilibrium [77] is depicted in Fig. 375. At pressures of less than 1000 bar, two monovariant curves are found, representing the equilibria $\text{CaO} + \text{Ca(OH)}_2 \rightleftharpoons$ vapor and $\text{CaO} + \text{liquid} \rightleftharpoons$ vapor. At invariant point E, at which four P-t curves intersect, four phases coexist: $\text{CaO} + \text{Ca(OH)}_2 + \text{liquid} + \text{vapor}$.

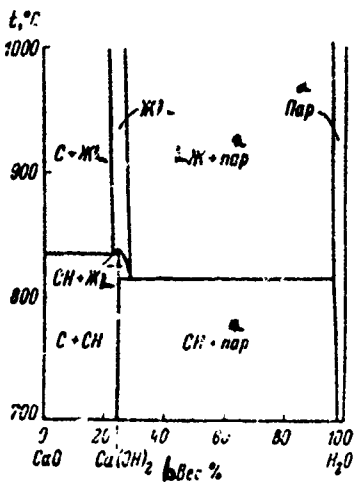


Fig. 374. Phase diagram of CaO -- H₂O system for pressure of 1000 bar (from Wyllie and Tuttle).

Key:

- a. Vapor
- b. Weight %

The Ca(OH)₂ -- H₂O system, at 21° and high pressure, studied by Weir [75], is presented in Fig. 376.

Majumdar and Roy [53] have studied the dissociation of Ca(OH)₂ at various water vapor pressures. An equilibrium curve of the reaction Ca(OH)₂ ⇌ CaO + H₂O, at high water vapor pressures, is presented in Fig. 377. According to Majumdar and Roy, the dissociation temperature of Ca(OH)₂ is 740° at a pressure of 1000 bar. The data of Johnston [15] on the dependence of the temperature of the dissociation Ca(OH)₂ ⇌ CaO + H₂O on pressure are valid at the present time.

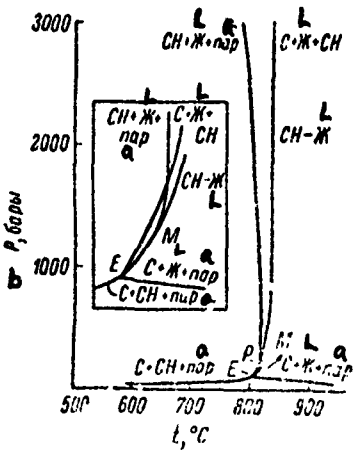


Fig. 375. P-t projection of mono-variant equilibrium in $\text{CaO} - \text{H}_2\text{O}$ system (from Wyllie and Tuttle): Four monovariant curves meet at invariant point E; curve CH-L extends from singular point M and fuses with curve $\text{C} + \text{L} + \text{CH}$.

Key:

- a. Vapor
- b. P, bar

The $\text{Ca}(\text{OH})_2 \rightleftharpoons \text{CaO} + \text{H}_2\text{O}$ equilibrium has been studied by Pistorius [60], at pressures up to 20,000 atm. Pistorius showed that, at pressures over 7000 atm, the dissociation temperature is almost independent of pressure and is close to 790° .

The only compound in the $\text{Ca}(\text{OH})_2$ system (portlandite) has hexagonal symmetry, and it has the appearance of thin, six-sided plates [1, 11, 63, 64].

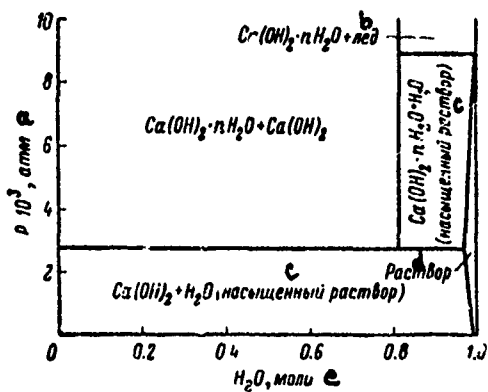


Fig. 376. Hypothetical "pressure-composition" diagram of $\text{Ca}(\text{OH})_2$ -- H_2O system at 21° (from Weir).

Key:

- | | |
|-----------------------|-------------|
| a. atm | d. Solution |
| b. Ice | e. Moles |
| c. Saturated solution | |

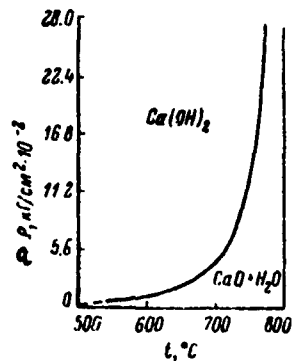


Fig. 377. Equilibrium curve of reaction $\text{Ca}(\text{OH})_2 \rightleftharpoons \text{CaO} + \text{H}_2\text{O}$ at high water vapor pressures (from Majumdar and Roy).

Key:

- a. P , $\text{kgf}/\text{cm}^2 \cdot 10^{-2}$

and others]. The crystal system is hexagonal. The unit cell parameters: $a = 3.585$, $c = 4.895 \text{ kX}$. The indices of refraction are $N_g = 1.574$ and $N_p = 1.547$. Uniaxial, negative. Density 2.23 g/cm^3 . Tippmann refers to crystallization of Ca(OH)_2 , in the form of needles or fibers [73].

Weir [75] found, in addition to Ca(OH)_2 , a crystalline hydrate of the composition $\text{Ca(OH)}_2 \cdot n\text{H}_2\text{O}$, where n is not less than 4 and not over 6. Ca(OH)_2 also has been found in the form of an amorphous variety, which usually is formed by hydration of calcium silicates and portland cement [8].

Many works have been devoted to investigation of the CaO slaking process [10, 11, 13, 14, 19, 28, 29, 31, 38, 44, 52, 54, 55, 59, 65, 76, 78].

Solubility of Ca(OH)_2 in water has been studied. Hedin [40-42] obtained solubility data in the temperature range from 24 to 57° , Bassett [30], in the $0-150^\circ$ temperature range and Peppler and Wells [57], up to 250° .

Segalova, Kontorovich and Rebinder [25] determined the solubility in water at 21.6° of calcium oxide proper, by means of incorporating additives of sulfite-alcohol residues, glucose, preventing the rapid growth of Ca(OH)_2 nuclei.

Fratini [37], Hedin [40], D'Ans and Eick [34], Budnikov [9] and others have studied the solubility of Ca(OH)_2 in caustic alkali solutions (NaOH and KOH) at various temperatures, in solutions of chloride salts, in a solution of gypsum at 20° and in sugar solution.

Ratinov and Grigoryan [18] have determined the coefficient of diffusion of Ca(OH)_2 in solution at temperatures from 28 to 85° .

Ringqvist [61] has studied the electrical conductivity of Ca(OH)_2 solutions of various concentrations at $0-100^\circ$.

SiO_2 -- H_2O . A schematic diagram of the phase relationships of the SiO_2 -- H_2O system were first plotted by Smits [66] in 1930, although Fenner [36] had already begun study of this system in 1913.

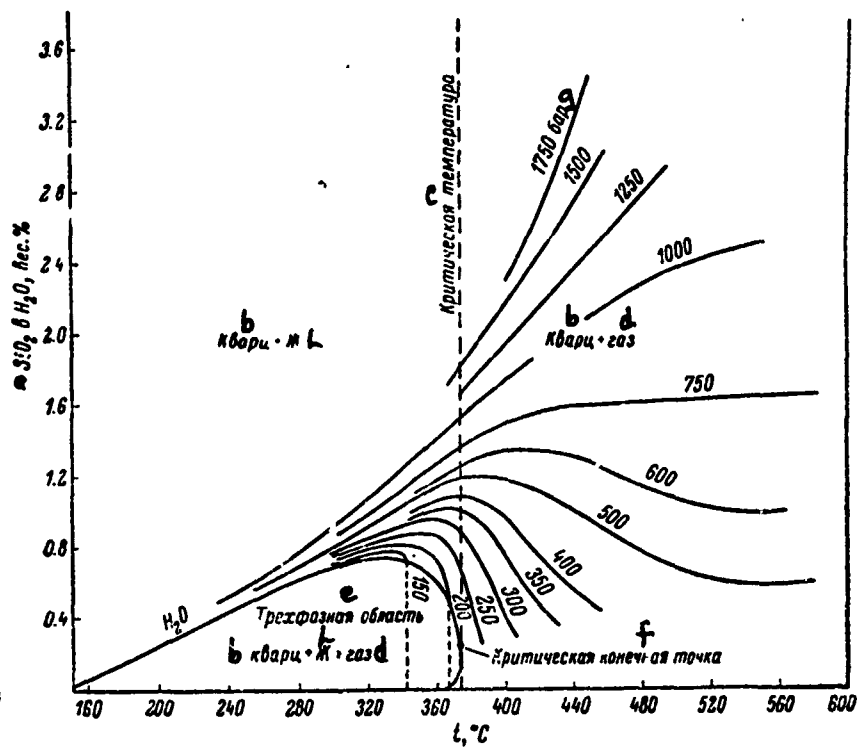
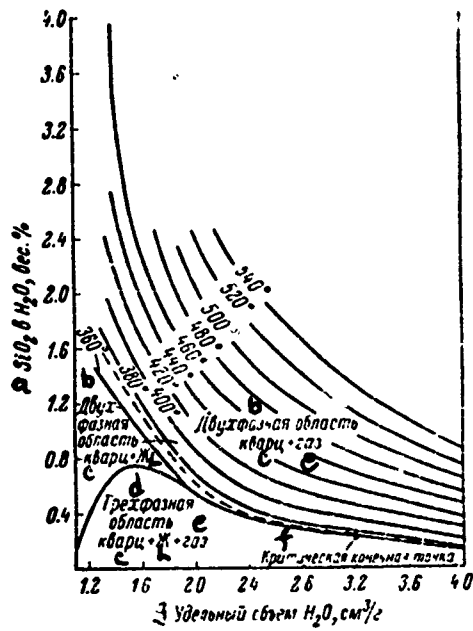


Fig. 378. SiO_2 -- H_2O system, isobaric quartz solubility curves (from Kennedy).

Key:

- a. SiO_2 in H_2O , weight %
- b. Quartz
- c. Critical temperature
- d. Gas
- e. Three-phase region
- f. Critical final point
- g. Bar



Reproduced from
best available copy.

Fig. 379. SiO_2 -- H_2O system, isothermal quartz solubility curves (from Kennedy).

Key:

- a. SiO_2 in H_2O , weight %
- b. Two-phase region
- c. Quartz
- d. Three-phase region
- e. Gas
- f. Critical final point
- g. Specific volume H_2O , cm^3/g

Kennedy [47-49] has studied the system over a broad range of temperatures and pressures. The SiO_2 -- H_2O system is depicted in Fig. 378, in the form of isobars of solubility of quartz in water, from the experimental data of Kennedy. The pressure in bars is indicated on each curve. Quartz solubility isotherms, according to Kennedy, are presented in Fig. 379 and, in Fig. 380, a P-t diagram of a part of the silica-water system, from Tuttle and England [74].

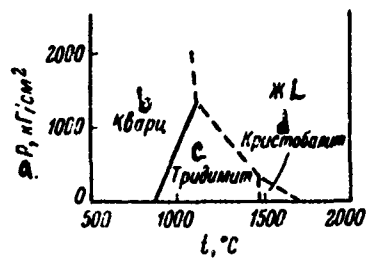


Fig. 380. SiO_2 -- H_2O system,
P-t diagram for silica-rich region
of system (from Tuttle and England).

Key:

- | | |
|-----------------------------------|-----------------|
| a. P , kgf/cm^2 | c. Tridymite |
| b. Quartz | d. Cristobalite |

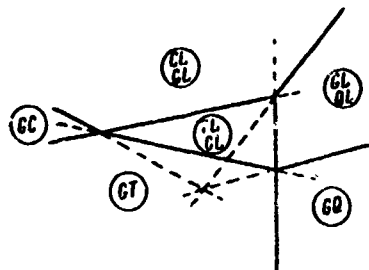


Fig. 381. Theoretical arrangement of P-t diagram
of SiO_2 -- H_2O system (from Ostrovskiy and colleagues):
in circles divariant phase combinations, stable in the
corresponding fields of the diagram; T. tridymite,
C. cristobalite, Q. quartz, L. melt, G. vapor.

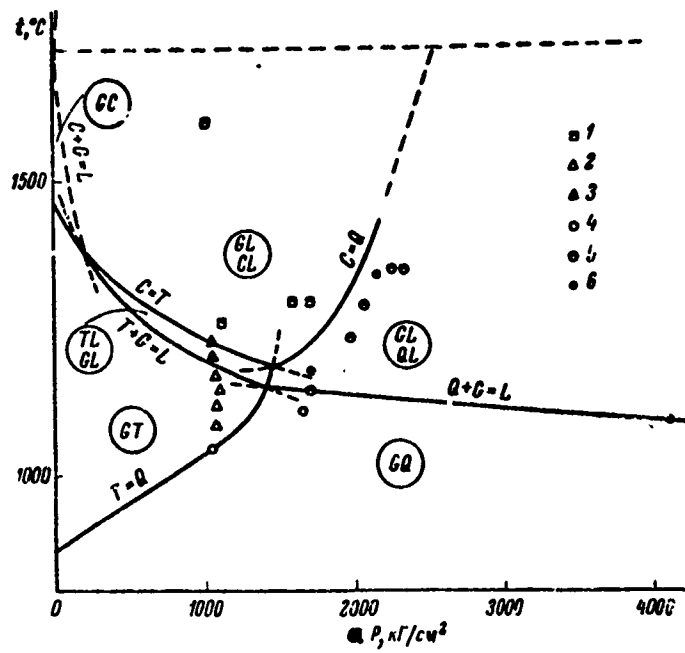


Fig. 382. Experimental P-t diagram of part of $\text{SiO}_2 - \text{H}_2\text{O}$ system (Ostrovskiy and colleagues): 1. cristobalite + melt; 2. tridymite; 3. tridymite + melt; 4. quartz; quartz + melt; 6. melt; remaining designations same as in Fig. 381.

Key:

a. $P, \text{kgf/cm}^2$

Ostrovskiy and colleagues [16, 17] have presented a theoretical (Fig. 381) and an experimental (Fig. 382) P-t diagram of part of the $\text{SiO}_2 - \text{H}_2\text{O}$ system. The fact that the tridymite -- cristobalite transformation curve has a negative slope and bounds a narrow field, in which coexistence of tridymite and melt is possible, from the top attracts attention. Of the invariant points,

in which cristobalite, tridymite and quartz are in equilibrium, the cristobalite -- quartz equilibrium curve stands out; its position was determined experimentally up to a temperature of 1360° and it was extrapolated further to the melting temperature of silica. The diagram shows that neither cristobalite nor tridymite are stable at high pressure. Thus, according to the data of Ostrovskiy, the cristobalite + tridymite + quartz invariant point lies at 1190° and 1430 kgf/cm^2 . According to the thermodynamic calculations of Mosesman and Pitzer [56], it is assumed to be approximately at 1420° and 660 atm. The position of the equilibrium of quartz with the melt and vapor on the Ostrovskiy diagram passes 15° higher than Stewart gives [68]: 1130° at 2000 bar and 1065° at 5000 bar.

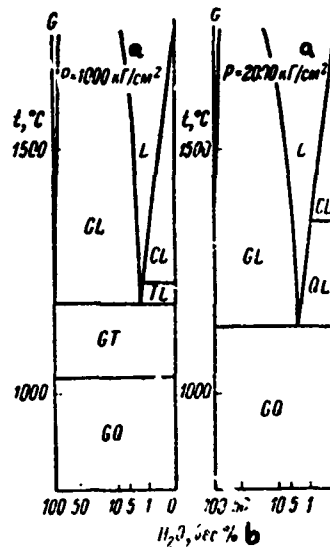


Fig. 383. Schematic representation of "pressure-temperature-composition" section of diagram of SiO_2 -- H_2O system at 1000 and 2000 kgf/cm^2 (from Ostrovskiy and colleagues); designations same as in Fig. 381.
Key:

a. kgf/cm^2

b. Weight %

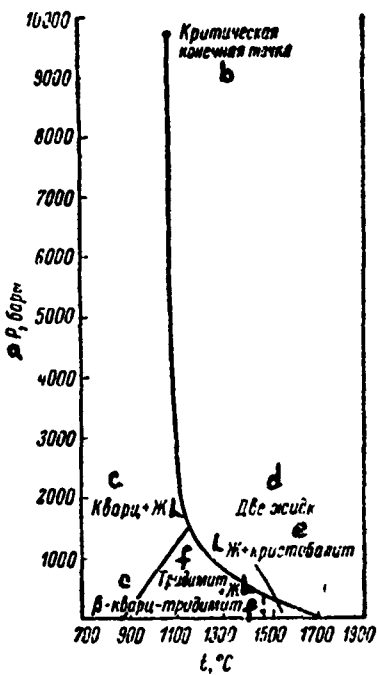


Fig. 384. P-t projection of monovariant equilibrium in SiO_2 -- H_2O system (from Kennedy).

Key:

- a. P bar
- b. Critical final point
- c. Quartz
- d. Two liquids
- e. Cristobalite
- f. Tridymite

Ostrovskiy has plotted schematic isobaric sections for pressures of 1000 and 2000 kgf/cm² (Fig. 383).

A P-t projection of the phase diagram of the SiO_2 -- H_2O system, obtained by Kennedy [48, 49], is presented in Fig. 384. As is evident from the

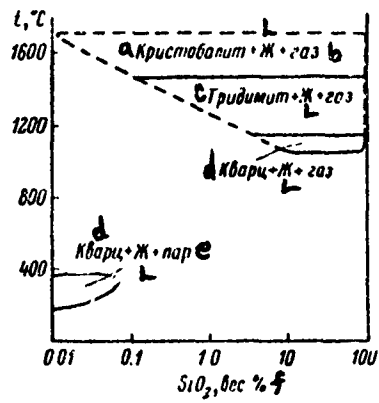


Fig. 385. Phase diagram of SiO_2 -- H_2O system, upper and lower three-phase regions (from Kennedy).

Key:

- | | |
|-----------------|-------------|
| a. Cristobalite | d. Quartz |
| b. Gas | e. Vapor |
| c. Tridymite | f. Weight % |

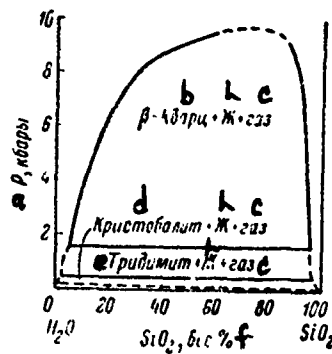


Fig. 386. Phase diagram of SiO_2 -- H_2O system, compositions along upper three-phase boundary curve (from Kennedy).

Key:

- | | |
|------------|-----------------|
| a. P, kbar | d. Cristobalite |
| b. Quartz | e. Tridymite |
| c. Gas | f. Weight % |

figure, the results of Kennedy mainly coincide with the data of Ostrovskiy.

The SiO_2 -- H_2O system according to Kennedy [49], showing the upper and lower three-phase region, is depicted in Fig. 385. The compositions along the upper three-phase boundary curve, according to Kennedy [49] are shown on the phase diagram in Fig. 386.

BIBLIOGRAPHY

1. Andriyevskiy, A. I., V. A. Tikhonov, L. G. Shpynova, I. D. Nabitovich, Stroit. mater., 3, 1959, p. 33.
2. Babushkin, V. I., G. M. Matveyev, O. P. Mcchedlov-Petrosyan, Termodinamika silikatov [Thermodynamics of Silicates], Gosstroyizdat Press, Moscow, 1962.
3. Bazhenov, N. M., A. I. Kol'tsov, N. P. Kirpichnikova, Ya. I. Ryskin, G. P. Stavitskaya, A. I. Boykova, N. A. Toropov, Izv. AN SSSR, ser. khim., 3, 1964, p. 409.
4. Belov, N. V., Kristallokhimiya silikatov s krupnymi kationami [Crystal-chemistry of Silicates with Large Cations], AN SSSR Press, Moscow, 1961.
5. Berkovich, T. M., D. M. Kheyker, O. I. Gracheva, L. S. Zevin, N. I. Kupreyeva, DAN SSSR, 120, 4, 1958, p. 853.
6. Bernal, D., in the collection Tretiy mezhdunarodnyy kongress po khimii tsementa [Third International Congress on Cement Chemistry], Gosstroyizdat Press, Moscow, 1958, p. 137.
7. Bozhenov, P. I., G. F. Suvorova, Obrabotka stroitel'nykh materialov parom vysokogo davleniya [Treatment of Structural Materials with High Pressure Steam], Gosstroyizdat Press, Moscow, 1961.
8. Brunauer, S., S. A. Grinberg, in the collection Chetvertyy mezhdunarodnyy kongress po khimii tsementa [Fourth International Congress on Cement Chemistry], Stroyizdat Press, Moscow, 1964, p. 123.
9. Budnikov, P. P., M. A. Matveyeva, S. P. Yurchik, DAN SSSR, 84, 5, 1952, p. 1021.
10. Budnikov, P. P., N. V. Pertovykh, Mineral'noye tsyr'ye, 2, 1961, p. 164.
11. Butt, Yu. M., L. N. Rashkovich, Tverdeniye vyazhushchikh pri povyshennykh temperaturakh [Hardening of Binders at Elevated Temperatures], Stroyizdat Press, Moscow, 1965.

12. Grineva, M. K., Yu. M. Butt, V. V. Timashev, V. S. Bakshutov, V. V. Plyukhin, Trudy MXTI im. D.I. Mendeleyeva, Issue 73, "Silicates," 1969, p. 218.
13. Kontorovich, S. I., Ye. Ye. Segalova, P. A. Rebinder, DAN SSSR, 129, 4, 1959, p. 847.
14. Kontorovich, S. I., Ye. Ye. Segalova, P. A. Rebinder, Kolloidn. zhurn., 25, 5, 1963, p. 561.
15. Krzheminskiy, S. A., L. A. Kroychuk, N. K. Sudina, Sb. trudov Vses. nauchno-issled. inst. stroymaterialov i konstruktsiy, 14(42), 1969, p. 3.
16. Ostrovskiy, I. A., G. P. Mishina, V. M. Povilaytis, DAN SSSR, 126, 3, 1959, p. 645.
17. Ostrovskiy, I. A., G. P. Mishina, V. M. Povilaytis, Izv. AN SSSR, ser. geol., 1, 1957, p. 116.
18. Ratinov, V. B., V. A. Grigoryan, Stroit. mater., 3, 1960, p. 32.
19. Rashkovich, L. N., Ibid., 6, 1962, p. 31.
20. Roy, D. M., R. I. Harker, in the collection Chetvertyy mezhdunarodnyy kongress po khimii tsementa [Fourth International Congress on Cement Chemistry], Stroyizdat Press, Moscow, 1964, p. 193.
21. Ryskin, Ya. I., G. P. Stavitskaya, Optika i spektroskopiya, 8, 5, 1960, p. 606.
22. Ryskin, Ya. I., G. P. Stavitskaya, Izv. AN SSSR, OKhN, 5, 1964, p. 793.
23. Ryskin, Ya. I., G. P. Stavitskaya, S. P. Zhdanov, N. A. Mitropol'skiy, Izv. AN SSSR, Neorg. mater., 5, 5, 1969, p. 954.
24. Ryskin, Ya. I., G. P. Stavitskaya, N. A. Mitropol'skiy, Ibid., 3, p. 577.
25. Segalova, Ye. Ye., S. I. Kontorovich, P. A. Rebinder, DAN SSSR, 123, 3, 1958, p. 509.
26. Taylor, H. F., in the collection Chetvertyy mezhdunarodnyy kongress po khimii tsementa [Fourth International Congress on Cement Chemistry], Stroyizdat Press, Moscow, 1964, p. 159.
27. Khant, Ch. M., Ibid., p. 240.
28. Adams, E. W., Ind. Eng. Chem., 19, 5, 1927, p. 589.
29. Backman, A., Zement -- Kalk -- Gips, 9, 6, 1956, p. 262.

30. Bassett, H., J. Chem. Soc., 1, Sept. 1934, p. 1270.
31. Birss, F., T. Thorvaldson, Can. J. Chem., 33, 5, 1955, p. 870.
32. Buckner, E.A., D.M. Roy, R. Roy, Amer. J. Sci., 258, 2, 1960, p. 132.
33. Chalmers, R.A., A.W. Nicol, H.F.W. Taylor, Mineral. Magaz., 33, 256, 1962, p. 70.
34. D'Ans, J., H. Fick, Zement -- Kalk -- Gips, 6, 9, 1953, p. 302.
35. Farmer, V.C., J. Jeevaratnam, K. Speakman, H.F.W. Taylor, Symp. on Structure of Portland Cement Paste and Concrete, Washington, 1966, p. 291.
36. Fenner, K.N., Amer. J. Sci., 4, 36, 1913, p. 331.
37. Fratini, N., Ann. di chim. applicata, 39, 10-11, 1949, p. 616.
38. Glasson, D.R., J. Appl. Chem., 8, 12, 1958, p. 793; 10, 1, 1960, p. 38.
39. Grudemo, A. An electronographic study of the morphology and crystallization properties of calcium silicate hydrates. Handlingar 26, Stockholm, 1955.
40. Hedin, R., Chemical process in the hardening of portland cement. Handlingar 3, Stockholm, 1945.
41. Hedin, R., Saturation concentration of calcium hydroxide, Handlingar, 27, Stockholm, 1955.
42. Hedin, R., Processes of diffusion, solution and crystallisation in system Ca(OH)₂ -- H₂O, Handlingar, 33, Stockholm, 1962.
43. Heller, L., H.F.W. Taylor, Crystallographic data for the calcium silicates, London, 1956.
44. Holms, M.E., G.J. Fink, F.C. Mathers, Chem. a. Metall Eng., 27, 24, 1922, p. 1212.
45. Johnston, J., Zs. phys. Chem., 62, 3, 1908, p. 330.
46. Kloysek, G., R. Roy, J. Amer. Ceram. Soc., 40, 7, 1957, p. 236.
47. Kennedy, G.C., Econ. Geol., 45, 7, 1950, p. 644.
48. Kennedy, G.C., in: Progress in Very High Pressure Res., New York, 1960, pp. 304,314.
49. Kennedy, G.C., G.J. Wasserburg, H.C. Heard, R.C. Newton, Amer. J. Sci., 260, 7, 1962, p. 501.

50. Kondo, R., Proc. 5th Int. Symp. on the Chem. of Cement, pt. II, Tokyo, 1969, p. 203.
51. Kullerud, G., Norsk. Geol. Tidsskrift, 33, 3-4, 1954, p. 197.
52. Kurdowski, W., Cement -- Wapno -- Gips, 11, 9, 1955, p. 196.
53. Majumdar, A.J., R. Roy, J. Amer. Ceram. Soc., 39, 12, 1956, p. 434.
54. Mikhail, R. Sh., J. Phys. Chem., 67, 10, 1963, p. 2050.
55. Miller, T. C., A study of the reaction between calcium oxide and water, Washington, 1960.
56. Mosesman, M.A., K.S. Pitzer, J. Amer. Chem. Soc., 63, 9, 1941, p. 2348.
57. Peppler, R.B., L.S. Wells, J. Res. Nat. Bur. Stand., 52, 2, 1954, p. 75.
58. Petch, H.E., N. Sheppard, H.D. Megaw, Acta crystallogr., 9, 1, 1956, p. 29.
59. Pischinger, E., S. Kaminski, Cement -- Wapno -- Gips, 18, 4, 1961, p. 73.
60. Pistorius, C.W.F.T., Amer. J. Sci., 261, 1, 1963, p. 79.
61. Ringqvist, G., Concentration of pure calcium hydroxide solution as a function of electrolytic conductivity in the temperature range from 0 to 100° C., Handlingar No. 19, Stockholm, 1955.
62. Roy, D.M., Amer. Mineralogist, 43, 11/12, 1958, p. 1009.
63. Schimmel, G., Zement -- Kalk -- Gips, 10, 4, 1957, p. 134.
64. Schimmel, G., Zement -- Kalk -- Gips, 11, 2, 1958, p. 46.
65. Sersale, R., Ind. ital. cemento, 31, 11, 1961.
66. Smits, A., Rec. trav. chim., Pays-Bas, 49, 9/10, 1930, p. 962.
67. Spangenberg, K., Tagungsber. d. Zement Industrie, 4, 1951, p. 102.
68. Stewart, D.B., Carnegie Inst. Washington Year Book, 56, 1957.
69. Taylor, H.F.W. (ed.), The chemistry of cements, London, New York, 1964.
70. Taylor, H.F.W., Proc. 7th Conf. Silicate Industry, Budapest, 1965, p. 199.

71. Taylor, H.F.W., Proc. 5th Int. Symp. on the Chem. of Cement, pt. II, Tokyo, 1, 1969.
72. Taylor, H.F.W., G.E. Bessey, Mag. Concrete Res., 2, 4, 1950, p. 15.
73. Tippmann, F.F., Zement, 19, 52, 1225, 1930; 20, 34, 1931.
74. Tuttle, O.F., J.L. England, Bull. Geol. Soc. Amer., 66, 1, 1955, p. 150.
75. Weir, C.E., J. Res. Nat. Bur. Stand., 54, 1, 1955, p. 40.
76. Wuhrer, J., Zement -- Kalk -- Gips, 6, 10, 1953, p. 354.
77. Wyllie, P.J., O.F. Tuttle, J. Amer. Ceram. Soc., 42, 9, 1959, p. 449.
78. Zander van H., Zement -- Kalk -- Gips, 11, 2, 1958, p. 41.



The system has been studied by Roy and Mumpton [5] (Fig. 387). Two zinc hydrosilicates are known, hemimorphite $\text{Zn}_4\text{Si}_2\text{O}_7(\text{OH})_2 \cdot \text{H}_2\text{O}$ and sauconite $\text{Zn}_6(\text{Si}_{8-x}\text{Zn}_x\text{O}_{20})(\text{OH})_4$ [1, 3, 4]. Hemimorphite is in the rhombic crystal system [1], and the unit cell parameters are $a = 8.38$, $b = 10.70$, $c = 5.11$ kX. Density is 3.45 g/cm^3 . The indices of refraction are $N_g = 1.636$, $N_p = 1.614$ and $N_m = 1.317$.

Roy and Mumpton have studied the mutual transitions of sauconite and hemimorphite at pressures up to 40,000 psi. They found that the temperature of the hemimorphite \rightleftharpoons willemite + H_2O reaction varies from 240° at 10,000 psi to 260° at 40,000 psi.

The monovariant P-t curves for the hemimorphite \rightleftharpoons willemite + H_2O reaction, at 100 kbar, according to Pistorius [3], are represented in Fig. 388. Taylor [6] has shown that hemimorphite changes into willemite Zn_2SiO_4 at 700° . The phase relations in the system and dehydration also have been studied by Markham [2].

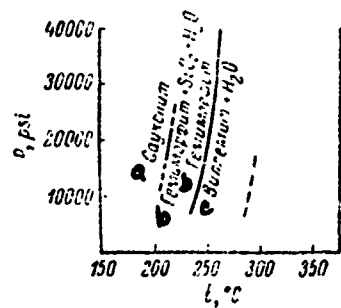


Fig. 387. Monovariant P-t curves of $\text{ZnO} - \text{SiO}_2 - \text{H}_2\text{O}$ system (from Rey and Mumpton).

Key:

- a. Sauconite
- b. Hemimorphite
- c. Willemite

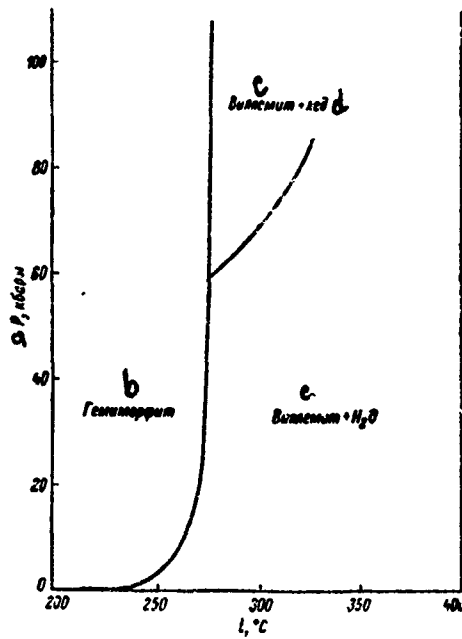


Fig. 388. Monovariant P-t curve for hemimorphite \rightleftharpoons willemitite + water reaction at 100 kbar (from Pistorius).

Key:

- | | |
|-----------------|--------------|
| a. P, kbar | c. Willemite |
| b. Hemimorphite | d. Ice |

BIBLIOGRAPHY

1. Ito, T., J. West, Zs. Kristallogr., 83, 1/2, 1932, p. 1.
2. Markham, N.L., Econ. Geol., 55, 4, 1960, p. 844.
3. Pistorius, C.W.F.T., Neues Jahrb. Mineral., Monatshefte, 2/3, 1963, p. 30.
4. Roy, D.M., R. Roy, Amer. Mineralogist, 39, 11-12, 1954, p. 957.
5. Roy, D.M., F.A. Mumpton, Econ. Geol., 51, 5, 1956, p. 432.
6. Taylor, H.F.W., Amer. Mineralogist, 47, 7-8, 1962, p. 932.



The system has not been studied. Carlson and Wells [1] have synthesized individual compounds under hydrothermal conditions. Powder X-ray photos and differential-thermal analysis curves have been obtained for all phases. The composition of compounds in the system and their crystallo-optical characteristics are presented in the table.

CHARACTERISTICS OF STRONTIUM HYDROSILICATES

α Соединение	N_E	N_M	N_P	β Габитус кристаллов
SrO · 2SiO ₂ · H ₂ O		$N_{M} = 1.574$		Округлые зерна ^c
SrO · SiO ₂ · H ₂ O		$N_{M} = 1.604$		Чешуйки ^d
2SrO · 2SiO ₂ · 3H ₂ O		$N_{M} = 1.60$		Кристаллы неправильной формы
3SrO · 2SiO ₂ · 3H ₂ O	1.614	1.602	1.602	Вытянутые призмы
3SrO · 2SiO ₂ · 4H ₂ O	{ 1.627 1.637	— —	{ 1.595 1.617	} Дендриты ^e
2SrO · SiO ₂ · H ₂ O	1.641	—	1.638	Ламкообразные призмы
3SrO · SiO ₂ · 2H ₂ O	1.595	—	1.575	Иголки или пластинки

Key:

- | | |
|---------------------------------|----------------------------|
| a. Compound | f. Elongated prisms |
| b. Appearance of crystals | g. Dendrites |
| c. Rounded grains | h. Lath-shaped prisms |
| d. Lamella | i. Small needles or plates |
| e. Crystals of irregular shapes | |

BIBLIOGRAPHY

1. Carlson, E. T., L. S. Wells, J. Res. Nat. Bur. Stand., 51, 2, 1953, p. 73.



The system has not been studied. Only individual compounds of the system have been synthesized and investigated [1, 2], the barium hydrosilicates: BaO · SiO₂ · 6H₂O, BaO · SiO₂ · 3H₂O, BaO · 2SiO₂ · 0.5H₂O, BaO · SiO₂ · 1-1.3H₂O (I), BaO · SiO₂ · 1-1.3H₂O (II). Kruger and Wieker [3] present the formulas BaO · SiO₂ · 1.5H₂O (I) and BaO · SiO₂ · H₂O (II), respectively, for the last two, as well as X ray photos of them.

Funk [1] describes conditions for synthesis of barium hydrosilicates, and he presents X-ray photos and differential-thermal analysis curves of them.

The structure of barium hydrosilicate hexahydrate has been determined [2]. The crystal system is rhombic and the unit cell parameters are $a = 8.43$, $b = 12.96$ and $c = 15.01 \text{ \AA}$; density is $2.59-2.60 \text{ g/cm}^3$; indices of refraction: $N_g = 1.549$, $N_p = 1.542$ and $N_m = 1.548$ [5].

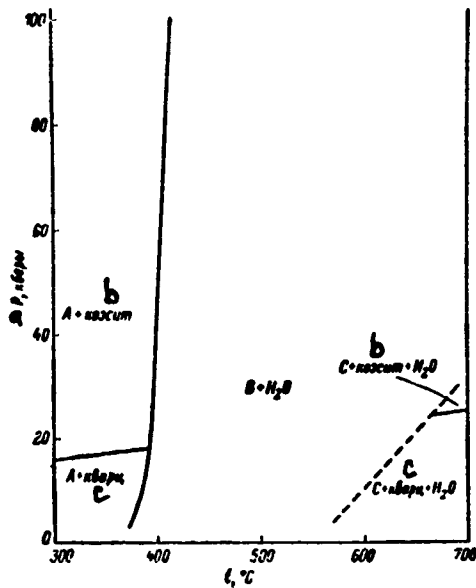


Fig. 389. Approximate phase relationships in silica-rich region of $\text{BaO} - \text{SiO}_2 - \text{H}_2\text{O}$ system; phases A, B and C not identified (from Pistorius).

Key:

- a. P , kbar
- b. Coesite
- c. Quartz.

A diagram of the conjectural phase relationships in the silica-rich region of the system, according to Pistorius [4], is represented in Fig. 389. Phases A, B and C, found in study of the system, were not successfully identified. The author presents X-ray photos of these phases and indicates that they do not coincide with the X-ray photos of known barium hydrosilicates.

BIBLIOGRAPHY

1. Funk, H., Zs. anorgan. allgem. Chem., 296, 106, 1958, p. 46.
2. Höhne, E., K. Dornberger-Schiff, Acta crystallogr., 14, 12, 1961, p. 1298.
3. Krüger, G., W. Wieker, Zs. anorgan allgem. Chem., 340, 5-6, 1965, p. 277.
4. Pistorius, C.W.F.T., Neues Jahrb. Mineral., Monatshefte, 2/3, 1963, p. 27.
5. Wahl, W., Zs. Kristallogr., 36, 2, 1902, p. 156.



The phase diagram of the system, at pressures up to 10,000 psi, has been studied by Roy and Osborn [29] (Fig. 390). Monovariant curves are presented in Fig. 391, in which the triangles correspond to the triangles of Fig. 390. The aluminum hydrosilicates are characterized in Fig. 392 and in the table.

In 1963, Roy and Aramaki [5] made a revision of the system. Two new phases AS(H)-I and AS(H)-II, were described. Some investigators [13, 36-38] relate phase AS(H)-II to andalusite.

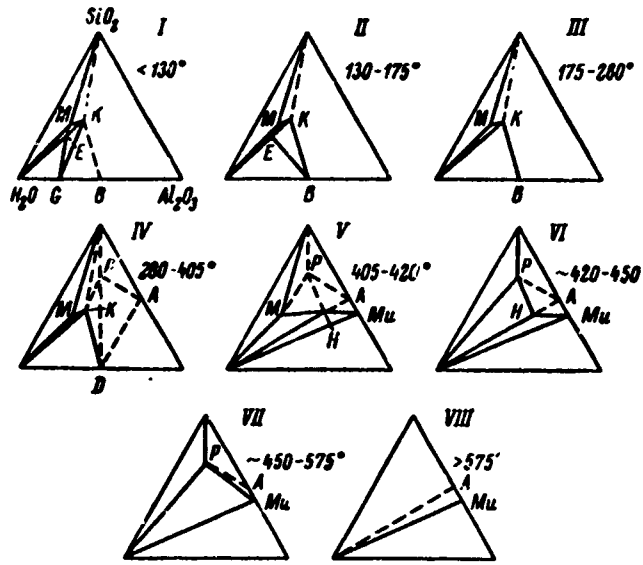


Fig. 390. Coexisting phase triangles for various temperatures and pressures of about 10,000 psi of the Al_2O_3 -- SiO_2 -- H_2O system (from Roy and Osborn); solid lines, experimental data; dashed, conjectural relationships; A. andalusite; B. boehmite; D. diaspore; E. endellite; G. gibbsite; H. hydralsite; K. kaolinite, nacrite, dickite or halloysite; M. Al-montmorillonite; Mu. mullite; P. pyrophyllite.

P-t curves of some reactions in the Al_2O_3 -- SiO_2 -- H_2O system, according to Kennedy [16], are depicted in Fig. 393. The data of this author from study of the system under hydrostatic conditions also are presented in work [21]. Curves characterizing the equilibrium of the pyrophyllite = kyanite + quartz (coesite) + H_2O and pyrophyllite + corundum = kyanite reactions are shown in Fig. 394.

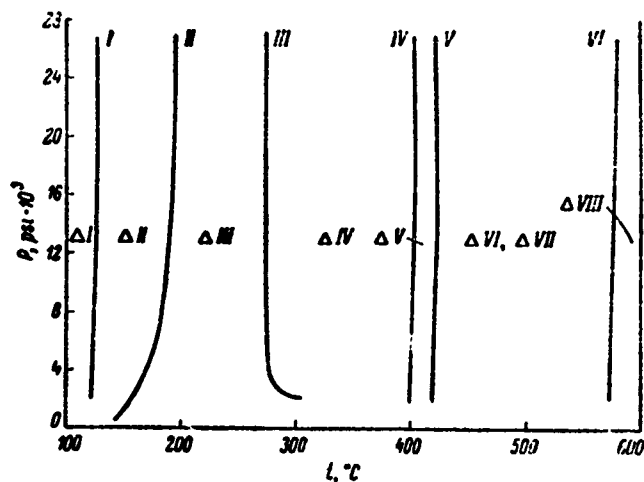


Fig. 391. Monovariant P-t curves of Al_2O_3 -- SiO_2 -- H_2O system (from Roy and Osborn); the triangles correspond to the triangles of Fig. 390: I. gibbsite = boehmite + H_2O ; II. endellite = halloysite + H_2O ; III. boehmite = diaspore; IV. diaspore = corundum + H_2O and kaolinite = hydralsite + pyrophyllite + montmorillonite; V. montmorillonite + pyrophyllite + hydralsite + H_2O ; VI. pyrophyllite = mullite (or andalusite) + quartz + H_2O .

The results of Kennedy have been supplemented by Robinson [28]. The data of Robinson concerns stable and metastable equilibria close to the invariant points (Fig. 395). The objections of Robinson concern the pyrophyllite + corundum = kyanite + H_2O and pyrophyllite + diaspore = kyanite + H_2O

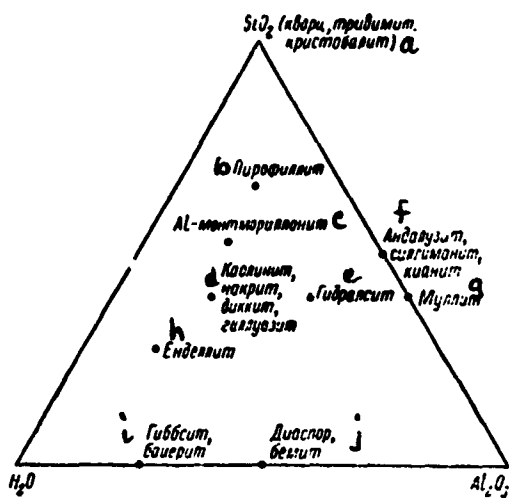


Fig. 392. Crystalline phases in Al_2O_3 -- SiO_2 -- H_2O system (from Roy and Osborn).

Key:

- a. Quartz, tridymite, cristobalite
- b. Pyrophyllite
- c. Al-montmorillonite
- d. Kaolinite, nacrite, dickite, halloysite
- e. Hydralsite
- f. Andalusite, sillimanite, kyanite
- g. Mullite
- h. Endellite
- i. Gibbsite, bayerite
- j. Diaspor, boehmite

reactions. Robinson points out that these reactions become metastable when they intersect the reaction curve of diaspore = corundum + H_2O . The pyrophyllite = kyanite + quartz + H_2O reaction also becomes metastable upon intersecting the kyanite -- sillimanite curve in the low pressure region and the quartz-coesite curve in the high pressure region.

ALUMINUM HYDROSILICATE CHARACTERISTICS

A Соединение	N_g	N_p	Плотность, г/см ³	Сингония	Параметры элементарной ячейки					
					a , Å	b , Å	c , Å	α	β	γ
$Al_2O_3 \cdot 2SiO_2 \cdot 4H_2O$ (галлуазит) енделлит)	$N_{g\beta} = 1.526-1.532$		2.0-2.2	-						
$Al_2O_3 \cdot 2SiO_2 \cdot 2H_2O$ (галлуазит) метагаллуазит)	$N_{g\beta} = 1.548-1.556$		2.56-2.53	-						
$Al_2O_3 \cdot 2SiO_2 \cdot 2H_2O$	каолинит i нектарит j диккит k	1.560-1.570 1.563-1.566 1.566-1.571	1.553-1.563 1.557-1.560 1.560-1.562	2.60-2.427 * 2.5 2.62	Триклиническая Ромбодирическая Моноклинная Псевдооктахедральная	5.16 5.15	8.94 8.96	7.38 43.0	91.8 —	104.5° 90°20'° 96°50'°
$2Al_2O_3 \cdot 2SiO_2 \cdot H_2O$ (гидраллит)	$N_{g\beta} = 1.600$		-							
$Al_2O_3 \cdot 4SiO_2 \cdot H_2O$ (Al-монтмориллонит)	1.515-1.630	1.480-1.590	2.348-1.772 *	-						
$Al_2O_3 \cdot 4SiO_2 \cdot H_2O$ (пирофиллит)	1.800	1.552	2.74	Моноклинная	5.15	8.98	18.60	—	99°35'	—
$Al_2O_3 \cdot SiO_2(H_2O)-I$ (AS(H)-I)	$N_{g\beta} = 1.71$		-							
$Al_2O_3 \cdot SiO_2(H_2O)-II$ (AS(H)-II)	1.640	1.625	-							

* The density limits, depending on moisture, are indicated.

Key:

- | | |
|-------------------------------|-----------------------|
| a. Compound | j. Nacrite |
| b. Density, g/cm ³ | k. Dickite |
| c. Crystal system | l. Triclinic |
| d. Unit cell parameters | m. Rhombic |
| e. Halloysite | n. Monoclinic |
| f. Endellite | o. Hydralsite |
| g. Metahalloysite | p. Pseudohexagonal |
| h. Basal interplane distance | q. Al-montmorillonite |
| i. Kaolinite | r. Pyrophyllite |

Kittrick [18] has plotted a phase diagram of the $Al_2O_3 - SiO_2 - H_2O$ system at 25° and 1 atm.

Althaus [4] carried out a revision of the equilibrium relations in the system at pressures up to 12,000 bar. According to his data, the kaolinite + quartz ⇌ pyrophyllite + water phase boundary passes through the points: 500 bar and 340°, 1000 bar and 368°, 2000 bar and 390°, 6900 bar and 405°. The following equilibrium conditions have been found for the pyrophyllite ⇌

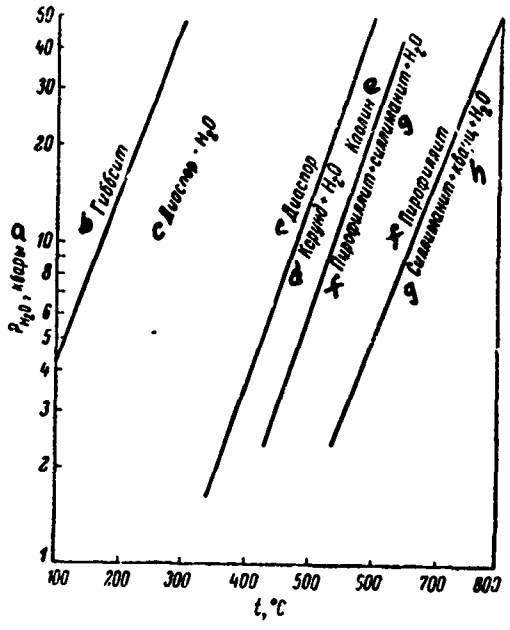


Fig. 393. P-t curves for some reactions in Al_2O_3 -- SiO_2 -- H_2O system (from Kennedy).

Key:

- | | |
|-------------|-----------------|
| a. Kbar | e. Kaolinite |
| b. Gibbsite | f. Pyrophyllite |
| c. Diaspore | g. Sillimanite |
| d. Corundum | h. Quartz |

andalusite + quartz + water reaction: $487 \pm 5^\circ$ at 2000 bar and $513 \pm 10^\circ$ at 6900 bar; for pyrophyllite \rightleftharpoons kyanite + quartz + water reaction, $512 \pm 10^\circ$ at 7000 bar and $528 \pm 10^\circ$ at 12000 bars. The equilibrium relationships between phases and their characteristics also are presented in the works of Brindley [7] (kaolinite structure), Gruner [10] (dickite), Hendricks [14] (nacrite), Blount and colleagues [6] (nacrite), Newton [23] (kyanite -- sillimanite and

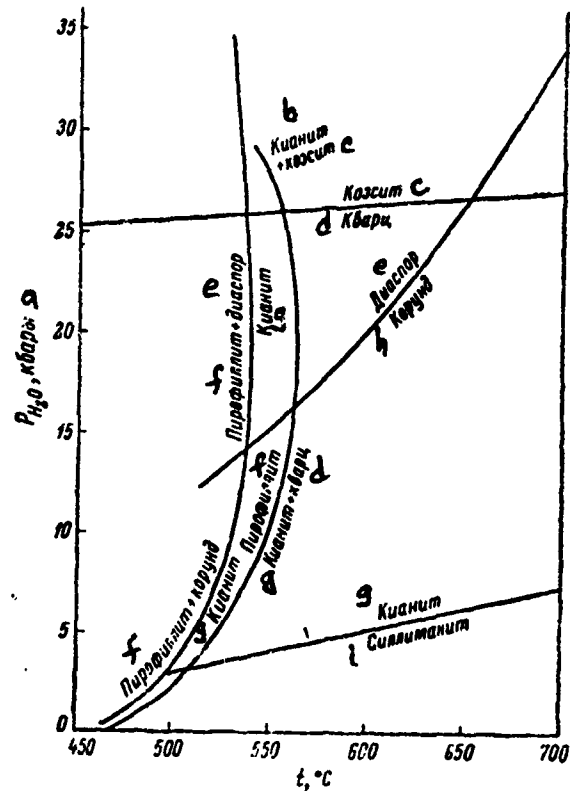


Fig. 394. P-t curves of pyrophyllite = kyanite + quartz (coesite) + H_2O and pyrophyllite + corundum = kyanite reactions (from Kennedy).

Key:

- | | |
|------------|-----------------|
| a. Kbar | e. Diaspor |
| b. Kyanite | f. Pyrophyllite |
| c. Coesite | g. Kyanite |
| d. Quartz | h. Corundum |
| | i. Sillimanite |

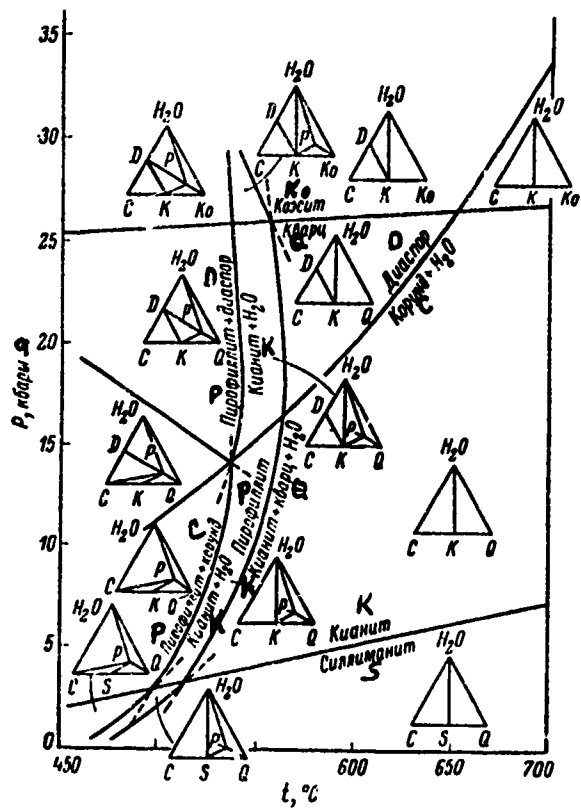


Fig. 395. P-t curves of reactions and coexisting phase triangles in Al_2O_3 -- SiO_2 -- H_2O system (from Robinson); D. diaspore; P. pyrophyllite; K. kyanite; S. sillimanite; Q. quartz; C. corundum; Ko. coesite.

Key:

a. Kbar

kyanite -- andalusite equilibria), Newton and Kennedy [24], Schreyer and Yoder [31], Ved' and Litvinova [2] (study of Al_2O_3 -- SiO_2 -- H_2O system under autoclave conditions), Bulygin [1] (dehydration and rehydration of natural and synthetic aluminosilicate hydrates of kaolinite composition), Niggli [25] and Kerrik [17].

Study of equilibria in the Al_2O_3 -- SiO_2 -- H_2O system would be incomplete without examination of the data on the Al_2O_3 -- H_2O system, some information on which is contained in volume 1 of the handbook [N. A. Toropov, V. P. Barzakovskiy, V. V. Lapin, N. N. Kurtseva, Diagrammy sostoyaniya silikatnykh sistem, I. Dvoynyye sistemy [Phase Diagrams of Silicate Systems: I. Binary Systems], Nauka Press, Leningrad, 1965, p. 459].

Al_2O_3 -- H_2O . The Al_2O_3 -- H_2O system is presented in P-t coordinates in Fig. 396, from Torkar and Worel [34]. The system has been studied by Kennedy [16], in the 100-600° temperature range and pressures from 5000 to 40,000 atm. Phase diagrams at low and high pressures are depicted in Fig. 397. At a pressure of 40,000 atm and a temperature of 295°, the trihydrate (gibbsite) is stable. The monohydrate (diaspore) is stable at 40,000 atm and 590°. The monohydrate exists in two polymorphic modifications, diaspore and boehmite. Boehmite is a metastable phase. Jamaguchi and colleagues have obtained a new hydrate $5\text{Al}_2\text{O}_3 \cdot \text{H}_2\text{O}$ (todite), under hydrothermal conditions [15]. A hexagonal cell has been established with parameters: $a = 5.575$, $b = 8.761$ Å.

Three polymorphic varieties of aluminum oxide trihydrate $\text{Al}_2\text{O}_3 \cdot 3\text{H}_2\text{O}$ are known: gibbsite, bayelite and the new mineral nordstrandite, synthesized by Nordstrand and colleagues [26]. Nordstrandite was obtained from solutions of aluminum chloride or nitrate and ammonium hydroxide.

Nordstrand presents a X-ray photo of the new mineral. According to his data, the basal interplane distance of the new phase is 4.875 Å. Dehydration of nordstrandite takes place at a temperature of about 200°, with

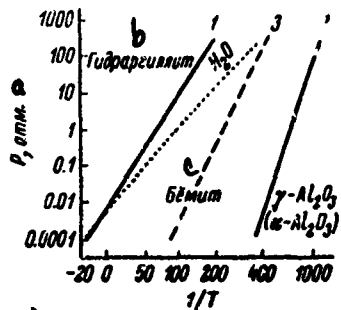
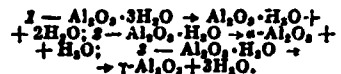


Fig. 396. Phase diagram of $\text{Al}_2\text{O}_3 - \text{H}_2\text{O}$ system, P-t curves (from Torkar and Worel);



Key:

- a. Atm
- b. Hydrargyllite
- c. Boehmite

formation of $\eta\text{-Al}_2\text{O}_3$. The mineral is known in nature [11, 35]. Nordstrandite from Borneo [35] has a density of 2.43 g/cm^3 and indices of refraction $\text{Ng} = 1.613$, $\text{Nm} = 1.583$ (calculation) and $\text{Np} = 1.580$. Nordstrandite from Guam [12] has a density of 2.436 g/cm^3 and indices of refraction $\text{Ng} = 1.596$, $\text{Nm} = 1.580$ and $\text{Np} = 1.580$.

Aldcroft [3] has studied the formation and thermal decomposition of nordstrandite. A series of works has been devoted to production and study of various properties of this mineral [12, 20, 27, 32]. Saalfeld and Mehrotra [30]

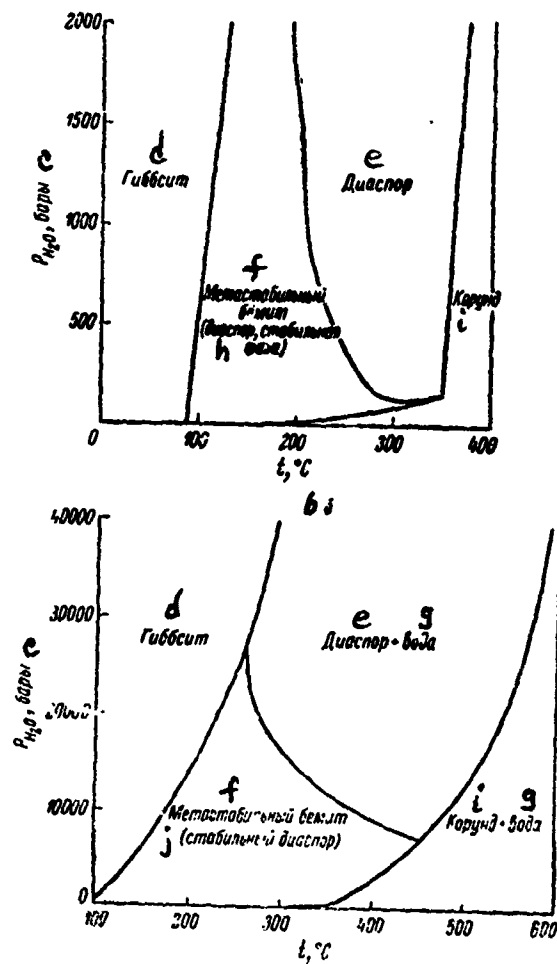


Fig. 397. Phase diagram of $\text{Al}_2\text{O}_3 - \text{H}_2\text{O}$ system (from Kennedy); a. at low H_2O pressure; b. at high H_2O pressure.

Key:

- | | |
|------------------------|---------------------------|
| c. Bar | g. Water |
| d. Gibbsite | h. Diaspore, stable phase |
| e. Diaspore | i. Corundum |
| f. Metastable boehmite | j. Stable diaspore |

have presented a X-ray study of monocrystals of natural nordstrandite.

According to their data, nordstrandite is in the triclinic crystal system.

There is a hypothesis that nordstrandite has various modifications.

The system also was studied earlier by Friecke and Hüttig [9], Ervin and Osborn [8], Thompson [33] and Yoder and Weir [39]. The system has been studied under hydrothermal conditions by Neuhaus and Heide [22] and by Laubengayer and Weisz [19].

BIBLIOGRAPHY

1. Bulygin, L. A., "Dehydration and rehydration of natural and synthetic aluminosilicate hydrates of kaolinite composition," author's abstract, candidate's dissertation, Simferopol', 1964.
2. Ved', Ye.I., Z.S. Litvinova, Vestn. Khar'k. politekhn. inst., No. 13 (61), "Chemical technology of inorganic substances," 1st Ed., 1966, p. 49.
3. Aldcroft, D., G.C. Bye, Sci. Ceram., 3, 1967, p. 75.
4. Althaus, E., Neues Jahrb. Mineral., Abh., 111, 1, 1969, p. 74.
5. Aramaki, Sh., R. Roy, Amer. Mineralogist, 48, 11-12, 1963, p. 1322.
6. Blount, A.M., I.M. Threadgold, S.W. Bailey, Clay a. Clay Minerals, 17, 3, 1969, p. 185.
7. Brindley, G.W., X-ray identification and crystal structures of clay minerals., London, 1951.
8. Ervin, G., E.F. Osborn, J. Geol., 59, 4, 1951, p. 381.
9. Friecke, R., G.F. Hüttig, Hydroxide and oxyhydrate, Ann Arbor, Michigan, 1944.
10. Gruner, J.W., Zs. Kristallogr., 83, 5/6, 1932, p. 394.
11. Hathaway, J.C., S.O. Schlanger, Nature, 196, 4851, 1962, p. 265.
12. Hauschild, U., Zs. anorgan. allgem. Chem., 324, 1-2, 1964, p. 15.
13. Hemley, J.J., J. Phys. Chem., 63, 2, 1959, p. 320.

14. Hendricks, S. B., Zs. Kristallogr., 100, 6, 1939, p. 509.
15. Jamaguchi, G., M. Okumiya, Sh. Ono., Bull. Chem. Soc. Japan, 42, 8, 1969, p. 2247.
16. Kennedy, G. C., Amer. J. Sci., 257, 8, 1959, p. 563.
17. Kerrik, D. M., Amer. J. Sci., 266, 3, 1968, p. 204.
18. Kittrick, J. A., Clay a. Clay Minerals, 17, 3, 1969, p. 157.
19. Laubengayer, A. W., R. S. Weisz, J. Amer. Chem. Soc., 65, 2, 1943, p. 250.
20. Lippens, B. C., Structure and texture of aluminas. Delft. 1961.
21. Matsushima, Sh., G. C. Kennedy, J. Akella, J. Haygarth, Amer. J. Sci., 265, 1, 1967, p. 28.
22. Neuhaus, A., H. Heide, Ber. Dtsch. keram. Ges., 42, 5, 1965, p. 167.
23. Newton, R. C., Science, 151, 3715, 1222; 153, 3732, 1966, p. 170.
24. Newton, R. C., G. C. Kennedy, J. Geophys. Res., 68, 1964 p. 2967.
25. Niggli, P., Rocks and mineral deposits, San Francisco, California, 1954.
26. Nordstrand, J. I., van, W. P. Hettinger, C. D. Keith, Nature, 177, 4511, 1956, p. 13.
27. Papé, D., R. Teptian, R. Biais, Bull. Soc. Franç. Chim., 11-12, 1958, p. 130.
28. Robinson, P., Amer. J. Sci., 265, 9, 1967, p. 831.
29. Roy, R., E. F. Osborn, Amer. Mineralogist, 39, 11-12, 1954, p. 853.
30. Saalfeld, H., B. B. Mehrotra, Naturwissenschaften, 53, 5, 1966, p. 128.
31. Schreyer, W., H. S. Yoder, Ann. Rept. Geophys. Lab. Carnegie Inst. Washington, 100, 1958-1959.
32. Shimizu, Y., S. Miyashige, K. Funaki, J. Chem. Soc. Japan, Industr. Chem. sect., 61, 1958, p. 475.
33. Thompson, J. B., Amer. J. Sci., 253, 2, 1955, p. 65.
34. Torkar, K., H. Worel, Monatsh. Chem., 88, 5, 1957, p. 739.

35. Wall, J.R.D., E.B. Wolfensen, E.H. Beard, T. Deans, Nature, 196, 4851, 1962, p. 264.
36. Warshaw, C.W., Proc. 7th Nat. Conf. Clays and Clay Minerals, 1958, Washington, 1960, p. 303.
37. Winkler, H.G.F., Geochim. cosmochim. acta, 13, 1, 1957, p. 42.
38. Yoder, H.S., Amer. J. Sci., Bowen vol., 1952, p. 569.
39. Yoder, H.S., C.F. Weir, Amer. J. Sci., 249, 9, 1951, p. 683.



The phase diagram of the system has not been studied. Individual compounds of the system, gallium hydrosilicates, have been synthesized: gallium kaolinite $\text{Ga}_2\text{O}_3 \cdot 2\text{SiO}_2 \cdot 2\text{H}_2\text{O}$, at temperatures from 200 to 500° and pressures from 6000 to 10,000 psi, and gallium montmorillonite $\text{Ga}_2\text{O}_3 \cdot 4\text{SiO}_2 \cdot \text{H}_2\text{O}$, having an appearance typical of montmorillonite, namely in the form of extremely thin plates and "fluffy" particles, sometimes with rounded corners [1].

BIBLIOGRAPHY

1. Roy, D.M., R. Roy, Amer. Mineralogist, 39, 11-12, 1954, p. 972.



The system has been studied by Maurice [1]. The formation of zirconium hydrosilicates has not been found. In water solution, at 400° and a pressure of 900 atm, zircon and anhydrous zirconium minerals have been obtained.

BIBLIOGRAPHY

1. O.D. Maurice, Econ. Geol., 44, 8, 1949, p. 721.



The phase diagram of the system has not been studied. A series of compounds of the system, phosphorus hydrosilicates, has been synthesized, and the conditions for producing them and some properties have been described [1-7]: $\text{P}_2\text{O}_5 \cdot \text{SiO}_2 \cdot \text{H}_2\text{O}$, $\text{P}_2\text{O}_5 \cdot \text{SiO}_2 \cdot 2\text{H}_2\text{O}$, $3\text{P}_2\text{O}_5 \cdot 2\text{SiO}_2 \cdot \text{H}_2\text{O}$, $2\text{P}_2\text{O}_5 \cdot \text{SiO}_2 \cdot 4\text{H}_2\text{O}$. Only an approximate composition is indicated for the latter compound. The X-ray photo of this hydrosilicate practically coincides with the X-ray photo of the compound $\text{P}_2\text{O}_5 \cdot \text{SiO}_2 \cdot 2\text{H}_2\text{O}$.

Lelong and Boulle have studied the conditions of formation of $\text{P}_2\text{O}_5 \cdot \text{SiO}_2 \cdot \text{H}_2\text{O}$ from H_3PO_4 and SiO_2 (or SiCl_4). These investigators [6] subsequently obtained and proved chromatographically the existence of two new phosphorus hydrosilicates, $\text{P}_2\text{O}_5 \cdot \text{SiO}_2 \cdot 2\text{H}_2\text{O}$ and $3\text{P}_2\text{O}_5 \cdot 2\text{SiO}_2 \cdot \text{H}_2\text{O}$, containing ortho-and triphosphate anions, respectively. The authors also carried out X-ray studies and studied the thermal behavior of these compounds. Lecomte and colleagues [3] have studied the structure of compounds of the system by means of infrared spectroscopy.

BIBLIOGRAPHY

1. Boulle, A., R. Jary, Compt. rend., 237, 3, 1953, p. 258.
2. Hautefeuille, P., J. Margottet, Bull. Soc. Chim., 47, 1, 1887, p. 952.
3. Lecomte, J., A. Boulle, C. Doremieux-Morin, B. Lelong, Compt. rend., 255, 4, 1962, p. 621.
4. Lelong, B., Ann. Chim., 9, 5-6, 1964, p. 229.
5. Lelong, B., A. Boulle, Compt. rend., 255, 3, 1962, p. 530.
6. Lelong, B., A. Boulle, Compt. rend., 257, 22, 1963, p. 3437.
7. Schwarz, R., Zs. anorgan. allgem. Chem., 176, 1-3, 1928, p. 236.



Only preliminary results have been obtained from investigation of the system [1]. Compounds with a layered structure have not been obtained. $\text{CrO}(\text{OH})$ crystallized out in certain tests in the 200-275° temperature range.

BIBLIOGRAPHY

1. Roy, D. M., R. Roy, Amer. Mineralogist, 39, 11-12, 1954, p. 972.



The difficulty in study of this system consists of the presence of oxides with cations of variable valence. A phase diagram of the system has not been produced. Efforts to study the system have been made by D. Roy and R. Roy [1].

BIBLIOGRAPHY

1. Roy, D. M., R. Roy, Amer. Mineralogist, 39, 11-12, 1954, p. 972.



Flaschen and Osborn [2] have studied the system at low oxygen partial pressure. Study of the system was complicated by the presence of a cation with variable valence. In practice, study of the $\text{FeO} \text{ -- Fe}_2\text{O}_3 \text{ -- SiO}_2 \text{ -- H}_2\text{O}$ system was required. A series of tetrahedra, depicting the equilibrium relationships between the phases in the four-component system in the 250-480° temperature range, is presented in Fig. 398.

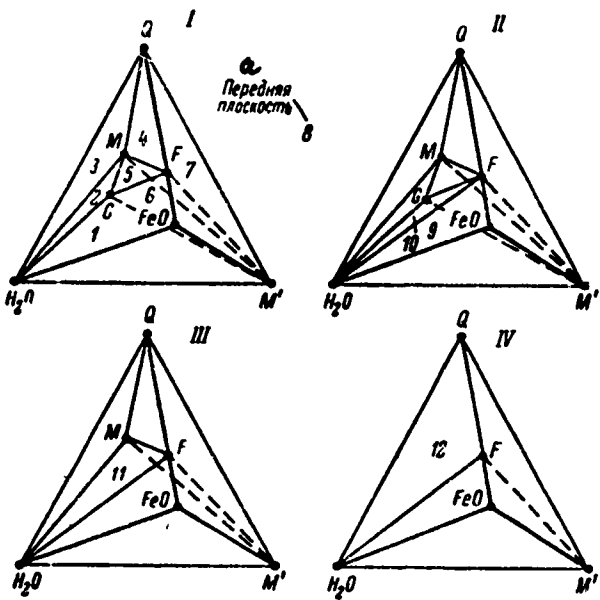


Fig. 398. Stable phase emsembles in $\text{FeO} - \text{Fe}_2\text{O}_3 - \text{SiO}_2 - \text{H}_2\text{O}$ system at various temperatures (from Flaschen and Osborn); I. $< 250^\circ$; II. $250-470^\circ$; III. $470-480^\circ$; IV. $> 480^\circ$; 1-12. stability fields of three or four condensed phases; M'. magnetite; Q. quartz; F. fayalite; M. minnesotaite; G. greenalite.

Key:

a. Anterior plane

The tetrahedra include 2's coexisting phase triangles, showing the equilibria among the following phases: magnetite -- greenalite -- water (1), minnesotaite -- greenalite -- water (2), quartz -- minnesotaite -- water (3), quartz -- minnesotaite -- fayalite (4), minnesotaite -- greenalite -- water (5), greenalite -- fayalite -- water (6), quartz -- fayalite -- magnetite (7), magnetite -- quartz -- water (8), magnetite -- fayalite -- water (9), greenalite --

fayalite -- water (10), minnesotaite -- fayalite -- water (11) and fayalite -- quartz -- water (12).

The following crystalline phases, iron hydrosilicates, in the system are known:

1. Minnesotaite $\text{Fe}_3\text{Si}_4\text{O}_{10}(\text{OH})_2$, the iron analog of talc [4], monoclinic; unit cell parameters $a = 5.4$, $b = 9.4$, $c \sin \beta = 19.1 \text{ \AA}$; indices of refraction $\text{Ng} = \text{Nm} = 1.618$ and $\text{Np} = 1.586$; density $3.0-3.1 \text{ g/cm}^3$;

2. Greenalite $\text{Fe}_3\text{Si}_2\text{O}_5(\text{OH})_2$ belongs to the serpentine group of minerals; Gruner [3] proposed the formula $(\text{OH})_{12}\text{Fe}_9^2\text{Fe}_2^3\text{Si}_8\text{O}_{22} \cdot 2\text{H}_2\text{O}$; monoclinic, unit cell parameters $a = 14.5$, $c = 18.6 \text{ \AA}$, parameter b has not been determined; density 3.0 g/cm^3 ;

3. Grunerite $\text{Fe}_7\text{Si}_8\text{O}_{22}(\text{OH})_2$ is an iron amphibole, monoclinic; indices of refraction $\text{Ng} = 1.729$, $\text{Np} = 1.686$ and $\text{Nm} = 1.709$ [1].

Greenalite and minnesotaite are metastable phases up to 470 and 480° , respectively. Above 470° , greenalite decomposes into minnesotaite, fayalite and water and minnesotaite, into quartz, fayalite and water.

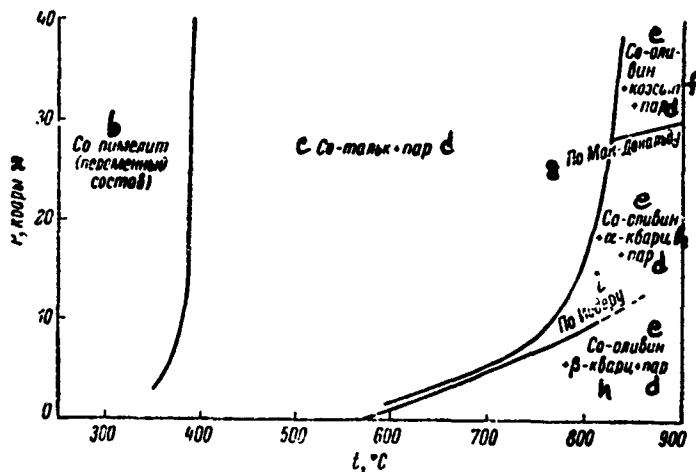
The system also has been studied by D. Roy and R. Roy [5]. Iron muscovite has been synthesized under hydrothermal conditions. Trivalent iron is in both octahedral and tetrahedral coordination in the structure.

BIBLIOGRAPHY

1. Bowen, N. L., J. F. Schairer, Amer. Mineralogist, 20, 8, 1935, p. 543.
2. Flaschen, W. W., F. F. Osborn, Econ. Geol., 52, 8, 1957, p. 923.
3. Gruner, J. W., Amer. Mineralogist, 21, 7, 1936, p. 449.
4. Gruner, J. W., Amer. Mineralogist, 29, 9-10, 1944, p. 363.
5. Roy, D. M., R. Roy, Amer. Mineralogist, 39, 11-12, 1954, p. 970.



The phase diagram of the system has not been investigated. Pistorius [5] has studied only the silica-rich region of the system (Fig. 399). The data of Yoder and MacDonald [2, 7] also is presented in the figure. Three phases have been found: Co-olivine, Co-talc and Co-pimelite. The unit cell parameters of Co-talc $3\text{CoO} \cdot 4\text{SiO}_2 \cdot \text{H}_2\text{O}$ have been determined: $a_0 \sin \beta = 18.90$, $b_0 = 9.17$ and $c_0 = 5.29 \text{ \AA}$; monoclinic crystal system.



Reproduced from
best available copy.

Fig. 399. Phase relationships in silica-rich portion of $\text{CoO} \text{ -- } \text{SiO}_2 \text{ -- } \text{H}_2\text{O}$ system at temperatures up to 900° and pressures up to 40 kbar (from Pistorius).

Key:

- | | |
|---------------------------------------|-------------------|
| a. Kbar | f. Coesite |
| b. Co-pimelite (variable composition) | g. From MacDonald |
| c. Co-talc | h. Quartz |
| d. Vapor | i. From Yoder |
| e. Co-olivine | |

Individual compounds, cobalt hydrosilicates, of the system have been synthesized by Pukall [6] who obtained $\text{CoSiO}_3 \cdot 2\text{H}_2\text{O}$, Feitknecht and Berger [1], $7.4 \text{ CoO} \cdot 4\text{SiO}_2 \cdot 8\text{H}_2\text{O}$, Noll, Kircher and Sybertz [3, 4], Co-chrysotile $\cdot \text{CoO} \cdot 2\text{SiO}_2 \cdot 2\text{H}_2\text{O}$.

BIBLIOGRAPHY

1. Feitknecht, W., A. Berger, Helv. chim. acta, 25, 7-8, 1942, p. 1543.
2. MacDonald, G.J.F., Amer. J. Sci., 254, 12, 1956, p. 713.
3. Noll, W., H. Kircher, W. Sybertz, Naturwissenschaften, 45, 20, 1958, p. 489.
4. Noll, W., H. Kircher, W. Sybertz, Beitr. Miner. Petrogr., 7, 4, 1960, p. 232.
5. Pistorius, C.W.F.T., Neues Jahrb. Mineral., Monatshefte, 2/3, 1963, p. 30.
6. Pukall, W., Silikate Zeitschr., 2, H. 4-6, 1914, p. 65.
7. Yoder, H.S., Trans. Amer. Geophys. Union, 31, 6, 1950, p. 827.



The system has been studied by D. Roy and R. Roy [8]. Coexisting phase triangles for certain temperatures are presented in Fig. 400. Pistorius [7] presented a diagram of the phase relationships in the silica-rich region of the system studied up to 350° at a pressure of 40 kbar (Fig. 401). A curve from Yoder [10] also is presented in the figure. Nickel hydrosilicates of differing compositions have been synthesized. Garnierite (chrysotile) $3\text{NiO} \cdot 2\text{SiO}_2 \cdot 2\text{H}_2\text{O}$ was obtained by D. Roy and R. Roy [8]. Noll and Kircher [6], Caillère [3, 4] and others. Ni-sepiolite $3\text{NiO} \cdot 4\text{SiO}_2 \cdot n\text{H}_2\text{O}$ [4], Ni-talc $3\text{NiO} \cdot 4\text{SiO}_2 \cdot \text{H}_2\text{O}$,

Ni-pimelite $3\text{NiO} \cdot 4\text{SiO}_2 \cdot \text{H}_2\text{O}$ and Ni-serpentine $3\text{NiO} \cdot 2\text{SiO}_2 \cdot 2\text{H}_2\text{O}$ also have been obtained. Prikhod'ko and colleagues [2] synthesized $\text{NiO} \cdot \text{SiO}_2 \cdot 2.42\text{H}_2\text{O}$ under hydrothermal conditions and Feitknecht and Berger [5], $5\text{NiO} \cdot 8\text{SiO}_2 \cdot 8\text{H}_2\text{O}$. Nickel hydrosilicates also have been studied by Spangenberg [9], Alekseyeva and Godlevskiy [1] and others.

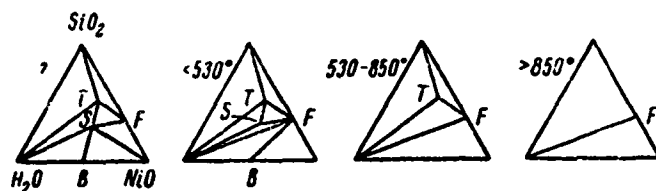


Fig. 400. Coexisting phase triangles of $\text{NiO} - \text{SiO}_2 - \text{H}_2\text{O}$ system (from D. Roy and R. Roy); T. talc; F. forsterite; S. serpentine; B. brucite.

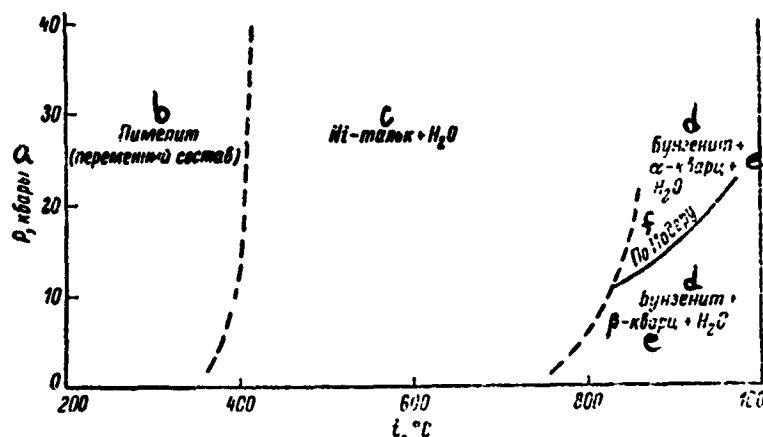


Fig. 401. Conjectural phase relationships in $\text{NiO} - \text{SiO}_2 - \text{H}_2\text{O}$ system in silica-rich region, at temperatures up to 950° and pressures up to 40 kbar (from Pistorius).

Key:

- | | |
|------------------------------------|---------------|
| a. Kbar | d. Bunsenite |
| b. Pimelite (variable composition) | e. Quartz |
| c. Talc | f. from Yoder |

BIBLIOGRAPHY

1. Alekseyeva, Ye.F., M.N. Godlevskiy, Zap. Russk. mineral. obshch., 66, 1, 1937, p. 51.
2. Prikhod'ko, N.Ye., V.S. Molchanov, O.S. Molchanova, DAN SSSR, nov. ser., 86, 1, 1952, p. 83.
3. Caillère, S., Bull. Soc. Franc. Miner., 59, April 1936, p. 163.
4. Caillère, S., S. Hénin, J. Esquevin, Compt. rend., 241, 13, 1955, p. 810.
5. Feitknecht, W., A. Berger, Helv. chim. acta, 25, 7-8, 1942, p. 1543.
6. Noll, W., H. Kircher, Naturwissenschaften, 39, 10, 1952, p. 233.
7. Pistorius, C.W.F.T., Neues Jahrb. Mineral., Monatshefte, 2/3, 1963, p. 30.
8. Roy, D.M., R. Roy, Amer. Mineralogist, 39, 11-12, 1954, p. 972.
9. Spangenberg, K., Naturwissenschaften, 26, 35, 1938, p. 578.
10. Yoder, H.S., Trans. Amer. Geophys. Union, 31, 6, 1950, p. 827.

SUPPLEMENT



Shahid and Glasser [4] have obtained the high-silica compound $\text{Na}_2\text{O} \cdot \text{CaO} \cdot 5\text{SiO}_2$, rhombic crystal system, with space group $P2_12_12_1$; $a = 7.74$, $b = 9.83$, $c = 13.88 \text{ \AA}$; $Nm = 1.545$, $Ng-Np = 0.007$, with density of 2.619 g/cm^3 , undergoing a reversible polymorphic transformation at 720° .

Shahid and Glasser [5] have studied the high-silica region by the quenching method. A section found here, distinguished by low melting temperature, is in the primary crystallization field $\text{Na}_2\text{O} \cdot \text{CaO} \cdot 5\text{SiO}_2$ and $3\text{Na}_2\text{O} \cdot 8\text{SiO}_2$. The latter melts incongruently, with formation of sodium disilicate and liquid, and not silica and liquid, as was mentioned by Williamson and Glasser [6].

There are three eutectic points between the fields: NCS_5 , NS_2 and N_3S_8 (775°); NCS_5 , N_3S_8 and quartz (755°); and N_3S_8 and quartz (788°); they contain the following amounts of Na_2O , CaO and SiO_2 (weight %), respectively; 24.4, 3.6, 72.0; 22.0, 3.8, 74.2; 27.2, 0.0, 72.8. There are four peritectic points among the fields: NC_3S_6 , NCS_5 and quartz (827°); NC_3S_6 , NC_2S_3 and NS_2 (785°); NC_3S_6 , NCS_5 and NS_2 (785°); and NS_2 and N_3S_8 (793°); they contain Na_2O , CaO and SiO_2 in the following amounts (weight %), respectively:

19.0, 6.8, 74.2; 25.4, 5.4, 69.2; 25.0, 5.4, 69.6; and 26.2, 0.0, 73.8.

Akhmetov and colleagues, by crystallization of the corresponding glasses [2] or hydrothermally [1], obtained a new ternary compound $\text{Na}_2\text{O} \cdot \text{CaO} \cdot 2\text{SiO}_2$ ($\text{Na}_2\text{CaSi}_2\text{O}_6$) in the cubic crystal system, $a_0 = 7.48 \pm 0.01 \text{ \AA}$, density 2.87 g/cm³ and Nm = 1.585.

Upon heating, $\text{Na}_2\text{O} \cdot \text{CaO} \cdot 2\text{SiO}_2$ apparently changes into a tetragonal modification, which, in the opinion of the authors, Kröger and Blömer [3] obtained, erroneously taking it for $\text{Na}_2\text{O} \cdot \text{CaO} \cdot 3\text{SiO}_2$.

BIBLIOGRAPHY

1. Akhmetov, S. F., G. L. Akhmetova, I. P. Baymurzina, R. D. Simbinov, Trudy Khimiko-metallurg. inst. AN Kazakhsk. SSR, 1, 1969.
2. Akhmetov, S. F., G. L. Akhmetova, L. P. Strel'chenko, Ibid., 15 1970, p. 141.
3. Kröger, C., J. Blömer, Zs. anorgan. allgem. Chem., 280, 1-2, 1955, p. 61.
4. Shahid, K. A., F. P. Glasser, J. Amer. Ceram. Soc., 53, 7, 1970, p. 423.
5. Shahid, K. A., F. P. Glasser, Phys. Chem. Glasses, 12, 2, 1971, p. 50.
6. Williamson, J., F. P. Glasser, Science, 148, 3677, 1965, p. 1589.



Hatfield and Richmond [1] have studied the solubility of monticellite (CaMgSiO_4) in forsterite (Mg_2SiO_4), using a reflecting microscope on quenched samples. In earlier investigations, when the X-ray radiographic method was used, an overstated concentration of the dissolved monticellite was obtained. According to Hatfield and Richmond, the limiting solution at 1500° contains 9 weight % and, at 1700°, 4 weight % of monticellite (from Ricker and Osborne, 28 weight % at 1500°, from Biggar and O'Hara, 19 mole % at 1490°).

Panek and Kanclir [4] have studied the thermal breakdown of merwinite $3\text{CaO} \cdot \text{MgO} \cdot 2\text{SiO}_2$. Upon heating in vacuum, the breakdown is accompanied by formation of $\alpha' 2\text{CaO} \cdot \text{SiO}_2$ and, in air, $\alpha' 2\text{CaO} \cdot \text{SiO}_2$.

Spencer and colleagues [5] showed that the solubility of CaO in magnesium oxide depends on the silica content in mixtures annealed at 1800° . Silica can occur in the form of monticellite, merwinite or calcium silicates. With a constant SiO_2 content, the solubility of CaO in periclase (MgO) increases in proportion to increase in the CaO/SiO_2 ratio (see table).

CaO CONTENT IN SOLID SOLUTION OF PERICLASE vs. NATURE AND AMOUNT OF SILICATE PRESENT IN THE BATCH

a Добавка, мол.-%	b Состав, вес.-%			c Содержание CaO в твердом растворе периклаза, вес.-%
	CaO	MgO	SiO ₂	
0.5 CMS	0.69	98.58	0.73	0.10
0.25 C ₃ MS ₂	1.03	98.24	0.73	0.22
0.5 C ₂ S	1.37	97.90	0.73	0.30
0.5 C ₂ S	2.04	97.23	0.73	0.75
1.0 CMS	1.35	97.23	1.42	0.10
0.5 C ₃ MS ₂	2.01	96.57	1.42	0.30
1.0 C ₂ S	2.69	95.89	1.42	0.51
1.0 C ₃ S	3.98	94.60	1.42	1.46

Key:

- a. Additive, moles
- b. Composition, weight %
- c. CaO content in periclase solid solution, weight %

Henney and Jones [3] found that the amount of calcium oxide dissolved in periclase increased in proportion to addition of $2\text{CaO} \cdot \text{SiO}_2$ to magnesium oxide, and reached 0.8 weight % at 1750° .

Hatfield and colleagues [2] showed that the periclase phase, occurring in equilibrium with the melt, contains calcium oxide in solid solution.

Spencer and Coleman [6] studied sintering of magnesium oxide (1400-1890°), to which small (0.5 and 10 mole %) amounts of forsterite, monticellite, merwinite, calcium silicates and CaO were added. In the first half hour at all temperatures, consolidation of the magnesium oxide took place, but addition of silicates hampered consolidation with further exposure.

BIBLIOGRAPHY

1. Hatfield, T., C. Richmond, Trans. Brit. Ceram. Soc., 69, 3, 1970, p. 90.
2. Hatfield, T., C. Richmond, W.F. Ford, J. White, Trans. Brit. Ceram. Soc., 69, 2, 1970, p. 53.
3. Henney, J.W., J.W.S. Jones, Trans. Brit. Ceram. Soc., 68, 4, 1969, p. 202.
4. Panek, Z., E. Kanclíř, Silikaty, 13, 3, 1966, p. 203.
5. Spencer, D.R.F., R.W. Beamond, D.S. Coleman, Trans. Brit. Ceram. Soc., 70, 1, 1971, p. 31.
6. Spencer, D.R.F., D.S. Coleman, in: Science of Ceramics, vol. 5, Ed. C. Brosset, E. Knopp, Gothenburg, 1970, p. 15.



Fields and colleagues [1] obtained the ternary compound $\text{BaSrSi}_3\text{O}_8$, melting congruently at $1325 \pm 15^\circ$. Limited solubility was found in the $\text{Ba}_2\text{SiO}_4 \text{ -- } \text{Sr}_2\text{SiO}_4$ profile: 70 mole % Sr_2SiO_4 in Ba_2SiO_4 and 5 mole % Ba_2SiO_4 in Sr_2SiO_4 at the eutectic temperature. In the metasilicate profile at the eutectic temperature of $1210 \pm 15^\circ$, 40 mole % SrSiO_3 dissolves in BaSiO_3 and 20 mole % BaSiO_3 in SrSiO_3 .

BIBLIOGRAPHY

1. Fields, J.M., B.S. Dear, I.I. Brown, Bull. Amer. Ceram. Soc., 50, 4, 1971, p. 372.



Lam [1] found the compound $2\text{Li}_2\text{O} \cdot 4\text{ZnO} \cdot 3\text{SiO}_2$ and limited solid solutions in the orthosilicate section. At 900° , 5 mole % Zn_2SiO_4 dissolves in $\text{Li}_2\text{ZnSiO}_4$ and from 62 to 72 mole % Zn_2SiO_4 dissolves in $2\text{Li}_2\text{O} \cdot 4\text{ZnO} \cdot 3\text{SiO}_2$.

West and Glasser [2] studied completely the partial system $\text{Li}_4\text{SiO}_4 \text{ -- } \text{Zn}_2\text{SiO}_4$, by quenching and differential-thermal analysis.

The compound $\text{Li}_2\text{ZnSiO}_4$ melts congruently at $1472 \pm 20^\circ$. The eutectic of this compound and Zn_2SiO_4 , containing 84 ± 4 mole % Zn_2SiO_4 , melts at $1340 \pm 20^\circ$. Zn_2SiO_4 -base solid solutions do not form. The authors assume four modifications for Li_4SiO_4 , with transition temperatures of 608 , 666 and 724° . A Li_4SiO_4 -base solid solution forms, up to a content of approximately 18 mole % Zn_2SiO_4 (900 - 950°).

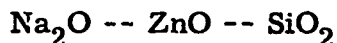
Two types of solid solutions were found in the central part of the diagram: phases γ and β , with some fields of homogeneity. Phase β apparently forms on a base of the compound $\text{Li}_2\text{ZnSiO}_4$, and it consists of two modifications, with a transition point of 650° . The γ phase, adjacent to the β phase, extends in the Li_4SiO_4 direction. It has three polymorphic forms: γ_{11} (high-temperature), γ_1 and γ_0 .

The authors established a more zinc oxide-rich rhombic C phase, with some region of homogeneity. It is proposed that the "ideal formula" of this phase corresponds to the compound $\text{Li}_3\text{Zn}_6\text{Si}_5\text{O}_{20}$ or $\text{Li}_6\text{Zn}_5\text{Si}_4\text{O}_{16}$.

West and Glasser [2], besides stable ones, plotted metastable phase diagrams of the Li_4SiO_4 -- Zn_2SiO_4 system. The first was obtained at a rate of cooling from the melt or from the solidus temperature of 2-20° per minute and the second, at a rate of 50-500° per minute. In the metastable diagram (cooling at 2-20° per minute), a new phase D figures, which apparently is some variety of solid solution, based on the low-temperature modification of Li_4SiO_4 .

BIBLIOGRAPHY

1. Lam, A. H., Ph. D. Thesis Univ. of Sheffield, 1964.
2. West, A. R., F. P. Glasser, J. Mater. Sci., 5, 7, p. 557; 8, p. 676, 1970.



Belokoneva and colleagues [1] have studied the crystal structure of $\text{Na}_2\text{ZnSi}_2\text{O}_6$, called zinc chkalovite. The parameters of the rhombic cell of this compound are $a = 21.503 \pm 0.05$, $b = 7.120 \pm 0.02$ and $c = 7.400 \pm 0.002$ Å. With a density of 3.1 g/cm^3 , a unit parallelepiped contains eight formula units.

Joubert-Bettan and colleagues [2] assume that $\text{Na}_2\text{ZnSiO}_4$ is a derivative of the rhombic $\beta \text{Na}_2\text{Fe}_2\text{O}_4$. The authors think that $\text{Na}_2\text{ZnSiO}_4$ is the first compound which can be treated as a hexagonal diamond structure.

BIBLIOGRAPHY

1. Belokoneva, Ye. L., Ya. K. Yegorov-Tismenko, M. A. Simonov, N. V. Belov, Kristallografiya, 14, 6, 1969, p. 1060.
2. Joubert-Bettan, C. A., R. Lachenal, E. F. Bertaut, E. Parthé, J. Solid State Chem., 1, 1, 1969, p. 1.

$\text{CaO} - \text{ZnO} - \text{SiO}_2$

Eysel and Hahn [1] have studied the stabilizing effect of zinc oxide on the polymorphic modifications of $3\text{CaO} \cdot \text{SiO}_2$. The authors consider that the monoclinic forms M_{II} and M_I occur in two forms a and b. With increase in amount of ZnO , the modifications are stabilized in the following sequence: T_I , T_{II} , M_{Ib} , M_{IIB} and R (see page 106 for designations).

BIBLIOGRAPHY

1. Eysel, W., Th. Hahn, Zs. Kristallogr., 131, 1-2, 1970, p. 40.

$\text{BaO} - \text{ZnO} - \text{SiO}_2$

The system has been studied by Segnit and Holland [1]. Five ternary compounds have been found and described, with the mole ratios BaO : ZnO : SiO_2 , 1:1:1, 1:1:3, 1:2:2, 2:1:2, 2:3:3. 50 invariant points are presented in the triple phase diagram, and six of them are eutectics, one of which, with a minimum melting temperature of 1100° , has the composition 41.7 weight % BaO , 17.0 ZnO and 41.3 SiO_2 .

BIBLIOGRAPHY

1. Segnit, E. R., A. E. Holland, Austral. J. Chem., 23, 6, 1970, p. 1077.

$\text{Na}_2\text{O} - \text{CoO} - \text{SiO}_2$

Lacy and Pask [1] present a likely phase diagram of the partial system $\text{CoO} - \text{Na}_2\text{O} \cdot 2\text{SiO}_2$, which is of the simple eutectic type.

The eutectic contains 40 mole % CoO at 630° .

BIBLIOGRAPHY

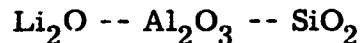
1. Lacy, A. M., J. A. Pask, J. Amer. Ceram. Soc., **54**, 5, 1971, p. 236.



The system has not been studied completely. Lapin and Solovova [1] have synthesized cobalt akermanite $\text{Ca}_2\text{CoSi}_2\text{O}_7$ from a mixture of CaCO_3 , $\text{Co}(\text{NO}_3)_2$ and $\text{SiO}_2 \cdot \text{H}_2\text{O}$. Its melting temperature is 1285° . It forms a continuous series of solid solutions with magnesium akermanite $\text{Ca}_2\text{MgSi}_2\text{O}_7$. Cobalt akermanite is uniaxial and negative; the indices of refraction are $N_o = 1.680$, $N_e = 1.668$. The glass has $N = 1.690$. A distinct pleochroism along N_o is blue and along N_e is violet. These same authors have shown experimentally that manganese and nickel akermanites cannot be synthesized in pure form, but MnO (up to 4.65 weight %) and NiO (up to 9.75 weight %) can be incorporated in the composition of magnesium akermanite.

BIBLIOGRAPHY

1. Lapin, V. V., K. P. Solovova, Avtoreferaty rabot cotrudnikov IGEM AN SSSR za 1970 g. [Authors' Abstracts of Work of Colleagues of USSR Academy of Sciences Institute of Geology of Ores, Mineralogy, Petrography and Geochemistry in 1970], Moscow, 1971, p. 123.

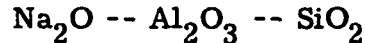


Tscherry and Laves [3] have obtained a colorless monocrystal of β eucryptite, with a diameter of more than 20 mm, from a melt of the composition (weight %): 46.4 eucryptite, 29.2 LiF , 10.3 AlF_3 and 14.1 V_2O_5 . The mixture was fused (0.5 hour) at 1200° , then cooled (0.5-1.0°/hour) to 1010° . The crystals are hexagonal bipyramids and, rarely, prisms.

Li Chi-tang [1] has studied the structure of $\text{Li}_2\text{Al}_2\text{Si}_3\text{O}_{10}$, one of the members of a solid solution with the high-temperature quartz structure. The basic structure is a skeleton, consisting of 6 and 8 member rings, with the lithium atoms located in the cavities. He also [2] showed the mechanism of reconstructive (with breaking of chemical bonds) transition of the high-temperature phase of $\text{LiAlSi}_2\text{O}_6$ (see p. 212) into the kitite form.

BIBLIOGRAPHY

1. Li Chi-tang, Zs. Kristallogr., 132, 1-2, 1970, p. 15.
2. Li Chi-tang, Acta crystallogr., 27B, 6, 1971, p. 1132.
3. Tscherry, V., F. Laves, Naturwissenschaften, 57, 1, 1970, p. 194.



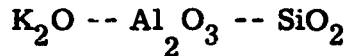
Grundy and Brown [2, 3] have accomplished a high-temperature (up to 850°) X-ray study (powder and monocrystal methods) of natural and of a large number of synthetic albites, obtained by prolonged (up to 3000 hours) crystallization of glasses at 500-1000° and elevated pressure. The authors discuss the effect of "order-disorder" transitions on the unit cell parameters.

Grundy and colleagues [4] have shown that "high" albite becomes monoclinic at about 930°. Eberhard [1] and Stewart and colleagues [5-7] also have been occupied with the structural investigations of albite at elevated temperatures.

BIBLIOGRAPHY

1. Eberhard, E., Schweiz. Min. Petrogr. Mitt., 47, 2, 1967, pp. 351, 385.
2. Grundy, H. D., W. L. Brown, Schweiz. Min Petrogr. Mitt., 47, 1, 1967, p. 21.

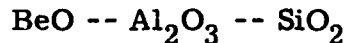
3. Grundy, H. D., W.L. Brown, Mineral. Magaz., 37, 286, 1969, p. 156.
4. Grundy, H. D., W.L. Brown, W.S. MacKenzie, Mineral. Magaz., 36, 277, 1967, p. 83.
5. Stewart, D.B., D. Limbach, Amer. Mineralogist, 52, 3-4, 1967, p. 389.
6. Stewart, D.B., G.W. Walker, T.L. Wright, J. Fahey, Amer. Mineralogist, 51, 1-2, 1966, p. 177.
7. Stewart, D.B., T.L. Wright, Amer. Mineralogist, 53, 1-2, 1968, p. 38.



Yamaguchi [1] obtained $K_2O \cdot Al_2O_3 \cdot SiO_2$, by annealing a mixture of $K_2O \cdot Al_2O_3$ and SiO_2 . There is a continuous series of solid solutions between cubic $K_2O \cdot Al_2O_3 \cdot SiO_2$ and $K_2O \cdot Al_2O_3$. These solid solutions are formed by the action of K_2CO_3 vapors on mullite.

BIBLIOGRAPHY

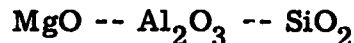
1. Yamaguchi, A., J. Ceram. Assoc. Japan, 78, 894, 1970, p. 74.



Bahat [1] has studied the kinetics of the hexacelsian-celsian transformation, proceeding from powders of various particle sizes. The transformation takes place slowly for powders with 0.635 cm grains. If the powder is ground to 200 mesh, the transformation is accelerated and takes place in three stages: the first stage is controlled by the crystal growth rate, the second, by both the rate of nucleus formation and crystal growth rate and the third stage is controlled by the rate of nucleus formation. The crystal growth activation energy in the first period is 20 kcal/mole.

BIBLIOGRAPHY

1. Bahat, D., J. Mater. Sci., 5, 9, 1970, p. 805.



Langer and Schreyer [1], proceeding from pure cordierite glass ($2\text{MgO} \cdot 2\text{Al}_2\text{O}_3 \cdot 5\text{SiO}_2$), by means of crystallization of it at 980° , obtained a metastable solid solution, designated as "high quartz." The maximum amount of this product was obtained in 50 min, and an increase in the amount of "high cordierite" then took place. For transformation of "high cordierite" into "low cordierite," a temperature of 1400° and prolonged exposure was required. The authors demonstrated the fruitfulness of using infrared spectroscopy for study of cordierite polymorphism.

For characterization of the initial stages of structural transformations from "high" to "low" cordierite, the authors propose introduction of a "width index" $W_{1/3}$, which is a more sensitive X-radiographic parameter than the "orderliness index" Δ usually used.

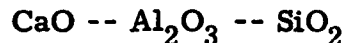
Zeck [3] thinks that it is advisable to use the $K\mathcal{Q}_1$ reflections, observed in X-ray diffraction images for a more detailed characterization of the orderliness of cordierite.

Schulz and colleagues [2] have obtained a new compound of variable composition $\text{MgO} \cdot \text{Al}_2\text{O}_3 \cdot x\text{SiO}_2$, where $x = 3-4$, hexagonal crystal system with the high-temperature quartz structure.

BIBLIOGRAPHY

1. Langer, K., W. Schreyer, Amer. Mineralogist, 54, 9-10, 1969, p. 1442.
2. Schulz, H., W. Hoffman, G.M. Muchow, Naturwissenschaften, 57, 5, 1970, p. 242.

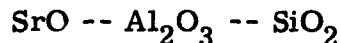
3. Zeck, H.P., Amer. Mineralogist, 54, 11-12, 1969, p. 1728.



Thermal expansion of monocrystals of anorthite $\text{CaAl}_2\text{Si}_2\text{O}_8$ over a wide temperature region has been studied [1], by means of a new, improved Siemens diffractometer. A decrease in volume was observed from 20 to 240° , and then an increase (up to 1500°). At 300° , the volume of anorthite became equal to its volume at room temperature. In the $20-1000^\circ$ temperature region, the average coefficient of thermal expansion was $\alpha = 11 \cdot 10^{-6}$. An increase in temperature causes a change in the monoclinic lattice from primitive to body-centered.

BIBLIOGRAPHY

1. Czank, M., H. Schulz, Naturwissenschaften, 58, 2, 1971, p. 94.



Reid and Ringwood [1] have shown that $\text{SrAl}_2\text{Si}_2\text{O}_8$ is converted into a new, dense phase, at a pressure of 100-120 kbar and 920° , having a tetragonal hollandite structure, with six-fold coordination of silicon and aluminum. The composition of this compound differs from the initial one, and it has the formula $\text{Sr}_x\text{Al}_{2x}\text{Si}_{4-2x}\text{O}_8$, where x is close to 2.75. The unit cell parameters are $a = 9.32$ and $c = 2.72$ Å.

BIBLIOGRAPHY

1. Reid, A.F., A.E. Ringwood, J. Solid State Chem., 1, 1, 1969, p. 6.

$\text{BaO} \text{ -- } \text{Al}_2\text{O}_3 \text{ -- } \text{SiO}_2$

Semler and Foster [2] have given a new version of the section included in the "celsian -- silica -- alumina" triangle. Compared with the diagram proposed by Toropov and colleagues, the mullite field is decreased and the celsian field is expanded, a . . result of which celsian and silica became co-existing phases. In the section of the triangle being discussed, there are two invariant points: a eutectic among the celsian, silica and mullite fields, containing 19 weight % BaO, 15 Al_2O_3 and 66 SiO_2 , melting at $1296 \pm 3^\circ$, and a reaction point among the celsian, mullite and alumina fields, with a temperature of $1554 \pm 4^\circ$, containing 26 weight % BaO, 27 Al_2O_3 and 47 SiO_2 . Triple solid solutions were not found.

Reid and Ringwood [1] have shown that $\text{BaAl}_2\text{Si}_2\text{O}_8$ is transformed into a new dense phase at a pressure of 100-120 kbar and 900° , having the tetragonal hollandite structure, with six-fold coordination of silicon and aluminum. The composition of this compound differs from the initial one, and it is expressed by the formula $\text{Ba}_x\text{Al}_{2x}\text{Si}_{4-2x}\text{O}_8$, where x is close to 0.75. The unit cell parameters are a = 9.41 and c = 2.72 Å.

BIBLIOGRAPHY

1. Reid, A.F., A.E. Ringwood, J. Solid State Chem., 1, 1, 1969, p. 6.
2. Semler, C.E., W.R. Foster, J. Amer. Ceram. Soc., 53, 11, 1970, p. 595.

$\text{EuO} \text{ -- } \text{Al}_2\text{O}_3 \text{ -- } \text{SiO}_2$

Jaffe [1] has synthesized three divalent europium aluminosilicates, $\text{EuAl}_2\text{Si}_2\text{O}_8$ (isomorphic with $\text{SrAl}_2\text{Si}_2\text{O}_8$), $\text{Eu}_2\text{Al}_2\text{SiO}_7$ and $\text{Eu}_6\text{Al}_{18}\text{Si}_2\text{O}_{37}$, having structures similar to the corresponding strontium compounds. The

initial materials were Eu_2O_3 , $\text{Al}(\text{OH})_3$ and SiO_2 . Annealing was carried out in silica or alumina crucibles, in an atmosphere of NH_3 or a mixture of H_2 and N_2 , at 1250-1350°. A small single-phase region is introduced in the triple diagram, surrounding the compound $\text{EuAl}_2\text{Si}_2\text{O}_8$, although the author does not introduce any indications of solid solutions.

The substances obtained are phosphors, activated by divalent europium.

BIBLIOGRAPHY

1. Jaffe, P. M., J. Electrochem. Soc., 116, 5, 1969, p. 629.



Eysel and Hahn [2], studying the partial system Ca_2SiO_4 -- Ca_2GeO_4 by the differential-thermal analysis method, found that continuous solid solutions are formed in both the high-temperature region (α solid solution) and in the low-temperature (below 725°) regions (γ solid solution). Limited solid solutions are formed adjacent to dicalcium silicate, not only based on the α' modification of Ca_2SiO_4 , but based on the metastable $\beta\text{Ca}_2\text{SiO}_4$.

Eysel and Hahn [1] have studied the partial system $3\text{CaO}\cdot\text{SiO}_2$ -- $3\text{CaO}\cdot\text{GeO}_2$; they also found complete compatibility here and they confirmed the results of Boykova, Toropov and Vavilonova, concerning the polymorphic forms of tricalcium germanate.

The authors showed that a small number of foreign ions can stabilize various high-temperature modifications of $3\text{CaO}\cdot\text{GeO}_2$. The effect of ZnO was studied in special detail.

Pure $3\text{CaO}\cdot\text{GeO}_2$ is thermodynamically unstable below 1335°.

BIBLIOGRAPHY

1. Eysel, W., Th. Hahn, Zs. Kristallogr., 131, 1-2, 1970, p. 40.
2. Eysel, W., Th. Hahn, Zs. Kristallogr., 131, 4-5, 1970, p. 322.



Berberova and colleagues [1] have studied the fusibility diagram (crystallization surface) by the drop point method (noncrucible fusing) described by Molokhovich and colleagues [2]. They took the temperature at which drops of the melt broke away from the sample as the melting temperature.

In the central portion of the triple diagram, there are fields of BaTiSiO_5 , BaTiO_3 , Ba_2TiO_4 , Ba_2SiO_4 and BaSiO_3 . Three triple eutectics: 1. of BaTiO_3 , Ba_2SiO_4 and Ba_2TiO_4 (1450°); 2. of BaTiO_3 , BaTiSiO_5 and Ba_2SiO_4 (1245°); and 3. Ba_2SiO_4 , BaSiO_3 and BaTiSiO_5 (1286°), contain , respectively: 57.0, 46.0 and 54.0 mole % BaO , 41.0, 30.0 and 7.0 mole % TiO_2 and 2.0, 24.0 and 39.0 mole % SiO_2 .

The BaTiO_3 -- BaSiO_3 section is not a stable section (these compounds do not coexist). Reactions take place among them, leading to formation of BaTiSiO_5 (barium sphene) and Ba_2SiO_4 . The BaTiSiO_5 -- Ba_2SiO_4 section also is not stable. The reaction $\text{BaTiSiO}_5 + 2\text{BaTiO}_3 = \text{Ba}_2\text{SiO}_4 + 3\text{BaTiO}_3$ takes place here. Coexisting compounds are $\text{BaTiO}_3 + \text{Ba}_2\text{SiO}_4$ and $\text{BaTiSiO}_5 + \text{Ba}_2\text{SiO}_4$.

Robbins [5], in study of the BaTiO_3 -- SiO_2 system, obtained the compound $\text{Ba}_2\text{TiSi}_2\text{O}_8$, which, by optical, crystallographic and X-ray data, corresponds to the natural mineral fresnoite, described by Alfors and colleagues [3]. The natural mineral is in the tetragonal crystal system, with space group P4/mnb

(or P4bm), $a = 8.52$, $c = 5.21 \text{ \AA}$, $c/a = 0.6115$, experimental density 4.43 g/cm^3 , calculated 4.45 g/cm^3 ; $Z = 2$, uniaxial (-), $No = 1.775$, $Ne = 1.765$, and it is pleochroic from colorless to yellow. Monocrystals of $2\text{BaCO}_3 \cdot \text{TiO}_2 \cdot 2\text{SiO}_2$ were obtained by heating a mixture of BaCO_3 , TiO_2 and SiO_2 at 1425° and cooling at a rate of 3° per hour (see also [4]).

The authors demonstrate that BaTiSiO_5 , barium sphene, was not obtained synthetically, but that, actually, the compound $\text{Ba}_2\text{TiSi}_2\text{O}_8$ always was formed, with an X-ray photo coinciding exactly with that which was ascribed to "barium sphene." The BaTiO_3 -- SiO_2 system cannot be considered to be binary.

The solubility of $\text{Ba}_2\text{TiSi}_2\text{O}_8$ in a melt of the composition $1\text{BaO} + 1\text{TiO}_2 + 1\text{SiO}_2$, somewhat enriched in titanium dioxide, is 86 weight % at 1400° . The congruent melting temperature of 1400° , adopted by Reese and Roy for BaTiSiO_5 , actually is the point at which the compound $\text{Ba}_2\text{TiSi}_2\text{O}_8$ begins to crystallize from the melt. Robbins found little solution of TiO_2 in $\text{Ba}_2\text{TiSi}_2\text{O}_8$.

BIBLIOGRAPHY

1. Berberova, L. M., M. L. Molokhovich, I. N. Belyayev, Zhurn. neorgan. khim., 16, 2, 1971, p. 539.
2. Molokhovich, M. L., O. N. Kramarov, L. M. Berberova, Fizicheskaya khimiya rasplavlenykh soley [Physical Chemistry of Molten Salts], Moscow, 1965.
3. Alfors, J. T., M. C. Stinson, B. A. Matthews, A. Pabst, Amer. Mineralogist, 50, 3-4, 1965, p. 314.
4. Masse, R., J. C. Grenier, A. Durif, Bull. Soc. franc. mineralogie, cristallogr., 90, 1, 1967, p. 20.
5. Robbins, C. R., J. Res. Nat. Bur. Stand., 74A, Phys. a. Chem., 2, 1970, p. 229.

Cr_2O_3 -- TiO_2 -- SiO_2

Berezhnay [1], on the basis of his studies, notes that ternary compounds and triple solid solutions are not formed in the system. It was shown that, up to 1627° , $\text{Cr}_2\text{Ti}_2\text{O}_7$ coexists with silica. A large region of immiscibility of the liquids is assumed.

BIBLIOGRAPHY

1. Berezhnay, A. S., Mnogokomponentnye sistemy okislov [Multicomponent Oxide Systems], Naukova dumka Press, Kiev, 1970, p. 237.

FeO -- TiO_2 -- SiO_2

Lamprecht and Woermann [1] have studied the system in the subsolidus region at 1130° and various pressures. The following three phases are in equilibrium at atmospheric pressure (the compatibility triangles are being considered):
1. FeO (wüstite) + Fe_2SiO_4 + Fe_2TiO_4 ; 2. Fe_2SiO_4 + SiO_2 + Fe_2TiO_4 ;
3. Fe_2TiO_4 + SiO_2 + FeTiO_3 ; 4. FeTiO_3 + SiO_2 + FeTi_2O_5 ; 5. FeTi_2O_5 + SiO_2 + TiO_2 .

An increase in pressure causes the following reactions: at 10 kbar,
 $2\text{Fe}_2\text{TiO}_4 + \text{SiO}_2 = 2\text{FeTiO}_3 + \text{Fe}_2\text{SiO}_4$ and $\text{FeTi}_2\text{O}_5 = \text{FeTiO}_3 + \text{TiO}_2$;
at 20 kbar, $\text{Fe}_2\text{SiO}_4 + \text{SiO}_2 = 2\text{FeSiO}_3$; at 30 kbar, $\text{Fe}_2\text{TiO}_4 = \text{FeTiO}_3 + \text{FeO}$.

BIBLIOGRAPHY

1. Lamprecht, A., E. Woermann, Naturwissenschaften, 57, 1, 1970, p. 191.

$\text{Na}_2\text{O} \text{-- } \text{ZrO}_2 \text{-- } \text{SiO}_2$

Sircar and Brett [1], using sealed platinum ampules, found that all ternary compounds found in the system -- $\text{Na}_2\text{O}\cdot\text{ZrO}_2\cdot\text{SiO}_2$, $2\text{Na}_2\text{O}\cdot2\text{ZrO}_2\cdot3\text{SiO}_2$ and $\text{Na}_2\text{O}\cdot\text{ZrO}_2\cdot2\text{SiO}_2$ -- melt incongruently at 1480, 1545 and 1460-1500°, respectively, forming ZrO_2 and liquid. All of these compounds occur in the zirconium dioxide field.

The authors introduce a diagram in which seven fields are observed (not considering the small sodium silicate fields): ZrO_2 , Na_2ZrO_3 , $\text{Na}_2\text{O}\cdot\text{ZrO}_2\cdot\text{SiO}_2$, $2\text{Na}_2\text{O}\cdot2\text{ZrO}_2\cdot3\text{SiO}_2$, $\text{Na}_2\text{O}\cdot\text{ZrO}_2\cdot2\text{SiO}_2$, ZrSiO_4 and SiO_2 . The three invariant peritectic points among the $\text{NZ} \text{-- NZS} \text{-- Z}$, $\text{NZS} \text{-- N}_2\text{Z}_2\text{S}_3 \text{-- Z}$ and $\text{N}_2\text{Z}_2\text{S}_3 \text{-- NZS}_2 \text{-- Z}$ fields contain, respectively: 38.5, 43.0 and 32.0 weight % Na_2O ; 36.0, 14.0 and 7.0 weight % ZrO_2 ; 25.5, 43.0 and 61.0 weight % SiO_2 , and have temperatures of 1380, 1446 and 1450°.

The authors were the first to draw the contours of the zircon field, which is located along the silica field, in the form of a narrow ribbon.

The liquidus temperature in the very large zirconium dioxide field exceeds 1700°, with a ZrO_2 content of more than 70 weight %.

The triangulation carried out showed that ZrO_2 coexists with all three ternary compounds; zircon coexists with $\text{Na}_2\text{O}\cdot2\text{SiO}_2$, $\text{Na}_2\text{O}\cdot3\text{SiO}_2$ and $\text{Na}_2\text{O}\cdot\text{ZrO}_2\cdot2\text{SiO}_3$; the compound NZS coexists with, beside ZrO_2 , $\text{Na}_2\text{O}\cdot\text{ZrO}_2$, $2\text{Na}_2\text{O}\cdot\text{SiO}_2$ and $\text{Na}_2\text{O}\cdot\text{SiO}_2$.

BIBLIOGRAPHY

1. Sircar, A., N.H. Brett, Trans. Brit. Ceram. Soc., 69, 3, 1970, p. 131.



Ramakrishnan and colleagues [2] have investigated the breakdown of zircon ZrSiO_4 , occurring in a solid solution with hafnium silicate HfSiO_4 . Spectrally pure ZrSiO_4 dissociates into ZrO_2 and SiO_2 at 1677° , according to Bitterman and Foster [1]. ZrSiO_4 , occurring in a solid solution with HfSiO_4 , increases its stability: dissociation of zircon is decreased with increase in HfSiO_4 content in the solid solution.

BIBLIOGRAPHY

1. Bitterman, W.C., W.R. Foster, Amer. Mineralogist, 52, 5-6, 1967, p. 880.
2. Ramakrishnan, S.S., E.C. Subbarao, K.V. Gokhale, Mater. Res. Bull., 5, 11, 1970, p. 965.



Ramakrishnan and colleagues [1] have found 4 mole % ThSiO_4 dissolves in zircon ZrSiO_4 at 1630° . It was found that dissociation of zircon is facilitated by the presence of ThSiO_4 . The effect of ThSiO_4 on dissociation of ZrSiO_4 is opposite to the effect of HfSiO_4 .

BIBLIOGRAPHY

1. Ramakrishnan, S.S., E.C. Subbarao, K.V. Gokhale, Mater. Res. Bull., 5, 11, 1970, p. 965.



Jones and colleagues [1], in the process of investigation of the quaternary system $\text{FeO} \text{ -- Fe}_2\text{O}_3 \text{ -- ZrO}_2 \text{ -- SiO}_2$, studied the partial system iron oxide -- $\text{ZrO}_2 \text{ -- SiO}_2$ in air, and they plotted a diagram for it which is a projection

of the liquidus surface, with the zirconium dioxide, zircon, magnetite, tridymite and cristobalite phase fields and isotherms for temperatures from 1450 to 2600° plotted on it. The spinel phase (magnetite) contains a little ZrO_2 , in the form of a solid solution. There are two "piercing points." This term is used here to designate the intersections between the four liquidus, monovariant curves and the oxygen isobaric surface ($P_{O_2} = 0.2$ atm). Since the oxygen pressure was fixed beforehand in this case, one degree of freedom was eliminated and, therefore, the compositions of all phases are fixed, as in a true invariant situation. The "piercing points" are characterized by the following equilibrium phase associations: 1. at 1425°, spinel, silica (tridymite or cristobalite), zircon and liquid of composition (weight %) $76Fe_3O_4$, $10ZrO_2$ and $14SiO_2$ are in equilibrium. 2. at 1438°, spinel, zircon, zirconium dioxide and liquid of the composition $74Fe_3O_4$, $17ZrO_2$ and $9SiO_2$. Moreover, the invariant situation at 1660° is characterized by an equilibrium association of silica, zircon, zirconium dioxide and liquid of the composition $47Fe_3O_4$, $23ZrO_2$ and $30SiO_2$, and a second liquid of the composition $5Fe_3O_4$, $4ZrO_2$ and $91SiO_4$.

BIBLIOGRAPHY

1. Jones, T.S., S. Kimura, A. Muan, J. Amer. Ceram. Soc., 50, 3, 1967, p. 137.



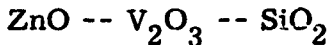
Grebenshchikov and Parfenenkov have studied the phase diagram of the partial systems HfO_2 -- Y_2SiO_5 [1] and HfO_2 -- $Y_2Si_2O_7$ [2] (quenching, using a molybdenum vacuum furnace at 2800° and the differential -thermal method).

In both systems, a HfO_2 -base monoclinic solid solution contains about 2.5 mole % of the corresponding yttrium silicate as a limit, at 1700°. A tetragonal solid solution is observed above 1900°. The cubic solid solutions contain from 17 to 47 mole % Y_2SiO_5 (index of refraction changes in this case from 1.817 to 1.946) and from 21 to 48 mole % $\text{Y}_2\text{Si}_2\text{O}_7$, respectively, under normal conditions, with expansion of this region upon increase in temperature; the index of refraction changes here from 1.880 to 1.900.

The eutectics of the cubic solid solutions and yttrium silicates contain 82.5 mole % Y_2SiO_5 (1800°) and 87.5 mole % $\text{Y}_2\text{Si}_2\text{O}_7$ (1600°), respectively.

BIBLIOGRAPHY

1. Grebenschchikov, R.G., V.N. Parfenenkov, Izv. AN SSSR, Neorg. mater., 7, 8, 1971, p. 1393.
2. Grebenschchikov, R.G., V.N. Parfenenkov, Zhurn. prikl. khim., 44, 3, 1971, p. 501.



Turne and colleagues [1] have studied the partial system ZnV_2O_4 -- SiO_2 in the subsolidus region (heating of mixtures of the extreme members in a sealed quartz tube). Formation of a limited solid solution based on ZnV_2O_4 , expressed by the formula $(1-x)\text{ZnV}_2\text{O}_4 \cdot 2x\text{SiO}_2$, was found. In the limiting solid solution at 1000°, $x = 0.055$. With decrease in temperature, solubility of SiO_2 decreases.

BIBLIOGRAPHY

1. Turne, G., J. Schaffner, B. Cros, Compt. rend., 272C, 13, 1971, p. 1219.

$\text{CaO} \text{ -- } \text{Nb}_2\text{O}_5 \text{ -- } \text{SiO}_2$

Jongejan and Wilkins [2] have studied the system with the aid of a heating microscope. One ternary compound $10\text{CaO} \cdot \text{Nb}_2\text{O}_5 \cdot 6\text{SiO}_2$, niokalite, having its field on the diagram, has been found.

In a study, Jongejan [1] demonstrated that the compound $3\text{CaO} \cdot \text{Nb}_2\text{O}_5$ does not exist, and he proves the formation of $4\text{CaO} \cdot \text{Nb}_2\text{O}_5$, $5\text{CaO} \cdot \text{Nb}_2\text{O}_5$ and $11\text{CaO} \cdot 2\text{Nb}_2\text{O}_5$. These compounds, together with the previously determined $\text{CaO} \cdot \text{Nb}_2\text{O}_5$ and $2\text{CaO} \cdot \text{Nb}_2\text{O}_5$, have their fields on the triple diagram.

Five peritectic points in the calcium oxide-enriched region, with the temperatures indicated below, have the compositions (weight %): 1790° , among the CaO , C_3S and C_{11}N_2 fields; 54.5 CaO , $34.5 \text{ Nb}_2\text{O}_5$ and 11.0 SiO_2 ; 1735° , among the C_3S , C_{11}N_2 and C_5N fields: 50.5 CaO , $38.5 \text{ Nb}_2\text{O}_5$ and 11SiO_2 ; 1645° among the C_2S , C_5N and C_4N fields: 48 CaO , $42 \text{ Nb}_2\text{O}_5$ and 10 SiO_2 ; 1505° , among the C_3S , C_2S and C_4N fields: 44CaO , $44.5\text{Nb}_2\text{O}_5$ and 11.5SiO_2 ; 1400° , among the C_2S , C_4N and C_2N fields: 41.5CaO , $46\text{Nb}_2\text{O}_5$ and 12.5SiO_2 .

BIBLIOGRAPHY

1. Jongejan, A., J. Less-Common Metals, 19, 3, 1969, p. 193.
2. Jongejan, A., A. L. Wilkins, J. Less-Common Metals, 19, 3, 1969, p. 203.

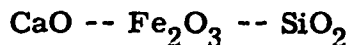
$\text{BaO} \text{ -- } \text{Ta}_2\text{O}_5 \text{ -- } \text{SiO}_2$

Shannon and Katz [1] obtained the compound $3\text{BaO} \cdot 4\text{SiO}_2 \cdot 3\text{Ta}_2\text{O}_5$ ($\text{Ba}_3\text{Si}_4\text{Ta}_6\text{O}_{26}$) by a complex route, initially synthesizing $\text{Ba}_3\text{Si}_4\text{Ta}_6\text{O}_{23}$ (heating a mixture of BaO , Ta_2O_5 and tantalum metal in a sealed, evacuated

quartz tube), with subsequent oxidation of it (heating in air at 1000°). The compound obtained has hexagonal symmetry, with unit cell parameters $a = 8.99 \pm 0.01$ and $c = 7.79 \pm 0.01$ Å.

BIBLIOGRAPHY

1. Shannon, J., L. Katz, J. Solid State Chem., 1, 3-4, 1970, p. 399.



Strictly speaking, this system is not a three-component one, since a magnetite (Fe_3O_4) field, containing divalent iron, occurs in it. There is a hematite field in it, as well as fields of calcium silicates ($\text{CaO} \cdot \text{SiO}_2$, $3\text{CaO} \cdot 2\text{SiO}_2$, $2\text{CaO} \cdot \text{SiO}_2$ and $3\text{CaO} \cdot \text{SiO}_2$) and calcium ferrites ($\text{CaO} \cdot 2\text{Fe}_2\text{O}_3$, $\text{CaO} \cdot \text{Fe}_2\text{O}_3$ and $2\text{CaO} \cdot \text{Fe}_2\text{O}_3$). In the region adjacent to silica, there is an extensive region of immiscibility of the liquids.

The partial system $\text{CaO} \cdot \text{SiO}_2 -- 2\text{CaO} \cdot \text{Fe}_2\text{O}_3$ has been studied by Iwase and Nishioka [8], who treat it as a simple eutectic (eutectic is 1185°, 45 weight % $\text{CaO} \cdot \text{SiO}_2$); however, Burdick [2], in a study of the triple system, showed that the $\text{CaO} \cdot \text{SiO}_2 -- 2\text{CaO} \cdot \text{Fe}_2\text{O}_3$ section intersects the field of dicalcium silicate and the compound $3\text{CaO} \cdot 2\text{SiO}_2$.

The eutectic easiest to melt (1192°) among the $2\text{CaO} \cdot \text{SiO}_2$, $\text{CaO} \cdot \text{Fe}_2\text{O}_3$ and $\text{CaO} \cdot 2\text{Fe}_2\text{O}_3$ fields has the composition 7.5 weight % SiO_2 , 66 Fe_2O_3 and 26.5 CaO .

The question of ternary compounds in the system has remained obscure up to the present time. The compound $\text{CaFe}_2\text{SiO}_6$, described by Kohl Meyer [9], apparently does not exist, although solid solutions between this compound and other metasilicates, diopside, for example, are observed.

Hansen and Bogue [4], studying the concentration fields between di and tricalcium silicate and calcium ferrites, also reject this compound.

At a pressure of 20 kbar and 900°, the garnet andradite $\text{Ca}_3\text{Fe}_2(\text{SiO}_4)_3$ forms; it also probably can be obtained in the metastable state, according to Ito and Frondel [7], from coprecipitated gels of the appropriate oxides, by heating at 900°.

Huckenholz and Yoder [5] have obtained the garnet andradite, starting from glasses of this composition or mixtures of wollastonite and hematite. Tests were carried out in sealed platinum tubes in the presence of PtO_2 , used as an oxygen source, or under hydrothermal conditions in the presence of hydrogen peroxide.

In air, andradite, having an index of refraction of 1.887 ± 0.002 and $a = 12.056 \pm 0.003$ Å, is stable up to $1137 \pm 5^\circ$, when it dissociates into wollastonite and hematite. In an oxygen-rich atmosphere and at a pressure of 30 kbar, andradite is stable up to 1510° .

The authors present phase diagrams of the partial system $\text{CaSiO}_3 - \text{Fe}_2\text{O}_3$, at pressures of 1, 5, 10, 15 and 20 kbar (in the presence of oxygen), from which it is evident that the stability of andradite from 1150° (at 1 kbar) increases to 1365° at 15 kbars, and at this garnet melts congruently at 1428° and 20 kbar.

Hugill [6] proposes the existence of a rhombic, pyroxene-related phase, called "mellorite," formed by the action of slags containing calcium ferrites on Dinas brick (a type of silica refractory brick).

Fletcher [3] has studied the solubility of Fe_2O_3 in tricalcium silicate $3\text{CaO} \cdot \text{SiO}_2$ at $1400-1500^\circ$. The author considers the solid solution formed to be a series $3\text{CaO} \cdot \text{SiO}_2 - "3\text{CaO} \cdot \text{Fe}_2\text{O}_3"$ (hypothetical compound). The solubility limit at 1400° is 1.5 mole % " $3\text{CaO} \cdot \text{Fe}_2\text{O}_3$ " or 1.05 weight % Fe_2O_3 . The

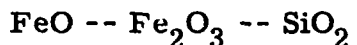
author assumes that the substitution takes place according to the scheme:
 $3\text{Ca}^{2+} \rightarrow 3\text{Fe}^{3+}$ and $6\text{Si}^{4+} \rightarrow 6\text{Fe}^{3+}$. To balance the charges of the ions,
part of the Fe^{3+} is located in the interstices.

The system has been studied by Phillips and Muan [11].

A phase diagram of the triple system was presented by Berezhnoy [1],
and it also is in the handbook of Levin and colleagues [10].

BIBLIOGRAPHY

1. Berezhnoy, A. S., Mnogokomponentnyye sistemy okislov [Multicomponent Oxide Systems], Naukova dumka Press, Kiev, 1970, p. 180.
2. Burdick, M. D., J. Res. Nat. Bur. Stand., 25, 4, 1940, p. 475.
3. Fletcher, K. E., Trans. Brit. Ceram. Soc., 64, 8, 1965, p. 377.
4. Hansen, W. C., R. H. Bogue, J. Amer. Chem. Soc., 48, 1926, p. 1261.
5. Huckenholz, H. G., H. S. Yoder, Neues Jahrbuch Mineralogie, Abh., 114, 3, 1971, v. 246.
6. Hugill, W., Trans. Brit. Ceram. Soc., 41, 1, 1942, p. 46.
7. Ito, J., C. Frondel, Amer. Mineralogist, 52, 5-6, 1967, p. 773.
8. Iwase, K., N. Nishicka, Sci. Rep. Tohoku Imp. Univ. (ser. 1), 26, 1938, p. 597.
9. Kohlmeyer, E. J., Metall u. Erz, 7, 1910, p. 301.
10. Levin, E. M., C. R. Robbins, H. F. McMurdie, Phase Diagrams for Ceramists, Amer. Ceram. Soc., USA, Ohio, 1964.
11. Phillips, B., A. Muan, J. Amer. Ceram. Soc., 42, 9, 1959, p. 422.



The relationships between these oxides should be considered as part of
the Fe -- Si -- O system. In the diagram of the $\text{FeO} -- \text{Fe}_2\text{O}_3 -- \text{SiO}_2$ system

presented by Muan [3], two immiscible liquids, metallic iron and a silicate melt, occur next to wüstite.

In the regions adjacent to silica, a large area of immiscibility of liquids is observed, with a critical temperature of 1698°. According to Gibbon and Tuttle [2], liquation is preserved under hydrothermal conditions. In the partial section Fe_3O_4 -- SiO_2 , studied by Muan, liquation is observed at a silica content of from 26 to 94 weight %, with a critical temperature of 1670°.

A eutectic with a minimum melting temperature (1140°) was formed by the Fe_2SiO_4 , Fe_3O_4 and SiO_2 phases, and it contains 35 weight % SiO_2 , 11 Fe_2O_3 and 54FeO; iron metasilicate FeSiO_3 is not observed in an atmosphere of air.

Berezhnay [1], who presents a triple diagram, proposes that a garnet $\text{Fe}_3^{2+}\text{Fe}_2^{3+}(\text{SiO}_4)_3$ should exist at very high pressures.

BIBLIOGRAPHY

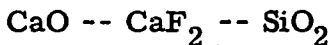
1. Berezhnay, A. S., Mnogokomponentnyye sistemy okislov [Multicomponent Oxide Systems], Naukova dumka Press, Kiev, 1970, p. 225.
2. Gibbon, D. L., O. F. Tuttle, Amer. Mineralogist, 52, 5-6, 1967, p. 886.
3. Muan, A., J. Metals, 7, Trans. Metallurg. Soc. AIME, 203, 1955, p. 965.



In investigation of the crystallization of glasses, Willgallis [1] has roughly studied the partial triple system Na_2SiO_3 -- $\text{Na}_2\text{Si}_2\text{O}_5$ -- NaF. A previously undescribed effect of transformation of sodium metasilicate was discovered. The system behaves as a simple eutectic, without formation of new compounds.

BIBLIOGRAPHY

1. Willgallis, A., Glastechn. Ber., 42, 12, 1969, p. 506.



Gutt and Osborne [1] have studied the partial system $3\text{CaO} \cdot \text{SiO}_2 \text{ -- CaF}_2$, in which the compound $(3\text{CaO} \cdot \text{SiO}_2)_3 \cdot \text{CaF}_2$ exists. There is a two-phase field $(3\text{CaO} \cdot \text{SiO}_2)_3 \cdot \text{CaF}_2 + \text{CaF}_2$ in the $1120\text{--}1100^\circ$ range; the compound being discussed occurs in combination with liquid in the $1175\text{--}1120^\circ$ range. Above 1175° and below 1100° , the compound $(3\text{CaO} \cdot \text{SiO}_2)_3 \cdot \text{CaF}_2$ is not observed.

The compound $(3\text{CaO} \cdot \text{SiO}_2)_3 \cdot \text{CaF}_2$ has a small field, surrounded by the fields of the solid solutions $3\text{CaO} \cdot \text{SiO}_2$, $2\text{CaO} \cdot \text{SiO}_2$, CaF_2 and CaO , in the phase diagram of the partial triple system $\text{CaO} \text{ -- } 2\text{CaO} \cdot \text{SiO}_2 \text{ -- CaF}_2$. The four eutectics existing here have melting temperatures between 1113 and 1175° .

Heiman and Franke [2] have studied the reaction between SiO_2 and a melt of $\text{CaF}_2 + \text{CaCl}_2$. Initially (at $840\text{--}860^\circ$), metastable pseudowollastonite is formed. Subsequently, under conditions of a high fluorine content, cuspidine is formed.

BIBLIOGRAPHY

1. Gutt, W., G.J. Osborne, Trans. Brit. Ceram. Soc., 69, 3, 1970, p. 125.
2. Heiman, R., W. Franke, Ber. Dtsch. keram. Ges., 47, 3, 1970, p. 169.



Three new natural sodium hydrosilicates have been found in Magadi (Kenya): magadiite $\text{NaSi}_7\text{O}_{13}(\text{OH})_3 \cdot 3\text{H}_2\text{O}$, kenyatite $\text{NaSi}_{11}\text{O}_{20.5}(\text{OH}) \cdot 3\text{H}_2\text{O}$

and makatite $\text{Na}_2\text{Si}_4\text{O}_9 \cdot 5\text{H}_2\text{O}$ or $\text{NaSi}_2\text{O}_3(\text{OH})_3 \cdot \text{H}_2\text{O}$. The first two minerals have been described by Eugster [2]. The author points out that they are well-crystallized lamellar silicates, with a large basal interplane distance.

Makatite has been characterized by Sheppard and colleagues [4]. The mineral is in the orthorhombic crystal system, with unit cell parameters $a = 16.840 \pm 8$, $b = 10.256 \pm 4$, $c = 19.146 \pm 7 \text{ \AA}$, $V = 3.3069 \pm 1.5 \text{ \AA}^3$; the indices of refraction $N_g = 1.487 \pm 0.001$ and $N_p = 1.472 \pm 0.001$.

A differential-thermal analysis curve has been obtained, with strongly endothermic effects at 80, 100 and 185°, extensive endothermic effects at 530 and 810° and an extensive exothermic effect at 675°.

Ryskin [1] has investigated the structure of some sodium hydrosilicates, on the basis of infrared spectroscopy data.

Freund [3] and colleagues presents the results of study of sodium hydrosilicates by proton magnetic resonance.

Williams and Dent-Glasser [5] have investigated the position of the hydrogen atoms in the compound $\text{Na}_2\text{O} \cdot \text{SiO}_2 \cdot 6\text{H}_2\text{O}$, with the aid of neutron diffraction.

BIBLIOGRAPHY

1. Ryskin, Ya.I., Izv AN SSSR, Neorg. mater., 7, 3, 1971, p. 375.
2. Eugster, H.P., Science, 157, 3793, 1967, p. 1177.
3. Freund, E., C. Doremieux-Morin, Compt. rend., 273, ser C, 20, 1971, p. 1344.
4. Sheppard, R.A., J. Gude, III, R.L. Hay, Am. Mineralogist, 55, 3-4, 1970, p. 358.
5. Williams, P.P., L.S. Dent-Glasser, Acta crystallogr., B27, 11, 1971, p. 2269.



Khitarov & colleagues [2] have investigated equilibrium transformations in the system at high temperatures and pressures from thermodynamic data. Over a broad range of temperatures and pressures, thermodynamic calculations of the following reactions were carried out: $\text{T} + 3\text{B} = 2\text{Sp}$ (I), $\text{Sp} + \text{B} = 2\text{F} + 3\text{V}$ (II), $5\text{Sp} = 6\text{F} + \text{T} + 9\text{V}$ (III), $\text{T} + 5\text{B} = 4\text{F} + 6\text{V}$ (IV), $\text{T} + \text{B} = 2\text{E} + 2\text{V}$ (V), $\text{T} + \text{F} = 5\text{E} + \text{V}$ (VI), $\text{B} + \text{E} = \text{F} + \text{V}$ (VII), $\text{B} + 6\text{E} = 2\text{F} + \text{T}$ (VIII) (Sp is serpentine, T is talc, F is forsterite, E is enstatite, B is brucite and V is H_2O).

The authors calculated a series of equilibrium phase boundaries in the $\text{MgO} \text{ -- } \text{SiO}_2 \text{ -- } \text{H}_2\text{O}$ system, on the basis of a critical, comprehensive selection of thermochemical data of the minerals. A P-t diagram of the phase relationships in the system, plotted from thermodynamic data, is presented, as well as a schematic P-t diagram, showing the stability fields of the mineral associations vs. temperature and pressure. The authors point out that, of all the equilibria established, only 8 are stable from thermodynamics considerations; only three are encountered and recorded in nature: $\text{Sp} + \text{B} = 2\text{F} + 3\text{V}$ (II), $5\text{Sp} = 6\text{F} + \text{T} + 9\text{V}$ (III), $\text{F} + \text{T} = 5\text{E} + \text{V}$ (VI).

Khitarov and colleagues [3] and Korytkova and Makarova [1] have investigated the serpentinization process. Electron microscopic studies of synthetic and natural chrysotile have been carried out [4]. Scarf and Garrison [7] have studied the dependence of serpentine stability on pressure, with limited temperatures. Scarfe and Wyllie [6] also have investigated the behavior of serpentine under various conditions.

MgO -- H₂O. The phase equilibria in the MgO -- H₂O system have been investigated by Yamaoka and colleagues [5], at temperatures from 500 to 1450° and pressures from 5 to 40 kbar. The authors present a P-t curve of the equilibrium between brucite, on the one hand, and periclase and water vapors on the other. The curve passes through the points 810° and 10 kbar, 945° and 20 kbar, 1000° and 32 kbar and 975° and 40 kbar. Extrapolation of this curve to lower pressures agrees with the data of other investigators, who used the hydrothermal technique. The authors also present data on the growth of brucite crystals at high pressure.

BIBLIOGRAPHY

1. Korytkova, E.N., T.A. Makarova, DAN SSSR, ser. geol., 196, 4, 1971, p. 927.
2. Kuskov, O.L., V.A. Pugin, N.I. Khitarov, Geokhimiya, 12, 1970, p. 1423.
3. Pugin, V.A., N.I. Khitarov, A.B. Slutskiy, N.I. Revin, O.L. Kuskov, Ibid., 10, 1969, p. 1188.
4. Khadzhi, I.P., L.I. Tsinober, T.A. Makarova, DAN SSSR, ser. geol., 200, 4, 1971, p. 953.
5. Yamacka, Sh., O. Fukunada, Sh. Saito, J. Amer. Ceram. Soc., 53, 4, 179, 1970; 54, 9, 472, 1971.
6. Scarfe, C.M., P.J. Wyllie, Nature, 215, 5104, 1967, p. 945.
7. Sclar, C.B., L.C. Garrison, Science, 153, 3741, 1964, p. 1285.

CaO -- SiO₂ -- H₂O

In study of the CaO -- SiO₂ -- H₂O system at the present time, the principal attention is given to study of the structure and structural singularities of both individual phases of the system and of their analogs. Belov and colleagues [1, 16] and Butt and colleagues [2] have synthesized monocrystals

of calcium hydrosilicates hydrothermally. The structure of the hydrosilicate of composition $6\text{CaO} \cdot 3\text{SiO}_2 \cdot \text{H}_2\text{O}$ (Y phase or dellaite) has been studied [4]. Monocrystals of this hydrosilicate have been obtained by hydrothermal crystallization in the $\text{Na}_2\text{O} \text{-- CaO} \text{-- SiO}_2 \text{-- H}_2\text{O}$ system [1, 12, 13, 16]. The structural formula of phase Y is $\text{Ca}_6(\text{Si}_2\text{O}_7)\cdot(\text{SiO}_4)(\text{OH})$, triclinic crystal system, unit cell parameters $a = 6.85$, $b = 6.95$, $c = 12.90 \text{ \AA}$, $\alpha = 90^\circ 45'$, $\beta = 97^\circ 20'$, $\gamma = 98^\circ 15'$, $Z = 2\text{C}_6\text{S}_3\text{H}$. Works of Dornberger-Shiff and Organova [5], studying rustamite, Taylor and colleagues [14] on thaumasite, a calcium hydrosilicate with $\text{SO}_4(\text{CO}_3)$ groups in the structure, Mamedov and colleagues [6], on calcium hydrosilicate and their analogs, Debinder and colleagues on the role of chemical condensation in the processes of hydrothermal transformations of tobermorite-like calcium hydrosilicates, also have been devoted to study of the structural singularities of calcium hydrosilicates. The correlating work of Ryskin Structure and Infrared Spectra of Acid Silicates [7] also concerns the calcium hydrosilicates $\text{Ca}_2(\text{HSiO}_4)\cdot\text{OH}$ (α -hydrate), $\text{Ca}_3(\text{HSiO}_4)_2 \cdot 2\text{H}_2\text{O}$ (afwillite), $\text{Ca}_3\text{F}_2(\text{HSiO}_4)_2 \cdot 2\text{H}_2\text{O}$, 11.3 A-tobermorite.

Nikol [19] presents new data on the composition and thermal dehydration of nekoite.

Sereda and colleagues [8] have investigated the microstructure of calcium hydrosilicates by the electron microscope and X-ray methods. The authors have studied the morphological and microstructural changes over time of hydrated tricalcium silicate pastes. A large amount of work has been devoted to study of hydration of $3\text{CaO} \cdot \text{SiO}_2$, the kinetics and the mechanism of this process and investigation of the hydration products [9, 15, 17, 18, 21, 22]. One

of the structural singularities of the calcium hydrosilicates is their capacity for isomorphic substitutions [10, 11]. An exhaustive bibliography on this question has been presented by Taylor [20].

BIBLIOGRAPHY

1. Bakshutov, V.S., R.M. Ganiyev, V.A. Kuznetsov, V.V. Ilyukhin, N.V. Belov, Izv. AN SSSR, Neorg. mater., 4, 12, 1968, p. 2146.
2. Butt, Yu.M., V.V. Timashev, V.V. Ilyukhin, V.A. Kuznetsov, M.K. Grineva, V.S. Bakshutov, in the collection Obrazovaniye i strukturnyye prevrashcheniya tsementnykh mineralov. Kratkiye tezisy dokladov [Formation and Structural Transformations of Cement Minerals: Short Summaries of Reports], Leningrad, 1971, p. 8.
3. Varlamov, V.P., O.I. Luk'yanova, P.A. Rebinder, DAN SSSR, 190, 1-3, 1970, p. 625.
4. Ganiyev, R.M., V.V. Ilyukhin, E.A. Kuz'mina, N.V. Belov, Kristallografiya, 16, 4, 1971, p. 731.
5. Dornberger-Shiff, K., N.I. Organova, Ibid., 1, p. 228.
6. Mamedov, Kh.S., S.T. Amirov, Ibid., 2, p. 314.
7. Ryskin, Ya.I., Izv. AN SSSR, Neorg. mater., 4, 3, 1971, p. 375.
8. Ciach, T.D., J.E. Gillott, E.G. Swenson, P.J. Sereda, Cement a. Concrete Res., 1, 1, 13, 1971.
9. Collepardi, M., L. Massidda, J. Amer. Ceram. Soc., 54, 9, 1971, p. 419.
10. Copeland, L.E., E. Bodor, T.N. Chang, C.H. Weise, J.P.C.A. Res.a. Dev. Labs., 9, 81, 1967.
11. Diamond, S., J.L. White, W.L. Dolch, Amer. Mineralogist, 51, 3-4, 1966, p. 388.
12. Dent-Glasser, L.S., H. Funk, W. Hilmer, H.F.W. Taylor, J. Appl. Chem., 11, 5, 1961, p. 186.
13. Dent-Glasser, L.S., D.M. Roy, Amer. Mineralogist, 44, 3-4, 1959, p. 447.

14. Edge, R.A., H.F.W. Taylor, Acta crystallogr., B27, 3, 1971, p. 594.
15. Englert, G., F. Wittmann, Zement -- Kalk -- Gips, 7, 1971, p. 312.
16. Ganiev, R.M., W.A. Kuznezov, W.W. Lijuchin, A.N. Lobačev, N.V. Belov, Kristall u. Technik, 5, 3, 1970, p. 309.
17. Grutzeck, M.W., D.M. Roy, Nature, 223, 5205, 1969, p. 492.
18. Kondo, R., M. Daimon, J. Amer. Ceram. Soc., 52, 9, 1969, p. 503.
19. Nikol, A.W., Acta crystallogr., B27, 3, 1971, p. 469.
20. Taylor, H.F.W., Proc. 5th Int. Symp. on the Chem. of Cement, pt. II, Tokyo, 1, 1969.
21. Tenoutasse, N., Cement -- Wapno -- Gips, 5-6, 1971, p. 171.
22. Tenoutasse, N., A. DeDonder, Silikates Industriels, 35, 12, 1970, p. 301.

ALPHABETICAL INDEX OF SYSTEMS

$\text{Al}_2\text{O}_3-\text{B}_2\text{O}_3-\text{SiO}_2$	201	$\text{BaO}-\text{B}_2\text{O}_3-\text{SiO}_2$	195
$\text{Al}_2\text{O}_3-\text{BaF}_2-\text{SiO}_2$	516	$\text{BaO}-\text{BaF}_2-\text{SiO}_2$	513
$\text{Al}_2\text{O}_3-\text{BaO}-\text{SiO}_2$	286, 626	$\text{BaO}-\text{BeO}-\text{SiO}_2$	79
$\text{Al}_2\text{O}_3-\text{BeO}-\text{SiO}_2$	246, 624	$\text{BaO}-\text{CaO}-\text{SiO}_2$	86
$\text{Al}_2\text{O}_3-\text{CaF}_2-\text{SiO}_2$	516	$\text{BaO}-\text{CrO}_3-\text{SiO}_2$	368
$\text{Al}_2\text{O}_3-\text{CaO}-\text{SiO}_2$	272, 625a	$\text{BaO}-\text{H}_2\text{O}-\text{SiO}_2$	591
$\text{Al}_2\text{O}_3-\text{CoO}-\text{SiO}_2$	320	$\text{BaO}-\text{Li}_2\text{O}-\text{SiO}_2$	73
$\text{Al}_2\text{O}_3-\text{Cr}_2\text{O}_3-\text{SiO}_2$	306	$\text{BaO}-\text{MgO}-\text{SiO}_2$	80
$\text{Al}_2\text{O}_3-\text{EuO}-\text{SiO}_2$	626	$\text{BaO}-\text{Na}_2\text{O}-\text{SiO}_2$	75
$\text{Al}_2\text{O}_3-\text{FeO}-\text{SiO}_2$	314	$\text{BaO}-\text{PbO}-\text{SiO}_2$	122
$\text{Al}_2\text{O}_3-\text{Fe}_2\text{O}_3-\text{SiO}_2$	317	$\text{BaO}-\text{SrO}-\text{SiO}_2$	93, 618
$\text{Al}_2\text{O}_3-\text{Ga}_2\text{O}_3-\text{SiO}_2$	327	$\text{BaO}-\text{Ta}_2\text{O}_5-\text{SiO}_2$	635
$\text{Al}_2\text{O}_3-\text{GeO}_2-\text{SiO}_2$	372	$\text{BaO}-\text{TiO}_2-\text{SiO}_2$	392, 628
$\text{Al}_2\text{O}_3-\text{H}_2\text{O}$	601	$\text{BaO}-\text{ZnO}-\text{SiO}_2$	108, 621
$\text{Al}_2\text{O}_3-\text{H}_2\text{O}-\text{SiO}_2$	593	$\text{BaO}-\text{ZrO}_2-\text{SiO}_2$	427
$\text{Al}_2\text{O}_3-\text{K}_2\text{O}-\text{SiO}_2$	237, 624	$\text{BeO}-\text{Al}_2\text{O}_3-\text{SiO}_2$	246, 624
$\text{Al}_2\text{O}_3-\text{Li}_2\text{O}-\text{SiO}_2$	206, 622	$\text{BeO}-\text{BaO}-\text{SiO}_2$	79
$\text{Al}_2\text{O}_3-\text{MgF}_2-\text{SiO}_2$	516	$\text{BeO}-\text{SrO}-\text{SiO}_2$	71
$\text{Al}_2\text{O}_3-\text{MgO}-\text{SiO}_2$	253, 625		
$\text{Al}_2\text{O}_3-\text{MnO}-\text{SiO}_2$	310		
$\text{Al}_2\text{O}_3-\text{Na}_2\text{O}-\text{SiO}_2$	222, 623	$\text{CaF}_2-\text{Al}_2\text{O}_3-\text{SiO}_2$	516
$\text{Al}_2\text{O}_3-\text{Na}_3\text{AlF}_6-\text{SiO}_2$	515	$\text{CaF}_2-\text{CaO}-\text{SiO}_2$	505, 640
$\text{Al}_2\text{O}_3-\text{Nd}_2\text{O}_3-\text{SiO}_2$	303	$\text{CaF}_2-\text{KF}-\text{SiO}_2$	520
$\text{Al}_2\text{O}_3-\text{NiO}-\text{SiO}_2$	323	$\text{CaF}_2-\text{NaF}-\text{SiO}_2$	520
$\text{Al}_2\text{O}_3-\text{P}_2\text{O}_5-\text{SiO}_2$	460	$\text{CaF}_2-\text{Na}_2\text{O}-\text{SiO}_2$	520
$\text{Al}_2\text{O}_3-\text{PbO}-\text{SiO}_2$	304	$\text{CaO}-\text{Al}_2\text{O}_3-\text{SiO}_2$	272, 625a
$\text{Al}_2\text{O}_3-\text{SrF}_2-\text{SiO}_2$	516	$\text{CaO}-\text{B}_2\text{O}_3-\text{SiO}_2$	191
$\text{Al}_2\text{O}_3-\text{SrO}-\text{SiO}_2$	283, 625a	$\text{CaO}-\text{BaO}-\text{SiO}_2$	86
$\text{Al}_2\text{O}_3-\text{TiO}_2-\text{SiO}_2$	394	$\text{CaO}-\text{CaF}_2-\text{SiO}_2$	505, 640
$\text{Al}_2\text{O}_3-\text{Y}_2\text{O}_3-\text{SiO}_2$	301	$\text{CaO}-\text{CaS}-\text{SiO}_2$	529
$\text{Al}_2\text{O}_3-\text{ZnO}-\text{SiO}_2$	300	$\text{CaO}-\text{Cr}_2\text{O}_3-\text{SiO}_2$	476
$\text{Al}_2\text{O}_3-\text{ZrO}_2-\text{SiO}_2$	429	$\text{CaO}-\text{FeO}-\text{SiO}_2$	152
$\text{B}_2\text{O}_3-\text{Al}_2\text{O}_3-\text{SiO}_2$	201	$\text{CaO}-\text{Fe}_2\text{O}_3-\text{SiO}_2$	636
$\text{B}_2\text{O}_3-\text{BaO}-\text{SiO}_2$	195	$\text{CaO}-\text{GeO}_2-\text{SiO}_2$	362, 627
$\text{B}_2\text{O}_3-\text{CaO}-\text{SiO}_2$	191	$\text{CaO}-\text{H}_2\text{O}$	568
$\text{B}_2\text{O}_3-\text{Li}_2\text{O}-\text{SiO}_2$	182	$\text{CaO}-\text{H}_2\text{O}-\text{SiO}_2$	558, 643
$\text{B}_2\text{O}_3-\text{MgO}-\text{SiO}_2$	188	$\text{CaO}-\text{K}_2\text{O}-\text{SiO}_2$	40
$\text{B}_2\text{O}_3-\text{Na}_2\text{O}-\text{SiO}_2$	184	$\text{CaO}-\text{La}_2\text{O}_3-\text{SiO}_2$	334
$\text{B}_2\text{O}_3-\text{P}_2\text{O}_5-\text{SiO}_2$	458	$\text{CaO}-\text{Li}_2\text{O}-\text{SiO}_2$	28
$\text{B}_2\text{O}_3-\text{PbO}-\text{SiO}_2$	203	$\text{CaO}-\text{MgO}-\text{SiO}_2$	46, 616
$\text{B}_2\text{O}_3-\text{ZnO}-\text{SiO}_2$	200	$\text{CaO}-\text{MnO}-\text{SiO}_2$	132
$\text{BaF}_2-\text{Al}_2\text{O}_3-\text{SiO}_2$	516	$\text{CaO}-\text{Na}_2\text{O}-\text{SiO}_2$	30, 615
$\text{BaF}_2-\text{BaO}-\text{SiO}_2$	513	$\text{CaO}-\text{Nb}_2\text{O}_5-\text{SiO}_2$	635
$\text{BaF}_2-\text{NaF}-\text{SiO}_2$	520	$\text{CaO}-\text{Nd}_2\text{O}_3-\text{SiO}_2$	342
$\text{BaO}-\text{Al}_2\text{O}_3-\text{SiO}_2$	286, 626	$\text{CaO}-\text{NiO}-\text{SiO}_2$	179
		$\text{CaO}-\text{P}_2\text{O}_5-\text{SiO}_2$	446
		$\text{CaO}-\text{SrO}-\text{SiO}_2$	64

$\text{CaO}-\text{Ta}_2\text{O}_5-\text{SiO}_2$	469	$\text{Ga}_2\text{O}_3-\text{Al}_2\text{O}_3-\text{SiO}_2$	327
$\text{CaO}-\text{TiO}_4-\text{SiO}_2$	387	$\text{Ga}_2\text{O}_3-\text{H}_2\text{O}-\text{SiO}_2$	606
$\text{CaO}-\text{Y}_2\text{O}_3-\text{SiO}_2$	329	$\text{Ga}_2\text{O}_3-\text{P}_2\text{O}_5-\text{SiO}_2$	462
$\text{CaO}-\text{ZnO}-\text{SiO}_2$	105, 621	$\text{Gd}_2\text{O}_3-\text{Dy}_2\text{O}_3-\text{SiO}_2$	350
$\text{CaO}-\text{ZrO}_2-\text{SiO}_2$	415	$\text{GeO}_2-\text{Al}_2\text{O}_3-\text{SiO}_2$	372
$\text{CaS}-\text{CaO}-\text{SiO}_2$	529	$\text{GeO}_2-\text{BaO}-\text{SiO}_2$	368
$\text{CeO}_2-\text{Li}_2\text{O}-\text{SiO}_2$	339	$\text{GeO}_2-\text{CaO}-\text{SiO}_2$	362, 627
$\text{Ce}_2\text{O}_3-\text{Lu}_2\text{O}_3-\text{SiO}_2$	341	$\text{GeO}_2-\text{Li}_2\text{O}-\text{SiO}_2$	358
$\text{Ce}_2\text{O}_3-\text{Li}_2\text{O}-\text{SiO}_2$	339	$\text{GeO}_2-\text{MgO}-\text{SiO}_2$	359
$\text{Ce}_2\text{O}_3-\text{Nd}_2\text{O}_3-\text{SiO}_2$	342	$\text{GeO}_2-\text{Nd}_2\text{O}_3-\text{SiO}_2$	374
$\text{Ce}_2\text{O}_3-\text{Y}_2\text{O}_3-\text{SiO}_2$	340	$\text{GeO}_2-\text{NiO}-\text{SiO}_2$	376
$\text{CoO}-\text{Al}_2\text{O}_3-\text{SiO}_2$	320	$\text{GeO}_2-\text{PbO}-\text{SiO}_2$	375
$\text{CoO}-\text{Fe}_3\text{O}_4-\text{SiO}_2$	498	$\text{GeO}_2-\text{Sc}_2\text{O}_3-\text{SiO}_2$	372
$\text{CoO}-\text{H}_2\text{O}-\text{SiO}_2$	611	$\text{GeO}_2-\text{SrO}-\text{SiO}_2$	367
$\text{CoO}-\text{MnO}-\text{SiO}_2$	173	$\text{GeO}_2-\text{Y}_2\text{O}_3-\text{SiO}_2$	373
$\text{CoO}-\text{Na}_2\text{O}-\text{SiO}_2$	621	$\text{GeO}_2-\text{ZnO}-\text{SiO}_2$	371
$\text{CoO}-\text{Yb}_2\text{O}_3-\text{SiO}_2$	354		
$\text{CoO}-\text{ZrO}_2-\text{SiO}_2$	438	$\text{H}_2\text{O}-\text{Al}_2\text{O}_3$	411
$\text{Cr}_2\text{O}_3-\text{Al}_2\text{O}_3-\text{SiO}_2$	306	$\text{H}_2\text{O}-\text{Al}_2\text{O}_3-\text{SiO}_2$	593
$\text{Cr}_2\text{O}_3-\text{CaO}-\text{SiO}_2$	476	$\text{H}_2\text{O}-\text{BaO}-\text{SiO}_2$	591
$\text{Cr}_2\text{O}_3-\text{Fe}_3\text{O}_4-\text{SiO}_2$	482	$\text{H}_2\text{O}-\text{CaO}$	388
$\text{Cr}_2\text{O}_3-\text{H}_2\text{O}-\text{SiO}_2$	608	$\text{H}_2\text{O}-\text{CaO}-\text{SiO}_2$	568
$\text{Cr}_2\text{O}_3-\text{MgO}-\text{SiO}_2$	473	$\text{H}_2\text{O}-\text{CaO}-\text{SiO}_2$	558, 643
$\text{Cr}_2\text{O}_3-\text{TiO}_2-\text{SiO}_2$	630	$\text{H}_2\text{O}-\text{CoO}-\text{SiO}_2$	611
$\text{Cr}_2\text{O}_3-\text{ZrO}_2-\text{SiO}_2$	435	$\text{H}_2\text{O}-\text{Cr}_2\text{O}_3-\text{SiO}_2$	608
$\text{CuO}-\text{MgO}-\text{SiO}_2$	15	$\text{H}_2\text{O}-\text{Fe}_3\text{O}_4-\text{SiO}_2$	608
$\text{Dy}_2\text{O}_3-\text{Gd}_2\text{O}_3-\text{SiO}_2$	350	$\text{H}_2\text{O}-\text{Ga}_2\text{O}_3-\text{SiO}_2$	606
$\text{Er}_2\text{O}_3-\text{Y}_2\text{O}_3-\text{SiO}_2$	351	$\text{H}_2\text{O}-\text{K}_2\text{O}-\text{SiO}_2$	543
$\text{EuO}-\text{Al}_2\text{O}_3-\text{SiO}_2$	626	$\text{H}_2\text{O}-\text{MgO}$	550, 643
$\text{FeO}-\text{Al}_2\text{O}_3-\text{SiO}_2$	314	$\text{H}_2\text{O}-\text{MgO}-\text{SiO}_2$	545, 642
$\text{FeO}-\text{CaO}-\text{SiO}_2$	152	$\text{H}_2\text{O}-\text{MnO}-\text{SiO}_2$	608
$\text{FeO}-\text{Fe}_2\text{O}_3-\text{SiO}_2$	638	$\text{H}_2\text{O}-\text{Na}_2\text{O}-\text{SiO}_2$	533, 640
$\text{FeO}-\text{FeS}-\text{SiO}_2$	530	$\text{H}_2\text{O}-\text{NiO}-\text{SiO}_2$	612
$\text{FeO}-\text{K}_2\text{O}-\text{SiO}_2$	142	$\text{H}_2\text{O}-\text{P}_2\text{O}_5-\text{SiO}_2$	607
$\text{FeO}-\text{MgO}-\text{SiO}_2$	144	$\text{H}_2\text{O}-\text{SiO}_2$	577
$\text{FeO}-\text{MnO}-\text{SiO}_2$	165	$\text{H}_2\text{O}-\text{SrO}-\text{SiO}_2$	590
$\text{FeO}-\text{Na}_2\text{O}-\text{SiO}_2$	138	$\text{H}_2\text{O}-\text{ZnO}-\text{SiO}_2$	588
$\text{FeO}-\text{TiO}_2-\text{SiO}_2$	630	$\text{H}_2\text{O}-\text{ZrO}_2-\text{SiO}_2$	606
$\text{FeO}-\text{ZnO}-\text{SiO}_2$	163	$\text{H}_2\text{O}-\text{Y}_2\text{O}_3-\text{SiO}_2$	633
$\text{Fe}_2\text{O}_3-\text{Al}_2\text{O}_3-\text{SiO}_2$	317	$\text{H}_2\text{O}_2-\text{ZrO}_2-\text{SiO}_2$	434, 632
$\text{Fe}_2\text{O}_3-\text{CaO}-\text{SiO}_2$	636		
$\text{Fe}_2\text{O}_3-\text{FeO}-\text{SiO}_2$	638	$\text{KF}-\text{BaF}_2-\text{SiO}_2$	520
$\text{Fe}_2\text{O}_3-\text{H}_2\text{O}-\text{SiO}_2$	608	$\text{KF}-\text{CaF}_2-\text{SiO}_2$	520
$\text{Fe}_2\text{O}_3-\text{K}_2\text{O}-\text{SiO}_2$	493	$\text{KF}-\text{MgF}_2-\text{SiO}_2$	520
$\text{Fe}_2\text{O}_3-\text{MgO}-\text{SiO}_2$	496	$\text{KF}-\text{SrF}_2-\text{SiO}_2$	520
$\text{Fe}_2\text{O}_3-\text{Na}_2\text{O}-\text{SiO}_2$	486	$\text{K}_2\text{O}-\text{Al}_2\text{O}_3-\text{SiO}_2$	237, 624
$\text{Fe}_2\text{O}_3-\text{PbO}-\text{SiO}_2$	497	$\text{K}_2\text{O}-\text{CaO}-\text{SiO}_2$	40
$\text{Fe}_2\text{O}_3-\text{CoO}-\text{SiO}_2$	498	$\text{K}_2\text{O}-\text{FeO}-\text{SiO}_2$	142
$\text{Fe}_2\text{O}_3-\text{Cr}_2\text{O}_3-\text{SiO}_2$	482	$\text{K}_2\text{O}-\text{Fe}_3\text{O}_4-\text{SiO}_2$	493
$\text{Fe}_2\text{O}_3-\text{ZrO}_2-\text{SiO}_2$	632	$\text{K}_2\text{O}-\text{H}_2\text{O}-\text{SiO}_2$	543
$\text{Fe}_2\text{O}_3-\text{FeO}-\text{SiO}_2$	530	$\text{K}_2\text{O}-\text{Li}_2\text{O}-\text{SiO}_2$	10

La ₂ O ₃ --CaO--SiO ₂	334	MnO--FeO--SiO ₂	165
La ₂ O ₃ --Ce ₂ O ₃ --SiO ₂	341	MnO--H ₂ O--SiO ₂	608
La ₂ O ₃ --MgO--SiO ₂	334	MnO--MgO--SiO ₂	127
La ₂ O ₃ --Sm ₂ O ₃ --SiO ₂	349	MnO--Na ₂ O--SiO ₂	126
La ₂ O ₃ --SrO--SiO ₂	336	MnO--TiO ₂ --SiO ₂	401
La ₂ O ₃ --Y ₂ O ₃ --SiO ₂	338		
La ₂ O ₃ --Yb ₂ O ₃ --SiO ₂	353		
Li ₂ O--Al ₂ O ₃ --SiO ₂	206, 622	Na ₃ AlF ₆ --Al ₂ O ₃ --SiO ₂	515
Li ₂ O--B ₂ O ₃ --SiO ₂	182	NaF--BaF ₂ --SiO ₂	520
Li ₂ O--BaO--SiO ₂	73	NaF--CaF ₂ --SiO ₂	520
Li ₂ O--CaO--SiO ₂	28	NaF--MgF ₂ --SiO ₂	520
Li ₂ O--CeO ₂ --SiO ₂	339	NaF--Na ₂ O--SiO ₂	501, 639
Li ₂ O--Ce ₂ O ₃ --SiO ₂	339	NaF--SrF ₂ --SiO ₂	520
Li ₂ O--GeO ₂ --SiO ₂	358	Na ₂ O--Al ₂ O ₃ --SiO ₂	222, 623
Li ₂ O--K ₂ O--SiO ₂	10	Na ₂ O--B ₂ O ₃ --SiO ₂	164
Li ₂ O--MgO--SiO ₂	16	Na ₂ O--BaO--SiO ₂	75
Li ₂ O--Nd ₂ O--SiO ₂	6	Na ₂ O--CaF ₂ --SiO ₂	520
Li ₂ O--TiO ₂ --SiO ₂	378	Na ₂ O--CaO--SiO ₂	30, 615
Li ₂ O--ZnO--SiO ₂	97, 619	Na ₂ O--CoO--SiO ₂	621
Li ₂ O--ZrO ₂ --SiO ₂	403	Na ₂ O--FeO--SiO ₂	138
		Na ₂ O--Fe ₂ O ₃ --SiO ₂	486
		Na ₂ O--H ₂ O--SiO ₂	533, 640
MgF ₂ --Al ₂ O ₃ --SiO ₂	516	Na ₂ O--O--SiO ₂	13
MgF ₂ --KF--SiO ₂	520	Na ₂ O--Li ₂ O--SiO ₂	6
MgF ₂ --MgO--SiO ₂	502	Na ₂ O--MgO--SiO ₂	18
MgF ₂ --NaF--SiO ₂	520	Na ₂ O--MnO--SiO ₃	126
MgO--Al ₂ O ₃ --SiO ₂	253, 625	Na ₂ O--NaF--SiO ₂	501, 639
MgO--B ₂ O ₃ --SiO ₂	188	Na ₂ O--P ₂ O ₅ --SiO ₂	439
MgO--BaO--SiO ₂	80	Na ₂ O--PbO--SiO ₂	109
MgO--CaO--SiO ₂	46, 616	Na ₂ O--SrO--SiO ₂	69
MgO--Cr ₂ O ₃ --SiO ₂	473	Na ₂ O--TiO ₂ --SiO ₂	380
MgO--CuO--SiO ₂	15	Na ₂ O--ZnO--SiO ₂	97, 620
MgO--FeO--SiO ₂	144	Na ₂ O--ZrO ₂ --SiO ₂	405, 631
MgO--Fe ₂ O ₃ --SiO ₂	496	Nb ₂ O ₅ --CaO--SiO ₂	635
MgO--GeO ₂ --SiO ₂	359	Nb ₂ O ₅ --ZnO--SiO ₂	468
MgO--H ₂ O	550, 643	Nd ₂ O ₃ --Al ₂ O ₃ --SiO ₂	303
MgO--H ₂ O--SiO ₂	545, 642	Nd ₂ O ₃ --CaO--SiO ₂	342
MgO--K ₂ O--SiO ₂	21	Nd ₂ O ₃ --Ce ₂ O ₃ --SiO ₂	342
MgO--La ₂ O ₃ --SiO ₂	334	Nd ₂ O ₃ --CaO ₂ --SiO ₂	374
MgO--Lu ₂ O ₃ --SiO ₂	16	Nd ₂ O ₃ --SrO--SiO ₂	346
MgO--MgF ₂ --SiO ₂	502	NiO--Al ₂ O ₃ --SiO ₂	323
MgO--Mg ₃ O ₂	528	NiO--CaO--SiO ₂	179
MgO--MnO--SiO ₂	127	NiO--GeO ₂ --SiO ₂	376
MgO--Na ₂ O--SiO ₂	18	NiO--H ₂ O--SiO ₂	612
MgO--NiO--SiO ₂	175	NiO--MgO--SiO ₂	175
MgO--P ₂ O ₅ --SiO ₂	444	NiO--Yb ₂ O ₃ --SiO ₂	356
MgO--U ₃ O ₈ --SiO ₂	119	NiO--ZrO ₂ --SiO ₂	438
MgO--ScO--SiO ₂	72		
MgO--TiO ₂ --SiO ₂	381		
MgO--Y ₂ O ₃ --SiO ₂	329		
MgO--ZnO--SiO ₂	102	P ₂ O ₅ --Al ₂ O ₃ --SiO ₂	460
MgO--ZrO ₂ --SiO ₂	410	P ₂ O ₅ --B ₂ O ₃ --SiO ₂	458
Mg ₂ O--MgO--SiO ₂	528	P ₂ O ₅ --CaO--SiO ₂	446
MnO--Al ₂ O ₃ --SiO ₂	310	P ₂ O ₅ --Ga ₂ O ₃ --SiO ₂	462
MnO--CaO--SiO ₄	132	P ₂ O ₅ --H ₂ O--SiO ₂	607
MnO--CeO--SiO ₂	173	P ₂ O ₅ --MgO--SiO ₂	444

$P_2O_5-Na_2O-SiO_2$	439	$UO_4-ZrO_2-SiO_2$	437
$P_2O_5-PbO-SiO_2$	463	$V_2O_3-ZnO-SiO_2$	634
$P_2O_5-ZnO-SiO_2$	457	$V_2O_5-ZnO-SiO_2$	466
$PbO-Al_2O_3-SiO_2$	304	$V_2O_5-TiO_2-SiO_2$	467
$PbO-B_2O_3-SiO_2$	203		
$PbO-BaO-SiO_2$	122		
$PbO-Fe_2O_3-SiO_2$	497	$Y_2O_3-Al_2O_3-SiO_2$	301
$PbO-GeO_2-SiO_2$	375	$Y_2O_3-CaO-SiO_2$	329
$PbO-K_2O-SiO_2$	115	$Y_2O_3-Ce_2O_3-SiO_2$	340
$PbO-MgO-SiO_2$	119	$Y_2O_3-Er_2O_3-SiO_2$	351
$PbO-Na_2O-SiO_2$	109	$Y_2O_3-GeO_2-SiO_2$	373
$PbO-P_2O_5-SiO_2$	463	$Y_2O_3-HfO_2-SiO_2$	633
$Rb_2O-ZrO_2-SiO_2$	409	$Y_2O_3-La_2O_3-SiO_2$	338
$Se_2O_3-GeO_2-SiO_2$	372	$Y_2O_3-MgO-SiO_2$	329
$Sm_2O_3-La_2O_3-SiO_2$	349	$Y_2O_3-SrO-SiO_2$	331
$SrF_2-Al_2O_3-SiO_2$	516	$Yb_2O_3-CoO-SiO_2$	354
$SrF_2-KF-SiO_2$	520	$Yb_2O_3-La_2O_3-SiO_2$	353
$SrF_2-KaF-SiO_2$	520	$Yb_2O_3-NiO-SiO_2$	356
$SiF_2-SiO-SiO_2$	512		
$SrO-Al_2O_3-SiO_2$	283, 625a	$ZnO-Al_2O_3-SiO_2$	300
$SrO-BaO-SiO_2$	93, 618	$ZnO-B_2O_3-SiO_2$	200
$SrO-BeO-SiO_2$	71	$ZnO-BaO-SiO_2$	108, 621
$SrO-CaO-SiO_2$	64	$ZnO-CaO-SiO_2$	105, 621
$SrO-GeO_2-SiO_2$	367	$ZnO-FeO-SiO_2$	163
$SrO-H_2O-SiO_2$	590	$ZnO-GeO_2-SiO_2$	371
$SrO-La_2O_3-SiO_2$	336	$ZnO-H_2O-SiO_2$	588
$SrO-MgO-SiO_2$	72	$ZnO-K_2O-SiO_2$	100
$SrO-Na_2O-SiO_2$	69	$ZnO-Li_2O-SiO_2$	97, 619
$SrO-Nd_2O_3-SiO_2$	346	$ZnO-MgO-SiO_2$	102
$SiO-SrF_2-SiO_2$	512	$ZnO-Na_2O-SiO_2$	97, 620
$SrO-TiO_2-SiO_2$	392	$ZnO-Nb_2O_5-SiO_2$	468
$SrO-Y_2O_3-SiO_2$	331	$ZnO-P_2O_5-SiO_2$	457
$SrO-ZnO-SiO_2$	107	$ZnO-SrO-SiO_2$	107
$SrO-ZrO_2-SiO_2$	426	$ZnO-Ta_2O_5-SiO_2$	472
$Ta_2O_5-BaO-SiO_2$	635	$ZnO-V_2O_3-SiO_2$	634
$Ta_2O_5-CaO-SiO_2$	469	$ZnO-V_2O_5-SiO_2$	466
$Ta_2O_5-ZnO-SiO_2$	472	$ZrO_2-Al_2O_3-SiO_2$	429
$ThO_2-ZrO_2-SiO_2$	434, 632	$ZrO_2-BaO-SiO_2$	427
$TiO_2-Al_2O_3-SiO_2$	394	$ZrO_2-CaO-SiO_2$	415
$TiO_2-BaO-SiO_2$	392, 628	$ZrO_2-CoO-SiO_2$	438
$TiO_2-CaO-SiO_2$	387	$ZrO_2-Cr_2O_3-SiO_2$	435
$TiO_2-Cr_2O_3-SiO_2$	630	$ZrO_2-Fe_2O_3-SiO_2$	632
$TiO_2-FeO-SiO_2$	630	$ZrO_2-H_2O-SiO_2$	606
$TiO_2-Li_2O-SiO_2$	378	$ZrO_2-HfO_2-SiO_2$	434, 632
$TiO_2-MgO-SiO_2$	381	$ZrO_2-Li_2O-SiO_2$	403
$TiO_2-MnO-SiO_2$	401	$ZrO_2-MgO-SiO_2$	410
$TiO_2-Na_2O-SiO_2$	380	$ZrO_2-Na_2O-SiO_2$	405, 631
$TiO_2-SrO-SiO_2$	392	$ZrO_2-NiO-SiO_2$	438
$TiO_2-Ti_2O_3-SiO_2$	398	$ZrO_2-Rb_2O-SiO_2$	409
$TiO_2-ZrO_2-SiO_2$	399	$ZrO_2-SrO-SiO_2$	426
$Ti_2O_3-Ti_3O_2-SiO_2$	398	$ZrO_2-ThO_2-SiO_2$	434, 632

TABLE OF CONTENTS

Foreword	3
Alkali Silicate Systems	6
Cuprite-Silicate Systems	15
Magnesia-Silicate Systems	16
Calcium Silicate Systems	28
Strontium Silicate Systems	69
Barium Silicate Systems	73
Zinc Silicate Systems	97
Lead Silicate Systems	109
Manganese Silicate Systems	126
Ferrosilicate Systems	138
Cobalt Silicate Systems	173
Nickel Silicate Systems	175
Borosilicate Systems	182
Aluminosilicate Systems	206
Gallium Silicate Systems	327
Yttrium Silicate Systems	329
Lanthanide-Silicate Systems	334
Germanium Silicate Systems	358
Titanosilicate Systems	378
Zirconosilicate Systems	403
Silicophosphate Systems	439
Vanadate-Silicate Systems	466
Niobate-Silicate Systems	468
Tantalate-Silicate Systems	469
Chromosilicate Systems	473
Ferrisilicate Systems	486
Systems Containing Fluorine	501
Systems Containing Sulfides	528
Systems Containing Water	533
Supplement	615
Alphabetical Index	647